P. Lambropoulos
D. Petrosyan

Fundamentals of Quantum Optics and Quantum Information

Springer

Peter Lambropoulos · David Petrosyan

Fundamentals of Quantum Optics and Quantum Information

Peter Lambropoulos
David Petrosyan

Fundamentals of Quantum Optics and Quantum Information

With 95 Figures

Springer

Prof. Dr. Peter Lambropoulos
Foundation for Research
and Technology Hellas (FORTH)
IESL and University of Crete
P.O. Box 1527
711 10 Heraklion, Crete
Greece
e-mail: labro@iesl.forth.gr

Dr. David Petrosyan
Foundation for Research
and Technology Hellas (FORTH)
IESL
P.O. Box 1527
711 10 Heraklion, Crete
Greece
e-mail: dap@iesl.forth.gr

Library of Congress Control Number: 2006932725

ISBN-10 3-540-34571-X Springer Berlin Heidelberg New York
ISBN-13 978-3-540-34571-8 Springer Berlin Heidelberg New York

Springer is a part of Springer Science+Business Media

springer.com

Typesetting: Camera ready by authors
Production: LE-TEX Jelonek, Schmidt & Vöckler GbR, Leipzig
Cover Design: WMXDesign GmbH, Heidelberg

Printed on acid-free paper 57/3100/YL 5 4 3 2 1 0

To Olympia
P. L.

To Anna and Mika
D. P.

Preface

Another book on Quantum Optics? or Quantum Information? Well, not exactly. A more descriptive title might be: "A guided tour through basic quantum mechanics, quantum optics and quantum information". Even better, a few words on its origin and our motivation for undertaking the task might be useful to the potential reader in deciding whether to turn the pages beyond this preface.

For more than ten years now, a graduate course on quantum optics has been taught in the physics department of the University of Crete. Spanning two semesters, it originally consisted of a collection of topics representative of what can be found in the numerous by now excellent books on quantum optics. Over the last four years or so, however, the course acquired a gradually increasing segment of what is broadly referred to as quantum information, which at this point is approximately half of the material. Inevitably, the topics on standard quantum optics had to be reduced or compressed accordingly.

The connection between quantum optics and quantum information is not accidental. Strictly speaking, quantum optics represents the set of phenomena in radiation–matter interaction in which the state and quantum statistical properties of the radiation play a role, but in a broader sense it also involves the study of few-state and often single quantum systems interacting with radiation. Quantum information is a more recent arrival in physics and, to some extent, computer science. It revolves around the notion of physical information and its processing in the context of quantum mechanics, where the principle of superposition and entanglement play fundamental roles. Owing to tremendous progress in coherent radiation sources and signal detection, now it is indeed possible to conduct experiments involving only one or few atoms and photons at a time. Many arrangements of this type provide a convenient and fertile testing ground for at least proof-of-principle experiments pertaining to physical implementations of quantum information processing. Conversely, demands arising from such implementations motivate and shape a great deal of current research in quantum optics.

In our collection of topics, we endeavored to cover the fundamentals, in the sense of providing the tools and phenomenology needed for an uninterrupted and self consistent flow of the material, as well as presenting to the students as broad a landscape of the field as two semesters allow. Although the majority of the students taking the class came from departments of physics, with a two-semester exposure to quantum mechanics, their level of mastery of the subject was not uniform, especially on aspects relevant to coherent interactions and quantum optics. Moreover, occasionally a student or two from mathematics or computer science might appear, if for no other reason simply out of curiosity. As a consequence, the necessity of establishing a common language arose. Of course many aspects of quantum information could be discussed only in terms of vector spaces. Physical implementations were, however, all along meant to be an essential part of the course, for which quantum optics provides an ideal vehicle. With such a plan in mind, instead of waiting until gaps in the quantum theoretical background of some students became evident, half-way through the course, we found it more expedient to simply provide a crash course on basic quantum theory. And that is how we arrived at the structure of the book.

Although the skeleton of the course has remained more or less fixed, some topics have varied from year to year, reflecting our preferences at the time; inevitably influenced by recent developments. Thus the content of the pages that follow represents the sum total of the various versions of the course over the last two or three years, optimized for economic, but hopefully self-contained, presentation within a book of reasonable length. To the best of our knowledge, the material can not be found in one single book. Most of it can of course be found in a collection of excellent books—a fairly extensive list of which is given in our bibliography—through which the student would have to sort, a task which can be disorienting for the novice and apt to lead to discouragement.

The broad scope and inevitable limitations in the size of the book dictated choices as to topics included, which were guided by the need to provide the necessary background, in a self-contained fashion, so that the material can be followed without recourse to other texts. Thus the chapters on quantum theory represent a preparation for the understanding of quantum optics, which in turn serves the purpose of illustrating physical implementations of quantum information processing. The discussion of quantum information and computation emphasizes the physical rather than the computer science aspects or the underlying mathematical structure. Obviously, a number of topics found in texts of quantum optics or quantum information and computation have been left out. On the other hand, a few topics representing relatively recent developments, not yet in books, have been included, as they seem, at least to us, to complement the tools and physical concepts for the implementation of quantum computation. The assumption is that equipped with the tools and phenomenology provided in this book, the student should be prepared to handle more specialized texts.

It must be already clear that the book was prepared with the advanced undergraduate and beginning graduate student in mind; or perhaps a researcher from a different field. Yet, it should also be useful to instructors in providing a selection of topics and ways of presentation in a course along similar lines. In fact, although the two parts of the book are to some extent interconnected, its structure is such that Parts I and II could serve as concise independent texts for short courses on, respectively, quantum optics and quantum information. These two subjects come together in a synthesis represented by Chap. 10, the only chapter that requires a background in both. As for Chap. 1, which provides a prerequisite for both subjects, it can simply serve as a convenient reference to those thoroughly familiar with quantum theory.

Given its scope, the book does not contain an extensive list of research journals' articles. We have instead endeavored to provide as extensive a list of related books as we know, and in some cases reference to original research or review articles that we deemed useful complements to our discussion of certain topics. Inevitably, our selection of such articles is not immune to omissions for which we hasten to apologize and assure the reader that they certainly were not intentional.

After submission to the publisher, Steven van Enk took the initiative to read through many parts of the book, with admirable speed and efficiency. His comments and suggestions, many of which were implemented, despite the time pressure, have proven very valuable in improving the text, for which we are very grateful. Needless to add that the responsibility for whatever rough edges persist rests with the authors.

Heraklion,
June 2006

Peter Lambropoulos
David Petrosyan

Contents

Part I

Quantum Optics

Preamble

Quantum optics is a relatively mature field of physics, having quickly developed shortly after the inventions of masers and lasers in the late 50's and early 60's. It usually deals with quantum effects associated with the light–matter interaction. Recently, the research in quantum optics was largely driven by the rapid progress in microfabrication technologies, precision measurements and coherent radiation sources. Many quantum optical systems can and are employed to test and illustrate the fundamental notions of quantum theory, not to mention various practical applications for optical communications or quantum information processing, whose physical aspects have by now become an integral part of quantum optics.

This Part of the book is devoted to the fundamentals of quantum optics. In Chap. 1 we give a brief review of quantum theory. Chap. 2 introduces the quantization of the electromagnetic field, its quantum states and various representations of the field. In Chap. 3 we study the interaction of an atom with the classical and quantized electromagnetic fields. We then describe several formalisms to deal with the decoherence and dissipation of quantum systems coupled to an environment and illustrate these techniques in the context of atomic spontaneous decay in Chap. 4 and decay of electromagnetic field confined within a cavity in Chap. 5. Finally, in Chap. 6 we consider several illustrative examples of weak field propagation in atomic media

1

Quantum Mechanical Background

To make this book self-contained and accessible to a broader audience, we begin with an outline of the mathematical framework of quantum theory, introducing vector spaces and linear operators, the postulates of quantum mechanics, the Schrödinger equation, and the density operator. In order to illustrate as well as motivate much of the discussion, we review the properties of the simplest, yet very important quantum mechanical system—the quantized harmonic oscillator, which is encountered repeatedly in the sections that follow.

Our presentation of the fundamental principles of quantum theory follows the traditional approach based on the standard set of postulates found in most textbooks. It could be viewed as a "pragmatic" approach in which quantum mechanics is accepted as an operational theory geared to predicting the outcomes of measurements on physical systems under well defined conditions. We have deliberately stayed clear of, depending on disposition, semi-philosophical issues pertaining to the relation of quantum theory and some of its counterintuitive notions vis a vis our macroscopic experience. Thus issues such as the collapse of the wavefunction upon measurement; the quantum correlations—entanglement—between spatially separated systems, or else, the non-local character of such correlations; the transition from the quantum to the classical world; etc., are treated according to the rules of the theory, without any excursion into philosophical implications, as they would be beyond the scope, as well as the needs, of this book. Discussions pertaining to such issues can be found in the relevant literature cited at the end of this book under the title Further Reading.

1.1 The Mathematical Framework

The language of physics is mathematics and in particular it is analysis for classical physics. The fundamental laws in mechanics, electromagnetism and

even relativity are formulated in terms of differential and/or integral equations and so are their applications to specific problems. Quantum mechanics, initially called wave mechanics, was also formulated in terms of differential equations: The Schrödinger equation, often still called wave-equation, being a case in point. Eventually, it was realized, however, that the essence and natural language of quantum mechanics is that of vector spaces which means linear algebra and functional analysis. This does not mean that one does not have to solve differential equations in some specific applications of the theory. But it does mean that a thorough picture of the structure of quantum systems, their states and eigenvalues, as well as their interaction with other systems can be obtained by studying the algebra of a suitably chosen set of operators and the corresponding vector spaces. Thus we begin with a brief summary of the algebra of vector space and linear operators.

1.1.1 Complex Vector Spaces

A complex vector space is a set $\mathbb{V}$ of elements ϕ_i, called vectors, in which an operation of summation $\phi_i + \phi_j$ as well as multiplication $a\phi_i$ by a complex number (c-number) a can be defined. For a vector space, the following properties are assumed to hold true:

(a) If $\phi_i, \phi_j \in \mathbb{V}$ then $\phi_i + \phi_j \in \mathbb{V}$
  (a_1) $\phi_i + \phi_j = \phi_j + \phi_i$
  (a_2) $(\phi_i + \phi_j) + \phi_k = \phi_i + (\phi_j + \phi_k)$
(b) There exists in $\mathbb{V}$ a zero element 0 such that $\phi_i + 0 = \phi_i$ for all $\phi_i \in \mathbb{V}$
(c) If $\phi_i \in \mathbb{V}$ then $a\phi_i \in \mathbb{V}$
  (c_1) $ab\phi_i = a(b\phi_i)$
  (c_2) $1 \cdot \phi_i = \phi_i$
  (c_3) $0 \cdot \phi_i = 0$, which means that ϕ_i multiplied by the number 0 gives the zero element of $\mathbb{V}$
(d_1) $a(\phi_i + \phi_j) = a\phi_i + a\phi_j$
(d_2) $(a + b)\phi_i = a\phi_i + b\phi_i$

The element resulting from the operation $(-1)\phi_i$ is denoted by $-\phi_i$, and using the above properties we have

$$\phi_i + (-\phi_i) = (1 + (-1))\phi_i = 0 \cdot \phi_i = 0.$$

A subset $\mathbb{S}$ of the elements of $\mathbb{V}$ is called a subspace of $\mathbb{V}$ if for all $\phi_i \in \mathbb{S}$, all of the above properties hold true with respect to $\mathbb{S}$, i.e., if for all $\phi_i, \phi_j \in \mathbb{S}$ it follows that $\phi_i + \phi_j \in \mathbb{S}$, $a\phi_i \in \mathbb{S}$, etc.

An expression of the form $\sum_{i=1}^{n} c_i\phi_i$, with c_i complex numbers, is referred to as a linear combination of the vectors $\phi_1, \phi_2, \ldots, \phi_n$. A set of vectors $\phi_1, \phi_2, \ldots, \phi_n$ are said to be linearly independent if the relation $\sum_{i=1}^{n} c_i\phi_i = 0$ is satisfied only for all $c_i = 0$.

A vector space $\mathbb{V}$ is N-dimensional if there are N and not more linearly independent vectors in $\mathbb{V}$, for which the notation $\mathbb{V}^{(N)}$ shall be used when

necessary. If the number of linearly independent vectors in a space can be arbitrarily large, the space is called infinite-dimensional. Every set of N linearly independent vectors in an N-dimensional space is a basis. If $e_1, e_2, \ldots, e_N$ are the vectors of a basis, every vector ϕ_i of the space can be expressed as a linear combination of the form

$$\phi_i = c_1 e_1 + c_2 e_2 + \ldots + c_N e_N \ , \tag{1.1}$$

with the coefficients c_j $(j = 1, 2, \ldots N)$ referred to as the coordinates of ϕ_i in that particular basis. Obviously, when vectors are added or multiplied by a c-number a, their coordinates are added or multiplied by that number, respectively.

From two (or more) different vector spaces $\mathbb{V}_{\rm A}^{(N_{\rm A})}$ and $\mathbb{V}_{\rm B}^{(N_{\rm B})}$, with the corresponding dimensions $N_{\rm A}$ and $N_{\rm B}$, one can construct a new vector space $\mathbb{V}^{(N)} = \mathbb{V}_{\rm A}^{(N_{\rm A})} \otimes \mathbb{V}_{\rm B}^{(N_{\rm B})}$, called tensor-product space, whose dimension is given by $N = N_{\rm A} N_{\rm B}$. If $\phi^{\rm A}$ is a vector in space $\mathbb{V}_{\rm A}^{(N_{\rm A})}$ and $\phi^{\rm B}$ is a vector in space $\mathbb{V}_{\rm B}^{(N_{\rm B})}$, the vector $\phi = \phi^{\rm A} \otimes \phi^{\rm B}$ is called the tensor product of $\phi^{\rm A}$ and $\phi^{\rm B}$ and it belongs to $\mathbb{V}^{(N)}$. For the tensor product vectors, the following properties are satisfied:

(a) If $\phi^{\rm A} \in \mathbb{V}_{\rm A}^{(N_{\rm A})}$ and $\phi^{\rm B} \in \mathbb{V}_{\rm B}^{(N_{\rm B})}$ and a is any c-number, then
$a(\phi^{\rm A} \otimes \phi^{\rm B}) = (a\phi^{\rm A}) \otimes \phi^{\rm B} = \phi^{\rm A} \otimes (a\phi^{\rm B}) \in \mathbb{V}^{(N)}$

($\rm b_1$) If $\phi_i^{\rm A}, \phi_j^{\rm A} \in \mathbb{V}_{\rm A}^{(N_{\rm A})}$ and $\phi^{\rm B} \in \mathbb{V}_{\rm B}^{(N_{\rm B})}$, then
$(\phi_i^{\rm A} + \phi_j^{\rm A}) \otimes \phi^{\rm B} = \phi_i^{\rm A} \otimes \phi^{\rm B} + \phi_j^{\rm A} \otimes \phi^{\rm B} \in \mathbb{V}^{(N)}$

($\rm b_2$) If $\phi^{\rm A} \in \mathbb{V}_{\rm A}^{(N_{\rm A})}$ and $\phi_i^{\rm B}, \phi_j^{\rm B} \in \mathbb{V}_{\rm B}^{(N_{\rm B})}$, then
$\phi^{\rm A} \otimes (\phi_i^{\rm B} + \phi_j^{\rm B}) = \phi^{\rm A} \otimes \phi_i^{\rm B} + \phi^{\rm A} \otimes \phi_j^{\rm B} \in \mathbb{V}^{(N)}$

Any vector $\phi \in \mathbb{V}^{(N)}$ can be expressed as a linear superposition

$$\phi = \sum_{i=1}^{N_{\rm A}} \sum_{j=1}^{N_{\rm B}} c_{ij}\, e_{ij} \ , \tag{1.2}$$

where $e_{ij} \equiv e_i^{\rm A} \otimes e_i^{\rm B}$ with $e_i^{\rm A}$ and $e_j^{\rm B}$ being the basis vectors of spaces $\mathbb{V}_{\rm A}^{(N_{\rm A})}$ and $\mathbb{V}_{\rm B}^{(N_{\rm B})}$, respectively. All of the above properties for vector spaces hold for the tensor product vector space $\mathbb{V}^{(N)} = \mathbb{V}_{\rm A}^{(N_{\rm A})} \otimes \mathbb{V}_{\rm B}^{(N_{\rm B})}$ which is thus a vector space itself.

A vector space is called a scalar product space if a function (ϕ_i, ϕ_j) can be defined in it, which has the properties

$$(\phi, \phi) \geq 0 \quad \text{with} \quad (\phi, \phi) = 0 \ \text{ iff } \ \phi = 0 \ , \tag{1.3}$$

$$(\phi_i, \phi_j) = (\phi_j, \phi_i)^* \ , \tag{1.4}$$

where $(\ldots)^*$ denotes the complex conjugate of $(\ldots)$.

$$(\phi_i + \phi_j, \phi_k) = (\phi_i, \phi_k) + (\phi_j, \phi_k) \ , \tag{1.5}$$

and for any c-number a

$$(\phi_i, a\phi_j) = a(\phi_i, \phi_j) \ , \tag{1.6}$$

which in combination with (1.4) yields $(a\phi_i, \phi_j) = a^*(\phi_i, \phi_j)$. The function (ϕ_i, ϕ_j) is called the scalar product of the elements ϕ_i and ϕ_j, and the two elements are said to be orthogonal if

$$(\phi_i, \phi_j) = 0 \ . \tag{1.7}$$

Given the notion of the scalar product, the norm of the vector ϕ is defined as

$$||\phi|| \equiv +\sqrt{(\phi, \phi)} \ . \tag{1.8}$$

From the definition of the scalar product in (1.3) it follows that (ϕ, ϕ) is a real and positive number. The vector $\hat{\phi} \equiv \phi/||\phi||$ is said to be normalized, since $||\hat{\phi}|| = 1$.

With the above properties of the scalar product, it is easy to prove the Cauchy–Schwarz inequality

$$|(\phi_i, \phi_j)|^2 \leq (\phi_i, \phi_i)(\phi_j, \phi_j) \tag{1.9}$$

which holds for any two vectors $\phi_i, \phi_j \in \mathbb{V}^{(N)}$. To this end, consider

$$(\phi_i - a\phi_j, \phi_i - a\phi_j) \geq 0 \ ,$$

which can be expanded as

$$(\phi_i, \phi_i) - a(\phi_i, \phi_j) - a^*(\phi_j, \phi_i) + aa^*(\phi_j, \phi_j) \geq 0 \ . \tag{1.10}$$

Choosing $a = (\phi_j, \phi_i)/(\phi_j, \phi_j)$, from (1.10) we obtain the Cauchy–Schwarz inequality (1.9).

The above notions and notation in connection with the scalar product and its properties represent a generalization of what is usually called scalar (or inner) product in the 3-dimensional space of traditional vector calculus. From now on, we will adopt the, usual in quantum mechanics, Dirac notation $|\phi\rangle$ for vectors of the space and $\langle\phi_i|\phi_j\rangle$ for the scalar product, while $|\phi\rangle$ and $\langle\phi|$ are also referred to, respectively, as *ket* and *bra* vectors. It can be shown that the bra vectors belong to the space dual to that of the kets.

1.1.2 Bases and Vector Decomposition

In an N-dimensional scalar product space $\mathbb{V}^{(N)}$, as in a 3-dimensional space, one can always choose a set of N orthonormal and therefore linearly independent vectors $|e_i\rangle$,

$$\langle e_i|e_j\rangle = \delta_{ij} \ , \quad i, j = 1, 2, \ldots, N \ ,$$

where

$$\delta_{ij} = \begin{cases} 1 & \text{if } i = j \\ 0 & \text{if } i \neq j \end{cases}$$

is the Kronecker delta. This set of vectors is said to form a basis $\{|e_i\rangle\}$ in terms of which any vector $|\phi\rangle \in \mathbb{V}^{(N)}$ can be expressed as a linear combination of the basis unit vectors

$$|\phi\rangle = \sum_{i=1}^{N} c_i |e_i\rangle \ , \tag{1.11}$$

with the c-number coefficients $c_i = \langle e_i|\phi\rangle$, which is an immediate consequence of the orthonormality and completeness of the basis. Thus any $|\phi\rangle$ can be written as

$$|\phi\rangle = \sum_{i=1}^{N} \langle e_i|\phi\rangle |e_i\rangle \ , \tag{1.12}$$

which is said to be a decomposition of vector $|\phi\rangle$ in terms of the basis $\{|e_i\rangle\}$, with the decomposition coefficients being a generalization of the components of a vector in 3-dimensional space on the axes of the basis chosen for the description of the system under consideration, whether it be a point mass, an extended rigid body, etc.

Any nonzero vector $|\phi\rangle$ in a finite scalar product space can, as is often desirable in quantum mechanics, be normalized. In that case, we have $\langle\phi|\phi\rangle = 1$, which implies

$$\sum_{i=1}^{N} |c_i|^2 = \sum_{i=1}^{N} |\langle e_i|\phi\rangle|^2 = 1 \ . \tag{1.13}$$

This again follows from the orthonormality of the basis vectors and we can state that, for any vector $|\phi\rangle$ normalized or not, the decomposition

$$|\hat{\phi}\rangle = \frac{1}{||\phi||} \sum_{i=1}^{N} \langle e_i|\phi\rangle |e_i\rangle \ , \tag{1.14}$$

with $||\phi|| \equiv +\sqrt{\langle\phi|\phi\rangle} = (\sum_i |\langle e_i|\phi\rangle|^2)^{1/2}$, represents a normalized vector.

Considering now a two-component tensor product vector space $\mathbb{V}^{(N)} = \mathbb{V}_{\rm A}^{(N_{\rm A})} \otimes \mathbb{V}_{\rm B}^{(N_{\rm B})}$, we state without proof an important theorem of linear algebra, known as the Schmidt (or polar) decomposition: For any vector $|\phi\rangle \in \mathbb{V}^{(N)}$, it is possible to construct the orthonormal sets of vectors $|\phi_i^{\rm A}\rangle \in \mathbb{V}_{\rm A}^{(N_{\rm A})}$ and $|\phi_i^{\rm B}\rangle \in \mathbb{V}_{\rm B}^{(N_{\rm B})}$, where $i = 1, 2, \ldots, \min(N_{\rm A}, N_{\rm B})$, in terms of which $|\phi\rangle$ can be represented as

$$|\phi\rangle = \sum_i s_i \, |\phi_i^{\rm A}\rangle \otimes |\phi_i^{\rm B}\rangle \ , \tag{1.15}$$

where the Schmidt coefficients s_i are real non-negative numbers. Comparing this with the expansion (1.2) which involves double summation over

$i = 1, 2, \ldots, N_{\mathrm{A}}$ and $j = 1, 2, \ldots, N_{\mathrm{B}}$, we see that the Schmidt decomposition allows one to represent a vector $|\phi\rangle$ through a single sum over $i = 1, 2, \ldots, \min(N_{\mathrm{A}}, N_{\mathrm{B}})$.

Most of the above features and properties can be generalized to the case of infinite-dimensional ($N \to \infty$) discrete spaces, for which the summations over i extend from from 1 to ∞, and the respective quantities, as for example the square of the norm $||\phi||^2 = \sum_{i=1}^{\infty} |\langle e_i|\phi\rangle|^2$, are to be understood as the limit of the infinite series. A further generalization having to do with transition from a discrete to a continuous vector decomposition is discussed below, after we introduce the notion of linear operators in a vector space and review their properties. Infinite-dimensional discrete vector spaces, as well as continuous, represent the most basic tool in the formulation of quantum theory, as the possible states of any physical system correspond to the vectors of suitably chosen and constructed vector spaces.

The vector spaces describing quantum systems are habitually said to be Hilbert spaces, the term being most meaningful for infinite dimensional vector spaces. Strictly speaking, a Hilbert space $\mathbb{H}$ is a vector space with a scalar product, a metric generated through that scalar product and which is complete with respect to that metric. What is meant by metric is the distance between two vectors ϕ_i and ϕ_j, given in this case by the norm of their difference, i.e., $||\phi_i - \phi_j||$. The space is complete if every Cauchy sequence ϕ_i of vectors in the space converges to some vector ϕ in that space, in the sense that

$$\lim_{i \to \infty} ||\phi_i - \phi|| = 0 \, .$$

An infinite sequence of vectors is said to be Cauchy if $||\phi_i - \phi_j|| \to 0$ as $i, j \to \infty$. For all practical purposes, it is justified to use the term Hilbert space for all vector spaces encountered in this book.

1.1.3 Linear Operators

Let $\mathcal{A}$ be a function (an operation) that maps any vector of a linear space $\mathbb{S}$ into another vector of the same space; symbolically

$$\mathcal{A}\phi_i = \phi_j \, . \tag{1.16}$$

Such a function is called a linear operator if it satisfies the conditions

$$\mathcal{A}(\phi_i + \phi_j) = \mathcal{A}\phi_i + \mathcal{A}\phi_j \, , \tag{1.17a}$$

$$\mathcal{A}(c\phi_i) = c\mathcal{A}\phi_i \, , \tag{1.17b}$$

for $\phi_i, \phi_j \in \mathbb{S}$ and c a c-number.

The multiplication of an operator by a c-number, the addition $\mathcal{A} + \mathcal{B}$ and the product $\mathcal{A}\mathcal{B}$ of two operators are defined via

$$(c\mathcal{A})\phi = c(\mathcal{A}\phi) \,, \tag{1.18a}$$

$$(\mathcal{A}+\mathcal{B})\phi = \mathcal{A}\phi + \mathcal{B}\phi \,, \tag{1.18b}$$

$$(\mathcal{A}\mathcal{B})\phi = \mathcal{A}(\mathcal{B}\phi) \,, \tag{1.18c}$$

the order of $\mathcal{A}$ and $\mathcal{B}$ in the two sides of the last equation being an essential part of the definition. It is easy to show that if $\mathcal{A}$ and $\mathcal{B}$ are linear operators then $\mathcal{A}+\mathcal{B}$ and $\mathcal{A}\mathcal{B}$ also are linear operators.

In any vector space $\mathbb{S}$ there is the zero operator defined via $0\phi = 0$, the 0 in the left side represents the operator, while on the right side it denotes the zero vector of the space $\mathbb{S}$. The identity operator I is defined via $I\phi = \phi$. Both definitions are valid for any $\phi \in \mathbb{S}$. Linear operators are fully defined only when the vector space on which they operate, so to speak, is also defined.

To every linear operator $\mathcal{A}$ on $\mathbb{S}$, its adjoint operator $\mathcal{A}^\dagger$ can also be defined by the relation

$$\langle \mathcal{A}^\dagger \phi_i | \phi_j \rangle = \langle \phi_i | \mathcal{A}\phi_j \rangle \,. \tag{1.19}$$

If it so happens that $\mathcal{A}^\dagger = \mathcal{A}$, then the operator $\mathcal{A}$ is said to be self-adjoint, which for our purposes in this book is equivalent to $\mathcal{A}$ being Hermitian, in the standard sense of quantum mechanics texts.

The operator $\mathcal{B}$ is the inverse of an operator $\mathcal{A}$ if

$$\mathcal{A}\mathcal{B} = \mathcal{B}\mathcal{A} = I \,, \tag{1.20}$$

and is denoted by $\mathcal{A}^{-1}$.

If the inverse of a linear operator $\mathcal{U}$ is its Hermitian adjoint $\mathcal{U}^\dagger$, in which case

$$\mathcal{U}^\dagger \mathcal{U} = I \,, \tag{1.21}$$

then $\mathcal{U}$ is said to be unitary. Equivalently, $\mathcal{U}$ is unitary if $\mathcal{U}^\dagger = \mathcal{U}^{-1}$.

Given two operators $\mathcal{A}$ and $\mathcal{B}$, their commutator is defined as

$$[\mathcal{A}, \mathcal{B}] = \mathcal{A}\mathcal{B} - \mathcal{B}\mathcal{A} \,, \tag{1.22}$$

and anticommutator as

$$[\mathcal{A}, \mathcal{B}]_+ = \mathcal{A}\mathcal{B} + \mathcal{B}\mathcal{A} \,. \tag{1.23}$$

The operators are said to commute (anticommute) if their commutator (anticommutator) is zero.

A vector $|\phi\rangle$, other that the zero vector, is said to be an eigenvector of operator $\mathcal{A}$, with eigenvalue the c-number a, if it satisfies the relation

$$\mathcal{A}\,|\phi\rangle = a\,|\phi\rangle \,. \tag{1.24}$$

If the operator is Hermitian, its eigenvalues and eigenvectors have two important properties:

(i) All eigenvalues are real.

(ii) If $|\phi_i\rangle$ and $|\phi_j\rangle$ are two eigenvectors of $\mathcal{A}$, with respective eigenvalues a_i and a_j, which are not equal ($a_i \neq a_j$), then the two eigenvectors are orthogonal to each other $\langle\phi_i|\phi_j\rangle = 0$.

These two properties follow from the definitions of hermiticity and the scalar product.

A special case of the operator product is an operator $\mathcal{A}$ raised to some integer power p, i.e., $\mathcal{A}^p$, whose eigenvectors obviously coincide with the eigenvectors of $\mathcal{A}$, while the eigenvalues are given by a_i^p. In general, any function $f(\mathcal{A})$ of an operator $\mathcal{A}$ is defined through the Taylor series (assuming it exists)

$$f(\mathcal{A}) = \sum_{p=0}^{\infty} \frac{f^{(p)}(0)}{p!} \mathcal{A}^p \ , \tag{1.25}$$

which is thus given by the action of the powers of $\mathcal{A}$. Using the series expansion, one can prove the operator (Baker–Hausdorff) relation

$$\mathrm{e}^{\mathcal{A}+\mathcal{B}} = \mathrm{e}^{-\frac{1}{2}[\mathcal{A},\mathcal{B}]} \mathrm{e}^{\mathcal{A}} \, \mathrm{e}^{\mathcal{B}} \ , \tag{1.26}$$

which holds when $[\mathcal{A}, [\mathcal{A}, \mathcal{B}]] = [[\mathcal{A}, \mathcal{B}], \mathcal{B}] = 0$ (see Prob. 1.1).

In quantum mechanics, it is convenient and useful to adopt as a basis the normalized eigenvectors of Hermitian operators. The set of eigenvalues a_i of a linear operator $\mathcal{A}$, which are real for a Hermitian operator, is called the spectrum of $\mathcal{A}$, and the expression or expansion of a vector $|\phi\rangle$ in the basis $\{|e_i\rangle\}$ of eigenvectors of $\mathcal{A}$, i.e., $|\phi\rangle = \sum_i c_i |e_i\rangle$, is also referred to as spectral decomposition.

In a finite-dimensional space, for every Hermitian operator there exists a set of eigenvectors which can serve as a basis for the spectral decomposition of any vector of the space. The spaces that are needed for the description of physical systems, however, more often than not are infinite-dimensional and, in many cases, at least part of the spectrum of eigenvalues is continuous. This is indeed the case for the energy operator or Hamiltonian of the simplest atomic system, the hydrogen atom. On the other hand, the Hamiltonian of another basic and simple system studied below, namely the harmonic oscillator, has an infinite but discrete spectrum. Thus, a basis must include a discrete as well as a continuous part, which is accomplished through a generalization of the finite-dimensional case.

Let then $\mathcal{K}$ be a Hermitian operator that has a discrete infinite-dimensional spectrum with eigenvalues κ_n, i.e., $\mathcal{K}|\kappa_n\rangle = \kappa_n |\kappa_n\rangle$ ($n = 0, 1, 2 \ldots$), and a continuous part with eigenvalues κ, i.e., $\mathcal{K}|\kappa\rangle = \kappa |\kappa\rangle$, where the values of κ range from some lower value to in principle infinity. In such a case, any vector $|\phi\rangle$ can be decomposed as follows,

$$|\phi\rangle = \sum_{n=0}^{\infty} |\kappa_n\rangle\langle\kappa_n|\phi\rangle + \int_{\kappa_l}^{\kappa_u} \mathrm{d}\kappa \, |\kappa\rangle\langle\kappa|\phi\rangle \ , \tag{1.27}$$

where κ_l and κ_u denote the lower and upper limits of the integration. The condition of normalization of the vector $|\phi\rangle$ decomposed as above now reads

$$\sum_{n=0}^{\infty} |\langle \kappa_n | \phi \rangle|^2 + \int_{\kappa_l}^{\kappa_u} \mathrm{d}\kappa \, |\langle \kappa | \phi \rangle|^2 < \infty \ ,$$

which means that the series must be summable and the integral must converge when κ_u is not finite.

Dirac delta function

The case of continuous spectra in quantum optics appears not so much through the atomic continuum as through the interaction of a small system (few degrees of freedom) with the outside world (environment), which is the cause of dissipation and decoherence. The mathematical treatments of the continua in those cases are discussed as they arise. In that context, we will often encounter the Dirac delta function $\delta(x)$ of a real variable x. This may be a good place to introduce and discuss some of its properties. Despite its name, $\delta(x)$ is not really a function, in the sense of a pointwise interpretation of its value for every value of the variable x; although it is often said that $\delta(x)$ can be thought of as being zero for every $x \neq 0$, while it tends to infinity at $x = 0$, so that

$$\int_{-\infty}^{\infty} \delta(x) \, \mathrm{d}x = 1 \ . \tag{1.28}$$

Strictly speaking, however, such an object can not be a function—hence the term generalized function or distribution,—although its properties can be defined rigorously through sequences of bona fide functions. It can, for example, be shown that, if $F(x)$ is continuous and bounded on $x \in (-\infty, +\infty)$, then

$$\lim_{\epsilon \to 0^+} \frac{1}{\sqrt{\pi \epsilon}} \int_{-\infty}^{\infty} \mathrm{e}^{-x^2/\epsilon} \, F(x) \, \mathrm{d}x = F(0) \ ,$$

which is exactly what $\delta(x)$ does. Representations of $\delta(x)$ through a variety of alternative sequences are given at the end of this section. It has been proven that all such sequences are equivalent, in the sense that they lead to the same action on the function $F(x)$.

The delta function owes its origin to the need for dealing with the derivative $\theta'(x)$ of the Heaviside step function

$$\theta(x) = \begin{cases} 0 & \text{if } x < 0 \\ 1 & \text{if } x > 1 \end{cases} \ , \tag{1.29}$$

with a discontinuity at $x = 0$ where the derivative does not exist in the ordinary sense. Properly speaking, the delta function is a linear functional (or operator) which, to every complex valued function $F(x)$ of the real variable

x, assigns the value $F(0)$, symbolically written as $\langle \delta, F \rangle = \int \delta(x) F(x)\,\mathrm{d}x = F(0)$. The class of complex functions relevant to the definition must be locally integrable, which means that $\int \delta(x) F(x)\,\mathrm{d}x$ exists on every bounded interval $x \in [x_l, x_u]$

From the above definition and a change of variable, it is obvious that

$$\int_{x_l}^{x_u} \delta(x - x_0) F(x)\,\mathrm{d}x = F(x_0)\ , \quad x_l < x_0 < x_u\ .$$

It is also instructive to show that, if the rules of integration by parts apply, then $\langle \theta', F \rangle = -\langle \theta, F' \rangle = \langle \delta, F \rangle$, under the assumption that the class of functions $F(x)$ vanish at $\pm\infty$. Pursuing this argument further, one can define the derivatives of a generalized function such as $\delta(x)$ through $\langle \delta', F \rangle = -\langle \delta, F' \rangle = -F'(0)$, and in general

$$\langle \delta^{(n)}, F \rangle = (-1)^n \langle \delta, F^{(n)} \rangle = (-1)^n F^{(n)}(0)\ ,$$

assuming of course that the functions $F(x)$ are differentiable to arbitrary order n. It should be evident now that the properties of generalized functions, of which $\delta(x)$ is one example, are determined by the properties of the class of functions on which they operate, also referred to as test functions.

It is possible to represent functions on the real axis by analytic functions in the complex plane through the following theorem that we state without proof: If $F(x)$ is a bounded continuous function on the real axis, then there exists a function $F(z)$, analytic in the whole z-plane, except on the real x-axis, such that

$$\lim_{\epsilon \to 0^+} \big[F(x + \mathrm{i}\epsilon) - F(x - \mathrm{i}\epsilon)\big] = F(x) \quad \text{for all } x\ .$$

The difference inside the square brackets is the "jump" that $F(x)$ makes as we cross the real axis from above. Therefore, although it is impossible to represent an arbitrary $F(x)$ —notably one with a discontinuity—as the restriction of an analytic function, any $F(x)$ can be represented by such a jump.

The above theorem has an immediate application to the representation of generalized functions. It can be stated as follows: If $\mathcal{G}$ is a generalized function, then there exists a function $g(z)$, analytic everywhere except possibly on the real axis, such that

$$\lim_{\epsilon \to 0^+} \int \big[g(x + \mathrm{i}\epsilon) - g(x - \mathrm{i}\epsilon)\big] F(x)\mathrm{d}x = \langle \mathcal{G}, F \rangle$$

for any test function of the appropriate class. $g(z)$ is called the analytic representation of $\mathcal{G}$. Through the use of such analytic representations of generalized functions one can show that

$$\lim_{\epsilon \to 0^+} \frac{1}{x \pm \mathrm{i}\epsilon} = \mathrm{P}\frac{1}{x} \mp \mathrm{i}\pi\delta(x)\ , \tag{1.30}$$

where P indicates the principal value part in an integration over x. The above relation will prove necessary in later sections, where we deal with the coupling of a system with discrete spectrum to a continuum.

Finally, the following alternative expressions involving the delta function are often useful,

$$\delta(x) = \frac{1}{2\pi}\int_{-\infty}^{\infty} \mathrm{d}k\, \mathrm{e}^{\mathrm{i}kx} \,, \tag{1.31a}$$

$$\delta(x) = \lim_{\epsilon\to 0^+} \frac{1}{\pi}\,\frac{\epsilon}{x^2+\epsilon^2} \,, \tag{1.31b}$$

$$\delta(x) = \lim_{\epsilon\to 0^+} \frac{1}{\sqrt{\pi\epsilon}}\,\exp\left(-\frac{x^2}{\epsilon}\right) \,, \tag{1.31c}$$

$$\delta(x) = \lim_{\epsilon\to 0^+} \frac{1}{\pi}\,\frac{\sin(x/\epsilon)}{x} \,, \tag{1.31d}$$

$$\delta(x) = \lim_{\epsilon\to 0^+} \frac{\epsilon}{\pi}\,\frac{\sin^2(x/\epsilon)}{x^2} \,, \tag{1.31e}$$

using which, one can, in particular, prove that

$$\delta(\alpha x) = \frac{1}{|\alpha|}\delta(x) \,, \tag{1.32a}$$

$$\delta(x^2-\alpha^2) = \frac{1}{2|\alpha|}[\delta(x-\alpha)+\delta(x+\alpha)] \,, \tag{1.32b}$$

for $\alpha \neq 0$ (see Prob. 1.3).

1.1.4 Matrix Representation of Operators

Let us for the moment consider the case of a discrete spectrum of a Hermitian operator $\mathcal{K}$, assuming its eigenvectors $|\kappa_n\rangle$ are normalized. Then for any vector $|\phi\rangle$ we have

$$|\phi\rangle = \sum_{n=0}^{\infty} |\kappa_n\rangle\langle\kappa_n|\phi\rangle \,. \tag{1.33}$$

Since this is valid for any $|\phi\rangle$, it must be that

$$\sum_{n=0}^{\infty} |\kappa_n\rangle\langle\kappa_n| = I \,. \tag{1.34}$$

This is valid for any orthonormal basis and is referred to as the spectral resolution of the identity operator I. From this resolution, and using the definition of the basis as eigenvectors of $\mathcal{K}$, i.e., $\mathcal{K}\,|\kappa\rangle = \kappa\,|\kappa\rangle$, we obtain

$$\mathcal{K} = \sum_{n=0}^{\infty} \kappa_n\,|\kappa_n\rangle\langle\kappa_n| \,, \tag{1.35}$$

referred to as spectral resolution of the Hermitian operator $\mathcal{K}$. The object $\Pi_n \equiv |\kappa_n\rangle\langle\kappa_n|$ is called projection operator and in fact the expansion of vector $|\phi\rangle$ in (1.33) can be viewed as the vector sum of the projections of $|\phi\rangle$ on all vectors of the basis; because $\Pi_n |\phi\rangle = |\kappa_n\rangle\langle\kappa_n|\phi\rangle$ indeed represents the $|\kappa_n\rangle$ component of $|\phi\rangle$. Generally, a Hermitian operator having the property $\Pi^2 = \Pi$ is called a projection operator.

Let now $\mathcal{A}$ be an arbitrary linear operator in the space and consider its action on $|\phi\rangle$,

$$\mathcal{A}|\phi\rangle = \sum_{n=0}^{\infty} \mathcal{A}|\kappa_n\rangle\langle\kappa_n|\phi\rangle = \sum_{m,n=0}^{\infty} |\kappa_m\rangle\langle\kappa_m|\mathcal{A}|\kappa_n\rangle\langle\kappa_n|\phi\rangle \ , \tag{1.36}$$

where in each step we have used the resolution of the identity operator in (1.34). Since the above equation is valid for all $|\phi\rangle$, we conclude that

$$\mathcal{A} = \sum_{m,n=0}^{\infty} |\kappa_m\rangle\langle\kappa_m|\mathcal{A}|\kappa_n\rangle\langle\kappa_n| = \sum_{m,n=0}^{\infty} \langle\kappa_m|\mathcal{A}|\kappa_n\rangle\,|\kappa_m\rangle\langle\kappa_n| \ , \tag{1.37}$$

which is called the representation of operator $\mathcal{A}$ in the basis $\{|\kappa_n\rangle\}$. It becomes the spectral resolution only when $\mathcal{A}$ is Hermitian and the basis is that of its eigenvectors. The above representation is quite general, being valid even for operators that do not have eigenvectors. The quantities $\langle\kappa_m|\mathcal{A}|\kappa_n\rangle \equiv \mathcal{A}_{mn}$, which in general are complex numbers, form an infinite matrix—N^2 in an N-dimensional space—often called matrix realization or representation of an operator. The generalization of the matrix representation of an operator for the case of discrete and continuous spectrum has the form

$$\mathcal{A} = \sum_{m,n=0}^{\infty} \langle\kappa_m|\mathcal{A}|\kappa_n\rangle\,|\kappa_m\rangle\langle\kappa_n| + \int\!\!\int \mathrm{d}\kappa\,\mathrm{d}\kappa'\,\langle\kappa|\mathcal{A}|\kappa'\rangle\,|\kappa\rangle\langle\kappa'| \ . \tag{1.38}$$

Clearly, the representation of an operator refers to a (chosen) specific basis (e.g., $\{|\kappa_n\rangle\}$). But as in the usual three-dimensional space, one may wish to change the basis. Let $\{|\chi_n\rangle\}$ be another orthonormal basis which represents the eigenvectors of another Hermitian operator $\mathcal{X}$ having a discrete spectrum, i.e.

$$\mathcal{X}|\chi_n\rangle = \chi_n|\chi_n\rangle \ , \quad n = 0, 1, 2, \ldots \tag{1.39}$$

Again, for any arbitrary vector of the space we can write

$$|\phi\rangle = \sum_{n=0}^{\infty} |\chi_n\rangle\langle\chi_n|\phi\rangle \ . \tag{1.40}$$

But the vectors $|\kappa_m\rangle$ can also be decomposed in the new basis as

$$|\kappa_m\rangle = \sum_{n=0}^{\infty} |\chi_n\rangle\langle\chi_n|\kappa_m\rangle \ . \tag{1.41}$$

Using this decomposition for any two vectors $|\kappa_m\rangle$ and $|\kappa_{m'}\rangle$, we have

$$\langle\kappa_{m'}|\kappa_m\rangle = \delta_{mm'} = \sum_{n,n'}\langle\kappa_{m'}|\chi_{n'}\rangle\langle\chi_{n'}|\chi_n\rangle\langle\chi_n|\kappa_m\rangle \ . \tag{1.42}$$

Since $\langle\chi_{n'}|\chi_n\rangle = \delta_{nn'}$, we obtain

$$\sum_n \langle\chi_n|\kappa_{m'}\rangle^* \langle\chi_n|\kappa_m\rangle = \delta_{mm'} \ . \tag{1.43}$$

Similarly, one can show that

$$\sum_m \langle\kappa_m|\chi_{n'}\rangle^* \langle\kappa_m|\chi_n\rangle = \delta_{nn'} \ . \tag{1.44}$$

The quantities $\langle\chi_n|\kappa_m\rangle \equiv \mathcal{T}_{nm}$ are the matrix elements of a matrix $\mathcal{T}$ that transforms the coefficients of the decomposition of any vector $|\phi\rangle$ in one basis to the coefficients of its decomposition in the other basis. It is referred to as the transformation (from one to another basis) matrix. The inverse transformation is realized by the matrix $\mathcal{T}^\dagger$ whose elements are $(\mathcal{T}^\dagger)_{mn} \equiv \langle\kappa_m|\chi_n\rangle = \mathcal{T}^*_{nm}$. The components $\langle\chi_n|\phi\rangle$ of any vector $|\phi\rangle$ on the basis $\{|\chi_n\rangle\}$ can be viewed as a column matrix, as can its components in another basis. The two column matrices are obtained one from the other through multiplication by the transformation matrix.

A matrix $\mathcal{U}$ whose matrix elements satisfy the condition $\sum_n \mathcal{U}^*_{nm}\mathcal{U}_{nm'} = \delta_{mm'}$ is said to be unitary, consistently with the definition of the unitary operator in (1.21). It is called orthogonal if in addition its matrix elements happen to be real, $\mathcal{U}^*_{nm} = \mathcal{U}_{nm}$. Obviously, the transformation matrix $\mathcal{T}$ is unitary, $\mathcal{T}^\dagger\mathcal{T} = \mathcal{T}\,\mathcal{T}^\dagger = I$.

The matrix representation of an operator in different bases are also related through the transformation matrix. This is easily seen if we consider the matrix element $\langle\kappa_{m'}|\,\mathcal{A}\,|\kappa_m\rangle$ of $\mathcal{A}$ and express the vectors $|\kappa_m\rangle$ in terms of $\{|\chi_n\rangle\}$ as in (1.41). We then have

$$\langle\kappa_{m'}|\,\mathcal{A}\,|\kappa_m\rangle = \sum_{n,n'}\langle\kappa_{m'}|\chi_{n'}\rangle\langle\chi_{n'}|\,\mathcal{A}\,|\chi_n\rangle\langle\chi_n|\kappa_m\rangle \ , \tag{1.45}$$

where the right side represents a typical expression found in the multiplication of matrices. Let us define $\mathcal{A}_{n'n}(\chi) \equiv \langle\chi_{n'}|\,\mathcal{A}\,|\chi_n\rangle$ and $\mathcal{A}_{m'm}(\kappa) \equiv \langle\kappa_{m'}|\,\mathcal{A}\,|\kappa_m\rangle$, where by $\mathcal{A}(\chi)$ or $\mathcal{A}(\kappa)$ we denote the matrix representing the operator $\mathcal{A}$ in the respective basis. Then (1.45) can be written in matrix form as

$$\mathcal{A}(\kappa) = \mathcal{T}^\dagger\mathcal{A}(\chi)\mathcal{T} \ , \tag{1.46}$$

which also shows explicitly that changing bases in the representation of an operator involves, or is equivalent to, a unitary transformation. An operator is thus completely defined if its representation in some basis is known.

The careful reader may notice that the above relations emerge from repeated application of the resolution of the identity operator in terms of orthonormal bases, $I = \sum_n |\chi_n\rangle\langle\chi_n|$.

The trace of an operator is defined as the sum of the diagonal elements of its matrix representation,

$$\mathrm{Tr}(\mathcal{A}) \equiv \sum_n \mathcal{A}_{nn} \ . \tag{1.47}$$

It has the following obvious properties

(i) $\mathrm{Tr}(\mathcal{A}+\mathcal{B}) = \mathrm{Tr}(\mathcal{A}) + \mathrm{Tr}(\mathcal{B})$.
(ii) $\mathrm{Tr}(c\mathcal{A}) = c\mathrm{Tr}(\mathcal{A})$ with c a c-number.
(iii) $\mathrm{Tr}(\mathcal{A}\mathcal{B}) \equiv \sum_n \sum_m \mathcal{A}_{nm}\mathcal{B}_{mn} = \sum_m \sum_n \mathcal{B}_{mn}\mathcal{A}_{nm} = \mathrm{Tr}(\mathcal{B}\mathcal{A})$.

It then follows that for any unitary operator $\mathcal{U}$ we have

$$\mathrm{Tr}(\mathcal{U}^\dagger \mathcal{A}\mathcal{U}) = \mathrm{Tr}(\mathcal{U}\mathcal{U}^\dagger\mathcal{A}) = \mathrm{Tr}(\mathcal{A}) \ . \tag{1.48}$$

An important consequence of this is that the trace is invariant under the basis transformations (1.46), since the transformation matrix $\mathcal{T}$ is unitary.

1.2 Description of Quantum Systems

Having outlined the most relevant properties of vector spaces and linear operators, we turn now to the formulation of quantum theory which rests upon the fundamental postulates stated below.

1.2.1 Physical Observables

The first postulate of quantum theory can be formulated as follows. Any physical observable is represented by a Hermitian operator in the Hilbert space associated with the system's degrees of freedom. The complete description of a system may require more than one physical variable and therefore the respective operators. The possible physical states of a system are represented by vectors in the space spanned by the eigenstates of all necessary operators. These operators obey commutation relations which are related to the measurement procedure, as detailed in Sect. 1.2.4.

The system under consideration may be inseparable or composite, in the latter case the complete vector space spanned by the degrees of freedom of the system is given by the tensor product of vector spaces corresponding to its constituent subsystems.

The most fundamental property of an isolated physical system is its energy which is constant. In quantum theory, the energy is represented by the Hamiltonian $\mathcal{H}$—a Hermitian operator. One or more other observables (operators) may enter in the expression of the Hamiltonian.

Linear Harmonic Oscillator

To give a brief example, we consider the one-dimensional harmonic oscillator. Classically, it corresponds to a point mass M on a straight line x subject to a restoring force κx, where κ is a constant. The potential energy is $\frac{1}{2}\kappa x^2$, while the kinetic energy is $\frac{1}{2M}p^2$ with p being the momentum of the particle. Then the total energy is

$$E = \frac{1}{2M}\, p^2 + \frac{M\omega^2}{2}\, x^2 \,, \tag{1.49}$$

where $\omega = \sqrt{\kappa/M}$ is the frequency of the oscillator.

In the transition to quantum theory, the coordinate x and momentum p variables become operators $\mathcal{Q}$ and $\mathcal{P}$. In particular, $\mathcal{P}$ is the differential operator $-\mathrm{i}\hbar\partial_x$, while $\mathcal{Q} = x$. As a consequence, their commutator is

$$[\mathcal{P}, \mathcal{Q}] = \mathcal{P}\mathcal{Q} - \mathcal{Q}\mathcal{P} = -\mathrm{i}\hbar I \,, \tag{1.50}$$

which is a c-number multiplying the identity operator I. The crucial point is that the commutator is nonzero; otherwise stated, $\mathcal{Q}$ and $\mathcal{P}$ do not commute, which is what sets apart quantum mechanics from the classical counterpart cast in terms of the same set of variables (physical observables). The c-number in the right-hand side of commutator (1.50) is the universal number $\hbar = h/2\pi$ with h known as Planck's constant ($h = 6.619 \times 10^{-34}$ J s). The roots of this constant and its value reach back to the origins of the quantum theory in the early 20th century. The discussion of how this came about is outside the scope of this book, but can of course be found in most books on quantum theory.

The Hamiltonian operator of the harmonic oscillator therefore is

$$\mathcal{H} = \frac{1}{2M}\, \mathcal{P}^2 + \frac{M\omega^2}{2}\, \mathcal{Q}^2 \,, \tag{1.51}$$

where $\mathcal{H}$, $\mathcal{P}$ and $\mathcal{Q}$ are all linear Hermitian operators.

The quantum description of the harmonic oscillator, as of any system, requires the complete specification of the vector space spanned by the vectors corresponding to all possible states of the system. The initial approach to this problem, although not cast in this language, was through the stationary Schrödinger equation. This means that one considers the differential equation

$$\mathcal{H}\,\Psi(x) = \left(-\frac{\hbar^2}{2M}\, \frac{\partial^2}{\partial x^2} + \frac{M\omega^2}{2}\, x^2 \right) \Psi(x) = E\,\Psi(x) \,, \tag{1.52}$$

where $\Psi(x)$ are functions of x, and E the respective eigenvalues of energy which is represented by the differential operator $\mathcal{H}$. The variable x takes values in the continuum $-\infty \le x \le \infty$, as dictated by the nature of the physical system. If the function $\Psi(x)$ is to correspond to a physically permissible state denoted by $|\Psi\rangle$, it must be normalizable. The space thus consists of c-valued one variable functions $\Psi(x)$. If the scalar product is defined via

$$\langle \Psi | \Psi' \rangle \equiv \int_{-\infty}^{\infty} \mathrm{d}x \, \Psi^*(x) \Psi'(x) \, , \tag{1.53}$$

the square of the norm of $\Psi(x)$ is

$$\langle \Psi | \Psi \rangle = \int_{-\infty}^{\infty} \mathrm{d}x \, |\Psi(x)|^2 \, . \tag{1.54}$$

For the norm to be finite, the permissible functions $\Psi(x)$ must be square integrable. Typically, one uses a power series expansion for the solutions $\Psi(x)$ with the requirement that they approach zero sufficiently fast as $|x| \to \infty$ for the square $|\Psi(x)|^2$ to be integrable. This leads to a discrete set of infinitely many solutions $\Psi_n(x)$ with the corresponding states $|\Psi_n\rangle$ indexed by $n = 0, 1, 2, \ldots$ having the respective energy eigenvalues

$$E_n = \hbar\omega(n + \tfrac{1}{2}) \, . \tag{1.55}$$

The normalized functions can be expressed in terms of Hermite polynomials $H_n(x) = (-1)^n \mathrm{e}^{x^2} \frac{\mathrm{d}^n}{\mathrm{d}x^n} \mathrm{e}^{-x^2}$ as

$$\Psi_n(x) = \left(\frac{M\omega}{\pi\hbar} \right)^{1/4} \frac{2^{-n/2}}{\sqrt{n!}} \exp\left(-\frac{M\omega}{2\hbar} \, x^2 \right) H_n\left(\sqrt{\frac{M\omega}{\hbar}} \, x \right) \, . \tag{1.56}$$

In particular, for the lowest $n = 0$ (or ground) state $|\Psi_0\rangle$ with energy $E_0 = \frac{1}{2}\hbar\omega$, one has

$$\Psi_0(x) = \left(\frac{M\omega}{\pi\hbar} \right)^{1/4} \exp\left(-\frac{M\omega}{2\hbar} \, x^2 \right) \, . \tag{1.57}$$

Let us look back at what we have done. Starting with the classical Hamiltonian for the system, we have replaced the momentum p by the differential operator $-\mathrm{i}\hbar\partial_x$ converting thus the Hamiltonian to an operator. Then we sought solutions to the differential equation $\mathcal{H}\Psi(x) = E\Psi(x)$ under the appropriate boundary conditions, which defined an eigenvalue problem. The resulting eigenvalues E_n are the values of the energy dictated by quantum theory, with the respective eigenfunctions $\Psi_n(x)$ representing the state of the system $|\Psi_n\rangle$ with that energy. Thus a system, which in classical physics can have any energy from zero to infinity, in quantum theory has energy that is restricted to discrete values determined by the eigenvalues of a differential operator, and its state (physical properties) is characterized by the respective eigenfunctions $\Psi_n(x)$ (or eigenvectors $|\Psi_n\rangle$) in the space spanned by these eigenvectors. Moreover, the lowest possible energy is not zero, but the finite quantity $\frac{1}{2}\hbar\omega$, referred to as zero-point energy. This is directly related to the non-commutativity of $\mathcal{P}$ and $\mathcal{Q}$ as discussed later on.

1.2.2 Quantum Mechanical Hamiltonian

In the approach just outlined, we have solved a differential equation, which is what one does in classical physics. Where does quantum mechanics come in

then? It is in the interpretation based on the postulates that relate the vectors to the observation (measurement) of the physical variable, and of course in the replacement of the dynamical variables by operators.

The procedure for the quantization of the Hamiltonian of the harmonic oscillator represents a special case of a more general scheme. If we have a system with k degrees of freedom represented by the coordinates $q_1, q_2, \ldots, q_k$ and their canonically conjugate momenta $p_1, p_2, \ldots, p_k$, the Hamiltonian of the system will, in general, be a function of q's and p's, i.e.,

$$\mathcal{H} = \mathcal{H}(p_1, p_2, \ldots, p_k; q_1, q_2, \ldots, q_k) \; . \tag{1.58}$$

Classically, the Hamilton's equations

$$\frac{\mathrm{d}q_i}{\mathrm{d}t} = \frac{\partial \mathcal{H}}{\partial p_i} \quad \text{and} \quad \frac{\mathrm{d}p_i}{\mathrm{d}t} = \frac{\partial \mathcal{H}}{\partial q_i} \; , \quad i = 1, 2, \ldots, k \; , \tag{1.59}$$

determine the equations of motion of the system. The transition to quantum mechanics is accomplished by identifying p_i with the differential operator $-\mathrm{i}\hbar\partial_{q_i}$ and solving the eigenvalue problem defined by the partial differential equation

$$\mathcal{H}\Psi(q_1, q_2, \ldots, q_k) = E\,\Psi(q_1, q_2, \ldots, q_k) \; , \tag{1.60}$$

under the appropriate boundary conditions, to determine the eigenfunctions $\Psi_n(q_1, q_2, \ldots, q_k)$ and the corresponding energy eigenvalues E_n, with n running over an infinite set of discrete and/or continuous values. In general, n can, and usually does, represent a group of indices, each running over the appropriate range of values. The scalar product is now given as

$$\langle \Psi_n | \Psi_{n'} \rangle = \int \mathrm{d}q_1 \mathrm{d}q_2 \ldots \mathrm{d}q_k \, \Psi_n^*(q_1, q_2, \ldots, q_k) \Psi_{n'}(q_1, q_2, \ldots, q_k) \; . \tag{1.61}$$

The set of eigenstates $|\Psi_n\rangle$ forms an orthonormal basis for the space of the physical system described by $\mathcal{H}$. Identifying q_i and p_i with the operators $\mathcal{Q}_i$ and $\mathcal{P}_i$, and imposing the commutation relations

$$[\mathcal{Q}_j, \mathcal{P}_i] = \mathrm{i}\hbar\delta_{ij} I \; , \quad [\mathcal{Q}_i, \mathcal{Q}_j] = [\mathcal{P}_i, \mathcal{P}_j] = 0 \; , \quad i, j = 1, 2, \ldots, k \; , \tag{1.62}$$

we have what is referred to as canonical quantization of the system. The route to quantization in non-relativistic quantum theory, which is the context of this book, is to obtain the Hamiltonian appropriate to the system under consideration and proceed with the canonical quantization. If the system does not have a classical Hamiltonian, e.g., quantum mechanical spin, we must define for it a suitable vector space.

1.2.3 Algebraic Approach for the Harmonic Oscillator

Having outlined an example of the wavefunction approach through the explicit solution of the differential (Schrödinger) equation, it is instructive to show

how, for the same quantum system, the eigenvectors and eigenvalues of $\mathcal{H}$ can be obtained from the algebraic properties of the operators of the system, without solving any differential equation. This approach not only underscores the fundamental relation between vector spaces and quantum theory, but it also provides a powerful and elegant tool.

To this end, we introduce the operators a and $a^\dagger$, defined as

$$a = \frac{1}{\sqrt{2M\hbar\omega}} \left(M\omega\mathcal{Q} + \mathrm{i}\mathcal{P}\right) \ , \quad a^\dagger = \frac{1}{\sqrt{2M\hbar\omega}} \left(M\omega\mathcal{Q} - \mathrm{i}\mathcal{P}\right) \ . \tag{1.63}$$

Clearly they are non-Hermitian, with $a^\dagger$ being the Hermitian adjoint of a. Their commutator is

$$[a, a^\dagger] = 1 \ , \tag{1.64}$$

which follows directly from the commutator of $\mathcal{Q}$ and $\mathcal{P}$ in (1.50). We introduce in addition a Hermitian operator $\mathcal{N} = a^\dagger a$, which upon substitution of a and $a^\dagger$ from (1.63) is found to be

$$\mathcal{N} = \frac{1}{\hbar\omega} \left(\mathcal{H} - \frac{\hbar\omega}{2} I\right) \ .$$

We can then write

$$\mathcal{H} = \hbar\omega\big(\mathcal{N} + \tfrac{1}{2}\big) = \hbar\omega\big(a^\dagger a + \tfrac{1}{2}\big) \ . \tag{1.65}$$

Since $\mathcal{H}$ is the energy of the harmonic oscillator, evidently $\mathcal{N}$ is also a measure of energy in units of $\hbar\omega$. Being a Hermitian operator, $\mathcal{N}$ possesses eigenstates with real eigenvalues, if it possesses any at all. A purely algebraic approach can lead us to the answer as follows.

Assume there is an eigenvector χ_λ with eigenvalue λ, which means

$$\mathcal{N}\chi_\lambda = \lambda\chi_\lambda \ . \tag{1.66}$$

Calculate $\mathcal{N}a\chi_\lambda$ using (1.64):

$$\mathcal{N}a\chi_\lambda = a^\dagger aa\chi_\lambda = (aa^\dagger - 1)a\chi_\lambda = a(a^\dagger a - 1)\chi_\lambda = (\lambda - 1)(a\chi_\lambda) \ .$$

Therefore $a\chi_\lambda$ is also an eigenvector of $\mathcal{N}$ with eigenvalue $(\lambda-1)$, $a\chi_\lambda = \chi_{\lambda-1}$. Repeating the procedure m times, we see that $a^m\chi_\lambda = \chi_{\lambda-m}$, provided it is not the zero eigenvector. Similarly, we find that

$$\mathcal{N}a^\dagger\chi_\lambda = (\lambda + 1)(a^\dagger\chi_\lambda) \ ,$$

which means that $a^\dagger\chi_\lambda = \chi_{\lambda+1}$, i.e., an eigenvector of $\mathcal{N}$ with eigenvalue $\lambda + 1$, unless it is the zero vector. We now show that in can not be the zero vector. If it were, i.e., if $a^\dagger\chi_\lambda = 0$, we would have $\langle a^\dagger\chi_\lambda | a^\dagger\chi_\lambda\rangle = 0$. But from the definition of the Hermitian adjoint we have

$$\langle a^\dagger\chi_\lambda | a^\dagger\chi_\lambda\rangle = \langle\chi_\lambda | aa^\dagger\chi_\lambda\rangle = \langle\chi_\lambda | (a^\dagger a + 1)\chi_\lambda\rangle = \langle a\chi_\lambda | a\chi_\lambda\rangle + \langle\chi_\lambda | \chi_\lambda\rangle \neq 0 \ ,$$

because by hypothesis $\chi_\lambda \neq 0$. Repeating the procedure m times, we find that $(a^\dagger)^m \chi_\lambda = \chi_{\lambda+m}$. Therefore, if we have an eigenvector χ_λ of the operator $\mathcal{N}$, the sequence of vectors $\chi_{\lambda+m}$ generated as $(a^\dagger)^m \chi_\lambda$ for $m = 0, 1, 2, \ldots$ constitutes a sequence of eigenvectors of $\mathcal{N}$, which are non-zero, with respective eigenvalues $\lambda + m$.

It remains to determine whether the sequence $a^m \chi_\lambda = \chi_{\lambda-m}$ leads to the zero eigenvector. Note that

$$\langle \chi_{\lambda-m} | \mathcal{N} \chi_{\lambda-m} \rangle = (\lambda - m) \langle \chi_{\lambda-m} | \chi_{\lambda-m} \rangle \ ,$$

and also

$$\langle \chi_{\lambda-m} | \mathcal{N} \chi_{\lambda-m} \rangle = \langle \chi_{\lambda-m} | a^\dagger a \chi_{\lambda-m} \rangle = \langle a \chi_{\lambda-m} | a \chi_{\lambda-m} \rangle \ .$$

Combining the two results, we obtain

$$\lambda - m = \frac{\langle a \chi_{\lambda-m} | a \chi_{\lambda-m} \rangle}{\langle \chi_{\lambda-m} | \chi_{\lambda-m} \rangle} \geq 0 \ ,$$

because both numerator and denominator, being the norms of two vectors, are non-negative. Consequently, the sequence of eigenvectors $\chi_{\lambda-m}$ must eventually terminate to an eigenvector χ_0, such that $a\chi_0 = 0$, with χ_0 being the eigenvector of $\mathcal{N}$ with eigenvalue 0,

$$\mathcal{N}\chi_0 = a^\dagger a \chi_0 = a^\dagger 0 = 0 \ , \tag{1.67}$$

This is the eigenvector with the lowest eigenvalue. Assume it is normalized, $\langle \chi_0 | \chi_0 \rangle = 1$. All other eigenvectors can now be produced (or constructed) from χ_0 through the repeated application of $a^\dagger$. Thus

$$\chi_n = k_n (a^\dagger)^n \chi_0 \ , \tag{1.68}$$

with k_n a normalization constant, to be determined from the requirement $\langle \chi_n | \chi_n \rangle = 1$. We thus have $\mathcal{N}\chi_n = n\chi_n$ and the condition

$$|k_n|^2 \langle (a^\dagger)^n \chi_0 | (a^\dagger)^n \chi_0 \rangle = 1 \ .$$

One now seeks a relation between k_n and k_{n-1}, obtained as follows,

$$\begin{aligned} \chi_{n-1} &= k_{n-1} (a^\dagger)^{n-1} \chi_0 \ , \\ a^\dagger \chi_{n-1} &= k_{n-1} (a^\dagger)^n \chi_0 = \frac{k_{n-1}}{k_n} \chi_n \ , \\ \text{or} \quad \chi_n &= \frac{k_n}{k_{n-1}} a^\dagger \chi_{n-1} \ , \end{aligned} \tag{1.69}$$

where both χ_n and χ_{n-1} must be normalized. In terms of (1.69), this normalization implies

$$\begin{aligned}\langle\chi_n|\chi_n\rangle = 1 &= \frac{|k_n|^2}{|k_{n-1}|^2}\langle a^\dagger\chi_{n-1}|a^\dagger\chi_{n-1}\rangle = \frac{|k_n|^2}{|k_{n-1}|^2}\langle\chi_{n-1}|aa^\dagger\chi_{n-1}\rangle \\ &= \frac{|k_n|^2}{|k_{n-1}|^2}\langle\chi_{n-1}|(a^\dagger a+1)\chi_{n-1}\rangle \\ &= \frac{|k_n|^2}{|k_{n-1}|^2}(n-1+1)\langle\chi_{n-1}|\chi_{n-1}\rangle \\ &= \frac{|k_n|^2}{|k_{n-1}|^2}n\ ,\end{aligned} \tag{1.70}$$

from which we obtain the recursion relation

$$|k_n|^2 = \frac{1}{n}\,|k_{n-1}|^2\ . \tag{1.71}$$

Since χ_0 is assumed normalized, we have $k_0 = 1$, from which repeated application of the recursion relation (1.71) leads to

$$k_n = \sqrt{\frac{1}{n!}}\ . \tag{1.72}$$

The derivation above is compatible with the more general choice $k_n = \mathrm{e}^{\mathrm{i}\vartheta}\sqrt{1/n!}$, with ϑ any real number. This phase will not be significant in our considerations, as far as determining the eigenvectors is concerned, and is set equal to 0.

We have thus determined the eigenvectors of operator $\mathcal{N}$ to be

$$|\chi_n\rangle = \frac{1}{\sqrt{n!}}(a^\dagger)^n\,|\chi_0\rangle\ , \tag{1.73}$$

with eigenvalues $n = 0, 1, 2, \ldots$ They are orthogonal to each other, $\langle\chi_n|\chi_{n'}\rangle = \delta_{nn'}$, because they all have distinct eigenvalues. Since the Hamiltonian $\mathcal{H}$ is given by (1.65), it is evident that

$$\mathcal{H}\,|\chi_n\rangle = \hbar\omega\big(n+\tfrac{1}{2}\big)\,|\chi_n\rangle\ , \tag{1.74}$$

which shows that the vectors $|\chi_n\rangle$ are the eigenvectors of the Hamiltonian, with eigenvalues $\hbar\omega(n+\frac{1}{2})$, in agreement with the results obtained above through the solution of the differential (Schrödinger) equation. Here, however, the eigenvectors and eigenvalues of $\mathcal{H}$ were obtained from the algebraic properties of the operators of the system without ever solving a differential equation.

If we want to have the analytic expressions for χ_n as functions of x, all we need is the expression for χ_0. According to (1.57), it is given by

$$\chi_0 = \Psi_0(x) = \left(\frac{M\omega}{\pi\hbar}\right)^{1/4}\exp\left(-\frac{M\omega}{2\hbar}x^2\right)\ . \tag{1.75}$$

Then the eigenfunctions χ_n are obtained by successive application of the differential operator

$$a^\dagger = \frac{1}{\sqrt{2}} \left(\sqrt{\frac{M\omega}{\hbar}}\, x - \sqrt{\frac{\hbar}{M\omega}}\, \frac{\partial}{\partial x} \right) , \tag{1.76}$$

with the result $\chi_n = \Psi_n(x)$ given by (1.56). Using the properties of $|\chi_n\rangle$, it is straightforward to show that

$$a\,|\chi_n\rangle = \sqrt{n}\,|\chi_{n-1}\rangle \quad \text{and} \quad a^\dagger\,|\chi_n\rangle = \sqrt{n+1}\,|\chi_{n+1}\rangle\ . \tag{1.77}$$

Although for reasons of expediency, in deriving the above results we invoked the expression for $\chi_0 = \Psi_0(x)$ obtained through the differential equation (1.52), that was not necessary. One can obtain χ_n as functions of x within the algebraic procedure, using only the properties of the operators a and $a^\dagger$. Briefly, to this end, one seeks the eigenvectors $|x\rangle$ of operator $\mathcal{Q}$ with the (continuous) eigenvalues x. Formally, one seeks solutions of

$$\mathcal{Q}\,|x\rangle = x\,|x\rangle\ , \tag{1.78}$$

and uses the basis $\{\,|\chi_n\rangle\}$ to obtain the coefficients $\langle\chi_n|x\rangle$ transforming one set of eigenvectors into the other. One expresses $\mathcal{Q}$ in terms of a and $a^\dagger$, and exploits their action on $|\chi_n\rangle$, defining in the process

$$f_n(y) = \sqrt{2^n n!}\,\frac{\langle\chi_n|x\rangle}{\langle\chi_0|x\rangle}$$

with $y = \sqrt{m\omega/\hbar}\,x$. One then arrives at the difference equations (or recursion relations)

$$f_n(y) = 2y f_{n-1}(y) - 2(n-1) f_{n-2}(y) \tag{1.79}$$

with $f_0(y) = 1$ and $f_1(y) = 2y f_0(y)$. The above recursion relations are known to be those of the Hermite polynomials, and for real y are given by

$$f_n(y) = H_n(y) = (-1)^n \mathrm{e}^{y^2}\,\frac{\mathrm{d}^n \mathrm{e}^{-y^2}}{\mathrm{d}y^n}\ ,$$

yielding finally

$$\langle\chi_n|x\rangle = \frac{1}{\sqrt{2^n n!}}\langle\chi_0|x\rangle H_n\left(\sqrt{\frac{M\omega}{\hbar}}\,x\right) \quad \text{for} \quad -\infty < x < \infty\ . \tag{1.80}$$

Having established that according to the fundamental structure of quantum theory the harmonic oscillator can have only the energies $E_n = \hbar\omega(n+\frac{1}{2})$, it is said that its energy is quantized in units of $\hbar\omega$, which is referred to as one quantum. Since the action of operator a or $a^\dagger$ on $|\chi_n\rangle$ results, respectively, in the decrease or increase of the energy by one quantum $\hbar\omega$, they are called,

respectively, the annihilation (lowering) or creation (raising) operators. Both are said to be ladder operators.

The infinite set $\{|\chi_n\rangle\}$ of eigenvectors of $\mathcal{H}$ constitutes an orthonormal basis for the infinite-dimensional space that contains all possible states (vectors) of the harmonic oscillator allowed by quantum theory. An arbitrary state $|\Psi\rangle$ of the system can therefore be written as

$$|\Psi\rangle = \sum_{n=0}^{\infty} c_n |\chi_n\rangle \ , \tag{1.81}$$

with the condition $\sum_{n=0}^{\infty} |c_n|^2 < \infty$. The space of all $|\Psi\rangle$ that satisfy this condition, with the scalar product defined via (1.53), i.e.

$$\langle \Psi | \Psi' \rangle \equiv \int_{-\infty}^{\infty} \mathrm{d}x \, \Psi^*(x) \Psi'(x) \ ,$$

constitutes a Hilbert space.

More generally, the eigenvectors of the harmonic oscillator constitute an orthonormal set of vectors that can be, and often is, used as a basis for the description of the states of any system in one dimension in the real interval $(-\infty, \infty)$, under the condition that its states are square integrable in that interval. Given the equivalence of the two approaches that led to the eigenvectors of $\mathcal{H}$, we can condense the notation by using $|n\rangle$ for the eigenvectors of $\mathcal{N}$, called the number states, i.e.,

$$\mathcal{N} |n\rangle \equiv a^\dagger a |n\rangle = n |n\rangle \ , \tag{1.82}$$

as is very common in the literature. Clearly,

$$\mathcal{H} |n\rangle = \hbar\omega\big(n + \tfrac{1}{2}\big) |n\rangle \ . \tag{1.83}$$

Coherent States of the Harmonic Oscillator

In addition to providing a fundamental quantum system for the elaboration and illustration of the principles of quantum theory, the harmonic oscillator represents a building block in the description of many physical systems, such as the electromagnetic field, vibrations of nuclei in crystals or molecules, etc. It is thus of interest to explore several of its properties as they will be found useful in the subsequent chapters.

A very special feature of the harmonic oscillator is the existence of a set of states quite different from the eigenstates $|n\rangle$ of the Hamiltonian $\mathcal{H}$. They are known as coherent states and can be obtained as eigenstates of the (non-Hermitian) annihilation operator a. Clearly, if they exist at all, these eigenstates can not be expected to be necessarily real.

Let $|\alpha\rangle$ be such a state, with the complex number α denoting its eigenvalue. By definition, we thus have

$$a\,|\alpha\rangle = \alpha\,|\alpha\rangle\ . \tag{1.84}$$

But whatever $|\alpha\rangle$ is, it has to be a state of the harmonic oscillator and can therefore be decomposed in the basis $\{\,|n\rangle\}$, which means

$$|\alpha\rangle = \sum_{n=0}^{\infty} \langle n|\alpha\rangle\,|n\rangle\ . \tag{1.85}$$

Using the definition of $|\alpha\rangle$ in (1.84) we can write

$$\langle n|\,a\,|\alpha\rangle = \alpha\langle n|\alpha\rangle\ .$$

On the other hand, we have

$$\langle n|\,a\,|\alpha\rangle = \langle\alpha|\,a^{\dagger}\,|n\rangle^{*} = \sqrt{n+1}\,\langle\alpha|n+1\rangle^{*}\ .$$

Equating these two expressions for $\langle n|\,a\,|\alpha\rangle$, we obtain

$$\langle n+1|\alpha\rangle = \frac{\alpha}{\sqrt{n+1}}\,\langle n|\alpha\rangle\ . \tag{1.86}$$

Starting from the lowest $n = 0$, by induction we find

$$\langle n|\alpha\rangle = \frac{\alpha^n}{\sqrt{n!}}\,\langle 0|\alpha\rangle\ , \tag{1.87}$$

which enables us to represent $|\alpha\rangle$ as

$$|\alpha\rangle = \langle 0|\alpha\rangle \sum_{n=0}^{\infty} \frac{\alpha^n}{\sqrt{n!}}\,|n\rangle\ , \tag{1.88}$$

where the only unknown is the multiplicative constant $\langle 0|\alpha\rangle$, a c-number. Requiring that $|\alpha\rangle$ be normalized, i.e. $\langle\alpha|\alpha\rangle = 1$, we have

$$\langle\alpha|\alpha\rangle = |\langle 0|\alpha\rangle|^2 \sum_{n=0}^{\infty} \frac{|\alpha|^{2n}}{n!} = |\langle 0|\alpha\rangle|^2 \exp(|\alpha|^2) = 1\ ,$$

from where $\langle 0|\alpha\rangle = \mathrm{e}^{\mathrm{i}\vartheta}\mathrm{e}^{-\frac{1}{2}|\alpha|^2}$ with ϑ being a real number representing the phase of the state vector. Unless one has a reason to expect the phase to play a role in a particular context, it can be set equal to zero. Thus a well-defined eigenstate of the annihilation operator a is

$$|\alpha\rangle = \mathrm{e}^{-\frac{1}{2}|\alpha|^2} \sum_{n=0}^{\infty} \frac{\alpha^n}{\sqrt{n!}}\,|n\rangle\ , \tag{1.89}$$

which exists for any c-number α.

Let us also express the coherent state $|\alpha\rangle$ through the lowest energy state of the harmonic oscillator $|0\rangle$ as

$$|\alpha\rangle = \mathrm{e}^{-\frac{1}{2}|\alpha|^2} \sum_{n=0}^{\infty} \frac{(\alpha a^\dagger)^n}{n!} |0\rangle = \mathrm{e}^{-\frac{1}{2}|\alpha|^2} \mathrm{e}^{\alpha a^\dagger} |0\rangle \ . \tag{1.90}$$

Using the fact that $\mathrm{e}^{-\alpha^* a} |0\rangle = |0\rangle$ (since $a|0\rangle = 0$) and the operator relation (1.26), we can rewrite (1.90) as

$$|\alpha\rangle = \mathcal{D}(\alpha) |0\rangle \ , \quad \mathcal{D}(\alpha) \equiv \mathrm{e}^{\alpha a^\dagger - \alpha^* a} \ . \tag{1.91}$$

Thus, formally, the coherent state $|\alpha\rangle$ can be generated from the lowest (ground) state $|0\rangle$ by acting upon it with the operator $\mathcal{D}(\alpha)$ known as the displacement operator.

Consider now the scalar product of two coherent states $|\alpha\rangle$ and $|\beta\rangle$,

$$\langle\alpha|\beta\rangle = \mathrm{e}^{-\frac{1}{2}(|\alpha|^2+|\beta|^2)} \sum_n \frac{(\alpha^*)^n \beta^n}{n!} = \exp\left[\alpha^*\beta - \frac{1}{2}(|\alpha|^2 + |\beta|^2)\right] .$$

We thus have

$$|\langle\alpha|\beta\rangle|^2 = \mathrm{e}^{-|\alpha-\beta|^2} \ , \tag{1.92}$$

which is small for $|\alpha - \beta|^2 \gg 1$, but never zero, i.e., the coherent states are non-orthogonal. However, the farther from each other (on the complex plane) the eigenvalues α and β are, the more "orthogonal" (less overlap) the two state are, but each state still contains all of the others. Thus the set of coherent states $\{|\alpha\rangle\}$ is continuous, normalized, but not orthogonal and overcomplete. It can nevertheless be used as a basis which is particularly useful in calculating the expectation values of correlation functions of $a^\dagger$ and a, as will be illustrated in the next chapter.

1.2.4 Operators and Measurement

In the beginning of Sect. 1.2, we formulated the first postulate of quantum theory that relates physical observables with Hermitian operators in the Hilbert space in which the possible state vectors of the system are defined. The second postulate of quantum theory states that the measurement of a physical observable corresponds to an action of the respective operator on the state of the system. In addition, the result of the measurement can only be one of the eigenvalues of the operator, with a probability determined by the respective coefficient in the expansion of the state vector in terms of eigenvectors of that operator, which is often refereed to as the Born rule.

To state this postulate formally, let $\mathcal{A}$ be the Hermitian operator, $|a_i\rangle$ its eigenvectors with eigenvalues a_i, and $|\Psi\rangle$ the state of the system. Then we can write

$$|\Psi\rangle = \sum_i \langle a_i|\Psi\rangle \, |a_i\rangle \ , \tag{1.93}$$

from which

$$\mathcal{A}\,|\Psi\rangle = \sum_i \langle a_i|\Psi\rangle\, a_i\, |a_i\rangle \ . \tag{1.94}$$

The probability $P(a_i)$ for obtaining the result a_i in one given measurement is

$$P(a_i) = |\langle a_i|\Psi\rangle|^2 = \langle\Psi|\, \Pi_i\, |\Psi\rangle \ , \tag{1.95}$$

where $\Pi_i \equiv |a_i\rangle\langle a_i|$ is the corresponding projection operator. Since we always assume the state vector $|\Psi\rangle$ to be normalized, we have

$$\sum_i P(a_i) = \sum_i |\langle a_i|\Psi\rangle|^2 = 1 \ , \tag{1.96}$$

as it should be if $P(a_i)$ are to fulfill the necessary conditions for probabilities. The average value to be expected from the measurement of $\mathcal{A}$ on an ensemble of systems identically prepared in state $|\Psi\rangle$ will obviously be

$$\sum_i a_i P(a_i) = \sum_i a_i |\langle a_i|\Psi\rangle|^2 = \langle\Psi|\, \mathcal{A}\, |\Psi\rangle \equiv \langle\mathcal{A}\rangle \ , \tag{1.97}$$

and is called the expectation (or expected) value of $\mathcal{A}$ for a system in state $|\Psi\rangle$. It simply represents in ket notation the scalar product of $|\Psi\rangle$ with the vector $\mathcal{A}\,|\Psi\rangle$ resulting from the action of operator $\mathcal{A}$ on $|\Psi\rangle$.

In general, there is a variance $\sigma^2_{\mathcal{A}} \equiv (\Delta\mathcal{A})^2$ associated with the measurement of $\mathcal{A}$,

$$(\Delta\mathcal{A})^2 \equiv \langle\mathcal{A}^2\rangle - \langle\mathcal{A}\rangle^2 = \langle\Psi|\, \mathcal{A}^2\, |\Psi\rangle - |\langle\Psi|\, \mathcal{A}\, |\Psi\rangle|^2 \ , \tag{1.98}$$

which is consistent with the definition of the variance in probability theory, since (1.98) also represents the quantity

$$\sum_i a_i^2 P(a_i) - \Big(\sum_i a_i P(a_i)\Big)^2 = \sigma^2_{\mathcal{A}} \ .$$

Clearly, if $|\Psi\rangle$ coincides with one of the eigenstates of $\mathcal{A}$, the result of the measurement will be its corresponding eigenvalue with zero variance. It is only in that case that the expectation value of the physical observable can be determined with no uncertainty whatsoever.

Post-measurement State

As stated above, the measurement of a physical observable described by an operator $\mathcal{A}$ yields one of its the eigenvalues a_i. In turn, the state of the system immediately after the measurement is given by the eigenvector corresponding to the measured eigenvalue of $\mathcal{A}$. Thus, for an arbitrary state $|\Psi\rangle$, if the outcome of the measurement is a_i, immediately after the measurement the system is in state $|a_i\rangle$. This is often referred to as the collapse of the state

vector $|\Psi\rangle$ to $|a_i\rangle$. The outcome of the measurement can therefore be associated with the corresponding projection operator $\Pi_i \equiv |a_i\rangle\langle a_i|$ acting on the system initially in state $|\Psi\rangle$ to generate the post-measurement state $|\Psi^{\rm pm}\rangle$ according to

$$|\Psi^{\rm pm}\rangle = \frac{\Pi_i |\Psi\rangle}{\sqrt{P(a_i)}} = |a_i\rangle \,, \tag{1.99}$$

where the denominator with $P(a_i)$ given by (1.95) ensures the renormalization of $|\Psi^{\rm pm}\rangle$.

Often in quantum mechanics one encounters more general types of measurement, in which the detection process involves an intermediate system (or environment) which is correlated with the interrogated system through an interaction. In general, this interaction may result in transitions between the eigenstates $|a_i\rangle$ of the measured system. Examples of such measurements will be given in Sect. 2.3 and Sect. 4.2. Then, with each outcome of the measurement performed on the intermediate system (environment) we can associate an operator $\alpha_i = |a_j\rangle\langle a_i|$, where $|a_j\rangle$ and $|a_i\rangle$ may represent different eigenstates. The so-called quantum jump operator α_i acts on the system initially in state $|\Psi\rangle$ to generate the post-measurement state $|\Psi^{\rm pm}\rangle$ given by

$$|\Psi^{\rm pm}\rangle = \frac{\alpha_i |\Psi\rangle}{\sqrt{\langle\Psi| \alpha_i^\dagger \alpha_i |\Psi\rangle}} = \frac{|a_j\rangle\langle a_i|\Psi\rangle}{\sqrt{P(a_i)}} = |a_j\rangle \,, \tag{1.100}$$

where we have used $\langle\Psi| \alpha_i^\dagger \alpha_i |\Psi\rangle = \langle\Psi|a_i\rangle\langle a_i|\Psi\rangle = P(a_i)$. In the special case of $\alpha_i = |a_i\rangle\langle a_i| = \Pi_i$ we recover the post-measurement state (1.99). The measurement schemes resulting in the post-measurement states (1.99) and (1.100) are sometimes called measurements of the first and second kind, respectively.

1.2.5 Heisenberg Uncertainty Principle

A quantum system is determined fully by the necessary operators whose number depends on the nature of the system and its degrees of freedom. In the simple case of the linear harmonic oscillator, with one degree of freedom, we have the position $\mathcal{Q}$ and momentum $\mathcal{P}$ operators which do not commute. On the other hand, we have seen that for k degrees of freedom we have k operators $\mathcal{Q}_i$ and $\mathcal{P}_i$, each of which commutes with all others as per (1.62). This often means that the Hamiltonian $\mathcal{H}$ can be written in terms of the sum of operators acting on different non-overlapping subspaces whose union constitutes the complete space of the system. These partial Hamiltonian operators commute with each other as they involve different degrees of freedom represented by commuting operators. Thus we are led to the following very useful property (theorem): If two operators $\mathcal{A}$ and $\mathcal{B}$ have the same set of eigenvectors, they must commute, $[\mathcal{A}, \mathcal{B}] = 0$. The converse is also true: If two operators commute, their eigenvectors coincide.

Let $\{|\phi_i\rangle\}$ be the common set of eigenvectors, i.e., $\mathcal{A}|\phi_i\rangle = a_i|\phi_i\rangle$ and $\mathcal{B}|\phi_i\rangle = b_i|\phi_i\rangle$ with a_i and b_i the respective eigenvalues and $i = 0, 1, 2, \ldots, N$ or ∞. Obviously

$$\mathcal{A}\mathcal{B}|\phi_i\rangle = \mathcal{A}b_i|\phi_i\rangle = b_i\mathcal{A}|\phi_i\rangle = b_i a_i|\phi_i\rangle = \mathcal{B}\mathcal{A}|\phi_i\rangle \,. \tag{1.101}$$

Therefore $\mathcal{A}\mathcal{B} - \mathcal{B}\mathcal{A} = 0$ because (1.101) holds for all $|\phi_i\rangle$. To prove the converse, assume $\mathcal{A}\mathcal{B} = \mathcal{B}\mathcal{A}$ and let $\{|a_i\rangle\}$ be the complete set of eigenvectors of $\mathcal{A}$, i.e., $\mathcal{A}|a_i\rangle = a_i|a_i\rangle$. Consider now $\mathcal{A}\mathcal{B}|a_i\rangle = \mathcal{B}\mathcal{A}|a_i\rangle = a_i\mathcal{B}|a_i\rangle$. This implies that $\mathcal{B}|a_i\rangle$ is an eigenvector of $\mathcal{A}$ with the eigenvalue a_i. Consequently $\mathcal{B}|a_i\rangle = \lambda_i|a_i\rangle$, where λ_i is a c-number coefficient. But this means that $|a_i\rangle$ is an eigenvector of $\mathcal{B}$ as well.

Thus, if two operators $\mathcal{A}$ and $\mathcal{B}$ commute, they possess a common set of eigenvectors $\{|\phi_i\rangle\}$ with corresponding eigenvalues $\{a_i\}$ and $\{b_i\}$. It is now evident that if the system is in one of those common eigenstates, say $|\phi_i\rangle$, measurement of both $\mathcal{A}$ and $\mathcal{B}$ will yield values a_i and b_i with no uncertainty. Otherwise, if $\mathcal{A}$ and $\mathcal{B}$ do not commute, each of them has its own distinct set of eigenvectors $\{|a_i\rangle\}$ and $\{|b_i\rangle\}$, respectively. Then if the system is in one of the eigenstates of $\mathcal{A}$, say $|a_i\rangle$, the measurement of observable associated with $\mathcal{A}$ will yield a_i with no uncertainty. But because $|a_i\rangle$ is not an eigenstate of $\mathcal{B}$, the result of measurement of $\mathcal{B}$ will be uncertain. This fundamental feature of quantum theory was first articulated by Heisenberg in what is now known as Heisenberg uncertainty principle, which states that the product of uncertainties of two variables represented by operators $\mathcal{A}$ and $\mathcal{B}$ must be no smaller than half of the expectation value of their commutator,

$$\Delta\mathcal{A}\,\Delta\mathcal{B} \geq \tfrac{1}{2}|\langle[\mathcal{A}, \mathcal{B}]\rangle| \,. \tag{1.102}$$

For two canonically conjugate variables, represented by two non-commuting operators, such as position $\mathcal{Q}$ and momentum $\mathcal{P}$, we thus have

$$\Delta\mathcal{Q}\,\Delta\mathcal{P} \geq \hbar/2 \,, \tag{1.103}$$

which is a consequence of the commutation relation (1.50)

To illustrate the foregoing discussion, let us revert again to the harmonic oscillator in the coherent state $|\alpha\rangle$. Since $|\alpha\rangle$, as given by (1.89), is a linear combination of the energy eigenstates $|n\rangle$, the energy of the system in such a state involves an uncertainty. Clearly, upon measurement, the probability of obtaining the value $n\hbar\omega$ is

$$P(n) = |\langle n|\alpha\rangle|^2 = \frac{|\alpha|^{2n}}{n!}\,\mathrm{e}^{-|\alpha|^2} \,, \tag{1.104}$$

while the average value of n is

$$\langle\alpha|\, a^\dagger a\,|\alpha\rangle = \sum_n nP(n) = |\alpha|^2 \equiv \bar{n} \,. \tag{1.105}$$

This implies that $P(n)$ can also be expressed as

$$P(n) = \frac{\bar{n}^n \mathrm{e}^{-\bar{n}}}{n!} \,, \tag{1.106}$$

which demonstrates that the probability of obtaining n quanta is given by the Poisson distribution. The variance $(\Delta n)^2 = \langle \mathcal{N}^2 \rangle - \langle \mathcal{N} \rangle^2$ can easily be calculated, by noting that

$$\begin{aligned} \langle \alpha | \, \mathcal{N}^2 \, | \alpha \rangle &= \langle \alpha | \, a^\dagger a a^\dagger a \, | \alpha \rangle = \langle \alpha | \, a^\dagger (a^\dagger a + 1) a \, | \alpha \rangle \\ &= \langle \alpha | \, a^\dagger a^\dagger a a \, | \alpha \rangle + \langle \alpha | \, a^\dagger a \, | \alpha \rangle = |\alpha|^4 + |\alpha|^2 \,, \end{aligned}$$

where we have used the fact that $\langle \alpha | \, a^\dagger = (a \, | \alpha \rangle)^* = \alpha^* \langle \alpha | \,$, i.e., $a^\dagger$ operates to the left (on the bra), while a operates to the right (on the ket). We thus have $(\Delta n)^2 = |\alpha|^4 + |\alpha|^2 - |\alpha|^4 = |\alpha|^2$, or

$$\Delta n = |\alpha| = \sqrt{\bar{n}} \,, \tag{1.107}$$

as also expected from the Poisson distribution (1.106).

Let us also calculate the uncertainties in the position $\mathcal{Q}$ and momentum $\mathcal{P}$ measurement of the harmonic oscillator in the coherent state $|\alpha\rangle$. Using

$$\mathcal{Q} = \sqrt{\frac{\hbar}{2M\omega}} \, (a^\dagger + a) \,, \quad \mathcal{P} = \mathrm{i} \sqrt{\frac{M\hbar\omega}{2}} \, (a^\dagger - a) \,, \tag{1.108}$$

we have

$$\langle \mathcal{Q} \rangle = \sqrt{\frac{2\hbar}{M\omega}} \, \mathrm{Re}(\alpha) \,, \quad \langle \mathcal{P} \rangle = \sqrt{2M\hbar\omega} \, \mathrm{Im}(\alpha) \,,$$

and

$$\langle \mathcal{Q}^2 \rangle = \frac{\hbar}{2M\omega} \left[\big(2\mathrm{Re}(\alpha) \big)^2 + 1 \right] \,, \quad \langle \mathcal{P}^2 \rangle = \frac{M\hbar\omega}{2} \left[\big(2\mathrm{Im}(\alpha) \big)^2 + 1 \right] \,.$$

The variances are thus given by

$$(\Delta \mathcal{Q})^2 = \langle \mathcal{Q}^2 \rangle - \langle \mathcal{Q} \rangle^2 = \frac{\hbar}{2M\omega} \,, \quad (\Delta \mathcal{P})^2 = \langle \mathcal{P}^2 \rangle - \langle \mathcal{P} \rangle^2 = \frac{M\hbar\omega}{2} \,, \tag{1.109}$$

from which

$$\Delta \mathcal{Q} \, \Delta \mathcal{P} = \hbar/2 \,, \tag{1.110}$$

i.e., the coherent state of the harmonic oscillator is a minimum uncertainty state in the sense that $\Delta \mathcal{Q} \, \Delta \mathcal{P}$ is the minimum allowed. In addition, the uncertainties of the position $\mathcal{Q}$ and momentum $\mathcal{P}$ are equal (except for the dimensional factors $\sqrt{M\omega}$ in the denominator and numerator, respectively), as shown in Fig. 1.1(a).

A more general class of minimum uncertainty states are the squeezed coherent states for which the uncertainty of one of the variables is smaller than

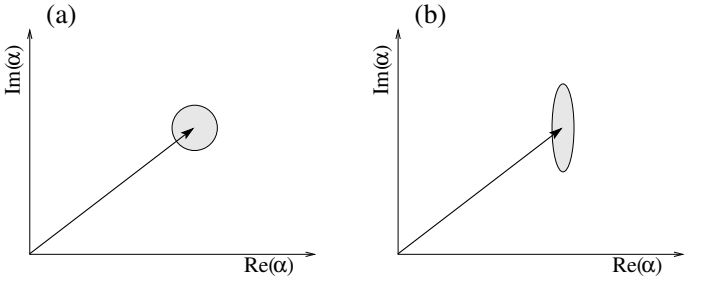

Fig. 1.1. Amplitudes ($\langle\mathcal{Q}\rangle \propto \mathrm{Re}(\alpha)$ and $\langle\mathcal{P}\rangle \propto \mathrm{Im}(\alpha)$) and uncertainties (shaded error contours) for the (a) coherent and (b) squeezed states.

that of the coherent state, $\sqrt{\hbar/2}$, with the uncertainty of the conjugate variable larger than $\sqrt{\hbar/2}$, so that their product is equal to $\hbar/2$, as required by the uncertainty principle. A squeezed state denoted by $|\alpha,\zeta\rangle$ can formally be generated by acting with the unitary squeezing operator $\mathcal{S}(\zeta)$ upon the coherent state $|\alpha\rangle$,

$$|\alpha,\zeta\rangle = \mathcal{S}(\zeta)\,|\alpha\rangle\ , \quad \mathcal{S}(\zeta) \equiv \exp\left(\tfrac{1}{2}\zeta^* a^2 - \tfrac{1}{2}\zeta a^{\dagger 2}\right)\ . \tag{1.111}$$

Given a harmonic oscillator in the squeezed state $|\alpha,\zeta\rangle$, where $\zeta = r\mathrm{e}^{i\phi}$ is a complex number, it is convenient to define the Hermitian amplitude operators

$$\mathcal{Y}_1(\phi) = (a^\dagger \mathrm{e}^{\mathrm{i}\phi/2} + a\mathrm{e}^{-\mathrm{i}\phi/2})\ , \quad \mathcal{Y}_2(\phi) = \mathrm{i}(a^\dagger \mathrm{e}^{\mathrm{i}\phi/2} - a\mathrm{e}^{-\mathrm{i}\phi/2})\ , \tag{1.112}$$

which are proportional to the position $\mathcal{Q}$ and momentum $\mathcal{P}$ operators rotated by the angle $\phi/2$ in the complex α plain. Using the following properties of the squeezing operator (see Prob. 1.5),

$$\mathcal{S}^\dagger(\zeta) a \mathcal{S}(\zeta) = a\cosh r - a^\dagger \mathrm{e}^{i\phi}\sinh r\ , \tag{1.113a}$$
$$\mathcal{S}^\dagger(\zeta) a^\dagger \mathcal{S}(\zeta) = a^\dagger\cosh r - a\mathrm{e}^{-i\phi}\sinh r\ , \tag{1.113b}$$

it is a simple exercise to obtain

$$\langle\mathcal{Y}_1\rangle = \langle\alpha|\,\mathcal{S}^\dagger(\zeta) d_1 \mathcal{S}(\zeta)\,|\alpha\rangle = (\alpha^*\mathrm{e}^{i\phi/2} + \alpha\mathrm{e}^{-i\phi/2})\,\mathrm{e}^{-r}\ ,$$
$$\langle\mathcal{Y}_2\rangle = \langle\alpha|\,\mathcal{S}^\dagger(\zeta) d_2 \mathcal{S}(\zeta)\,|\alpha\rangle = \mathrm{i}(\alpha^*\mathrm{e}^{i\phi/2} - \alpha\mathrm{e}^{-i\phi/2})\,\mathrm{e}^{r}\ ,$$

and

$$\langle\mathcal{Y}_1^2\rangle = \left[1 + (\alpha^*\mathrm{e}^{i\phi/2} + \alpha\mathrm{e}^{-i\phi/2})^2\right]\mathrm{e}^{-2r}\ ,$$
$$\langle\mathcal{Y}_2^2\rangle = \left[1 - (\alpha^*\mathrm{e}^{i\phi/2} - \alpha\mathrm{e}^{-i\phi/2})^2\right]\mathrm{e}^{2r}\ .$$

The variances of $\mathcal{Y}_1$ and $\mathcal{Y}_2$ are therefore

$$(\Delta\mathcal{Y}_1)^2 = \mathrm{e}^{-2r}\ , \quad (\Delta\mathcal{Y}_2)^2 = \mathrm{e}^{2r}\ , \tag{1.114}$$

which yields

$$\Delta\mathcal{Y}_1\,\Delta\mathcal{Y}_2 = 1\,. \tag{1.115}$$

Thus the parameter r determines the amount of squeezing of the uncertainty of one of the amplitudes, while the uncertainty of the other (conjugate) amplitude is stretched by the corresponding amount, such that their product is a constant equal to 1. When $\phi = 0$, the amplitudes $\mathcal{Y}_1$ and $\mathcal{Y}_2$ correspond, respectively, to the position $\mathcal{Q}$ and momentum $\mathcal{P}$ operators, for which we readily obtain

$$\Delta\mathcal{Q} = \sqrt{\frac{\hbar}{2M\omega}}\,\mathrm{e}^{-r}\,, \quad \Delta\mathcal{P} = \sqrt{\frac{M\hbar\omega}{2}}\,\mathrm{e}^{r}\,. \tag{1.116}$$

For $r > 0$ we have a position-squeezed state, meaning that the uncertainty in the position measurement is smaller than that for the coherent state (see Fig. 1.1(b)), while for $r < 0$ the harmonic oscillator is in a momentum-squeezed state.

1.2.6 Time Evolution: The Schrödinger Equation

The third postulate of non-relativistic quantum theory states that the time-evolution of a system is governed by the Schrödinger equation

$$\mathrm{i}\hbar\frac{\partial}{\partial t}\,|\Psi(t)\rangle = \mathcal{H}\,|\Psi(t)\rangle\,. \tag{1.117}$$

For an isolated system, the Hamiltonian $\mathcal{H} = \mathcal{H}^0$ is time-independent and the total energy of the system is conserved. We can then expand the state of the system $|\Psi\rangle$ in terms of the eigenstates $|E_n\rangle$ of the Hamiltonian, $\mathcal{H}^0\,|E_n\rangle = E_n\,|E_n\rangle$ with E_n the corresponding energy eigenvalues, as

$$|\Psi\rangle = \sum_n c_n\,|E_n\rangle\,.$$

Substituting this into the Schrödinger equation (1.117) we have

$$\sum_n \dot{c}_n\,|E_n\rangle = -\frac{\mathrm{i}}{\hbar}\sum_n E_n c_n\,|E_n\rangle\,, \tag{1.118}$$

with the solution $c_n(t) = c_n(0)\,\mathrm{e}^{-\mathrm{i}\omega_n t}$, where $\omega_n = E_n/\hbar$. Thus the amplitudes c_n of the decomposition of the state vector, while preserving their absolute value $|c_n(t)| = |c_n(0)|$, oscillate in time with the frequencies ω_n determined by the corresponding energy eigenvalues E_n, with the result

$$|\Psi(t)\rangle = \sum_n c_n(0)\mathrm{e}^{-\mathrm{i}\omega_n t}\,|E_n\rangle\,. \tag{1.119}$$

Consider now the case of a system under an external (in general time-dependent) perturbation $\mathcal{V}(t)$ which acts through some dynamic variable

(operator) of the system contained in $\mathcal{V}$. The total Hamiltonian now is $\mathcal{H} = \mathcal{H}^0 + \mathcal{V}$. It is often convenient to expand the state of the systems in terms of the eigenstates $|E_n\rangle$ of the unperturbed Hamiltonian $\mathcal{H}^0$ as

$$|\Psi(t)\rangle = \sum_n c_n(t)\,|E_n\rangle = \sum_n \tilde{c}_n(t)\mathrm{e}^{-\mathrm{i}\omega_n t}\,|E_n\rangle\ .$$

Then, from the Schrödinger equation (1.117) we obtain the following set of differential equations for the slowly-varying coefficients $\tilde{c}_n(t)$,

$$\frac{\partial}{\partial t}\tilde{c}_n(t) = -\frac{\mathrm{i}}{\hbar}\sum_m \tilde{\mathcal{V}}_{nm}(t)\tilde{c}_m(t)\ , \quad \tilde{\mathcal{V}}_{nm}(t) \equiv \mathrm{e}^{\mathrm{i}\omega_{nm}t}\langle E_n|\,\mathcal{V}(t)\,|E_m\rangle\ , \quad (1.120)$$

where $\omega_{nm} = \omega_n - \omega_m$. These equations govern the time evolution of the systems in the so-called *interaction picture*, in which the rapid oscillations of the coefficients of the state vector expansion in terms of the energy eigenstates $|E_n\rangle$ were removed via the transformation

$$|\tilde{\Psi}(t)\rangle = \mathrm{e}^{\frac{\mathrm{i}}{\hbar}\mathcal{H}^0 t}\,|\Psi(t)\rangle = \sum_n \tilde{c}_n(t)\,|E_n\rangle\ . \quad (1.121)$$

The Schrödinger equation for $|\tilde{\Psi}(t)\rangle$ then reads

$$\mathrm{i}\hbar\frac{\partial}{\partial t}\,|\tilde{\Psi}(t)\rangle = \tilde{\mathcal{V}}(t)\,|\tilde{\Psi}(t)\rangle\ , \quad \tilde{\mathcal{V}}(t) \equiv \mathrm{e}^{\frac{\mathrm{i}}{\hbar}\mathcal{H}^0 t}\,\mathcal{V}(t)\,\mathrm{e}^{-\frac{\mathrm{i}}{\hbar}\mathcal{H}^0 t}\ , \quad (1.122)$$

which is an equivalent way of writing (1.120). Thus to determine the state of the system at time $t > 0$, given its state at time $t = 0$, one has to solve the set of coupled differential equations (1.120) with the corresponding initial conditions defined by the amplitudes $c_n(0) = \tilde{c}_n(0)$.

When the interaction $\mathcal{V}$ is time independent (or its time-dependence is harmonic), the time evolution of the state vector $|\Psi(t)\rangle$ can, in principle, be determined through the solution of the eigenvalue problem $\mathcal{H}\,|\Psi\rangle = \hbar\lambda\,|\Psi\rangle$. The roots of the determinant $\det(\mathcal{H} - \hbar\lambda I)$ give the eigenfrequencies λ_n or the eigenenergies $\hbar\lambda_n$ of the total Hamiltonian $\mathcal{H}$. The corresponding eigenvectors $|\Psi_n\rangle$, which satisfy $\mathcal{H}\,|\Psi_n\rangle = \hbar\lambda_n\,|\Psi_n\rangle$, are the eigenstates of the system "dressed" by the interaction $\mathcal{V}$. Then, the state of the system at any time $t \geq 0$ is given by

$$|\Psi(t)\rangle = \sum_n \mathrm{e}^{-\mathrm{i}\lambda_n t}\,|\Psi_n\rangle\langle\Psi_n|\Psi(0)\rangle\ , \quad (1.123)$$

where $|\Psi(0)\rangle$ is the initial state. For an isolated system, $\mathcal{V} = 0$, we obviously have $\hbar\lambda_n = E_n$ and $|\Psi_n\rangle = |E_n\rangle$, where E_n and $|E_n\rangle$ are the energy eigenvalues and the corresponding eigenstates of $\mathcal{H}^0$. Then the above equation reduces to (1.119) with $c_n(0) = \langle E_n|\Psi(0)\rangle$.

1.2.7 Heisenberg Picture

The time-dependent Schrödinger equation (1.117) admits the formal solution

$$|\Psi(t)\rangle = \mathcal{U}(t)\,|\Psi(0)\rangle\ , \tag{1.124}$$

where the evolution operator is defined via $\mathcal{U}(t) \equiv \exp[-\frac{\mathrm{i}}{\hbar}\mathcal{H}t]$, assuming that the Hamiltonian $\mathcal{H}$ does not explicitly depend on time. The evolution operator $\mathcal{U}(t)$ acts upon the state vector $|\Psi(0)\rangle$ at initial time $t = 0$ to change it to $|\Psi(t)\rangle$. In calculating the expectation value $\langle\mathcal{A}(t)\rangle$ of some operator $\mathcal{A}$ at time t, the time dependence can formally be incorporated in the operator itself,

$$\langle\mathcal{A}(t)\rangle = \langle\Psi(t)|\,\mathcal{A}\,|\Psi(t)\rangle = \langle\Psi(0)|\,\mathcal{U}^\dagger(t)\,\mathcal{A}\mathcal{U}(t)\,|\Psi(0)\rangle = \langle\Psi(0)|\,\mathcal{A}(t)\,|\Psi(0)\rangle\ , \tag{1.125}$$

where the time-dependent Heisenberg operator is defined as

$$\mathcal{A}(t) = \mathcal{U}^\dagger(t)\,\mathcal{A}\mathcal{U}(t)\ , \tag{1.126}$$

while the state of the system is that at $t = 0$. The equation governing the time evolution of $\mathcal{A}(t)$ can be obtained by differentiating (1.126),

$$\frac{\mathrm{d}}{\mathrm{d}t}\mathcal{A}(t) = \frac{\mathrm{d}\mathcal{U}^\dagger(t)}{\mathrm{d}t}\,\mathcal{A}\mathcal{U}(t) + \mathcal{U}^\dagger(t)\,\frac{\partial\mathcal{A}}{\partial t}\,\mathcal{U}(t) + \mathcal{U}^\dagger(t)\,\mathcal{A}\,\frac{\mathrm{d}\mathcal{U}(t)}{\mathrm{d}t}\ .$$

Using the definition of $\mathcal{U}$ and the fact that $\mathcal{U}$ and $\mathcal{H}$ commute, since $\mathcal{U}$ is a function of $\mathcal{H}$, we have

$$\frac{\mathrm{d}}{\mathrm{d}t}\mathcal{A}(t) = \frac{\mathrm{i}}{\hbar}[\mathcal{H}\mathcal{A} - \mathcal{A}\mathcal{H}] + \mathcal{U}^\dagger\,\frac{\partial\mathcal{A}}{\partial t}\,\mathcal{U}\ . \tag{1.127}$$

If in the Schrödinger picture the operator $\mathcal{A}$ is not explicitly time-dependent, $\partial_t\mathcal{A} = 0$, this equation becomes

$$\frac{\mathrm{d}}{\mathrm{d}t}\mathcal{A}(t) = \frac{\mathrm{i}}{\hbar}[\mathcal{H}, \mathcal{A}]\ , \tag{1.128}$$

and is referred to as the Heisenberg equation of motion of operator $\mathcal{A}$.

1.3 Density Operator

So far we have been describing the behavior of quantum systems in terms of state vectors. As discussed below, however, it is not always possible to ascribe a state vector to a quantum system that is not isolated but is a part of a larger compound system. In this section, we introduce the density operator and its matrix representation—the density matrix—an indispensable tool of quantum theory, allowing the rigorous treatment of interacting quantum systems.

1.3.1 Pure and Mixed States

When the state of a quantum system can be represented as a linear superposition of basis vectors $|n\rangle$, $|\Psi\rangle = \sum_n c_n |n\rangle$, the system is said to be in a pure state, *not* necessarily an eigenstate, although that is a special case of a pure state too. The density operator ρ for the system in a pure state is defined as

$$\rho = |\Psi\rangle\langle\Psi| \ . \tag{1.129}$$

Using the expansion of $|\Psi\rangle$ above, we have

$$\rho = \sum_n \sum_m c_n c_m^* |n\rangle\langle m| = \sum_{n,m} \rho_{nm} |n\rangle\langle m| \ , \tag{1.130}$$

where $\rho_{nm} = \langle n| \rho |m\rangle$ are the matrix elements of the density operator, which for pure states are given by $\rho_{nm} = c_n c_m^*$. The diagonal matrix elements of ρ have a physical meaning: If a measurement is made on the system, the probability of finding it in state $|n\rangle$ is ρ_{nn}. That is why the matrix elements ρ_{nn} are also called populations. For the off-diagonal matrix elements we have the relations $\rho_{nm} = \rho_{mn}^*$. They are often called coherences because they depend on the relative phase of c_n and c_m. To see why, let us write these amplitudes in the polar form as $c_n = r_n e^{i\varphi_n}$ and $c_m = r_m e^{i\varphi_m}$. Obviously $\rho_{nm} = r_n r_m e^{i(\varphi_n - \varphi_m)}$ which shows the dependence on $\Delta\varphi_{nm} \equiv \varphi_n - \varphi_m$. In the quantum language, equilibrium statistical mechanics and thermodynamics are concerned only with ρ_{nn}, because equilibrium in the thermodynamic sense means complete loss of phase information.[1] On the other hand, quantum optics often deals with situations in which phase relations between the amplitudes of states (or coherences) are very important. And in fact, in quantum information the coherence is absolutely necessary; loss of coherence, or decoherence, is the mortal enemy of quantum information processing.

The density operator for a pure state has the properties:

$$\mathrm{Tr}(\rho) \equiv \sum_n \rho_{nn} = 1 \ \text{ and } \ |\rho_{mn}|^2 = \rho_{mm}^2 \rho_{nn}^2 \ , \tag{1.131}$$

from which it also follows that

$$\mathrm{Tr}(\rho^2) = 1 \ \text{ and } \ \rho^2 = \rho \ . \tag{1.132}$$

This is also evident from $\rho^2 = |\Psi\rangle\langle\Psi|\Psi\rangle\langle\Psi|$, which means that ρ is idempotent.

A quantum system, however, may not be in a pure state. In fact, in most cases of physical systems, their state is not pure. A basic reason for this is that the quantum system may have interacted with other systems, which

[1] For an illustration of this statement, see Sect. 5.1.1 and, in particular, equations (5.16) and (5.17).

have resulted in inseparability of the state vectors of individual systems, called entanglement, as discussed below. For the moment, assume that all we know is that the system is in a mixture (not a superposition) of states $|\Psi\rangle$, not necessary orthogonal to each other, each $|\Psi\rangle$ having a different expansion in the basis of eigenvectors $|n\rangle$. Let $P_\Psi \geq 0$ be the probability that the system is in some particular state $|\Psi\rangle$. Then the density operator must be written as

$$\rho = \sum_\Psi P_\Psi \, |\Psi\rangle\langle\Psi| \ , \tag{1.133}$$

which is clearly a Hermitian operator, $\rho = \rho^\dagger$. For each $|\Psi\rangle$ we have $|\Psi\rangle = \sum_n c_n^\Psi \, |n\rangle$ with no relation between the expansion coefficients c_n^Ψ for different $|\Psi\rangle$. For all $|\Psi\rangle$ we have $\langle\Psi|\Psi\rangle = 1$, which means $\sum_n |c_n^\Psi|^2 = 1$. We can now write

$$\rho = \sum_\Psi \sum_{nm} P_\Psi c_n^\Psi (c_m^\Psi)^* \, |n\rangle\langle m| \ , \tag{1.134}$$

$$\mathrm{Tr}(\rho) \equiv \sum_n \rho_{nn} = \sum_\Psi P_\Psi \sum_n |c_n^\Psi|^2 = \sum_\Psi P_\Psi \ . \tag{1.135}$$

In order for $\mathrm{Tr}(\rho) = 1$, we must have $\sum_\Psi P_\Psi = 1$, which is consistent with the interpretation of P_Ψ as the probability for the system to be in state $|\Psi\rangle$. Under these conditions, we say that the system is in a mixed state, which can not be represented by a state vector. Note that for the mixed density operator we have $\rho_{nn} = \sum_\Psi P_\Psi |c_n^\Psi|^2$ and $\rho_{nm} = \sum_\Psi P_\Psi c_n^\Psi (c_m^\Psi)^*$, from which we obtain

$$\begin{aligned} \rho_{nm}\rho_{mn} &= \sum_\Psi \sum_{\Psi'} P_\Psi P_{\Psi'} c_n^\Psi (c_n^{\Psi'})^* \, c_m^{\Psi'} (c_m^\Psi)^* \ , \\ \rho_{nn}\rho_{mm} &= \sum_\Psi \sum_{\Psi'} P_\Psi P_{\Psi'} |c_n^\Psi|^2 \, |c_m^{\Psi'}|^2 \neq \rho_{nm}\rho_{mn} \ . \end{aligned} \tag{1.136}$$

This is an important difference between the pure and mixed state density operators.

1.3.2 Expectation Value of an Operator

When a system is in a pure state $|\Psi\rangle = \sum_n c_n \, |n\rangle$, according to (1.97) the expectation value of an operator $\mathcal{A}$ is given by

$$\langle\mathcal{A}\rangle \equiv \langle\Psi| \, \mathcal{A} \, |\Psi\rangle = \sum_n \sum_m c_n c_m^* \langle m| \, \mathcal{A} \, |n\rangle \ .$$

Since $c_n c_m^* = \rho_{nm}$ and $\langle m| \, \mathcal{A} \, |n\rangle = \mathcal{A}_{mn}$, we have

$$\langle\mathcal{A}\rangle = \sum_n \Big(\sum_m \rho_{nm} \mathcal{A}_{mn} \Big) = \sum_n (\rho\mathcal{A})_{nn} = \mathrm{Tr}(\rho\mathcal{A}) = \mathrm{Tr}(\mathcal{A}\rho) \ , \tag{1.137}$$

which shows that once the density matrix of the system is known, the expectation value of any operator can be calculated by taking the trace of the product of that operator in matrix representation with the density matrix, in any order. This rule can be generalized to the case of a system in mixed state and therefore described by a mixed density operator of (1.134), i.e., $\rho = \sum_\Psi \sum_{nm} P_\Psi \rho^\Psi_{nm} |n\rangle\langle m|$ with $\rho^\Psi_{nm} \equiv c^\Psi_n (c^\Psi_m)^*$. We then have

$$\begin{aligned}\langle \mathcal{A} \rangle = \mathrm{Tr}(\rho\mathcal{A}) &= \sum_n (\rho\mathcal{A})_{nn} = \sum_{nm} \rho_{nm}\mathcal{A}_{mn} = \sum_\Psi \sum_{nm} P_\Psi \rho^\Psi_{nm}\mathcal{A}_{mn} \\ &= \sum_\Psi P_\Psi \mathrm{Tr}(\rho^\Psi \mathcal{A}) = \sum_\Psi P_\Psi \langle\Psi| \mathcal{A} |\Psi\rangle \ , \end{aligned} \tag{1.138}$$

which shows that the expectation value of operator $\mathcal{A}$ is given by the statistical average of its expectation values $\langle\Psi| \mathcal{A} |\Psi\rangle$ in the pure states $|\Psi\rangle$. Note that this is consistent with defining the trace via $\mathrm{Tr}(\ldots) = \sum_n \langle n| \ldots |n\rangle$, in which case

$$\mathrm{Tr}(\rho) = \sum_n \langle n| \sum_\Psi P_\Psi |\Psi\rangle\langle\Psi| n\rangle = \sum_\Psi P_\Psi \sum_n |c^\Psi_n|^2 = \sum_\Psi P_\Psi = 1 \ .$$

Since ρ is Hermitian, its eigenvalues are real, and from the above equation it is clear that they must lie between 0 and 1.

Let $|a_i\rangle$ be the eigenvectors and a_i the corresponding eigenvalues of operator $\mathcal{A}$. The probability $P(a_i)$ for obtaining the result a_i in a single measurement is given by

$$\begin{aligned} P(a_i) &= \sum_\Psi P_\Psi \langle\Psi|a_i\rangle\langle a_i|\Psi\rangle = \sum_\Psi \sum_{nm} P_\Psi \langle\Psi|m\rangle\langle m|a_i\rangle\langle a_i|n\rangle\langle n|\Psi\rangle \\ &= \sum_{nm} \sum_\Psi P_\Psi c^\Psi_n (c^\Psi_m)^* \langle m|a_i\rangle\langle a_i|n\rangle = \sum_{nm} \rho_{nm} \langle m|a_i\rangle\langle a_i|n\rangle \ . \end{aligned}$$

With $\Pi_i \equiv |a_i\rangle\langle a_i|$ denoting the corresponding projection operator, the above expression reads

$$P(a_i) = \sum_n (\rho\Pi_i)_{nn} = \mathrm{Tr}(\rho\Pi_i) \ , \tag{1.139}$$

which is thus consistent with the general rule of (1.138).

Consider now an operator $\mathcal{A}$ acting on a quantum system A which is coupled to another system B. As we know, the complete vector space associated with the compound system A+B is given by the tensor product of the vector spaces of the individual subsystems A and B with the corresponding basis vectors $|n^\mathrm{A}\rangle$ and $|n^\mathrm{B}\rangle$. With ρ denoting the density operator of the compound system, for the expectation value of $\mathcal{A}$ we can write

$$\begin{aligned}\langle \mathcal{A} \rangle = \mathrm{Tr}(\rho\mathcal{A}) &= \sum_{n^\mathrm{A}} \sum_{n^\mathrm{B}} \langle n^\mathrm{A}| \otimes \langle n^\mathrm{B}| \, \rho\mathcal{A} \, |n^\mathrm{A}\rangle \otimes |n^\mathrm{B}\rangle \\ &= \sum_{n^\mathrm{A} m^\mathrm{A}} \sum_{n^\mathrm{B} m^\mathrm{B}} \langle n^\mathrm{A} n^\mathrm{B}| \, \rho \, |m^\mathrm{A} m^\mathrm{B}\rangle\langle m^\mathrm{A} m^\mathrm{B}| \, \mathcal{A} \, |n^\mathrm{A} n^\mathrm{B}\rangle \ , \end{aligned} \tag{1.140}$$

where $|n^{\rm A}n^{\rm B}\rangle$ is a simplified notation for $|n^{\rm A}\rangle \otimes |n^{\rm B}\rangle$ and similarly for other ket's and bra's. Since the operator $\mathcal{A}$ acts only on the subsystem A, we have $\langle m^{\rm A}m^{\rm B}|\,\mathcal{A}\,|n^{\rm A}n^{\rm B}\rangle = \langle m^{\rm A}|\,\mathcal{A}\,|n^{\rm A}\rangle\langle m^{\rm B}|n^{\rm B}\rangle$ and (1.140) becomes

$$\langle\mathcal{A}\rangle = {\rm Tr}(\rho\mathcal{A}) = \sum_{n^{\rm A}m^{\rm A}} \langle n^{\rm A}|\,\rho^{\rm A}\,|m^{\rm A}\rangle\langle m^{\rm A}|\,\mathcal{A}\,|n^{\rm A}\rangle = {\rm Tr}(\rho^{\rm A}\mathcal{A})\;, \tag{1.141}$$

where

$$\rho^{\rm A} = \sum_{n^{\rm B}} \langle n^{\rm B}|\,\rho\,|n^{\rm B}\rangle = {\rm Tr}_{\rm B}(\rho) \tag{1.142}$$

is called the reduced density operator of system A, obtained by taking the partial trace of the total density operator ρ with respect to system B.

1.3.3 Reduced Density Operator

Assume that the compound system A+B is in a pure state $|\Phi\rangle$ and therefore its density operator is given by $\rho = |\Phi\rangle\langle\Phi|$. For the reduced density operator of system A we can then write,

$$\rho^{\rm A} = \sum_{n^{\rm B}} \langle n^{\rm B}|\Phi\rangle\langle\Phi|n^{\rm B}\rangle = \sum_{n^{\rm B}} P_{n^{\rm B}}\,|\Psi^{\rm A}_{n^{\rm B}}\rangle\langle\Psi^{\rm A}_{n^{\rm B}}|\;, \tag{1.143}$$

where the probabilities are given by

$$P_{n^{\rm B}} = |\langle n^{\rm B}|\Phi\rangle|^2\;,$$

and the normalized state vectors of system A are defined through

$$|\Psi^{\rm A}_{n^{\rm B}}\rangle = \frac{\langle n^{\rm B}|\Phi\rangle}{\sqrt{P_{n^{\rm B}}}} = \frac{1}{\sqrt{P_{n^{\rm B}}}} \sum_{n^{\rm A}} |n^{\rm A}\rangle\langle n^{\rm A}n^{\rm B}|\Phi\rangle\;.$$

Obviously, the mixed state density operator of (1.133) is equivalent to the above expansion (1.143) of the reduced density operator $\rho^{\rm A}$ in terms of the state vectors $|\Psi^{\rm A}_{n^{\rm B}}\rangle$ of system A. Clearly, both $|\Psi^{\rm A}_{n^{\rm B}}\rangle$ and the corresponding probabilities $P_{n^{\rm B}}$ depend on the particular basis $\{\,|n^{\rm B}\rangle\}$ used for tracing over the degrees of freedom of system B. In Sect. 8.5 we will elaborate more on this observation in the simplest context of two correlated (or entangled) two-level quantum systems—qubits. Here let us note that if the state vector of the compound system A+B factorizes into the product of individual state vectors of systems A and B, $|\Phi\rangle = |\Psi^{\rm A}\rangle\otimes|\Psi^{\rm B}\rangle$, then $\rho^{\rm A}$ reduces to the density matrix of system A in the pure state $|\Psi^{\rm A}\rangle$. Indeed, from (1.143) we have

$$\rho^{\rm A} = \sum_{n^{\rm B}} \langle n^{\rm B}|\Psi^{\rm B}\rangle\langle\Psi^{\rm B}|n^{\rm B}\rangle\,|\Psi^{\rm A}\rangle\langle\Psi^{\rm A}|\;=\sum_{n^{\rm B}} P_{n^{\rm B}}\,|\Psi^{\rm A}\rangle\langle\Psi^{\rm A}|\;=\;|\Psi^{\rm A}\rangle\langle\Psi^{\rm A}|\;, \tag{1.144}$$

since for normalized $|\Psi^{\rm B}\rangle$ the sum of probabilities $P_{n^{\rm B}} = |\langle n^{\rm B}|\Psi^{\rm B}\rangle|^2$ over all basis states $|n^{\rm B}\rangle$ is unity. The state of a compound system that does not admit

a factorization into a product of states of its subsystems, $|\Phi\rangle \neq |\Psi^{\mathrm{A}}\rangle \otimes |\Psi^{\mathrm{B}}\rangle$, is called an entangled state. The Schmidt decomposition of Sect. 1.1.2 states, however, that for any pure state $|\Phi\rangle$ of the compound system A+B there exist orthonormal bases $\{|\psi_i^{\mathrm{A}}\rangle\}$ for A and $\{|\psi_i^{\mathrm{B}}\rangle\}$ for B in terms of which we can expand $|\Phi\rangle$ as

$$|\Phi\rangle = \sum_i s_i \, |\psi_i^{\mathrm{A}}\rangle \otimes |\psi_i^{\mathrm{B}}\rangle \; . \tag{1.145}$$

It then follows that the reduced density matrix of system A in this basis is diagonal,

$$\rho^{\mathrm{A}} = \sum_i p_i \, |\psi_i^{\mathrm{A}}\rangle\langle\psi_i^{\mathrm{A}}| \; , \tag{1.146}$$

i.e., $|\psi_i^{\mathrm{A}}\rangle$ are eigenstates of ρ^{A} with eigenvalues $p_i = s_i^2$. Similarly, $|\psi_i^{\mathrm{B}}\rangle$ are eigenstates of the reduced density operator ρ^{B} of system B with the same eigenvalues p_i. The number of nonzero eigenvalues $p_i \neq 0$ is called the Schmidt number, and clearly the two systems are entangled if the Schmidt number for the compound state $|\Phi\rangle$ is larger than one, i.e., the Schmidt decomposition (1.145) has more than one term.

1.3.4 Time Evolution: The Von Neumann Equation

From the Schrödinger equation (1.117) for the state vector $|\Psi\rangle$, we can derive the equation of motion for the density operator ρ of an isolated quantum system. In general, the initial state of the system is described by the mixed density operator of (1.133), meaning that the system may have interacted in the past with another system, whose degrees of freedom have now been eliminated by taking the partial trace in an appropriate basis. The assumption that the system has become isolated implies that the probabilities P_Ψ will not depend on time, with the time dependence of ρ originating from that of $|\Psi\rangle$. Differentiating (1.133) with respect to time and using (1.117), we then have

$$\frac{\partial}{\partial t}\rho = \sum_\Psi P_\Psi \left[\frac{\partial \, |\Psi\rangle}{\partial t}\langle\Psi| \, + \, |\Psi\rangle \frac{\partial \langle\Psi|}{\partial t} \right] = -\frac{\mathrm{i}}{\hbar} \sum_\Psi P_\Psi \left[\mathcal{H} \, |\Psi\rangle\langle\Psi| \, - \, |\Psi\rangle\langle\Psi| \, \mathcal{H} \right] \; ,$$

or

$$\frac{\partial}{\partial t}\rho = -\frac{\mathrm{i}}{\hbar}[\mathcal{H}, \rho] \; , \tag{1.147}$$

which, in the case of a pure state, is the Schrödinger equation in terms of ρ. Equation (1.147) is known as the von Neumann or Liouville equation. In analogy with (1.124), the formal solution for ρ can be written as $\rho(t) = \mathcal{U}(t)\rho(0)\mathcal{U}^\dagger(t)$. Later we shall see, however, that the von Neumann equation can be generalized to account for various dephasing (decoherence) and relaxation processes not amenable to treatment through the Schrödinger equation.

From (1.147), we obtain the equations governing the time-evolution of the matrix elements ρ_{nm} of the density operator,

$$\frac{\partial}{\partial t}\rho_{nm} = -\frac{\mathrm{i}}{\hbar}[\langle n|\,\mathcal{H}\rho\,|m\rangle - \langle n|\,\rho\mathcal{H}\,|m\rangle] = -\frac{\mathrm{i}}{\hbar}\sum_k [\mathcal{H}_{nk}\rho_{km} - \rho_{nk}\mathcal{H}_{km}]\ . \tag{1.148}$$

As in Sect. 1.2.6, let us assume that the total Hamiltonian of the system $\mathcal{H} = \mathcal{H}^0 + \mathcal{V}$ consists of the free Hamiltonian $\mathcal{H}^0$ and an external perturbation $\mathcal{V}$. We can then write (1.147) and (1.148) as

$$\frac{\partial}{\partial t}\rho = -\frac{\mathrm{i}}{\hbar}[\mathcal{H}^0, \rho] - \frac{\mathrm{i}}{\hbar}[\mathcal{V}, \rho]\ , \tag{1.149}$$

$$\frac{\partial}{\partial t}\rho_{nm} = -\mathrm{i}\omega_{nm}\rho_{nm} - \frac{\mathrm{i}}{\hbar}\sum_k [\mathcal{V}_{nk}\rho_{km} - \rho_{nk}\mathcal{V}_{km}]\ , \tag{1.150}$$

where, as before, $\omega_{nm} \equiv (E_n - E_m)/\hbar$. Alternatively, making the transformation $\rho = \mathrm{e}^{-\frac{\mathrm{i}}{\hbar}\mathcal{H}^0 t}\,\tilde{\rho}\,\mathrm{e}^{\frac{\mathrm{i}}{\hbar}\mathcal{H}^0 t}$, we obtain the von Neumann equation in the interaction picture

$$\frac{\partial}{\partial t}\tilde{\rho} = -\frac{\mathrm{i}}{\hbar}[\tilde{\mathcal{V}}, \tilde{\rho}]\ , \tag{1.151}$$

where $\tilde{\mathcal{V}} \equiv \mathrm{e}^{\frac{\mathrm{i}}{\hbar}\mathcal{H}^0 t}\,\mathcal{V}\,\mathrm{e}^{-\frac{\mathrm{i}}{\hbar}\mathcal{H}^0 t}$. For the matrix elements of $\tilde{\rho}$, we thus have

$$\frac{\partial}{\partial t}\tilde{\rho}_{nm} = -\frac{\mathrm{i}}{\hbar}\sum_k [\tilde{\mathcal{V}}_{nk}\tilde{\rho}_{km} - \tilde{\rho}_{nk}\tilde{\mathcal{V}}_{km}]\ , \tag{1.152}$$

where the slowly varying density matrix elements $\tilde{\rho}_{nm}$ are related to the original ones through $\tilde{\rho}_{nm} = \rho_{nm}\,\mathrm{e}^{\mathrm{i}\omega_{nm}t}$. The set of differential equations (1.152) is obviously the analog of equations (1.120) in the language of density matrix.

Problems

1.1. Prove the operator identity

$$\mathrm{e}^{\mathcal{A}}\mathcal{B}\mathrm{e}^{-\mathcal{A}} = \mathcal{B} + [\mathcal{A}, \mathcal{B}] + \frac{1}{2!}[\mathcal{A}, [\mathcal{A}, \mathcal{B}]] + \ldots \tag{1.153}$$

Given operators $\mathcal{A}$ and $\mathcal{B}$ satisfying the conditions $[\mathcal{A}, [\mathcal{A}, \mathcal{B}]] = [[\mathcal{A}, \mathcal{B}], \mathcal{B}] = 0$, prove the Baker–Hausdorff relation (1.26).

1.2. Consider the integral

$$\int_{-\infty}^{\infty} \theta(x)\,\theta'(x)\,\mathrm{d}x\ ,$$

where $\theta(x)$ is the Heaviside step function and $\theta'(x)$ its derivative. Show that the value of the integral is zero. Now, make the replacement $\theta'(x) = \delta(x)$. What is the value of the resulting integral? Is there a contradiction?

1.3. Prove the relations (1.32).

1.4. Verify that Hermite polynomials $H_n(x) = (-1)^n \mathrm{e}^{x^2} \frac{\mathrm{d}^n}{\mathrm{d}x^n} \mathrm{e}^{-x^2}$ satisfy the differential equation

$$\left(\frac{\mathrm{d}^2}{\mathrm{d}x^2} - 2x \frac{\mathrm{d}}{\mathrm{d}x} + 2n \right) H_n(x) = 0 \,. \tag{1.154}$$

1.5. Prove the relations (1.113). (*Hint*: Use the operator identity (1.153).) Then verify the derivation of (1.114) and (1.115).

1.6. Consider a harmonic oscillator initially (at $t = 0$) in a coherent state $|\Psi(0)\rangle = |\alpha\rangle$. Using the formal solution $|\Psi(t)\rangle = \mathrm{e}^{-\frac{\mathrm{i}}{\hbar}\mathcal{H}t} |\Psi(0)\rangle$ of the Schrödinger equation (1.117) with the free Hamiltonian $\mathcal{H}$ of (1.65) show that the time evolution of its state is given by $|\Psi(t)\rangle = |\alpha \, \mathrm{e}^{-\mathrm{i}\omega t}\rangle$, i.e., for a free harmonic oscillator, a coherent state remains coherent. (*Hint*: Prove and then use the equality $\mathrm{e}^{-\frac{\mathrm{i}}{\hbar}\mathcal{H}t} |n\rangle = \mathrm{e}^{-\mathrm{i}\omega(n+\frac{1}{2})t} |n\rangle$.)

1.7. Given the density operator ρ^{A} of system A in a mixed state, construct a pure state $|\Phi\rangle$ of the compound system A+B, which would yield ρ^{A} upon taking the partial trace of $\rho = |\Phi\rangle\langle\Phi|$ over B. Show that any two such "purifications" $|\Phi_1\rangle$ and $|\Phi_2\rangle$ of ρ^{A} are related by a unitary basis transformation $\mathcal{T}_{\mathrm{B}}$ of system B only, i.e., $|\Phi_1\rangle = (I_{\mathrm{A}} \otimes \mathcal{T}_{\mathrm{B}}) |\Phi_2\rangle$. This is the Gisin–Hughston–Jozsa–Wootters (GHJW) theorem.

2

Quantum Theory of Radiation

Having summarized the fundamental notions of quantum theory in Chap. 1, here we employ the classical Maxwell equations to quantize the electromagnetic field in vacuum. We then consider various quantum states of the field, followed by the discussion of the photon measurement and the information that it can yield. In the last section of this chapter, we develop several quantum mechanical representations of the field, which can be employed to conveniently evaluate the expectation values of various functions of field operators.

2.1 Maxwell's Equations and Field Quantization

The two fundamental quantities defining the electromagnetic field are the electric $\boldsymbol{E}(\boldsymbol{r},t)$ and magnetic $\boldsymbol{H}(\boldsymbol{r},t)$ fields which, in classical physics, are functions of space and time satisfying the Maxwell's equations. In the non-relativistic form and SI units, they are given by

$$\boldsymbol{\nabla}\times\boldsymbol{E}+\frac{\partial\boldsymbol{B}}{\partial t}=0\,, \tag{2.1a}$$

$$\boldsymbol{\nabla}\times\boldsymbol{H}-\frac{\partial\boldsymbol{D}}{\partial t}=\boldsymbol{J}\,, \tag{2.1b}$$

$$\boldsymbol{\nabla}\cdot\boldsymbol{D}=\sigma\,, \tag{2.1c}$$

$$\boldsymbol{\nabla}\cdot\boldsymbol{B}=0\,, \tag{2.1d}$$

where $\boldsymbol{J}$ and σ are the densities of currents and free charges, respectively, which are the sources of the fields. In empty space (vacuum), these are zero, $\boldsymbol{J}=0$ and $\sigma=0$, while $\boldsymbol{D}=\varepsilon_0\boldsymbol{E}$ and $\boldsymbol{B}=\mu_0\boldsymbol{H}$ with ε_0 the electric permittivity and μ_0 the magnetic permeability of vacuum. The fields can be expressed in terms of the scalar $\phi(\boldsymbol{r},t)$ and vector $\boldsymbol{A}(\boldsymbol{r},t)$ potentials as

$$\boldsymbol{E}=-\boldsymbol{\nabla}\phi-\frac{\partial\boldsymbol{A}}{\partial t}\,,\quad \boldsymbol{B}=\boldsymbol{\nabla}\times\boldsymbol{A}\,, \tag{2.2}$$

which is easily verified by substitution into (2.1a) and (2.1d). The Maxwell equations are invariant under gauge transformations. Specifically, if ϕ and $\boldsymbol{A}$ are changed to

$$\phi' = \phi - \frac{\partial \chi}{\partial t} \quad \text{and} \quad \boldsymbol{A}' = \boldsymbol{A} + \boldsymbol{\nabla}\chi \,,$$

where $\chi = \chi(\boldsymbol{r}, t)$ is any scalar function of the position $\boldsymbol{r}$ and time t, equations (2.2) do not change. As a result, we can choose $\phi = 0$ and $\boldsymbol{\nabla} \cdot \boldsymbol{A} = 0$, a choice that goes by the names of Coulomb, radiation or transverse gauge. Then the fields are given by

$$\boldsymbol{E} = -\frac{\partial \boldsymbol{A}}{\partial t} \,, \quad \boldsymbol{B} = \boldsymbol{\nabla} \times \boldsymbol{A} \,, \tag{2.3}$$

which means that if we know the vector potential $\boldsymbol{A}(\boldsymbol{r}, t)$ we can easily obtain the fields. As seen from (2.1c), in the absence of charges, the electric field $\boldsymbol{E}$ has a transverse part only. Substituting (2.3) into the remaining equation (2.1b) and using the vector identity $\boldsymbol{\nabla} \times \boldsymbol{\nabla} \times \boldsymbol{A} = \boldsymbol{\nabla}(\boldsymbol{\nabla} \cdot \boldsymbol{A}) - \nabla^2 \boldsymbol{A}$ and the Coulomb gauge conditions, we obtain

$$\left(\nabla^2 - \frac{1}{c^2} \frac{\partial^2}{\partial t^2} \right) \boldsymbol{A}(\boldsymbol{r}, t) = 0 \,, \tag{2.4}$$

where $c = (\mu_0 \varepsilon_0)^{-1/2}$ is the speed of light in vacuum. Thus, Maxwell's equations condense into the single equation for $\boldsymbol{A}(\boldsymbol{r}, t)$, known also as the wave equation.

The total energy stored in the electromagnetic field is given by

$$E = \frac{1}{2} \int_V \mathrm{d}^3 r \big(\varepsilon_0 \boldsymbol{E}^2 + \mu_0^{-1} \boldsymbol{B}^2 \big) \,, \tag{2.5}$$

where the spatial integration extends over the volume V in which the field is to be considered. It can be the whole space, as in the case of the open field usually employed in quantum electrodynamics (QED), or a finite volume of a specific geometry, within which the field is confined by perfectly conducting walls, representing the typical situation in cavity QED. This is an issue to which we return below.

In preparation for the transition to the quantum theory of electromagnetic fields, we can concentrate for the moment on the vector potential $\boldsymbol{A}(\boldsymbol{r}, t)$ which satisfies the homogeneous wave equation (2.4). As already noted above, we must specify the volume in which the fields are confined, even if that is infinite. In other words, we must specify the boundary conditions to be satisfied by the fields. Let us begin with the case of open space without any material boundaries. We consider the field within a cube of linear dimension L shown in Fig. 2.1 and assume periodic boundary conditions. If we write $\boldsymbol{A}(\boldsymbol{r}, t)$ as a product of a spatial and a temporal part—the typical separation of variables approach—we find that the solutions of the spatial part have the form $\exp(\pm \mathrm{i} \boldsymbol{k} \cdot \boldsymbol{r})$ and the corresponding solutions of the temporal part have the form $\exp(\mp \mathrm{i} ckt)$ with $k \equiv |\boldsymbol{k}|$. Because of the boundary conditions,

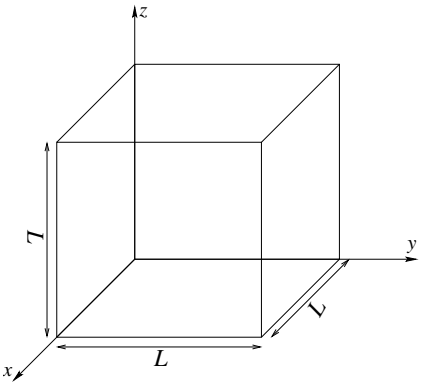

Fig. 2.1. Cubic volume of linear dimensions L.

however, the allowed values of the vectors $\boldsymbol{k}$ are restricted to $k_x = 2\pi n_x/L$, $k_y = 2\pi n_y/L$ and $k_z = 2\pi n_z/L$, where $n_{x,y,z} = \pm 1, \pm 2, \pm 3, \ldots$. To account for the vector character of $\boldsymbol{A}$, we consider the solutions $\hat{\boldsymbol{e}}_{\boldsymbol{k}\lambda} \exp(\pm \mathrm{i}\boldsymbol{k}\cdot\boldsymbol{r})$, where $\hat{\boldsymbol{e}}_{\boldsymbol{k}\lambda}$ are unit vectors, which must be chosen such that the condition $\boldsymbol{\nabla}\cdot\boldsymbol{A} = 0$ is satisfied. This means that for every $\boldsymbol{k}$, we should choose two unit vectors, perpendicular to each other and of course to $\boldsymbol{k}$, labeled as $\hat{\boldsymbol{e}}_{\boldsymbol{k}\lambda}$ with λ assuming the values 1 and 2,

$$\hat{\boldsymbol{e}}_{\boldsymbol{k}\lambda} \cdot \hat{\boldsymbol{e}}_{\boldsymbol{k}\lambda'} = \delta_{\lambda\lambda'} \ , \qquad \boldsymbol{k} \cdot \hat{\boldsymbol{e}}_{\boldsymbol{k}\lambda} = 0 \ . \tag{2.6}$$

These two unit vectors, known as polarization vectors because they represent the polarization properties of the radiation, together with $\boldsymbol{k}$ are usually chosen so as to form a right handed system of orthogonal vectors. In general, $\hat{\boldsymbol{e}}_{\boldsymbol{k}\lambda}$ can be complex, but for our purposes here we can take them to be real, without loss of generality. The three spatial components $\hat{e}^x_{\boldsymbol{k}\lambda}$, $\hat{e}^y_{\boldsymbol{k}\lambda}$ and $\hat{e}^z_{\boldsymbol{k}\lambda}$ of the polarization vectors satisfy the relation

$$\sum_{\lambda=1,2} \hat{e}^i_{\boldsymbol{k}\lambda} \hat{e}^j_{\boldsymbol{k}\lambda} = \delta_{ij} - \frac{k_i k_j}{\boldsymbol{k}^2} \ , \quad i,j = x,y,z \ . \tag{2.7}$$

The above spatial solutions denoted as $\boldsymbol{u}_{\boldsymbol{k}\lambda}(\boldsymbol{r}) = \hat{\boldsymbol{e}}_{\boldsymbol{k}\lambda} \exp(\mathrm{i}\boldsymbol{k}\cdot\boldsymbol{r})$, satisfy the orthogonality condition

$$\frac{1}{V} \int_V \mathrm{d}^3 r \, \boldsymbol{u}^*_{\boldsymbol{k}\lambda}(\boldsymbol{r}) \, \boldsymbol{u}_{\boldsymbol{k}'\lambda'}(\boldsymbol{r}) = \delta_{\boldsymbol{k}\boldsymbol{k}'} \delta_{\lambda\lambda'} \ , \tag{2.8}$$

where $V = L^3$. Now the vector potential can be expanded as

$$\boldsymbol{A}(\boldsymbol{r},t) = \sum_{\boldsymbol{k}\lambda} \left[A_{\boldsymbol{k}\lambda}(t) \boldsymbol{u}_{\boldsymbol{k}\lambda}(\boldsymbol{r}) + A^*_{\boldsymbol{k}\lambda}(t) \boldsymbol{u}^*_{\boldsymbol{k}\lambda}(\boldsymbol{r}) \right] \ , \tag{2.9}$$

where the temporal functions $A_{\boldsymbol{k}\lambda}(t)$ must satisfy the differential equation

$$\left(c^2k^2 + \frac{\partial^2}{\partial t^2}\right) A_{\boldsymbol{k}\lambda}(t) = 0 \,,$$

which has the obvious solution

$$A_{\boldsymbol{k}\lambda}(t) = A_{\boldsymbol{k}\lambda}\, \mathrm{e}^{-\mathrm{i}\omega_k t} \,. \tag{2.10}$$

The frequency ω_k and the wavevector $\boldsymbol{k}$ are related through $\omega_k = ck$ which is known as the dispersion relation. Due to the particular form of the spatial eigenfunctions of open space, the expansion of $\boldsymbol{A}(\boldsymbol{r}, t)$ in (2.9) happens to also represent a Fourier expansion in both space and time. The Fourier expansions of the fields follow readily from their expression (2.3) in terms of $\boldsymbol{A}$,

$$\boldsymbol{E}(\boldsymbol{r}, t) = \mathrm{i} \sum_{\boldsymbol{k}\lambda} \omega_k \big[A_{\boldsymbol{k}\lambda} \mathrm{e}^{-\mathrm{i}\omega_k t} \boldsymbol{u}_{\boldsymbol{k}\lambda}(\boldsymbol{r}) - A^*_{\boldsymbol{k}\lambda} \mathrm{e}^{\mathrm{i}\omega_k t} \boldsymbol{u}^*_{\boldsymbol{k}\lambda}(\boldsymbol{r})\big] \,, \tag{2.11a}$$

$$\boldsymbol{B}(\boldsymbol{r}, t) = \mathrm{i} \sum_{\boldsymbol{k}\lambda} \boldsymbol{k} \times \big[A_{\boldsymbol{k}\lambda} \mathrm{e}^{-\mathrm{i}\omega_k t} \boldsymbol{u}_{\boldsymbol{k}\lambda}(\boldsymbol{r}) - A^*_{\boldsymbol{k}\lambda} \mathrm{e}^{\mathrm{i}\omega_k t} \boldsymbol{u}^*_{\boldsymbol{k}\lambda}(\boldsymbol{r})\big] \,. \tag{2.11b}$$

If we consider the corresponding Fourier components of the fields $\boldsymbol{E}$ and $\boldsymbol{B}$ and substitute them into the Maxwell equations, we find that (2.1a) is satisfied identically, while (2.1b) reduces to

$$\ddot{A}_{\boldsymbol{k}\lambda} + \omega_k^2 A_{\boldsymbol{k}\lambda} = 0 \,, \tag{2.12}$$

which is basically what we have obtained from the differential equation for $\boldsymbol{A}$ and is nothing else but the differential equation for the harmonic oscillator. This also implies that $A_{\boldsymbol{k}\lambda}$ and $\dot{A}_{\boldsymbol{k}\lambda}$ are canonically conjugate variables.

Using the Fourier expansion for $\boldsymbol{A}$ in (2.9), and the orthogonality of the spatial eigenfunctions (2.8), we find that the energy of the field is given by

$$E = \varepsilon_0 V \sum_{\boldsymbol{k}\lambda} \omega_k^2 \big(A_{\boldsymbol{k}\lambda} A^*_{\boldsymbol{k}\lambda} + A^*_{\boldsymbol{k}\lambda} A_{\boldsymbol{k}\lambda}\big) = 2\varepsilon_0 V \sum_{\boldsymbol{k}\lambda} \omega_k^2 \left|A_{\boldsymbol{k}\lambda}\right|^2 \,, \tag{2.13}$$

the last step being valid only in the classical case.

We can express the Fourier components $A_{\boldsymbol{k}\lambda}$ of the vector potential as $A_{\boldsymbol{k}\lambda} = \sqrt{\frac{\hbar}{2\varepsilon_0 V \omega_k}}\, \alpha_{\boldsymbol{k}\lambda}$, which upon substitution into (2.13) yields

$$E = \frac{1}{2} \sum_{\boldsymbol{k}\lambda} \hbar\omega_k \big(\alpha_{\boldsymbol{k}\lambda} \alpha^*_{\boldsymbol{k}\lambda} + \alpha^*_{\boldsymbol{k}\lambda} \alpha_{\boldsymbol{k}\lambda}\big) \,. \tag{2.14}$$

If we now introduce the new real variables $q_{\boldsymbol{k}\lambda}$ and $p_{\boldsymbol{k}\lambda}$ defined by

$$q_{\boldsymbol{k}\lambda} \equiv \sqrt{\frac{\hbar}{2\omega_k}}\, (\alpha_{\boldsymbol{k}\lambda} + \alpha^*_{\boldsymbol{k}\lambda}) \,, \quad p_{\boldsymbol{k}\lambda} \equiv -\mathrm{i}\sqrt{\frac{\hbar\omega_k}{2}}\, (\alpha_{\boldsymbol{k}\lambda} - \alpha^*_{\boldsymbol{k}\lambda}) \,,$$

the expression for the energy becomes

$$E = \frac{1}{2} \sum_{\boldsymbol{k}\lambda} \big(p^2_{\boldsymbol{k}\lambda} + \omega_k^2 q^2_{\boldsymbol{k}\lambda}\big) \,, \tag{2.15}$$

which explicitly shows that it is the sum of the energies of an infinite set of independent harmonic oscillators with $q_{\boldsymbol{k}\lambda}$ and $p_{\boldsymbol{k}\lambda}$ playing the role of position and its conjugate momentum, respectively.

2.1.1 Field Quantization in Open Space

The route to the quantum description is now evident. As in Sect. 1.2.2, we replace the position $q_{\boldsymbol{k}\lambda}$ and its conjugate momentum $p_{\boldsymbol{k}\lambda}$ variables by the Hermitian operators $\mathcal{Q}_{\boldsymbol{k}\lambda}$ and $\mathcal{P}_{\boldsymbol{k}\lambda}$ obeying the commutation relations

$$[\mathcal{Q}_{\boldsymbol{k}\lambda}, \mathcal{P}_{\boldsymbol{k}'\lambda'}] = \mathrm{i}\hbar\delta_{\boldsymbol{k}\boldsymbol{k}'}\delta_{\lambda\lambda'} \ , \quad [\mathcal{Q}_{\boldsymbol{k}\lambda}, \mathcal{Q}_{\boldsymbol{k}'\lambda'}] = [\mathcal{P}_{\boldsymbol{k}\lambda}, \mathcal{P}_{\boldsymbol{k}'\lambda'}] = 0 \ . \tag{2.16}$$

We define further the annihilation and creation operators

$$a_{\boldsymbol{k}\lambda} = \frac{1}{\sqrt{2\hbar\omega_k}} \left(\omega_k \mathcal{Q}_{\boldsymbol{k}\lambda} + \mathrm{i}\mathcal{P}_{\boldsymbol{k}\lambda}\right) \ , \quad a^\dagger_{\boldsymbol{k}\lambda} = \frac{1}{\sqrt{2\hbar\omega_k}} \left(\omega_k \mathcal{Q}_{\boldsymbol{k}\lambda} - \mathrm{i}\mathcal{P}_{\boldsymbol{k}\lambda}\right) \ , \tag{2.17}$$

which obey the bosonic commutation relations

$$[a_{\boldsymbol{k}\lambda}, a^\dagger_{\boldsymbol{k}'\lambda'}] = \delta_{\boldsymbol{k}\boldsymbol{k}'}\delta_{\lambda\lambda'} \ , \quad [a_{\boldsymbol{k}\lambda}, a_{\boldsymbol{k}'\lambda'}] = [a^\dagger_{\boldsymbol{k}\lambda}, a^\dagger_{\boldsymbol{k}'\lambda'}] = 0 \ , \tag{2.18}$$

as well as the Hermitian *number operators* $\mathcal{N}_{\boldsymbol{k}\lambda} \equiv a^\dagger_{\boldsymbol{k}\lambda} a_{\boldsymbol{k}\lambda}$ which have the following commutation properties

$$[a_{\boldsymbol{k}\lambda}, \mathcal{N}_{\boldsymbol{k}'\lambda'}] = \delta_{\boldsymbol{k}\boldsymbol{k}'}\delta_{\lambda\lambda'} a_{\boldsymbol{k}\lambda} \ , \quad [a^\dagger_{\boldsymbol{k}\lambda}, \mathcal{N}_{\boldsymbol{k}'\lambda'}] = -\delta_{\boldsymbol{k}\boldsymbol{k}'}\delta_{\lambda\lambda'} a^\dagger_{\boldsymbol{k}\lambda} \ . \tag{2.19}$$

The operators $a_{\boldsymbol{k}\lambda}$ and $a^\dagger_{\boldsymbol{k}\lambda}$ clearly are those defined in Sect. 1.2.3 for the harmonic oscillator. They have the same mathematical properties but different physical content, as they now represent dynamical variables of the electromagnetic field instead of those of a particle bound to a quadratic potential.

The Hamiltonian of the quantized electromagnetic field written in terms of the creation and annihilation operators is

$$\mathcal{H} = \frac{1}{2} \sum_{\boldsymbol{k}\lambda} \hbar\omega_k \left(a^\dagger_{\boldsymbol{k}\lambda} a_{\boldsymbol{k}\lambda} + a_{\boldsymbol{k}\lambda} a^\dagger_{\boldsymbol{k}\lambda}\right) = \sum_{\boldsymbol{k}\lambda} \hbar\omega_k \left(a^\dagger_{\boldsymbol{k}\lambda} a_{\boldsymbol{k}\lambda} + \tfrac{1}{2}\right) \ , \tag{2.20}$$

which is seen to contain an infinity, since $\sum_{\boldsymbol{k}\lambda} \frac{1}{2}\hbar\omega_k = \infty$. This has to do with the fact that the lowest energy of the quantized harmonic oscillator is not zero but is equal to the energy of one half quantum. Since the Hamiltonian of the electromagnetic field consists of infinitely many oscillators, the infinity noted above is simply the sum of the zero point energies of all the oscillators of the field. As long as the processes in which this Hamiltonian enters describe the exchange of energy between the field and some other system, it is only energy differences that matter, in which case the zero point energy can be omitted from the Hamiltonian. Thus we will most of the time write $\mathcal{H}$ as

$$\mathcal{H} = \sum_{\boldsymbol{k}\lambda} \hbar\omega_k a^\dagger_{\boldsymbol{k}\lambda} a_{\boldsymbol{k}\lambda} \ . \tag{2.21}$$

The vector potential and the electric and magnetic fields are now operators which can be expressed in terms of $a_{\boldsymbol{k}\lambda}$ and $a^\dagger_{\boldsymbol{k}\lambda}$ as

$$\boldsymbol{A}(\boldsymbol{r},t) = \sum_{\boldsymbol{k}\lambda} \hat{\boldsymbol{e}}_{\boldsymbol{k}\lambda} \sqrt{\frac{\hbar}{2\varepsilon_0 V \omega_k}} \left[a_{\boldsymbol{k}\lambda} \mathrm{e}^{\mathrm{i}(\boldsymbol{k}\cdot\boldsymbol{r}-\omega_k t)} + a^\dagger_{\boldsymbol{k}\lambda} \mathrm{e}^{-\mathrm{i}(\boldsymbol{k}\cdot\boldsymbol{r}-\omega_k t)} \right] , \tag{2.22a}$$

$$\boldsymbol{E}(\boldsymbol{r},t) = \mathrm{i} \sum_{\boldsymbol{k}\lambda} \hat{\boldsymbol{e}}_{\boldsymbol{k}\lambda} \sqrt{\frac{\hbar\omega_k}{2\varepsilon_0 V}} \left[a_{\boldsymbol{k}\lambda} \mathrm{e}^{\mathrm{i}(\boldsymbol{k}\cdot\boldsymbol{r}-\omega_k t)} - a^\dagger_{\boldsymbol{k}\lambda} \mathrm{e}^{-\mathrm{i}(\boldsymbol{k}\cdot\boldsymbol{r}-\omega_k t)} \right] , \tag{2.22b}$$

$$\boldsymbol{B}(\boldsymbol{r},t) = \mathrm{i} \sum_{\boldsymbol{k}\lambda} \frac{\hat{\boldsymbol{k}} \times \hat{\boldsymbol{e}}_{\boldsymbol{k}\lambda}}{c} \sqrt{\frac{\hbar\omega_k}{2\varepsilon_0 V}} \left[a_{\boldsymbol{k}\lambda} \mathrm{e}^{\mathrm{i}(\boldsymbol{k}\cdot\boldsymbol{r}-\omega_k t)} - a^\dagger_{\boldsymbol{k}\lambda} \mathrm{e}^{-\mathrm{i}(\boldsymbol{k}\cdot\boldsymbol{r}-\omega_k t)} \right] , \tag{2.22c}$$

where $\hat{\boldsymbol{k}} = \boldsymbol{k}/k$ is the unit vector along the $\boldsymbol{k}$. Sometimes it proves convenient to separate the electric field operator $\boldsymbol{E}(\boldsymbol{r},t)$ into the positive and negative frequency parts,

$$\boldsymbol{E}(\boldsymbol{r},t) = \boldsymbol{E}^{(+)}(\boldsymbol{r},t) + \boldsymbol{E}^{(-)}(\boldsymbol{r},t) , \tag{2.23}$$

where $\boldsymbol{E}^{(+)}(\boldsymbol{r},t)$ contains the sum of annihilation operators $a_{\boldsymbol{k}\lambda}$ oscillating as $\mathrm{e}^{-\mathrm{i}\omega_k t}$, while $\boldsymbol{E}^{(+)}(\boldsymbol{r},t)$ is given by the sum of creation operators $a^\dagger_{\boldsymbol{k}\lambda}$ oscillating as $\mathrm{e}^{\mathrm{i}\omega_k t}$. Obviously $\boldsymbol{E}^{(+)}(\boldsymbol{r},t) = \left(\boldsymbol{E}^{(-)}(\boldsymbol{r},t)\right)^\dagger$.

The electromagnetic field quantized within a box consists of a denumerable, infinite set of harmonic oscillators. One obvious basis for this quantum system can be constructed by combining the eigenstates of the Hamiltonians of all the oscillators. In an obvious generalization of the notation established in Sect. 1.2.3, we denote by $|n_{\boldsymbol{k}\lambda}\rangle$ the eigenstates of the $\boldsymbol{k}\lambda$ oscillator. Thus a general state of the electromagnetic field can be expressed through the eigenstates of its Hamiltonian (2.20) having the form

$$|n_{\boldsymbol{k}_1\lambda_1}\rangle \otimes |n_{\boldsymbol{k}_2\lambda_2}\rangle \otimes \ldots \otimes |n_{\boldsymbol{k}_l\lambda_l}\rangle \ldots = \bigotimes_{\boldsymbol{k}\lambda} |n_{\boldsymbol{k}\lambda}\rangle , \tag{2.24}$$

also referred to as a tensor product of the infinitely many eigenvectors. It specifies the number of quanta (called in this case photons) in each of the oscillators (called also modes of the field). Clearly each $n_{\boldsymbol{k}\lambda}$ can assume non negative integer values. Somewhat abbreviated forms for the notation of these states are $|n_{\boldsymbol{k}_1\lambda_1}, n_{\boldsymbol{k}_2\lambda_2}, \ldots, n_{\boldsymbol{k}_l\lambda_l}, \ldots\rangle$ or even $|\{n_{\boldsymbol{k}\lambda}\}\rangle$. The total energy for the field in such a state is given by

$$\langle\{n_{\boldsymbol{k}\lambda}\}|\,\mathcal{H}\,|\{n_{\boldsymbol{k}\lambda}\}\rangle = \sum_{\boldsymbol{k}\lambda} \hbar\omega_k n_{\boldsymbol{k}\lambda} , \tag{2.25}$$

where it should be kept in mind that for each $\boldsymbol{k}$, we have two terms corresponding to $\lambda = 1, 2$. The expectation value of the operator $\mathcal{N} \equiv \sum_{\boldsymbol{k}\lambda} \mathcal{N}_{\boldsymbol{k}\lambda}$ gives the total number of photons in all of the field modes,

$$\langle\mathcal{N}\rangle = \sum_{\boldsymbol{k}\lambda} \langle\mathcal{N}_{\boldsymbol{k}\lambda}\rangle = \sum_{\boldsymbol{k}\lambda} n_{\boldsymbol{k}\lambda} . \tag{2.26}$$

This completes the transition to the quantum description of the electromagnetic field, often also called radiation field. Having established that it is

equivalent to a collection of infinitely many harmonic oscillators, the formalism developed in Sect. 1.2.3 is directly transferable to this system. For convenience in referencing later on, we collect here the most important relations for the creation and annihilation operators,

$$a^\dagger_{\boldsymbol{k}\lambda}\,|n_{\boldsymbol{k}\lambda}\rangle = \sqrt{n_{\boldsymbol{k}\lambda}+1}\,|n_{\boldsymbol{k}\lambda}+1\rangle\;, \tag{2.27a}$$

$$a_{\boldsymbol{k}\lambda}\,|n_{\boldsymbol{k}\lambda}\rangle = \sqrt{n_{\boldsymbol{k}\lambda}}\,|n_{\boldsymbol{k}\lambda}-1\rangle\;,\quad a_{\boldsymbol{k}\lambda}\,|0\rangle = 0\;, \tag{2.27b}$$

$$\mathcal{N}_{\boldsymbol{k}\lambda}\,|n_{\boldsymbol{k}\lambda}\rangle \equiv a^\dagger_{\boldsymbol{k}\lambda}a_{\boldsymbol{k}\lambda}\,|n_{\boldsymbol{k}\lambda}\rangle = n_{\boldsymbol{k}\lambda}\,|n_{\boldsymbol{k}\lambda}\rangle\;, \tag{2.27c}$$

where $|0\rangle$ is the ground or vacuum (zero photon) state, from which the n-photon state of the field mode $\boldsymbol{k}\lambda$ is obtained by successive application of the creation operator,

$$|n_{\boldsymbol{k}\lambda}\rangle = \frac{(a^\dagger_{\boldsymbol{k}\lambda})^{n_{\boldsymbol{k}\lambda}}}{\sqrt{n_{\boldsymbol{k}\lambda}!}}\,|0\rangle\;. \tag{2.28}$$

As long as we are dealing with the electromagnetic field quantized within a box, the eigenstates $|n_{\boldsymbol{k}\lambda}\rangle$ for various modes are normalizable, as the spatial eigenfunctions of the corresponding modes are square-integrable (L^2-integrable), so that we have a legitimate Hilbert space. Of course the physical open field does not have any boundaries, which means that its spectrum is not discrete. To account for this, we need to let the dimension L of the quantization box go to infinity, which is one and the simplest way to accommodate the continuum in our mathematical framework here.[1] Recalling the boundary conditions for the wave vector $\boldsymbol{k}$, $k_{x,y,z} = 2\pi n_{x,y,z}/L$, the summation over the field modes $\sum_{\boldsymbol{k}\lambda}$ can then be replaced by integration according to

$$\sum_{\boldsymbol{k}\lambda} \to \left(\frac{L}{2\pi}\right)^3 \int \mathrm{d}^3k\;, \tag{2.29}$$

where $\mathrm{d}^3k = \mathrm{d}k_x\,\mathrm{d}k_y\,\mathrm{d}k_z$ is the volume element in the $\boldsymbol{k}$ space. In spherical coordinates, this is given by $\mathrm{d}^3k = (\omega_k^2/c^3)\mathrm{d}\omega_k\,\sin\theta\mathrm{d}\theta\,\mathrm{d}\phi$. We can then calculate the total number of modes $\mathrm{d}N$ in volume $V = L^3$ in the frequency interval between ω_k and $\omega_k + \mathrm{d}\omega_k$ as

$$\mathrm{d}N = 2\left(\frac{L}{2\pi}\right)^3 \frac{\omega_k^2}{c^3}\,\mathrm{d}\omega_k \int_0^\pi \sin\theta\mathrm{d}\theta \int_0^{2\pi} \mathrm{d}\phi = \frac{L^3\omega_k^2}{\pi^2c^3}\,\mathrm{d}\omega_k \equiv \varrho(\omega_k)\,\mathrm{d}\omega_k\;, \tag{2.30}$$

where the factor 2 accounts for the two possible polarizations of each $\boldsymbol{k}$ mode. The function $\varrho(\omega_k)$ is known as the density of modes. In Sects. 3.5.2 and 4.1.2, where we derive the atomic spontaneous decay in free space, we will use the replacement (2.29) at the appropriate stage of calculations.

[1] Strictly speaking, the continuum wavefunctions in this case are not normalizable, at least not in the sense of the inner product being a c-number, which is not necessarily compatible with a Hilbert space. In a generalization of the notion, they are said to be delta-function, or even simply delta, normalized. The procedure outlined above is a straightforward, yet mathematically justifiable, way of approaching the limit to the continuum through a legitimate Hilbert space.

2.1.2 Field Quantization in a Cavity

It is now straightforward to show how the above formalism is adapted to the quantization of the electromagnetic field confined within a finite volume. The typical, somewhat idealized, case of interest here is that of an enclosure—cavity—with perfectly reflecting walls. The boundary condition appropriate to that physical situation is to require that the electric field vanish on the walls. Again, the solution of the spatial part of Maxwell's equations under this condition leads to a set of infinitely many eigensolutions with a discrete spectrum. Since the space of integration is now finite, these eigenfunctions are obviously normalizable. Their analytic expressions, if such are feasible, depend on the geometry of the cavity. We can therefore assume that the form of the expressions for the expansion of $\boldsymbol{A}$, $\boldsymbol{E}$ and $\boldsymbol{B}$ in terms of the spatial eigenfunctions is still valid, except for their particular form in each case. The respective operators $a_{\boldsymbol{k}\lambda}$ and $a^\dagger_{\boldsymbol{k}\lambda}$ now refer to the photons in that particular mode of the cavity. Since the field is confined within the cavity, we expect that we will now have standing instead of running waves.

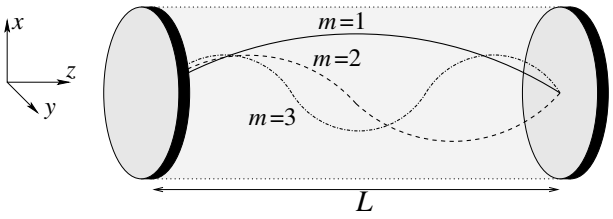

Fig. 2.2. One-dimensional optical cavity of length L.

As a simple example, which in fact is often quite relevant to problems in quantum optics, we consider the case of a quasi one-dimensional (1D) cavity. The quasi refers to the fact that, although the structure in reality is three-dimensional (3D), it is only modes with photons propagating in one direction that are of interest. As sketched in Fig. 2.2, such a cavity could be thought of as a tube with transparent walls, except for the two ends whose inside is perfectly reflecting. The expressions for the fields now simplify to $\boldsymbol{E}(\boldsymbol{r},t) \to \hat{\boldsymbol{e}}E(z,t) = \hat{x}E(z,t)$, and $\boldsymbol{B}(\boldsymbol{r},t) \to \hat{\boldsymbol{k}} \times \hat{\boldsymbol{e}}\, B(z,t) = \hat{y}B(z,t)$, where we have assumed that the electric field is propagating along the z axis and polarized along the x, as required in the transverse gauge. Imposing the boundary conditions $E(z=0,t) = E(z=L,t) = 0$, vanishing of the electric field at the two end walls at all times, we easily find that the spatial eigensolutions must be of the form $\sin(k_m z)$, where $k_m = \pi m/L$, $m = 1,2,3,\ldots$, with the respective wavelengths $\lambda_m = 2L/m$ and frequencies $\omega_m = k_m c$. The quantized fields in the k_m mode can now be written as

$$E_m(z,t) = \sqrt{\frac{\hbar\omega_m}{\varepsilon_0 V}}\left[a_m(t) + a_m^\dagger(t)\right]\sin(k_m z)\,, \tag{2.31a}$$

$$B_m(z,t) = -\frac{\mathrm{i}}{c}\sqrt{\frac{\hbar\omega_m}{\varepsilon_0 V}}\left[a_m(t) - a_m^\dagger(t)\right]\cos(k_m z)\,, \tag{2.31b}$$

with the creation and annihilation operators $a_m^\dagger(t) \equiv a_m^\dagger \mathrm{e}^{\mathrm{i}\omega_m t}$ and $a_m(t) \equiv a_m \mathrm{e}^{-\mathrm{i}\omega_m t}$ referring to the particular mode under consideration. The reduction of the problem to one dimension is most meaningful and useful in situations where we are interested in the interaction of the field inside the cavity with an atom chosen so that only one of the cavity modes is effective in coupling to the atom, reducing thus the physical problem to a two-level atom coupled to a field of a single frequency. It should be noted here that in the coefficients appearing in (2.31), the volume V pertaining to the particular mode of the cavity appears in the denominator. Therefore the smaller V is, the stronger the field is, for a given expectation value of the amplitude operators a_m and $a_m^\dagger$. When we study the interaction of a bound electron with a quantized field in Sect. 3.3.2, this will be shown to be intimately connected to the strength with which the atom undergoes Rabi oscillations in a cavity.

2.2 Quantum States of the Field

Above we have already encountered the number states of the electromagnetic field, which are the eigenstates of the field Hamiltonian. Of course the possible states of the field are not restricted to the number states, other most commonly considered pure states being the coherent and squeezed states. Here we discuss in some detail the properties of such pure states as as well as the chaotic field produced by a thermal source.

2.2.1 Single-Mode Cavity Field

Consider the electromagnetic field in one mode of frequency ω in a 1D cavity and assume that the field contains precisely n photons, i.e., it is in the number state $|n\rangle$. Using (2.31a), we have

$$\langle n|\, E(z,t)\,|n\rangle = \epsilon_\omega \langle n|\, a(t) + a^\dagger(t)\,|n\rangle \sin(kz)\,, \tag{2.32}$$

where we have introduced $\epsilon_\omega \equiv \sqrt{\hbar\omega/\varepsilon_0 V}$. Since $\langle n|\, a\,|n\rangle = \sqrt{n}\,\langle n|n-1\rangle = 0$ and $\langle n|\, a^\dagger\,|n\rangle = \sqrt{n+1}\,\langle n|n+1\rangle = 0$, we find that the expectation value of the electric field, or the magnetic field for that matter, is zero when the electromagnetic field is in a pure number state (sometimes also referred to as Fock state), which is an eigenstate of the energy. That is true, no matter how large n is. This is worth noting here, because occasionally it is said that when the electromagnetic field contains large numbers of photons, its state approaches the classical one. Obviously, this can not be true if the field is in a

number state, because a classical field has a non-zero value of the electric field, unless its energy is zero. As we have already seen for the harmonic oscillator, it is the coherent state that provides the "best" quantum approximation to a classical state, which is also true for the electromagnetic field, as will be discussed shortly.

Continuing with the number state, we consider now the so-called root mean square deviation or the uncertainty of the electric field. Recall that for any operator $\mathcal{A}$, the uncertainty $\Delta\mathcal{A}$ is defined as the square-root of the variance $\langle\mathcal{A}^2\rangle - \langle\mathcal{A}\rangle^2 \equiv (\Delta\mathcal{A})^2$. For the electric field in this specific case, we have $\langle n|\, E(z,t)\,|n\rangle = 0$ and

$$\begin{aligned}\langle n|\, E^2(z,t)\,|n\rangle &= \epsilon_\omega^2 \sin^2(kz)\langle n|\, a^\dagger a^\dagger \mathrm{e}^{\mathrm{i}2\omega t} + aa^\dagger + a^\dagger a + aa\mathrm{e}^{-\mathrm{i}2\omega t}\,|n\rangle \\ &= \epsilon_\omega^2 \sin^2(kz)\langle n|\, 2a^\dagger a + 1\,|n\rangle \\ &= 2\epsilon_\omega^2 \sin^2(kz)(n+\tfrac{1}{2})\ ,\end{aligned}$$

from which

$$\Delta E = \sqrt{2}\epsilon_\omega |\sin(kz)| \sqrt{n+\tfrac{1}{2}}\ . \tag{2.33}$$

As expected, the uncertainty is non-zero, proportional to the square-root of the number of photons in the field and it also depends on the position in the cavity, determined by the spatial distribution of the field strength in the mode under consideration. The most counterintuitive aspect of this result, however, is the non-zero uncertainty in the electric field even for $n = 0$ which is the vacuum state $|0\rangle$. Indeed, for $n = 0$ the uncertainty is $\epsilon_\omega |\sin(kz)|$. This points to the physical meaning of the coefficient ϵ_ω defined above, namely an effective field at frequency ω due to quantum mechanical fluctuations of the vacuum, which despite its misleading name appears to be "full of life". A non-zero value of the uncertainty implies that the quantized electric field exhibits fluctuations even when no photons are present. As a result of such fluctuations, random values of the field appear and disappear. Although not directly observable, these random fields have indirect effects on charged particles, such as electrons, and the quantum states of systems to which they may be bound, such as atoms. Specifically, these fluctuations are responsible for the spontaneous decay and the energy shift of excited atomic state, discussed in Sects. 3.5.2 and 4.1.2.

Each photon that is added to the field contributes an additional $\sqrt{2}\epsilon_\omega$ to the uncertainty. And the fact that ϵ_ω is inversely proportional to the square-root of the cavity volume V implies that the smaller the cavity is, the stronger this effective field is. A numerical example is quite illuminating. Assuming a cavity of linear dimension $100\,\mu\mathrm{m} = 0.1\,\mathrm{mm}$ and optical radiation of wavelength about $0.5\,\mu\mathrm{m} = 500\,\mathrm{nm}$, we obtain $\epsilon_\omega \simeq 1\,\mathrm{V\,cm^{-2}}$, which is of the same order as the field strengths of a laser with intensity $1\,\mathrm{mW\,cm^{-2}}$. Such a laser could cause damage to the retina of the eye if looked at straight on! We also see now, why it can be said that the electromagnetic field in state $|n\rangle$ has an effective amplitude of the electric field proportional to $\sqrt{n}$, but its phase being random between 0 and 2π makes the average (expectation) value zero; a useful picture for the state $|n\rangle$, up to a point.

In complete analogy with the harmonic oscillator, we can define coherent states as the eigenstates of the annihilation operator, $a\,|\alpha\rangle = \alpha\,|\alpha\rangle$ and $\langle\alpha|\,a^\dagger = \alpha^*\langle\alpha|$ with $\alpha = |\alpha|\mathrm{e}^{\mathrm{i}\varphi}$ being any complex number. Again, formally, the coherent state $|\alpha\rangle = \mathcal{D}(\alpha)\,|0\rangle$ results from applying the displacement operator $\mathcal{D}(\alpha)$ to the vacuum state $|0\rangle$. Note that using the Baker–Hausdorff operator relation (1.26) and the commutation relation $[a, a^\dagger] = 1$, the displacement operator can be written in three equivalent forms

$$\mathcal{D}(\alpha) = \mathrm{e}^{\alpha a^\dagger - \alpha^* a} = \mathrm{e}^{-\frac{1}{2}|\alpha|^2}\mathrm{e}^{\alpha a^\dagger}\mathrm{e}^{-\alpha^* a} = \mathrm{e}^{\frac{1}{2}|\alpha|^2}\mathrm{e}^{-\alpha^* a}\mathrm{e}^{\alpha a^\dagger}\ , \tag{2.34}$$

in which the creation $a^\dagger$ and annihilation a operators appear, respectively, in what is called symmetric, normal and antinormal order. We can expand the coherent state $|\alpha\rangle$ in terms of the number states $|n\rangle$ of the field as

$$|\alpha\rangle = \mathrm{e}^{-\frac{1}{2}|\alpha|^2}\sum_{n=0}^{\infty}\frac{\alpha^n}{\sqrt{n!}}\,|n\rangle\ . \tag{2.35}$$

The probability to find n photons in the field is thus

$$P_\alpha(n) = \langle\alpha|\,\Pi_n\,|\alpha\rangle = \mathrm{e}^{-|\alpha|^2}\frac{|\alpha|^{2n}}{n!}\ ,\quad \Pi_n \equiv |n\rangle\langle n|\ , \tag{2.36}$$

which is shown in Fig. 2.3(a). This is the Poisson distribution with the average photon number $\bar{n} = \sum nP_\alpha(n) = |\alpha|^2$. The corresponding root mean square deviation (uncertainty) of the number of photons in the field is

$$\Delta\mathcal{N} = \sqrt{\langle\alpha|\,a^\dagger a a^\dagger a\,|\alpha\rangle - \langle\alpha|\,a^\dagger a\,|\alpha\rangle^2} = \sqrt{\bar{n}} = |\alpha|\ . \tag{2.37}$$

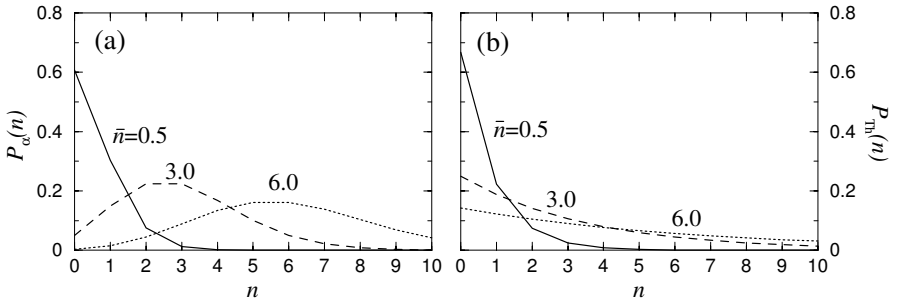

Fig. 2.3. Photon probability distributions for (a) coherent, and (b) chaotic (thermal) electromagnetic fields.

We have seen above that the expectation value of the electric field in the number state is zero. The situation is entirely different for the coherent state $|\alpha\rangle$, for which we have

$$\langle\alpha|\, E(z,t)\,|\alpha\rangle = \epsilon_\omega \langle\alpha|\, a(t) + a^\dagger(t)\,|\alpha\rangle \sin(kz) = \epsilon_\omega \big(2|\alpha|\cos(\omega t - \varphi)\big)\sin(kz)\ . \tag{2.38}$$

Let us calculate the uncertainty for the field in the coherent state. With

$$\langle\alpha|\, E^2(z,t)\,|\alpha\rangle = \epsilon_\omega^2 \big[\big(2|\alpha|\cos(\omega t - \varphi)\big)^2 + 1\big]\sin^2(kz)\ , \tag{2.39}$$

we obtain

$$\Delta E = \sqrt{\langle E^2\rangle - \langle E\rangle^2} = \epsilon_\omega |\sin(kz)|\ , \tag{2.40}$$

which does not depend on α. Thus the electric field operator E is analogous to the position operator $\mathcal{Q}$ of the harmonic oscillator, while the magnetic field operator B of (2.31b) corresponds to the momentum operator $\mathcal{P}$. Exploring this analogy even further, we can define the squeezed state of the electromagnetic field $|\alpha,\zeta\rangle = \mathcal{S}(\zeta)\,|\alpha\rangle$ generated by the squeezing operator $\mathcal{S}(\zeta) \equiv \exp\big(\frac{1}{2}\zeta^* a^2 - \frac{1}{2}\zeta a^{\dagger 2}\big)$ possessing all the properties discussed in Sect. 1.2.4. In particular, when $\zeta = r$ is purely real, the uncertainties of electric and magnetic fields are

$$\Delta E = \epsilon_\omega |\sin(kz)|\, \mathrm{e}^{-r}\ , \quad \Delta B = \epsilon_\omega/c\, |\cos(kz)|\, \mathrm{e}^{r}\ , \tag{2.41}$$

which is the optical equivalent of (1.116).

Finally, thermal light sources produce a chaotic (or thermal) field. Often referred to as the black body radiation, it was studied by Max Planck at the turn of the twentieth century, which initiated the birth of quantum theory. The history of this discovery and detailed derivation of the Planck's law can be found in most books on quantum mechanics. By definition, the chaotic field is in thermal equilibrium with the surrounding environment at finite temperature T. Its state is, therefore, characterized by the density operator

$$\rho = \frac{\exp(-\mathcal{H}/k_\mathrm{B}T)}{\mathrm{Tr}\big[\exp(-\mathcal{H}/k_\mathrm{B}T)\big]}\ , \tag{2.42}$$

where k_B is Boltzmann's constant. A single or few modes of such field can be filtered out of the Planck distribution, or in the case of a cavity, its walls and the surrounding environment radiate thermal photons into the discrete modes of the cavity. Then, with the density operator for a mode of frequency ω,

$$\rho = \frac{\mathrm{e}^{-\hbar\omega a^\dagger a/k_\mathrm{B}T}}{\mathrm{Tr}\big(\mathrm{e}^{-\hbar\omega a^\dagger a/k_\mathrm{B}T}\big)}\ , \tag{2.43}$$

the probability to find n photons is

$$P_\mathrm{Th}(n) = \mathrm{Tr}(\rho\Pi_n) = \frac{\mathrm{e}^{-\hbar\omega n/k_\mathrm{B}T}}{\sum_n \mathrm{e}^{-\hbar\omega n/k_\mathrm{B}T}} = \mathrm{e}^{-\hbar\omega n/k_\mathrm{B}T}\big(1 - \mathrm{e}^{-\hbar\omega/k_\mathrm{B}T}\big)\ , \tag{2.44}$$

and the mean number of photons is

$$\bar{n} = \sum_n n P_\mathrm{Th}(n) = \frac{1}{\mathrm{e}^{\hbar\omega/k_\mathrm{B}T} - 1}\ . \tag{2.45}$$

In terms of $\bar{n}$, the probability distribution for the chaotic field can then be cast as

$$P_{\rm Th}(n) = \frac{1}{1+\bar{n}} \left(\frac{\bar{n}}{1+\bar{n}} \right)^n = \frac{\bar{n}^n}{(1+\bar{n})^{n+1}} \,, \tag{2.46}$$

and is shown in Fig. 2.3(b). The root mean square deviation of the photon number is given by

$$\Delta\mathcal{N} = \sqrt{\langle \mathcal{N}^2 \rangle - \langle \mathcal{N} \rangle^2} = \sqrt{\bar{n}^2 + \bar{n}} \,, \tag{2.47}$$

which in the limit of $\bar{n} \gg 1$ yields $\Delta\mathcal{N} \simeq \bar{n}$, clearly much different from that of a coherent state given by (2.37).

2.2.2 Free Electromagnetic Field

We have considered above the quantum states of a single standing-wave mode of the electromagnetic field in a cavity. These considerations apply equally to individual modes of the free electromagnetic field quantized within a box, the only difference being that ϵ_ω should be taken as $\epsilon_\omega \equiv \sqrt{\hbar\omega/2\varepsilon_0 V}$, while $\sin(kz)$ (and $\cos(kz)$) should be dropped all together since these are running-wave modes. In a complete description, however, we should specify the states of all the relevant modes of the field. Since the spatial eigenfunctions $\boldsymbol{u}_{\boldsymbol{k}\lambda}(\boldsymbol{r})$ for different modes are mutually orthogonal (2.8), the total state of the field $|\Psi_{\rm total}\rangle$ is simply a tensor product of the states of individual modes $|\Psi_{\boldsymbol{k}\lambda}\rangle$,

$$|\Psi_{\rm total}\rangle = \bigotimes_{\boldsymbol{k}\lambda} |\Psi_{\boldsymbol{k}\lambda}\rangle \,. \tag{2.48}$$

In particular, we have seen above that the multimode number state (2.24) is an eigenstate of Hamiltonian (2.20) with eigenvalue given by (2.25). As we have noted there, any pure state of the field can be represented as a superposition of the number states. The simplest example of such a superposition is the single-photon state $|1\rangle$ given by

$$|1\rangle \equiv \sum_{\boldsymbol{k}\lambda} \xi_{\boldsymbol{k}\lambda} \, |1_{\boldsymbol{k}\lambda}\rangle \,, \quad |1_{\boldsymbol{k}\lambda}\rangle \equiv a^\dagger_{\boldsymbol{k}\lambda} \, |0\rangle \,, \tag{2.49}$$

with the normalization condition $\sum_{\boldsymbol{k}\lambda} |\xi_{\boldsymbol{k}\lambda}|^2 = 1$. Recall that the positive frequency part $\boldsymbol{E}^{(+)}(\boldsymbol{r},t)$ of the electric field operator contains the sum of annihilation operators of all the field modes. With $\epsilon_k \equiv \sqrt{\hbar\omega_k/2\varepsilon_0 V}$ denoting the vacuum field at frequency ω_k, we then have

$$\langle 0| \, \boldsymbol{E}^{(+)}(\boldsymbol{r},t) \, |1\rangle = \mathrm{i} \sum_{\boldsymbol{k}\lambda} \hat{\boldsymbol{e}}_{\boldsymbol{k}\lambda} \epsilon_k \, \xi_{\boldsymbol{k}\lambda} \, \mathrm{e}^{\mathrm{i}(\boldsymbol{k}\cdot\boldsymbol{r} - \omega_k t)} = \boldsymbol{F}(\boldsymbol{r},t) \,, \tag{2.50}$$

where $\boldsymbol{F}(\boldsymbol{r},t)$ is the spatio-temporal envelope of the single-photon wavepacket. Assume that only modes having a common polarization direction $\hat{\boldsymbol{e}}$ and frequencies lying within a narrow band around some frequency ω are significantly

populated. For example, the radiation emitted by a suitably excited atom has a bandwidth several orders of magnitude smaller than the frequency of the atomic transition. In another example studied in Sect. 5.3, the carrier frequency and the bandwidth of a single-photon pulse emitted from the cavity are determined by the mode frequency and its decay rate (or width), the latter being typically orders of magnitude smaller than the former. We can then write

$$F(\boldsymbol{r},t) = \mathrm{i}\epsilon_\omega \sum_{\boldsymbol{k}} \xi_{\boldsymbol{k}}(t)\, \mathrm{e}^{\mathrm{i}\boldsymbol{k}\cdot\boldsymbol{r}} \equiv \mathrm{i}\epsilon_\omega\, f(\boldsymbol{r},t)\ , \tag{2.51}$$

which shows that the amplitudes $\xi_{\boldsymbol{k}}(t)$ play the role of the Fourier coefficients in the mode expansion of the normalized envelope function $f(\boldsymbol{r},t)$. Clearly, the normalized spatio-temporal intensity distribution of the single-photon pulse is $R(\boldsymbol{r},t) = |f(\boldsymbol{r},t)|^2$. Conversely, the knowledge of $f(\boldsymbol{r},t)$ (or $F(\boldsymbol{r},t)$) at time t allows one to calculate the amplitudes $\xi_{\boldsymbol{k}}(t)$ of state (2.49) via the inverse Fourier transform

$$\xi_{\boldsymbol{k}}(t) = \frac{1}{V}\int f(\boldsymbol{r},t)\, \mathrm{e}^{-\mathrm{i}\boldsymbol{k}\cdot\boldsymbol{r}}\, \mathrm{d}^3 r\ . \tag{2.52}$$

Another instructive example is the multimode coherent state $|\boldsymbol{\alpha}\rangle$, which is a tensor product of single-mode coherent states,

$$|\boldsymbol{\alpha}\rangle = \bigotimes_{\boldsymbol{k}\lambda} |\alpha_{\boldsymbol{k}\lambda}\rangle\, . \tag{2.53}$$

It is the eigenstate of the operator $\boldsymbol{E}^{(+)}(\boldsymbol{r},t)$,

$$\boldsymbol{E}^{(+)}(\boldsymbol{r},t)\, |\boldsymbol{\alpha}\rangle = \boldsymbol{\mathcal{E}}(\boldsymbol{r},t)\, |\boldsymbol{\alpha}\rangle\ , \tag{2.54}$$

with the eigenvalue function $\boldsymbol{\mathcal{E}}(\boldsymbol{r},t)$ given by

$$\boldsymbol{\mathcal{E}}(\boldsymbol{r},t) = \mathrm{i}\sum_{\boldsymbol{k}\lambda} \hat{\boldsymbol{e}}_{\boldsymbol{k}\lambda}\epsilon_k\, \alpha_{\boldsymbol{k}\lambda}\, \mathrm{e}^{\mathrm{i}(\boldsymbol{k}\cdot\boldsymbol{r}-\omega_k t)}\ .$$

If, as before, we assume that only the modes with common polarization direction and similar frequencies are populated, the eigenvalue function for the multimode coherent state becomes

$$\mathcal{E}(\boldsymbol{r},t) = \mathrm{i}\epsilon_\omega \sum_{\boldsymbol{k}} \alpha_{\boldsymbol{k}\lambda} \mathrm{e}^{\mathrm{i}(\boldsymbol{k}\cdot\boldsymbol{r}-\omega_k t)} \equiv \mathrm{i}\epsilon_\omega\, \alpha(\boldsymbol{r},t)\ .$$

We have thus seen that the free electromagnetic field can be decomposed into an infinite set of independent eigenmodes. The total state of the field then factorizes into the states of individual modes, each described by its own set of dynamical variables (operators). We will therefore often consider only a single mode field, which will simplify the notation while retaining all of the essential physics.

2.3 Photon Detection and Correlation Functions

Thus far we have quantized the electromagnetic field and considered several most important quantum states. Here we address the question of measurement and the information that can be extracted towards determining the state of the field.

Photons are typically counted by photodetectors via photon absorption, which, in the first place, results in a certain change in the microscopic state of the detector. It is then amplified to yield a macroscopic, classical signal, e.g., current in an electric circuit, which is observed and/or recorded by the experimenter. Various photodetectors have different response time (inverse bandwidth) and sensitivity to the frequency of the detected photons. The precise nature of the detection device is not of our concern here, but one has to keep in mind that good understanding of the particular mechanism of photon absorption and subsequent amplification of the signal is crucial in interpreting experiments involving photon detection. Typical photodetectors in the optical range employ photo-ionization in which the absorption of a single photon by an atom at some position $\boldsymbol{r}$ and time t creates a free electron and an ion. These charges are then accelerated by a strong gradient electric field, so that they acquire enough energy to ionize subsequent atoms, causing an avalanche of electrons and ions, which produce a macroscopic current in the electric circuit that closes the photosensitive medium. Alternatively, in semiconductor photodetectors, the absorption of a photon with the energy above a certain band-gap energy leads to the excitation of a conduction band electron and a hole, which in the strong electric field propagate in opposite directions acquiring in the process enough energy to cause an avalanche of electron–hole pairs, producing again a macroscopic current in the circuit.

Assume that prior to detection the field is in some pure state $|\Psi\rangle$. As the photon is absorbed, the resulting state of the field $|\Psi_f\rangle$ is obtained by acting with the operator $E^{(+)}(\boldsymbol{r},t)$, containing the annihilation operators of the field modes, on the initial state, $|\Psi_f\rangle \propto E^{(+)}(\boldsymbol{r},t)\,|\Psi\rangle$. For simplicity, we have assumed that the field is linearly polarized and can thus be described by scalar operators $E^{(\pm)}(\boldsymbol{r},t)$. The probability of photon detection, accompanied by the transition $|\Psi\rangle \to |\Psi_f\rangle$ is therefore proportional to

$$|\langle\Psi_f|\,E^{(+)}(\boldsymbol{r},t)\,|\Psi\rangle|^2\ .$$

The total probability of photodetection $w_1(\boldsymbol{r},t)$ is given by the sum over all possible final states $|\Psi_f\rangle$,

$$w_1(\boldsymbol{r},t)=\sum_f |\langle\Psi_f|\,E^{(+)}(\boldsymbol{r},t)\,|\Psi\rangle|^2=\sum_f \langle\Psi|\,E^{(-)}(\boldsymbol{r},t)\,|\Psi_f\rangle\langle\Psi_f|\,E^{(+)}(\boldsymbol{r},t)\,|\Psi\rangle\ . \tag{2.55}$$

Although some subsets of final states may not contribute to the transition $|\Psi\rangle \to |\Psi_f\rangle$, we can still sum over a complete set of states $|\Psi_f\rangle$, knowing that the terms corresponding to the non-contributing states will simply be zero.

Since $\sum_f |\Psi_f\rangle\langle\Psi_f|$ is then the identity operator, the above equation reduces to

$$w_1(\boldsymbol{r},t) = \langle\Psi|\, E^{(-)}(\boldsymbol{r},t)\, E^{(+)}(\boldsymbol{r},t)\, |\Psi\rangle \ . \tag{2.56}$$

Note that if $|\Psi\rangle$ is a single-photon state of (2.49), the detection probability is given by $w_1(\boldsymbol{r},t) = F^*(\boldsymbol{r},t)\, F(\boldsymbol{r},t) = |F(\boldsymbol{r},t)|^2$, where the envelope function $F(\boldsymbol{r},t)$ defined in (2.50) plays here the role of photodetection amplitude. If instead of the pure state $|\Psi\rangle$ the field is in a mixed state described by the density operator

$$\rho = \sum_{\Psi} P_\Psi\, |\Psi\rangle\langle\Psi| \ , \tag{2.57}$$

the photodetection probability is given by

$$w_1(\boldsymbol{r},t) = \mathrm{Tr}\big(\rho E^{(-)}(\boldsymbol{r},t)\, E^{(+)}(\boldsymbol{r},t)\big) \ . \tag{2.58}$$

If we now define the first-order correlation function of the field via

$$G^{(1)}(\boldsymbol{r}_1,\boldsymbol{r}_2;t_1,t_2) = \mathrm{Tr}\big(\rho E^{(-)}(\boldsymbol{r}_1,t_1)\, E^{(+)}(\boldsymbol{r}_2,t_2)\big) \ , \tag{2.59}$$

the detection probability can be expressed as

$$w_1(\boldsymbol{r},t) = G^{(1)}(\boldsymbol{r},\boldsymbol{r};t,t) \equiv G^{(1)}(\boldsymbol{r};t) \ , \tag{2.60}$$

where the choice $\boldsymbol{r}_1 = \boldsymbol{r}_2 = \boldsymbol{r}$ and $t_1 = t_2 = t$ simply reflects the fact that we are dealing with one event at a particular position and time. An important property of the two-time correlation function $G^{(1)}(\boldsymbol{r};t_1,t_2) \equiv \langle E^{(-)}(\boldsymbol{r},t_1)\, E^{(+)}(\boldsymbol{r},t_2)\rangle$ is that the power spectrum $S(\boldsymbol{r},\omega_k)$ of the field at position $\boldsymbol{r}$ is proportional to

$$S(\boldsymbol{r},\omega_k) \propto \lim_{T\to\infty} \int_0^T \int_0^T G^{(1)}(\boldsymbol{r};t_1,t_2) \mathrm{e}^{\mathrm{i}\omega_k(t_2-t_1)} \mathrm{d}t_1 \mathrm{d}t_2 \ .$$

For stochastic stationary fields, $G^{(1)}$ depends only on the time difference $\tau = t_2 - t_1$, and we have

$$S(\boldsymbol{r},\omega_k) = \frac{\varepsilon_0 c}{2\pi}\, \mathrm{Re} \int_0^\infty \langle E^{(-)}(\boldsymbol{r},0)\, E^{(+)}(\boldsymbol{r},\tau)\rangle \mathrm{e}^{\mathrm{i}\omega_k\tau} \mathrm{d}\tau \ , \tag{2.61}$$

i.e., the power spectrum and the first order correlation function are related by the Fourier transform.

Consider next the joint probability of detection of two photons, one at $\boldsymbol{r}_1$ and t_1 and the other at $\boldsymbol{r}_2$ and t_2. Clearly, for the field in a pure state $|\Psi\rangle$, it is given by

$$\begin{aligned} w_2(\boldsymbol{r}_1,t_1;\boldsymbol{r}_2,t_2) &= \sum_f |\langle\Psi_f|\, E^{(+)}(\boldsymbol{r}_2,t_2)\, E^{(+)}(\boldsymbol{r}_1,t_1)\, |\Psi\rangle|^2 \\ &= \langle\Psi|\, E^{(-)}(\boldsymbol{r}_1,t_1)\, E^{(-)}(\boldsymbol{r}_2,t_2)\, E^{(+)}(\boldsymbol{r}_2,t_2)\, E^{(+)}(\boldsymbol{r}_1,t_1)\, |\Psi\rangle \ , \end{aligned} \tag{2.62}$$

while for the mixed state (2.57), it becomes

$$w_2(\boldsymbol{r}_1,t_1;\boldsymbol{r}_2,t_2)=\mathrm{Tr}\big(\rho E^{(-)}(\boldsymbol{r}_1,t_1)\,E^{(-)}(\boldsymbol{r}_2,t_2)\,E^{(+)}(\boldsymbol{r}_2,t_2)\,E^{(+)}(\boldsymbol{r}_1,t_1)\big)\,. \tag{2.63}$$

This leads to the definition of the second-order correlation function via

$$\begin{aligned}&G^{(2)}(\boldsymbol{r}_1,\boldsymbol{r}_2,\boldsymbol{r}_3,\boldsymbol{r}_4;t_1,t_2,t_3,t_4)\\&=\mathrm{Tr}\big(\rho E^{(-)}(\boldsymbol{r}_1,t_1)\,E^{(-)}(\boldsymbol{r}_2,t_2)\,E^{(+)}(\boldsymbol{r}_3,t_3)\,E^{(+)}(\boldsymbol{r}_4,t_4)\big)\,,\end{aligned} \tag{2.64}$$

in terms of which the joint detection probability is given by

$$w_2(\boldsymbol{r}_1,t_1;\boldsymbol{r}_2,t_2)=G^{(2)}(\boldsymbol{r}_1,\boldsymbol{r}_2,\boldsymbol{r}_2,\boldsymbol{r}_1;t_1,t_2,t_2,t_1)\equiv G^{(2)}(\boldsymbol{r}_1,\boldsymbol{r}_2;t_1,t_2)\,. \tag{2.65}$$

Three or more photon detection and the corresponding higher-order correlation functions can similarly be defined as a straightforward generalization of the above formalism.

It is convenient to introduce the dimensionless (normalized) forms of the above correlation functions,

$$g^{(1)}(\boldsymbol{r}_1,\boldsymbol{r}_2;t_1,t_2)=\frac{G^{(1)}(\boldsymbol{r}_1,\boldsymbol{r}_2;t_1,t_2)}{\big[G^{(1)}(\boldsymbol{r}_1;t_1)\,G^{(1)}(\boldsymbol{r}_2;t_2)\big]^{1/2}}\,, \tag{2.66}$$

$$\begin{aligned}&g^{(2)}(\boldsymbol{r}_1,\boldsymbol{r}_2,\boldsymbol{r}_3,\boldsymbol{r}_4;t_1,t_2,t_3,t_4)\\&\quad=\frac{G^{(2)}(\boldsymbol{r}_1,\boldsymbol{r}_2,\boldsymbol{r}_3,\boldsymbol{r}_4;t_1,t_2,t_3,t_4)}{\big[G^{(1)}(\boldsymbol{r}_1;t_1)\,G^{(1)}(\boldsymbol{r}_2;t_2)\,G^{(1)}(\boldsymbol{r}_3;t_3)\,G^{(1)}(\boldsymbol{r}_4;t_4)\big]^{1/2}}\,,\end{aligned} \tag{2.67}$$

and similarly for $g^{(m)}$ with any $m\geq 1$. It is easy to see that if one considers individual modes of the electromagnetic field, the calculations of dimensionless correlations functions $g^{(m)}$ reduce to calculations of expectation values of normally ordered products of creation and annihilation operators.

Consider first a setup in which one detector monitors the electromagnetic field in a single mode. Quite obviously, the corresponding first-order correlation function is $g^{(1)}=\langle a^\dagger(t)\,a(t)\rangle/\langle a^\dagger a\rangle=1$. Imagine, however, that the field is first split and then recombined at the position of the detector, as shown in Fig. 2.4(a). Then the detector signal is proportional to

$$g^{(1)}(\delta s)=\frac{\langle a^\dagger(t-s_1/c)\,a(t-s_2/c)\rangle}{\langle a^\dagger a\rangle}=\mathrm{e}^{\mathrm{i}k\delta s}\,, \tag{2.68}$$

where $\delta s=s_2-s_1$ is the corresponding optical paths difference. This is a purely classical result, in the spirit of the Young's double-slit experiment, which does not provide any information on the quantum state of the field and the corresponding photon statistics.

We consider next the Hanbury–Brown and Twiss detection scheme of Fig. 2.4(b), in which the field is directed onto a 50/50 beam-splitter whose

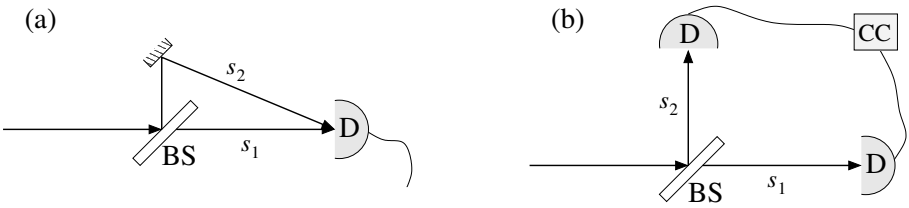

Fig. 2.4. Photon detection schemes: (a) single photon interference setup, and (b) two-photon coincidence setup. BS is beam-splitter, D is detector and CC is coincidence counting device.

outputs are monitored by two photodetectors. We are interested in the two-photon detection probability, which is represented by the second-order correlation function

$$g^{(2)}(t_1, t_2) = \frac{\langle a^\dagger(t_1)\, a^\dagger(t_2)\, a(t_2)\, a(t_1)\rangle}{\langle a^\dagger(t_1) a(t_1)\rangle \langle a^\dagger(t_2) a(t_2)\rangle} \,. \tag{2.69}$$

If the field is stationary, $g^{(2)}$ depends only on the time difference $\tau = t_2 - t_1$, and we can write

$$g^{(2)}(\tau) = \frac{\langle a^\dagger(0)\, a^\dagger(\tau)\, a(\tau)\, a(0)\rangle}{\langle a^\dagger a\rangle^2} \,. \tag{2.70}$$

It is instructive to compare the results of two-photon coincidence measurements for various initial states of the field. Consider first the field in a coherent state $|\alpha\rangle$, for which we obviously have

$$g^{(2)}(0) = \frac{\langle\alpha|\, a^\dagger a^\dagger a a\, |\alpha\rangle}{\langle\alpha|\, a^\dagger a\, |\alpha\rangle^2} = 1 \,. \tag{2.71}$$

In fact, all higher order normalized correlation functions $g^{(m)}$ for the coherent state are equal to 1. This is because the expectation values of the operator products of the form $\langle a^\dagger \ldots a^\dagger\, a \ldots a\rangle$ factorize into $\alpha^* \ldots \alpha^*\, \alpha \ldots \alpha = |\alpha|^{2m}$. The coherent state is therefore said to possess all orders of coherence, which is also true for the classical monochromatic field.

Consider now the field in a number state $|n\rangle$. Obviously, for $n = 1$ we have $g^{(2)}(0) = 0$, because the single photon can only be detected by one photodetector at a time, and therefore no coincidence of the detector clicks are possible. For $n > 1$, by direct calculation we obtain

$$g^{(2)}(0) = \frac{n(n-1)}{n^2} = 1 - \frac{1}{n} < 1 \,, \tag{2.72}$$

a strikingly non-classical result!

Before continuing with the chaotic field, let us prove a useful relation for the second-order correlation function

$$g^{(2)}(0) = \frac{\langle a^\dagger a^\dagger a a \rangle}{\langle a^\dagger a \rangle^2} = \frac{\langle (a^\dagger a)^2 \rangle - \langle a^\dagger a \rangle}{\langle a^\dagger a \rangle^2} \,, \tag{2.73}$$

where we have used the commutator $[a, a^\dagger] = 1$. Since $\langle a^\dagger a \rangle = \bar{n}$ is the mean number of photons and $\langle (a^\dagger a)^2 \rangle - \langle a^\dagger a \rangle^2 = (\Delta \mathcal{N})^2$ is the variance in the photon number, the above expression can be cast as

$$g^{(2)}(0) = 1 + \frac{(\Delta \mathcal{N})^2 - \bar{n}}{\bar{n}^2} \,. \tag{2.74}$$

Using now (2.47), for the field in a chaotic state we obtain

$$g^{(2)}(0) = 2 \,, \tag{2.75}$$

which indicates that the photons have the tendency to arrive at the two detectors simultaneously, in pairs. This effect is called photon bunching, as opposed to photon antibunching, $g^{(2)}(0) < 1$, corresponding to the field in a number state. Interestingly, however, the second order correlation function $g^{(2)}(\tau)$ for both types of fields, i.e., thermal and number-state, approaches the value 1 as $\tau \to \infty$.

2.4 Representations of the Field

As we have already seen, a natural basis for representing the states of the radiation field can be constructed from the eigenstates of its Hamiltonian, which are the number states $|n\rangle$. The density operator for the field can be expanded in this basis as

$$\rho = \sum_n \sum_m |n\rangle\langle n| \, \rho \, |m\rangle\langle m| = \sum_{n,m} \rho_{nm} \, |n\rangle\langle m| \,, \quad \rho_{nm} \equiv \langle n| \, \rho \, |m\rangle \,. \tag{2.76}$$

This, however, is not the only possible basis, nor always the most convenient. In this section we examine several alternative representations of the field which employ the coherent states as a basis.

2.4.1 Coherent State Representation

Let us recall the properties of the coherent states studied in Sect. 1.2.3, and in particular the fact that the scalar product of two coherent states $|\alpha\rangle$ and $|\beta\rangle$ is given by

$$\langle \alpha | \beta \rangle = \exp\left[\alpha^* \beta - \tfrac{1}{2}(|\alpha|^2 + |\beta|^2)\right] \,, \tag{2.77}$$

which yields $|\langle \alpha | \beta \rangle|^2 = \mathrm{e}^{-|\alpha - \beta|^2} \neq 0$. As a consequence of this non-orthogonality of the coherent states, any coherent state $|\alpha\rangle$ can be expanded in terms of all coherent states $|\beta\rangle$ as

$$|\alpha\rangle = \frac{1}{\pi}\int |\beta\rangle \exp\left[\alpha\beta^* - \tfrac{1}{2}(|\alpha|^2 + |\beta|^2)\right] \mathrm{d}^2\beta \,, \tag{2.78}$$

where $\mathrm{d}^2\beta \equiv \mathrm{d}\,\mathrm{Re}(\beta)\,\mathrm{d}\,\mathrm{Im}(\beta)$, which demonstrates the overcompleteness of the coherent states. Since the coherent states are not orthogonal to each other, their use as a basis might at first sight seem at best inconvenient. Yet, such a basis has indeed been proven to not only be convenient, but also to have advantages in certain contexts and especially in the representation of the density operator of the radiation field.

To develop the relevant formalism, we begin by noting that the identity operator I can be expanded as

$$I = \frac{1}{\pi}\int |\alpha\rangle\langle\alpha| \, \mathrm{d}^2\alpha \,, \tag{2.79}$$

where $\mathrm{d}^2\alpha \equiv \mathrm{d}\,\mathrm{Re}(\alpha)\,\mathrm{d}\,\mathrm{Im}(\alpha)$. This expression is readily proven by considering the expansion of $|\alpha\rangle$ in terms of the photon number states $|n\rangle$ that leads to

$$\int |\alpha\rangle\langle\alpha| \, \mathrm{d}^2\alpha = \pi \sum_n |n\rangle\langle n| \, = \pi I \,.$$

The density operator ρ can now be written as

$$\rho = I\rho I = \frac{1}{\pi^2}\iint |\alpha\rangle\langle\alpha|\,\rho\,|\beta\rangle\langle\beta| \, \mathrm{d}^2\alpha \, \mathrm{d}^2\beta \,, \tag{2.80}$$

which seems to suggest a representation of ρ in terms of the coherent states, with the quantities $\langle\alpha|\,\rho\,|\beta\rangle$ appearing as weight functions in the integral (2.80). Strictly speaking, they can not be called matrix elements of ρ, owing to the lack of orthogonality between $|\alpha\rangle$ and $|\beta\rangle$. Recall that in establishing the existence and properties of the coherent states, we reverted to their expansion in terms of the orthonormal basis $\{\,|n\rangle\}$ of photon number states. We follow a similar course in order to establish the properties of the weight functions $\langle\alpha|\,\rho\,|\beta\rangle$. To this end, we use the expansion (2.35), noting at the same time that in terms of the number state basis the density operator ρ is given by (2.76), or equivalently by

$$\rho = \sum_{n,m} \frac{\rho_{nm}}{\sqrt{n!m!}} (a^\dagger)^n \, |0\rangle\langle 0| \, (a)^m \,.$$

The above relations suggest that we define the quantity

$$R(\alpha^*, \beta) = \sum_{n,m} \rho_{nm} \frac{(\alpha^*)^n (\beta)^m}{\sqrt{n!m!}} \,, \tag{2.81}$$

in terms of which $\langle\alpha|\,\rho\,|\beta\rangle$ is written as

$$\langle\alpha|\,\rho\,|\beta\rangle = R(\alpha^*, \beta)\,\langle\alpha|0\rangle\langle 0|\beta\rangle = R(\alpha^*, \beta)\,\mathrm{e}^{-\frac{1}{2}(|\alpha|^2 + |\beta|^2)} \,, \tag{2.82}$$

which is a function of two complex variables α^* and β. We can now rewrite (2.80) as

$$\rho = \frac{1}{\pi^2} \iint R(\alpha^*, \beta)\, |\alpha\rangle\langle\beta|\, \mathrm{e}^{-\frac{1}{2}(|\alpha|^2+|\beta|^2)}\, \mathrm{d}^2\alpha\, \mathrm{d}^2\beta\,. \tag{2.83}$$

Since ρ is a bounded operator, in the sense that $\mathrm{Tr}(\rho^2) = \sum_n \sum_m \rho_{nm}\rho_{mn} = \sum_{nm} |\rho_{nm}|^2 \leq 1$, the Taylor series representing $R(\alpha^*, \beta)$ converges for all finite values of α and β. It is therefore an entire function. The above relation representing the density operator in terms of coherent states is applicable to any operator $\mathcal{T}$ of the system. Given its matrix elements $\mathcal{T}_{nm}$ in the $\{\,|n\rangle\}$ basis, the operator is represented by the integral

$$\mathcal{T} = \frac{1}{\pi^2} \iint T(\alpha^*, \beta)\, |\alpha\rangle\langle\beta|\, \mathrm{e}^{-\frac{1}{2}(|\alpha|^2+|\beta|^2)}\, \mathrm{d}^2\alpha\, \mathrm{d}^2\beta \tag{2.84}$$

over two complex variables of the function $T(\alpha^*, \beta)$ defined by

$$T(\alpha^*, \beta) = \sum_{n,m} \mathcal{T}_{nm} \frac{(\alpha^*)^n (\beta)^m}{\sqrt{n!m!}}\,. \tag{2.85}$$

Such a representation has in fact many of the properties of the usual representations in terms of orthonormal bases. For example, if $\mathcal{T}$ is a product of two operators, i.e., $\mathcal{T} = \mathcal{T}_1\mathcal{T}_2$, one can readily prove the relations (see Prob. 2.1)

$$\langle\alpha|\, \mathcal{T}\, |\beta\rangle = \langle\alpha|\, \mathcal{T}_1\mathcal{T}_2\, |\beta\rangle = \frac{1}{\pi} \int \langle\alpha|\, \mathcal{T}_1\, |\gamma\rangle\langle\gamma|\, \mathcal{T}_2\, |\beta\rangle\, \mathrm{d}^2\gamma\,, \tag{2.86}$$

and

$$T(\alpha^*, \beta) = \frac{1}{\pi} \int T_1(\alpha^*, \gamma)\, T_2(\gamma^*, \beta)\, \mathrm{e}^{-|\gamma|^2}\, \mathrm{d}^2\gamma\,. \tag{2.87}$$

The calculation of expectation values of operators requires the calculation of traces of the type $\mathrm{Tr}(\rho\mathcal{T})$ and we need to establish the rules for its calculation in terms of the coherent state representation. To this end, we consider first the trace of the operator $|\alpha\rangle\langle\beta|\, \mathcal{T}$ which is easily obtained if we use the expansion of the coherent states in the $\{\,|n\rangle\}$ basis, with the result

$$\mathrm{Tr}(\,|\alpha\rangle\langle\beta|\, \mathcal{T}) = T(\alpha^*, \beta)\, \mathrm{e}^{-\frac{1}{2}(|\alpha|^2+|\beta|^2)} = \langle\alpha|\, \mathcal{T}\, |\beta\rangle\,. \tag{2.88}$$

We can now obtain an expression for the expectation value of operator $\mathcal{T}$ as follows:

$$\begin{aligned} \langle\mathcal{T}\rangle = \mathrm{Tr}(\rho\mathcal{T}) &= \frac{1}{\pi^2} \iint R(\alpha^*, \beta)\langle\beta|\, \mathcal{T}\, |\alpha\rangle\, \mathrm{e}^{-\frac{1}{2}(|\alpha|^2+|\beta|^2)}\, \mathrm{d}^2\alpha\, \mathrm{d}^2\beta \\ &= \frac{1}{\pi^2} \iint R(\alpha^*, \beta)\, T(\beta^*, \alpha)\, \mathrm{e}^{-(|\alpha|^2+|\beta|^2)}\, \mathrm{d}^2\alpha\, \mathrm{d}^2\beta\,. \end{aligned} \tag{2.89}$$

The trace of ρ, which we know must be unity, is obtained from the above relation by setting $\mathcal{T} = I$, with the result

$$\mathrm{Tr}(\rho) = \frac{1}{\pi^2} \iint R(\alpha^*, \beta)\, \mathrm{e}^{(\beta^*\alpha - |\alpha|^2 - |\beta|^2)}\, \mathrm{d}^2\alpha\, \mathrm{d}^2\beta\ . \tag{2.90}$$

Using $\frac{1}{\pi} \int R(\alpha^*, \beta)\, \exp(\beta^*\alpha - |\alpha|^2)\, \mathrm{d}^2\alpha = R(\beta^*, \beta)$ we find that $R(\alpha^*, \beta)$ must satisfy the condition

$$\frac{1}{\pi} \int R(\beta^*, \beta)\, \mathrm{e}^{-|\beta|^2}\, \mathrm{d}^2\beta = 1\ . \tag{2.91}$$

Note that for any wavefunction $|\Psi\rangle$ of the system, we must have $\langle\Psi|\, \rho\, |\Psi\rangle \geq 0$, which must also hold for $|\Psi\rangle = |\alpha\rangle$, yielding the condition $R(\alpha^*, \alpha) \geq 0$.

2.4.2 Quasi-Probability Distributions

The density operator is a rather special operator and it can be shown that for most conceivable states of the field that are apt to be of physical interest, the density operator can quite generally be represented in the "diagonal–looking" form

$$\rho = \int P(\alpha)\, |\alpha\rangle\langle\alpha|\, \mathrm{d}^2\alpha\ , \tag{2.92}$$

which involves an integration over only one complex variable α. This is a consequence of the overcompleteness of the coherent states. Obviously, the lack of orthogonality of the coherent states precludes the strict meaning of diagonality in this case. The Hermitian character of ρ is guaranteed by the condition $P(\alpha) = [P(\alpha)]^*$, while the condition $\mathrm{Tr}(\rho) = 1$ is satisfied by $\int P(\alpha)\mathrm{d}^2\alpha = 1$. This representation of the density operator is referred to as P-representation, where $P(\alpha)$ is a real-valued function of the single complex variable. It is related to the R-representation outlined above via (see Prob. 2.2)

$$R(\beta^*, \gamma) = \int P(\alpha)\, \mathrm{e}^{(\beta^*\alpha + \gamma\alpha^* - |\alpha|^2)}\, \mathrm{d}^2\alpha\ . \tag{2.93}$$

It is easy to show that in the P-representation the expectation value of an operator $\mathcal{T}$ is given by

$$\langle\mathcal{T}\rangle = \mathrm{Tr}(\rho\mathcal{T}) = \int P(\alpha)\langle\alpha|\, \mathcal{T}\, |\alpha\rangle\, \mathrm{d}^2\alpha = \int P(\alpha)\, T(\alpha)\, \mathrm{d}^2\alpha\ , \tag{2.94}$$

where $T(\alpha) \equiv \langle\alpha|\, \mathcal{T}\, |\alpha\rangle$. In general, $P(\alpha)$ may not even be a function, but a generalized function of the complex variable α. As an example, for a field mode in a coherent state $|\beta\rangle$, it is given by $P(\alpha) = \delta^{(2)}(\alpha - \beta)$, as will be shown below. Nevertheless, the fact that $\delta^{(2)}(\alpha - \beta)$ satisfies the necessary conditions for the hermiticity and completeness of ρ suggests that the P-representation admits a bit more generality than our wording above, if taken literally, implied. In any case, $P(\alpha)$ can not be interpreted as a probability, as the diagonal matrix elements of the density operator normally do, if not for any other reason, simply because the coherent states are not orthogonal

to each other. Thus a $P(\alpha)$ that is not even a function does not present a contradiction.

The density operator is essential in calculating expectation values of operators representing quantities of physical interest. An example of particular interest in our context are the correlation functions of the field, discussed in the previous section. In principle, one can simply employ the operator form of the correlation function and proceed to the direct calculation of the trace, using, for example, the P-representation of the density operator. It turns out, however, that an alternative approach through auxiliary tools known as characteristic functions can facilitate the task considerably. Moreover, in the study of the dynamics of the density operator of the field in interaction with other systems, it is often more convenient to obtain the evolution of the appropriate characteristic function rather than the density operator itself. We shall not trace here the motivation for this approach to its origins but shall proceed directly to the definition and brief description of the most important characteristic functions in our context.

Such a characteristic function is defined by

$$C(\gamma) = \mathrm{Tr}\big(\rho\, \mathrm{e}^{\gamma a^\dagger - \gamma^* a}\big)\ , \tag{2.95}$$

in which the operators $a^\dagger$ and a appear in a symmetric order. Evaluating the trace in a representation that diagonalizes ρ, one can show that $|C(\gamma)| \leq 1$ for all γ. Obviously, the above expression represents the expectation value of the displacement operator $\mathcal{D}(\gamma) = \mathrm{e}^{\gamma a^\dagger - \gamma^* a}$. Two additional characteristic functions of interest are defined by

$$C_{\mathrm{N}}(\gamma) = \mathrm{Tr}\big(\rho\, \mathrm{e}^{\gamma a^\dagger}\, \mathrm{e}^{-\gamma^* a}\big)\ , \tag{2.96}$$

$$C_{\mathrm{A}}(\gamma) = \mathrm{Tr}\big(\rho\, \mathrm{e}^{-\gamma^* a}\, \mathrm{e}^{\gamma a^\dagger}\big)\ , \tag{2.97}$$

and are referred to as normally and antinormally, respectively, ordered characteristic functions. The usefulness of these characteristic functions becomes evident if we expand $C_{\mathrm{N}}(\gamma)$ and $C_{\mathrm{A}}(\gamma)$ in powers of γ and γ^*. Taking partial derivatives with respect to γ and $-\gamma^*$ evaluated at $\gamma = 0$, it is straightforward to show that (see Prob. 2.3)

$$\frac{\partial^n}{\partial \gamma^n} \frac{\partial^m}{\partial(-\gamma^*)^m}\, C_{\mathrm{N}}(\gamma)\bigg|_{\gamma=0} = \mathrm{Tr}\big(\rho\, (a^\dagger)^n a^m\big)\ , \tag{2.98}$$

$$\frac{\partial^n}{\partial \gamma^n} \frac{\partial^m}{\partial(-\gamma^*)^m}\, C_{\mathrm{A}}(\gamma)\bigg|_{\gamma=0} = \mathrm{Tr}\big(\rho\, a^n (a^\dagger)^m\big)\ . \tag{2.99}$$

These relations demonstrate that the normally and antinormally ordered characteristic functions are, respectively, convenient for the calculation of normally and antinormally ordered products of the field operators. Using the operator relation (1.26) or, equivalently, relations (2.34), we obtain

$$C(\gamma) = \mathrm{e}^{-\frac{1}{2}|\gamma|^2} C_{\mathrm{N}}(\gamma) = \mathrm{e}^{\frac{1}{2}|\gamma|^2} C_{\mathrm{A}}(\gamma)\ , \tag{2.100}$$

which, in view of the property $|C(\gamma)| \leq 1$, imply that $|C_{\rm A}(\gamma)|$ decreases at least as fast as $\mathrm{e}^{-\frac{1}{2}|\gamma|^2}$, while $|C_{\rm N}(\gamma)|$ may diverge as rapidly as $\mathrm{e}^{\frac{1}{2}|\gamma|^2}$ for $|\gamma| \to \infty$. Thus the three characteristic functions discussed above are related to each other through Gaussian factors.

Considering now expectation values of more general expressions, we can write

$$\begin{aligned}\mathrm{Tr}\big(\rho U(a)V(a^\dagger)\big) = \mathrm{Tr}\big(V(a^\dagger)\rho U(a)\big) &= \frac{1}{\pi}\int \langle\alpha|\, V(a^\dagger)\rho U(a)\,|\alpha\rangle\, \mathrm{d}^2\alpha \\ &= \frac{1}{\pi}\int V(\alpha^*)\langle\alpha|\,\rho\,|\alpha\rangle U(\alpha)\,\mathrm{d}^2\alpha \end{aligned} \tag{2.101}$$

for any functions $U(a)$ and $V(a^\dagger)$ of the operators a and $a^\dagger$, respectively. Using these relations for $C_{\rm A}(\gamma)$, we obtain

$$\begin{aligned} C_{\rm A}(\gamma) = \mathrm{Tr}\big(\rho\,\mathrm{e}^{-\gamma^* a}\,\mathrm{e}^{\gamma a^\dagger}\big) &= \frac{1}{\pi}\int \langle\alpha|\,\rho\,|\alpha\rangle\,\mathrm{e}^{\gamma\alpha^* - \gamma^*\alpha}\,\mathrm{d}^2\alpha \\ &= \int Q(\alpha)\,\mathrm{e}^{\gamma\alpha^* - \gamma^*\alpha}\,\mathrm{d}^2\alpha\,, \end{aligned} \tag{2.102}$$

where $Q(\alpha) \equiv \frac{1}{\pi}\langle\alpha|\,\rho\,|\alpha\rangle$ is known as the Q quasiprobability distribution function. Clearly, $Q(\alpha)$ is a positive–definite bounded function, since the density operator ρ is a positive operator, $0 \leq Q(\alpha) \leq 1/\pi$. If we write $\alpha = \alpha_1 + \mathrm{i}\alpha_2$ and $\gamma = \gamma_1 + \mathrm{i}\gamma_2$, where all $\alpha_{1,2}$ and $\gamma_{1,2}$ are real, we have $\gamma\alpha^* - \gamma^*\alpha = \mathrm{i}2(\gamma_2\alpha_1 - \gamma_1\alpha_2)$, and (2.102) becomes

$$C_{\rm A}(\gamma) = \int Q(\alpha)\,\mathrm{e}^{\mathrm{i}2\gamma_2\alpha_1}\mathrm{e}^{-\mathrm{i}2\gamma_1\alpha_2}\,\mathrm{d}^2\alpha\,, \quad \mathrm{d}^2\alpha \equiv \mathrm{d}\alpha_1\,\mathrm{d}\alpha_2\,. \tag{2.103}$$

This implies that $C_{\rm A}(\gamma)$ is the two-dimensional (2D) Fourier transform of $Q(\alpha)$, establishing thus a connection between the "diagonal" matrix elements $\langle\alpha|\,\rho\,|\alpha\rangle = \pi Q(\alpha)$ of the density operator and the antinormally ordered characteristic function. Conversely, $Q(\alpha)$ is given by the inverse Fourier transform

$$Q(\alpha) = \frac{1}{\pi^2}\int \mathrm{e}^{\alpha\gamma^* - \alpha^*\gamma}\, C_{\rm A}(\gamma)\,\mathrm{d}^2\gamma\,. \tag{2.104}$$

We have thus seen that $C_{\rm A}(\gamma)$ and $Q(\alpha)$ are the 2D Fourier transforms of each other.

Consider now the Fourier transform of the symmetrically ordered characteristic function $C(\gamma)$,

$$W(\alpha) = \frac{1}{\pi^2}\int \mathrm{e}^{\alpha\gamma^* - \alpha^*\gamma}\, C(\gamma)\,\mathrm{d}^2\gamma\,, \tag{2.105}$$

known as the Wigner function. Integrating by parts, one can show that

$$\int (\alpha^*)^n \alpha^m W(\alpha)\, \mathrm{d}^2\alpha = \int \delta^{(2)}(\gamma)\, \frac{\partial^n}{\partial \gamma^n} \frac{\partial^m}{\partial(-\gamma^*)^m}\, C(\gamma)\, \mathrm{d}^2\gamma$$
$$= \frac{\partial^n}{\partial \gamma^n} \frac{\partial^m}{\partial(-\gamma^*)^m}\, C(\gamma)\Big|_{\gamma=0} , \qquad (2.106)$$

from which it follows that for $n = m = 0$ one has $\int W(\alpha)\mathrm{d}^2\alpha = 1$, a result that seems to be compatible with $W(\alpha)$ satisfying one of the necessary conditions for a probability distribution. A well know difficulty with this function, however, is that it can also assume negative values, which precludes the literal interpretation as a probability distribution. It can nevertheless, with a proper caveat, provide useful insight into the connection of the state of a quantum system with the analogous classical situation. $W(\alpha)$ is therefore also referred to as the Wigner quasiprobability distribution. In addition, it is more convenient for the calculation of products of operators with symmetric ordering.

If we assume now that $P(\alpha)$ exists, we can write $C_{\mathrm{N}}(\gamma)$ as

$$C_{\mathrm{N}}(\gamma) = \int P(\alpha)\, \langle\alpha|\, \mathrm{e}^{\gamma a^\dagger} \mathrm{e}^{-\gamma^* a}\, |\alpha\rangle\, \mathrm{d}^2\alpha = \int P(\alpha)\, \mathrm{e}^{\gamma\alpha^* - \gamma^*\alpha}\, \mathrm{d}^2\alpha , \qquad (2.107)$$

which is the 2D Fourier transform of $P(\alpha)$. Conversely, we can obtain $P(\alpha)$ through the inverse Fourier transform, namely

$$P(\alpha) = \frac{1}{\pi^2} \int \mathrm{e}^{\alpha\gamma^* - \alpha^*\gamma}\, C_{\mathrm{N}}(\gamma)\, \mathrm{d}^2\gamma , \qquad (2.108)$$

assuming of course that the integral exists, which it should if $P(\alpha)$ does. As we have noted before, this statement admits generalized functions, such as, e.g., $P(\alpha) = \delta^{(2)}(\alpha)$ corresponding to the ground state of the harmonic oscillator (vacuum) which is equivalent to the coherent state with $\beta = 0$.

The Wigner distribution $W(\alpha)$, as well as the $Q(\alpha)$ and $P(\alpha)$ distributions, represent the relative weight of each coherent state $|\alpha\rangle$ in the representation of the density operator of the field in the basis of coherent states. It is therefore natural for them to be related to each other through rather simple integral transforms, i.e.

$$W(\alpha) = \frac{2}{\pi} \int P(\beta)\, \mathrm{e}^{-2|\alpha-\beta|^2}\, \mathrm{d}^2\beta , \qquad (2.109)$$

$$Q(\alpha) = \frac{2}{\pi} \int W(\beta)\, \mathrm{e}^{-2|\alpha-\beta|^2}\, \mathrm{d}^2\beta$$
$$= \frac{1}{\pi} \int P(\beta)\, \mathrm{e}^{-|\alpha-\beta|^2}\, \mathrm{d}^2\beta . \qquad (2.110)$$

As an illustration of the above formalism, we consider its application to the coherent, number-state and chaotic fields.

Coherent field: For a pure coherent state $|\beta\rangle$, we have $\rho = |\beta\rangle\langle\beta|$ which can obviously be written as

$$\rho = \int \delta^{(2)}(\alpha - \beta)\, |\alpha\rangle\langle\alpha|\, \mathrm{d}^2\alpha \,. \tag{2.111}$$

Therefore

$$P(\alpha) = \delta^{(2)}(\alpha - \beta) \equiv \delta\big(\mathrm{Re}(\alpha - \beta)\big)\delta\big(\mathrm{Im}(\alpha - \beta)\big) \,, \tag{2.112}$$

from which we easily obtain

$$C_{\mathrm{N}}(\gamma) = \langle\beta|\, \mathrm{e}^{\gamma a^\dagger} \mathrm{e}^{-\gamma^* a}\, |\beta\rangle = \mathrm{e}^{\gamma\beta^* - \gamma^*\beta} \,, \tag{2.113}$$

and

$$W(\alpha) = \frac{2}{\pi}\, \mathrm{e}^{-2|\alpha-\beta|^2} \,, \tag{2.114a}$$

$$Q(\alpha) = \frac{1}{\pi}\, \mathrm{e}^{-|\alpha-\beta|^2} \,. \tag{2.114b}$$

Field in a number (Fock) state: The density operator for a single-mode field in a number state $|n\rangle$ is $\rho = |n\rangle\langle n|$. We therefore have

$$Q(\alpha) = \frac{1}{\pi}\langle\alpha|\, \rho\, |\alpha\rangle = \frac{|\alpha|^{2n}}{\pi n!}\, \mathrm{e}^{-|\alpha|^2} \,, \tag{2.115}$$

which is a well behaved non-negative function. Calculation of the Wigner function yields

$$W(\alpha) = \frac{2}{\pi}(-1)^n\, \mathrm{e}^{-2|\alpha|^2} L_n(4|\alpha|^2) \,, \tag{2.116}$$

where L_n is a Laguerre polynomial. In particular, for $n = 1$ we have

$$W(\alpha) = \frac{2}{\pi}\, \mathrm{e}^{-2|\alpha|^2}\, (4|\alpha|^2 - 1) \,,$$

which is clearly negative in the vicinity of $|\alpha| = 0$, where its value is $W(0) = -2/\pi$. In general, for a number state with $n > 0$, the Wigner $W(\alpha)$ (as well as $P(\alpha)$) distribution takes negative values and therefore does not represent a well-defined probability distribution. The negativity of the Wigner (or $P(\alpha)$) function is thus a signature of the highly non-classical character of the corresponding quantum state.

Chaotic field: The density operator has the form

$$\rho = \upsilon\, \mathrm{e}^{\mu a^\dagger a} = \upsilon \sum_n \mathrm{e}^{\mu n}\, |n\rangle\langle n| \,, \tag{2.117}$$

where

$$\upsilon = \frac{1}{1 + \bar{n}} \,, \quad \mu = \ln \frac{\bar{n}}{1 + \bar{n}} \,,$$

with $\bar{n}$ being the average photon number of (2.45). Through a direct application of the formalism, we obtain

$$Q(\alpha) = v\,\mathrm{e}^{-v|\alpha|^2}\ , \tag{2.118}$$

and, using (2.103),

$$C_{\mathrm{A}}(\gamma) = \mathrm{e}^{-|\gamma|^2/v}\ , \tag{2.119}$$

which in turn determines $C(\gamma)$ and $C_{\mathrm{N}}(\gamma)$ through multiplication by the Gaussian factors as in (2.100). Inverting the Fourier transform, we find

$$W(\alpha) = \frac{1}{\pi}\frac{1}{1+\bar{n}}\,\exp\left(-\frac{|\alpha|^2}{\frac{1}{2}+\bar{n}}\right)\ , \tag{2.120}$$

$$P(\alpha) = \frac{1}{\pi\bar{n}}\exp\left(-\frac{|\alpha|^2}{\bar{n}}\right)\ , \tag{2.121}$$

which yields the density matrix

$$\rho = \frac{1}{\pi\bar{n}}\int \mathrm{e}^{-|\alpha|^2/\bar{n}}\,|\alpha\rangle\langle\alpha|\,\mathrm{d}^2\alpha\ . \tag{2.122}$$

For the sake of formal completeness, in closing this section, we note that all of the above characteristic functions can be expressed in a unified way by defining

$$C(\gamma,\lambda) = C(\gamma)\,\mathrm{e}^{-\frac{1}{2}\lambda|\gamma|^2}\ , \tag{2.123}$$

from which, with (2.100), we have

$$C(\gamma) = C(\gamma,0)\ ,\quad C_{\mathrm{N}}(\gamma) = C(\gamma,1)\ ,\quad C_{\mathrm{A}}(\gamma) = C(\gamma,-1)\ . \tag{2.124}$$

If we further define

$$W(\alpha,\lambda) = \frac{1}{\pi}\int \mathrm{e}^{\alpha\gamma^*-\alpha^*\gamma}\,C(\gamma,\lambda)\,\mathrm{d}^2\gamma\ , \tag{2.125}$$

it is straightforward to show that

$$W(\alpha) = W(\alpha,0)\ ,\quad P(\alpha) = W(\alpha,1)\ ,\quad Q(\alpha) = W(\alpha,-1)\ . \tag{2.126}$$

Problems

2.1. Prove the relations (2.86), (2.87) and (2.88).

2.2. Prove the relations (2.93) and (2.94).

2.3. Prove the relations (2.98), (2.99) and (2.106).

2.4. Show that

$$\frac{\partial}{\partial\alpha}\,|\alpha\rangle\langle\alpha| = (a^\dagger-\alpha^*)\,|\alpha\rangle\langle\alpha|\ ,\quad \frac{\partial}{\partial\alpha^*}\,|\alpha\rangle\langle\alpha| = |\alpha\rangle\langle\alpha|\,(a-\alpha)\ . \tag{2.127}$$

(*Hint*: Express $|\alpha\rangle$ through $|0\rangle$ as in (1.90).)

2.5. Show that a system initially in the coherent state $|\alpha\rangle$ evolving in time under the Hamiltonian

$$\mathcal{H} = \hbar\omega a^\dagger a + \hbar(g^* a + g a^\dagger) \,,$$

where g and g^* are c-numbers, remains in a coherent state at all times.

3

Atom in an External Radiation Field

In this chapter, after a brief outline of the physics of an one-electron atom, we discuss its interaction with an external electromagnetic field. In particular, we focus on a two-level atom interacting with a near-resonant monochromatic (single–frequency) field which can be treated classically in the case of a strong coherent field produced by a laser, or quantum mechanically when the field is very weak, as is the case in optical or microwave cavities containing only a few photons at a time. We then discuss the coupling of the atom to the continuum of empty modes of the open radiation field and derive the Weisskopf–Wigner law of spontaneous decay of an excited atomic state. Finally, in order to illustrate certain effects associated with atomic coherence and interference, we consider the interaction of a three-level atom with a bichromatic classical field.

3.1 One Electron Atom

In this section, we review the properties of the simplest (one-electron) atom and its coupling with the radiation, which results in the transitions between the atomic energy levels accompanied by the photon emission or absorption.

3.1.1 Electronic States of an Atom

For the purposes of this book, the one-electron atom consists of a single electron of mass m_{e} bound to a central force potential $V(r)$, $r = |\boldsymbol{r}|$ being the distance of the electron from the origin of the potential, which makes the system spherically symmetric. We need not be concerned with the translational motion of the nucleus in space but only with the motion of the electron with respect to the nucleus, which being much heavier than the electron will be taken as the fixed in space origin of the system of coordinates. Given the spherical symmetry of the system, it is most convenient to use spherical coordinates (r, θ, ϕ). The Hamiltonian of the system, being the sum of the kinetic

and potential energy, is given by $\mathcal{H}^{\mathrm{A}} = \boldsymbol{\mathcal{P}}^2/2m_{\mathrm{e}} + V(r)$. For the special case of a hydrogen–like atom, the potential is due to a point charge and has the Coulomb form $V(r) \propto -r^{-1}$. To determine the eigenstates and the corresponding energy eigenvalues of this system, we need to solve the stationary Schrödinger equation

$$\left(-\frac{\hbar^2}{2m_{\mathrm{e}}}\,\boldsymbol{\nabla}^2 + V(r)\right)\Psi(\boldsymbol{r}) = E\,\Psi(\boldsymbol{r})\;, \tag{3.1}$$

under the condition that the solutions are square integrable, which implies that they must approach zero sufficiently fast as $|\boldsymbol{r}| \to \infty$. The form of the Hamiltonian operator and the spherical symmetry of the potential allow the separation of variables. We therefore seek solutions of the form

$$\Psi(\boldsymbol{r}) = R(r)\,Y(\theta,\phi) = R(r)\,\Theta(\theta)\,\Phi(\phi)\;.$$

Substitution of this form into (3.1) leads to the three separate differential equations

$$\frac{\mathrm{d}^2\Phi}{\mathrm{d}\phi^2} = -m^2\Phi\;, \tag{3.2a}$$

$$-\frac{1}{\sin\theta}\,\frac{\mathrm{d}}{\mathrm{d}\theta}\left(\sin\theta\,\frac{\mathrm{d}\Theta}{\mathrm{d}\theta}\right) + \frac{m^2}{\sin^2\theta}\,\Theta = l(l+1)\,\Theta\;, \tag{3.2b}$$

$$\frac{1}{r^2}\,\frac{\mathrm{d}}{\mathrm{d}r}\left(r^2\,\frac{\mathrm{d}R}{\mathrm{d}r}\right) - \frac{l(l+1)}{r^2}\,R - \frac{2m_{\mathrm{e}}}{\hbar^2}V(r)R + \frac{2m_{\mathrm{e}}E}{\hbar^2}\,R = 0\;, \tag{3.2c}$$

where $-m^2$ and $l(l+1)$ are separation constants with physical significance discussed below.

Irrespective of the particular form of $V(r)$, as long as it is central, the resulting solutions for $\Phi(\phi)$ and $\Theta(\theta)$ are always the same, namely

$$\Phi_m = \frac{1}{\sqrt{2\pi}}\,\mathrm{e}^{\mathrm{i}m\phi}\;, \tag{3.3a}$$

$$\Theta_l^m = (-1)^m\left[\frac{(2l+1)}{2}\,\frac{(l-m)!}{(l+m)!}\right]^{1/2} P_l^m(\cos\theta)\;. \tag{3.3b}$$

Here $P_l^m(x)$ are known functions, specifically polynomials of degree l referred to as associated Legendre polynomials, where $l = 0, 1, 2, \ldots$ and m is also an integer whose absolute value is restricted by $|m| \le l$ which ensures that $\Phi(\phi)$ and $\Theta(\theta)$ are single-valued functions; not a postulate of quantum theory but a requirement for their unambiguous interpretation. Combining (3.2a) and (3.2b), we obtain the differential equation

$$\left[-\frac{1}{\sin\theta}\,\frac{\partial}{\partial\theta}\left(\sin\theta\,\frac{\partial}{\partial\theta}\right) - \frac{1}{\sin^2\theta}\,\frac{\partial^2}{\partial\phi^2}\right] Y = l(l+1)\,Y \tag{3.4}$$

for the function $Y(\theta,\phi)$ incorporating the complete angular dependence of the wavefunction $\Psi(\boldsymbol{r})$. Its solutions are the functions

$$Y_l^m = \Phi_m \Theta_l^m = (-1)^m \left[\frac{(2l+1)}{4\pi}\frac{(l-m)!}{(l+m)!}\right]^{1/2} P_l^m(\cos\theta)\,\mathrm{e}^{\mathrm{i}m\phi}\ , \quad (3.5a)$$

$$Y_l^{-m} = (-1)^m (Y_l^m)^*\ , \quad \text{for} \quad m \geq 0\ , \quad (3.5b)$$

known as spherical harmonics which satisfy the orthonormality conditions

$$\int (Y_l^m)^*\, Y_{l'}^{m'}\,\mathrm{d}\Omega = \int_0^{2\pi}\mathrm{d}\phi \int_0^{\pi}\sin\theta\mathrm{d}\theta\,(Y_l^m)^*\, Y_{l'}^{m'} = \delta_{mm'}\delta_{ll'}\ .$$

The solutions of the equation for the radial part depend on the form of $V(r)$. For the case of a pure Coulomb potential, as is the case for a hydrogen–like atom with a nucleus of charge Ze, $V(r) = -Ze^2/4\pi\varepsilon_0 r$, the solutions can be expressed in terms of functions known as the Laguerre polynomials. Briefly, if we introduce the variables $\rho = r/\alpha$ and $\lambda = 2m_\mathrm{e}Ze^2\alpha/4\pi\varepsilon_0\hbar^2$, where $\alpha^2 = -\hbar^2/8m_\mathrm{e}E$, the radial equation (3.2c) becomes

$$\frac{1}{\rho^2}\frac{\mathrm{d}}{\mathrm{d}\rho}\left(\rho^2\frac{\mathrm{d}R}{\mathrm{d}\rho}\right) + \left[\frac{\lambda}{\rho} - \frac{1}{4} - \frac{l(l+1)}{\rho^2}\right]R = 0\ , \quad (3.6)$$

whose solutions are

$$R(\rho) = \mathrm{e}^{-\rho/2}\rho^l F(\rho)\ , \quad (3.7)$$

with $F(\rho)$ being a polynomial related to the so-called associated Laguerre polynomials $L_n^k(\rho)$. The expression for $R(\rho)$ explicitly shows its asymptotic behavior $R \sim \mathrm{e}^{-\rho/2}$ as $\rho \to \infty$ and $R \sim \rho^l$ as $\rho \to 0$. The solutions (3.7) are obtained through a power series expansion in terms of ρ. The requirement that the power series terminate leads to the condition that λ be an integer: $\lambda = n$, where $n \geq l+1$ or $n = l+1+n'$ with $n' = 0, 1, 2, \ldots$ Thus the solutions for $R(r)$ are labeled by two indices, $n = 1, 2, 3, \ldots$ and $l \leq n-1$. They obey the orthonormality condition

$$\int_0^\infty R_{nl}^* R_{n'l'}\, r^2\mathrm{d}r = \delta_{nn'}\delta_{ll'}\ .$$

The complete set of eigenfunctions for the hydrogen–like atom, labeled by the three indices, is

$$\Psi_{nlm}(\boldsymbol{r}) = R_{nl}(r)Y_l^m(\theta,\phi)\ , \quad (3.8)$$

with the orthonormality condition

$$\int_0^\infty r^2\mathrm{d}r \int_0^{2\pi}\mathrm{d}\phi \int_0^{\pi}\sin\theta\mathrm{d}\theta\,\Psi_{nlm}^*\Psi_{n'l'm'} = \delta_{nn'}\delta_{ll'}\delta_{mm'}\ .$$

The three indices nlm are referred to as quantum numbers of the states of the system. This suggests the more compact ket notation $|nlm\rangle$ for the eigenstates, with the orthonormality condition now reading as

$$\langle nlm|n'l'm'\rangle = \delta_{nn'}\delta_{ll'}\delta_{mm'} \ . \tag{3.9}$$

The corresponding eigenvalues of the energy then are

$$E_n = -\frac{1}{(4\pi\varepsilon_0)^2}\,\frac{Z^2 e^4 m_\mathrm{e}}{2\hbar^2 n^2} \ , \tag{3.10}$$

which means that, for a pure Coulomb potential, the eigenvalues depend only on one of the indices, namely n. By convention, the energies are negative, indicating that the electron is bound to the center (nucleus). Since for $n > 1$ the quantum numbers l and m can have more than one value, we have the case of a set of eigenfunctions separated in subsets with the same eigenvalue. In other words, there are more than one eigenstate with the same energy. The spectrum is then said to be degenerate. This is due to the spherical symmetry of the system as well as the special form of the Coulomb potential. For a potential which is central but not Coulomb, the degeneracy in m remains, which is a direct consequence of spherical symmetry, but the degeneracy in l is lifted. It is customary to also call n the principal quantum number and l the orbital angular momentum quantum number. That is because, for an electron in state $|nlm\rangle$, the square of the angular momentum of the electron in its motion around the center of the attractive force is given by $l(l+1)$, while m ($-l \le m \le l$) represents the possible values of the projection of the orbital angular momentum (measured in units of $\hbar$) on the quantization axis z chosen for the description of the system. The degeneracy in m is lifted if the atom is placed in a magnetic field, known as the Zeeman effect, because of which m is also referred to as the magnetic quantum number. As expected on the basis of the general structure of quantum theory, we have found that the classical quantities energy and angular momentum of the electron bound to a center of attractive force can only assume discrete values in the quantum description of the system. By convention, due to historical reasons, states with $l = 0, 1, 2, 3, 4, 5, 6, 7, \ldots$ are denoted by s,p,d,f,g,h,i,k, $\ldots$ and often the electronic states of the atom are abbreviated as ns, np, etc.

The atoms of interest in quantum optics most often are the alkali atoms and especially Li, Na, Rb and Cs, their common feature being that they have one electron (the so-called valence electron) moving around a center of force determined by the charge of the nucleus and all of the other electrons belonging to the atom and forming a spherically symmetric shell. The net charge that the outer electron feels still is practically $Z = 1$, but the force, although central, is not a pure Coulomb force. As a result, the radial parts of the wavefunction are now much more complicated and the energy eigenvalues depend on l as well. Also, depending on which of the alkalies we are dealing with, the lowest value of n is no longer 1, because the other electrons have occupied lower orbits. Thus, it is $n = 2$ for Li, $n = 3$ for Na, $n = 5$ for Rb and $n = 6$ for Cs. The angular momentum quantum number for the lowest (ground) state of the valence electron still is $l = 0$. For our purposes in this book, we can consider the atom as an effectively one-electron (but

not hydrogen–like) atom, since the other more tightly bound electrons are insensitive to the processes of interest to us here. We can still work with the formalism for the wavefunctions established above for the hydrogen atom, keeping in mind that the radial parts are more complicated, although the overall features retain their character.

The electron which classically, as a particle, should have a definitive orbit eventually collapsing into the nucleus, now is represented by a wave extending in principle over all space. The quantity $|\Psi(\boldsymbol{r})|^2\,\mathrm{d}^3r$ provides the probability for the electron to be found within the volume element d^3r around the position $\boldsymbol{r}$. For that reason, $|\Psi(\boldsymbol{r})|^2$ is called probability density. If we examine the eigenfunctions $\Psi_{nlm}(\boldsymbol{r})$, we find that the lower n and l are, the more concentrated is the probability density $|\Psi_{nlm}(\boldsymbol{r})|^2$ closer to the center of attraction, spreading outward as n and l increase, retaining thus some analogy to the classical behavior. All radial parts vanish at $\boldsymbol{r} = 0$, with the exception of the states of zero angular momentum s which have a maximum at $\boldsymbol{r} = 0$. The quantity

$$a_0 = \frac{4\pi\varepsilon_0\hbar^2}{m_\mathrm{e}e^2} = 0.5292 \times 10^{-10}\,\mathrm{m} \tag{3.11}$$

is referred to as the Bohr radius of the hydrogen atom in its ground state, providing an order of magnitude estimate of the radial extent of the atom, in the sense of the region in which the electron is to be found most of the time. The proper quantum mechanical measure of the "extent" of the wavefunction of the electron, however, is provided by the expectation values of the type

$$\langle r^k\rangle \equiv \int \mathrm{d}^3r\,\Psi^*(\boldsymbol{r})|\boldsymbol{r}|^k\Psi(\boldsymbol{r}) = \int_0^\infty R_{nl}^* r^k R_{nl}\,r^2\mathrm{d}r\ .$$

Thus for $k = 1$, we have the expectation value of the radial position in state $|nlm\rangle$ given by the analytical expression

$$\langle r\rangle = \left[3n^2 - l(l+1)\right]\frac{a_0}{2Z}\ ,$$

which for the ground state $n = 1$ and $l = 0$ of hydrogen ($Z = 1$) is indeed quite close to the Bohr radius, $\langle r\rangle = \frac{3}{2}a_0$.

The behavior of the wavefunction under the change of $\boldsymbol{r}$ to $-\boldsymbol{r}$ is said to characterize the parity of the state. If we define the parity operator $\hat{P}$ by the operation $\hat{P}\Psi(\boldsymbol{r}) = \Psi(-\boldsymbol{r})$, we easily see that

$$\hat{P}^2\Psi(\boldsymbol{r}) = \hat{P}\Psi(-\boldsymbol{r}) = \Psi(\boldsymbol{r})\ , \tag{3.12}$$

which means that $\Psi(\boldsymbol{r})$ is an eigenstate of $\hat{P}^2$ with eigenvalue $P^2 = 1$ and also an eigenstate of $\hat{P}$ with eigenvalue $P = \pm 1$. Consequently, the eigenfunctions $\Psi(\boldsymbol{r})$ must either change sign or remain unchanged, under the parity operation. They are said to be of odd parity in the first case and of even parity in the second. The parity of the eigenfunctions in a central potential is even for even

values and odd for odd values of l. An immediate consequence of this property is that the matrix element

$$\langle nlm|\,\boldsymbol{r}\,|n'l'm'\rangle \equiv \int \mathrm{d}^3 r\, \Psi^*_{nlm}(\boldsymbol{r})\,\boldsymbol{r}\,\Psi_{n'l'm'}(\boldsymbol{r})\ , \tag{3.13}$$

can be non zero only between the states $|nlm\rangle$ and $|n'l'm'\rangle$ having even and odd angular momentum (i.e., states of different parity), because in (3.13) $\boldsymbol{r}$ is itself an odd function. This property in needed in the interaction of the atom with an electromagnetic field.

3.1.2 Angular Momentum and Spin in Quantum Theory

Orbital angular momentum was encountered in the previous section trough the solution of the Schrödinger equation for a particle in a central potential. The relevant quantum operator is the differential operator in (3.4) involving the angles θ and ϕ. Its eigenstates are the spherical harmonics $Y_l^m(\theta,\phi)$ with eigenvalues $l(l+1)$ and m. The explicit differential form of the operator has to do with the particular system of coordinates chosen. It is useful to generalize the notion of angular momentum by distilling its essential properties as an operator. First, note that it is a vector operator and as such, it has three components. Thus if we denote by $\boldsymbol{J}$ a general, dimensionless, Hermitian angular momentum operator, in a system of Cartesian coordinates, it will have the components J_x, J_y, J_z. The essential property that defines an angular momentum operator is that its components obey the commutation relations

$$[J_x, J_y] = \mathrm{i}J_z\ , \quad [J_y, J_z] = \mathrm{i}J_x\ , \quad [J_z, J_x] = \mathrm{i}J_y\ , \tag{3.14}$$

which can be written in the more compact form $\boldsymbol{J}\times\boldsymbol{J} = \mathrm{i}\boldsymbol{J}$. The operator $\boldsymbol{J}^2 = \boldsymbol{J}\cdot\boldsymbol{J} = J_x^2 + J_y^2 + J_z^2$, representing the square of the angular momentum $\boldsymbol{J}$, commutes with its three components J_x, J_y, J_z, which, however, do not commute with each other. We expect therefore to be able to find a set of eigenstates common to $\boldsymbol{J}^2$ and one of its components, usually chosen to be J_z. That is exactly what was done in the previous section through the differential equation. The spherical harmonics Y_l^m indeed are simultaneous eigenstates of the orbital angular momentum operators $\boldsymbol{l}^2$ and l_z with respective eigenvalues $l(l+1)$ and m. Thus if a system is known to involve a dynamical variable corresponding to an angular momentum operator $\boldsymbol{J}$, the relevant eigenstates can be labeled as $|J,M\rangle$ which satisfy the equations

$$\boldsymbol{J}^2\,|J,M\rangle = J(J+1)\,|J,M\rangle\ , \quad J_z\,|J,M\rangle = M\,|J,M\rangle\ , \tag{3.15}$$

where the values of M range from $-J$ to J, with J being positive. There are therefore $2J+1$ eigenstates of J_z for a given J. It also follows that J can only have integer or half integer values. We are simply stating here without proof the above properties; the relevant derivation is obtained most succinctly through an algebraic procedure which almost parallels that for the harmonic

oscillator and can be found in most books on quantum theory. In the process of the derivation, one introduces the non-Hermitian operators

$$J_\pm = J_x \pm \mathrm{i} J_y \tag{3.16}$$

referred to as raising and lowering operators because of their action on $|J, M\rangle$, namely

$$J_\pm \, |J, M\rangle = \big[J(J+1) - M(M \pm 1)\big]^{1/2} \, |J, M \pm 1\rangle \; . \tag{3.17}$$

They are the analogues of the creation and annihilation operators of Sect. 1.2.3. In addition, they obey the following commutation relations

$$[J_+, J_-] = 2J_z \; , \quad [J_\pm, J_z] = \mp J_\pm \; , \tag{3.18}$$

from which we can easily prove the useful relations

$$\boldsymbol{J}^2 = J_z^2 + \tfrac{1}{2}(J_+ J_- + J_- J_+) \; , \quad J_\pm J_\mp = \boldsymbol{J}^2 - J_z(J_z \mp 1) \; . \tag{3.19}$$

All of the above algebra, which fully determines the space and the eigenstates, is quite general, independent of whether there is a classical dynamical variable whose operator $\boldsymbol{J}$ is the quantum analogue—as is the case of orbital angular momentum—or an abstract quantum property without classical analogue. A case in point is the spin of the electron or any other elementary particle for that matter. Although there is a classical notion of spin, it can not serve as a strict analogue in the sense of something spinning inside the electron. Thus we adopt the notion of an intrinsic angular momentum, obeying the algebra described above with $J = \frac{1}{2}$ for which the symbol s is commonly used. The corresponding dimensionless spin operator is denoted as $\boldsymbol{s} \equiv \frac{1}{2}\boldsymbol{\sigma}$.

Since $s = \frac{1}{2}$, the possible values of the projection on the quantization axis z are $m_s = \frac{1}{2}$ and $m_s = -\frac{1}{2}$. We have thus two eigenstates labeled as $|s, m_s\rangle$, namely $|\frac{1}{2}, \frac{1}{2}\rangle$ and $|\frac{1}{2}, -\frac{1}{2}\rangle$. They can serve as a basis for a two-dimensional vector space. This is a case of a veritable two-level system, the relevant operators being $\boldsymbol{s}^2$, s_x, s_y, s_z, as well as $s_\pm = s_x + \mathrm{i} s_y$, obeying the general commutation relations (3.14) and (3.18). Alternative notations for the two eigenstates are

$$|\tfrac{1}{2}, \tfrac{1}{2}\rangle = |\uparrow_z\rangle = \begin{bmatrix} 1 \\ 0 \end{bmatrix} \; , \quad |\tfrac{1}{2}, -\tfrac{1}{2}\rangle = |\downarrow_z\rangle = \begin{bmatrix} 0 \\ 1 \end{bmatrix} \; . \tag{3.20}$$

The operators s_x, s_y, s_z can therefore be represented by the matrices

$$s_x \equiv \tfrac{1}{2}\sigma_x = \tfrac{1}{2}\begin{bmatrix} 0 & 1 \\ 1 & 0 \end{bmatrix} \; , \quad s_y \equiv \tfrac{1}{2}\sigma_y = \tfrac{1}{2}\begin{bmatrix} 0 & -\mathrm{i} \\ \mathrm{i} & 0 \end{bmatrix} \; , \quad s_z \equiv \tfrac{1}{2}\sigma_z = \tfrac{1}{2}\begin{bmatrix} 1 & 0 \\ 0 & -1 \end{bmatrix} \; , \tag{3.21}$$

where $\sigma_x, \sigma_y, \sigma_z$ are known as the Pauli spin matrices or simply Pauli matrices.

The electron happens to have an internal magnetic moment $\boldsymbol{\mu}_\mathrm{e}$ connected with its intrinsic spin through the relation $\boldsymbol{\mu}_\mathrm{e} = 2\mu_\mathrm{B}\boldsymbol{s}$, where $\mu_\mathrm{B} = -e\hbar/2m_\mathrm{e}c$

is a physical constant known as the Bohr magneton. When placed in a constant magnetic field $\boldsymbol{B}$, the magnetic moment couples to $\boldsymbol{B}$ through the interaction $\mathcal{V} = -\boldsymbol{\mu}_\mathrm{e} \cdot \boldsymbol{B}$. If the magnetic field is oriented along the z-axis, $\boldsymbol{B} = \hat{z}B$, the interaction leads to the lifting of the degeneracy between the two states with $m_s = \pm\frac{1}{2}$ which now have the energies $E_\pm = \pm e\hbar B/2m_\mathrm{e}c$, respectively. The spin precesses around the magnetic field with the frequency $\omega_0 = (E_+ - E_-)/\hbar = eB/m_\mathrm{e}c$, in analogy to the precession of a top spinning with its axis inclined with respect to the vertical.

3.1.3 Spin–Orbit Coupling

Since the electron carries electric charge, its orbital motion around the nucleus is equivalent to an electric current. An electric current generates a magnetic moment which in this case is called orbital magnetic moment $\boldsymbol{\mu} = \mu_\mathrm{B}\boldsymbol{l}$. This magnetic moment interacts with the spin magnetic moment and affects the energies of the atomic levels obtained in Sect. 3.1.1 without consideration of the spin. The correct energy of interaction, as obtained from the relativistic generalization of the theory, through the Dirac equation, is

$$\mathcal{V}_{ls} = \frac{\hbar^2}{2m_\mathrm{e}^2c^2}\frac{1}{r}\frac{\mathrm{d}V(r)}{\mathrm{d}r}\,\boldsymbol{l}\cdot\boldsymbol{s} = \frac{\hbar^2 Ze^2}{2m_\mathrm{e}^2c^2}\frac{\boldsymbol{l}\cdot\boldsymbol{s}}{4\pi\varepsilon_0 r^3}\,. \tag{3.22}$$

Before discussing what happens to the energies, however, we need to examine what happens to the angular momentum of the electron. We now have two angular momenta, the orbital $\boldsymbol{l}$ and the spin $\boldsymbol{s}$, which are coupled though a mutual interaction. Each of them has its own vector space but a complete description of the atom incorporating both requires the combination (tensor product) of the two spaces. This means that we need consider states of the form $|nlm_l\rangle\,|sm_s\rangle$ specifying the orbital as well as the spin state, in terms of uncoupled product states.

There is, however, an alternative approach. Briefly, it consists of considering the vector operator $\boldsymbol{j} = \boldsymbol{l} + \boldsymbol{s}$ resulting from the addition of two vector operators. Since both $\boldsymbol{l}$ and $\boldsymbol{s}$ are angular momentum operators, so is $\boldsymbol{j}$, as one can easily verify by examining the commutation relations of $\boldsymbol{j}$ and its components, taking into account the commutation relations for $\boldsymbol{l}$ and $\boldsymbol{s}$, as well as the fact that all components of $\boldsymbol{l}$ commute with those of $\boldsymbol{s}$, since they refer to different spaces. Therefore $\boldsymbol{j}$ possesses eigenstates of the form $|jm\rangle$ obtainable through the procedure of Sect. 3.1.2. If we combine the entire basis $\{\,|lm_l\rangle\}$ with the basis $\{\,|sm_s\rangle\}$, we obtain a basis for the tensor product space, whose vectors describe both the orbital and the spin state of the system. Thus any state of the system could be written as a linear combination of tensor products of the eigenstates of the form $|lm_l\rangle\,|sm_s\rangle$. Such a basis must be equivalent to the basis of the eigenstates $|j,m\rangle$ containing all eigenstates in this representation, which includes all j's resulting from the combination of all l's with s. The two bases are related by a transformation matrix. The

quantity j is called total angular momentum. Its eigenstates can in general be expressed as

$$|j,m\rangle = \sum_{\substack{m_l,m_s \\ (m_l+m_s=m)}} C^j_{m_l m_s} \, |lm_l\rangle \, |sm_s\rangle \ , \tag{3.23}$$

where the coefficients $C^j_{m_l m_s} \equiv \langle lm_l; sm_s|j,m\rangle$, referred to as Clebsch–Gordan coefficients, are known, well-studied quantities that can be found in books on angular momentum. They are non-zero only for values of m_l and m_s such that $m_l + m_s = m$. Obviously the inverse transformation can also be obtained.

We need not dwell upon the detailed mathematical description of this addition of angular momenta here, but we do need to know some of the consequences. Each atomic state in a one-electron atom is characterized by the total angular momentum j. According to the algebra of this vector addition of angular momenta, each state $|nlm_l\rangle$ of the electron without spin when coupled with the spin states leads to two new states with total angular momenta $j = l + \frac{1}{2}$ and $j = l - \frac{1}{2}$, with m-values according to the rules described above. Thus a state that was labeled as $|nlm_l\rangle$ before, when combined with the electron spin, gives rise to the states labeled as $|nlm_l; l+\frac{1}{2}, m\rangle$ and $|nlm_l; l-\frac{1}{2}, m\rangle$. The principal quantum number n remains unaffected as it has nothing to do with angular momentum. Since the value of the spin s is always $\frac{1}{2}$, it is often omitted in the notation. For example, a state with $l = 0$ (s-state; not to be confused with the spin s) gives rise to one new state with $j = \frac{1}{2}$, often denoted in the abbreviated notation as $\mathrm{s}_{1/2}$. In this notation, the ground state of the Na atom, which has principal quantum number 3, is denoted by $3\mathrm{s}_{1/2}$. The first excited state, which has $n = 3$ and $l = 1$ (p-state), generates two states with $j = \frac{1}{2}$ and $\frac{3}{2}$, denoted by $3\mathrm{p}_{1/2}$ and $3\mathrm{p}_{3/2}$, respectively. The energies of the new states are shifted from the position of the energy of the nl state, typically the one with $j = l + \frac{1}{2}$ upwards and $j = l - \frac{1}{2}$ downwards. This change of energies, known as the fine structure splitting of the energy levels characterized by the same principal n and orbital l quantum numbers, is due to the interaction between the orbital and spin magnetic moments given by (3.22).

3.2 Coupling of Radiation Field with Atomic Electron

The non-relativistic Hamiltonian for an electron of charge $-e$ bound by a central potential $V(r)$ and placed in an electromagnetic field, in the Coulomb gauge, is given by

$$\mathcal{H} = \frac{1}{2m_\mathrm{e}} \big[\boldsymbol{\mathcal{P}} - e\boldsymbol{A}(\boldsymbol{r})\big]^2 + V(r) \ , \tag{3.24}$$

with $\boldsymbol{\mathcal{P}} = -\mathrm{i}\hbar\boldsymbol{\nabla}$ the momentum operator of the electron and $\boldsymbol{A}(\boldsymbol{r})$ the vector potential of the field at the electron's position $\boldsymbol{r}$. Due to the Coulomb gauge

(transversality) condition $\boldsymbol{\nabla}\cdot\boldsymbol{A}=0$, we have $\boldsymbol{\mathcal{P}}\cdot\boldsymbol{A}=\boldsymbol{A}\cdot\boldsymbol{\mathcal{P}}$, which allows us to write $\big[\boldsymbol{\mathcal{P}}-e\boldsymbol{A}\big]^2=\boldsymbol{\mathcal{P}}^2-2e\,\boldsymbol{\mathcal{P}}\cdot\boldsymbol{A}+e^2\boldsymbol{A}^2$. Equation (3.24) then takes the form

$$\mathcal{H}=\mathcal{H}^{\mathrm{A}}+\mathcal{V}^{\mathrm{AF}}\ , \tag{3.25}$$

with

$$\mathcal{H}^{\mathrm{A}}=\frac{\boldsymbol{\mathcal{P}}^2}{2m_{\mathrm{e}}}+V(r)\ , \tag{3.26a}$$

$$\mathcal{V}^{\mathrm{AF}}=-\frac{e}{m_{\mathrm{e}}}\boldsymbol{\mathcal{P}}\cdot\boldsymbol{A}+\frac{e^2}{2m_{\mathrm{e}}}\boldsymbol{A}^2\ . \tag{3.26b}$$

Here $\mathcal{H}^{\mathrm{A}}$ is the Hamiltonian of the atom alone, whose eigenstates were discussed in Sect. 3.1.1, while $\mathcal{V}^{\mathrm{AF}}$ represents the interaction (coupling) of the atom with the field. Although the nucleus is also charged, for our purposes in this book, namely the interaction of atoms with radiation of optical and longer wavelengths, its interaction with the electromagnetic field is negligible. Thus if we are to investigate what happens to an atom, initially in one of its eigenstates, placed in an electromagnetic field, we need to calculate the matrix elements of $\mathcal{V}^{\mathrm{AF}}$ between eigenstates of the unperturbed atomic Hamiltonian $\mathcal{H}^{\mathrm{A}}$.

If the field is described classically, the vector potential $\boldsymbol{A}$ can be expanded in terms of c-numbers, as in (2.9). If on the other hand the field is described quantum mechanically, the Hamiltonian of the free field $\mathcal{H}^{\mathrm{F}}=\sum_{\boldsymbol{k}\lambda}\hbar\omega_k a^\dagger_{\boldsymbol{k}\lambda}a_{\boldsymbol{k}\lambda}$ must be included in (3.25), in which case the total Hamiltonian is

$$\mathcal{H}=\mathcal{H}^{\mathrm{A}}+\mathcal{H}^{\mathrm{F}}+\mathcal{V}^{\mathrm{AF}}\ , \tag{3.27}$$

where now $\boldsymbol{A}$ is an operator given by (2.22a). In the first case, we have matrix elements between atomic eigenstates. In the second, we have matrix elements between product eigenstates specifying the atomic and field states.

In either case, the vector potential $\boldsymbol{A}(\boldsymbol{r})$ in general depends on $\boldsymbol{r}$ through the expansion in terms of the spatial eigenfunctions $\boldsymbol{u}_{\boldsymbol{k}\lambda}(\boldsymbol{r})=\hat{\boldsymbol{e}}_{\boldsymbol{k}\lambda}\exp(\mathrm{i}\boldsymbol{k}\cdot\boldsymbol{r})$ as in (2.9). As long as one is interested in phenomena involving radiation of long wavelength, meaning large compared to the size of the atom a_0, which is certainly the case here, the spatial dependence of the field can be neglected. That is, taking the power series expansion

$$\exp(\mathrm{i}\boldsymbol{k}\cdot\boldsymbol{r})=1+\mathrm{i}\boldsymbol{k}\cdot\boldsymbol{r}-\tfrac{1}{2}(\boldsymbol{k}\cdot\boldsymbol{r})^2+\ldots$$

and retaining only the first term, since $\boldsymbol{k}\cdot\boldsymbol{r}\lesssim ka_0\ll 1$, we obtain

$$\boldsymbol{A}(\boldsymbol{r})\simeq\boldsymbol{A}(0)=\sum_{\boldsymbol{k}\lambda}\hat{\boldsymbol{e}}_{\boldsymbol{k}\lambda}\big[A_{\boldsymbol{k}\lambda}+A^*_{\boldsymbol{k}\lambda}\big]\ , \tag{3.28}$$

which is known as the dipole approximation. We thus need to calculate the matrix elements of $\mathcal{V}^{\mathrm{AF}}$ between pairs of atomic eigenstates $|nlm_l\rangle$ and $|n'l'm'_l\rangle$,

$$\langle nlm_l|\,\mathcal{V}^{\mathrm{AF}}\,|n'l'm'_l\rangle = -\boldsymbol{A}\frac{e}{m_{\mathrm{e}}}\langle nlm_l|\,\boldsymbol{\mathcal{P}}\,|n'l'm'_l\rangle\ , \tag{3.29}$$

where we have ignored the term containing $\boldsymbol{A}^2$ which, strictly speaking, is part of the interaction (3.26b). In the dipole approximation, however, this term does not involve atomic operators and, consequently, its matrix elements between orthogonal atomic states are zero. The problem thus reduces to the calculation of the matrix elements of $\boldsymbol{\mathcal{P}}$. It is more common in quantum optics, however, to discuss the atom–field interaction in terms of the dipole coupling

$$\mathcal{V}^{\mathrm{AF}} = -e\boldsymbol{r}\cdot\boldsymbol{E}\ , \tag{3.30}$$

which is more intuitive physically, since classically the potential energy of a dipole $e\boldsymbol{r}$ placed in an electric field $\boldsymbol{E}$ is given precisely by (3.30). It is not difficult to find the relation between the matrix elements of operators $\boldsymbol{\mathcal{P}}$ and $\boldsymbol{r}$. Using the relation

$$[\boldsymbol{r},\mathcal{H}^{\mathrm{A}}] = \mathrm{i}\frac{\hbar}{m_{\mathrm{e}}}\boldsymbol{\mathcal{P}}\ , \tag{3.31}$$

which is easy to prove taking into account the commutation relation between $\boldsymbol{r}$ and $\boldsymbol{\mathcal{P}}$ (see Prob. 3.1), we have

$$\begin{aligned}\frac{e}{m_{\mathrm{e}}}\langle nlm_l|\,\boldsymbol{\mathcal{P}}\,|n'l'm'_l\rangle &= -\mathrm{i}\frac{e}{\hbar}\langle nlm_l|\,\boldsymbol{r}\mathcal{H}^{\mathrm{A}} - \mathcal{H}^{\mathrm{A}}\boldsymbol{r}\,|n'l'm'_l\rangle \\ &= \mathrm{i}\omega_{nn'}e\,\langle nlm_l|\,\boldsymbol{r}\,|n'l'm'_l\rangle\ ,\end{aligned} \tag{3.32}$$

where $\omega_{nn'} = (E_n - E_{n'})/\hbar$ is the frequency of the atomic transition $|n'l'm'_l\rangle \rightarrow |nlm_l\rangle$. For a monochromatic field of frequency $\omega \simeq \omega_{nn'}$, the electric field can be expressed through the vector potential as $\boldsymbol{E} = \mathrm{i}\omega\boldsymbol{A}$. One can then verify that the two forms of the atom–field interaction Hamiltonian, (3.26b) and (3.30), are equivalent.

For the sake of completeness, it is perhaps worth noting here that the dipole approximation can also be arrived at from a different, more formal and, depending on taste, more systematic approach, discussed, e.g., in Cohen-Tannoudji, Dupont-Roc and Grynberg (1989). It consists of a canonical transformation of the Lagrangian of an electron in the electromagnetic field. Through the transformation, the interaction between the electron and the field is expressed in the form of an expansion, known as the multipole expansion, the first term of which is $-e\boldsymbol{r}\cdot\boldsymbol{E}$, this being expression (3.30) above. The atomic operator $e\boldsymbol{r} \equiv \boldsymbol{\wp}$ is often referred to as the dipole moment operator and transitions involving this operator as dipole transitions.

The conditions under which the matrix elements of $\mathcal{V}^{\mathrm{AF}}$ do not vanish are referred to as selection rules. These rules can equivalently be discussed in terms of the matrix elements $\langle nlm_l|\,\hat{\boldsymbol{e}}\cdot\boldsymbol{\mathcal{P}}\,|n'l'm'_l\rangle$ or $\langle nlm_l|\,\hat{\boldsymbol{e}}\cdot\boldsymbol{r}\,|n'l'm'_l\rangle$; for concreteness we employ the latter. For linearly polarized radiation, it is customary to take the polarization (unit) vector of the radiation $\hat{\boldsymbol{e}}$ as the z-axis, in which case $\hat{\boldsymbol{e}}\cdot\boldsymbol{r} = z$ and the matrix element is $\langle nlm_l|\,z\,|n'l'm'_l\rangle$.

This matrix element is non-zero only when $l - l' = \pm 1$ and $m_l = m_{l'}$. For circularly polarized radiation, the z-axis is taken along the propagation direction (wavevector) $\boldsymbol{k}$ of the radiation. Then, the unit polarization vectors are $\hat{\boldsymbol{e}}_\pm = \hat{x} \pm \mathrm{i}\hat{y}$, the "+" corresponding to right and the "−" to left circularly polarized radiation. The respective atomic matrix elements are then non-vanishing when $m_l - m_{l'} = \pm 1$, with the selection rule for the orbital angular momenta l, l' remaining the same. Mathematically, these rules follow from the properties of the spherical harmonics, since the polarization vectors can also be expressed in terms of spherical harmonics. Physically, they are due to the fact that the photon, in the dipole approximation, has one unit of angular momentum which must be accommodated—absorbed or emitted—between the atomic states; hence the condition $l - l' = \pm 1$ which also follows from (3.13). When the atomic states are described in the angular momentum basis $|ls; jm\rangle$, the selection rules for m are identical to those for m_l. The selection rules for l remain the same, while the rule for j in a matrix element of the type $\langle nls; jm| \, \hat{\boldsymbol{e}} \cdot \boldsymbol{r} \, |n'l's'; j'm'\rangle$ is $j - j' = 0, \pm 1$, with the restriction that $j = j' = 0$ is forbidden.

We have thus outlined the basic principles of atomic physics and the selection rules for the dipole–coupling of an atom to electromagnetic fields. In the next section, we study the dynamical evolution of an atom placed in a monochromatic (single mode) classical or quantum field whose frequency is close to a particular atomic transition frequency, while in the Sect. 3.5.2 we derive the exponential (Weisskopf–Wigner) law of spontaneous decay of an excited atom.

3.3 Two-Level Atom Interacting with Monochromatic Fields

An elementary but basic tool in quantum optics is the two-level system. In the context of quantum information studied in Part II, the two-level system plays an even more fundamental role, as it can be employed to represent and manipulate the elementary unit of quantum information called quantum bit, or qubit for short. Physically, the two-level system can, in principle, be any quantum system two levels of which have been selected for involvement in the necessary operations, which are nothing more than combinations of transformations in the appropriate vector space representing the quantum states under consideration. Mathematically, the two-level system is equivalent to a spin-$\frac{1}{2}$ system.

The transformations mentioned above correspond to physical processes implemented through the interaction of the two-level system with another quantum or even classical system. In quantum optics, such interactions serve the purpose of exploring and elucidating the quantum and statistical properties of the electromagnetic field. Their understanding proves later helpful in selecting the systems and processes that may be useful and hopefully practical

in implementing quantum information processing. An atom interacting with an electromagnetic field whose frequency is close to the frequency of transition between a particular pair of atomic eigenstates represents, to a very good approximation, a two-level system that involves all aspects essential to our purpose. As will be seen in later chapters, it is thus useful to discuss the dynamical behavior of the atom–field interaction in some detail.

3.3.1 Interaction of an Atom with a Classical Field

Let $|g\rangle$ and $|e\rangle$ denote the lower (ground) and upper (excited) states of an atom, with respective energies $E_g = \hbar\omega_g$ and $E_e = \hbar\omega_e > E_g$, as depicted schematically in Fig. 3.1. The corresponding frequency of the atomic transition $|g\rangle \leftrightarrow |e\rangle$ is $\omega_{eg} = \omega_e - \omega_g$. Then the Hamiltonian for the atom placed in an electromagnetic field is

$$\mathcal{H} = \mathcal{H}^{\mathrm{A}} + \mathcal{V}^{\mathrm{AF}}(t) \,, \tag{3.33}$$

with the atomic and interaction terms given by

$$\mathcal{H}^{\mathrm{A}} = \hbar\omega_g \, |g\rangle\langle g| \, + \hbar\omega_e \, |e\rangle\langle e| \;, \tag{3.34a}$$

$$\mathcal{V}^{\mathrm{AF}}(t) = -\boldsymbol{\wp} \cdot \boldsymbol{E}(t) = -\wp E(t) \,, \tag{3.34b}$$

where $\wp = \boldsymbol{\wp} \cdot \hat{\boldsymbol{e}}$ is the projection of the electric dipole operator on the polarization direction $\hat{\boldsymbol{e}}$ of the electric field of amplitude

$$E(t) = \mathcal{E}\mathrm{e}^{-\mathrm{i}\omega t} + \mathcal{E}^{*}\mathrm{e}^{\mathrm{i}\omega t} = 2|\mathcal{E}| \cos(\omega t - \varphi) \,, \tag{3.35}$$

with ω being its frequency and φ the phase. We are for the moment assuming an externally imposed and controlled classical monochromatic field. Its polarization $\hat{\boldsymbol{e}}$ for simplicity is taken here to be linear, but of course could be chosen circular, if needed. Note that by simply replacing $\boldsymbol{\wp}$ by the magnetic moment $\boldsymbol{\mu}$, and $\boldsymbol{E}(t)$ by a harmonically varying magnetic field $\boldsymbol{B}(t)$, the problem changes to the standard textbook case of magnetic resonance.

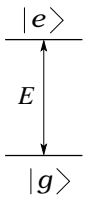

Fig. 3.1. Two-level atom interacting with a monochromatic field E.

Although a more thorough description of the dynamics of the two-level atom is obtained through the use of the density matrix discussed in Sect. 4.1.3, for reasons of simplicity we shall in this chapter proceed with the wavefunction

approach of Sect. 1.2.6. The state of the atom at any time can be expressed as

$$|\Psi(t)\rangle = c_g(t)\,|g\rangle + c_e(t)\,|e\rangle\ , \tag{3.36}$$

where c_g and c_e are the time-dependent complex amplitudes of the atomic eigenstates $|g\rangle$ and $|e\rangle$. The time-evolution of $|\Psi(t)\rangle$ is governed by the Schrödinger equation (1.117), i.e.,

$$\frac{\partial}{\partial t}\,|\Psi(t)\rangle = -\frac{\mathrm{i}}{\hbar}\mathcal{H}\,|\Psi(t)\rangle\ , \tag{3.37}$$

which for completeness requires an initial condition on $|\Psi(0)\rangle$. For concreteness, we take $c_g(0) = 1$ and $c_e(0) = 0$, i.e., the system is assumed to be initially in its ground state $|g\rangle$. Substituting (3.36) into (3.37), taking the inner product first with $|g\rangle$ and then with $|e\rangle$, and using the orthonormality of the eigenstates $|g\rangle$ and $|e\rangle$, we obtain

$$\frac{\partial}{\partial t}c_g = -\mathrm{i}\omega_g c_g + \mathrm{i}c_e\frac{\wp_{ge}}{\hbar}\big(\mathcal{E}\mathrm{e}^{-\mathrm{i}\omega t} + \mathcal{E}^*\mathrm{e}^{\mathrm{i}\omega t}\big)\ , \tag{3.38a}$$

$$\frac{\partial}{\partial t}c_e = -\mathrm{i}\omega_e c_e + \mathrm{i}c_g\frac{\wp_{eg}}{\hbar}\big(\mathcal{E}\mathrm{e}^{-\mathrm{i}\omega t} + \mathcal{E}^*\mathrm{e}^{\mathrm{i}\omega t}\big)\ , \tag{3.38b}$$

where $\wp_{ij} \equiv \langle i|\,\wp\,|j\rangle$ are the matrix elements of the dipole operator $\wp$. We have assumed that the diagonal matrix elements of $\wp$ are zero, $\wp_{gg} = \wp_{ee} = 0$, which is practically always valid in this context, while as usual $\wp_{ge} = \wp_{eg}^*$ and often these matrix elements can be taken real. Making the transformations $c_\mu(t) = \tilde{c}_\mu(t)\mathrm{e}^{-\mathrm{i}\omega_\mu t}$ $(\mu = g, e)$, which is equivalent to adopting the interaction picture, we obtain the differential equations for the slowly varying amplitudes $\tilde{c}_\mu(t)$ as

$$\frac{\partial}{\partial t}\tilde{c}_g = \mathrm{i}\tilde{c}_e\frac{\wp_{ge}}{\hbar}\big(\mathcal{E}\mathrm{e}^{-\mathrm{i}(\omega+\omega_{eg})t} + \mathcal{E}^*\mathrm{e}^{\mathrm{i}(\omega-\omega_{eg})t}\big) \simeq \mathrm{i}\tilde{c}_e\frac{\wp_{ge}}{\hbar}\mathcal{E}^*\mathrm{e}^{\mathrm{i}\Delta t}\ , \tag{3.39a}$$

$$\frac{\partial}{\partial t}\tilde{c}_e = \mathrm{i}\tilde{c}_g\frac{\wp_{eg}}{\hbar}\big(\mathcal{E}\mathrm{e}^{-\mathrm{i}(\omega-\omega_{eg})t} + \mathcal{E}^*\mathrm{e}^{\mathrm{i}(\omega+\omega_{eg})t}\big) \simeq \mathrm{i}\tilde{c}_g\frac{\wp_{eg}}{\hbar}\mathcal{E}\mathrm{e}^{-\mathrm{i}\Delta t}\ , \tag{3.39b}$$

where we have defined the detuning $\Delta \equiv \omega - \omega_{eg}$ of the radiation frequency from the resonance frequency ω_{eg} of the atomic transition. With the understanding that we shall be interested in near-resonant transitions, in the sense that $\Delta \ll \omega_{eg} \approx \omega$, we have adopted the rotating wave approximation (RWA), which amounts to neglecting the terms involving the exponentials $\mathrm{e}^{\pm\mathrm{i}(\omega+\omega_{eg})}$, i.e., oscillating with the sum frequencies $\pm(\omega + \omega_{eg})$, as opposed to those oscillating with the small difference frequencies $\pm\Delta$.

Although the above differential equations are easily solved by the elementary technique of substitution, we shall instead proceed through the method of Laplace transforms, in order to prepare the ground for somewhat more complicated problems that follow. Let

$$L_j(s) = \int_0^\infty \mathrm{d}t\,\mathrm{e}^{-st}\tilde{c}_j(t)$$

be the Laplace transform of $\tilde{c}_j(t)$. Taking the transforms of both sides of equations (3.39) we have

$$sL_g(s) - 1 = \mathrm{i}\frac{\wp_{ge}\mathcal{E}}{\hbar} L_e(s - \mathrm{i}\Delta) , \tag{3.40a}$$

$$sL_e(s) = \mathrm{i}\frac{\wp_{eg}\mathcal{E}^*}{\hbar} L_g(s + \mathrm{i}\Delta) , \tag{3.40b}$$

where we have used the following properties of the Laplace transform,

$$\int_0^\infty \mathrm{d}t\, \mathrm{e}^{-st}\dot{c}(t) = sL(s) - c(0) ,$$

$$\int_0^\infty \mathrm{d}t\, \mathrm{e}^{-st}\mathrm{e}^{pt}c(t) = L(s - p) .$$

From (3.40b) we have

$$(s - \mathrm{i}\Delta)L_e(s - \mathrm{i}\Delta) = \mathrm{i}\frac{\wp_{eg}\mathcal{E}^*}{\hbar} L_g(s) .$$

Solving for $L_e(s - \mathrm{i}\Delta)$ and substituting into (3.40a), we obtain an algebraic equation for $L_g(s)$, whose solution is

$$L_g(s) = \frac{s - \mathrm{i}\Delta}{s^2 - \mathrm{i}\Delta s + \Omega^2} , \tag{3.41}$$

where we have introduced the quantity $\Omega = \wp_{ge}|\mathcal{E}|/\hbar$ referred to as the Rabi frequency of the transition $|g\rangle \leftrightarrow |e\rangle$ under the field $\mathcal{E}$. The roots of the denominator in (3.41) are

$$s_\pm = \mathrm{i}\left[\frac{\Delta}{2} \pm \sqrt{\Omega^2 + \left(\frac{\Delta}{2}\right)^2}\right] .$$

Thus we have

$$L_g(s) = \frac{s - \mathrm{i}\Delta}{(s - s_+)(s - s_-)} , \tag{3.42}$$

from which it follows that the inverse Laplace transform of $L_g(s)$, which is $\tilde{c}_g(t)$, is given by

$$\tilde{c}_g(t) = \frac{s_+ - \mathrm{i}\Delta}{s_+ - s_-}\,\mathrm{e}^{s_+ t} - \frac{s_- - \mathrm{i}\Delta}{s_+ - s_-}\,\mathrm{e}^{s_- t} . \tag{3.43}$$

To compress notation somewhat, we define $\bar{\Omega} \equiv \sqrt{\Omega^2 + (\Delta/2)^2}$, which is an effective Rabi frequency for non-zero detuning Δ, reducing to the Rabi frequency Ω when $\Delta = 0$. Obviously $s_+ - s_- = \mathrm{i}2\bar{\Omega}$. Expressing the roots $s_\pm$ in terms of $\bar{\Omega}$ and after a few straightforward steps of trigonometric algebra, we obtain

$$\tilde{c}_g(t) = \mathrm{e}^{\mathrm{i}\frac{\Delta}{2}t}\left[\cos(\bar{\Omega}t) - \mathrm{i}\frac{\Delta}{2\bar{\Omega}}\sin(\bar{\Omega}t)\right] , \tag{3.44a}$$

$$\tilde{c}_e(t) = \mathrm{i}\mathrm{e}^{-\mathrm{i}\frac{\Delta}{2}t-\mathrm{i}\varphi}\frac{\Omega}{\bar{\Omega}}\sin(\bar{\Omega}t) , \tag{3.44b}$$

which satisfy the initial conditions, as well as the normalization condition $|\tilde{c}_g(t)|^2 + |\tilde{c}_e(t)|^2 = 1$ for all $t \geq 0$.

Clearly, for exact resonance $\Delta = 0$, we have

$$\tilde{c}_g(t) = \cos(\Omega t) , \quad \tilde{c}_e(t) = \mathrm{i}\mathrm{e}^{-\mathrm{i}\varphi}\sin(\Omega t) , \tag{3.45}$$

which explain why Ω is the Rabi frequency, as it represents the frequency of the oscillation of the two-level system between its two states under the driving by the external field. From the expression in (3.44), it is evident that for $\Delta \neq 0$ we have an additional phase difference Δt between the oscillations of the amplitudes $\tilde{c}_j(t)$ of the two states, while the phase difference is $\pi/2 - \varphi$ for exact resonance $\Delta = 0$. What we have here is a quantum system with its own resonance frequency ω_{eg} driven by an external classical field $E(t)$ oscillating at its own characteristic frequency ω. It is reasonable therefore that when the two frequencies match, the oscillation of the quantum system is most efficient, as illustrated in Fig. 3.2

So far, the discussion has been focused on the atom initially in the lower state $|g\rangle$. But for the atom initially in the upper state $|e\rangle$, the same steps obviously yield similar solutions, with the roles of the amplitudes $\tilde{c}_g$ and $\tilde{c}_e$ in (3.44) interchanged. In particular, for exact resonance $\Delta = 0$, we obtain

$$\tilde{c}_g(t) = \mathrm{i}\mathrm{e}^{\mathrm{i}\varphi}\sin(\Omega t) , \quad \tilde{c}_e(t) = \cos(\Omega t) . \tag{3.46}$$

We can thus write the evolution operator for the atom as

$$\mathcal{U}(t) \equiv \exp\left[-\tfrac{\mathrm{i}}{\hbar}\tilde{\mathcal{V}}t\right] = \begin{bmatrix} \cos\Omega t & \mathrm{i}\mathrm{e}^{\mathrm{i}\varphi}\sin\Omega t \\ \mathrm{i}\mathrm{e}^{-\mathrm{i}\varphi}\sin\Omega t & \cos\Omega t \end{bmatrix} , \tag{3.47}$$

where the interaction Hamiltonian is given by $\tilde{\mathcal{V}} = -\hbar\Omega\left[\mathrm{e}^{\mathrm{i}\varphi}\,|e\rangle\langle g| + \mathrm{H.c.}\right]$ with H.c. standing for the Hermitian conjugate. Clearly, when $\Omega t = \pi/2, 3\pi/2$, etc, the populations of states $|g\rangle$ and $|e\rangle$ are interchanged. For a pulsed field of certain duration τ (rectangular pulse), the quantity $\theta = 2\Omega\tau$ is called the pulse area; a more general definition of the pulse area is given in (6.42).

A quantity that will prove very useful in probing the effect of the quantum nature of the driving field is the so-called population inversion, or simply inversion for short, defined by

$$D_{\mathrm{cl}}(\mathcal{E}, t) = |c_e(t)|^2 - |c_g(t)|^2 . \tag{3.48}$$

Using (3.44), we have

$$\begin{aligned} D_{\mathrm{cl}}(\mathcal{E}, t) &= \frac{\Omega^2 - (\Delta/2)^2}{\Omega^2 + (\Delta/2)^2}\sin^2(\bar{\Omega}t) - \cos^2(\bar{\Omega}t) \\ &= -\left(\frac{\Omega}{\bar{\Omega}}\right)^2\cos(2\bar{\Omega}t) - \left(\frac{\Delta}{2\bar{\Omega}}\right)^2 , \end{aligned} \tag{3.49}$$

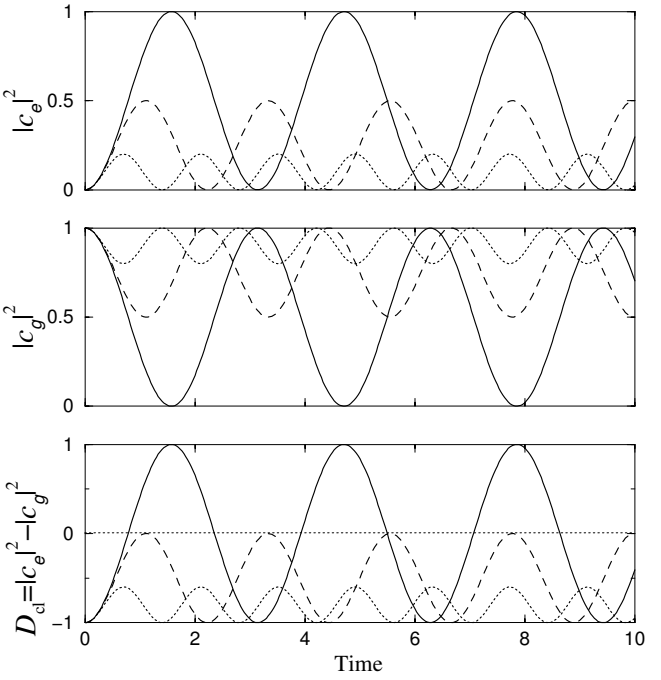

Fig. 3.2. Time-dependence of the populations $|\tilde{c}_e(t)|^2$ and $|\tilde{c}_g(t)|^2$ and the inversion $D_{\rm cl}$ for the driven two-level atom for the detunings $\Delta = 0$ (solid line), $\Delta = 2\Omega$ (dashed line) and $\Delta = 4\Omega$ (dotted line). The time is measured in units of Ω^{-1}.

which for $\Delta = 0$ obviously reduces to

$$D_{\rm cl}(\mathcal{E}, t) = -\cos(2\Omega t) \; . \tag{3.50}$$

The subscript of $D_{\rm cl}(\mathcal{E}, t)$ is meant to remind us that the field has been treated classically, with $\mathcal{E}$ denoting the magnitude of the field. Clearly, it is the combination of $\mathcal{E}$ with the coupling constant (dipole matrix element) $\wp_{ge}$ that determines the effectiveness of the oscillation, the measure of which is the Rabi frequency $\Omega = \wp_{ge}|\mathcal{E}|/\hbar$. The next step is to contrast the above behavior with that obtained when the field is treated quantum mechanically.

3.3.2 Interaction of an Atom with a Quantized Field: Jaynes–Cummings Model

Consider now the interaction of a single atom with the quantized field of a cavity, such as the one discussed in Sect. 2.1.2. We assume that the frequency ω of one of the cavity modes is near-resonant with the frequency ω_{eg} of the atomic transition $|g\rangle \leftrightarrow |e\rangle$, so that the atom effectively interacts only with that mode, while all of the other modes do not couple to the atom due to the

large frequency mismatch and can therefore be neglected, as is in fact the case in many experimental situations; later on we will specify more precisely the conditions under which this assumption is well justified. The total Hamiltonian for the system,

$$\mathcal{H} = \mathcal{H}^{\mathrm{A}} + \mathcal{H}^{\mathrm{F}} + \mathcal{V}^{\mathrm{AF}} \,, \tag{3.51}$$

has now three terms describing the two-level atom $\mathcal{H}^{\mathrm{A}}$, the cavity field $\mathcal{H}^{\mathrm{F}}$, and the atom–field interaction $\mathcal{V}^{\mathrm{AF}}$. Let us introduce the atomic operators $\sigma_z \equiv |e\rangle\langle e| - |g\rangle\langle g|$, $\sigma_+ \equiv |e\rangle\langle g|$ and $\sigma_- \equiv |g\rangle\langle e|$. Casting them in matrix form in the $\{|e\rangle, |g\rangle\}$ basis,

$$\sigma_z = \begin{bmatrix} 1 & 0 \\ 0 & -1 \end{bmatrix} \,, \quad \sigma_+ = \begin{bmatrix} 0 & 1 \\ 0 & 0 \end{bmatrix} \,, \quad \sigma_- = \begin{bmatrix} 0 & 0 \\ 1 & 0 \end{bmatrix} \,, \tag{3.52}$$

we see that σ_z coincides with the corresponding Pauli spin matrix, while the pseudo-spin raising σ_+ and lowering σ_- operators can be related to the Pauli matrices through $\sigma_\pm = \frac{1}{2}[\sigma_x \pm \mathrm{i}\sigma_y]$. In terms of these operators, the atomic Hamiltonian is given by

$$\mathcal{H}^{\mathrm{A}} = \tfrac{1}{2}\hbar\omega_{eg}\sigma_z = \tfrac{1}{2}\hbar\omega_{eg}\,|e\rangle\langle e| - \tfrac{1}{2}\hbar\omega_{eg}\,|g\rangle\langle g| \,, \tag{3.53}$$

i.e., the energy of state $|e\rangle$ is $E_e = \frac{1}{2}\hbar\omega_{eg}$ and that of $|g\rangle$ is $E_g = -\frac{1}{2}\hbar\omega_{eg}$. In other words, we choose the zero point of energy half-way between levels $|e\rangle$ and $|g\rangle$. Denoting by $\mathcal{U}_{\mathrm{A}}(t) = \mathrm{e}^{-\frac{\mathrm{i}}{\hbar}\mathcal{H}^{\mathrm{A}}t}$ the free evolution operator for the atom, we have

$$\mathcal{U}_{\mathrm{A}}^{\dagger}(t)\,\sigma_\pm\,\mathcal{U}_{\mathrm{A}}(t) = \sigma_\pm\,\mathrm{e}^{\pm\mathrm{i}\omega_{eg}t} \,.$$

which is equivalent to transforming the corresponding operators into the interaction picture. The Hamiltonian for the cavity field is $\mathcal{H}^{\mathrm{F}} = \hbar\omega a^\dagger a$, where $a^\dagger$ and a are the creation and annihilation operators for the field mode under consideration. In analogy with the atomic operators, in the interaction picture with $\mathcal{U}_{\mathrm{F}}(t) = \mathrm{e}^{-\frac{\mathrm{i}}{\hbar}\mathcal{H}^{\mathrm{F}}t}$ we have

$$\mathcal{U}_{\mathrm{F}}^{\dagger}(t)\,a\,\mathcal{U}_{\mathrm{F}}(t) = a\,\mathrm{e}^{-\mathrm{i}\omega t} \,, \quad \mathcal{U}_{\mathrm{F}}^{\dagger}(t)\,a^\dagger\,\mathcal{U}_{\mathrm{F}}(t) = a\,\mathrm{e}^{\mathrm{i}\omega t} \,.$$

Finally, in the dipole approximation, the atom–field interaction has the standard form $\mathcal{V}^{\mathrm{AF}} = -\wp E(z_0)$, where the electric field at the atomic position z_0 is given by $E(z_0) = \epsilon_\omega(a + a^\dagger)\sin(kz_0)$ with $\epsilon_\omega = \sqrt{\hbar\omega/\varepsilon_0 V}$ being the field per photon within the cavity volume V. Expressing the dipole moment operator as

$$\wp = |g\rangle\langle g|\,\wp\,|e\rangle\langle e| + |e\rangle\langle e|\,\wp\,|g\rangle\langle g| \equiv \wp_{ge}\sigma_- + \wp_{eg}\sigma_+ \,,$$

and defining the atom–cavity field coupling constant $g \equiv -(\wp_{ge}\epsilon_\omega/\hbar)\sin(kz_0)$, we can write

$$\mathcal{V}^{\mathrm{AF}} = \hbar g(\sigma_- + \sigma_+)(a + a^\dagger) \,, \tag{3.54}$$

where g is assumed real, without loss of generality. Let us denote by $\mathcal{H}^0 = \mathcal{H}^{\mathrm{A}} + \mathcal{H}^{\mathrm{F}}$ the sum of the free atomic and field Hamiltonians. Then in the interaction picture we have

$$\tilde{\mathcal{V}} \equiv \mathrm{e}^{\frac{\mathrm{i}}{\hbar}\mathcal{H}^0 t}\,\mathcal{V}^{\mathrm{AF}}\,\mathrm{e}^{-\frac{\mathrm{i}}{\hbar}\mathcal{H}^0 t} = \hbar g\big(a^\dagger\sigma_-\,\mathrm{e}^{\mathrm{i}(\omega-\omega_{eg})t} + \sigma_+ a\,\mathrm{e}^{-\mathrm{i}(\omega-\omega_{eg})t} + a^\dagger\sigma_+\,\mathrm{e}^{\mathrm{i}(\omega+\omega_{eg})t} + \sigma_- a\,\mathrm{e}^{-\mathrm{i}(\omega+\omega_{eg})t}\big)\,. \tag{3.55}$$

In this interaction Hamiltonian, the term of the form $a^\dagger\sigma_-$ corresponds to the process of atomic transition from the upper to the lower state and creation of one photon, while the term $\sigma_+ a$ describes the inverse process, both of which are near-resonant, $\Delta \equiv \omega - \omega_{eg} \ll \omega_{eg} \approx \omega$. On the other hand, the terms $a^\dagger\sigma_+$ and $\sigma_- a$, which in the interaction picture oscillate with the sum frequencies $\pm(\omega + \omega_{eg})$, describe the nonresonant processes in which the atom and the field are excited or de-excited simultaneously. In analogy with the classical case, these nonresonant terms, which do not conserve the total energy of the system, are dropped in the rotating wave approximation,

$$\mathcal{V}^{\mathrm{AF}} = \hbar g(\sigma_+ a + a^\dagger\sigma_-)\,, \tag{3.56}$$

and the total Hamiltonian becomes

$$\mathcal{H} = \tfrac{1}{2}\hbar\omega_{eg}\sigma_z + \hbar\omega a^\dagger a + \hbar g(\sigma_+ a + a^\dagger\sigma_-)\,. \tag{3.57}$$

A two-level system coupled to a single-mode electromagnetic field is known as the Jaynes–Cummings model.

Since we consider the problem of atom–field interaction in the fully quantized version, the complete state of the system should be specified via the states of both atom and field. In the energy eigenstate representation, the basis states of the field are the number states $|n\rangle$, with $n = 0, 1, 2, \ldots$ In the above Hamiltonian, the interaction $\mathcal{V}^{\mathrm{AF}}$ couples the states $|e\rangle\,|n\rangle \equiv |e, n\rangle$ and $|g\rangle\,|n+1\rangle \equiv |g, n+1\rangle$,

$$\langle g, n+1|\,\mathcal{H}\,|e, n\rangle = \langle e, n|\,\mathcal{H}\,|g, n+1\rangle = \hbar g\sqrt{n+1}\,. \tag{3.58}$$

The energies of these states are given by

$$E_{e,n} = \langle e, n|\,\mathcal{H}\,|e, n\rangle = \hbar\big(\omega n + \tfrac{1}{2}\omega_{eg}\big)\,, \tag{3.59a}$$

$$E_{g,n+1} = \langle g, n+1|\,\mathcal{H}\,|g, n+1\rangle = \hbar\big(\omega(n+1) - \tfrac{1}{2}\omega_{eg}\big) = E_{e,n} + \hbar\Delta\,, \tag{3.59b}$$

where $\Delta \equiv \omega - \omega_{eg}$ is the detuning. Thus the total Hilbert space $\mathbb{H}$ of the system consists of the mutually decoupled subspaces $\mathbb{H}_n = \{\,|e, n\rangle,\, |g, n+1\rangle\}$ for $n = 0, 1, 2, \ldots$ The Hamiltonian (3.57) can then be split into the sum $\mathcal{H} = \sum_n \mathcal{H}_n$ with each term

$$\mathcal{H}_n = E_{e,n}\begin{bmatrix} 1 & 0 \\ 0 & 1 \end{bmatrix} + \hbar\begin{bmatrix} 0 & g\sqrt{n+1} \\ g\sqrt{n+1} & \Delta \end{bmatrix}\,, \tag{3.60}$$

acting on its own subspace $\mathbb{H}_n$. Diagonalizing the matrix in (3.60), we find the eigenvalues

$$\lambda_{\pm}^{(n)} = \tfrac{1}{\hbar}E_{e,n} + \tfrac{1}{2}\Delta \pm \bar{\Omega}\,, \tag{3.61}$$

with $\bar{\Omega} \equiv \sqrt{g^2(n+1) + (\Delta/2)^2}$, and the corresponding eigenstates

$$|\pm_n\rangle = \frac{1}{\sqrt{N_\pm}}\big[\big(\bar{\Omega} \mp \tfrac{1}{2}\Delta\big)\,|e,n\rangle \pm g\sqrt{n+1}\,|g,n+1\rangle\big]\,, \tag{3.62}$$

where $N_\pm = \big(\bar{\Omega} \mp \frac{1}{2}\Delta\big)^2 + g^2(n+1)$ are the normalization constants. These are known as the dressed states of $\mathcal{H}_n$ (see Prob. 3.2). At resonance, $\Delta = 0$, we have

$$\lambda_{\pm}^{(n)} = \tfrac{1}{\hbar}E_{e,n} \pm g\sqrt{n+1}\,, \tag{3.63}$$

and

$$|\pm_n\rangle = \frac{1}{\sqrt{2}}\big[\,|e,n\rangle \pm |g,n+1\rangle\big]\,. \tag{3.64}$$

Thus the dressed states are given by the symmetric $|+_n\rangle$ and antisymmetric $|-_n\rangle$ superposition of the bare states $|e,n\rangle$ and $|g,n+1\rangle$ and are split by the amount $\lambda_+^{(n)} - \lambda_-^{(n)} = 2g\sqrt{n+1}$, which is twice the matrix element of (3.58). Below we consider the dynamics of the compound system for various given initial states of the atom and the cavity field.

Field in number (Fock) state (Q1)

Assume that initially, at $t = 0$, the atom is in the lower state $|g\rangle$ and the cavity contains precisely n photons, i.e., the field is in a number (Fock) state $|n\rangle$, $n = 1, 2, \ldots$ We will call this case quantum case 1 (Q1). Then the initial state of the system is $|g,n\rangle$, while the interaction term of the Hamiltonian (3.57) connects this initial state to the final state $|e,n-1\rangle$,

$$\langle e,n-1|\,\mathcal{V}^{\mathrm{AF}}\,|g,n\rangle = \langle g,n|\,\mathcal{V}^{\mathrm{AF}}\,|e,n-1\rangle = \hbar g\sqrt{n}\,. \tag{3.65}$$

In the interaction picture, the state vector of the compound system at any time has the form

$$|\tilde{\Psi}(t)\rangle = \tilde{c}_{g,n}(t)\,|g,n\rangle + \tilde{c}_{e,n-1}(t)\,|e,n-1\rangle\,, \tag{3.66}$$

and its time-evolution is governed by the Schrödinger equation (1.122), namely

$$\frac{\partial}{\partial t}\,|\tilde{\Psi}(t)\rangle = -\frac{\mathrm{i}}{\hbar}\tilde{\mathcal{V}}\,|\tilde{\Psi}(t)\rangle\,. \tag{3.67}$$

We assume exact resonance $\Delta \equiv \omega - \omega_{eg} = 0$, for which we obviously have $\tilde{\mathcal{V}}_{if} = \mathcal{V}_{if}^{\mathrm{AF}}$. We then obtain the following differential equations for the probability amplitudes of (3.66),

$$\frac{\partial}{\partial t}\tilde{c}_{g,n} = -\mathrm{i}\tilde{c}_{e,n-1}g\sqrt{n}\,, \tag{3.68a}$$

$$\frac{\partial}{\partial t}\tilde{c}_{e,n-1} = -\mathrm{i}\tilde{c}_{g,n}g\sqrt{n}\,, \tag{3.68b}$$

with the initial conditions $c_{g,n}(0) = 1$ and $c_{e,n-1}(0) = 0$. These equations have the same form as the corresponding amplitude equations for the two-level atom interacting with a resonant classical field. We can therefore immediately write their solution as

$$\tilde{c}_{g,n}(t) = \cos(g\sqrt{n}\,t)\ , \quad \tilde{c}_{e,n-1}(t) = -\mathrm{i}\sin(g\sqrt{n}\,t)\ , \tag{3.69}$$

yielding $|c_{g,n}(t)|^2 = \cos^2(g\sqrt{n}\,t)$ and $|c_{e,n-1}(t)|^2 = \sin^2(g\sqrt{n}\,t)$, which shows that the compound system "atom+field" oscillates between its two states $|g,n\rangle$ and $|e,n-1\rangle$ with the Rabi frequency $g\sqrt{n} = \frac{\wp_{ge}}{\hbar}\epsilon_\omega\sqrt{n}$, where for convenience we took $\sin(kz_0) = -1$. At intermediate times, when neither of the amplitudes $\tilde{c}_{g,n}(t)$ and $\tilde{c}_{e,n-1}(t)$ is zero, the compound system is in an entangled state, as the state vector $|\tilde{\Psi}(t)\rangle$ of (3.66) can not be written as a product of individual state vectors of the atom and the field. For the atomic population inversion

$$D_{\mathrm{Q1}}(n,t) \equiv \langle\tilde{\Psi}(t)|\,\sigma_z\,|\tilde{\Psi}(t)\rangle\ , \tag{3.70}$$

i.e., the expectation value of the σ_z operator, we obtain $D_{\mathrm{Q1}}(n,t) = -\cos(2g\sqrt{n}\,t)$, which is the same as in the case of a classical field—a rather strange result one may think, since, as we have seen, a field in state $|n\rangle$ is very different from classical.

But what if at time $t = 0$ the atom is in the upper state $|e\rangle$ and the field state is $|n\rangle$, $n = 0, 1, 2, \ldots$ We then have the initial state $|e,n\rangle$ coupled to the state $|g,n+1\rangle$, the corresponding matrix element of the interaction being $\langle g,n+1|\,\mathcal{V}^{\mathrm{AF}}\,|e,n\rangle = \hbar g\sqrt{n+1}$. The state vector of the system reads

$$|\tilde{\Psi}(t)\rangle = \tilde{c}_{e,n}(t)\,|e,n\rangle + \tilde{c}_{g,n+1}(t)\,|g,n+1\rangle\ . \tag{3.71}$$

Repeating the same procedure as before, we find

$$\tilde{c}_{e,n}(t) = \cos(g\sqrt{n+1}\,t)\ , \quad \tilde{c}_{g,n+1}(t) = -\mathrm{i}\sin(g\sqrt{n+1}\,t)\ , \tag{3.72}$$

from which we have $|c_{e,n}(t)|^2 = \cos^2(g\sqrt{n+1}\,t)$, $|c_{g,n+1}(t)|^2 = \sin^2(g\sqrt{n+1}\,t)$ and

$$D_{\mathrm{Q1}}(n,t) = \cos(2g\sqrt{n+1}\,t)\ . \tag{3.73}$$

This means that the atom periodically returns to the upper state with Rabi frequency $g\sqrt{n+1}$ which is non-zero even if $n = 0$, and hence is different from the Rabi frequency $g\sqrt{n}$ corresponding to the case of the atom being initially in the lower state $|g\rangle$. Thus an excited atom placed in an empty cavity ($n = 0$) undergoes periodic, *reversible* spontaneous decay. This is the basis of cavity quantum electrodynamics (cavity QED) discussed in more detail in Chap. 5. Note in addition that this result can not be obtained with a classical field of zero amplitude.

Field in coherent state (Q2)

Consider now the situation in which at $t = 0$ the atom is in the ground state $|g\rangle$ but the cavity field is in a coherent state $|\alpha\rangle$. The initial state of the compound system "atom+field" is thus $|g\rangle\,|\alpha\rangle \equiv |g, \alpha\rangle$. Upon expanding the coherent state in terms of the number state as in (2.35), we can write

$$|g, \alpha\rangle = \mathrm{e}^{-\frac{1}{2}|\alpha|^2} \sum_{n=0}^{\infty} \frac{\alpha^n}{\sqrt{n!}}\, |g, n\rangle \,. \tag{3.74}$$

The interaction Hamiltonian (3.56) couples each term $|g, n\rangle$ of this sum to the corresponding state $|e, n-1\rangle$, and every such pair of states evolves according to (3.68) with the corresponding solution given by (3.69). The state $|g, 0\rangle$ is an exception, since $\mathcal{V}^{\mathrm{AF}}\,|g, 0\rangle = 0$ and therefore it does not evolve in time under the action of $\mathcal{V}^{\mathrm{AF}}$. We can thus write the wavefunction of the system at any time $t \geq 0$ as

$$|\tilde{\Psi}(t)\rangle = \mathrm{e}^{-\frac{1}{2}|\alpha|^2} \left[|g, 0\rangle + \sum_{n=1}^{\infty} \frac{\alpha^n}{\sqrt{n!}} \left[\cos(g\sqrt{n}\, t)\, |g, n\rangle - \mathrm{i} \sin(g\sqrt{n}\, t)\, |e, n-1\rangle \right] \right] . \tag{3.75}$$

It is useful to consider also the case of an initial state corresponding to the excited atom,

$$|e, \alpha\rangle = \mathrm{e}^{-\frac{1}{2}|\alpha|^2} \sum_{n=0}^{\infty} \frac{\alpha^n}{\sqrt{n!}}\, |e, n\rangle \,. \tag{3.76}$$

so that the system can be driven even by the vacuum $\alpha = 0$. Now the initial states $|e, n\rangle$ are coupled via the interaction $\mathcal{V}^{\mathrm{AF}}$ to the states $|g, n+1\rangle$, and the corresponding solution for every such pair is given by (3.72). Consequently, the wavefunction of the system is

$$|\tilde{\Psi}(t)\rangle = \mathrm{e}^{-\frac{1}{2}|\alpha|^2} \sum_{n=0}^{\infty} \frac{\alpha^n}{\sqrt{n!}} \left[\cos(g\sqrt{n+1}\, t)\, |e, n\rangle - \mathrm{i} \sin(g\sqrt{n+1}\, t)\, |g, n+1\rangle \right] . \tag{3.77}$$

Note that the summation includes also the term with $n = 0$. We are interested in the atomic population inversion

$$D_{\mathrm{Q2}}(\alpha, t) \equiv \langle \tilde{\Psi}(t)|\, \sigma_z\, |\tilde{\Psi}(t)\rangle = \sum_{n=0}^{\infty} P_\alpha(n) D_{\mathrm{Q1}}(n, t) \,, \tag{3.78}$$

where $P_\alpha(n)$ is the probability of finding n photons in the coherent field given by (2.36) and $D_{\mathrm{Q1}}(n, t)$ is the atomic inversion of (3.73). We thus obtain

$$D_{\mathrm{Q2}}(\alpha, t) = \sum_{n=0}^{\infty} \mathrm{e}^{-\bar{n}} \frac{\bar{n}^n}{n!} \cos(2g\sqrt{n+1}t) \,, \quad \bar{n} \equiv |\alpha|^2 \,. \tag{3.79}$$

There exists no known closed form expression for $D_{\mathrm{Q2}}(\alpha, t)$ and it must be calculated numerically. For sufficiently short time and strong field, so that $t \ll |\alpha|/g$, the sum (3.79) can be shown to reduce to the approximate form

$$D_{\mathrm{Q2}} = \tfrac{1}{2}\left[1 + \cos(2|\alpha|gt)\, \exp(-g^2 t^2)\right] .$$

The long time behavior of the inversion for an atom placed in the quantum coherent field is shown in Fig. 3.3(a). Obviously, it is very different from that for a classical field of Fig. 3.2, even though $|\alpha\rangle$ is as close to a classical field as possible. Yet, the behavior under a quantum field in a number state $|n\rangle$ and classical field are identical. That is because the atomic inversion depends on the energy, and $|n\rangle$ is an eigenstate of the Hamiltonian of the field and has no fluctuations. We would need another process to detect a difference in behavior caused by a classical field and a field in a number state $|n\rangle$.

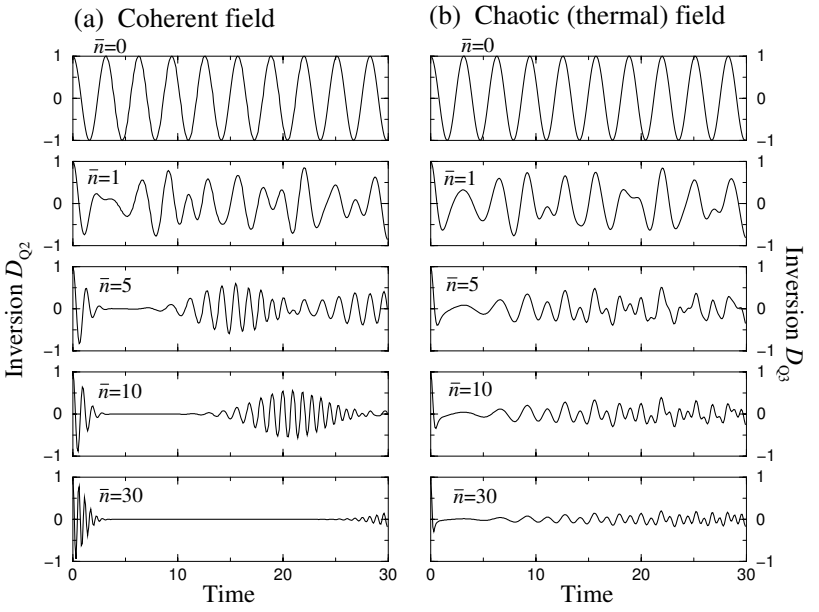

Fig. 3.3. Time-dependence of the inversion of a two-level atom interacting with a quantum single-mode coherent field (a), and chaotic (thermal) field (b).

The coherent state $|\alpha\rangle$, however, consists of a superposition of states $|n\rangle$ with fixed amplitudes $\alpha^n/\sqrt{n!}$. As is evident from (3.75) or (3.77), each component $|n\rangle$ of $|\alpha\rangle$ tends to drive the atom with its own Rabi frequency $g\sqrt{n}$ or $g\sqrt{n+1}$. As a result, the oscillations collapse, reviving later because of the quantum nature of the field and the particular relations between the coefficients of various $|n\rangle$. It is said that the inversion undergoes collapses and revivals, the time-scale of which depends on $g\sqrt{\bar{n}} = g|\alpha|$.

Chaotic (thermal) field (Q3)

There is one more quantum case of interest, in which the field is quantized but chaotic. In the case of a single-mode cavity, its walls and the surrounding environment of finite temperature T radiate thermal photons, which make up the chaotic field. Since there are no fixed phase relations between the coefficients of various $|n\rangle$, the state of the chaotic field can not be expressed through a wavefunction. But we know that the photon number distribution $P_{\rm Th}(n)$ is given by (2.46). With the atom initially in the excited state $|e\rangle$, the inversion reads

$$D_{\rm Q3} = \sum_{n=0}^{\infty} P_{\rm Th}(n) D_{\rm Q1}(n,t) = \sum_{n=0}^{\infty} \frac{\bar{n}^n}{(1+\bar{n})^{n+1}} \cos(2g\sqrt{n+1}t) \;, \qquad (3.80)$$

where $\bar{n} = (\mathrm{e}^{\hbar\omega/k_{\rm B}T} - 1)^{-1}$ is the average number of thermal photons in the mode. For $T = 0$, we have the vacuum $\bar{n} = 0$. For finite temperatures, the inversion must again be calculated numerically, and the results for various values of $\bar{n}$ are shown in Fig. 3.3(b). Clearly, there is no pattern, no revivals, completely chaotic behavior, no matter how long we wait, in striking contrast to the case of a coherent field having a Poissonian distribution of the occupation probabilities of the states $|n\rangle$.

3.4 Two-Level Atom in a Harmonic Potential

In Chap. 1, the harmonic oscillator has served the purpose of illustrating the transition from classical to quantum description of physical systems. In quantum optics, one interesting and important example of mechanical harmonic oscillator is an atom, or an ion, trapped in a nearly parabolic potential and subjected to an external driving field. Here we will not be concerned much with the nature of the trapping potential, noting briefly that neutral atoms can be confined relatively weakly by the dipole force mediated by off-resonant optical fields, while charged ions can be strongly confined by the combination of static and oscillating (radio-frequency) electric fields, as in the case of ion-traps described in Sect. 10.3. As will be seen shortly, a two-level atom (alias ion) driven by a near-resonant classical field and tightly confined in a harmonic trap, can closely resemble the Jaynes–Cummings model studied in the previous section. Here, however, it is the quantized motional (external) degrees of freedom of the atom that play a role analogous to that of the quantized cavity field, while the classical field couples the internal and external degrees of freedom of the atom.

We thus consider an atom of mass $M_{\rm A}$ confined in a parabolic potential $\frac{1}{2}M_{\rm A}\nu^2 x^2$, where ν is the frequency associated with the atomic motion in the trap, and x the atomic position. For simplicity we discuss here only the motion in one dimension (along x), noting that the other two dimensions

(along y and z) can be treated analogously. Such a treatment can in fact be a valid approximation when one deals with one-dimensional trap geometry, in which the confinement of the atom along the y and z directions is much stronger than that along x. The trapped two-level atom interacts with the coherent classical field of amplitude

$$E(\boldsymbol{r},t) = \mathcal{E}\mathrm{e}^{\mathrm{i}(\boldsymbol{k}\cdot\boldsymbol{r}-\omega t)} + \mathcal{E}^*\mathrm{e}^{-\mathrm{i}(\boldsymbol{k}\cdot\boldsymbol{r}-\omega t)} = 2|\mathcal{E}|\cos(\boldsymbol{k}\cdot\boldsymbol{r}-\omega t+\varphi)\ , \tag{3.81}$$

with $\boldsymbol{k}$ being its wavevector, ω the frequency and φ the phase. Now, the total Hamiltonian has three terms,

$$\mathcal{H} = \mathcal{H}^{\mathrm{A}} + \mathcal{H}^{\mathrm{M}} + \mathcal{V}^{\mathrm{AF}}\ , \tag{3.82}$$

the first term describing the internal degrees of freedom of the two-level atom,

$$\mathcal{H}^{\mathrm{A}} = \tfrac{1}{2}\hbar\omega_{eg}\sigma_z\ , \tag{3.83}$$

the second term representing the atomic motion in the trap,

$$\mathcal{H}^{\mathrm{M}} = \frac{1}{2M_{\mathrm{A}}}\,p^2 + \frac{M_{\mathrm{A}}\nu^2}{2}\,x^2\ , \tag{3.84}$$

and the last term being responsible for the position-dependent coupling of the atom with the classical field,

$$\begin{aligned}\mathcal{V}^{\mathrm{AF}} = -\wp E(\boldsymbol{r},t) &= -\big(\wp_{eg}\sigma_+ + \wp_{ge}\sigma_-\big)\big[\mathcal{E}\mathrm{e}^{\mathrm{i}(k_x x-\omega t)} + \mathcal{E}^*\mathrm{e}^{-\mathrm{i}(k_x x-\omega t)}\big] \\ &= -\hbar\Omega\big(\sigma_+ + \sigma_-\big)\big[\mathrm{e}^{\mathrm{i}(k_x x-\omega t+\varphi)} + \mathrm{e}^{-\mathrm{i}(k_x x-\omega t+\varphi)}\big]\ ,\end{aligned} \tag{3.85}$$

where k_x is the projection of $\boldsymbol{k}$ on the direction of atomic motion x, and $\Omega = \wp_{ge}|\mathcal{E}|/\hbar$ is the Rabi frequency. We are concerned here with the quantized motion of the atom in the harmonic potential. The general procedure for canonical quantization was described in Sect. 1.2. We therefore proceed along the lines of Sect. 1.2.3, replacing in the above expressions the classical position x and momentum p variables with the corresponding operators $\mathcal{Q}$ and $\mathcal{P}$ which obey the commutation relations (1.62). We further introduce the creation $b^\dagger$ and annihilation b operators for the harmonic oscillator as in (1.63), through which the position and momentum operators are expressed as

$$\mathcal{Q} = \sqrt{\frac{\hbar}{2M_{\mathrm{A}}\nu}}\big(b+b^\dagger\big)\ ,\quad \mathcal{P} = -\mathrm{i}\sqrt{\frac{M_{\mathrm{A}}\hbar\nu}{2}}\big(b-b^\dagger\big)\ . \tag{3.86}$$

With these definitions, omitting the zero point energy $\frac{1}{2}\hbar\nu$, the harmonic oscillator Hamiltonian (3.84) becomes $\mathcal{H}^{\mathrm{M}} = \hbar\nu b^\dagger b$, while in the atom-field interaction Hamiltonian (3.85) the quantity $k_x x$ is replaced with $\eta(b+b^\dagger)$, where

$$\eta \equiv k_x\,\Delta x_0 = k_x\sqrt{\frac{\hbar}{2M_{\mathrm{A}}\nu}}$$

is the so-called Lamb–Dicke parameter given by the product of wavevector k_x and the spatial extent $\Delta x_0 \equiv \sqrt{\hbar/(2M_{\rm A}\nu)}$ of the ground-state wavefunction of (1.57). Since k_x is inversely proportional to the wavelength, the Lamb–Dicke parameter quantifies the amplitude of the atomic oscillations in the trap relative to the wavelength of the applied field. The interaction Hamiltonian then reads

$$\mathcal{V}^{\rm AF} = -\hbar\Omega\big(\sigma_+ + \sigma_-\big)\big(\mathrm{e}^{\mathrm{i}[\eta(b+b^\dagger)-\omega t+\varphi]} + \mathrm{e}^{-\mathrm{i}[\eta(b+b^\dagger)-\omega t+\varphi]}\big)\ . \tag{3.87}$$

The dynamics of the atom driven by the classical field becomes most transparent if we make the transformation to the interaction picture. With $\mathcal{H}^0 = \mathcal{H}^{\rm A} + \mathcal{H}^{\rm M}$ denoting the Hamiltonian of the trapped atom alone, for the interaction picture Hamiltonian we have

$$\begin{aligned}\tilde{\mathcal{V}} &\equiv \mathrm{e}^{\frac{\mathrm{i}}{\hbar}\mathcal{H}^0 t}\,\mathcal{V}^{\rm AF}\,\mathrm{e}^{-\frac{\mathrm{i}}{\hbar}\mathcal{H}^0 t}\\ &= -\hbar\Omega\,\mathrm{e}^{\frac{\mathrm{i}}{\hbar}\mathcal{H}^{\rm A} t}\big(\sigma_+ + \sigma_-\big)\mathrm{e}^{-\frac{\mathrm{i}}{\hbar}\mathcal{H}^{\rm A} t}\\ &\quad\times \mathrm{e}^{\frac{\mathrm{i}}{\hbar}\mathcal{H}^{\rm M} t}\big[\mathrm{e}^{\mathrm{i}\eta(b+b^\dagger)}\,\mathrm{e}^{-\mathrm{i}(\omega t-\varphi)} + \mathrm{e}^{-\mathrm{i}\eta(b+b^\dagger)}\,\mathrm{e}^{\mathrm{i}(\omega t-\varphi)}\big]\mathrm{e}^{-\frac{\mathrm{i}}{\hbar}\mathcal{H}^{\rm M} t}\ .\end{aligned} \tag{3.88}$$

Recall that $\mathcal{U}_{\rm A}(t) = \mathrm{e}^{-\frac{\mathrm{i}}{\hbar}\mathcal{H}^{\rm A} t}$ and $\mathcal{U}_{\rm M}(t) = \mathrm{e}^{-\frac{\mathrm{i}}{\hbar}\mathcal{H}^{\rm M} t}$ represent the free evolution operators. We thus obtain

$$\mathcal{U}_{\rm A}^\dagger(t)\,\sigma_\pm\,\mathcal{U}_{\rm A}(t) = \sigma_\pm\,\mathrm{e}^{\pm\mathrm{i}\omega_{eg} t}\ .$$

Multiplying now the various terms of (3.88), and assuming that the field is near-resonant with the atomic transition, $\Delta \equiv \omega - \omega_{eg} \ll \omega_{eg} \approx \omega$, we can drop the terms oscillating with the sum frequencies $\pm(\omega+\omega_{eg})$, while keeping the terms oscillating with the small frequencies $\pm\Delta$, which amounts to making the rotating wave approximation. Next, for the harmonic oscillator operators we obviously have

$$\mathcal{U}_{\rm M}^\dagger(t)\,b\,\mathcal{U}_{\rm M}(t) = b\,\mathrm{e}^{-\mathrm{i}\nu t}\ ,\quad \mathcal{U}_{\rm M}^\dagger(t)\,b^\dagger\,\mathcal{U}_{\rm M}(t) = b^\dagger\,\mathrm{e}^{\mathrm{i}\nu t}\ ,$$

from where it follows that (Prob. 3.3)

$$\mathcal{U}_{\rm M}^\dagger(t)\,\mathrm{e}^{\pm\mathrm{i}\eta(b+b^\dagger)}\,\mathcal{U}_{\rm M}(t) = \exp\big[\pm\mathrm{i}\eta(b\,\mathrm{e}^{-\mathrm{i}\nu t} + b^\dagger\,\mathrm{e}^{\mathrm{i}\nu t})\big]\ . \tag{3.89}$$

We can now write the interaction Hamiltonian (3.88) in its final form,

$$\begin{aligned}\tilde{\mathcal{V}} = -\hbar\Omega\Big\{&\sigma_+\,\mathrm{e}^{-\mathrm{i}(\Delta t-\varphi)}\exp\big[\mathrm{i}\eta(b\,\mathrm{e}^{-\mathrm{i}\nu t} + b^\dagger\,\mathrm{e}^{\mathrm{i}\nu t})\big]\\ &+\sigma_-\,\mathrm{e}^{\mathrm{i}(\Delta t-\varphi)}\exp\big[-\mathrm{i}\eta(b\,\mathrm{e}^{-\mathrm{i}\nu t} + b^\dagger\,\mathrm{e}^{\mathrm{i}\nu t})\big]\Big\}\ .\end{aligned} \tag{3.90}$$

Let us note at this point that if $\eta = 0$, i.e., the wavevector $\boldsymbol{k}$ is normal to the x direction and therefore $k_x = 0$, the classical field does not couple the internal and motional degrees of freedom of the atom. Then (3.90) becomes $\tilde{\mathcal{V}} = -\hbar\Omega\,\sigma_+\,\mathrm{e}^{-\mathrm{i}(\Delta t-\varphi)} + \mathrm{H.c}$, which is just the interaction Hamiltonian for the driven two-level atom studied in Sect. 3.3.1.

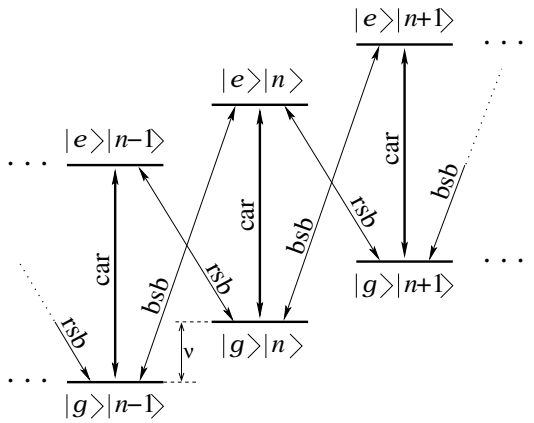

Fig. 3.4. Energy level diagram for a two-level atom in a harmonic potential. The lines with arrows indicate the carrier (car), red-sideband (rsb) and blue-sideband (bsb) resonances of the coherent coupling field.

For nonzero values of the Lamb–Dicke parameter, depending on the values of the Rabi frequency Ω and detuning Δ, the interaction Hamiltonian (3.90) can couple internal states of the atom to certain motional states, for which we will use the standard notation $|n\rangle$ denoting the state of the harmonic oscillator containing n motional excitations, called phonons. A particularly simple picture emerges in the Lamb–Dicke regime $\eta \ll 1$, when the atom is confined in a region of space Δx_0 small compared to $1/k_x$. Then, provided that the number of excitations of the harmonic oscillator is small enough for the condition $\eta\sqrt{\langle (b+b^\dagger)^2\rangle} \ll 1$ to hold for all times, we can expand the exponential operators of (3.90) to the lowest (first) order in η, obtaining

$$\tilde{\mathcal{V}} = -\hbar\Omega\Big\{\sigma_+ \,\mathrm{e}^{-\mathrm{i}(\Delta t-\varphi)}\big[1+\mathrm{i}\eta(b\,\mathrm{e}^{-\mathrm{i}\nu t}+b^\dagger\,\mathrm{e}^{\mathrm{i}\nu t})\big] + \sigma_-\,\mathrm{e}^{\mathrm{i}(\Delta t-\varphi)}\big[1-\mathrm{i}\eta(b\,\mathrm{e}^{-\mathrm{i}\nu t}+b^\dagger\,\mathrm{e}^{\mathrm{i}\nu t})\big]\Big\}\,. \tag{3.91}$$

Clearly, we can identify three values of detuning Δ for which the system exhibits resonant behavior, as can be seen from Fig. 3.4. The first one is trivial, $\Delta = 0$, and is called the carrier resonance. Neglecting the off-resonant terms oscillating with the frequencies $\pm\nu$, from (3.91) we obtain the effective Hamiltonian

$$\tilde{\mathcal{V}}^{\mathrm{car}} = -\hbar\Omega\big[\sigma_+\,\mathrm{e}^{\mathrm{i}\varphi}+\sigma_-\,\mathrm{e}^{-\mathrm{i}\varphi}\big]\,, \tag{3.92}$$

which couples only the internal atomic states $|g\rangle$ and $|e\rangle$ with the usual Rabi frequency Ω, and does not change the motional state of the atom. More precisely, the coupling strength associated with the nonresonant terms of the form $\sigma_\pm b\,\mathrm{e}^{-\mathrm{i}\nu t}$ and $\sigma_\pm b^\dagger\,\mathrm{e}^{\mathrm{i}\nu t}$ is given by $\Omega\eta$, which should be smaller than ν so that the nonresonant transitions can be neglected.

The second resonance $\Delta = -\nu$ is called the first red-sideband resonance. Similarly, neglecting the off-resonant terms oscillating with the frequencies $\pm\nu$ and $\pm 2\nu$, from (3.91) we have

$$\tilde{\mathcal{V}}^{\mathrm{rsb}} = -\hbar\Omega\eta\left[\mathrm{i}\,\mathrm{e}^{\mathrm{i}\varphi}\sigma_+ b - \mathrm{i}\,\mathrm{e}^{-\mathrm{i}\varphi}\sigma_- b^\dagger\right] . \tag{3.93}$$

Neglecting now the nonresonant terms containing only the atomic operators $\sigma_\pm\,\mathrm{e}^{\pm\mathrm{i}\nu t}$ imposes a more stringent condition upon the Rabi frequency, namely $\Omega \ll \nu$. If we introduce $g \equiv \Omega\eta$ and choose $\varphi = \pi/2$, the effective Hamiltonian becomes

$$\tilde{\mathcal{V}}^{\mathrm{rsb}} = \hbar g(\sigma_+ b + b^\dagger\sigma_-) , \tag{3.94}$$

which is precisely the same Jaynes–Cummings Hamiltonian of (3.56) that governs the evolution of the compound system "atom+quantized cavity field". Here, however, the Hamiltonian (3.94) couples the states $|g\rangle\,|n\rangle$ and $|e\rangle\,|n-1\rangle$ where n denotes the number of phonons, i.e., motional excitations of the harmonic oscillator. In other words, the classical field induces the transition $|g\rangle\,|n\rangle \leftrightarrow |e\rangle\,|n-1\rangle$ with the effective Rabi frequency $g\sqrt{n} = \Omega\eta\sqrt{n}$, and the dynamics of the system is formally the same as that in Sect. 3.3.2.

Consider finally the case of the first blue-sideband resonance $\Delta = \nu$. The effective Hamiltonian is then

$$\tilde{\mathcal{V}}^{\mathrm{bsb}} = -\hbar\Omega\eta\left[\mathrm{i}\,\mathrm{e}^{\mathrm{i}\varphi}\sigma_+ b^\dagger - \mathrm{i}\,\mathrm{e}^{-\mathrm{i}\varphi}\sigma_- b\right] , \tag{3.95}$$

which upon the substitution $g \equiv \Omega\eta$ and $\varphi = \pi/2$ becomes

$$\tilde{\mathcal{V}}^{\mathrm{bsb}} = \hbar g(\sigma_+ b^\dagger + b\sigma_-) . \tag{3.96}$$

This Hamiltonian couples the states $|g\rangle\,|n\rangle$ and $|e\rangle\,|n+1\rangle$ with the effective Rabi frequency $g\sqrt{n+1} = \Omega\eta\sqrt{n+1}$, i.e., excitation of the atom is accompanied by the excitation of the harmonic oscillator. The analogous process in the context of cavity QED is not allowed due to the energy conservation constraint. Here, however, the energy conservation is not violated because the excitation energy of both the atom and the phonon add up to the energy of a single photon drawn from the classical coupling field. Systems described by Hamiltonian (3.96) are sometimes said to represent the anti-Jaynes–Cummings model.

Let us finally note that, if in the expansion of the exponential operators in (3.90) we kept the terms of second (or higher) order in η, we would have obtained terms of the form $\sigma_\pm bb$ and $\sigma_\pm b^\dagger b^\dagger$ responsible for the two- (or more) phonon transitions for $\Delta = \pm 2\nu$. However, the corresponding coupling strength is given by $\Omega\eta^2/2$, and therefore in the Lamb–Dicke regime these transitions can be safely neglected.

3.5 Quantum System Coupled to a Reservoir

A problem that recurs often and in more than one facet, in quantum optics, is the coupling of a small quantum system, having only a few states, to a large

system, often referred to as reservoir, with many, in principle infinitely many, closely spaced energy states. The mathematical limit is that of a continuum of states, which does in fact correspond to a real physical situation. Some examples are: The spontaneous decay of an excited atomic state by photon emission into the open radiation filed, the loss of energy from the electromagnetic field inside a cavity through absorbing and transmitting walls, the ejection of an electron from a bound state by photoionization. The physical nature of the small and large systems may vary from case to case, but the basic mathematical structure and the physical conditions that lead to the conclusions as to what happens to the small system are essentially the same and can in fact be discussed most simply in the formal context of this section.

3.5.1 Single State Coupled to a Continuum of States

In the spirit of stripping the model down to the bare essentials, let us consider a quantum system which initially, at time $t = 0$, has been put to a particular state $|i\rangle$ of energy $E_i = \hbar\omega_i$. Let this state be coupled to a continuum of states denoted by $|r\rangle$ with respective energies $E_r = \hbar\omega_r$. Assume further that $|i\rangle$ is coupled to states $|r\rangle$ through a harmonically varying time-dependent perturbation $\mathcal{V}(t) = -\hbar\Omega(\mathrm{e}^{-\mathrm{i}\omega t} + \mathrm{e}^{\mathrm{i}\omega t})$, where Ω is an operator whose non-zero matrix elements are $\Omega_{ir} \equiv \langle i|\,\Omega\,|r\rangle$. The similarity to the problem of an electron interacting with a time-dependent electromagnetic field is intentional, but the structure of the problem is more general.

In a straightforward extension of the formal development of the previous section, the state of the system at any time $t \geq 0$ can be written as

$$|\Psi(t)\rangle = c_i(t)\,|i\rangle + \int \mathrm{d}\omega_r\, c_r(t)\,|r\rangle\ , \tag{3.97}$$

where the integration is understood over the complete continuum which, depending on the particulars of the physical system, may or may not have a threshold. For the moment, we leave the limits of integration unspecified. Substituting $|\Psi(t)\rangle$ in the time-dependent Schrödinger equation (3.37), and following the procedure of Sect. 3.3.1, we obtain the following differential equations for the expansion amplitudes,

$$\frac{\partial}{\partial t}c_i = -\mathrm{i}\omega_i c_i + \mathrm{i}\int \mathrm{d}\omega_r \Omega_{ir}\,\mathrm{e}^{\mathrm{i}\omega t}c_r\ , \tag{3.98a}$$

$$\frac{\partial}{\partial t}c_r = -\mathrm{i}\omega_r c_r + \mathrm{i}\Omega_{ri}\,\mathrm{e}^{-\mathrm{i}\omega t}c_i\ . \tag{3.98b}$$

Adopting the RWA, we have kept only one of the exponentials $\mathrm{e}^{\pm\mathrm{i}\omega t}$ in each of the equations above; a point to which we return later on. Taking now the Laplace transforms of both sides of the equations, under the initial conditions $c_i(0) = 1$ and $c_r(0) = 0$ and using the properties of the transform, we obtain a system of algebraic equations satisfied by the Laplace transforms $L_i(s)$ and $L_r(s)$ of $c_i(t)$ and $c_r(t)$, namely

$$sL_i(s) - 1 = -\mathrm{i}\omega_i L_i(s) + \mathrm{i}\int \mathrm{d}\omega_r \Omega_{ir}\, L_r(s - \mathrm{i}\omega)\ , \tag{3.99a}$$

$$sL_r(s) = -\mathrm{i}\omega_r L_r(s) + \mathrm{i}\Omega_{ri}\, L_i(s + \mathrm{i}\omega)\ . \tag{3.99b}$$

From (3.99b) we have $[s - \mathrm{i}(\omega - \omega_r)]L_r(s - \mathrm{i}\omega) = \mathrm{i}\Omega_{ri}\, L_i(s)$. Substituting from here $L_r(s - \mathrm{i}\omega)$ into (3.99a), we obtain

$$L_i(s) = \frac{1}{s + \mathrm{i}\omega_i + G_i(s)}\ , \quad G_i(s) = \int \mathrm{d}\omega_r \frac{|\Omega_{ri}|^2}{s - \mathrm{i}(\omega - \omega_r)}\ . \tag{3.100}$$

The essential point to be kept in mind is that Ω_{ri} is a parameter that depends on the energy $E_r = \hbar\omega_r$ of state $|r\rangle$ and is responsible for the coupling of the initial discrete state $|i\rangle$ to the continuum. The subscript i in $G_i(s)$ is intended to underscore the fact that this quantity refers to the particular initial state. Our objective is to obtain the time evolution of the amplitude $c_i(t)$, which enables us to predict the probability $|c_i(t)|^2$ that the system is still in state $|i\rangle$ at a later time $t > 0$. For this, we need to invert the Laplace transform in (3.100); not an easy task, if possible at all in general. The complication arises from the obvious fact that the denominator contains the function $G_i(s)$ for which an analytic expression can be contemplated only if the analytic form of $|\Omega_{ri}|^2$ allows it and if the integral converges. What we are about to do, however, is to explore the general conditions under which the integral can be performed, irrespective of the particular analytic form of $|\Omega_{ri}|^2$. Let us therefore proceed in steps as simple as possible.

First, note that $G_i(s)$ is a complex-valued function of s. Let us then call $\frac{1}{2}\Gamma_i(s)$ its real and $S_i(s)$ its imaginary part, so that we can write $G_i(s) = \mathrm{i}S_i(s) + \frac{1}{2}\Gamma_i(s)$. Obviously, if $G_i(s)$ could be approximated by a constant, so that $G_i(s) \equiv G_i = \mathrm{i}S_i + \frac{1}{2}\Gamma_i$, the inversion of the transform (3.100) would be trivial, leading to

$$c_i(t) = \mathrm{e}^{-\mathrm{i}(\omega_i + S_i)t - \frac{1}{2}\Gamma_i t}\ , \tag{3.101}$$

indicating that the coupling to the continuum would lead to the decay of the amplitude $c_i(t)$ with rate $\frac{1}{2}\Gamma_i$ and of course of the probability $|c_i(t)|^2$ with rate Γ_i; assuming that Γ_i is positive. It would be a disaster if it were not, as the probability would grow indefinitely violating unitarity. But not knowing yet which is the case, we simply keep it in mind. We note further that in addition to the decay, the amplitude oscillates at a frequency shifted by S_i from its original frequency ω_i. We have thus found that, under the above rather drastic assumptions, the coupling of a discrete state to a continuum leads to a decay and a shift of its energy.

The next question is whether and under what general conditions it is indeed possible, in the sense of a good approximation, to replace $G_i(s)$ by a constant, which implies by its value at some s; and if yes, at which value of s? To this end, note that when inverting the Laplace transform (3.100), the integrand has a pole at $s = -\mathrm{i}\omega_i - G_i(s)$. Now, if it could be argued, or justified even a posteriori, that: (a) $G_i(s) \ll \omega_i$ for all values of s, and

(b) $G_i(s)$ is a sufficiently slowly varying function in the vicinity of $s = -\mathrm{i}\omega_i$, then it seems a reasonable approximation to replace $G_i(s)$ in the denominator of (3.100) by $G_i(s = -\mathrm{i}\omega_i) \equiv \mathrm{i}S_i + \frac{1}{2}\Gamma_i$. Assuming that the above conditions are satisfied, it remains to extract the precise values of S_i and Γ_i from the general formal expression for $G_i(s)$ in (3.100). This can be accomplished by examining $G_i(s)$ on the complex plane, i.e., for complex values of s.

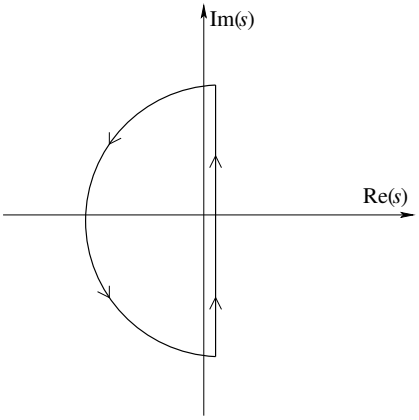

Fig. 3.5. Integration contour on the complex s-plane for performing inverse Laplace transform.

A brief interlude on the theory of Laplace transform is inevitable at this point. The general inversion theorem of the transform states that: To calculate the inversion integral, the transform must be extended on the complex s-plane and the integration performed counter-clockwise on a contour consisting of a straight line parallel to and to the right of the imaginary s-axis, closing with a circle on the left, as shown in Fig. 3.5. The straight line must be placed to the right of all singularities of the transform, so that they are enclosed by the contour in the limit that the line extends from $-\mathrm{i}\infty$ to $+\mathrm{i}\infty$ and therefore the circumference of the circle also goes to ∞. The proof includes the necessary and sufficient conditions on the behavior of the transform as $|s| \to \infty$ for the integral to exist.

In the case of $G_i(s)$, clearly all singularities lie on the imaginary axis. The conditions of the inversion theorem are therefore satisfied, if we displace the straight line to the right of $\mathrm{Im}(s)$ by a small distance $\epsilon > 0$. The straight line thus extends from $\epsilon - \mathrm{i}\infty$ to $\epsilon + \mathrm{i}\infty$. The idea now is to replace s by $\mathrm{i}y + \epsilon$ in our equations above, set $y = -\omega_i$ and take the limit of the integration over ω_r as $\epsilon \to 0$. In the process, the expression for $G_i(s)$ can be put in the form

$$G_i(s) = \mathrm{i} \int \mathrm{d}\omega_r \frac{|\Omega_{ri}|^2}{(\omega + \omega_i - \omega_r) + \mathrm{i}\epsilon} \ .$$

Since the limit for $\epsilon \to 0$ is understood, we can use the relation (1.30) involving the principal value part P of $1/x$ and the Dirac delta function $\delta(x)$, with $x = \omega+\omega_i-\omega_r$. The integral involving the delta function is performed immediately, irrespective of the analytic form of $|\Omega_{ri}|^2$, while the expression for S_i remains in integral form. Thus we obtain

$$\tfrac{1}{2}\Gamma_i = \pi|\Omega_{ri}|^2_{\omega_r=\omega+\omega_i} \ , \quad S_i = \mathrm{P}\int \mathrm{d}\omega_r \frac{|\Omega_{ri}|^2}{\omega+\omega_i-\omega_r} \ , \tag{3.102}$$

where in the expression for Γ_i, the coupling matrix element Ω_{ri} is evaluated at $\omega_r = \omega + \omega_i$. To calculate S_i, one needs to know the analytic form of Ω_{ri} as a function of ω_r which depends on the nature of the problem. In any case, however, the integration will yield a real number representing the shift mentioned above; assuming of course that the integral, whose limits of integration may extend to infinity, converges. That is not always the case, a well-known example being the Lamb shift of an excited atomic state due to its coupling to the radiation continuum of the open field. On the other hand, Γ_i is always given by the value of the respective coupling matrix element dictated by the delta function, which implies conservation of energy; precisely as in the so-called Fermi's golden rule.

In the above derivation, we have glossed over some mathematical details pertaining to the nature of the singularities of the integrand in (3.100). Our heuristic at times argumentation, for example, made no mention of the fact that a continuous spectrum entails a branch cut in the complex s-plane. The approximations we adopted led to a simple pole which is sufficient for our purposes here. A thorough treatment of these issues can be found, e.g., in Goldberger and Watson (1964).

The reader may have wondered about the absence of the density of states under the integral over the continuum. Indeed, in the standard treatment of a continuum, a density of states (modes) $\varrho(\omega_r)$, whose analytical form depends on the quantum system represented by the continuum, is included in the integrand. Its presence guarantees normalization, since true continuum states, e.g., plane waves, are not normalizable. Formally, we can assume that the continuum states denoted here by $|r\rangle$ have been multiplied by $\sqrt{\varrho(\omega_r)}$. Alternatively, $\varrho(\omega_r)$ can be incorporated in the expression for $|\Omega_{ri}|^2$. In either case, expressions (3.102) in the complete form read

$$\tfrac{1}{2}\Gamma_i = \pi\varrho(\omega_r = \omega+\omega_i)|\Omega_{ri}|^2_{\omega_r=\omega+\omega_i} \ , \quad S_i = \mathrm{P}\int \mathrm{d}\omega_r \frac{\varrho(\omega_r)|\Omega_{ri}|^2}{\omega+\omega_i-\omega_r} \ . \tag{3.103}$$

Note that consistency with our assumptions about $G_i(s)$ demands that $\varrho(\omega_r)$ also be a smooth, slowly varying function of ω_r, which restricts the type of systems amenable to this approach.

3.5.2 Spontaneous Decay of an Excited Atom in Open Space

As an example of the application of the formalism in the previous section, we consider now the spontaneous decay of an excited atomic state. In the

simplest possible context, we assume that an atom has somehow been put to an excited state $|e\rangle$, which has a non-vanishing dipole matrix element with a state $|g\rangle$ of lower energy. A radiative transition between the two states is therefore possible. We have already seen what happens in the presence of an externally imposed electromagnetic field, as well as a cavity environment with one mode near-resonant with the atomic transition. But what if the atom is in open space without any photons present? The quantized field now has an infinity of continuum modes, which is precisely the problem of the previous section.

Although in the previous section, we assumed a continuum, here we will approach the problem in two steps, following a procedure standard in non-relativistic quantum electrodynamics. We assume a field inside a box of linear dimension L as in Sect. 2.1. At time $t = 0$, the state of the compound system atom+field is $|i\rangle = |e\rangle\,|\{0_{\boldsymbol{k}\lambda}\}\rangle$, which is the direct product of the atomic state $|e\rangle$ and the vacuum state of the field $|\{0_{\boldsymbol{k}\lambda}\}\rangle \equiv |0_{\boldsymbol{k}_1\lambda_1}\rangle\,|0_{\boldsymbol{k}_2\lambda_2}\rangle\ldots$, with the energy $E_i = \hbar\omega_e$. This state is connected by the interaction to the state $|f_{\boldsymbol{k}\lambda}\rangle = |g\rangle\,|1_{\boldsymbol{k}\lambda}\rangle$ of the compound system, in which the atom is in the lower state $|g\rangle$ with one photon present in some arbitrary mode $\boldsymbol{k}\lambda$ of the field, $|1_{\boldsymbol{k}\lambda}\rangle \equiv |0_{\boldsymbol{k}_1\lambda_1}\rangle\ldots|1_{\boldsymbol{k}\lambda}\rangle\ldots|0_{\boldsymbol{k}_j\lambda_j}\rangle\ldots$, the corresponding energy being $E_{f_k} = \hbar\omega_g + \hbar\omega_k$. In the dipole approximation, the interaction between the two systems is given by

$$\mathcal{V}^{\mathrm{AF}} = -\wp\cdot\boldsymbol{E} = -\mathrm{i}\sum_{\boldsymbol{k}\lambda}(\wp\cdot\hat{\boldsymbol{e}}_{\boldsymbol{k}\lambda})\,\epsilon_k\big[a_{\boldsymbol{k}\lambda} - a^\dagger_{\boldsymbol{k}\lambda}\big]\,, \tag{3.104}$$

where $\wp = e\boldsymbol{r}$ is the atomic dipole moment and $\epsilon_k \equiv \sqrt{\hbar\omega_k/2\varepsilon_0 V}$ is the field per photon of frequency ω_k. Note that now $\mathcal{V}^{\mathrm{AF}}$ does not have the harmonic time dependence, because in the expression for the field $\boldsymbol{E}$ we take $t = 0$, as dictated by the initial condition. But the frequencies of the individual modes now appear through the energies E_i and E_{f_k} of the initial and final states, respectively, of the compound system. This has to do with the fact that in Sect. 3.5.1 the quantized system was fed energy through an external time-varying perturbation, while now we have a closed compound system in which the total energy is constant. Energy can, however, flow from one part to the other; in the present case from the atom to the field. The interaction (3.104), being linear in the field operators $a_{\boldsymbol{k}\lambda}$ and $a^\dagger_{\boldsymbol{k}\lambda}$, has a non-vanishing matrix element between the above states,

$$\langle i|\,\mathcal{V}^{\mathrm{AF}}\,|f_{\boldsymbol{k}\lambda}\rangle = -\mathrm{i}\,\langle e|\,\wp\cdot\hat{\boldsymbol{e}}_{\boldsymbol{k}\lambda}\,|g\rangle\sqrt{\frac{\hbar\omega_k}{2\varepsilon_0 V}}\,, \tag{3.105}$$

and similarly for $\langle f_{\boldsymbol{k}\lambda}|\,\mathcal{V}^{\mathrm{AF}}\,|i\rangle = \langle i|\,\mathcal{V}^{\mathrm{AF}}\,|f_{\boldsymbol{k}\lambda}\rangle^*$. Accordingly, the total wavefunction at any time $t \geq 0$ can be written as

$$|\Psi(t)\rangle = c_i(t)\,|i\rangle + \sum_{\boldsymbol{k}\lambda} c_{\boldsymbol{k}\lambda}(t)\,|f_{\boldsymbol{k}\lambda}\rangle\,, \tag{3.106}$$

where we have a summation over all possible modes of the field quantized in a box. The time-evolution of the amplitudes c_i and $c_{\boldsymbol{k}\lambda}$ of (3.106) is governed by the equations

$$\frac{\partial}{\partial t}c_i = -\mathrm{i}\omega_e c_i - \frac{\mathrm{i}}{\hbar}\sum_{\boldsymbol{k}\lambda}\langle i|\,\mathcal{V}^{\mathrm{AF}}\,|f_{\boldsymbol{k}\lambda}\rangle\, c_{\boldsymbol{k}\lambda}\ , \tag{3.107a}$$

$$\frac{\partial}{\partial t}c_{\boldsymbol{k}\lambda} = -\mathrm{i}(\omega_g+\omega_k)c_{\boldsymbol{k}\lambda} - \frac{\mathrm{i}}{\hbar}\langle f_{\boldsymbol{k}\lambda}|\,\mathcal{V}^{\mathrm{AF}}\,|i\rangle\, c_i\ . \tag{3.107b}$$

As in the previous section, we take the Laplace transforms of these equations, with the initial conditions $c_i(0)=1$ and $c_{\boldsymbol{k}\lambda}(0)=0$. Solving for the Laplace transform of $c_{\boldsymbol{k}\lambda}$ and substituting into the equation for $L_i(s)$—the Laplace transform of c_i—we obtain

$$L_i(s) = \frac{1}{s+\mathrm{i}\omega_e+G_i(s)}\ ,\quad G_i(s) = \sum_{\boldsymbol{k}\lambda}\frac{1}{\hbar^2}\frac{|\langle i|\,\mathcal{V}^{\mathrm{AF}}\,|f_{\boldsymbol{k}\lambda}\rangle|^2}{s+\mathrm{i}(\omega_g+\omega_k)}\ . \tag{3.108}$$

By letting the dimension of the quantization box L go to infinity, the sum over modes $\boldsymbol{k}\lambda$ in the expression for $G_i(s)$ can now be turned into an integral according to the procedure of (2.29), which corresponds to the spectrum of the field approaching the true continuum. Substituting the interaction matrix element from (3.105) and expressing the volume element d^3k in spherical coordinates, we have

$$G_i(s) = \frac{1}{4\pi\varepsilon_0}\frac{e^2}{4\pi^2\hbar c^3}\int_0^\infty \frac{\omega_k^3\,\mathrm{d}\omega_k}{s+\mathrm{i}(\omega_g+\omega_k)}\int|\langle e|\,\boldsymbol{r}\cdot\hat{\boldsymbol{e}}_{\boldsymbol{k}\lambda}\,|g\rangle|^2\mathrm{d}\Omega\ , \tag{3.109}$$

where $\mathrm{d}\Omega = \sin\theta\mathrm{d}\theta\,\mathrm{d}\phi$ is the solid angle element. Summing over the two polarizations and integrating over all possible propagation directions with the direction of $\boldsymbol{r}_{eg} = \langle e|\,\boldsymbol{r}\,|g\rangle$ fixed in space, the second integral in the above expression yields $2\frac{4\pi}{3}|\boldsymbol{r}_{eg}|^2$. Note that

$$|\boldsymbol{r}_{eg}|^2 = |r^+_{eg}|^2+|r^-_{eg}|^2+|r^0_{eg}|^2 \quad\text{with}\quad r^\pm \equiv \mp\frac{1}{\sqrt{2}}(x\pm\mathrm{i}y)\ ,\quad r^0\equiv z\ .$$

Following the prescription of the previous section, we make the replacement $s=-\mathrm{i}\omega_e+\epsilon$ and write $G_i(s)$ as

$$G_i(s) = \mathrm{i}\frac{2}{3\pi}\frac{\alpha}{c^2}|\boldsymbol{r}_{eg}|^2\int\frac{\omega_k^3\,\mathrm{d}\omega_k}{\omega_{eg}-\omega_k+\mathrm{i}\epsilon}\ , \tag{3.110}$$

where $\omega_{eg}=\omega_e-\omega_g$ is the atomic resonance frequency and

$$\alpha = \frac{1}{4\pi\varepsilon_0}\frac{e^2}{\hbar c}\simeq\frac{1}{137} \tag{3.111}$$

is a dimensionless constant known as the fine structure constant. From (3.110), taking the limit $\epsilon\to 0$, we obtain

$$\tfrac{1}{2}\Gamma_e = \frac{2\omega_{eg}^3\alpha|\boldsymbol{r}_{eg}|^2}{3c^2}\ , \quad S_e = -\frac{2\alpha|\boldsymbol{r}_{eg}|^2}{3\pi c^2}\,\mathrm{P}\int_0^\infty \frac{\omega_k^3\,\mathrm{d}\omega_k}{\omega_k-\omega_{eg}}\ , \tag{3.112}$$

representing, as we have established in the previous section, the decay rate and the energy shift of the excited atomic state $|e\rangle$. To emphasize this fact, the subscript i was replaced by e. The corresponding probability amplitude is then given by

$$c_i(t) = c_i(0)\,\mathrm{e}^{-\frac{1}{2}\Gamma_e t}\,\mathrm{e}^{-\mathrm{i}(\omega_e - S_e)t}\ . \tag{3.113}$$

and the probability to find the atom in the excited state $|e\rangle$ decays as $|\langle e|\Psi(t)\rangle|^2 \propto \mathrm{e}^{-\Gamma_e t}$. This is the Weisskopf–Wigner law of spontaneous decay of an excited atom. Note that the above expressions for Γ_e and S_e are the same in SI units as well as in CGS units, in which the fine structure constant is given by $\alpha = e^2/(\hbar c)$.

The problems we treated in this and the previous section encapsulate all of the conditions and elements needed to formulate and describe quantitatively what is referred to as quantum theory of dissipation or reservoir theory, which refers to the behavior of a small system (few degrees of freedom) coupled to a large system (infinitely many degrees of freedom). We have found that the small system decays irreversibly in a temporally exponential fashion, with the rate Γ_i also called width. We need to ask whether the conditions allowing the approximations leading to (3.103) are valid here. The first necessary condition is that the strength of the coupling between the small and the large systems must be much smaller than the energy difference between the two states of the transition, $\Gamma_e \ll \omega_{eg}$. Although this was imposed for mathematical reasons, it has a simple physical basis. If the question of how an initially prepared state decays is to be meaningful, that state must be clearly definable. If its coupling to another state is such that the width Γ_e is comparable to the energy separation ω_{eg} between the states, then the problem is ill-defined. The two states are strongly coupled and the requirement that at $t = 0$ the system is in one of the states is physically unrealistic. In that case, we would have the coupling to a reservoir of two or more strongly coupled states. The previous treatment can be generalized appropriately to deal with such situations, which, however, are beyond the needs in this book. The second condition implies that the dependence of the coupling matrix element on the energy of the large system (reservoir) states, as well as the density of states, must be smooth and slowly varying, at least in the range of the resonance frequency of the small system. This condition is indeed satisfied here, because both the interaction matrix element (3.105) and the free space density of states $\varrho(\omega_k)$, as given by (2.30), are slowly varying functions of ω_k. Physically, this condition means that the energy structure of the reservoir is such that there is no particular preference, or resonance, in the range of the system transition frequency. Viewed in the time domain, this implies that once the transition is made, the reservoir loses memory of the particular frequency "immediately", which is known as the Markov approximation. If that were not the case, the process is referred

to as non-Markovian and the resulting time evolution is much different from exponential decay.

It could be objected that in our treatment we tacitly assumed that the emission of one photon is the only way the atom can decay. In the language of perturbation theory, this means that we have limited the treatment to the lowest non-vanishing order; often referred to, in quantum optics, as Born approximation. The next order would be the emission of three photons and so on, since the parity selection rules allow only odd number of photons. The presence of the fine structure constant α in the above expressions, however, guarantees that higher orders decrease sufficiently fast to be negligible for most practical purposes. The fine structure constant is what characterizes the strength of the coupling in this problem, the simplest in quantum electrodynamics. And it is the magnitude, or rather the smallness, of this constant, $\alpha \ll 1$, that makes perturbation theory a valid approach in quantum electrodynamics. The shift still presents a problem, because an attempt to perform the integration leads to a logarithmic divergence, since formally the integration over the photon frequency extends to infinity. This is a celebrated divergence, known as ultraviolet divergence. It points to an inconsistency in the formalism of the non-relativistic treatment. A make-shift but insightful remedy, within the non-relativistic theory, was provided by Bethe 55 years ago, who argued that the integration over the frequency must be limited to the rest mass energy of the electron $m_e c^2$. The resulting value for the vacuum shift of the $2s_{1/2}$ state of the hydrogen atom, known now as the Lamb shift, turned out to be remarkably close to the experimental result of Lamb, providing at the same time the first theoretical explanation of the energy difference between the $2s_{1/2}$ and $2p_{1/2}$ states, which otherwise should have been degenerate. The rigorous and complete theoretical explanation came a few years later through the development of renormalization theory by Feynman, Schwinger and Tomonaga, which made quantum electrodynamics the first example of a complete and self-consistent quantum field theory in which perturbation theory works well in a quantitative systematic fashion.

Having treated the above problems in terms of the wavefunctions of the system, it is desirable to generalize the treatment to the description in terms of the density operator. If not for any other reason, simply because we know that it is only the density operator that provides the most general description of quantum systems. This will be the subject of the following chapter. We wish to stress, however, that although the relevant derivation will appear more involved, it is based on exactly the same physical conditions and assumptions.

3.6 Three-Level Atom

The set of energy levels of an atom consists of an infinite number of discrete levels, corresponding to the bound states of the electron, and a continuum of levels, corresponding to the system of positively charged ion and free electron

whose energy spans the continuum of energies that a particle can have in free space. In Sect. 3.3.1 we have studied the model two-level system which can adequately describe an atom interacting which a classical monochromatic field whose frequency is close to the frequency of transition between a pair of discrete atomic levels. We have also seen in Sect. 3.5.2 that the same model is applicable to the atom prepared initially in the first excited state which decays to a single ground state with the emission of a spontaneous photon. When an atom is subject to a radiation field containing many frequencies (and/or polarization components), other levels of the atom may have to be included in the model, since different atomic transitions may be near-resonant with different components of the field. Thus, as an extension of the simplest two-level model, let us consider a three-level atom whose energy levels will be designated as $|g\rangle$, $|e\rangle$ and $|s\rangle$. The three possible configurations of atomic levels are the ladder (or Ξ), V, and Λ configurations shown in Fig. 3.6.

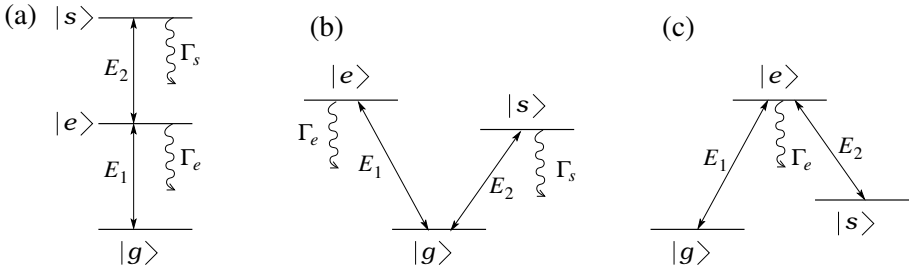

Fig. 3.6. Three possible configurations of the energy levels of a three-level atom: (a) Ξ, (b) V, and (c) Λ configuration.

In the ladder (Ξ) configuration, the dipole-allowed transitions are $|g\rangle \leftrightarrow |e\rangle$ and $|e\rangle \leftrightarrow |s\rangle$, while the transition $|g\rangle \leftrightarrow |s\rangle$ is dipole-forbidden. This means that states $|g\rangle$ and $|s\rangle$ have the same parity, i.e., the angular momentum quantum number l is either even or odd for both states, and the intermediate state $|e\rangle$ has the opposite parity with l being either odd or even. Obviously, when an atom with such level–configuration is excited to the uppermost level $|s\rangle$, it will decay to the ground state $|g\rangle$ via the sequential emission (cascade) of two spontaneous photons with frequencies close to the frequencies of the $|s\rangle \rightarrow |e\rangle$ and $|e\rangle \rightarrow |g\rangle$ transitions, provided that apart from the intermediate level $|e\rangle$ there are no other levels between $|s\rangle$ and $|g\rangle$. An important example of this situation is the radiative cascade $4p^2\ {}^1S_0 \rightarrow 4s4p\ {}^1P_1 \rightarrow 4s^2\ {}^1S_0$ in calcium, which has been employed in the experiments by Aspect and coworkers to produce pairs of correlated (polarization entangled) photons for the experimental tests of Bell's inequalities, as discussed in Sect. 8.8.

In the V configuration, the atom has a stable ground state $|g\rangle$ and two excited states $|e\rangle$ and $|s\rangle$, each coupled to the ground state via a dipole allowed

transition, but not to each other. Thus, if the atom is excited to either state $|e\rangle$ or $|s\rangle$, it can decay to the ground state $|g\rangle$ and emit a single spontaneous photon whose frequency is close to the resonant frequency of the corresponding transition. One interesting application of this model is related to the quantum jump experiments with single trapped ions, which are viable candidates for implementing qubits in an ion-trap quantum computer, as discussed in Sect. 4.2 and Sect. 10.3.

We shall consider the Λ configuration of atomic levels in somewhat more detail, in anticipation of its importance to later sections. In this configuration, the atom has two lower states $|g\rangle$ and $|s\rangle$ and the upper excited state $|e\rangle$ which can decay to either of the lower states or even to other states of the atom. In turn, the ground state $|g\rangle$ is, by definition, stable while $|s\rangle$ is metastable (long-lived). This is often called the Raman configuration, since in the presence of two fields E_1 and E_2 acting, respectively, on the atomic transitions $|g\rangle \leftrightarrow |e\rangle$ and $|e\rangle \leftrightarrow |s\rangle$, the two-photon transition $|g\rangle \leftrightarrow |s\rangle$ is known as the Raman transition. It is convenient to introduce the atomic operators $\sigma_{\mu\nu} \equiv |\mu\rangle\langle\nu|$, which are the rising and lowering operators for multilevel systems. The Hamiltonian for the three-level system takes the form

$$\mathcal{H} = \mathcal{H}^{\mathrm{A}} + \mathcal{V}^{\mathrm{AF}}(t) \,, \tag{3.114}$$

where the atomic Hamiltonian is

$$\mathcal{H}^{\mathrm{A}} = \hbar\omega_g \sigma_{gg} + \hbar\omega_e \sigma_{ee} + \hbar\omega_s \sigma_{ss} \,, \tag{3.115}$$

while the atom–field interaction is described by

$$\mathcal{V}^{\mathrm{AF}}(t) = -\boldsymbol{\wp} \cdot [\boldsymbol{E}_1(t) + \boldsymbol{E}_2(t)] \,, \tag{3.116}$$

with the two components $\boldsymbol{E}_j(t) = \hat{\boldsymbol{e}}_j E_j(t)$ $(j = 1, 2)$ of the total field given by $E_j = \mathcal{E}_j \mathrm{e}^{-\mathrm{i}\omega_j t} + \text{c.c.}$ As stated above, we assume that due to the choice of the frequencies ω_j and/or polarizations $\hat{\boldsymbol{e}}_j$ of the fields, the E_1 field interacts with the atom on the $|g\rangle \leftrightarrow |e\rangle$ transition, and E_2 on the $|e\rangle \leftrightarrow |s\rangle$ transition. We then have

$$\mathcal{V}^{\mathrm{AF}}(t) = -\wp_{ge}\mathcal{E}_1 \mathrm{e}^{-\mathrm{i}\omega_1 t} - \wp_{se}\mathcal{E}_2 \mathrm{e}^{-\mathrm{i}\omega_2 t} + \text{c.c.} \,, \tag{3.117}$$

where $\wp_{\mu\nu} \equiv \langle\mu| \boldsymbol{\wp} \cdot \hat{\boldsymbol{e}}_j |\nu\rangle$ is the dipole matrix element for the corresponding atomic transition $|\mu\rangle \leftrightarrow |\nu\rangle$. Using the the Schrödinger equation (3.37), for the amplitudes c_μ of the state vector of the system,

$$|\Psi(t)\rangle = c_g(t)\,|g\rangle + c_e(t)\,|e\rangle + c_s(t)\,|s\rangle \,, \tag{3.118}$$

we obtain, within the rotating wave approximation, the following equations,

$$\frac{\partial}{\partial t} c_g = -\mathrm{i}\omega_g c_g + \mathrm{i} c_e \Omega_1 \mathrm{e}^{\mathrm{i}\omega_1 t} \,, \tag{3.119a}$$

$$\frac{\partial}{\partial t} c_e = -\mathrm{i}\omega_e c_e + \mathrm{i} c_g \Omega_1 \mathrm{e}^{-\mathrm{i}\omega_1 t} + \mathrm{i} c_s \Omega_2 \mathrm{e}^{-\mathrm{i}\omega_2 t} \,, \tag{3.119b}$$

$$\frac{\partial}{\partial t} c_s = -\mathrm{i}\omega_s c_s + \mathrm{i} c_e \Omega_2 \mathrm{e}^{\mathrm{i}\omega_2 t} \,, \tag{3.119c}$$

where $\Omega_1 = \wp_{ge}\mathcal{E}_1/\hbar$ and $\Omega_2 = \wp_{se}\mathcal{E}_2/\hbar$ are the Rabi frequencies of the fields on the corresponding transitions, with $\wp_{\mu\nu}\mathcal{E}_j$ assumed real without loss of generality. Introducing the transformation $c_g(t) = c'_g(t)\,\mathrm{e}^{-\mathrm{i}\omega_g t}$, $c_e(t) = c'_e(t)\,\mathrm{e}^{-\mathrm{i}(\omega_g+\omega_1)t}$ and $c_s(t) = c'_s(t)\,\mathrm{e}^{-\mathrm{i}(\omega_g+\omega_1-\omega_2)t}$, from (3.119) we obtain

$$\frac{\partial}{\partial t}c'_g = \mathrm{i}\Omega_1 c'_e \;, \tag{3.120a}$$

$$\frac{\partial}{\partial t}c'_e = \mathrm{i}\Delta_1 c'_e + \mathrm{i}\Omega_1 c'_g + \mathrm{i}\Omega_2 c'_s \;, \tag{3.120b}$$

$$\frac{\partial}{\partial t}c'_s = \mathrm{i}(\Delta_1 - \Delta_2)c'_s + \mathrm{i}\Omega_2 c'_e \;, \tag{3.120c}$$

where $\Delta_1 = \omega_1 - \omega_{eg}$ and $\Delta_2 = \omega_2 - \omega_{es}$ are the detunings of the fields from the corresponding atomic transitions. Note that the above transformation is different from the transformation to the interaction picture $c_\mu = \tilde{c}_\mu \mathrm{e}^{-\mathrm{i}\omega_\mu t}$, the two obviously being related via $c'_g = \tilde{c}_g$, $c'_e = \tilde{c}_e\,\mathrm{e}^{\mathrm{i}\Delta_1 t}$ and $c'_s = \tilde{c}_s \mathrm{e}^{\mathrm{i}(\Delta_1-\Delta_2)t}$. Thus, instead of transforming to the frame rotating with the eigenfrequencies ω_μ ($\mu = e, g, s$) of the atomic levels, for reasons of convenience, we have transformed the set of amplitude equations (3.119) to the frame rotating with the frequencies of the optical fields ω_1 and ω_2. The equation for the amplitude of $|g\rangle$ is the same in both pictures (frames) because the transformation $\tilde{c}_g = c'_g = c_g\,\mathrm{e}^{\mathrm{i}\omega_g t}$ amounts to redefining the zero point energy to be the energy of level $|g\rangle$.

We can thus write the Hamiltonian of the Λ-configuration in the frame rotating with the frequencies of the optical fields as

$$\mathcal{H}_\Lambda = -\hbar\big[\Delta_1\sigma_{ee} + (\Delta_1 - \Delta_2)\sigma_{ss}\big] - \hbar\big[\Omega_1\sigma_{eg} + \Omega_2\sigma_{es} + \mathrm{H.c.}\big] \;, \tag{3.121}$$

where H.c. stands for the Hermitian conjugate. For the sake of completeness, we also state here the Hamiltonians for the three-level atoms interacting with two optical fields in the Ξ- and V-configurations, as shown in Fig. 3.6,

$$\mathcal{H}_\Xi = -\hbar\big[\Delta_1\sigma_{ee} + (\Delta_1 + \Delta_2)\sigma_{ss}\big] - \hbar\big[\Omega_1\sigma_{eg} + \Omega_2\sigma_{se} + \mathrm{H.c.}\big] \;, \tag{3.122}$$

$$\mathcal{H}_\mathrm{V} = -\hbar\big[\Delta_1\sigma_{ee} + \Delta_2\sigma_{ss}\big] - \hbar\big[\Omega_1\sigma_{eg} + \Omega_2\sigma_{sg} + \mathrm{H.c.}\big] \;, \tag{3.123}$$

which are easy to derive using the same reasoning as above (Prob. 3.4).

Continuing with the Λ-atom, note that so far we have not taken into account the decay of the excited state $|e\rangle$. In general, the atom in state $|e\rangle$ can emit a spontaneous photon and decay to either of the lower states $|g\rangle$ and $|s\rangle$ or to some other lower state. A rigorous treatment of this situation requires employing the density matrix formalism, which is the subject of the next chapter. Here we assume that $|e\rangle$ can decay to states other than $|g\rangle$ and $|s\rangle$, in which case, strictly speaking, the three-level system is not closed, because then the total population of the three states would not be conserved. This decay can be incorporated in the equation for c'_e by adding in the right-hand-side of (3.120b) a term of the form $-\gamma_e c'_e$. Indeed, as we have seen in

the previous section, in the absence of fields such a term would lead to the exponential decay of the amplitude of state $|e\rangle$ with the rate $\gamma_e \equiv \frac{1}{2}\Gamma_e$.

The analytic solution of the set of equations (3.120) for various amplitudes, time-dependencies and detunings of optical fields is in general a complex task that can often yield complicated expressions of little practical value. For such cases, numerical solutions are certainly much more useful and easier to obtain. However, for certain special cases of practical interest, simple analytical solutions are obtainable under reasonable, physically motivated approximations. We consider now one such case, corresponding to $|\Delta_1 - \Delta_2| \ll |\Delta_{1,2}|$, which will be employed in later sections on the physical implementation of quantum computers. To simplify the notation, from now on we shall denote the amplitudes of (3.120) without primes. Incorporating the decay of the excited level as described above, and assuming that $c_e(0) = 0$, we can write (3.120b) in the integral form as

$$c_e(t) = \mathrm{i}\int_0^t \mathrm{e}^{(\mathrm{i}\Delta_1 - \gamma_e)(t-t')}\big[\Omega_1(t')c_g(t') + \Omega_2(t')c_s(t')\big]\,\mathrm{d}t' \,. \tag{3.124}$$

If the Rabi frequencies Ω_1 and Ω_2 are smaller than $|\Delta_1|$ and $|\Delta_2|$, the amplitudes $c_g(t')$ and $c_s(t')$ will not change much during the time the exponent in (3.124) experiences many oscillations. Assuming further that the Rabi frequencies Ω_j change in time sufficiently slowly, so that the condition $|\dot{\Omega}_j/\Omega_j| \ll |\Delta_j|$ is satisfied for all $t' \in [0:t]$, the terms in the square brackets of (3.124) can be evaluated at time $t' = t$ and factored out of the integral,

$$c_e(t) = \mathrm{i}\big[\Omega_1(t)c_g(t) + \Omega_2(t)c_s(t)\big]\int_0^t \mathrm{e}^{(\mathrm{i}\Delta_1 - \gamma_e)(t-t')}\,\mathrm{d}t' \,.$$

The integration can then be performed, and for times $t \gg 1/\gamma_e$ we are left with the approximate expression

$$c_e(t) = -\frac{\Omega_1 c_g + \Omega_2 c_s}{\Delta_1 + \mathrm{i}\gamma_e} \,. \tag{3.125}$$

Note that this expression can be obtained directly from (3.120b) by taking $\partial_t c_e = 0$, which is a good approximation when $\sqrt{\Delta_{1,2}^2 + \gamma_e^2} \gg \Omega_{1,2}$. Substituting (3.125) into the remaining equations (3.120a) and (3.120c), for the amplitudes c_g and c_s we have

$$\frac{\partial}{\partial t}c_g = -\mathrm{i}\frac{|\Omega_1|^2}{\Delta_1 + \mathrm{i}\gamma_e}c_g - \mathrm{i}\frac{\Omega_1\Omega_2}{\Delta_1 + \mathrm{i}\gamma_e}c_s \,, \tag{3.126a}$$

$$\frac{\partial}{\partial t}c_s = \mathrm{i}\left(\Delta_1 - \Delta_2 - \frac{|\Omega_2|^2}{\Delta_1 + \mathrm{i}\gamma_e}\right)c_s - \mathrm{i}\frac{\Omega_2\Omega_1}{\Delta_1 + \mathrm{i}\gamma_e}c_g \,. \tag{3.126b}$$

Thus, we have adiabatically eliminated the intermediate excited state $|e\rangle$, obtaining coupled differential equations for the amplitudes of states $|g\rangle$ and $|s\rangle$. When $|\Delta_{1,2}| \gg \gamma_e, \Omega_{1,2}$, equations (3.126) reduce to

$$\frac{\partial}{\partial t}c_g = -(\mathrm{i}S_g + \gamma_g)c_g + \mathrm{i}\Omega_{\mathrm{eff}}\, c_e \ , \tag{3.127a}$$

$$\frac{\partial}{\partial t}c_s = -\big[\mathrm{i}(S_s - \Delta_1 + \Delta_2) + \gamma_s\big]c_s + \mathrm{i}\Omega_{\mathrm{eff}}\, c_g \ . \tag{3.127b}$$

Here $S_g = |\Omega_1|^2/\Delta_1$ and $S_s = |\Omega_2|^2/\Delta_1$ are the so-called ac Stark shifts of levels $|g\rangle$ and $|s\rangle$, respectively, while $\gamma_g = \gamma_e|\Omega_1|^2/\Delta_1^2 = \gamma_e S_g/\Delta_1$ and $\gamma_s = \gamma_e|\Omega_2|^2/\Delta_1^2 = \gamma_e S_s/\Delta_1$ are the effective relaxation (decay) rates, which due to our assumptions $\Omega_{1,2} \ll |\Delta_{1,2}|$ are much smaller than γ_e and therefore can be neglected for times $t < \gamma_{g,s}^{-1}$. Finally,

$$\Omega_{\mathrm{eff}} = \mathrm{i}\mathrm{e}^{\mathrm{i}\arctan(\frac{\Delta_1}{\gamma_e})}\frac{\Omega_1\Omega_2}{\Delta_1} \simeq -\frac{\Omega_1\Omega_2}{\Delta_1} \ , \quad (\Delta_1/\gamma_e \gg 1)$$

is the effective two-photon Rabi frequency for the transition $|g\rangle \leftrightarrow |s\rangle$. We can shift the zero point energy of the system by the amount S_g, via $c_{g,s} \to c_{g,s}\,\mathrm{e}^{-\mathrm{i}S_g t}$, obtaining finally

$$\frac{\partial}{\partial t}c_g = \mathrm{i}\Omega_{\mathrm{eff}}\, c_e \ , \tag{3.128a}$$

$$\frac{\partial}{\partial t}c_s = \mathrm{i}\Delta_{\mathrm{eff}}\, c_s + \mathrm{i}\Omega_{\mathrm{eff}}\, c_g \ , \tag{3.128b}$$

where $\Delta_{\mathrm{eff}} = \Delta_1 - \Delta_2 + S_g - S_s$ is the effective two-photon detuning, which obviously reduces to $\Delta_{\mathrm{eff}} = \Delta_1 - \Delta_2$ when $\Omega_1 = \Omega_2$. These equations have the same form with those of a two-level atom interacting with a monochromatic field studied in Sect. 3.3.1, except that equations (3.39) were written in the interaction picture. We can thus immediately write the solution of (3.128), for the initial conditions $c_g(0) = 1$ and $c_s(0) = 0$, as

$$c_g = \mathrm{e}^{\mathrm{i}\frac{\Delta_{\mathrm{eff}}}{2}t}\left[\cos(\bar{\Omega}_{\mathrm{eff}}t) - \mathrm{i}\frac{\Delta_{\mathrm{eff}}}{2\bar{\Omega}_{\mathrm{eff}}}\sin(\bar{\Omega}_{\mathrm{eff}}t)\right] \ , \tag{3.129a}$$

$$c_s = \mathrm{i}\mathrm{e}^{\mathrm{i}\frac{\Delta_{\mathrm{eff}}}{2}t}\frac{\Omega_{\mathrm{eff}}}{\bar{\Omega}_{\mathrm{eff}}}\sin(\bar{\Omega}_{\mathrm{eff}}t) \ , \tag{3.129b}$$

where $\bar{\Omega}_{\mathrm{eff}} \equiv \sqrt{\Omega_{\mathrm{eff}} + (\Delta_{\mathrm{eff}}/2)^2}$. When the two-photon (Raman) resonance condition is satisfied, $\Delta_{\mathrm{eff}} = 0$, we have

$$c_g(t) = \cos(\Omega_{\mathrm{eff}}t) \ , \quad c_s(t) = \mathrm{i}\sin(\Omega_{\mathrm{eff}}t) \ , \tag{3.130}$$

i.e., two-photon Rabi oscillations between states $|g\rangle$ and $|s\rangle$.

In the case of the ladder (Ξ) system, starting with the Hamiltonian (3.122) and following the same steps as above, one can adiabatically eliminate the nonresonant intermediate state $|e\rangle$, under the conditions $|\Delta_1 + \Delta_2| \ll |\Delta_{1,2}|$ and $|\Delta_{1,2}| \gg \gamma_e, \Omega_{1,2}$. The resulting effective two-level two-photon model is described by the coupled equations for the amplitudes c_g and c_s, which are similar to (3.128), with the effective two-photon detuning given by $\Delta_{\mathrm{eff}} = \Delta_1 +$

$\Delta_2 + S_g - S_e$. However, since the decay rate γ_s of the uppermost excited state $|s\rangle$ is large, it can not be neglected and should be included in the equation for c_s. Detailed derivation of these equations is left as an exercise (see Prob. 3.5). As for the V-atoms, in principle the same procedure can lead to the effective two-level model with states $|e\rangle$ and $|s\rangle$ which decay rapidly with the rates γ_e and γ_s, respectively. In practice, however, if in the course of time the ground state population becomes significant (due to the decay from $|e\rangle$ and $|s\rangle$), its adiabatic elimination becomes meaningless.

Returning back to the Λ-system, let us also consider the case of small and equal detunings $\Delta_1 = \Delta_2 = \Delta \lesssim \Omega_{1,2}$, i.e., exact two-photon (Raman) resonance. In the basis of "bare" atomic eigenstates $\{|g\rangle, |e\rangle, |s\rangle\}$, the Hamiltonian (3.121) can then be written in the matrix form as

$$\mathcal{H}_\Lambda = -\hbar \begin{bmatrix} 0 & \Omega_1 & 0 \\ \Omega_1 & \Delta & \Omega_2 \\ 0 & \Omega_2 & 0 \end{bmatrix} . \tag{3.131}$$

Our aim is to find the eigenstates of this Hamiltonian, i.e., eigenstates of the atom "dressed" by the fields E_1 and E_2. Solving the eigenvalue problem $\mathcal{H}_\Lambda |\Psi\rangle = \hbar\lambda |\Psi\rangle$, we find the eigenvalues of $\mathcal{H}_\Lambda$,

$$\lambda_0 = 0 , \quad \lambda_\pm = -(\Delta/2) \pm \bar{\Omega} , \tag{3.132}$$

with $\bar{\Omega} = \sqrt{\Omega_1^2 + \Omega_2^2 + (\Delta/2)^2}$, and the corresponding normalized eigenvectors

$$|D\rangle = \frac{1}{\sqrt{N_0}} [\Omega_2 |g\rangle - \Omega_1 |s\rangle] , \tag{3.133a}$$

$$|B_\pm\rangle = \frac{1}{\sqrt{N_\pm}} [\Omega_1 |g\rangle - \lambda_\pm |e\rangle + \Omega_2 |s\rangle] , \tag{3.133b}$$

with $N_0 = \Omega_1^2 + \Omega_2^2$ and $N_\pm = N_0 + \lambda_\pm^2$. We thus see that the eigenstate with zero energy $|D\rangle$ does not contain the intermediate state $|e\rangle$ which decays by emitting spontaneous photons with the rate γ_e. Therefore $|D\rangle$ is sometimes called the dark state, while $|B_\pm\rangle$ are called bright states. We can express the dark state as

$$|D\rangle = \cos\Theta |g\rangle - \sin\Theta |s\rangle , \tag{3.134}$$

where the mixing angle Θ is defined through $\tan\Theta = \Omega_1/\Omega_2$. This eigenstate is in fact decoupled from both fields E_1 and E_2, since $\mathcal{H}_\Lambda |D\rangle = 0$. This is a remarkable result, which means that if an atom, subject to two fields with Rabi frequencies Ω_1 and Ω_2, is prepared in a coherent superposition state (3.134), it will remain in this state, with the populations of levels $|g\rangle$, $|e\rangle$ and $|s\rangle$ given by $|c_g|^2 = \cos^2\Theta = \Omega_2^2/(\Omega_1^2 + \Omega_2^2)$, $|c_e|^2 = 0$ and $|c_s|^2 = \sin^2\Theta = \Omega_1^2/(\Omega_1^2 + \Omega_2^2)$. For this reason, the state $|D\rangle$ is also called coherent population trapping (CPT) state. In particular, when one of the two Rabi frequencies $\Omega_{1,2}$ is zero,

the CPT state coincides with the bare atomic state: $|D\rangle = |g\rangle$ for $\Omega_1 = 0$ and $\Omega_2 \neq 0$ ($\Omega_2 > 0$), and $|D\rangle = |s\rangle$ for $\Omega_1 \neq 0$ ($\Omega_1 < 0$) and $\Omega_2 = 0$.

So far, we have assumed that the field amplitudes $\mathcal{E}_{1,2}$ or the Rabi frequencies $\Omega_{1,2}$ do not change in time. When the fields are time-dependent, the eigenstates $|D(t)\rangle$ and $|B_\pm(t)\rangle$ also depend on time, their physical meaning being the instantaneous dressed eigenstate of the system at time t. Suppose now that at time t_i we prepare the atom in state $|\Psi(t_i)\rangle = |g\rangle$ and switch on only the $\mathcal{E}_2$ field, i.e., $\Omega_1(t_i) = 0$ and $\Omega_2(t_i) \neq 0$. Then the state of the atom coincides with the CPT state $|D(t_i)\rangle = |g\rangle = |\Psi(t_i)\rangle$. Next we slowly decrease Ω_2 and simultaneously increase Ω_1, so that at some later time t_f we have $\Omega_1(t_f) \neq 0$ and $\Omega_2(t_f) = 0$ and the CPT state is $|D(t_f)\rangle = |s\rangle$. If during all this time $t_i \leq t \leq t_f$ the state vector $|\Psi(t)\rangle$ followed the CPT state $|D(t)\rangle$, we would have transfered all of the atomic population from the initial state $|g\rangle$ to the final state $|s\rangle$, without ever populating the excited state $|e\rangle$ and loosing population due to its decay. In general, however, for a time-dependent perturbation, if a physical system at some instant of time is in one of its instantaneous eigenstates, at a later time other instantaneous eigenstates also acquire populations due to the transitions induced by the time-dependence of the perturbation. Only when the perturbation changes in time slowly enough—adiabatically—the state vector of the system can follow the initial eigenstate, which does not couple to other eigenstates. More precisely, the nonadiabatic coupling is small when the rate of change of the perturbation does not exceed the energy separation between the dressed eigenstates.

For the three-level Λ atom subject to two time-dependent pulsed fields, the above adiabatic following criterion yields $|\dot{\Theta}| \ll |\lambda_\pm - \lambda_0|$, or substituting for the time dependent mixing angle $\Theta(t) = \arctan\left[\Omega_1(t)/\Omega_2(t)\right]$ we obtain

$$\left| \frac{\dot{\Omega}_1 \Omega_2 - \Omega_1 \dot{\Omega}_2}{\Omega_1^2 + \Omega_2^2} \right| \ll |\lambda_\pm - \lambda_0| \,. \tag{3.135}$$

The procedure for coherent population transfer in the Λ atom can now be specified as follows (see Fig. 3.7). Initially, as the atom is in state $|g\rangle$, we switch on a pulsed field acting on the transition $|s\rangle \leftrightarrow |e\rangle$ with Rabi frequency Ω_2. We thus have $\Omega_1 \ll \Omega_2$ and $\Theta = 0$. At a later time, before the first pulse is off, we switch on the second pulsed field, acting on the transition $|g\rangle \leftrightarrow |e\rangle$ with Rabi frequency Ω_1. Once $\Omega_1 \gg \Omega_2$ and $\Theta = \pi/2$, the atomic state becomes $|s\rangle$ and remains so even after both pulses are off. Obviously, the two pulses should overlap in time sufficiently, so that the condition (3.135) remains satisfied during the transfer process. Careful consideration of (3.135) leads to the following constraint on the Rabi frequencies of the two fields, $\max(\Omega_{1,2})\,\tau \gg 1$, where τ is a characteristic time corresponding to the duration and the overlap of the pulses; see Bergmann, Theuer and Shore (1998). This technique of coherent population transfer in a three-level Λ-system is known as stimulated Raman adiabatic passage, or STIRAP. As discussed in later sections, the combination of STIRAP and cavity quantum

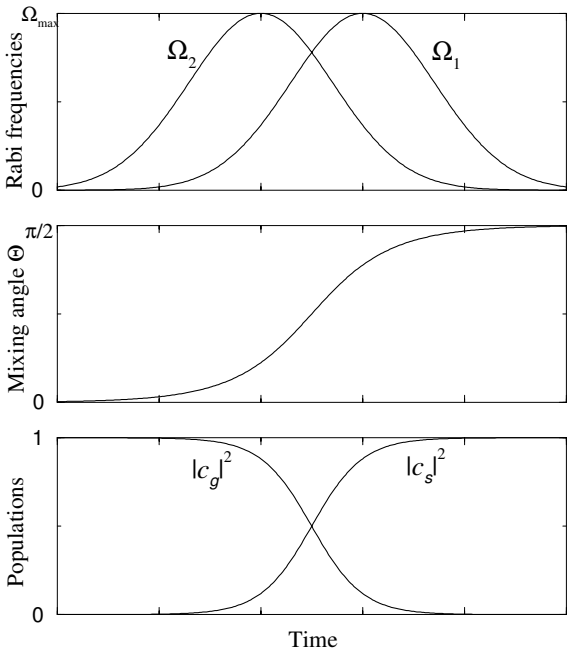

Fig. 3.7. Simulated Raman adiabatic passage in a three-level Λ atom. Time dependence of (a) the Rabi frequencies Ω_1 and Ω_2, (b) the mixing angle Θ, and (c) the populations of levels $|g\rangle$ and $|s\rangle$.

electrodynamics has many advantageous properties which can be employed in quantum information processing and communication. In Chap. 6 on field propagation in atomic media, we present yet another effect associated with the CPT states of three-level Λ atoms, namely electromagnetically induced transparency.

Problems

3.1. Prove the commutation relation (3.31).

3.2. Plot the energy eigenvalues $\lambda_{\pm}^{(n)}$ of (3.61) versus the detuning Δ for $g = 0$ and $g \neq 0$. Observe the avoided crossing at $\Delta = 0$ for the case of nonvanishing coupling constant g. Show that in the limit $(\Delta/2)^2 \gg g^2(n+1)$ the dressed states $|\pm_n\rangle$ approach the bare states $|e, n\rangle$ and $|g, n+1\rangle$; consider both cases $\Delta > 0$ and $\Delta < 0$ and deduce to which bare state corresponds the dressed state $|+_n\rangle$ (or $|-_n\rangle$).

3.3. Prove the equality (3.89). (*Hint*: Take the power series expansion of the exponential operator and use repetitively the fact that $\mathcal{U}_{\mathrm{M}}$ is a unitary operator, i.e., $\mathcal{U}_{\mathrm{M}}\mathcal{U}_{\mathrm{M}}^{\dagger} = I$.)

3.4. Derive the Hamiltonians (3.122) and (3.123) for the Ξ- and V-atoms interacting with two optical fields as shown in Fig. 3.6(a) and (b).

3.5. Starting with the Hamiltonian (3.122) for Ξ-atom and including the decays of levels $|e\rangle$ and $|s\rangle$, derive the coupled differential equations for the amplitudes c_g and c_s under the conditions $|\Delta_1 + \Delta_2| \ll |\Delta_{1,2}|$ and $\sqrt{\Delta_{1,2}^2 + \gamma_e^2} \gg \Omega_{1,2}$.

4

System-Reservoir Interaction

In this chapter, we begin with the general derivation of the so-called master equation, which is the equation of motion for the reduced density operator for a small system interacting with a large system, or a reservoir, having infinitely many densely spaced energy levels. We then describe an alternative approach to the same problem, based on the quantum Monte–Carlo stochastic wavefunctions, which is often convenient for numerical simulations of the dynamics of single quantum systems. Finally, we derive the quantum Langevin equations of motion for the system operators in the Heisenberg picture. The material of this chapter is illustrated with the driven two-level atom interacting with the open radiation field, while in the next chapter we employ the same general formalism in the context of cavity quantum electrodynamics. The spontaneous emission from the atom subject to a coherent driving field constitutes one of the central problems in quantum optics known as the resonance fluorescence, certain aspects of which are outlined below.

4.1 Reduced Density Operator

In the light of the results obtained and insight gained in Sect. 3.5, we proceed now to the formulation of the same question in terms of the density operator, which provides the most complete and general description of a quantum system.

4.1.1 General Master Equation

We consider a small quantum system, to be referred to from here on simply as the system (S), coupled to a large system with infinitely many states with a continuous spectrum to be referred to as the reservoir (R), for which also the term "bath" is often used in the literature. Let the Hamiltonians be, respectively, $\mathcal{H}^{\mathrm{S}}$ and $\mathcal{H}^{\mathrm{R}}$, with $\mathcal{V}$ the coupling between the two. Thus the total Hamiltonian of the compound system is

$$\mathcal{H} = \mathcal{H}^{\mathrm{S}} + \mathcal{H}^{\mathrm{R}} + \mathcal{V} \equiv \mathcal{H}^0 + \mathcal{V} \,. \tag{4.1}$$

The compound system is isolated, in the sense that its parts are not coupled to anything else but only to each other. Consequently, the total energy is a constant of motion. We assume that at some time to be taken as $t = 0$, we know the state of the system as described most generally by its density operator $\rho^{\mathrm{S}}(0)$ or, to compress somewhat notation, simply ρ_0^{S}. The reservoir is also described by its density operator ρ_0^{R} at $t = 0$, which, however, will not be affected by the interaction. This is one of the basic assumptions in the problem under consideration, which is based on the fact that in the actual physical situation the reservoir is too large to be affected by the small system. The objective therefore is to develop an equation of motion for the density operator of the system which incorporates the influence of the reservoir, in some approximation appropriate to the physical situation under consideration. The basic set of assumptions have already been discussed in the previous chapter. Here we not only formulate the problem in the more general context of the density operator, but we do in addition allow the reservoir to be at some finite temperature, generalizing thus the problem of Sect. 3.5.

It is most convenient and customary to model the reservoir by a set of infinitely many harmonic oscillators, with the corresponding creation and annihilation operators to be denoted here by $b_k^\dagger$ and b_k. This, as we have seen, is in fact the case with the open radiation field, as it would also be the case if the reservoir were the phonon field in a solid. It is therefore fair to say that no generality is lost by adopting this model and certainly that is the case in the context of quantum optics. The system could be another harmonic oscillator, as it is the case in the next chapter, or a two-level atom, which is discussed later in this chapter. In either case, we will describe it in terms of the appropriate raising and lowering operators, for which often the term ladder operators is also used. These, as we already know, correspond to the creation $a^\dagger$ and annihilation a operators in the case of harmonic oscillator, and to the pseudo-spin raising σ_+ and lowering σ_- operator in the case of a two-level atom.

Let $\tilde{\rho}(t)$ be the density operator of the compound system in the interaction picture. As established in Sect. 1.3.4, its time evolution is governed by the von Neumann equation

$$\frac{\partial}{\partial t}\tilde{\rho}(t) = -\frac{\mathrm{i}}{\hbar}[\tilde{\mathcal{V}}(t), \tilde{\rho}(t)] \,, \tag{4.2}$$

where the time-dependence of $\tilde{\mathcal{V}}(t)$ originates from the transformation to the interaction picture, $\tilde{\mathcal{V}}(t) = \mathrm{e}^{\frac{\mathrm{i}}{\hbar}\mathcal{H}^0 t}\,\mathcal{V}\,\mathrm{e}^{-\frac{\mathrm{i}}{\hbar}\mathcal{H}^0 t}$. In principle, $\mathcal{V}$ could be inherently time-dependent due to some external influence, which, however, will not be the case for our model here. Obviously at $t = 0$ we have $\tilde{\rho}(0) = \rho_0$. Solving the equation of motion (4.2) for the total density operator $\tilde{\rho}(t)$ is neither practical nor desirable. On physical grounds and without any mathematics, we know that the density operator $\tilde{\rho}^{\mathrm{R}}$ of the reservoir will not be significantly

affected. Our objective therefore is to extract another equation of motion for the density operator of the system $\tilde{\rho}^{\mathrm{S}}$, under a suitable set of approximations reflecting the underlying physical conditions. To this end, we consider the reduced density operator

$$\tilde{\rho}^{\mathrm{S}} \equiv \mathrm{Tr}_{\mathrm{R}}(\tilde{\rho}) \,, \tag{4.3}$$

obtained by taking the partial trace of the total $\tilde{\rho}$ with respect to R, also referred to as tracing out the degrees of freedom of the reservoir. If the two density operators are uncoupled, as is the case at $t = 0$, i.e., $\rho_0 = \rho_0^{\mathrm{S}} \otimes \rho_0^{\mathrm{R}}$, then obviously

$$\mathrm{Tr}_{\mathrm{R}}(\rho_0) = \rho_0^{\mathrm{S}} \,\mathrm{Tr}_{\mathrm{R}}(\rho_0^{\mathrm{R}}) = \rho_0^{\mathrm{S}} \,, \tag{4.4}$$

which is the exact density operator of S. Taking the trace over R in the general case of two interacting, and therefore entangled systems S and R does not result in a density operator depending only on the variables of S. However, as we know from Sect. 1.3.2, the density operator of system S determines the expectation value of any operator $\mathcal{T}$ acting only on S, according to $\langle \mathcal{T} \rangle = \mathrm{Tr}(\rho^{\mathrm{S}} \mathcal{T})$. Furthermore, the equation of motion for the density operator of S, often called master equation, is a convenient tool for the derivation of the equations of motion for the expectation values of various system operators.

One of the approximations to be adopted is perturbation theory, which is accomplished by developing a form of the equation of motion in powers of the interaction $\tilde{\mathcal{V}}$ and truncating it to the appropriate order. This suggests that the von Neumann equation (4.2) be written in the integral form

$$\tilde{\rho}(t) = \tilde{\rho}(0) - \frac{\mathrm{i}}{\hbar} \int_0^t \mathrm{d}t' \, [\tilde{\mathcal{V}}(t'), \tilde{\rho}(t')] \,. \tag{4.5}$$

Substituting this expression back into (4.2) and taking the trace over R, we obtain

$$\frac{\partial}{\partial t} \tilde{\rho}^{\mathrm{S}}(t) = -\frac{\mathrm{i}}{\hbar} \mathrm{Tr}_{\mathrm{R}}[\tilde{\mathcal{V}}(t), \tilde{\rho}(0)] - \frac{1}{\hbar^2} \int_0^t \mathrm{d}t' \, \mathrm{Tr}_{\mathrm{R}}[\tilde{\mathcal{V}}(t), [\tilde{\mathcal{V}}(t'), \tilde{\rho}(t')]] \,, \tag{4.6}$$

which is still an exact expression for $\partial_t \tilde{\rho}^{\mathrm{S}}$, even though the trace over R has been taken, because no approximation has yet been made. It simply is a formal expression for $\partial_t \tilde{\rho}^{\mathrm{S}}$ in the form of an integral equation. If needed, it can be iterated repeatedly, generating thus an expansion in powers of the interaction $\tilde{\mathcal{V}}$. But it is not needed for our purposes.

To begin with the type of applications and physical situations we have in mind, note first that the interaction $\tilde{\mathcal{V}}$ will always be linear in the system and reservoir operators, involving only products of operators of R with S. The density operator for R at $t = 0$ will be assumed diagonal in the energy eigenstates representation, because it represents a quantum system in equilibrium at some temperature. If it were not in equilibrium, it would mean that the reservoir was still interacting with another system of similar magnitude but different temperature. Under these two conditions, we have

$$\mathrm{Tr_R}[\tilde{\mathcal{V}}(t), \tilde{\rho}(0)] = \mathrm{Tr_R}[\tilde{\mathcal{V}}(t), \rho^{\mathrm{S}}(0) \otimes \rho^{\mathrm{R}}(0)] = 0 \,,$$

because when taking the trace over R, in the representation of the eigenstates of $\mathcal{H}^{\mathrm{R}}$ (i.e., eigenstates of $b_k^\dagger b_k$), the diagonal matrix elements of the reservoir operators $b_k^\dagger$ and b_k contained in $\tilde{\mathcal{V}}$ vanish. We are thus left with the equation

$$\frac{\partial}{\partial t}\tilde{\rho}^{\mathrm{S}}(t) = -\frac{1}{\hbar^2}\int_0^t \mathrm{d}t' \,\mathrm{Tr_R}[\tilde{\mathcal{V}}(t), [\tilde{\mathcal{V}}(t'), \tilde{\rho}(t')]] \,. \tag{4.7}$$

On the basis of our assumptions about the relative sizes of S and R, as well as the weakness of the coupling between the two, we can replace $\tilde{\rho}(t')$ by $\tilde{\rho}^{\mathrm{S}}(t')\,\rho_0^{\mathrm{R}}$ in the commutator of (4.7), obtaining

$$\frac{\partial}{\partial t}\tilde{\rho}^{\mathrm{S}}(t) = -\frac{1}{\hbar^2}\int_0^t \mathrm{d}t' \,\mathrm{Tr_R}[\tilde{\mathcal{V}}(t), [\tilde{\mathcal{V}}(t'), \tilde{\rho}^{\mathrm{S}}(t')\,\rho_0^{\mathrm{R}}]] \,. \tag{4.8}$$

As it stands, this equation relates the derivative of $\tilde{\rho}^{\mathrm{S}}(t)$ to $\tilde{\rho}^{\mathrm{S}}(t')$ at all previous times $t' \le t$. It does not imply that the system does not cause excitations in the reservoir, but that such excitations mediated by $\tilde{\mathcal{V}}$ decay very quickly into the equilibrium state. In other words, the reservoir attains the equilibrium during a time short compared to the time it takes for $\tilde{\rho}^{\mathrm{S}}(t')$ to change substantially, the latter time being inversely proportional to the coupling strength between S and R. Assuming that the reservoir decay times are sufficiently short, which is directly related to the assumption of a smooth density of states, we conclude that the reservoir correlations contained in products of the form $\tilde{\mathcal{V}}(t)\tilde{\mathcal{V}}(t')$ and $\tilde{\mathcal{V}}(t')\tilde{\mathcal{V}}(t)$ are sharply peaked around $t = t'$. We can therefore replace t' in $\tilde{\rho}^{\mathrm{S}}(t')$ by t, which is part of the Markov approximation, obtaining

$$\frac{\partial}{\partial t}\tilde{\rho}^{\mathrm{S}}(t) = -\frac{1}{\hbar^2}\int_0^t \mathrm{d}t' \,\mathrm{Tr_R}[\tilde{\mathcal{V}}(t), [\tilde{\mathcal{V}}(t'), \tilde{\rho}^{\mathrm{S}}(t)\,\rho_0^{\mathrm{R}}]] \,. \tag{4.9}$$

This equation is also known as the Redfield equation obtained several decades ago in the context of magnetic resonance. Note that the time evolution of the system governed by the differential equation (4.9) still depends on the initial state of the system at $t = 0$. This dependence is irrelevant as long as all the above conditions for the Markov approximation are met. It is eliminated by making a change of variable $t' \to t - t'$ and extending the limit of integration to ∞, with the final result

$$\frac{\partial}{\partial t}\tilde{\rho}^{\mathrm{S}}(t) = -\frac{1}{\hbar^2}\int_0^\infty \mathrm{d}t' \,\mathrm{Tr_R}[\tilde{\mathcal{V}}(t), [\tilde{\mathcal{V}}(t-t'), \tilde{\rho}^{\mathrm{S}}(t)\,\rho_0^{\mathrm{R}}]] \,, \tag{4.10}$$

which is a Born–Markov master equation. It involves two essential approximations, namely the Born approximation meaning that we have truncated the integral equation (4.5) to the lowest nonvanishing order in $\mathcal{V}$, and the Markov approximation discussed above.

In order to proceed beyond the general formal expression (4.10) for the quantum master equation, we need to specify somewhat further the components of the compound system. In this chapter we are concerned with the case of the system being a two level atom and the reservoir represented by the open radiation field, while in Chap. 5 we consider a single-mode cavity field damped by the absorption at the cavity walls and/or transmission losses into the outside field modes. In any case, the interaction would have the form

$$\mathcal{V} = \mathcal{A} \cdot \mathcal{B} \,, \tag{4.11}$$

where $\mathcal{A}$ and $\mathcal{B}$ are Hermitian operators for the system and reservoir, respectively, each of them being linear in the respective raising and lowering operators of the corresponding subsystem. It is also assumed that operators $\mathcal{A}$ and $\mathcal{B}$ have no nonvanishing diagonal matrix elements in the representation that diagonalizes the respective Hamiltonians $\mathcal{H}^{\mathrm{S}}$ and $\mathcal{H}^{\mathrm{R}}$, i.e., the energy eigenstates. Thus if we label the eigenstates of $\mathcal{H}^{\mathrm{S}}$ by $|i\rangle$, $|j\rangle, \ldots$, with the corresponding energy eigenvalues $\hbar\omega_i, \hbar\omega_j, \ldots$, we would have

$$\mathcal{A} = \sum_{ij} |i\rangle\langle i|\,\mathcal{A}\,|j\rangle\langle j| = \sum_{ij} |i\rangle\mathcal{A}_{ij}\langle j| \equiv \sum_{ij} \boldsymbol{\alpha}_{ij} = \sum_{ij} \boldsymbol{\alpha}_{ji}^{\dagger} \,, \tag{4.12}$$

which define the operators $\boldsymbol{\alpha}_{ij} \equiv \mathcal{A}_{ij}\,|i\rangle\langle j|$ in the Schrödinger picture. Observing that they obey

$$[\mathcal{H}^{\mathrm{S}}, \boldsymbol{\alpha}_{ij}] = \hbar\omega_{ij}\,\boldsymbol{\alpha}_{ij} \,, \quad [\mathcal{H}^{\mathrm{S}}, \boldsymbol{\alpha}_{ij}^{\dagger}] = -\hbar\omega_{ij}\,\boldsymbol{\alpha}_{ij}^{\dagger} \,, \quad [\mathcal{H}^{\mathrm{S}}, \boldsymbol{\alpha}_{ji}^{\dagger}\boldsymbol{\alpha}_{ij}] = 0 \,,$$

where $\omega_{ij} \equiv \omega_i - \omega_j$, it explains why $\boldsymbol{\alpha}_{ij}$ and $\boldsymbol{\alpha}_{ij}^{\dagger}$ are referred to as eigenoperators of $\mathcal{H}^{\mathrm{S}}$ with frequencies $\pm\omega_{ij}$. In the interaction picture, we then have

$$\tilde{\mathcal{A}}(t) \equiv \mathrm{e}^{\frac{\mathrm{i}}{\hbar}\mathcal{H}^{\mathrm{S}}t}\,\mathcal{A}\,\mathrm{e}^{-\frac{\mathrm{i}}{\hbar}\mathcal{H}^{\mathrm{S}}t} = \sum_{ij} \mathrm{e}^{\mathrm{i}\omega_i t}\,|i\rangle\mathcal{A}_{ij}\langle j|\,\mathrm{e}^{-\mathrm{i}\omega_j t} = \sum_{ij} \boldsymbol{\alpha}_{ij}\mathrm{e}^{\mathrm{i}\omega_{ij}t} \,, \tag{4.13a}$$

$$\tilde{\mathcal{B}}(t) \equiv \mathrm{e}^{\frac{\mathrm{i}}{\hbar}\mathcal{H}^{\mathrm{R}}t}\,\mathcal{B}\,\mathrm{e}^{-\frac{\mathrm{i}}{\hbar}\mathcal{H}^{\mathrm{R}}t} = \sum_{k} \tilde{\boldsymbol{\beta}}_k(t) \,, \tag{4.13b}$$

where we have indicated explicitly the form of operator $\tilde{\mathcal{B}}(t)$ as a sum over all the reservoir modes

$$\tilde{\boldsymbol{\beta}}_k(t) = \mathrm{i}\boldsymbol{\epsilon}_k(b_k^{\dagger}\mathrm{e}^{\mathrm{i}\omega_k t} - b_k\mathrm{e}^{-\mathrm{i}\omega_k t}) \,, \tag{4.14}$$

with ω_k denoting the frequencies of the corresponding modes. As we have already seen, this sum will eventually be turned into an integral. The system–reservoir interaction $\tilde{\mathcal{V}}(t)$ can now be written as

$$\tilde{\mathcal{V}}(t) = \tilde{\mathcal{A}}(t) \cdot \tilde{\mathcal{B}}(t) = \sum_{ij}\sum_{k} \mathrm{e}^{-\mathrm{i}\omega_{ji}t}\boldsymbol{\alpha}_{ij} \cdot \tilde{\boldsymbol{\beta}}_k(t) \,. \tag{4.15}$$

Since the reservoir is assumed to be in thermal equilibrium, its density operator is diagonal in the energy eigenstates representation, as a consequence of which we have

$$\langle\tilde{\boldsymbol{\beta}}_k(t)\rangle_{\mathrm{R}} = \mathrm{Tr}_{\mathrm{R}}\big(\tilde{\boldsymbol{\beta}}_k(t)\rho_0^{\mathrm{R}}\big) = 0\ . \tag{4.16}$$

Expanding now the commutators of the master equation (4.10) and inserting $\tilde{\mathcal{V}}(t)$ and $\tilde{\mathcal{V}}(t-t')$ expressed through operators $\boldsymbol{\alpha}_{ij}$ and $\tilde{\boldsymbol{\beta}}_k$ as in (4.15), we obtain

$$\frac{\partial}{\partial t}\tilde{\rho}^{\mathrm{S}}(t) = \sum_{ij,j'i'}\sum_{kk'}\ \mathrm{e}^{\mathrm{i}(\omega_{j'i'}-\omega_{ji})t}\Big[G_{kk'}(\omega_{ji})\big(\boldsymbol{\alpha}_{ij}\,\tilde{\rho}^{\mathrm{S}}(t)\,\boldsymbol{\alpha}_{j'i'} - \boldsymbol{\alpha}_{j'i'}\,\boldsymbol{\alpha}_{ij}\,\tilde{\rho}^{\mathrm{S}}(t)\big)$$
$$+\overline{G}_{kk'}(\omega_{ji})\big(\boldsymbol{\alpha}_{j'i'}\,\tilde{\rho}^{\mathrm{S}}(t)\,\boldsymbol{\alpha}_{ij} - \tilde{\rho}^{\mathrm{S}}(t)\,\boldsymbol{\alpha}_{ij}\,\boldsymbol{\alpha}_{j'i'}\big)\Big]\ , \tag{4.17}$$

where $G_{kk}(\omega_{ji})$ and $\overline{G}_{kk'}(\omega_{ji})$ are defined as

$$G_{kk'}(\omega_{ji}) \equiv \frac{1}{\hbar^2}\int_0^\infty \mathrm{d}t'\,\mathrm{e}^{\mathrm{i}\omega_{ji}t'}\,\langle\tilde{\boldsymbol{\beta}}_{k'}(t)\,\tilde{\boldsymbol{\beta}}_k(t-t')\rangle_{\mathrm{R}}\ , \tag{4.18a}$$

$$\overline{G}_{kk'}(\omega_{ji}) \equiv \frac{1}{\hbar^2}\int_0^\infty \mathrm{d}t'\,\mathrm{e}^{\mathrm{i}\omega_{ji}t'}\,\langle\tilde{\boldsymbol{\beta}}_k(t-t')\,\tilde{\boldsymbol{\beta}}_{k'}(t)\rangle_{\mathrm{R}}\ , \tag{4.18b}$$

and $\langle\,\cdot\,\rangle_{\mathrm{R}}$ is a short-hand notation for $\mathrm{Tr}_{\mathrm{R}}(\,\cdot\,\rho_0^{\mathrm{R}})$. These quantities represent thus the Fourier transforms of the respective correlation functions of the reservoir. For a reservoir in an equilibrium state, so that $[\mathcal{H}^{\mathrm{R}},\rho^{\mathrm{R}}]=0$, we have a stationary process $\partial_t\rho^{\mathrm{R}}=0$, which implies

$$\langle\tilde{\boldsymbol{\beta}}_{k'}(t)\,\tilde{\boldsymbol{\beta}}_k(t-t')\rangle_{\mathrm{R}} = \langle\tilde{\boldsymbol{\beta}}_{k'}(t')\,\tilde{\boldsymbol{\beta}}_k(0)\rangle_{\mathrm{R}}\ , \tag{4.19a}$$

$$\langle\tilde{\boldsymbol{\beta}}_k(t-t')\,\tilde{\boldsymbol{\beta}}_{k'}(t)\rangle_{\mathrm{R}} = \langle\tilde{\boldsymbol{\beta}}_k(0)\,\tilde{\boldsymbol{\beta}}_{k'}(t')\rangle_{\mathrm{R}}\ , \tag{4.19b}$$

i.e., the correlation functions depend only on the time difference t' and not on its origin t.

Recall that in (4.17) ω_{ji} and $\omega_{j'i'}$ represent the frequency differences $\omega_j-\omega_i$ and $\omega_{j'}-\omega_{i'}$, respectively. The rotating wave approximation in this context means that we should keep only the terms with $\omega_{ji}=\omega_{j'i'}$ for which the indices i,j and i',j' are obviously related by $i=i'$ and $j=j'$. With the notation

$$G_{ij} \equiv \sum_{kk'} G_{kk'}(\omega_{ji})\ ,\quad \overline{G}_{ij} \equiv \sum_{kk'}\overline{G}_{kk'}(\omega_{ji})\ , \tag{4.20}$$

where G_{ij} and $\overline{G}_{ij}$ are in general complex constants, the master equation (4.17) can then be written as

$$\frac{\partial}{\partial t}\tilde{\rho}^{\mathrm{S}}(t) = \sum_{ij}\ \Big[G_{ij}\big(\boldsymbol{\alpha}_{ij}\,\tilde{\rho}^{\mathrm{S}}(t)\,\boldsymbol{\alpha}_{ij}^\dagger - \boldsymbol{\alpha}_{ij}^\dagger\,\boldsymbol{\alpha}_{ij}\,\tilde{\rho}^{\mathrm{S}}(t)\big)$$
$$+\overline{G}_{ij}\big(\boldsymbol{\alpha}_{ij}^\dagger\,\tilde{\rho}^{\mathrm{S}}(t)\,\boldsymbol{\alpha}_{ij} - \tilde{\rho}^{\mathrm{S}}(t)\,\boldsymbol{\alpha}_{ij}\,\boldsymbol{\alpha}_{ij}^\dagger\big)\Big]\ . \tag{4.21}$$

We shall see later on that the real parts of G_{ij} and $\overline{G}_{ij}$ are responsible for the decay, while their imaginary parts modify the transition frequencies of the system due to the shift of its levels.

4.1.2 Spontaneous Decay of a Two-Level Atom

The general master equation (4.21) can further be reduced to a simpler form when the precise nature of the system and the reservoir is taken into consideration. A two-level atom interacting with the open radiation field is of particular interest here. Although we have examined this problem in Sect. 3.5.2, the master equation provides the necessary tool to generalize the treatment to a reservoir of finite (i.e., nonzero) temperature.

The system is thus a two-level atom with the lower and the upper states $|g\rangle$ and $|e\rangle$. It is described by the Hamiltonian $\mathcal{H}^{\mathrm{A}} = \sum_{i=g,e} \hbar\omega_i \, |i\rangle\langle i|$, which upon shifting the zero-point energy to $\frac{1}{2}\hbar(\omega_g + \omega_e)$ becomes $\mathcal{H}^{\mathrm{A}} = \frac{1}{2}\hbar\omega_{eg}\sigma_z$, where ω_{eg} is the $|e\rangle \to |g\rangle$ transition frequency and $\sigma_z = |e\rangle\langle e| - |g\rangle\langle g|$ is an atomic operator. In the notation of this chapter, the Hamiltonian of the reservoir—free radiation field—is given by $\mathcal{H}^{\mathrm{R}} = \sum_{\boldsymbol{k}\lambda} \hbar\omega_k b^\dagger_{\boldsymbol{k}\lambda} b_{\boldsymbol{k}\lambda}$. Finally, the atom–field interaction in the dipole approximation has the standard form

$$\mathcal{V} = -\wp \cdot \boldsymbol{E} \, , \tag{4.22}$$

where the atomic dipole operator $\wp$ can be expressed as

$$\wp = \wp_{eg}\sigma_{ge} + \wp_{ge}\sigma_{eg} \equiv \wp_{eg}\sigma_- + \wp_{ge}\sigma_+ \, , \tag{4.23}$$

with $\sigma_{ge} = |g\rangle\langle e|$ and $\sigma_{eg} = |e\rangle\langle g|$, while the electric field operator $\boldsymbol{E}$ reads

$$\boldsymbol{E} = \mathrm{i} \sum_{\boldsymbol{k}\lambda} \hat{\boldsymbol{e}}_{\boldsymbol{k}\lambda} \epsilon_k \left[b_{\boldsymbol{k}\lambda} - b^\dagger_{\boldsymbol{k}\lambda} \right] , \tag{4.24}$$

with $\epsilon_k \equiv \sqrt{\hbar\omega_k / 2\varepsilon_0 V}$. Thus, the atomic dipole operator $\wp$ represents the system's operator $\mathcal{A}$ of (4.12). Since by definition the two-level atom has only two levels $|e\rangle$ and $|g\rangle$, the indices ij in (4.21) run over ge and eg. Hence, the operator $\boldsymbol{\alpha}_{ij}$ and its Hermitian adjoint $\boldsymbol{\alpha}^\dagger_{ij}$ are given by

$$\boldsymbol{\alpha}_{ij} = \wp_{ji}\sigma_{ij} \, , \quad \boldsymbol{\alpha}^\dagger_{ij} = \wp_{ij}\sigma_{ij} \, , \quad (ij = ge, eg) \, .$$

On the other hand, the reservoir operator $\mathcal{B}$ corresponds to the electric field operator $\boldsymbol{E}$ with the minus sign. In the interaction picture, for the reservoir mode operators we therefore have

$$\tilde{\boldsymbol{\beta}}_{\boldsymbol{k}\lambda}(t) = -\mathrm{i}\hat{\boldsymbol{e}}_{\boldsymbol{k}\lambda} \sqrt{\frac{\hbar\omega_k}{2\varepsilon_0 V}} \left[b_{\boldsymbol{k}\lambda} \mathrm{e}^{-\mathrm{i}\omega_k t} - b^\dagger_{\boldsymbol{k}\lambda} \mathrm{e}^{\mathrm{i}\omega_k t} \right] . \tag{4.25}$$

The density matrix of the thermal reservoir, i.e., multimode electromagnetic field in a chaotic state, is just a tensor product of the density matrices (2.117) for all modes $\boldsymbol{k}\lambda$,

$$\rho^{\mathrm{R}}_0 = \bigotimes_{\boldsymbol{k}\lambda} \upsilon_k \, \mathrm{e}^{\mu_k b^\dagger_{\boldsymbol{k}\lambda} b_{\boldsymbol{k}\lambda}} = \bigotimes_{\boldsymbol{k}\lambda} \left[\upsilon_k \sum_{n_{\boldsymbol{k}\lambda}} \mathrm{e}^{\mu_k n_{\boldsymbol{k}\lambda}} \, |n_{\boldsymbol{k}\lambda}\rangle\langle n_{\boldsymbol{k}\lambda}| \right] , \tag{4.26}$$

where

$$\upsilon_k = \frac{1}{1+\bar{n}(\omega_k)} \,, \quad \mu_k = \ln \frac{\bar{n}(\omega_k)}{1+\bar{n}(\omega_k)} \,,$$

and $\bar{n}(\omega_k)$ is the mean number of quanta in the mode of frequency ω_k, which is given by Planck's law

$$\bar{n}(\omega_k) \equiv \langle b^\dagger_{\boldsymbol{k}\lambda} b_{\boldsymbol{k}\lambda} \rangle_{\mathrm{R}} = \frac{1}{\mathrm{e}^{\hbar\omega_k/k_{\mathrm{B}}T} - 1} \,. \tag{4.27}$$

Obviously ρ_0^{R} is diagonal in the basis $\{\bigotimes_{\boldsymbol{k}\lambda} |n_{\boldsymbol{k}\lambda}\rangle\}$. We have already assumed that the trace of the interaction $\mathcal{V}$ over the reservoir variables is zero, which in the present context translates into

$$\langle \boldsymbol{E} \rangle_{\mathrm{R}} = \mathrm{Tr}\big(\boldsymbol{E}(t)\rho_0^{\mathrm{R}}\big) = 0 \,.$$

On the other hand, the reservoir correlation functions are given by

$$\begin{aligned}
\langle \tilde{\boldsymbol{\beta}}_{\boldsymbol{k}'\lambda'}(t)\, \tilde{\boldsymbol{\beta}}_{\boldsymbol{k}\lambda}(t-t') \rangle_{\mathrm{R}} = & -\frac{\hbar\sqrt{\omega_{k'}\omega_k}}{2\varepsilon_0 V}\, \hat{\boldsymbol{e}}_{\boldsymbol{k}'\lambda'} \cdot \hat{\boldsymbol{e}}_{\boldsymbol{k}\lambda} \\
& \times \Big[\langle b_{\boldsymbol{k}'\lambda'} b_{\boldsymbol{k}\lambda} \rangle_{\mathrm{R}}\, \mathrm{e}^{-\mathrm{i}(\omega_{k'}+\omega_k)t}\, \mathrm{e}^{\mathrm{i}\omega_k t'} \\
& - \langle b_{\boldsymbol{k}'\lambda'} b^\dagger_{\boldsymbol{k}\lambda} \rangle_{\mathrm{R}}\, \mathrm{e}^{\mathrm{i}(\omega_k-\omega_{k'})t}\, \mathrm{e}^{-\mathrm{i}\omega_k t'} \\
& - \langle b^\dagger_{\boldsymbol{k}'\lambda'} b_{\boldsymbol{k}\lambda} \rangle_{\mathrm{R}}\, \mathrm{e}^{\mathrm{i}(\omega_{k'}-\omega_k)t}\, \mathrm{e}^{\mathrm{i}\omega_k t'} \\
& + \langle b^\dagger_{\boldsymbol{k}'\lambda'} b^\dagger_{\boldsymbol{k}\lambda} \rangle_{\mathrm{R}}\, \mathrm{e}^{\mathrm{i}(\omega_{k'}+\omega_k)t}\, \mathrm{e}^{-\mathrm{i}\omega_k t'} \Big] \,,
\end{aligned} \tag{4.28}$$

and similarly for $\langle \tilde{\boldsymbol{\beta}}_{\boldsymbol{k}\lambda}(t-t')\, \tilde{\boldsymbol{\beta}}_{\boldsymbol{k}'\lambda'}(t) \rangle_{\mathrm{R}}$. Due to the diagonality of the reservoir density matrix ρ_0^{R}, only two of the correlation tensors in the above expression are nonvanishing, namely

$$\langle b_{\boldsymbol{k}'\lambda'} b_{\boldsymbol{k}\lambda} \rangle_{\mathrm{R}} = \langle b^\dagger_{\boldsymbol{k}'\lambda'} b^\dagger_{\boldsymbol{k}\lambda} \rangle_{\mathrm{R}} = 0 \,, \tag{4.29a}$$

$$\langle b_{\boldsymbol{k}'\lambda'} b^\dagger_{\boldsymbol{k}\lambda} \rangle_{\mathrm{R}} = \big(1+\bar{n}(\omega_k)\big)\, \delta_{\boldsymbol{k}\boldsymbol{k}'}\, \delta_{\lambda\lambda'} \,, \tag{4.29b}$$

$$\langle b^\dagger_{\boldsymbol{k}'\lambda'} b_{\boldsymbol{k}\lambda} \rangle_{\mathrm{R}} = \bar{n}(\omega_k)\, \delta_{\boldsymbol{k}\boldsymbol{k}'}\, \delta_{\lambda\lambda'} \,. \tag{4.29c}$$

We thus see that the reservoir correlation functions are independent of t, depending only on the time difference t'.

We can now calculate the complex coefficients G_{ij} and $\overline{G}_{ij}$ of the general master equation (4.21). Upon substituting the correlation functions into (4.18) and taking into account the above expressions for the correlation tensors, we find that the double summation over the mode indices in (4.20) is turned into single summation, with the result

$$G_{ij} = \sum_{\boldsymbol{k}\lambda} \frac{\omega_k}{2\varepsilon_0\hbar V} \int_0^\infty \mathrm{d}t' \Big[\big(1+\bar{n}(\omega_k)\big) \mathrm{e}^{\mathrm{i}(\omega_{ji}-\omega_k)t'} + \bar{n}(\omega_k)\, \mathrm{e}^{\mathrm{i}(\omega_{ji}+\omega_k)t'} \Big] \,, \tag{4.30a}$$

$$\overline{G}_{ij} = \sum_{\boldsymbol{k}\lambda} \frac{\omega_k}{2\varepsilon_0\hbar V} \int_0^\infty \mathrm{d}t' \Big[\big(1+\bar{n}(\omega_k)\big) \mathrm{e}^{\mathrm{i}(\omega_{ji}+\omega_k)t'} + \bar{n}(\omega_k)\, \mathrm{e}^{\mathrm{i}(\omega_{ji}-\omega_k)t'} \Big] \,. \tag{4.30b}$$

As in Sect. 3.5.2, we now replace the sum over modes $\boldsymbol{k}\lambda$ by an integral according to the procedure of (2.29), i.e.

$$\sum_{\boldsymbol{k}\lambda} \to \frac{V}{(2\pi)^3}\int \mathrm{d}^3k = \frac{V}{(2\pi)^3 c^3}\int_0^\infty \mathrm{d}\omega_k\,\omega_k^2 \int \mathrm{d}\Omega\ ,$$

which corresponds to the continuous spectrum of the reservoir. Integrating over the solid angle Ω and using the relation

$$\int_0^\infty \mathrm{d}t' \mathrm{e}^{\mathrm{i}\omega t'} = \pi\delta(\omega) + \mathrm{i}\mathrm{P}\frac{1}{\omega}\ , \tag{4.31}$$

where P is the principal value part and $\delta(\omega)$ the Dirac delta function, we obtain (see Prob. 4.1)

$$\begin{aligned} G_{ij} &= \frac{1}{4\pi\varepsilon_0}\frac{2}{3\hbar c^3}\int_0^\infty \mathrm{d}\omega_k\,\omega_k^3\Big[\big(1+\bar{n}(\omega_k)\big)\delta(\omega_{ji}-\omega_k) + \bar{n}(\omega_k)\delta(\omega_{ji}+\omega_k)\Big] \\ &\quad +\mathrm{i}\frac{1}{4\pi\varepsilon_0}\frac{2}{3\pi\hbar c^3}\,\mathrm{P}\int_0^\infty \mathrm{d}\omega_k\,\omega_k^3\left[\frac{1+\bar{n}(\omega_k)}{\omega_{ji}-\omega_k} + \frac{\bar{n}(\omega_k)}{\omega_{ji}+\omega_k}\right]\ , \qquad (4.32a) \\ \overline{G}_{ij} &= \frac{1}{4\pi\varepsilon_0}\frac{2}{3\hbar c^3}\int_0^\infty \mathrm{d}\omega_k\,\omega_k^3\Big[\big(1+\bar{n}(\omega_k)\big)\delta(\omega_{ji}+\omega_k) + \bar{n}(\omega_k)\delta(\omega_{ji}-\omega_k)\Big] \\ &\quad +\mathrm{i}\frac{1}{4\pi\varepsilon_0}\frac{2}{3\pi\hbar c^3}\,\mathrm{P}\int_0^\infty \mathrm{d}\omega_k\,\omega_k^3\left[\frac{1+\bar{n}(\omega_k)}{\omega_{ji}+\omega_k} + \frac{\bar{n}(\omega_k)}{\omega_{ji}-\omega_k}\right]\ . \qquad (4.32b) \end{aligned}$$

Note that in the above equations the integration limits are taken as $\omega_k \in [0,\infty)$, i.e., ω_k is positive. On the other hand, the frequency difference ω_{ji} can be both positive and negative, depending on whether the energy of level $|j\rangle$ is higher or lower than that of level $|i\rangle$. Recall that the delta function is nonzero only when its argument is zero. Therefore when we evaluate the real parts of G_{ij} and $\overline{G}_{ij}$, only one term under each integral survives, corresponding to the argument of delta function being $(\omega_{ji}-\omega_k)$ for $\omega_{ji}>0$, and $(\omega_{ji}+\omega_k)$ for $\omega_{ji}<0$. Identifying the indices ij with either ge or eg, we then have

$$\begin{aligned} G_{ge}|\wp_{eg}|^2 &= \tfrac{1}{2}\Gamma_{eg}\big(1+\bar{n}(\omega_{ge})\big) + \mathrm{i}S_{ge}\ , \qquad (4.33a) \\ G_{eg}|\wp_{eg}|^2 &= \tfrac{1}{2}\Gamma_{eg}\bar{n}(\omega_{ge}) - \mathrm{i}S_{eg}\ , \qquad (4.33b) \\ \overline{G}_{ge}|\wp_{eg}|^2 &= \tfrac{1}{2}\Gamma_{eg}\bar{n}(\omega_{ge}) + \mathrm{i}S_{eg}\ , \qquad (4.33c) \\ \overline{G}_{eg}|\wp_{eg}|^2 &= \tfrac{1}{2}\Gamma_{eg}\big(1+\bar{n}(\omega_{ge})\big) - \mathrm{i}S_{ge}\ , \qquad (4.33d) \end{aligned}$$

where

$$\Gamma_{eg} = \frac{1}{4\pi\varepsilon_0}\frac{4\omega_{eg}^3|\wp_{eg}|^2}{3\hbar c^3} \tag{4.34}$$

is obviously the spontaneous decay rate of the excited atomic state $|e\rangle$, while

$$\begin{aligned} S_{ge} &= \frac{1}{4\pi\varepsilon_0}\frac{2|\wp_{eg}|^2}{3\pi\hbar c^3}\,\mathrm{P}\int_0^\infty \mathrm{d}\omega_k\,\omega_k^3\left[\frac{1+\bar{n}(\omega_k)}{\omega_{eg}-\omega_k} + \frac{\bar{n}(\omega_k)}{\omega_{eg}+\omega_k}\right]\ , \qquad (4.35a) \\ S_{eg} &= \frac{1}{4\pi\varepsilon_0}\frac{2|\wp_{eg}|^2}{3\pi\hbar c^3}\,\mathrm{P}\int_0^\infty \mathrm{d}\omega_k\,\omega_k^3\left[\frac{1+\bar{n}(\omega_k)}{\omega_{eg}+\omega_k} + \frac{\bar{n}(\omega_k)}{\omega_{eg}-\omega_k}\right]\ , \qquad (4.35b) \end{aligned}$$

represent the shift of the atomic transition frequency. In the limit $\bar{n}(\omega_k) \to 0$ (reservoir at zero temperature $T \to 0$), S_{ge} and S_{eg} correspond to the Lamb shift of the excited state $|e\rangle$. We can redefine the frequency of the atomic transition ω_{eg} so as to incorporate this shift. Then, expanding the sum over ij, from (4.21) we obtain finally the master equation for the two-level atom,

$$\frac{\partial}{\partial t}\tilde{\rho}^{\mathrm{A}} = \tfrac{1}{2}\Gamma\,(1+\bar{n})\left(2\sigma_-\tilde{\rho}^{\mathrm{A}}\sigma_+ - \sigma_+\sigma_-\tilde{\rho}^{\mathrm{A}} - \tilde{\rho}^{\mathrm{A}}\sigma_+\sigma_-\right) + \tfrac{1}{2}\Gamma\,\bar{n}\left(2\sigma_+\tilde{\rho}^{\mathrm{A}}\sigma_- - \sigma_-\sigma_+\tilde{\rho}^{\mathrm{A}} - \tilde{\rho}^{\mathrm{A}}\sigma_-\sigma_+\right), \tag{4.36}$$

where to simplify somewhat the notation, we denote Γ_{eg} by Γ while $\bar{n}$ is understood as $\bar{n}(\omega_{eg})$, i.e., mean number of thermal photons at the frequency of the atomic transition. In the limit $\bar{n} \to 0$, relevant when $k_{\mathrm{B}}T \ll \hbar\omega_{eg}$, we obtain

$$\frac{\partial}{\partial t}\tilde{\rho}^{\mathrm{A}} = \tfrac{1}{2}\Gamma\left(2\sigma_-\tilde{\rho}^{\mathrm{A}}\sigma_+ - \sigma_+\sigma_-\tilde{\rho}^{\mathrm{A}} - \tilde{\rho}^{\mathrm{A}}\sigma_+\sigma_-\right) \equiv \mathcal{L}\tilde{\rho}^{\mathrm{A}}\,, \tag{4.37}$$

which describes the spontaneous decay of a two-level atom via the coupling to the empty radiation reservoir.

4.1.3 Driven Two-Level Atom

In Sect. 3.3.1 we have considered, in terms of the amplitude equations, an "idealized" two-level atom interacting with a classical monochromatic field, whose frequency ω is near the frequency of the atomic resonance ω_{eg}. "Idealized" is meant to imply that no spontaneous decay of the excited atomic level or any other relaxation of the atomic coherence was included in the analysis and therefore only purely coherent dynamics, i.e., Rabi oscillations, of the atom was manifest. On the other hand, in Sect. 3.5.2 we have seen that in open space an atom prepared in the excited state $|e\rangle$ decays to a lower state with the emission of a spontaneous photon.

In this section, we consider a realistic two-level atom subject to a coherent classical field taking also into account the spontaneous decay and possibly additional coherence relaxation of the atom. In principle, one can modify the amplitude equations (3.38) to account for the decay of level $|e\rangle$ by adding the term $-\frac{1}{2}\Gamma c_e$ in the right-hand-side of the equation for c_e. If the two-level system is not closed, meaning that the atom decays to some lower state other than state $|g\rangle$, this procedure can provide an adequate description of the atomic dynamics. But then, if at the initial time $t = 0$ the sum of populations $|c_g|^2 + |c_e|^2$ of the two atomic states $|g\rangle$ and $|e\rangle$ was 1, in the course of time it will not be preserved and will in fact decrease. Here we are concerned with the closed two-level system, meaning that the atomic population decays from the upper to the lower state. In the presence of a strong coherent field, the atom can again be promoted to the upper state and emit another spontaneous photon, and so on, while the total population remains constant. Thus,

the rigorous description of the system requires the solution of the density matrix equations, which can incorporate the spontaneous decay process in a closed system where the decrease of population of the excited atomic state is accompanied by the corresponding increase of population of the lower state. This process is described by the Liouvillian on the right-hand-side of (4.37).

We thus consider a two-level atom interaction with an external classical monochromatic field $E(t) = \mathcal{E}\mathrm{e}^{-\mathrm{i}\omega t} + \text{c.c.}$ Here we have a situation in which a single mode of frequency ω corresponding to the field E coherently drives the atomic transition $|g\rangle \leftrightarrow |e\rangle$, while all other modes of the photonic continuum are empty. The coupling of the atom to the classical field should therefore be treated separately from the spontaneous decay of the excited state $|e\rangle$ due to the coupling with the empty modes of the reservoir. Since only one mode, out of the infinity of modes, is isolated for the special treatment, the spontaneous decay rate remains unaffected by the presence of the classical field E. The evolution of the density operator for the atom $\tilde{\rho}$ (dropping the superscript A) is thus given by

$$\frac{\partial}{\partial t}\tilde{\rho} = -\frac{\mathrm{i}}{\hbar}[\tilde{\mathcal{V}}^{\mathrm{AF}}, \tilde{\rho}] + \mathcal{L}\tilde{\rho}\,, \tag{4.38}$$

where the first term on the right-hand-side contains the atom–field interaction, while the second term describes the atomic spontaneous decay as in (4.37). Under the rotating-wave approximation, the interaction Hamiltonian is given by

$$\tilde{\mathcal{V}}^{\mathrm{AF}} = -\hbar\big[\sigma_+ \Omega\, \mathrm{e}^{-\mathrm{i}\Delta t} + \Omega^* \sigma_-\, \mathrm{e}^{\mathrm{i}\Delta t}\big]\,, \tag{4.39}$$

where $\Delta = \omega - \omega_{eg}$ is the detuning of the field E from the atomic resonance and $\Omega = \wp_{eg}\mathcal{E}/\hbar$ is the (complex) Rabi frequency of the field. Expanding (4.38) in the basis of atomic eigenstates $|g\rangle$ and $|e\rangle$, we obtain the following set of differential equations

$$\frac{\partial}{\partial t}\tilde{\rho}_{gg} = \Gamma\tilde{\rho}_{ee} + \mathrm{i}(\Omega^*\tilde{\rho}_{eg}\,\mathrm{e}^{\mathrm{i}\Delta t} - \tilde{\rho}_{ge}\Omega\,\mathrm{e}^{-\mathrm{i}\Delta t})\,, \tag{4.40a}$$

$$\frac{\partial}{\partial t}\tilde{\rho}_{ee} = -\Gamma\tilde{\rho}_{ee} + \mathrm{i}(\Omega\tilde{\rho}_{ge}\,\mathrm{e}^{-\mathrm{i}\Delta t} - \tilde{\rho}_{eg}\Omega^*\,\mathrm{e}^{\mathrm{i}\Delta t})\,, \tag{4.40b}$$

$$\frac{\partial}{\partial t}\tilde{\rho}_{eg} = -\gamma_{eg}\tilde{\rho}_{eg} + \mathrm{i}(\Omega\tilde{\rho}_{gg}\,\mathrm{e}^{-\mathrm{i}\Delta t} - \tilde{\rho}_{ee}\Omega\,\mathrm{e}^{-\mathrm{i}\Delta t})\,, \tag{4.40c}$$

and $\tilde{\rho}_{ge} = \tilde{\rho}^*_{eg}$. In these equations, Γ is the population decay rate of the excited state $|e\rangle$, while γ_{eg} is the relaxation rate of the atomic coherence $\tilde{\rho}_{eg}$. In general, this coherence relaxation rate can be represented as $\gamma_{eg} = \frac{1}{2}\Gamma + 2\Gamma_{\mathrm{phase}}$, where $\frac{1}{2}\Gamma$ is the contribution of the spontaneous decay of $|e\rangle$, which is contained in $\mathcal{L}\tilde{\rho}$, while Γ_{phase} accounts for all other possible mechanisms of coherence relaxation of the atom which do not affect the populations. These may include phase-changing elastic collisions with a buffer gas (see Prob. 4.2), and/or relaxation due to phase fluctuations of the classical field. Formally, such pure phase relaxations can be represented by a Liouvillian

$$\mathcal{L}_{\mathrm{phase}}\tilde{\rho} \equiv \tfrac{1}{2}\Gamma_{\mathrm{phase}}\left(2\sigma_z\tilde{\rho}\sigma_z - \sigma_z\sigma_z\tilde{\rho} - \tilde{\rho}\sigma_z\sigma_z\right) = \Gamma_{\mathrm{phase}}(\sigma_z\tilde{\rho}\sigma_z - \tilde{\rho})\,, \tag{4.41}$$

which should be added to the right-hand-site of (4.38). Γ is called diagonal relaxation and γ_{eg} is off-diagonal relaxation. Often Γ is denoted by $1/T_1$ and γ_{eg} by $1/T_2$, where T_1 and T_2 are the corresponding relaxation times.

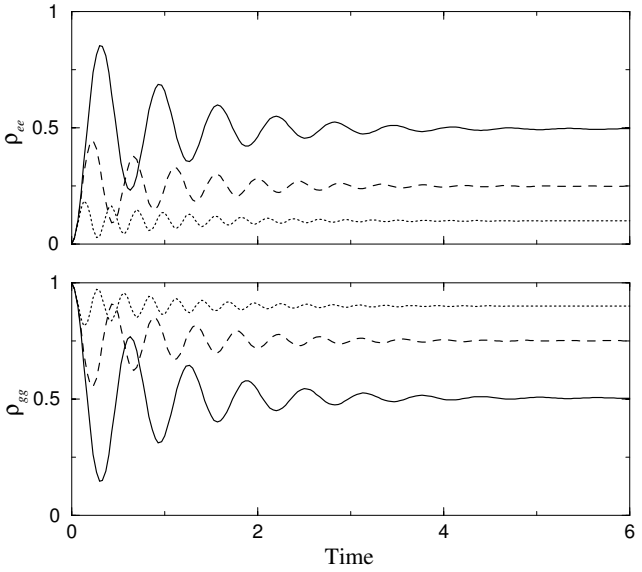

Fig. 4.1. Time-dependence of populations ρ_{gg} and ρ_{ee} of a driven two-level atom with $|\Omega| = 5\Gamma$, $\gamma_{eg} = \Gamma$ and detunings $\Delta = 0$ (solid line), $\Delta = 2|\Omega|$ (dashed line) and $\Delta = 4|\Omega|$ (dotted line). Time is measured in units of Γ^{-1}.

Before attempting to solve the density matrix equations (4.40), it is convenient to transform them into the frame rotating with the frequency of the external classical field E. This transformation is realized by substituting $\tilde{\rho}_{gg} = \rho_{gg}$, $\tilde{\rho}_{ee} = \rho_{ee}$ and $\tilde{\rho}_{eg} = \rho_{eg}\,\mathrm{e}^{-\mathrm{i}\Delta t}$, which yields

$$\frac{\partial}{\partial t}\rho_{gg} = \Gamma\rho_{ee} + \mathrm{i}(\Omega^*\rho_{eg} - \rho_{ge}\Omega)\,, \tag{4.42a}$$

$$\frac{\partial}{\partial t}\rho_{ee} = -\Gamma\rho_{ee} + \mathrm{i}(\Omega\rho_{ge} - \rho_{eg}\Omega^*)\,, \tag{4.42b}$$

$$\frac{\partial}{\partial t}\rho_{eg} = (\mathrm{i}\Delta - \gamma_{eg})\rho_{eg} - \mathrm{i}\Omega(\rho_{ee} - \rho_{gg})\,. \tag{4.42c}$$

In general, for constant Rabi frequency Ω and detuning Δ, the time-dependent solutions of the equations of motion (4.42) are expressed through the roots of a cubic equation, which yield rather cumbersome analytic expressions of little practical value. Of course, it is not difficult to obtain (numerical) solutions via numerical integration of equations (4.42) which is possible even for time-dependent Rabi frequencies $\Omega(t)$ and detunings $\Delta(t)$. In Fig. 4.1 we illustrate

the behavior of a two-level atom initially in the ground state $|g\rangle$, for given Ω, γ_{eg} and various values of the detuning Δ, all parameters being normalized by Γ. At short times, the atom undergoes Rabi oscillations, which, however, are damped with the rate γ_{eg}, and eventually, at longer times, the populations of levels $|g\rangle$ and $|e\rangle$ reach their steady state values. To obtain the analytical solution of (4.42) in the long-time limit, we write the equation for the coherence ρ_{eg} in an integral form,

$$\rho_{eg}(t) = -\mathrm{i}\Omega \int_0^t \mathrm{e}^{(\mathrm{i}\Delta - \gamma_{eg})(t-t')} D(t')\,\mathrm{d}t' \,, \tag{4.43}$$

where $D(t') \equiv \rho_{ee}(t') - \rho_{gg}(t')$ is the population inversion. Assuming that $D(t')$ does not change much for times $t > \gamma_{eg}^{-1}$, it can be evaluated at time $t' = t$ and factored out of the integral. The integration can then be performed, and in the limit $\gamma_{eg} t \gg 1$ we obtain

$$\rho_{eg}(t) = \frac{\Omega D(t)}{\Delta + \mathrm{i}\gamma_{eg}} \,. \tag{4.44}$$

Substituting this into the remaining equations of (4.42), we obtain two coupled rate equations for the populations of levels $|g\rangle$ and $|e\rangle$,

$$\frac{\partial}{\partial t}\rho_{gg} = \Gamma \rho_{ee} + RD \,, \tag{4.45a}$$

$$\frac{\partial}{\partial t}\rho_{ee} = -\frac{\partial}{\partial t}\rho_{gg} = -\Gamma \rho_{ee} - RD \,, \tag{4.45b}$$

where $R = 2\gamma_{eg}|\Omega|^2/(\Delta^2 + \gamma_{eg}^2)$ is the rate of stimulated transition $|g\rangle \leftrightarrow |e\rangle$. We thus see that the sum of populations of the two atomic levels is preserved in time, since $\partial_t(\rho_{gg} + \rho_{ee}) = 0$. For the initial conditions $\rho_{gg}(0) = 1$ and $\rho_{ee}(0) = 0$, from (4.45) we have

$$\frac{\partial}{\partial t}\rho_{ee} = -(\Gamma + 2R)\rho_{ee} + R \,, \quad \rho_{gg} = 1 - \rho_{ee}$$

with the solution

$$\rho_{ee}(t) = \frac{R}{\Gamma + 2R}\left[1 - \mathrm{e}^{-(\Gamma + 2R)t}\right] . \tag{4.46}$$

The steady-state is reached for times longer than $(\Gamma + 2R)^{-1}$, and for the population of the excited state we obtain

$$\rho_{ee}(\infty) = \frac{|\Omega|^2}{\frac{\Gamma}{2\gamma_{eg}}(\Delta^2 + \gamma_{eg}^2) + 2|\Omega|^2} \,. \tag{4.47}$$

In the absence of collisions and other sources of coherence relaxation, one has $\gamma_{eg} = \frac{1}{2}\Gamma$, and (4.47) becomes

$$\rho_{ee}(\infty) = \frac{|\Omega|^2}{\Delta^2 + \frac{1}{4}\Gamma^2 + 2|\Omega|^2} \,. \tag{4.48}$$

The steady-state is thus characterized by a dynamic equilibrium between two processes: spontaneous decay of the atom from $|e\rangle$ to $|g\rangle$, and stimulated by the field transition $|g\rangle \to |e\rangle$, as described by the rate equations (4.45). For a closed two-level system, the transition $|g\rangle \leftrightarrow |e\rangle$ is therefore called cycling transition, and the scattered light constitutes the resonance fluorescence.

The above equations indicate that the exited state population can take appreciable values only for large enough Rabi frequencies of the field, such that it is comparable to the detuning Δ and the width γ_{eg} of transition $|g\rangle \leftrightarrow |e\rangle$, $|\Omega|^2 \gtrsim \Delta^2, \Gamma\gamma_{eg}$. Off-resonant fields, $\Delta^2 \gg \Gamma^2, |\Omega|^2$, obviously induce little population of the excited state, $\rho_{ee} \ll 1$. In the opposite limit of a very strong, near resonant field, $|\Omega|^2 \gg \Delta^2 + \frac{1}{4}\Gamma^2$, the populations of states $|g\rangle$ and $|e\rangle$ tend to equalize, $\rho_{gg} \sim \rho_{ee} \to \frac{1}{2}$, and the transition $|g\rangle \leftrightarrow |e\rangle$ is said to saturate. Note that since Γ is the rate of spontaneous emission from the excited atomic state, in steady state the number of photons radiated by the atom per unit time (second) is given by $\Gamma\rho_{ee}$, which for strongly saturated transition becomes $\Gamma/2$ (see Prob. 4.3). The total power of the scattered light, i.e., radiation intensity integrated over 4π solid angle, is obviously $\hbar\omega\Gamma\rho_{ee}$.

Before closing this section, it may be instructive to show how the so-called Fermi's golden rule is obtained as a special case of the above more general formulation. Note that in the rate equations (4.45), the quantity R can be easily shown to be the rate of depopulation of state $|g\rangle$ for small times t such that $\rho_{ee} \ll 1$ and $\rho_{gg} \simeq 1$, i.e.,

$$\frac{\partial}{\partial t}\rho_{gg} = -R \, .$$

In the limit $\gamma_{eg} \to 0$, which implies $\Gamma \to 0$, this rate is given by

$$R = 2\pi|\Omega|^2\delta(\Delta) \, , \tag{4.49}$$

where we have used (1.31b) for the expression of the delta function. This result is equivalent to what is known as Fermi's golden rule for the rate of transition between two states $|g\rangle$ and $|e\rangle$ of sharply defined energies of a quantum system, induced by the coupling Ω. The delta function $\delta(\Delta)$ simply expresses energy conservation. Physically, small t and Γ means $\omega_{eg}^{-1} \ll t \ll \Gamma^{-1}$. Indeed, on the one hand, it is only for times $t \gg \omega_{eg}^{-1}$ that the notion of quantum mechanical transition is meaningful. On the other hand, for times $t \gtrsim \Gamma^{-1}$ the system has practically reached steady state and it makes no sense to talk about the transition probability per unit time, which R is. For the above inequality to be meaningful, it is necessary that $\Gamma \ll \omega_{eg}$, which simply means that the width(s) of the states involved is much smaller than the energy separation between them. This is the condition we encountered in Sect. 3.5, which, as pointed out there, guarantees that it is meaningful to talk about two separate states of sufficiently well defined energies.

4.2 Quantum Stochastic Wavefunctions

In the previous section, we have derived the master equation for the reduced density operator of a small system coupled to a reservoir, through which one can calculate the mean expectation value of any system operator corresponding to an ensemble averaged quantity. We have employed that formalism to study the dynamics of a two-level atom coherently driven by a monochromatic laser field, in the presence of spontaneous decay due to the coupling with the continuum of modes of the free electromagnetic field. Here we describe an alternative method for simulating the dissipative dynamics of quantum systems, which is based on stochastic, or Monte–Carlo, wavefunctions. Each such wavefunction describes a particular realization, or quantum trajectory, of a single thought (Gedanken-) experiment, in which the system undergoes a sequence of quantum jumps determined by random projective detection events. In fact, individual trajectories can closely mimic a realistic experimental situation in which a single quantum system, such as a coherently driven atom, is continuously monitored by a detector whose clicks at random times result in the projections of the system onto the corresponding state. Perhaps the best example is provided by the electron shelving or quantum jump experiments with single atoms discussed in the review article by Plenio and Knight (1998). On the other hand, by taking the ensemble average over the Monte–Carlo wavefunctions for independently simulated trajectories, one can derive the density matrix of the system and calculate the expectation values for any system operator.

4.2.1 General Formulation

We begin with the general formulation of the method and then adapt it to the case of a driven two-level atom. The time evolution of the reduced density operator $\rho^{\rm S}$ of a quantum system is governed by the master equation

$$\frac{\partial}{\partial t}\rho^{\rm S} = -\frac{\rm i}{\hbar}[\mathcal{H}_{\rm S}, \rho^{\rm S}] + \mathcal{L}\rho^{\rm S} \;, \tag{4.50}$$

where $\mathcal{H}_{\rm S}$ is the Hermitian Hamiltonian of the system ($\mathcal{H}_{\rm S}^{\dagger} = \mathcal{H}_{\rm S}$), which could be subject to an external classical control or driving, while $\mathcal{L}\rho^{\rm S}$ describes the non-Hermitian dynamics of the system due to the coupling to a Markovian reservoir. In general, the Liouvillian $\mathcal{L}\rho^{\rm S}$ has the so-called Lindblad form

$$\mathcal{L}\rho^{\rm S} = \sum_i \tfrac{1}{2}\Gamma_i\big(2\alpha_i\rho^{\rm S}\alpha_i^{\dagger} - \alpha_i^{\dagger}\alpha_i\rho^{\rm S} - \rho^{\rm S}\alpha_i^{\dagger}\alpha_i\big) \;, \tag{4.51}$$

where Γ_i is the decay or relaxation rate for channel i, and α_i and $\alpha_i^{\dagger}$ are the corresponding system operators. We define a non-Hermitian effective Hamiltonian of the system through

$$\mathcal{H}_{\rm eff} \equiv \mathcal{H}_{\rm S} - {\rm i}\hbar \sum_i \tfrac{1}{2}\Gamma_i \alpha_i^\dagger \alpha_i \ , \tag{4.52}$$

and the so-called jump superoperator $\mathcal{L}_{\rm jump}\rho^{\rm S} \equiv \sum_i \Gamma_i \alpha_i \rho^{\rm S} \alpha_i^\dagger$, in terms of which the master equation (4.50) can be cast in the form

$$\frac{\partial}{\partial t}\rho^{\rm S} = -\frac{\rm i}{\hbar}\big(\mathcal{H}_{\rm eff}\rho^{\rm S} - \rho^{\rm S}\mathcal{H}_{\rm eff}^\dagger\big) + \mathcal{L}_{\rm jump}\rho^{\rm S} \ , \tag{4.53}$$

which shows that the time-evolution of the density operator has two contributions. The first one, due to the effective Hamiltonian $\mathcal{H}_{\rm eff}$, is deterministic and continuous, although nonunitary, while the second one, due to $\mathcal{L}_{\rm jump}\rho^{\rm S}$, yields discontinuous projections $\alpha_i \rho^{\rm S} \alpha_i^\dagger$ called quantum jumps. Together, the two terms in the right-hand-side of (4.53) preserve the trace of $\rho^{\rm S}$ throughout its evolution. Recall from Sect. 1.3 that the density operator for a pure state $|\Psi\rangle$ is given by $\rho^{\rm S} = |\Psi\rangle\langle\Psi|$, while for the general case of a mixed initial state it can be represented as a statistical mixture $\rho^{\rm S} = \sum_\Psi P_\Psi |\Psi\rangle\langle\Psi|$. In either case, from (4.53) we have

$$\frac{\partial |\Psi\rangle}{\partial t}\langle\Psi| + |\Psi\rangle\frac{\partial \langle\Psi|}{\partial t} = -\frac{\rm i}{\hbar}\big(\mathcal{H}_{\rm eff}|\Psi\rangle\langle\Psi| - |\Psi\rangle\langle\Psi|\mathcal{H}_{\rm eff}^\dagger\big) + \sum_i \Gamma_i \alpha_i |\Psi\rangle\langle\Psi| \alpha_i^\dagger \ , \tag{4.54}$$

which suggests a very useful way of simulating the density operator of the system using the wavefunction approach and statistical averaging, as described below.

Consider a wavefunction of the system $|\Psi\rangle$ evolving according to the Schrödinger equation

$${\rm i}\hbar\frac{\partial}{\partial t}|\Psi\rangle = \mathcal{H}_{\rm eff}|\Psi\rangle \ . \tag{4.55}$$

Initially, at time $t = 0$, $|\Psi\rangle$ is assumed normalized, $\langle\Psi(0)|\Psi(0)\rangle = 1$. Since $\mathcal{H}_{\rm eff}$ is non-Hermitian, the norm of the wavefunction $||\,|\Psi(t)\rangle|| \equiv \sqrt{\langle\Psi(t)|\Psi(t)\rangle}$ decreases with time. Physically, this is due to the fact that the system is not isolated but is interacting with the reservoir. Therefore, as time evolves, various modes of the reservoir become correlated, or entangled, with the system. The missing population of the decaying states of the system is thus leaking into the reservoir. We can imagine that the reservoir is continuously monitored by an idealized detector. Mathematically, this is described by the last term of (4.54). Thus a click of the detector at a random time t_1 signifies the decay of the system along one of the possible decay channels and projects the wavefunction onto the corresponding state according to

$$|\Psi(t_1^+)\rangle = \frac{\alpha_i |\Psi(t_1)\rangle}{\sqrt{\langle\Psi(t_1)|\alpha_i^\dagger\alpha_i|\Psi(t_1)\rangle}} \ , \tag{4.56}$$

where t_1^+ denotes the instant of time immediately after the quantum jump, while the denominator ensures the renormalization of the wavefunction,

$\langle\Psi(t_1^+)|\Psi(t_1^+)\rangle = 1$. At any time $t \in [0, t_1]$, the probability density for the decay to occur into a particular channel i is given by

$$p_i(t) = ||\sqrt{\Gamma_i}\alpha_i\,|\Psi(t)\rangle||^2 = \Gamma_i||\alpha_i\,|\Psi(t)\rangle||^2 \ .$$

Then the total probability of decay $P(t)$ is obviously a monotonous function of time,

$$P(t) = \sum_i \int_0^t \mathrm{d}t' p_i(t') = 1 - \langle\Psi(t)|\Psi(t)\rangle \ , \tag{4.57}$$

where it is assumed that all decay channels are monitored with the same detector of unit efficiency.

We are now in a position to specify the procedure for performing the numerical simulation of the dissipative dynamics of the system. At time $t = 0$, we take a normalized wavefunction of the system $|\Psi(0)\rangle$ and propagate it with the Schrödinger equation (4.55) using the effective Hamiltonian $\mathcal{H}_{\text{eff}}$. This propagation is interrupted by a quantum jump, corresponding to the detector click, which is taken to occur at time t_1 for which $P(t_1) = r_1$, where r_1 is a uniformly distributed random number between zero and unity, $r_1 \in [0, 1]$. The decay channel i at this time t_1 is determined from the conditional probability density $p(i|t_1) = p_i(t_1)/\sum_i p_i(t_1)$ as follows. We divide the interval $[0, 1]$ into as many segments as there are decay channels, each segment having the corresponding length $p(i|t_1)$. We then generate another random number r_1' and decide which decay channel i was realized at this jump event by identifying the segment to which r_1' belongs. Accordingly, the normalized wavefunction after the jump is determined by (4.56). We then continue the time-evolution by repeating the above steps. Namely, stating from t_1, we propagate the new wavefunction up to the next jump time t_2 which is determined by comparing the decay probability $P(t > t_1)$ with another random number r_2. We then decide the decay channel according to conditional decay probability densities at t_2, accordingly project the wavefunction, and so on until we reach the desired final time t_{end}. This corresponds to the simulation of a single quantum trajectory, wherein the normalized wavefunction of the system $|\bar{\Psi}(t)\rangle$ at any time $t \in [0, t_{\text{end}}]$ is given by

$$|\bar{\Psi}(t)\rangle = \frac{|\Psi(t)\rangle}{||\,|\Psi(t)\rangle||} \ . \tag{4.58}$$

We can repeat this procedure $M \gg 1$ times, simulating M independent quantum trajectories, and record the corresponding wavefunctions $|\bar{\Psi}_m(t)\rangle$, $m = 1, 2, \ldots, M$. Then, by taking the ensemble average over these realizations, we obtain an approximate density operator of the system as

$$\rho(t) \simeq \frac{1}{M}\sum_m |\bar{\Psi}_m(t)\rangle\langle\bar{\Psi}_m(t)| \ . \tag{4.59}$$

Clearly, the larger the number of simulated trajectories M the better the approximation (4.59). Similarly, we can estimate the expectation value of any

system operator through

$$\langle \mathcal{T}(t)\rangle = \mathrm{Tr}\big(\rho(t)\mathcal{T}\big) \simeq \frac{1}{M}\sum_m \langle \bar{\Psi}_m(t)|\,\mathcal{T}(t)\,|\bar{\Psi}_m(t)\rangle\ . \tag{4.60}$$

On the other hand, if we follow only one realization of the wavefunction $|\bar{\Psi}(t)\rangle$ over times much longer than the decay times Γ_i^{-1}, we can use the ergodic hypothesis and approximate the stationary solution for the density matrix $\rho(\infty)$ by taking the time-average of $|\bar{\Psi}(t)\rangle\langle\bar{\Psi}(t)|$.

4.2.2 Application to a Driven Two-Level Atom

In order to illustrate the above formalism quantitatively, let us now apply it to a particular quantum system—driven two-level atom. In the frame rotating with the frequency ω of the driving field, the Hamiltonian for the atom is

$$\mathcal{H}_{\mathrm{A}} = -\hbar\big(\Delta\sigma_{ee} + \sigma_+\Omega + \Omega^*\sigma_-\big)\ , \tag{4.61}$$

where, as usual, $\Delta = \omega - \omega_{eg}$ is the detuning and Ω the Rabi frequency of the field on the transition $|g\rangle \leftrightarrow |e\rangle$, and $\sigma_{ee} \equiv |e\rangle\langle e| = \sigma_+\sigma_-$ is an atomic operator. For simplicity and lucidity of discussion, we consider only the decay channel due to the spontaneous emission from the excited atomic state $|e\rangle$, which is described by the Liouvillian

$$\mathcal{L}\rho = \tfrac{1}{2}\Gamma\left(2\sigma_-\rho\sigma_+ - \sigma_+\sigma_-\rho - \rho\sigma_+\sigma_-\right)\ . \tag{4.62}$$

We thus assume that there is no additional dephasing of atomic coherence, which, if present, could have been taken into account through the pure dephasing Liouvillian (4.41). The effective non-Hermitian Hamiltonian is then given by

$$\mathcal{H}_{\mathrm{eff}} = \mathcal{H}_{\mathrm{A}} - \mathrm{i}\hbar\tfrac{1}{2}\Gamma\sigma_+\sigma_- = -\hbar\big[(\Delta + \mathrm{i}\tfrac{1}{2}\Gamma)\sigma_{ee} + \sigma_+\Omega + \Omega^*\sigma_-\big]\ , \tag{4.63}$$

while the jump superoperator is $\mathcal{L}_{\mathrm{jump}}\rho = \Gamma\sigma_-\rho\sigma_+$. At time $t = 0$ we take the atom to be in the ground state, $|\Psi(0)\rangle = |g\rangle$. We draw the first random number $r_1 \in [0,1]$, and then start the propagation of the atomic wavefunction $|\Psi(t)\rangle = c_g(t)\,|g\rangle + c_e(t)\,|e\rangle$ with the Schroödinger equation using the effective Hamiltonian $\mathcal{H}_{\mathrm{eff}}$, which yields the amplitude equations

$$\frac{\partial}{\partial t}c_g = \mathrm{i}\Omega^* c_e\ , \tag{4.64a}$$

$$\frac{\partial}{\partial t}c_e = (\mathrm{i}\Delta - \tfrac{1}{2}\Gamma)c_e + \mathrm{i}\Omega c_g\ . \tag{4.64b}$$

The propagation is interrupted by the first quantum jump at time t_1, which is determined from the condition

$$P(t_1) = 1 - \langle\Psi(t_1)|\Psi(t_1)\rangle \equiv 1 - (|c_g|^2 + |c_e|^2) = r_1\ .$$

The wavefunction is then projected onto the ground state according to

$$|\Psi(t_1^+)\rangle = \frac{\sigma_- |\Psi(t_1)\rangle}{\sqrt{\langle\Psi(t_1)| \sigma_+\sigma_- |\Psi(t_1)\rangle}} = \frac{c_e(t_1)\,|g\rangle}{|c_e(t_1)|} \equiv c_g(t_1^+)\,|g\rangle\ , \tag{4.65}$$

where obviously $c_g(t_1^+) = \mathrm{e}^{i\phi}$, with ϕ being the argument of $c_e(t_1)$, i.e., $c_e(t_1) = |c_e(t_1)|\mathrm{e}^{i\phi}$, which can be set to zero as it represents an irrelevant overall phase of the wavefunction $|\Psi(t_1^+)\rangle$. We then continue the propagation, beginning with the new wavefunction $\Psi(t_1^+)$, until the next quantum jump at time t_2 which is determined by the second random number $r_2 = P(t_2)$, and so on till reaching the desired final time t_{end}.

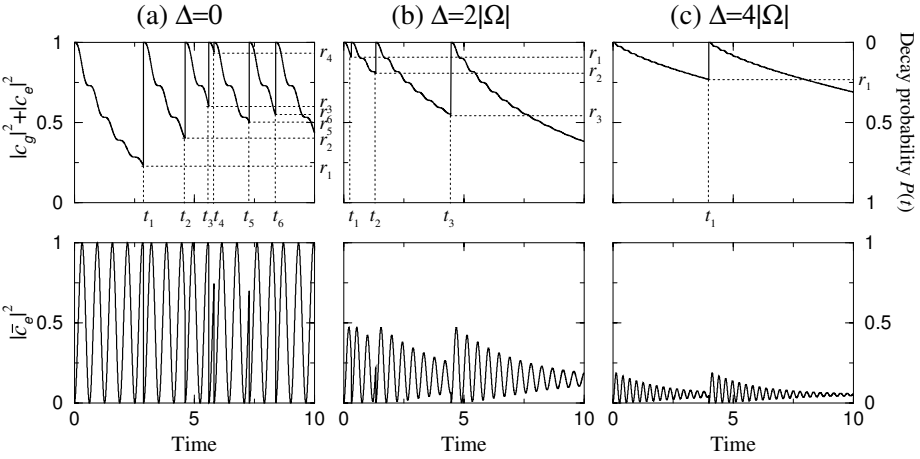

Fig. 4.2. Monte–Carlo simulations of the dynamics of a two-level atom driven by a laser field with $|\Omega| = 5\Gamma$ and detunings (a) $\Delta = 0$, (b) $\Delta = 2|\Omega|$ and (c) $\Delta = 4|\Omega|$. Upper graphs: time evolution of the square of wavefunction norm $\langle\Psi(t)|\Psi(t)\rangle = |c_g|^2 + |c_e|^2$, with the right vertical axis showing the decay probability $P(t) = 1 - \langle\Psi(t)|\Psi(t)\rangle$. Lower graphs: normalized population of the excited state $|\langle e|\bar{\Psi}(t)\rangle|^2 = |\bar{c}_e|^2$. Time is measured in units of Γ^{-1}.

In Fig. 4.2 we show single quantum trajectories for a two-level atom driven by a laser field with Rabi frequency $|\Omega| = 5\Gamma$ and various detunings Δ. There we plot the time evolution of the square of the norm of the wavefunction $|\Psi(t)\rangle$,

$$\langle\Psi(t)|\Psi(t)\rangle = |c_g|^2 + |c_e|^2\ ,$$

with the random numbers $r_1, r_2, \ldots$ and the corresponding jump times $t_1, t_2, \ldots$ indicated on the relevant axes, and the normalized population of the excited state,

$$|\langle e|\bar{\Psi}(t)\rangle|^2 \equiv |\bar{c}_e(t)|^2 = \frac{|c_e(t)|^2}{|c_g(t)|^2 + |c_e(t)|^2}\ .$$

Clearly, for the same Rabi frequency Ω of the field, increasing the detuning Δ results in the decrease of population of the excited state $|e\rangle$ and therefore slower buildup of the decay probability $P(t) = \int \mathrm{d}t' \Gamma |c_e(t')|^2$ between the quantum jumps. This, in turn, leads to the less frequent occurrences of quantum jumps, as can be seen from Fig. 4.2. In an idealized experiment with perfect photodetectors covering all space, each quantum jump corresponds to the detection of a spontaneous photon emitted by the atom. Since after the jump, the evolution of the atomic wavefunction starts from the ground state, the subsequent photon detection events are separated from each other by time intervals required by the atom to get promoted to the excited state $|e\rangle$ and then undergo spontaneous emission (Prob. 4.3). Recall from Sect. 2.3 that for a field in the number state $|n = 1\rangle$ the equal-time second order correlation function vanishes, $g^{(2)}(0) = 0$, indicating that the photons tend to arrive at the detectors one at a time. Thus a single driven two-level atom is a source of single photons exhibiting photon antibunching $g^{(2)}(0) < 1$.

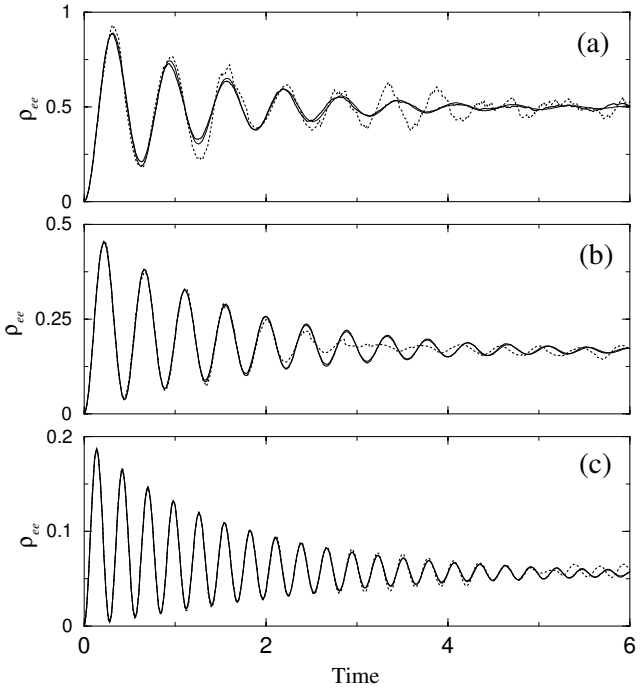

Fig. 4.3. Monte–Carlo simulations of the ensemble averaged population of the excited atomic state obtained from $M = 50$ (dotted lines) and $M = 1000$ (thick solid lines) independent realizations—trajectories. The parameters are those of Fig. 4.2, i.e., $|\Omega| = 5\Gamma$, and detunings (a) $\Delta = 0$, (b) $\Delta = 2|\Omega|$ and (c) $\Delta = 4|\Omega|$. The thin lines correspond to the exact solutions of the density matrix equations (4.42) with the same parameters.

Repeating the above procedure many times, we can generate M independent trajectories corresponding to different realizations of the atomic wavefunctions $|\bar{\Psi}_m(t)\rangle$, from which we can retrieve the approximate density operator of the system as prescribed by (4.59). In Fig. 4.3 we show the population of the excited atomic state $\rho_{ee}(t)$ obtained from averaging over $M = 50$ and $M = 1000$ independent trajectories. Clearly, the case of $M = 1000$ is hardly distinguishable from the exact solution of the density matrix equations (4.42) with the same parameters.

Of course, for a small system with only a few states, such as a two-level atom, solving the equations for the density matrix ρ seems to be a simpler task than generating many ($M \gg 1$) wave functions $|\bar{\Psi}_m(t)\rangle$ and then taking their ensemble average to approximate ρ, which clearly requires much longer computer CPU time. However, the particular advantage of the Monte–Carlo wavefunctions method becomes apparent when one has to simulate the dynamics of a large system with $N \gg 1$ degrees of freedom (eigenstates). Then the system wavefunction has N components (probability amplitudes), while the density matrix has N^2 elements. The wavefunction simulations then amount to repetitively solving N coupled differential equations, while numerical integration of the density matrix equations would require excessive computer memory for the storage and manipulation of N^2 elements, which may be prohibitive. There is thus a trade-off between memory and time, and depending on the availability of computational resources, one chooses one or the other approach to simulate the dissipative dynamics of a quantum system.

4.3 Heisenberg–Langevin Equations of Motion

So far we have worked in the Schrödinger picture, in which the dynamics of the system is described in terms of the time evolution of its wavefunction or, more generally, the density operator, while the relevant system operators are not explicitly time-dependent. The master equation for the reduced density operator ρ^{S} of the system can then be used to derive the equations of motion for the expectation values of various system operators. On the other hand, in the Heisenberg picture, the time-dependence is formally incorporated in the system operators, and the equations of motion for the corresponding observables are obtained by taking the quantum mechanical averages with the wavefunction or density matrix ρ_0^{S} pertaining to the initial state of the system. Thus, the expectation value of any system operator $\mathcal{T}$ at some time t is formally given by $\langle \mathcal{T}(t) \rangle = \mathrm{Tr}\big(\rho^{\mathrm{S}}(t)\mathcal{T}\big)$ in the Schrödinger picture, and by $\langle \mathcal{T}(t) \rangle = \mathrm{Tr}\big(\rho_0^{\mathrm{S}}\mathcal{T}(t)\big)$ in the Heisenberg picture.

Although in most practical situations it is more convenient to describe the dynamics of quantum systems in the Schrödinger picture, for the sake of completeness, we revisit here the problem of a small system coupled to a large reservoir employing the Heisenberg picture. We will see that the time evolution of the relevant system operators is governed by stochastic differential

equations having the form of the classical Langevin equation for a particle subject to a random force, such as a particle undergoing Brownian motion in a viscous medium.

4.3.1 General Formulation

As in Sect. 4.1.1, we consider the coupling of a small quantum system S with Hamiltonian $\mathcal{H}^{\rm S} = \sum_i \hbar\omega_i \, |i\rangle\langle i|$ to a reservoir R of harmonic oscillators described by Hamiltonian $\mathcal{H}^{\rm R} = \sum_k \hbar\omega_k b_k^\dagger b_k$. The system–reservoir coupling is given by $\mathcal{V} = :\mathcal{A}\cdot\mathcal{B}:$, where

$$\mathcal{A} = \sum_{ij} \mathcal{A}_{ij} \, |i\rangle\langle j| \equiv \sum_{ij} \boldsymbol{\alpha}_{ij} = \sum_{ij} \boldsymbol{\alpha}_{ji}^\dagger \, , \quad \mathcal{B} = \sum_k \boldsymbol{\beta}_k = \mathrm{i} \sum_k \boldsymbol{\epsilon}_k (b_k^\dagger - b_k) \, ,$$

are operators for the system and reservoir, respectively, each of them being linear in the corresponding raising and lowering operators. The symbol :: surrounding the operator product in $\mathcal{V}$ indicates the normal ordering of operators, with raising operators on the left-hand-side and lowering operators on the right-hand-side of the expressions involving operator products. Here we adhere to the normal ordering of operators; any other ordering would do, provided it is used consistently throughout the calculations. The normally ordered interaction Hamiltonian then takes the form

$$\mathcal{V} = \mathrm{i} \sum_k \boldsymbol{\epsilon}_k (b_k^\dagger \, \mathcal{A} - \mathcal{A} \, b_k) \, . \tag{4.66}$$

Clearly, at equal times the system and reservoir operators commute with each other. Consider any one of the system operators $\boldsymbol{\alpha}_{ij}$. The Heisenberg equation of motion reads

$$\frac{\mathrm{d}}{\mathrm{d}t}\boldsymbol{\alpha}_{ij}(t) = \frac{\mathrm{i}}{\hbar}[\mathcal{H}^{\rm S} + \mathcal{V}, \boldsymbol{\alpha}_{ij}] = \mathrm{i}\omega_{ij}\boldsymbol{\alpha}_{ij}(t) + \frac{1}{\hbar}\sum_k \boldsymbol{\epsilon}_k \left[b_k^\dagger(t) \aleph_{ij}(t) - \aleph_{ij}(t) b_k(t) \right] \, , \tag{4.67}$$

where $\omega_{ij} \equiv \omega_i - \omega_j$ is the frequency difference and $\aleph_{ij}$ denotes the commutator $[\boldsymbol{\alpha}_{ij}, \mathcal{A}]$. When the energy of state $|i\rangle$ is higher than that of state $|j\rangle$, $\boldsymbol{\alpha}_{ij}$ represents a raising operator and ω_{ij} is positive. In the opposite case of negative ω_{ij} ($\omega_i < \omega_j$) we have the lowering operator $\boldsymbol{\alpha}_{ij}$. On the other hand, for the reservoir mode operators $b_k(t)$ and $b_k^\dagger(t)$ we have

$$\frac{\mathrm{d}}{\mathrm{d}t} b_k(t) = \frac{\mathrm{i}}{\hbar}[\mathcal{H}^{\rm R} + \mathcal{V}, b_k] = -\mathrm{i}\omega_k b_k(t) + \frac{\boldsymbol{\epsilon}_k}{\hbar}\mathcal{A}(t) \, , \tag{4.68a}$$

$$\frac{\mathrm{d}}{\mathrm{d}t} b_k^\dagger(t) = \mathrm{i}\omega_k b_k^\dagger(t) + \frac{\boldsymbol{\epsilon}_k}{\hbar}\mathcal{A}(t) \, . \tag{4.68b}$$

where we have used the standard bosonic commutation relations $[b_k, b_{k'}] = [b_k^\dagger, b_{k'}^\dagger] = 0$ and $[b_k, b_{k'}^\dagger] = \delta_{kk'}$. The formal solution of these equations is given by

$$b_k(t) = b_k(0)\mathrm{e}^{-\mathrm{i}\omega_k t} + \frac{\boldsymbol{\epsilon}_k}{\hbar}\int_0^t \mathrm{d}t'\mathcal{A}(t')\mathrm{e}^{-\mathrm{i}\omega_k(t-t')} \,, \tag{4.69a}$$

$$b_k^\dagger(t) = b_k^\dagger(0)\mathrm{e}^{\mathrm{i}\omega_k t} + \frac{\boldsymbol{\epsilon}_k}{\hbar}\int_0^t \mathrm{d}t'\mathcal{A}(t')\mathrm{e}^{\mathrm{i}\omega_k(t-t')} \,, \tag{4.69b}$$

which should be substituted back into (4.67). Let us introduce slowly varying system operators $\hat{\boldsymbol{\alpha}}_{ij}(t) = \boldsymbol{\alpha}_{ij}(t)\mathrm{e}^{\mathrm{i}\omega_{ji}t}$, in terms of which the commutator $\aleph_{ij}$ is given by

$$\aleph_{ij}(t) = \sum_{j'i'} \big[\hat{\boldsymbol{\alpha}}_{ij}(t), \hat{\boldsymbol{\alpha}}_{j'i'}(t)\big]\mathrm{e}^{\mathrm{i}(\omega_{j'i'}-\omega_{ji})t} \,.$$

Substituting $\boldsymbol{\alpha}_{ij}(t) = \hat{\boldsymbol{\alpha}}_{ij}(t)\mathrm{e}^{\mathrm{i}\omega_{ij}t}$ into (4.67) and using the above solutions for the reservoir operators $b_k(t)$ and $b_k^\dagger(t)$, we have

$$\begin{aligned}\frac{\mathrm{d}}{\mathrm{d}t}\hat{\boldsymbol{\alpha}}_{ij}(t) = \mathrm{e}^{\mathrm{i}\omega_{ji}t}\frac{1}{\hbar}\sum_k \boldsymbol{\epsilon}_k\big[b_k^\dagger(0)\aleph_{ij}(t)\mathrm{e}^{\mathrm{i}\omega_k t} - \aleph_{ij}(t)b_k(0)\mathrm{e}^{-\mathrm{i}\omega_k t}\big] \\ +\frac{1}{\hbar^2}\sum_k \boldsymbol{\epsilon}_k^2\int_0^t \mathrm{d}t'\sum_{i'j'}\mathrm{e}^{\mathrm{i}(\omega_{ji}t-\omega_{j'i'}t')} \\ \times\big[\hat{\boldsymbol{\alpha}}_{i'j'}(t')\aleph_{ij}(t)\mathrm{e}^{\mathrm{i}\omega_k(t-t')} - \aleph_{ij}(t)\hat{\boldsymbol{\alpha}}_{i'j'}(t')\mathrm{e}^{-\mathrm{i}\omega_k(t-t')}\big] \,.\end{aligned} \tag{4.70}$$

As in Sect. 4.1.1, we can now make the rotating wave approximation. To this end, in the above equation we keep only the terms with $\omega_{j'i'} = \omega_{ji}$, for which $i' = i$ and $j' = j$. Then the commutator reduces to $\aleph_{ij} = [\hat{\boldsymbol{\alpha}}_{ij}, \hat{\boldsymbol{\alpha}}_{ji}] = [\boldsymbol{\alpha}_{ij}, \boldsymbol{\alpha}_{ji}]$ and (4.70) takes the following form

$$\frac{\mathrm{d}}{\mathrm{d}t}\hat{\boldsymbol{\alpha}}_{ij}(t) = \hat{\mathcal{D}}_{ij}(t) + \hat{\mathcal{F}}_{ij}(t) \,. \tag{4.71}$$

Here $\hat{\mathcal{D}}_{ij}(t)$ is known as the drift operator,

$$\begin{aligned}\hat{\mathcal{D}}_{ij}(t) = \frac{1}{\hbar^2}\sum_k \boldsymbol{\epsilon}_k^2\int_0^t \mathrm{d}t'\big[\hat{\boldsymbol{\alpha}}_{ij}(t')\aleph_{ij}(t)\mathrm{e}^{\mathrm{i}(\omega_{ji}+\omega_k)(t-t')} \\ -\aleph_{ij}(t)\hat{\boldsymbol{\alpha}}_{ij}(t')\mathrm{e}^{\mathrm{i}(\omega_{ji}-\omega_k)(t-t')}\big] \,,\end{aligned} \tag{4.72}$$

and $\hat{\mathcal{F}}_{ij}(t)$ represents the so-called noise operator,

$$\hat{\mathcal{F}}_{ij}(t) = \mathrm{e}^{\mathrm{i}\omega_{ji}t}\frac{1}{\hbar}\sum_k \boldsymbol{\epsilon}_k\big[b_k^\dagger(0)\aleph_{ij}(t)\mathrm{e}^{\mathrm{i}\omega_k t} - \aleph_{ij}(t)b_k(0)\mathrm{e}^{-\mathrm{i}\omega_k t}\big] \,. \tag{4.73}$$

The drift operator (4.72) contains the system operator $\hat{\boldsymbol{\alpha}}_{ij}(t')$ under the integral over the time interval $t' \in [0, t]$. Due to the contributions of all reservoir frequencies ω_k, the sum over the reservoir modes k amounts to a function which changes rapidly over the time scale of the order of the reservoir inverse bandwidth. On the other hand, if the system–reservoir coupling strength (inherent in $\boldsymbol{\alpha}_{ij}$) is small compared to the reservoir bandwidth, then $\hat{\boldsymbol{\alpha}}_{ij}(t')$ is

a slowly varying operator, which allows the Markov approximation. To that end, we replace t' by t and pull $\hat{\boldsymbol{\alpha}}_{ij}(t)$ out of the integral. We next change the variable t' to $t - t'$ and extend the limit of integration to ∞. These steps are obviously consistent with the approximations made in deriving the Markovian master equation (4.10). For the drift operator we thus obtain

$$\hat{\mathcal{D}}_{ij}(t) = g_{ij}^{(+)} \hat{\boldsymbol{\alpha}}_{ij}(t) \aleph_{ij}(t) - g_{ij}^{(-)} \aleph_{ij}(t) \hat{\boldsymbol{\alpha}}_{ij}(t) \,, \tag{4.74}$$

where $g_{ij}^{(\pm)}$ are complex constants given by

$$g_{ij}^{(\pm)} \equiv \frac{1}{\hbar^2} \sum_k \boldsymbol{\epsilon}_k^2 \int_0^\infty \mathrm{d}t' \mathrm{e}^{\mathrm{i}(\omega_{ji} \pm \omega_k)t'} \,. \tag{4.75}$$

Consider now the expression for the noise operator (4.73). Since the sum over the reservoir modes is a rapidly varying function of time, we may factor out the slowly varying system operator $\aleph_{ij}(t)$. Consistently with (4.14), we denote the reservoir mode operators as

$$\tilde{\boldsymbol{\beta}}_k(t) = \mathrm{i}\boldsymbol{\epsilon}_k \big[b_k^\dagger(0) \mathrm{e}^{\mathrm{i}\omega_k t} - b_k(0) \mathrm{e}^{-\mathrm{i}\omega_k t} \big] \,.$$

Hence, the noise operator

$$\mathcal{F}_{ij}(t) \equiv \mathrm{e}^{\mathrm{i}\omega_{ij} t} \hat{\mathcal{F}}_{ij}(t) = \aleph_{ij}(t) \frac{1}{\mathrm{i}\hbar} \sum_k \tilde{\boldsymbol{\beta}}_k(t)$$

depends linearly on the reservoir operators $b_k(0)$ and $b_k^\dagger(0)$. As in Sect. 4.1.1, we assume that the reservoir is in thermodynamic equilibrium and therefore its density operator ρ_0^{R} is diagonal in the energy eigenstates representation. Then the reservoir average of the noise operator vanishes at all times

$$\langle \mathcal{F}_{ij}(t) \rangle_{\mathrm{R}} = \mathrm{Tr}\big(\rho_0^{\mathrm{R}} \mathcal{F}_{ij}(t) \big) = 0 \,, \tag{4.76}$$

and (4.71) yields

$$\frac{\mathrm{d}}{\mathrm{d}t} \langle \hat{\boldsymbol{\alpha}}_{ij}(t) \rangle_{\mathrm{R}} = \langle \hat{\mathcal{D}}_{ij}(t) \rangle_{\mathrm{R}} \,. \tag{4.77}$$

However, various noise operators can have nonvanishing correlations. Indeed, the correlation functions for noise operators,

$$\langle \hat{\mathcal{F}}_{ij}(t) \, \hat{\mathcal{F}}_{i'j'}(t') \rangle_{\mathrm{R}} \propto \sum_{kk'} \langle \tilde{\boldsymbol{\beta}}_k(t) \, \tilde{\boldsymbol{\beta}}_{k'}(t') \rangle_{\mathrm{R}} \,,$$

contain a double summation over the reservoir mode operators $\tilde{\boldsymbol{\beta}}_k(t)$ and $\tilde{\boldsymbol{\beta}}_{k'}(t')$, which, as shown below, yields delta-correlations, i.e.,

$$\langle \hat{\mathcal{F}}_{ij}(t) \, \hat{\mathcal{F}}_{i'j'}(t') \rangle_{\mathrm{R}} = 2 \langle \hat{\mathcal{D}}_{ij;i'j'} \rangle_{\mathrm{R}} \delta(t - t') \,, \tag{4.78}$$

where $\langle\hat{\mathcal{D}}_{ij;i'j'}\rangle_{\rm R}$ is called the diffusion coefficient. Equation (4.71) thus governs the time-evolution of the system operator $\hat{\boldsymbol{\alpha}}_{ij}$ subject to a rapidly fluctuating quantum noise $\hat{\mathcal{F}}_{ij}$. Due to its similarity with the classical Langevin equation for a particle subject to a random force, the stochastic differential equation (4.71) is called a quantum Langevin equation.

Summarizing the above derivations, the equation of motion for the system operator $\hat{\boldsymbol{\alpha}}_{ij}$ reads (see Prob. 4.4)

$$\frac{\mathrm{d}}{\mathrm{d}t}\hat{\boldsymbol{\alpha}}_{ij}(t) = g_{ij}^{(+)}\hat{\boldsymbol{\alpha}}_{ij}(t)\aleph_{ij}(t) - g_{ij}^{(-)}\aleph_{ij}(t)\hat{\boldsymbol{\alpha}}_{ij}(t) + \hat{\mathcal{F}}_{ij}(t)\ , \tag{4.79}$$

and for the operator $\boldsymbol{\alpha}_{ij}(t)$ we have

$$\frac{\mathrm{d}}{\mathrm{d}t}\boldsymbol{\alpha}_{ij}(t) = \mathrm{i}\omega_{ij}\boldsymbol{\alpha}_{ij}(t) + g_{ij}^{(+)}\boldsymbol{\alpha}_{ij}(t)\aleph_{ij}(t) - g_{ij}^{(-)}\aleph_{ij}(t)\boldsymbol{\alpha}_{ij}(t) + \mathcal{F}_{ij}(t)\ . \tag{4.80}$$

We can also write the equation of motion for operator $\hat{\boldsymbol{\alpha}}_{ij}\hat{\boldsymbol{\alpha}}_{i'j'}$ as

$$\frac{\mathrm{d}}{\mathrm{d}t}\hat{\boldsymbol{\alpha}}_{ij}\hat{\boldsymbol{\alpha}}_{i'j'} = \frac{\mathrm{d}\hat{\boldsymbol{\alpha}}_{ij}}{\mathrm{d}t}\hat{\boldsymbol{\alpha}}_{i'j'} + \hat{\boldsymbol{\alpha}}_{ij}\frac{\mathrm{d}\hat{\boldsymbol{\alpha}}_{i'j'}}{\mathrm{d}t} = \hat{\mathcal{D}}_{ij}\hat{\boldsymbol{\alpha}}_{i'j'} + \hat{\boldsymbol{\alpha}}_{ij}\hat{\mathcal{D}}_{i'j'} + \hat{\mathcal{F}}_{ij}\hat{\boldsymbol{\alpha}}_{i'j'} + \hat{\boldsymbol{\alpha}}_{ij}\hat{\mathcal{F}}_{i'j'}\ . \tag{4.81}$$

In particular, for $i = j'$ and $j = i'$, we have $\hat{\boldsymbol{\alpha}}_{ij}\hat{\boldsymbol{\alpha}}_{ji} = \boldsymbol{\alpha}_{ij}\boldsymbol{\alpha}_{ji} \equiv \mathcal{N}_{ii}$.

Quantum Regression Theorem and Einstein Relation

Before proceeding with a specific application of the above formalism, let us outline some general features of the correlation functions between the system and noise operators. Multiplying the Langevin equation (4.71) from the right by $\boldsymbol{\alpha}_{i'j'}(t')$, with $t' < t$, and taking the reservoir average, we have

$$\frac{\mathrm{d}}{\mathrm{d}t}\langle\hat{\boldsymbol{\alpha}}_{ij}(t)\boldsymbol{\alpha}_{i'j'}(t')\rangle_{\rm R} = \langle\hat{\mathcal{D}}_{ij}(t)\boldsymbol{\alpha}_{i'j'}(t')\rangle_{\rm R} + \langle\hat{\mathcal{F}}_{ij}(t)\boldsymbol{\alpha}_{i'j'}(t')\rangle_{\rm R}\ . \tag{4.82}$$

Consistently with the Markov approximation, the system operator $\boldsymbol{\alpha}_{i'j'}(t')$ at time t' does not depend on the future noise source $\hat{\mathcal{F}}_{ij}(t)$. Therefore the correlation $\langle\hat{\mathcal{F}}_{ij}(t)\boldsymbol{\alpha}_{i'j'}(t')\rangle_{\rm R}$ vanishes and the above equation reduces to

$$\frac{\mathrm{d}}{\mathrm{d}t}\langle\hat{\boldsymbol{\alpha}}_{ij}(t)\boldsymbol{\alpha}_{i'j'}(t')\rangle_{\rm R} = \langle\hat{\mathcal{D}}_{ij}(t)\boldsymbol{\alpha}_{i'j'}(t')\rangle_{\rm R}\ , \tag{4.83}$$

which evidently has the same form as (4.77). Thus the two-time correlation function $\langle\hat{\boldsymbol{\alpha}}_{ij}(t)\boldsymbol{\alpha}_{i'j'}(t')\rangle_{\rm R}$ obeys the same equation of motion as the reservoir average of the system operator $\hat{\boldsymbol{\alpha}}_{ij}(t)$, which is the essence of the quantum regression theorem.

Next, using the identity

$$\hat{\boldsymbol{\alpha}}_{ij}(t) = \hat{\boldsymbol{\alpha}}_{ij}(t-\delta t) + \int_{t-\delta t}^{t}\mathrm{d}t'\left[\frac{\mathrm{d}}{\mathrm{d}t}\hat{\boldsymbol{\alpha}}_{ij}(t')\right]\ ,$$

and the Langevin equation (4.71), we have

$$\langle\hat{\boldsymbol{\alpha}}_{ij}(t)\hat{\mathcal{F}}_{i'j'}(t)\rangle_{\mathrm{R}} = \langle\hat{\boldsymbol{\alpha}}_{ij}(t-\delta t)\hat{\mathcal{F}}_{i'j'}(t)\rangle_{\mathrm{R}} + \int_{t-\delta t}^{t}\mathrm{d}t'\left[\langle\hat{\mathcal{D}}_{ij}(t')\hat{\mathcal{F}}_{i'j'}(t)\rangle_{\mathrm{R}} + \langle\hat{\mathcal{F}}_{ij}(t')\hat{\mathcal{F}}_{i'j'}(t)\rangle_{\mathrm{R}}\right] . \quad (4.84)$$

The operator $\boldsymbol{\alpha}_{ij}(t-\delta t)$ does not depend on the future noise source $\hat{\mathcal{F}}_{i'j'}(t)$ and the correlation $\langle\hat{\boldsymbol{\alpha}}_{ij}(t-\delta t)\hat{\mathcal{F}}_{i'j'}(t)\rangle_{\mathrm{R}}$ vanishes. Consider next the first term of the integral $\langle\hat{\mathcal{D}}_{ij}(t')\hat{\mathcal{F}}_{i'j'}(t)\rangle_{\mathrm{R}}$. Since the drift operator $\hat{\mathcal{D}}_{ij}(t')$, given by (4.74), is a function of system operators, it does not depend on $\hat{\mathcal{F}}_{i'j'}(t)$, except possibly at $t'=t$, at which point the integral is on a set of measure zero. We thus obtain

$$\langle\hat{\boldsymbol{\alpha}}_{ij}(t)\hat{\mathcal{F}}_{i'j'}(t)\rangle_{\mathrm{R}} = \int_{t-\delta t}^{t}\mathrm{d}t'\langle\hat{\mathcal{F}}_{ij}(t')\hat{\mathcal{F}}_{i'j'}(t)\rangle_{\mathrm{R}} = \langle\hat{\mathcal{D}}_{ij;i'j'}\rangle_{\mathrm{R}} , \quad (4.85)$$

where we have used (4.78). In the same way we find

$$\langle\hat{\mathcal{F}}_{ij}(t)\hat{\boldsymbol{\alpha}}_{i'j'}(t)\rangle_{\mathrm{R}} = \langle\hat{\mathcal{D}}_{ij;i'j'}\rangle_{\mathrm{R}} . \quad (4.86)$$

Taking the reservoir average of (4.81), we have

$$\frac{\mathrm{d}}{\mathrm{d}t}\langle\hat{\boldsymbol{\alpha}}_{ij}\hat{\boldsymbol{\alpha}}_{i'j'}\rangle_{\mathrm{R}} = \langle\hat{\mathcal{D}}_{ij}\hat{\boldsymbol{\alpha}}_{i'j'}\rangle_{\mathrm{R}} + \langle\hat{\boldsymbol{\alpha}}_{ij}\hat{\mathcal{D}}_{i'j'}\rangle_{\mathrm{R}} + \langle\hat{\mathcal{F}}_{ij}\hat{\boldsymbol{\alpha}}_{i'j'}\rangle_{\mathrm{R}} + \langle\hat{\boldsymbol{\alpha}}_{ij}\hat{\mathcal{F}}_{i'j'}\rangle_{\mathrm{R}} , \quad (4.87)$$

which, with the above expressions yields the so-called generalized Einstein relation,

$$2\langle\hat{\mathcal{D}}_{ij;i'j'}\rangle_{\mathrm{R}} = -\langle\hat{\boldsymbol{\alpha}}_{ij}\hat{\mathcal{D}}_{i'j'}\rangle_{\mathrm{R}} - \langle\hat{\mathcal{D}}_{ij}\hat{\boldsymbol{\alpha}}_{i'j'}\rangle_{\mathrm{R}} + \frac{\mathrm{d}}{\mathrm{d}t}\langle\hat{\boldsymbol{\alpha}}_{ij}\hat{\boldsymbol{\alpha}}_{i'j'}\rangle_{\mathrm{R}} . \quad (4.88)$$

This equation relates the diffusion coefficient $\langle\hat{\mathcal{D}}_{ij;i'j'}\rangle_{\mathrm{R}}$ to the drift terms $\hat{\mathcal{D}}_{ij}$ and $\hat{\mathcal{D}}_{i'j'}$, which is the essence of the quantum fluctuation–dissipation theorem. In many practical situations, when one can independently derive the equation of motion for $\langle\hat{\boldsymbol{\alpha}}_{ij}\hat{\boldsymbol{\alpha}}_{i'j'}\rangle_{\mathrm{R}}$, the Einstein relation provides a simple way to calculate the corresponding diffusion coefficient.

4.3.2 Application to a Two-Level Atom

The rather general operator equations derived above can be cast in a more compact and physically intuitive form once a specific physical system is considered. Here, as in the previous sections of this chapter, we apply the Heisenberg–Langevin formalism to the system represented by a two-level atom and the reservoir being the open radiation field. A somewhat simpler case of a single harmonic oscillator (single-mode cavity field) coupled to a reservoir of harmonic oscillators is discussed in Chap. 5.

We will generally follow the notation of Sect. 4.1.2. The Hamiltonian for the two-level atom with the lower state $|g\rangle$ and upper state $|e\rangle$ is $\mathcal{H}^{\rm A} = \sum_{i=g,e} \hbar\omega_i \, |i\rangle\langle i|$, which upon shifting the zero-point energy to $\frac{1}{2}\hbar(\omega_g + \omega_e)$ becomes $\mathcal{H}^{\rm A} = \frac{1}{2}\hbar\omega_{eg}\sigma_z$, where $\sigma_z = |e\rangle\langle e| - |g\rangle\langle g|$ is the atomic operator and $\omega_{eg} = \omega_e - \omega_g$ is the $|e\rangle \to |g\rangle$ transition frequency. The reservoir Hamiltonian is given by the sum over all modes of the open radiation field, $\mathcal{H}^{\rm R} = \sum_{\boldsymbol{k}\lambda} \hbar\omega_k b^\dagger_{\boldsymbol{k}\lambda} b_{\boldsymbol{k}\lambda}$. Finally, the atom–field interaction has the standard form $\mathcal{V} = -:\boldsymbol{\wp}\cdot\boldsymbol{E}:$, with the atomic dipole operator $\boldsymbol{\wp}$ and electric field $\boldsymbol{E}$ given, respectively, by (4.23) and (4.24). We can thus identify the system operators $\boldsymbol{\alpha}_{ij}$ as $\boldsymbol{\alpha}_{ge} = \boldsymbol{\wp}_{eg}\sigma_-$ and $\boldsymbol{\alpha}_{eg} = \boldsymbol{\alpha}^\dagger_{ge} = \boldsymbol{\wp}_{ge}\sigma_+$, and the commutators $\aleph_{ij}$ reduce to

$$\aleph_{eg} = |\boldsymbol{\wp}_{eg}|^2[\,|e\rangle\langle e| - |g\rangle\langle g|\,] = |\boldsymbol{\wp}_{eg}|^2\sigma_z \;, \quad \aleph_{ge} = -|\boldsymbol{\wp}_{eg}|^2\sigma_z \;.$$

In turn, the reservoir mode operators are given by $\boldsymbol{\beta}_{\boldsymbol{k}\lambda} = -{\rm i}\boldsymbol{\epsilon}_{\boldsymbol{k}\lambda}(b_{\boldsymbol{k}\lambda} - b^\dagger_{\boldsymbol{k}\lambda})$, with $\boldsymbol{\epsilon}_{\boldsymbol{k}\lambda} = \hat{\boldsymbol{e}}_{\boldsymbol{k}\lambda}\sqrt{\hbar\omega_k/2\varepsilon_0 V}$. For the coefficient g_{ij} we then have

$$\begin{aligned} g^{(\pm)}_{ij} &= \sum_{\boldsymbol{k}\lambda} \frac{\omega_k}{2\varepsilon_0\hbar V} \int_0^\infty {\rm d}t' \, {\rm e}^{{\rm i}(\omega_{ji}\pm\omega_k)t'} \\ &= \frac{1}{4\pi\varepsilon_0}\frac{2}{3\hbar c^3}\int_0^\infty {\rm d}\omega_k \, \omega_k^3 \delta(\omega_{ji}\pm\omega_k) \\ &\quad + {\rm i}\frac{1}{4\pi\varepsilon_0}\frac{2}{3\pi\hbar c^3}\,{\rm P}\int_0^\infty {\rm d}\omega_k \frac{\omega_k^3}{\omega_{ji}\pm\omega_k} \;, \end{aligned} \tag{4.89}$$

where we have used the standard procedure employed in evaluating the expressions in (4.30). In the same fashion, identifying the indices ij with either ge or eg and noting that $\omega_k \geq 0$, we obtain

$$g^{(-)}_{ge}|\boldsymbol{\wp}_{eg}|^2 = \tfrac{1}{2}\Gamma_{eg} + {\rm i}s^{(-)}_{ge} \;, \quad g^{(+)}_{ge}|\boldsymbol{\wp}_{eg}|^2 = 0 + {\rm i}s^{(+)}_{ge} \;, \tag{4.90a}$$

$$g^{(+)}_{eg}|\boldsymbol{\wp}_{eg}|^2 = \tfrac{1}{2}\Gamma_{eg} - {\rm i}s^{(-)}_{ge} \;, \quad g^{(-)}_{eg}|\boldsymbol{\wp}_{eg}|^2 = 0 - {\rm i}s^{(+)}_{ge} \;, \tag{4.90b}$$

where Γ_{eg} is obviously the spontaneous decay rate of (4.34), and

$$s^{(\pm)}_{eg} = \frac{1}{4\pi\varepsilon_0}\frac{2|\boldsymbol{\wp}_{eg}|^2}{3\pi\hbar c^3}\,{\rm P}\int_0^\infty {\rm d}\omega_k \, \frac{\omega_k^3}{\omega_{eg}\pm\omega_k} \;, \tag{4.91}$$

represent the Lamb shift of the atomic transition. Noting that $\sigma_z\sigma_\pm = \pm\sigma_\pm$ and $\sigma_\pm\sigma_z = \mp\sigma_\pm$, from (4.80) we then obtain the following equations for the atomic operators $\sigma_- = \boldsymbol{\alpha}_{ge}/\boldsymbol{\wp}_{eg}$ and $\sigma_+ = \boldsymbol{\alpha}_{eg}/\boldsymbol{\wp}_{ge}$,

$$\frac{\rm d}{{\rm d}t}\sigma_-(t) = -({\rm i}\omega_{eg} + \tfrac{1}{2}\Gamma_{eg})\,\sigma_-(t) + \mathcal{F}_-(t) \;, \tag{4.92a}$$

$$\frac{\rm d}{{\rm d}t}\sigma_+(t) = ({\rm i}\omega_{eg} - \tfrac{1}{2}\Gamma_{eg})\,\sigma_+(t) + \mathcal{F}_+(t) \;, \tag{4.92b}$$

where the Lamb shift is incorporated in the atomic transition frequency via

$$\omega_{eg} + s_{eg}^{(+)} + s_{eg}^{(-)} \to \omega_{eg} \ ,$$

and the noise operators are given by

$$\begin{aligned}\mathcal{F}_-(t) &= \wp_{ge}\sigma_z(t)\frac{\mathrm{i}}{\hbar}\sum_{\boldsymbol{k}\lambda}\tilde{\boldsymbol{\beta}}_{\boldsymbol{k}\lambda}(t) \\ &= \sigma_z(t)\frac{\wp_{ge}}{\hbar}\sum_{\boldsymbol{k}\lambda}\boldsymbol{\epsilon}_{\boldsymbol{k}\lambda}\big[b_{\boldsymbol{k}\lambda}(0)\mathrm{e}^{-\mathrm{i}\omega_k t} - b^\dagger_{\boldsymbol{k}\lambda}(0)\mathrm{e}^{\mathrm{i}\omega_k t}\big] \ , \qquad (4.93a)\\ \mathcal{F}_+(t) &= \big[\mathcal{F}_-(t)\big]^\dagger \ . \qquad (4.93b)\end{aligned}$$

From (4.92), for the slowly varying atomic operators $\hat{\sigma}_+(t) = \sigma_+(t)\mathrm{e}^{-\mathrm{i}\omega_{eg}t}$ and $\hat{\sigma}_-(t) = \sigma_-(t)\mathrm{e}^{\mathrm{i}\omega_{eg}t}$, we have

$$\frac{\mathrm{d}}{\mathrm{d}t}\hat{\sigma}_\pm(t) = -\tfrac{1}{2}\Gamma_{eg}\hat{\sigma}_\pm(t) + \hat{\mathcal{F}}_\pm(t) \ , \qquad (4.94)$$

with the corresponding noise operators $\hat{\mathcal{F}}_\pm(t) = \mathrm{e}^{\mp\mathrm{i}\omega_{eg}t}\mathcal{F}_\pm(t)$.

Consider now the correlation functions for the noise operators,

$$\langle\hat{\mathcal{F}}_\pm(t)\hat{\mathcal{F}}_\mp(t')\rangle_\mathrm{R} = \sigma_z(t)\sigma_z(t')|\wp_{eg}|^2 G^{(\pm)}_{eg}(t,t') \ , \qquad (4.95)$$

where

$$G^{(\pm)}_{eg}(t,t') \equiv \frac{1}{\hbar^2}\sum_{\boldsymbol{k}\lambda}\sum_{\boldsymbol{k}'\lambda'}\mathrm{e}^{\mp\mathrm{i}\omega_{eg}(t-t')}\langle\tilde{\boldsymbol{\beta}}_{\boldsymbol{k}\lambda}(t)\tilde{\boldsymbol{\beta}}_{\boldsymbol{k}'\lambda'}(t')\rangle_\mathrm{R} \ . \qquad (4.96)$$

We can calculate the reservoir correlation functions $\langle\tilde{\boldsymbol{\beta}}_{\boldsymbol{k}\lambda}(t)\tilde{\boldsymbol{\beta}}_{\boldsymbol{k}'\lambda'}(t')\rangle_\mathrm{R}$ using the same procedure as in (4.28). The correlation tensors are given by (4.29), which, upon substitution into the above expression yields

$$\begin{aligned}G^{(+)}_{eg}(t,t') = \sum_{\boldsymbol{k}\lambda}\frac{\omega_k}{2\varepsilon_0\hbar V}\big[\big(1+\bar{n}(\omega_k)\big)\,\mathrm{e}^{-\mathrm{i}(\omega_{eg}+\omega_k)(t-t')} \\ +\bar{n}(\omega_k)\,\mathrm{e}^{-\mathrm{i}(\omega_{eg}-\omega_k)(t-t')}\big] \ , \qquad (4.97a)\\ G^{(-)}_{eg}(t,t') = \sum_{\boldsymbol{k}\lambda}\frac{\omega_k}{2\varepsilon_0\hbar V}\big[\big(1+\bar{n}(\omega_k)\big)\,\mathrm{e}^{\mathrm{i}(\omega_{eg}-\omega_k)(t-t')} \\ +\bar{n}(\omega_k)\,\mathrm{e}^{\mathrm{i}(\omega_{eg}+\omega_k)(t-t')}\big] \ . \qquad (4.97b)\end{aligned}$$

We next replace the sum $\boldsymbol{k}\lambda$ by an integral over the continuous spectrum of the reservoir, and perform the integration over the solid angle Ω. Since in the remaining integral the reservoir frequencies ω_k are positive, we can drop the terms oscillating with the sum frequencies $(\omega_{eg}+\omega_k)$, obtaining

$$\begin{aligned}G^{(+)}_{eg}(t,t') &= \frac{1}{4\pi\varepsilon_0}\frac{4}{3\hbar c^3}\frac{1}{2\pi}\int_0^\infty \mathrm{d}\omega_k\,\omega_k^3\,\bar{n}(\omega_k)\,\mathrm{e}^{-\mathrm{i}(\omega_{eg}-\omega_k)(t-t')} \ , \qquad (4.98a)\\ G^{(-)}_{eg}(t,t') &= \frac{1}{4\pi\varepsilon_0}\frac{4}{3\hbar c^3}\frac{1}{2\pi}\int_0^\infty \mathrm{d}\omega_k\,\omega_k^3\big(1+\bar{n}(\omega_k)\big)\,\mathrm{e}^{\mathrm{i}(\omega_{eg}-\omega_k)(t-t')} \ . \qquad (4.98b)\end{aligned}$$

In the above equations, the functions $\omega_k^3\,\bar{n}(\omega_k)$ and $\omega_k^3\big(1+\bar{n}(\omega_k)\big)$ vary little over the frequency region $\omega_k \simeq \omega_{eg}$ where the exponents $\mathrm{e}^{\mp\mathrm{i}(\omega_{eg}-\omega_k)(t-t')}$ oscillate slowly. We can therefore evaluate these functions at $\omega_k = \omega_{eg}$ and pull them out of the integral. What remains is

$$\frac{1}{2\pi}\int_0^\infty \mathrm{d}\omega_k\,\mathrm{e}^{\pm\mathrm{i}(\omega_k-\omega_{eg})(t-t')} = \frac{1}{2\pi}\int_{-\infty}^\infty \mathrm{d}\omega\,\mathrm{e}^{\pm\mathrm{i}\omega(t-t')} = \delta(t-t')\,, \tag{4.99}$$

where in view of $\omega_{eg} > 0$, we have extended the lower limit of integration to $-\infty$ and denoted $(\omega_k - \omega_{eg})$ by ω, which results in the δ-function. We thus have

$$G_{eg}^{(+)}(t,t')|\wp_{eg}|^2 = \Gamma_{eg}\bar{n}(\omega_{eg})\,\delta(t-t')\,, \tag{4.100a}$$

$$G_{eg}^{(-)}(t,t')|\wp_{eg}|^2 = \Gamma_{eg}\big(1+\bar{n}(\omega_{eg})\big)\delta(t-t')\,. \tag{4.100b}$$

Since at $t = t'$ we have $\sigma_z(t)\sigma_z(t') = I$, for the noise correlation functions we finally obtain

$$\langle\hat{\mathcal{F}}_+(t)\hat{\mathcal{F}}_-(t')\rangle_{\mathrm{R}} = \Gamma_{eg}\bar{n}\,\delta(t-t')\,, \tag{4.101a}$$

$$\langle\hat{\mathcal{F}}_-(t)\hat{\mathcal{F}}_+(t')\rangle_{\mathrm{R}} = \Gamma_{eg}\big(1+\bar{n}\big)\delta(t-t')\,, \tag{4.101b}$$

where $\bar{n}$ stands for $\bar{n}(\omega_{eg})$ The corresponding diffusion coefficients are therefore given by

$$\langle\hat{\mathcal{D}}_{+-}\rangle_{\mathrm{R}} = \tfrac{1}{2}\Gamma_{eg}\bar{n} \quad \langle\hat{\mathcal{D}}_{-+}\rangle_{\mathrm{R}} = \tfrac{1}{2}\Gamma_{eg}\big(1+\bar{n}\big)\,. \tag{4.102}$$

Integrating the correlation functions (4.101), we obtain

$$\Gamma_{eg} = \frac{1}{\bar{n}}\int_{-\infty}^{-\infty}\mathrm{d}t'\langle\hat{\mathcal{F}}_+(t)\hat{\mathcal{F}}_-(t')\rangle_{\mathrm{R}} = \frac{1}{1+\bar{n}}\int_{-\infty}^{-\infty}\mathrm{d}t'\langle\hat{\mathcal{F}}_-(t)\hat{\mathcal{F}}_+(t')\rangle_{\mathrm{R}}\,, \tag{4.103}$$

which shows that the decay of the system Γ_{eg} is related to, or induced by, the reservoir fluctuations, which is another manifestation of the fluctuation–dissipation theorem.

Consider now the atomic operators $\sigma_{ee} \equiv |e\rangle\langle e| = \hat{\sigma}_+\hat{\sigma}_-$ and $\sigma_{gg} \equiv |g\rangle\langle g| = \hat{\sigma}_-\hat{\sigma}_+$. Using (4.94), their equations of motion are easily obtained as

$$\begin{aligned}\frac{\mathrm{d}}{\mathrm{d}t}\sigma_{ee}(t) &= \frac{\mathrm{d}\hat{\sigma}_+}{\mathrm{d}t}\hat{\sigma}_- + \hat{\sigma}_+\frac{\mathrm{d}\hat{\sigma}_-}{\mathrm{d}t}\\ &= -\Gamma_{eg}\sigma_{ee} + \hat{\mathcal{F}}_+\hat{\sigma}_- + \hat{\sigma}_+\hat{\mathcal{F}}_-\,,\end{aligned} \tag{4.104a}$$

$$\frac{\mathrm{d}}{\mathrm{d}t}\sigma_{gg}(t) = -\Gamma_{eg}\sigma_{gg} + \hat{\mathcal{F}}_-\hat{\sigma}_+ + \hat{\sigma}_-\hat{\mathcal{F}}_+\,. \tag{4.104b}$$

To calculate the reservoir averages of $\hat{\mathcal{F}}_+\hat{\sigma}_- + \hat{\sigma}_+\hat{\mathcal{F}}_-$ and $\hat{\mathcal{F}}_-\hat{\sigma}_+ + \hat{\sigma}_-\hat{\mathcal{F}}_+$, we can employ the formal solution of (4.94), namely

$$\hat{\sigma}_\pm(t) = \hat{\sigma}_\pm(0)\,\mathrm{e}^{-\frac{1}{2}\Gamma_{eg}t} + \int_0^t \mathrm{d}t'\hat{\mathcal{F}}_\pm(t')\,\mathrm{e}^{-\frac{1}{2}\Gamma_{eg}(t-t')}\,. \tag{4.105}$$

We then have

$$\langle\hat{\mathcal{F}}_+\hat{\sigma}_-\rangle_{\rm R} + \langle\hat{\sigma}_+\hat{\mathcal{F}}_-\rangle_{\rm R} = \big[\langle\hat{\mathcal{F}}_+(t)\rangle_{\rm R}\hat{\sigma}_-(0) + \hat{\sigma}_+(0)\langle\hat{\mathcal{F}}_-(t)\rangle_{\rm R}\big]{\rm e}^{-\frac{1}{2}\Gamma_{eg}t} + \int_0^t {\rm d}t'\big[\langle\hat{\mathcal{F}}_+(t)\hat{\mathcal{F}}_-(t')\rangle_{\rm R} + \langle\hat{\mathcal{F}}_+(t')\hat{\mathcal{F}}_-(t)\rangle_{\rm R}\big]{\rm e}^{-\frac{1}{2}\Gamma_{eg}(t-t')} .$$

Since the reservoir averages of the noise operators $\hat{\mathcal{F}}_\pm$ vanish, while the noise correlations are given by (4.101), the above expression yields

$$\langle\hat{\mathcal{F}}_+\hat{\sigma}_-\rangle_{\rm R} + \langle\hat{\sigma}_+\hat{\mathcal{F}}_-\rangle_{\rm R} = \Gamma_{eg}\bar{n} . \tag{4.106}$$

Similarly, we obtain

$$\langle\hat{\mathcal{F}}_-\hat{\sigma}_+\rangle_{\rm R} + \langle\hat{\sigma}_-\hat{\mathcal{F}}_+\rangle_{\rm R} = \Gamma_{eg}(1+\bar{n}) . \tag{4.107}$$

Defining the noise operators

$$\mathcal{F}_{ee}(t) = \hat{\mathcal{F}}_+\hat{\sigma}_- + \hat{\sigma}_+\hat{\mathcal{F}}_- - \Gamma_{eg}\bar{n} , \tag{4.108a}$$

$$\mathcal{F}_{gg}(t) = \hat{\mathcal{F}}_-\hat{\sigma}_+ + \hat{\sigma}_-\hat{\mathcal{F}}_+ - \Gamma_{eg}(1+\bar{n}) , \tag{4.108b}$$

which have the usual properties $\langle\hat{\mathcal{F}}_{ee}\rangle_{\rm R} = \langle\hat{\mathcal{F}}_{gg}\rangle_{\rm R} = 0$, we can cast (4.104) as

$$\frac{\rm d}{{\rm d}t}\sigma_{ee}(t) = -\Gamma_{eg}\sigma_{ee}(t) + \Gamma_{eg}\bar{n} + \mathcal{F}_{ee}(t) , \tag{4.109a}$$

$$\frac{\rm d}{{\rm d}t}\sigma_{gg}(t) = -\Gamma_{eg}\sigma_{gg}(t) + \Gamma_{eg}(1+\bar{n}) + \mathcal{F}_{gg}(t) . \tag{4.109b}$$

From these operator equations, we finally obtain the following equations of motion for the expectation values,

$$\frac{\rm d}{{\rm d}t}\langle\sigma_{ee}(t)\rangle = -\Gamma_{eg}\langle\sigma_{ee}(t)\rangle + \Gamma_{eg}\bar{n} , \tag{4.110a}$$

$$\frac{\rm d}{{\rm d}t}\langle\sigma_{gg}(t)\rangle = -\Gamma_{eg}\langle\sigma_{gg}(t)\rangle + \Gamma_{eg}(1+\bar{n}) = \Gamma_{eg}\langle\sigma_{ee}(t)\rangle + \Gamma_{eg}\bar{n} , \tag{4.110b}$$

where in the last step we have used the obvious relation $\langle\sigma_{gg}\rangle + \langle\sigma_{ee}\rangle = 1$, valid for a closed two-level atom. These are rate equations for a two-level atom in a thermal radiation reservoir.

Driven Two-Level Atom

Before closing this section, let us consider a two-level atom driven by a coherent classical field of frequency $\omega \simeq \omega_{eg}$. Under the rotating-wave approximation, the atom–field interaction Hamiltonian is given by

$$\mathcal{V}^{\rm AF} = -\hbar\big(\sigma_+\Omega\,{\rm e}^{-{\rm i}\omega t} + \Omega^*\sigma_-\,{\rm e}^{{\rm i}\omega t}\big) = -\hbar\big(\hat{\sigma}_+\Omega\,{\rm e}^{-{\rm i}\Delta t} + \Omega^*\hat{\sigma}_-\,{\rm e}^{{\rm i}\Delta t}\big) , \tag{4.111}$$

where, as in the previous sections, $\Delta = \omega - \omega_{eg}$ is the detuning and Ω is the Rabi frequency. Using the Heisenberg equation of motion, we then obtain the following set of coupled differential equations for the atomic operators,

$$\frac{\mathrm{d}}{\mathrm{d}t}\sigma_{gg} = \Gamma(1-\sigma_{gg}) + \mathrm{i}(\Omega^*\hat{\sigma}_- \,\mathrm{e}^{\mathrm{i}\Delta t} - \hat{\sigma}_+\Omega\,\mathrm{e}^{-\mathrm{i}\Delta t}) + \mathcal{F}_{gg}\ , \quad (4.112a)$$

$$\frac{\mathrm{d}}{\mathrm{d}t}\sigma_{ee} = -\Gamma\sigma_{ee} + \mathrm{i}(\Omega\hat{\sigma}_+ \,\mathrm{e}^{-\mathrm{i}\Delta t} - \hat{\sigma}_-\Omega^*\,\mathrm{e}^{\mathrm{i}\Delta t}) + \mathcal{F}_{ee}\ , \quad (4.112b)$$

$$\frac{\mathrm{d}}{\mathrm{d}t}\hat{\sigma}_- = -\tfrac{1}{2}\Gamma\hat{\sigma}_- + \mathrm{i}\Omega\,\mathrm{e}^{-\mathrm{i}\Delta t}(\sigma_{gg}-\sigma_{ee}) + \hat{\mathcal{F}}_-\ , \quad (4.112c)$$

$$\frac{\mathrm{d}}{\mathrm{d}t}\hat{\sigma}_+ = -\tfrac{1}{2}\Gamma\hat{\sigma}_+ - \mathrm{i}\Omega^*\,\mathrm{e}^{\mathrm{i}\Delta t}(\sigma_{gg}-\sigma_{ee}) + \hat{\mathcal{F}}_+\ , \quad (4.112d)$$

where Γ stands for Γ_{eg} and $\bar{n} \to 0$ is assumed. Taking the expectation value of these equations, and identifying the resulting quantities as

$$\langle\sigma_{gg}\rangle = \tilde{\rho}_{gg}\ , \quad \langle\sigma_{ee}\rangle = \tilde{\rho}_{ee}\ , \quad \langle\hat{\sigma}_-\rangle = \tilde{\rho}_{eg}\ , \quad \langle\hat{\sigma}_+\rangle = \tilde{\rho}_{ge}\ ,$$

we obviously recover the density matrix equations (4.40), with all the consequences discussed in Sect. 4.1.3.

Problems

4.1. Verify the derivation of equations (4.32) and (4.33)–(4.35).

4.2. Phase-changing collisions of the atom with a buffer gas can be described by the interaction Hamiltonian $\mathcal{V} = \sigma_z \sum_k g_k(b_k + b_k^\dagger)$, where b_k and $b_k^\dagger$ are the harmonic oscillator operators, g_k the corresponding coupling constants, and each collision is assumed to change by π the relative phase between the atomic states $|e\rangle$ and $|g\rangle$, hence the atomic operator σ_z. Using the formalism of Sect. 4.1.1, derive the Liouvillian (4.41) describing the atomic phase-relaxations.

4.3. For a driven two-level atom, what is the mean time interval δt between the emission of consecutive spontaneous photons? Show that for resonant driving $\Delta = 0$, the expression for δt reduces to $\delta t \simeq 2/\Gamma$ when $|\Omega| \gg \Gamma$, and $\delta t \simeq \Gamma/(4|\Omega|^2)$ when $|\Omega| \ll \Gamma$. How many clicks per unit time would an experimentalist record using a photodetector with finite efficiency $\eta < 1$?

4.4. Verify the derivation of equations (4.79) and (4.80).

4.5. Verify the derivation of equations (4.90), (4.92) and (4.101).

5

Cavity Quantum Electrodynamics

The dynamics of a small system coupled to a large reservoir can be described using several different formalisms developed in the previous chapter and illustrated with the system of a two-level atom in the open radiation field. Here we adapt this general theory to a system represented by a single-mode cavity field coupled to a reservoir of harmonic oscillators. We first derive the master equation, the Fokker–Planck equation and the Heisenberg–Langevin equations of motion for the cavity field. We then discuss certain aspects of cavity quantum electrodynamics (QED) which studies the behavior of an atom interacting with the cavity field. In particular, we consider a two-level atom in a leaky cavity and show that, depending on the parameters of the cavity, the atom–cavity system can exhibit damped Rabi oscillations, or the optical cavity can modify the rate of atomic spontaneous emission. Finally, we demonstrate that by employing the STIRAP techniques with a three-level atom confined in a leaky cavity, one can realize a deterministic source of single-photons. Other aspects of cavity QED will be discussed in Chap. 10 in the context of physical implementations of quantum information processing.

5.1 Single Mode Cavity Field Coupled to a Reservoir

As discussed in Sect. 2.1.2, the electromagnetic field confined within reflecting boundaries, such as a Fabry–Perot resonator consisting of two parallel mirrors, represents a quantum mechanical analog of the linear harmonic oscillator. The eigenmodes $k_m = \pi m/L$, $\omega_m = k_m c$ of such a cavity are equally spaced in frequency, the spacing $\delta\omega \equiv \omega_{m+1} - \omega_m = \pi c/L$ being inversely proportional to the distance between the mirrors L. In many practical situations, it is reasonable to consider only one of the infinitely many modes of the cavity, particularly when the field in this mode interacts near-resonantly with a system having sharp resonances (e.g., an atom), while the frequencies of all other modes are far away from the relevant transitions. More quantitatively, assuming for concreteness a two-level atom in the cavity as studied in Sect. 3.3.2,

we can neglect all those cavity modes k_m for which the atom–field coupling strength g is small compared to the frequency mismatch $\Delta_m = \omega_m - \omega_{eg}$ between the atomic transition resonance ω_{eg} and the mode frequency ω_m.

In this section we consider a single-mode cavity field coupled to a reservoir of harmonic oscillators resulting in the field relaxation. This problem is completely analogous to the problem studied in the previous chapter, wherein the coupling of a two-level atom with the continuum of modes of the open radiation field results in an irreversible decay of the excited atomic state. The cavity field is described by the creation $a^\dagger$ and annihilation a operators obeying the standard bosonic commutation relations

$$[a, a^\dagger] = 1 \ , \quad [a, a] = [a^\dagger, a^\dagger] = 0 \ . \tag{5.1}$$

Its Hamiltonian is given by $\mathcal{H}^{\rm F} = \hbar\omega a^\dagger a$, where ω is the mode frequency. The eigenstates of $\mathcal{H}^{\rm F}$ are the number or Fock states $|n\rangle$, with $n = 0, 1, 2, \ldots$ Then, obviously, in the energy eigenstate representation, the operators a and $a^\dagger$ can be expanded as

$$a = \sum_n \sqrt{n}\, |n-1\rangle\langle n| \ , \quad a^\dagger = \sum_n \sqrt{n}\, |n\rangle\langle n-1| \ ,$$

while the above Hamiltonian can be written as

$$\mathcal{H}^{\rm F} = \sum_n \hbar\omega_n\, |n\rangle\langle n| \ , \quad \omega_n \equiv n\omega \ ,$$

which has the same form as the system Hamiltonian $\mathcal{H}^{\rm S} = \sum_i \hbar\omega_i\, |i\rangle\langle i|$ employed throughout Chap. 4. In turn, the reservoir is composed of the infinite set of harmonic oscillators and is described by the Hamiltonian $\mathcal{H}^{\rm R} = \sum_k \hbar\omega_k b_k^\dagger b_k$, with $b_k^\dagger$ and b_k being the creation and annihilation operators of the corresponding mode. In the case of transmission losses, or leakage, through the imperfect (semi-transparent) mirrors of the cavity, the reservoir modes represent the photon modes of the free radiation field outside the cavity. Another mechanism of field relaxation is its absorption by the walls of the cavity, in which case the reservoir modes correspond to the phonon modes of the solid material enclosing the cavity. In either case, the interaction $\mathcal{V} = \mathcal{A}\cdot\mathcal{B}$ is bilinear in the corresponding system and reservoir operators, given, respectively, by

$$\mathcal{A} = \wp(a + a^\dagger) \ , \quad \mathcal{B} = \sum_k \boldsymbol{\beta}_k = {\rm i} \sum_k \boldsymbol{\epsilon}_k (b_k^\dagger - b_k) \ , \tag{5.2}$$

where $\wp$ is the coupling matrix element. In the case of transmission losses, $\wp$ is determined by the electric field transmission coefficient of the cavity mirrors. As for absorption losses, $\wp$ represents the coupling of the cavity field with bound electrons of the solid, which in turn excite the phonon modes of the material. In general, $\wp$ may be frequency depended, but here we consider only the situations in which the coupling between the system and reservoir is a slowly-varying function of ω_k in the vicinity of resonant frequency ω, where it can be well approximated by a constant.

5.1.1 Master Equation

We outline now the derivation of the master equation for the reduced density operator of the cavity field, $\tilde{\rho}^{\mathrm{F}} \equiv \mathrm{Tr}_{\mathrm{R}}(\tilde{\rho})$. Proceeding along the lines of Sect. 4.1, we adopt here similar notations, so as to emphasize the generality of the approach. We therefore define the system operators via

$$\boldsymbol{\alpha}_- = \wp a \ , \quad \boldsymbol{\alpha}_+ = \wp a^\dagger = (\boldsymbol{\alpha}_-)^\dagger \ , \tag{5.3}$$

and the corresponding frequencies $\omega_\pm = \pm\omega$. In the interaction picture, with $\mathcal{H}^0 = \mathcal{H}^{\mathrm{F}} + \mathcal{H}^{\mathrm{R}}$, we then have

$$\tilde{\mathcal{V}}(t) = \mathrm{e}^{\frac{\mathrm{i}}{\hbar}\mathcal{H}^0 t}\, \mathcal{V}\, \mathrm{e}^{-\frac{\mathrm{i}}{\hbar}\mathcal{H}^0 t} = \sum_{i=-,+} \sum_k \mathrm{e}^{\mathrm{i}\omega_i t} \boldsymbol{\alpha}_i \cdot \tilde{\boldsymbol{\beta}}_k(t) \ , \tag{5.4}$$

where the reservoir mode operators $\tilde{\boldsymbol{\beta}}_k(t)$ are given by (4.14). Substituting $\tilde{\mathcal{V}}(t)$ into the Markovian quantum master equation (4.10), we obtain

$$\begin{aligned} \frac{\partial}{\partial t}\tilde{\rho}^{\mathrm{F}}(t) = \sum_{i,i'} \sum_{kk'} \ \mathrm{e}^{\mathrm{i}(\omega_i+\omega_{i'})t} \Big[& G_{kk'}(\omega_i) \big(\boldsymbol{\alpha}_i \, \tilde{\rho}^{\mathrm{F}}(t)\, \boldsymbol{\alpha}_{i'} - \boldsymbol{\alpha}_{i'}\, \boldsymbol{\alpha}_i \, \tilde{\rho}^{\mathrm{F}}(t) \big) \\ & + \overline{G}_{kk'}(\omega_i) \big(\boldsymbol{\alpha}_{i'} \, \tilde{\rho}^{\mathrm{F}}(t)\, \boldsymbol{\alpha}_i - \tilde{\rho}^{\mathrm{F}}(t)\, \boldsymbol{\alpha}_i \, \boldsymbol{\alpha}_{i'} \big) \Big] \ , \end{aligned} \tag{5.5}$$

where

$$G_{kk'}(\omega_i) \equiv \frac{1}{\hbar^2} \int_0^\infty \mathrm{d}t' \, \mathrm{e}^{-\mathrm{i}\omega_i t'} \langle \tilde{\boldsymbol{\beta}}_{k'}(t)\, \tilde{\boldsymbol{\beta}}_k(t-t') \rangle_{\mathrm{R}} \ , \tag{5.6a}$$

$$\overline{G}_{kk'}(\omega_i) \equiv \frac{1}{\hbar^2} \int_0^\infty \mathrm{d}t' \, \mathrm{e}^{-\mathrm{i}\omega_i t'} \langle \tilde{\boldsymbol{\beta}}_k(t-t')\, \tilde{\boldsymbol{\beta}}_{k'}(t) \rangle_{\mathrm{R}} \ . \tag{5.6b}$$

We next perform the rotating-wave approximation, which amounts to neglecting the terms with indices $i = i'$ oscillating as $\mathrm{e}^{\pm 2\mathrm{i}\omega t}$, keeping only the terms with $i \neq i'$, for which we can obviously write $\boldsymbol{\alpha}_{i'} = \boldsymbol{\alpha}_i^\dagger$. With the notation

$$G_i \equiv \sum_{kk'} G_{kk'}(\omega_i) \ , \quad \overline{G}_i \equiv \sum_{kk'} \overline{G}_{kk'}(\omega_i) \ , \tag{5.7}$$

the master equation reads

$$\begin{aligned} \frac{\partial}{\partial t}\tilde{\rho}^{\mathrm{F}}(t) = \sum_i \ \Big[& G_i \big(\boldsymbol{\alpha}_i \, \tilde{\rho}^{\mathrm{F}}(t)\, \boldsymbol{\alpha}_i^\dagger - \boldsymbol{\alpha}_i^\dagger \, \boldsymbol{\alpha}_i \, \tilde{\rho}^{\mathrm{F}}(t) \big) \\ & + \overline{G}_i \big(\boldsymbol{\alpha}_i^\dagger \, \tilde{\rho}^{\mathrm{F}}(t)\, \boldsymbol{\alpha}_i - \tilde{\rho}^{\mathrm{F}}(t)\, \boldsymbol{\alpha}_i \, \boldsymbol{\alpha}_i^\dagger \big) \Big] \ . \end{aligned} \tag{5.8}$$

As in Sect. 4.1.2, we assume that the reservoir is in thermal equilibrium, with the correlation tensors given by (4.29). For the complex coefficients G_i and $\overline{G}_i$ we therefore have

$$G_i = \sum_k \frac{\boldsymbol{\epsilon}_k^2}{\hbar^2} \int_0^\infty \mathrm{d}t' \Big[\big(1 + \bar{n}(\omega_k)\big) \mathrm{e}^{-\mathrm{i}(\omega_i + \omega_k)t'} + \bar{n}(\omega_k)\, \mathrm{e}^{-\mathrm{i}(\omega_i - \omega_k)t'} \Big] , \tag{5.9a}$$

$$\overline{G}_i = \sum_{\boldsymbol{k}\lambda} \frac{\boldsymbol{\epsilon}_k^2}{\hbar^2} \int_0^\infty \mathrm{d}t' \Big[\big(1 + \bar{n}(\omega_k)\big) \mathrm{e}^{-\mathrm{i}(\omega_i - \omega_k)t'} + \bar{n}(\omega_k)\, \mathrm{e}^{-\mathrm{i}(\omega_i + \omega_k)t'} \Big] . \tag{5.9b}$$

The sum over modes k should be replaced by an integral,

$$\sum_k \to \int_0^\infty \mathrm{d}\omega_k \varrho(\omega_k) , \tag{5.10}$$

where $\varrho(\omega_k)$ is the density of modes of the reservoir around ω_k. If the reservoir is represented by the open radiation field outside the cavity, the density of modes $\varrho(\omega_k)$ is that of (2.30), while in the case of the reservoir being the phonon field of the solid material enclosing the cavity, the density of modes is determined by the parameters of the solid. In any case, however, we assume that both the reservoir density of modes $\varrho(\omega_k)$ and the coupling strength between the cavity field and the reservoir

$$g(\omega_k) = \frac{\wp \cdot \boldsymbol{\epsilon}_k}{\hbar} ,$$

are smooth and slowly-varying functions of ω_k in the vicinity of cavity resonance ω. Under these conditions, we evaluate the coefficients G_i and $\overline{G}_i$ using (4.31) and keeping in mind that ω is a positive quantity. Identifying the index i with either $-$ or $+$, we then obtain

$$G_-|\wp|^2 = \tfrac{1}{2}\kappa\big(1 + \bar{n}(\omega)\big) + \mathrm{i}S_- , \tag{5.11a}$$

$$G_+|\wp|^2 = \tfrac{1}{2}\kappa\, \bar{n}(\omega) - \mathrm{i}S_+ , \tag{5.11b}$$

$$\overline{G}_-|\wp|^2 = \tfrac{1}{2}\kappa\, \bar{n}(\omega) + \mathrm{i}S_+ , \tag{5.11c}$$

$$\overline{G}_+|\wp|^2 = \tfrac{1}{2}\kappa\big(1 + \bar{n}(\omega)\big) - \mathrm{i}S_- , \tag{5.11d}$$

where

$$\kappa = 2\pi\varrho(\omega)|g(\omega)|^2 , \tag{5.12}$$

is the decay rate or bandwidth of the cavity mode, and

$$S_- = \mathrm{P}\int_0^\infty \mathrm{d}\omega_k\, \varrho(\omega_k)|g(\omega_k)|^2 \left[\frac{1 + \bar{n}(\omega_k)}{\omega - \omega_k} + \frac{\bar{n}(\omega_k)}{\omega + \omega_k} \right] , \tag{5.13a}$$

$$S_+ = \mathrm{P}\int_0^\infty \mathrm{d}\omega_k\, \varrho(\omega_k)|g(\omega_k)|^2 \left[\frac{1 + \bar{n}(\omega_k)}{\omega + \omega_k} + \frac{\bar{n}(\omega_k)}{\omega - \omega_k} \right] , \tag{5.13b}$$

represent the frequency shifts which can be incorporated in the mode frequency ω. Then, expanding the sum over i, from (5.8) we finally arrive at the master equation for the cavity field,

$$\begin{aligned} \frac{\partial}{\partial t}\tilde{\rho}^{\mathrm{F}} = {} & \tfrac{1}{2}\kappa\,(1 + \bar{n}) \left(2a\tilde{\rho}^{\mathrm{F}}a^\dagger - a^\dagger a\tilde{\rho}^{\mathrm{F}} - \tilde{\rho}^{\mathrm{F}}a^\dagger a\right) \\ & + \tfrac{1}{2}\kappa\,\bar{n} \left(2a^\dagger\tilde{\rho}^{\mathrm{F}}a - aa^\dagger\tilde{\rho}^{\mathrm{F}} - \tilde{\rho}^{\mathrm{F}}aa^\dagger\right) , \end{aligned} \tag{5.14}$$

where $\bar{n}$ denotes $\bar{n}(\omega)$, i.e., the mean number of thermal photons at the frequency of the cavity mode. In the limit of $\bar{n} \to 0$ ($k_{\rm B}T \ll \hbar\omega$), we obtain

$$\frac{\partial}{\partial t}\tilde{\rho}^{\rm F} = \tfrac{1}{2}\kappa\left(2a\tilde{\rho}^{\rm F}a^\dagger - a^\dagger a\tilde{\rho}^{\rm F} - \tilde{\rho}^{\rm F}a^\dagger a\right) \equiv \mathcal{L}\tilde{\rho}^{\rm F} \ , \tag{5.15}$$

which describes the decay of the cavity field into the empty reservoir.

The above master equation can be used to derive equations of motion for the expectation values of various system operators, $\langle \mathcal{T}(t)\rangle = {\rm Tr}\big(\tilde{\rho}^{\rm F}(t)\mathcal{T}\big)$. The simplest example is the expectation value of the electric field $\langle E(t)\rangle = \epsilon_\omega\big(\langle a(t)\rangle + \langle a^\dagger(t)\rangle\big)$, where $\epsilon_\omega = \sqrt{\hbar\omega/\varepsilon_0 V}$ is the field per photon within the cavity volume V. In the interaction picture, we have (Prob. 5.2)

$$\frac{\rm d}{{\rm d}t}\langle a(t)\rangle = -\tfrac{1}{2}\kappa\langle a(t)\rangle \ , \tag{5.16}$$

and similarly for $\langle a^\dagger(t)\rangle$, which implies that the field amplitude decays exponentially with time according to $\langle a(t)\rangle = \langle a(0)\rangle {\rm e}^{-\frac{1}{2}\kappa t}$. Another example is the equation of motion for the mean number of photons in the cavity mode, given by the expectation value of the operator $\mathcal{N} \equiv a^\dagger a$,

$$\frac{\rm d}{{\rm d}t}\langle \mathcal{N}(t)\rangle = -\kappa\langle \mathcal{N}(t)\rangle + \kappa\bar{n} \ . \tag{5.17}$$

Its solution is

$$\langle \mathcal{N}(t)\rangle = \langle \mathcal{N}(0)\rangle {\rm e}^{-\kappa t} + \bar{n}(1 - {\rm e}^{-\kappa t}) \ , \tag{5.18}$$

which shows that for large times $t \gg \kappa^{-1}$, the average number of photons in the cavity mode approaches the number of thermal photons at the mode frequency ω, $\langle \mathcal{N}(\infty)\rangle \to \bar{n}(\omega) = ({\rm e}^{\hbar\omega/k_{\rm B}T} - 1)^{-1}$.

Consider finally the diagonal matrix elements $\langle n|\,\tilde{\rho}^{\rm F}\,|n\rangle \equiv P(n)$ of the density operator $\tilde{\rho}^{\rm F}$. Clearly, the physical meaning of $P(n)$ is the probability that the cavity mode contains precisely n photons, i.e., it is the expectation value of the projection operator $\mathit{\Pi}_n \equiv |n\rangle\langle n|$ as discussed in Sect. 2.2.1. Using the master equation (5.14), we obtain

$$\frac{\partial}{\partial t}P(n) = r_-(n+1)\,P(n+1) - \big[r_+(n) + r_-(n)\big]P(n) + r_+(n-1)\,P(n-1) \ , \tag{5.19}$$

where $r_-(n) = \kappa(1+\bar{n})n$ and $r_+(n) = \kappa\bar{n}(n+1)$ are the corresponding downward and upward transition rates from state $|n\rangle$. We thus have an infinite hierarchy of coupled rate equations for the probabilities $P(n)$ for the cavity field to contain $n = 0, 1, 2, \ldots$ photons. In the steady-state, $\partial_t P(n) = 0$, the above equation reduces to a three-term recursion relation for $P(n-1)$, $P(n)$ and $P(n+1)$, which implies the detailed balance condition

$$r_-(n)\,P(n) = r_+(n-1)\,P(n-1) \ , \tag{5.20}$$

stating that the probability of transition $|n\rangle \to |n-1\rangle$ is equal to that of the inverse transition $|n-1\rangle \to |n\rangle$. For the lowest pair of states $|0\rangle$ and $|1\rangle$, we have $r_-(1)\,P(1) = r_+(0)\,P(0)$, which gives

$$P(1) = \frac{\bar{n}}{1+\bar{n}} P(0) \,,$$

and by induction we find that

$$P(n) = \frac{\bar{n}}{1+\bar{n}} P(n-1) = \left(\frac{\bar{n}}{1+\bar{n}}\right)^n P(0) \,. \tag{5.21}$$

The normalization condition $\sum_n P(n) = 1$ yields $P(0) = (1+\bar{n})^{-1}$, using which we finally obtain

$$P(n) = \frac{1}{1+\bar{n}} \left(\frac{\bar{n}}{1+\bar{n}}\right)^n = \frac{\bar{n}^n}{(1+\bar{n})^{n+1}} = \mathrm{e}^{-\hbar\omega n/k_{\mathrm{B}}T} \big(1 - \mathrm{e}^{-\hbar\omega/k_{\mathrm{B}}T}\big) \,, \tag{5.22}$$

which is the same expression as (2.46), as it should be.

5.1.2 Stochastic Wavefunctions

We are now in the position to describe the procedure for performing the Monte–Carlo simulations of the dissipative dynamics of the cavity field. Following the general prescription of Sect. 4.2, we consider the evolution of a pure-state wavefunction of the system $|\Psi\rangle$ according to the Schrödinger equation

$$\mathrm{i}\hbar \frac{\partial}{\partial t} |\Psi\rangle = \mathcal{H}_{\mathrm{eff}} |\Psi\rangle \,, \tag{5.23}$$

where $\mathcal{H}_{\mathrm{eff}}$ is the effective Hamiltonian containing a Hermitian part $\mathcal{H}_{\mathrm{F}}$ plus non-Hermitian dissipative part. For simplicity, we assume that the surrounding environment, or the reservoir, is at zero temperature, $\bar{n} = 0$, and therefore only one relaxation channel of the cavity field is active, which is described by the Liouvillian $\mathcal{L}\rho$ of (5.15). Then the effective Hamiltonian reads

$$\mathcal{H}_{\mathrm{eff}} = \mathcal{H}_{\mathrm{F}} - \mathrm{i}\hbar \tfrac{1}{2} \kappa a^\dagger a \,, \tag{5.24}$$

while the jump superoperator is $\mathcal{L}_{\mathrm{jump}}\rho = \kappa a \rho a^\dagger$. To compress notation, we denote here the density operator $\tilde{\rho}^{\mathrm{F}}$ by ρ. Beginning with a pure normalized initial state $|\Psi(0)\rangle$, we propagate the Schrödinger equation (5.23) until the first quantum jump at time t_1 determined from the condition

$$P(t_1) = 1 - \langle \Psi(t_1) | \Psi(t_1) \rangle = r_1 \,, \tag{5.25}$$

where $r_1 \in [0,1]$ is a random number. The post-jump renormalized wavefunction is then given by the projection

$$|\Psi(t_1^+)\rangle = \frac{a\,|\Psi(t_1)\rangle}{\sqrt{\langle\Psi(t_1)|\,a^\dagger a\,|\Psi(t_1)\rangle}}\ . \tag{5.26}$$

We then continue the propagation, beginning with the new wavefunction $|\Psi(t_1^+)\rangle$, until the next quantum jump at time t_2 which is determined by the second random number $r_2 = P(t_2)$, and so on till reaching the desired final time $t_{\rm end}$. We thus simulate a single quantum trajectory, wherein the normalized wavefunction of the system $|\bar\Psi(t)\rangle$ at any time $t \in [0, t_{\rm end}]$ is given by $|\bar\Psi(t)\rangle = |\Psi(t)\rangle/||\,|\Psi(t)\rangle||$. We can repeat this procedure many times and average the results over a large number $M \gg 1$ of independent trajectories, to obtain an approximate density operator of the cavity field as

$$\rho(t) \simeq \frac{1}{M}\sum_m^M |\bar\Psi_j(t)\rangle\langle\bar\Psi_j(t)|\ . \tag{5.27}$$

To acquire an intuition on the outlined above Monte–Carlo simulations, consider first the simplest example of a cavity field prepared initially in a pure number state with precisely n photons, $|\Psi(0)\rangle = |n\rangle$. Before the first quantum jump, $t \le t_1$, the unnormalized wavefunction of the system evolves according to

$$|\Psi(t)\rangle = {\rm e}^{-\frac{\rm i}{\hbar}\mathcal{H}_{\rm eff}t}\,|\Psi(0)\rangle = {\rm e}^{-\frac{1}{2}\kappa n t}\,|n\rangle\ , \tag{5.28}$$

which shows that the decay rate is proportional to the number of photons n. The corresponding n-photon decay probability $P^{(n)}(t)$ is given by

$$P^{(n)}(t) = 1 - {\rm e}^{-\kappa n t}\ . \tag{5.29}$$

A random number r_1 determines the first quantum jump, $P^{(n)}(t_1) = r_1$, and projects the cavity field onto the state with $n-1$ photons,

$$|\Psi(t_1^+)\rangle = \frac{a\,|\Psi(t_1)\rangle}{\sqrt{\langle\Psi(t_1)|\,a^\dagger a\,|\Psi(t_1)\rangle}} = |n-1\rangle\ . \tag{5.30}$$

Between the first and second jump events, $t_1 < t \le t_2$, the field evolves according to

$$|\Psi(t)\rangle = {\rm e}^{-\frac{1}{2}\kappa(n-1)t}\,|n-1\rangle\ ,$$

with the corresponding decay probability $P^{(n-1)}(t) = 1 - {\rm e}^{-\kappa(n-1)t}$. This is followed by the second quantum jump, determined by r_2 and so on. After n quantum jumps, the field will reach the zero-photon state $|0\rangle$, which will not evolve any more.

In a more general case, the field may initially be prepared in some superposition state

$$|\Psi(0)\rangle = \sum_n^{n_{\rm max}} c_n(0)\,|n\rangle\ , \tag{5.31}$$

where $n_{\rm max}$ corresponds to the term with the largest number of photons, which could in principle be ∞, an example of which is the coherent state (2.35).

Then, between the quantum jumps $j-1$ and j ($j=1,2,\ldots$), each amplitude c_n of this superposition evolves with time $t \in (t_{j-1}, t_j]$ (with $t_0 = 0$) according to $c_n(t) = \mathrm{e}^{-\frac{1}{2}\kappa n t} c_n(t_{j-1}^+)$, and the total decay probability is given by

$$P(t) = 1 - \sum_n \mathrm{e}^{-\kappa n t} |c_n(t)|^2 \,. \tag{5.32}$$

A quantum jump at time t_j, $P(t_j) = r_j$, projects the system onto the state

$$|\Psi(t_j^+)\rangle = \frac{a\,|\Psi(t_j)\rangle}{\sqrt{\langle\Psi(t_j)|\,a^\dagger a\,|\Psi(t_j)\rangle}} = \sum_n^{n_{\max}-j} c_n(t_j^+)\,|n\rangle \,, \tag{5.33}$$

with the amplitudes $c_n(t_j^+)$ given by

$$c_n(t_j^+) = \frac{\mathrm{e}^{-\frac{1}{2}\kappa(n+1)t}\sqrt{n+1}}{\sum_{n'} \mathrm{e}^{-\kappa(n'+1)t}(n'+1)|c_{n'+1}(t_{j-1}^+)|^2}\, c_{n+1}(t_{j-1}^+) \,, \tag{5.34}$$

where the denominator ensures the normalization. We thus see that the quantum jump relates each amplitude c_n of state $|n\rangle$ with the pre-jump amplitude c_{n+1} corresponding to the state $|n+1\rangle$ with one more photon. With each jump, the amplitude c_0 of zero-photon state $|0\rangle$ is eliminated, while in the sum over the photon-number states in (5.33), the largest term contains one less photon. Consequently, if in the superposition (5.31) corresponding to the initial state, $n_{\max}$ is bound, after $j = n_{\max}$ quantum jumps the cavity field will be empty, $|\Psi(t_j^+)\rangle = |0\rangle$, with no further evolution. Clearly, this conclusion is valid only when the temperature T of the reservoir is so small, $k_\mathrm{B}T \ll \hbar\omega$, that we can assume that there are no thermal photons in the cavity, $\bar{n}(\omega) \simeq 0$. Otherwise, for $\bar{n}(\omega) \neq 0$, there will be a competing relaxation channel, corresponding to the addition of photons into the cavity from the thermal environment, which will eventually equilibrate the cavity field with the reservoir. As noted at the end of Sect. 4.2.1, under the ergodic hypothesis the long time-average of $|\bar{\Psi}(t)\rangle\langle\bar{\Psi}(t)|$ then yields an approximate density operator of the resulting thermal (chaotic) field (2.117).

Let us finally emphasize that above we have considered the free evolution of the cavity field, so that the Hermitian part of the effective Hamiltonian (5.24) does not contain any external control or coherent coupling of the field to other systems. The field was assumed to be initially prepared in state $|\Psi(0)\rangle$ by some process that ceased to act at time $t = 0$. Examples of such processes include field injection into the cavity by an outside source (e.g., laser), or an exchange of excitation between the cavity and an initially excited atom, which will be discussed later in this chapter.

5.1.3 Fokker–Planck Equation

In Sect. 2.4, we have presented several possible representations of the density operator of the electromagnetic field in the basis of coherent states. One such

representation is the P-representation of (2.92), which is convenient for evaluating the expectation values of normally–ordered operator products. Here we derive the equation of motion for the quasi-probability distribution function $P(\alpha)$. Remarkably, this equation will have the form of the classical Fokker–Planck equation, which arises in many problems involving stochastic processes and is equivalent to the corresponding Langevin equations.

The derivation of the quantum Fokker–Planck equation commences with the substitution of

$$\tilde{\rho}^{\mathrm{F}} = \int P(\alpha)\,|\alpha\rangle\langle\alpha|\,\mathrm{d}^2\alpha\,,$$

into the master equation (5.14), which yields

$$\begin{aligned}\int \frac{\partial P(\alpha)}{\partial t}\,|\alpha\rangle\langle\alpha|\,\mathrm{d}^2\alpha = \tfrac{1}{2}\kappa\,(1+\bar{n})\int P(\alpha)\big(2a\,|\alpha\rangle\langle\alpha|\,a^\dagger \\ -a^\dagger a\,|\alpha\rangle\langle\alpha| \;-\; |\alpha\rangle\langle\alpha|\,a^\dagger a\big)\mathrm{d}^2\alpha \\ +\tfrac{1}{2}\kappa\,\bar{n}\int P(\alpha)\big(2a^\dagger\,|\alpha\rangle\langle\alpha|\,a \\ -aa^\dagger\,|\alpha\rangle\langle\alpha| \;-\; |\alpha\rangle\langle\alpha|\,aa^\dagger\big)\mathrm{d}^2\alpha\,. \qquad (5.35)\end{aligned}$$

Using the relations (see Prob. 2.4)

$$a^\dagger\,|\alpha\rangle\langle\alpha| \;=\left(\frac{\partial}{\partial\alpha}+\alpha^*\right)|\alpha\rangle\langle\alpha|\;,\quad |\alpha\rangle\langle\alpha|\,a^\dagger = \alpha^*\,|\alpha\rangle\langle\alpha|\;, \qquad (5.36a)$$

$$|\alpha\rangle\langle\alpha|\,a = \left(\frac{\partial}{\partial\alpha^*}+\alpha\right)|\alpha\rangle\langle\alpha|\;,\quad a\,|\alpha\rangle\langle\alpha| \;=\alpha\,|\alpha\rangle\langle\alpha|\;, \qquad (5.36b)$$

we have

$$2a\,|\alpha\rangle\langle\alpha|\,a^\dagger - a^\dagger a\,|\alpha\rangle\langle\alpha| \;-\; |\alpha\rangle\langle\alpha|\,a^\dagger a = -\left(\alpha\frac{\partial}{\partial\alpha}+\alpha^*\frac{\partial}{\partial\alpha^*}\right)|\alpha\rangle\langle\alpha|\;,$$

$$2a^\dagger\,|\alpha\rangle\langle\alpha|\,a - aa^\dagger\,|\alpha\rangle\langle\alpha| \;-\; |\alpha\rangle\langle\alpha|\,aa^\dagger = \left(\alpha\frac{\partial}{\partial\alpha}+\alpha^*\frac{\partial}{\partial\alpha^*}+2\frac{\partial^2}{\partial\alpha\,\partial\alpha^*}\right)|\alpha\rangle\langle\alpha|\;,$$

which should be substituted into (5.35), with the result

$$\int \frac{\partial P(\alpha)}{\partial t}\,|\alpha\rangle\langle\alpha|\,\mathrm{d}^2\alpha = \frac{\kappa}{2}\int P(\alpha)\left(2\bar{n}\frac{\partial^2}{\partial\alpha\,\partial\alpha^*}-\alpha\frac{\partial}{\partial\alpha}-\alpha^*\frac{\partial}{\partial\alpha^*}\right)\big[\,|\alpha\rangle\langle\alpha|\,\big]\mathrm{d}^2\alpha\,. \qquad (5.37)$$

The terms under the integral on right-hand-side of this equation can be integrated by parts according to

$$\begin{aligned}\int \alpha P(\alpha)\frac{\partial}{\partial\alpha}\big[\,|\alpha\rangle\langle\alpha|\,\big]\mathrm{d}^2\alpha \\ = \alpha P(\alpha)\,|\alpha\rangle\langle\alpha|\,\Big|_{-\infty}^{\infty} - \int \frac{\partial}{\partial\alpha}\big[\alpha P(\alpha)\big]\,|\alpha\rangle\langle\alpha|\;\mathrm{d}^2\alpha\,, \qquad (5.38a)\end{aligned}$$

$$\int \alpha^* P(\alpha) \frac{\partial}{\partial \alpha^*} \big[\, |\alpha\rangle\langle\alpha| \,\big] \mathrm{d}^2\alpha$$
$$= \alpha^* P(\alpha)\, |\alpha\rangle\langle\alpha| \,\Big|_{-\infty}^{\infty} - \int \frac{\partial}{\partial \alpha^*} \big[\alpha^* P(\alpha)\big]\, |\alpha\rangle\langle\alpha| \, \mathrm{d}^2\alpha \,, \tag{5.38b}$$
$$\int P(\alpha) \frac{\partial^2}{\partial \alpha\, \partial \alpha^*} \big[\, |\alpha\rangle\langle\alpha| \,\big] \mathrm{d}^2\alpha$$
$$= P(\alpha) \frac{\partial}{\partial \alpha^*} \big[\, |\alpha\rangle\langle\alpha| \,\big] \Big|_{-\infty}^{\infty} - \int \frac{\partial}{\partial \alpha} \big[P(\alpha)\big] \frac{\partial}{\partial \alpha^*} \big[\, |\alpha\rangle\langle\alpha| \,\big] \mathrm{d}^2\alpha$$
$$= P(\alpha) \frac{\partial}{\partial \alpha^*} \big[\, |\alpha\rangle\langle\alpha| \,\big] \Big|_{-\infty}^{\infty} - \frac{\partial}{\partial \alpha} \big[P(\alpha)\big]\, |\alpha\rangle\langle\alpha| \,\Big|_{-\infty}^{\infty}$$
$$+ \int \frac{\partial^2}{\partial \alpha\, \partial \alpha^*} \big[P(\alpha)\big]\, |\alpha\rangle\langle\alpha| \, \mathrm{d}^2\alpha \,. \tag{5.38c}$$

Here the constants of integration disappear because the distribution $P(\alpha)$ vanishes for $|\alpha| \to \infty$. Thus, on the right-hand-side of the above equations, only the last terms containing integrals remain. Then, equation (5.37) yields

$$\int \frac{\partial P(\alpha)}{\partial t}\, |\alpha\rangle\langle\alpha| \, \mathrm{d}^2\alpha = \frac{\kappa}{2} \int \left(\frac{\partial}{\partial \alpha} \alpha + \frac{\partial}{\partial \alpha^*} \alpha^* + 2\bar{n} \frac{\partial^2}{\partial \alpha\, \partial \alpha^*} \right) \big[P(\alpha)\big]\, |\alpha\rangle\langle\alpha| \, \mathrm{d}^2\alpha \,. \tag{5.39}$$

Equating the coefficients of $|\alpha\rangle\langle\alpha|$ in the integrands on both sides of this equation, we obtain the following equation of motion for $P(\alpha)$,

$$\frac{\partial}{\partial t} P(\alpha) = \frac{\kappa}{2} \left(\frac{\partial}{\partial \alpha} \alpha + \frac{\partial}{\partial \alpha^*} \alpha^* \right) P(\alpha) + \kappa \bar{n} \frac{\partial^2}{\partial \alpha\, \partial \alpha^*} P(\alpha) \,. \tag{5.40}$$

This is the Fokker–Planck equation which governs the time-evolution of the quasi-probability $P(\alpha) \equiv P(\alpha, t)$ for the field to be in a coherent state $|\alpha\rangle$. The first term on the right-hand-side of this equation describes the deterministic motion of the peak of $P(\alpha, t)$, and thus the coefficients of the first derivatives represent the elements of the drift matrix. In turn, the second term causes the spreading or dispersion of $P(\alpha, t)$ due to the presence of thermal photons, and the coefficients of the second derivatives constitute the diffusion matrix.

Let us assume that at time $t = 0$ the field is in a pure coherent state $|\beta\rangle$, so its density operator is given by $\rho = |\beta\rangle\langle\beta|$. According to (2.112), we then have $P(\alpha, 0) = \delta^{(2)}(\alpha - \beta)$, which in the Gaussian representation can be expressed as

$$P(\alpha, 0) = \lim_{\epsilon \to 0} \frac{1}{\pi\epsilon} \exp\left(\frac{-|\alpha - \beta|^2}{\epsilon} \right) \,. \tag{5.41}$$

It can be verified (see Prob. 5.5) that the function

$$P(\alpha, t) = \frac{1}{\pi \bar{n} (1 - \mathrm{e}^{-\kappa t})} \exp\left(\frac{-|\alpha - \beta \mathrm{e}^{-\kappa t/2}|^2}{\bar{n}(1 - \mathrm{e}^{-\kappa t})} \right) \,, \tag{5.42}$$

constitutes the time-dependent solution of the Fokker–Planck equation (5.40). Here the quantity $D(t) \equiv \bar{n}(1 - \mathrm{e}^{-\kappa t})$ determines the dispersion of the Gaussian function. Consider first the case of the reservoir at zero temperature, so

that $\bar{n} \to 0$. Then the above solution can be cast as

$$P(\alpha,t) = \lim_{D\to 0} \frac{1}{\pi D} \exp\left(\frac{-|\alpha - \beta \mathrm{e}^{-\kappa t/2}|^2}{D}\right) = \delta^{(2)}(\alpha - \beta \mathrm{e}^{-\kappa t/2}) \,, \quad (5.43)$$

which indicates that, while the amplitude β of the initial coherent state decays exponentially with the rate $\kappa/2$, the field remains at all times in a pure coherent state represented by the density operator $\rho = |\beta \mathrm{e}^{-\kappa t/2}\rangle\langle\beta \mathrm{e}^{-\kappa t/2}|$. Consider next the case of a thermal reservoir with $\bar{n} > 0$. According to (5.42), again the amplitude β of the initial coherent state decays exponentially with time, but the dispersion $D(t) = \bar{n}(1 - \mathrm{e}^{-\kappa t})$ increases causing the quasi-probability to broaden and acquire a Gaussian form with the corresponding width. For large times $t \gg \kappa^{-1}$, the field equilibrates with the thermal reservoir and the steady-state value of $P(\alpha, t \to \infty)$ is given by

$$P(\alpha,\infty) = \frac{1}{\pi\bar{n}} \exp\left(-\frac{|\alpha|^2}{\bar{n}}\right) \,, \quad (5.44)$$

which is the same as in (2.121), as it should be.

5.1.4 Heisenberg–Langevin Equations of Motion

Let us finally derive the equations of motion for the cavity field operators in the Heisenberg picture. With the system $\mathcal{A}$ and reservoir $\mathcal{B}$ operators given by (5.2), the normally ordered interaction Hamiltonian reads

$$\mathcal{V} = :\mathcal{A}\cdot\mathcal{B}:= \mathrm{i}\sum_k \boldsymbol{\epsilon}_k \left(b_k^\dagger \boldsymbol{\alpha}_+ + b_k^\dagger \boldsymbol{\alpha}_- - \boldsymbol{\alpha}_+ b_k - \boldsymbol{\alpha}_- b_k\right) \,, \quad (5.45)$$

where the system operators $\boldsymbol{\alpha}_\pm$ are those of (5.3). In turn, the commutators $\aleph_\pm \equiv [\boldsymbol{\alpha}_\pm, \mathcal{A}]$ reduce to

$$\aleph_+ = -|\wp|^2 \,, \quad \aleph_- = |\wp|^2 \,,$$

which is a consequence of the commutation relations (5.1). Following the procedure of Sect. 4.3.1, we substitute the formal solution for reservoir operators $b_k(t)$ and $b_k^\dagger(t)$ into the Heisenberg equations of motion for the slowly varying system operators $\hat{\boldsymbol{\alpha}}_\mp(t) = \boldsymbol{\alpha}_\mp(t)\mathrm{e}^{\pm \mathrm{i}\omega t}$, obtaining

$$\begin{aligned}\frac{\mathrm{d}}{\mathrm{d}t}\hat{\boldsymbol{\alpha}}_\mp(t) = {} & \pm \mathrm{e}^{\pm\mathrm{i}\omega t}\frac{|\wp|^2}{\hbar}\sum_k \boldsymbol{\epsilon}_k \left[b_k^\dagger(0)\mathrm{e}^{\mathrm{i}\omega_k t} - b_k(0)\mathrm{e}^{-\mathrm{i}\omega_k t}\right] \\ & \pm \frac{|\wp|^2}{\hbar^2}\sum_k \boldsymbol{\epsilon}_k^2 \int_0^t \mathrm{d}t' \left[\hat{\boldsymbol{\alpha}}_+(t')\mathrm{e}^{\mathrm{i}\omega(t'\pm t)} + \hat{\boldsymbol{\alpha}}_-(t')\mathrm{e}^{-\mathrm{i}\omega(t'\mp t)}\right] \\ & \times \left[\mathrm{e}^{\mathrm{i}\omega_k(t-t')} - \mathrm{e}^{-\mathrm{i}\omega_k(t-t')}\right] \,, \end{aligned} \quad (5.46)$$

where the first term on the right-hand-side represents the corresponding noise operator $\hat{\mathcal{F}}_\pm$ and the second term is the drift operator $\hat{\mathcal{D}}_\pm$. In the expressions for the drift operators, we can drop the terms oscillating as $\mathrm{e}^{\pm\mathrm{i}\omega(t+t')}$, which amounts to the rotating wave approximation. For the remaining terms containing operators $\hat{\boldsymbol{\alpha}}_\mp(t')$, we then make the Markov approximation: we replace t' by t and pull $\hat{\boldsymbol{\alpha}}_\mp(t)$ out of the integral. We next change the variable t' by $t-t'$ and extend the limit of integration to ∞. The drift operators then read

$$\hat{\mathcal{D}}_- = \big[g_-^{(+)} - g_-^{(-)}\big]|\wp|^2\hat{\boldsymbol{\alpha}}_-(t)\;, \tag{5.47a}$$

$$\hat{\mathcal{D}}_+ = \big[g_+^{(-)} - g_+^{(+)}\big]|\wp|^2\hat{\boldsymbol{\alpha}}_+(t)\;, \tag{5.47b}$$

where $g_-^{(\pm)}$ and $g_+^{(\pm)}$ are complex coefficients given by

$$g_-^{(\pm)} = \frac{1}{\hbar^2}\sum_k \boldsymbol{\epsilon}_k^2 \int_0^\infty \mathrm{d}t' \mathrm{e}^{\mathrm{i}(\omega\pm\omega_k)t'}\;, \tag{5.48a}$$

$$g_+^{(\pm)} = \frac{1}{\hbar^2}\sum_k \boldsymbol{\epsilon}_k^2 \int_0^\infty \mathrm{d}t' \mathrm{e}^{-\mathrm{i}(\omega\mp\omega_k)t'}\;. \tag{5.48b}$$

To evaluate these coefficients, we use the relation (4.31) and then replace the sum over modes k by the integral (5.10), assuming that the density of modes of the reservoir $\varrho(\omega_k)$ and the coupling strength $g(\omega_k) = \wp\cdot\boldsymbol{\epsilon}_k/\hbar$ are smooth (non-singular) functions of ω_k in the vicinity of the cavity resonance $\omega > 0$. We thus obtain

$$g_-^{(-)}|\wp|^2 = \tfrac{1}{2}\kappa + \mathrm{i}s_-^{(-)}\;,\quad g_-^{(+)}|\wp|^2 = 0 + \mathrm{i}s_-^{(+)}\;, \tag{5.49a}$$

$$g_+^{(+)}|\wp|^2 = \tfrac{1}{2}\kappa - \mathrm{i}s_-^{(-)}\;,\quad g_+^{(-)}|\wp|^2 = 0 - \mathrm{i}s_-^{(+)}\;, \tag{5.49b}$$

where $\kappa = 2\pi\varrho(\omega)|g(\omega)|^2$ is the decay rate of the cavity eigenmode, and

$$s_-^{(\pm)} = \mathrm{P}\int_0^\infty \mathrm{d}\omega_k\, \frac{\varrho(\omega_k)|g(\omega_k)|^2}{\omega\pm\omega_k}\;, \tag{5.50}$$

are the frequency shifts which can be incorporated in the mode frequency via $\omega - s_-^{(+)} + s_-^{(-)} \to \omega$. We can now write the equations of motion for the cavity field operators $a = \boldsymbol{\alpha}_-/\wp$ and $a^\dagger = \boldsymbol{\alpha}_+/\wp$ as

$$\frac{\mathrm{d}}{\mathrm{d}t}a(t) = -(\mathrm{i}\omega + \tfrac{1}{2}\kappa)\,a(t) + \mathcal{F}(t)\;, \tag{5.51a}$$

$$\frac{\mathrm{d}}{\mathrm{d}t}a^\dagger(t) = (\mathrm{i}\omega - \tfrac{1}{2}\kappa)\,a^\dagger(t) + \mathcal{F}^\dagger(t)\;, \tag{5.51b}$$

where the noise operator $\mathcal{F}(t)$ is given by

$$\mathcal{F}(t) = \frac{\wp}{\mathrm{i}\hbar}\sum_k \tilde{\boldsymbol{\beta}}_k(t)\;,\quad \text{with}\quad \tilde{\boldsymbol{\beta}}_k(t) = \mathrm{i}\boldsymbol{\epsilon}_k\big[b_k^\dagger(0)\mathrm{e}^{\mathrm{i}\omega_k t} - b_k(0)\mathrm{e}^{-\mathrm{i}\omega_k t}\big]\;. \tag{5.52}$$

Equivalently, for the slowly varying field operator $\hat{a}(t) = a(t)\mathrm{e}^{\mathrm{i}\omega t} = \hat{\boldsymbol{\alpha}}_-(t)/\wp$, we have

$$\frac{\mathrm{d}}{\mathrm{d}t}\hat{a}(t) = -\tfrac{1}{2}\kappa\hat{a}(t) + \hat{\mathcal{F}}(t) \;, \tag{5.53}$$

with $\hat{\mathcal{F}}(t) = \mathrm{e}^{\mathrm{i}\omega t}\mathcal{F}(t)$, and similarly for $\hat{a}^\dagger(t) \equiv [\hat{a}(t)]^\dagger$.

Assuming, as before, that the reservoir is in thermal equilibrium, the reservoir average of the noise operator vanishes, $\langle\mathcal{F}(t)\rangle_\mathrm{R} = 0$. Then, using (5.53), the equation of motion for the expectation value of the slowly varying field operator reads

$$\frac{\mathrm{d}}{\mathrm{d}t}\langle\hat{a}(t)\rangle = -\tfrac{1}{2}\kappa\langle\hat{a}(t)\rangle \;, \tag{5.54}$$

which is the same as (5.16). Consider next the correlation functions for the noise operators,

$$\langle\hat{\mathcal{F}}^\dagger(t)\hat{\mathcal{F}}(t')\rangle_\mathrm{R} = |\wp|^2 G^{(+)}(t,t') \;, \quad \langle\hat{\mathcal{F}}(t)\hat{\mathcal{F}}^\dagger(t')\rangle_\mathrm{R} = |\wp|^2 G^{(-)}(t,t') \;, \tag{5.55}$$

where

$$G^{(\pm)}(t,t') \equiv \frac{1}{\hbar^2}\sum_{kk'} \mathrm{e}^{\mp\mathrm{i}\omega(t-t')}\langle\tilde{\boldsymbol{\beta}}_k(t)\tilde{\boldsymbol{\beta}}_{k'}(t')\rangle_\mathrm{R} \;. \tag{5.56}$$

As in Sect. 4.3.2, we expand the reservoir correlation functions $\langle\tilde{\boldsymbol{\beta}}_k(t)\tilde{\boldsymbol{\beta}}_{k'}(t')\rangle_\mathrm{R}$ and use the correlation tensors of (4.29) to obtain

$$G^{(\pm)}(t,t') = \sum_k \frac{\boldsymbol{\epsilon}_k^2}{\hbar^2}\big[\big(1+\bar{n}(\omega_k)\big)\,\mathrm{e}^{-\mathrm{i}(\omega_k\pm\omega)(t-t')} + \bar{n}(\omega_k)\,\mathrm{e}^{\mathrm{i}(\omega_k\mp\omega)(t-t')}\big] \;. \tag{5.57}$$

Next, we replace the sum over modes k by the integral (5.10), and drop the terms oscillating with the sum frequencies $(\omega + \omega_k)$. Assuming that $\varrho(\omega_k)|g(\omega_k)|^2\bar{n}(\omega_k)$ and $\varrho(\omega_k)|g(\omega_k)|^2\big(1 + \bar{n}(\omega_k)\big)$ vary little in the vicinity of ω, we can evaluate these functions at $\omega_k = \omega$ according to

$$\begin{aligned} G^{(+)}(t,t')|\wp|^2 &= \int_0^\infty \mathrm{d}\omega_k\, \varrho(\omega_k)|g(\omega_k)|^2\bar{n}(\omega_k)\,\mathrm{e}^{\mathrm{i}(\omega_k-\omega)(t-t')} \\ &\simeq \varrho(\omega)|g(\omega)|^2\bar{n}(\omega)\int_0^\infty \mathrm{d}\omega_k\,\mathrm{e}^{\mathrm{i}(\omega_k-\omega)(t-t')} \;, \end{aligned} \tag{5.58a}$$

$$\begin{aligned} G^{(-)}(t,t')|\wp|^2 &= \int_0^\infty \mathrm{d}\omega_k\, \varrho(\omega_k)|g(\omega_k)|^2\big(1+\bar{n}(\omega_k)\big)\,\mathrm{e}^{-\mathrm{i}(\omega_k-\omega)(t-t')} \\ &\simeq \varrho(\omega)|g(\omega)|^2\big(1+\bar{n}(\omega)\big)\int_0^\infty \mathrm{d}\omega_k\,\mathrm{e}^{-\mathrm{i}(\omega_k-\omega)(t-t')} \;. \end{aligned} \tag{5.58b}$$

Since $\omega > 0$, the above integrals yield the δ-function,

$$\int_0^\infty \mathrm{d}\omega_k\,\mathrm{e}^{\pm\mathrm{i}(\omega_k-\omega)(t-t')} = \int_{-\infty}^\infty \mathrm{d}\omega'\,\mathrm{e}^{\pm\mathrm{i}\omega'(t-t')} = 2\pi\delta(t-t') \;,$$

and for the noise correlation functions we finally obtain

$$\langle \hat{\mathcal{F}}^\dagger(t)\hat{\mathcal{F}}(t')\rangle_{\rm R} = \kappa\bar{n}\delta(t-t') \,, \tag{5.59a}$$
$$\langle \hat{\mathcal{F}}(t)\hat{\mathcal{F}}^\dagger(t')\rangle_{\rm R} = \kappa(1+\bar{n})\delta(t-t') \,, \tag{5.59b}$$

where $\bar{n} \equiv \bar{n}(\omega)$ is the mean number of thermal photons at the frequency of the cavity mode. Integrating the noise correlation functions, we have

$$\kappa = \frac{1}{\bar{n}} \int_{-\infty}^{-\infty} {\rm d}t' \langle \hat{\mathcal{F}}^\dagger(t)\hat{\mathcal{F}}(t')\rangle_{\rm R} = \frac{1}{1+\bar{n}} \int_{-\infty}^{-\infty} {\rm d}t' \langle \hat{\mathcal{F}}(t)\hat{\mathcal{F}}^\dagger(t')\rangle_{\rm R} \,, \tag{5.60}$$

as required by the fluctuation–dissipation theorem.

Let us derive now the equation of motion for the cavity photon number operator $\mathcal{N} = a^\dagger a = \hat{a}^\dagger\,\hat{a}$. Using (5.53), we have

$$\frac{\rm d}{{\rm d}t}\mathcal{N} = \frac{{\rm d}\hat{a}^\dagger}{{\rm d}t}\hat{a} + \hat{a}^\dagger \frac{{\rm d}\hat{a}}{{\rm d}t} = -\kappa\mathcal{N} + \hat{\mathcal{F}}^\dagger\hat{a} + \hat{a}^\dagger\hat{\mathcal{F}} \,. \tag{5.61}$$

The formal solution of (5.53) is given by

$$\hat{a}(t) = \hat{a}(0)\,{\rm e}^{-\frac{1}{2}\kappa t} + \int_0^t {\rm d}t' \hat{\mathcal{F}}(t')\,{\rm e}^{-\frac{1}{2}\kappa(t-t')} \,, \tag{5.62}$$

and similarly for $\hat{a}^\dagger(t)$. We then obtain

$$\begin{aligned}\langle \hat{\mathcal{F}}^\dagger\hat{a}\rangle_{\rm R} + \langle \hat{a}^\dagger\hat{\mathcal{F}}\rangle_{\rm R} &= \big[\langle \hat{\mathcal{F}}^\dagger(t)\rangle_{\rm R}\hat{a}(0) + \hat{a}^\dagger(0)\langle \hat{\mathcal{F}}(t)\rangle_{\rm R}\big]{\rm e}^{-\frac{1}{2}\kappa t} \\ &+ \int_0^t {\rm d}t' \big[\langle \hat{\mathcal{F}}^\dagger(t)\hat{\mathcal{F}}(t')\rangle_{\rm R} + \langle \hat{\mathcal{F}}^\dagger(t')\hat{\mathcal{F}}(t)\rangle_{\rm R}\big]{\rm e}^{-\frac{1}{2}\kappa(t-t')} = \kappa\bar{n} \,,\end{aligned} \tag{5.63}$$

where we have used $\langle \hat{\mathcal{F}}(t)\rangle_{\rm R} = \langle \hat{\mathcal{F}}^\dagger(t)\rangle_{\rm R} = 0$ and the expressions for the noise correlations (5.59). We can therefore define the noise operator

$$\mathcal{F}_{\mathcal{N}}(t) \equiv \hat{\mathcal{F}}^\dagger\hat{a} + \hat{a}^\dagger\hat{\mathcal{F}} - \kappa\bar{n} \,, \tag{5.64}$$

having the conventional property $\langle \mathcal{F}_{\mathcal{N}}(t)\rangle_{\rm R} = 0$, with which (5.61) takes the form

$$\frac{\rm d}{{\rm d}t}\mathcal{N} = -\kappa\mathcal{N} + \kappa\bar{n} + \mathcal{F}_{\mathcal{N}}(t) \,. \tag{5.65}$$

Taking the expectation value of this equation, we obtain

$$\frac{\rm d}{{\rm d}t}\langle \mathcal{N}(t)\rangle = -\kappa\langle \mathcal{N}(t)\rangle + \kappa\bar{n} \,, \tag{5.66}$$

which is the same as in (5.17), as it should be.

Consider finally the two-time correlation function for the cavity field $\langle a^\dagger(t_1)\,a(t_2)\rangle$. For consistency in notation, we denote the time difference by $\tau = t_2 - t_1$ and take $t_1 = 0$. Using (5.62), we have

$$\langle \hat{a}^\dagger(0)\,\hat{a}(\tau)\rangle = \langle \hat{a}^\dagger(0)\,\hat{a}(0)\rangle{\rm e}^{-\frac{1}{2}\kappa\tau} + \int_0^\tau {\rm d}t' \langle \hat{a}^\dagger(0)\,\hat{\mathcal{F}}(t')\rangle\,{\rm e}^{-\frac{1}{2}\kappa(\tau-t')} \,. \tag{5.67}$$

Since $\langle \hat{a}^\dagger(0)\,\hat{\mathcal{F}}(t')\rangle = \langle \hat{a}^\dagger(0)\rangle\,\langle \hat{\mathcal{F}}(t')\rangle = 0$, the above equation yields

$$\langle a^\dagger(0)\,a(\tau)\rangle = \langle \mathcal{N}(0)\rangle\,\mathrm{e}^{-\mathrm{i}\omega\tau-\frac{1}{2}\kappa\tau}\ , \tag{5.68}$$

i.e., the field correlation function decays exponentially with time. With (2.61), the power spectrum of the field is then given by

$$\begin{aligned} S(z,\omega_k) &= \frac{\varepsilon_0 c}{2\pi}\,\mathrm{Re}\int_0^\infty \epsilon_\omega^2 \sin^2(kz)\langle a^\dagger(0)\,a(\tau)\rangle \mathrm{e}^{\mathrm{i}\omega_k\tau}\mathrm{d}\tau \\ &= \hbar\omega\langle\mathcal{N}\rangle\,\frac{c\sin^2(kz)}{2V}\,\varrho_c(\omega_k)\ , \end{aligned} \tag{5.69}$$

where

$$\varrho_c(\omega_k) \equiv \frac{1}{\pi}\,\frac{\kappa/2}{(\omega_k-\omega)^2+(\kappa/2)^2} \tag{5.70}$$

is the density of modes inside the damped cavity, which is a Lorentzian with half-width $\kappa/2$ centered around the frequency ω of the cavity eigenmode. In other words, the eigenmode under consideration has a finite bandwidth κ. Consequently, for the single-mode treatment of the cavity field to be a valid approximation, the spacing $\delta\omega$ between the cavity eigenmodes should be sufficiently larger than their widths, $\delta\omega > \kappa$.

5.2 Atom in a Damped Cavity

In the Jaynes–Cummings model of Sect. 3.3.2, an excited atom placed in an empty cavity undergoes periodic, reversible spontaneous decay. Stated otherwise, in the absence of dissipation, the two-level atom and the cavity mode coherently exchange a single excitation, the process often called vacuum Rabi oscillations. In fact, such a system has been realized to a very good approximation in experiments with microwave cavities interacting with Rydberg atoms, as discussed in Sect. 10.2. In the optical domain, however, the rate of energy dissipation, due to the atomic spontaneous decay Γ and the decay of the cavity field κ, is comparable to the atom–field coupling constant g, and therefore can not be neglected. The spontaneous decay of an atom in the open radiation field was discussed in Sect. 3.5 and throughout Chap. 4, while the cavity field relaxation due to the absorption and transmission losses of the cavity walls was the subject of the previous section. In the present section, we incorporate these decay mechanisms into the Jaynes–Cummings model and derive the resulting dynamics of the system under the initial conditions of an excited atom and vacuum cavity field.

Thus, we consider the interaction of a two-level atom with a single mode of a cavity, as shown in Fig. 5.1. The Hamiltonian of the system is given by that of the Jaynes–Cummings model in (3.57), which in the frame rotating with the cavity mode frequency ω can be written as

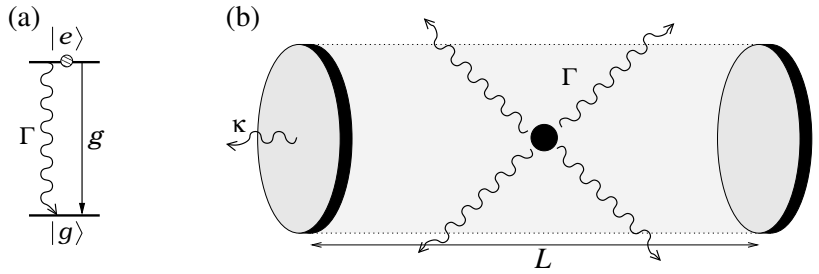

Fig. 5.1. Two-level atom in a cavity. (a) An excited atom decays with the rate Γ to the ground state and is coupled to a single-mode cavity field with the rate g. (b) The cavity mode is defined by a Fabry–Perot resonator of length L and decays with the rate κ.

$$\begin{aligned}\mathcal{H} &= \hbar\Delta\sigma_-\sigma_+ + \hbar g(\sigma_+ a + a^\dagger\sigma_-) \\ &= -\hbar\Delta\sigma_+\sigma_- + \hbar g(\sigma_+ a + a^\dagger\sigma_-)\,, \end{aligned} \tag{5.71}$$

where $\Delta = \omega - \omega_{eg}$ is the cavity field detuning from the atomic resonance frequency ω_{eg}. The two forms of the Hamiltonian are equivalent, differing only in the choice of the zero-point energy of the atom. The initial state of the compound system atom+cavity field is $|\Psi(0)\rangle = |e,0\rangle$, which is coupled by the above Hamiltonian to the state $|g,1\rangle$. If, as in Sect. 3.3.2, we disregard relaxation processes, we could determine the dynamics of the system by solving the Schrödinger equation (1.117) for the state vector

$$|\Psi(t)\rangle = c_{e,0}(t)\,|e,0\rangle + c_{g,1}(t)\,|g,1\rangle\,. \tag{5.72}$$

In the situation we consider here, however, both single excitation states $|e,0\rangle$ and $|g,1\rangle$ decay to the state $|g,0\rangle$, which is decoupled from the Hamiltonian (5.71): The decay of $|e,0\rangle$ is due to the atomic relaxation, while that of $|g,1\rangle$ is due to the cavity field relaxation.

As we know from the previous discussion, in free space the atom decays irreversibly to the ground state $|g\rangle$ with the emission of a spontaneous photon into a random direction within the 4π solid angle. When the atom is placed in a cavity, however, it interacts only with a subset of the free-space modes, as defined by the geometry of the cavity. Hence the spontaneous decay rate Γ of the excited atomic state $|e\rangle$ due to the photon emission into the continuum of free-space modes, excluding the cavity mode, is modified. In fact, with the remarkable progress in semiconductor technology, recently it has become possible to fabricate 2D and even 3D photonic–crystal nanocavities, wherein optically active quantum dots (sometimes called artificial atoms) do not see the free-space background, as a result of which one can have $\Gamma \to 0$. In turn, the total decay rate of the cavity field $\kappa = \kappa_{\rm abs} + \kappa_{\rm tr}$ is given by the sum of the absorption $\kappa_{\rm abs}$ and transmission $\kappa_{\rm tr}$ losses; for optical cavities the transmission losses usually dominate. It is customary to characterize such

cavities with the parameter $Q = \omega/\kappa$ called quality factor, which represents the number of oscillations of the cavity field during its relaxation time κ^{-1}.

At zero temperature, there are thus two relaxation channels, and the system described by the state vector (5.72) is not closed. Following the arguments of Sects. 4.2 and 5.1.2, we can then define an effective non-Hermitian Hamiltonian

$$\mathcal{H}_{\text{eff}} = H - \mathrm{i}\hbar\tfrac{1}{2}\Gamma\sigma_+\sigma_- - \mathrm{i}\hbar\tfrac{1}{2}\kappa a^\dagger a \,, \tag{5.73}$$

whose first term on the right-hand-side is the Hermitian Hamiltonian of (5.71), while the second and the third terms describe the atomic and photonic decays, respectively. Since both decay channels result in an irreversible loss of population from the single excitation states $|e,0\rangle$ and $|g,1\rangle$, we can propagate the state vector of the system $|\Psi(t)\rangle$ with the Schrödinger equation using the effective Hamiltonian (5.73), which yields the following differential equations,

$$\frac{\partial}{\partial t}c_{e,0} = -\tfrac{1}{2}\Gamma c_{e,0} - \mathrm{i}g c_{g,1} \,, \tag{5.74a}$$

$$\frac{\partial}{\partial t}c_{g,1} = -\big(\mathrm{i}\Delta + \tfrac{1}{2}\kappa\big)c_{g,1} - \mathrm{i}g c_{e,0} \,, \tag{5.74b}$$

with the initial conditions $c_{e,0}(0) = 1$ and $c_{g,1}(0) = 0$. These equations can be solved with the Laplace transform techniques employed in Sect. 3.3.1. Taking the Laplace transform of both sides of (5.74) we obtain the algebraic equations

$$sL_{e,0}(s) - 1 = -\tfrac{1}{2}\Gamma L_{e,0}(s) - \mathrm{i}g L_{g,1}(s) \,, \tag{5.75a}$$

$$sL_{g,1}(s) = -\big(\mathrm{i}\Delta + \tfrac{1}{2}\kappa\big)L_{g,1}(s) - \mathrm{i}g L_{e,0}(s) \,, \tag{5.75b}$$

whose solution is

$$L_{e,0}(s) = \frac{s + \mathrm{i}\Delta + \frac{1}{2}\kappa}{(s - s_+)(s - s_-)} \,, \quad L_{g,1}(s) = -\frac{\mathrm{i}g}{(s - s_+)(s - s_-)} \,, \tag{5.76}$$

with

$$s_\pm = -\frac{1}{2}\left[\frac{\kappa + \Gamma}{2} + \mathrm{i}\Delta \mp \sqrt{\left(\frac{\kappa - \Gamma}{2} + \mathrm{i}\Delta\right)^2 - 4g^2}\,\right] \,. \tag{5.77}$$

For simplicity, from now on we assume exact resonance, $\Delta = 0$, and consider two extreme cases of the atom–field coupling constant g being larger or smaller than the decay rates κ and Γ. Recall that in a standing-wave cavity the coupling $g(z_0) = -(\wp_{ge}\epsilon_\omega/\hbar)\sin(kz_0)$ is a function of the atomic position z_0.

In the strong coupling regime $g > \kappa, \Gamma$, the roots in (5.77) reduce to

$$s_\pm \simeq -\tfrac{1}{4}(\kappa + \Gamma) \pm \mathrm{i}g \,, \tag{5.78}$$

and the inverse Laplace transform of (5.76) gives

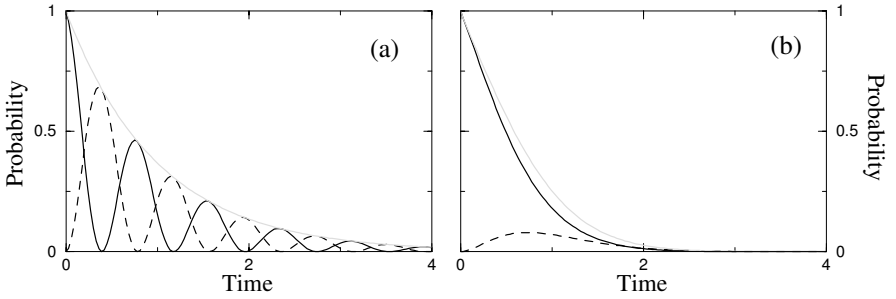

Fig. 5.2. Dynamics of a two-level atom undergoing spontaneous emission and coupled to a resonant ($\Delta = 0$) mode of a leaky cavity for (a) strong coupling regime, $g = 4\Gamma$, $\kappa = \Gamma$; and (b) weak coupling regime, $g = \Gamma$, $\kappa = 4\Gamma$. Solid lines: probability for the atom to be in the excited state, $|\langle e|\Psi(t)\rangle|^2 = |c_{e,0}(t)|^2$; Dashed lines: probability for the cavity mode to contain a single photon, $|\langle 1|\Psi(t)\rangle|^2 = |c_{g,1}(t)|^2$; Light-gray lines: square of the wavefunction norm $\langle\Psi(t)|\Psi(t)\rangle = |c_{e,0}(t)|^2 + |c_{g,1}(t)|^2$. Time is measured in units of Γ^{-1}.

$$c_{e,0}(t) = \mathrm{e}^{-\frac{1}{4}(\kappa+\Gamma)t}\left[\cos(gt) + \frac{\kappa-\Gamma}{4g}\sin(gt)\right]$$
$$\simeq \mathrm{e}^{-\frac{1}{4}(\kappa+\Gamma)t}\cos(gt)\ , \tag{5.79a}$$
$$c_{g,1}(t) = -\mathrm{i}\mathrm{e}^{-\frac{1}{4}(\kappa+\Gamma)t}\sin(gt)\ . \tag{5.79b}$$

In Fig. 5.2(a) we plot the time-dependence of probabilities for the atom to be in the excited state, $|\langle e|\Psi(t)\rangle|^2 = |c_{e,0}(t)|^2$, and for the cavity mode to contain a single photon, $|\langle 1|\Psi(t)\rangle|^2 = |c_{g,1}(t)|^2$. The system thus undergoes damped Rabi oscillations between the states $|e,0\rangle$ and $|g,1\rangle$, both of which decay with the respective rates Γ and κ to the state $|g,0\rangle$. The norm of the state vector $|\Psi(t)\rangle$ therefore decreases according to

$$\langle\Psi(t)|\Psi(t)\rangle = |c_{e,0}(t)|^2 + |c_{g,1}(t)|^2 \simeq \mathrm{e}^{-\frac{1}{2}(\kappa+\Gamma)t}\ , \tag{5.80}$$

i.e., it decays with the rate $\frac{1}{2}(\kappa+\Gamma)$

Consider now the case of weak coupling $g < \kappa$. In Fig. 5.2(b) we show the corresponding numerical solution of the amplitude equations (5.74). The system is in the overdamped regime in which no Rabi oscillations between the states $|e,0\rangle$ and $|g,1\rangle$ can be sustained. Simple analytical expressions for this case can be obtained in the limit of $g \ll \kappa$ ($\Gamma < \kappa$), in which the roots of (5.76) can be approximated as

$$s_+ \simeq -\tfrac{1}{2}\Gamma - \frac{2g^2}{\kappa-\Gamma}\ , \quad s_- \simeq -\tfrac{1}{2}\kappa\ . \tag{5.81}$$

The inverse Laplace transform of (5.76) then gives

$$c_{e,0}(t) = \mathrm{e}^{-\frac{1}{2}(\Gamma+\Gamma_c)t} \,, \tag{5.82a}$$

$$c_{g,1}(t) = \mathrm{i}\frac{2g(\kappa-\Gamma)}{(\kappa-\Gamma)^2-4g^2}\left[\mathrm{e}^{-\frac{1}{2}\kappa t} - \mathrm{e}^{-\frac{1}{2}(\Gamma+\Gamma_c)t}\right]$$

$$\simeq \mathrm{i}\frac{2g}{(\kappa-\Gamma)}\left[\mathrm{e}^{-\frac{1}{2}\kappa t} - \mathrm{e}^{-\frac{1}{2}(\Gamma+\Gamma_c)t}\right] \,, \tag{5.82b}$$

where

$$\Gamma_c = \frac{4g^2}{\kappa-\Gamma} \tag{5.83}$$

is the cavity contribution to the decay rate of the excited atom. Assuming that κ is much larger than Γ and expressing the spatially averaged value of g^2 through the free-space Γ given by (4.34), we obtain

$$\Gamma_c = 4\,\frac{\omega|\wp_{eg}|^2}{2\hbar\varepsilon_0 V}\,\frac{Q}{\omega} = \Gamma Q\left(\frac{6\pi}{Vk^3}\right) \,. \tag{5.84}$$

Thus the spontaneous emission rate of an atom placed in a resonant high-Q cavity can be substantially enhanced over its free-space value, as was first predicted by Purcell some 60 years ago. A simple and intuitive explanation of this effect can be given by considering the density of modes $\varrho(\omega_k)$ of the environment surrounding the atom. As we know from the previous discussion, the spontaneous decay rate can quite generally be expressed as

$$\Gamma = 2\pi\varrho(\omega_{eg})\langle|g(\omega_{eg})|^2\rangle_{\mathrm{sa}} \,, \tag{5.85}$$

where $\varrho(\omega_{eg})$ is the density of modes at the atomic resonance frequency ω_{eg}, and $|g(\omega_{eg})|^2 = |\wp_{eg}|^2\omega_{eg}/(2\hbar\varepsilon_0 V)$ is the atom–field couping strength, with $\langle\ldots\rangle_{\mathrm{sa}}$ denoting a spatial average. In free space, the density of modes is that of (2.30), while the angular average of the atomic dipole moment gives $\langle|\wp_{eg}|^2\rangle_{\mathrm{sa}} = \frac{1}{3}|\wp_{eg}|^2$. Then, from the above equation we obtain the spontaneous decay rate

$$\Gamma = \frac{\omega_{eg}^3|\wp_{eg}|^2}{3\pi\varepsilon_0\hbar c^3} \,,$$

which is the same as in (4.34). On the other hand, in a 1D cavity the density of modes around the eigenmode of frequency ω can be approximated as (see (5.70))

$$\varrho_c(\omega_k) = \frac{1}{\pi}\,\frac{\omega/2Q}{(\omega_k-\omega)^2+(\omega/2Q)^2} \,, \tag{5.86}$$

which for a resonant cavity $\omega = \omega_{eg}$ yields $\varrho_c(\omega_{eg}) = 2Q/(\pi\omega)$. In turn, the couping strength averaged over the atomic position z_0 is given by $|g(\omega_{eg})|^2 = |\wp_{eg}|^2\omega/(2\hbar\varepsilon_0 V)$, where $\wp_{eg}$ is the projection of the atomic dipole moment onto the polarization direction of the cavity mode. Equation (5.85) then yields

$$\Gamma_c = \frac{2Q|\wp_{eg}|^2}{\varepsilon_0\hbar V} \,,$$

which is the same as in (5.84). In the remainder of this chapter, we describe single-photon sources based on the cavity QED schemes closely related to the system studied here. Other cavity QED schemes for quantum information processing are discussed in Chap. 10.

5.3 Single Photons on Demand from Atom in a Cavity

In the previous section, we have seen that the spontaneous emission rate Γ_c of an atom placed in a damped cavity can be substantially enhanced over its free-space value Γ. The Purcell effect has been observed in experiments with atoms, molecules and more recently with semiconductor quantum dots (artificial atoms), placed in high-Q cavities. It results from the interplay between the atom–field coupling g and cavity field decay κ: Under the condition $\Gamma \lesssim g < \kappa$, the initially excited atom radiates a photon into the cavity mode which then quickly escapes from the cavity through partially transparent mirrors before it can be reabsorbed by the atom. If only one of the mirrors is partially transparent, with the other mirror completely reflective, the photon escaping through the transparent mirror forms a single-photon pulse propagating in a well-defined direction in space. In contrast, the spontaneous photon radiated by an excited atom in free space does not have any preferred direction of propagation. Therefore if the atom in the cavity can be excited easily to the state $|e\rangle$, it will realize an efficient source of single-photon pulses, which are required for optical quantum information processing and communication as discussed in Sect. 10.5.

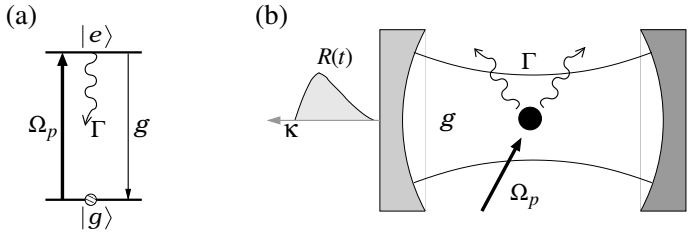

Fig. 5.3. Cavity QED single-photon source. (a) A two-level atom initially in the ground state $|g\rangle$ is excited by a pump field applied for time T such that $2\Omega_p T = \pi$ (π-pulse). (b) The excited atom emits into the cavity mode a single photon which leaves the cavity through the partially transmitting mirror with rate κ, forming a single-photon pulse with temporal shape $R(t)$.

Consider the compound system of atom + cavity field schematically shown in Fig. 5.3. Initially the atom is in the ground state $|g\rangle$ and the cavity mode is empty, $|0\rangle$. To excite the atom to the state $|e\rangle$, we can apply, from the side of the cavity, a strong classical pump field of frequency ω_p, which is resonant

with the atomic transition $|g\rangle \leftrightarrow |e\rangle$, i.e., $\omega_p = \omega_{eg}$. Denoting by Ω_p the Rabi frequency of the pump field and τ_p its duration, complete inversion of population can be achieved with a π-pulse, $2\Omega_p\tau_p = \pi$ (see (3.47)). The pulse duration τ_p should be much shorter than the excited state life-time Γ^{-1} and the inverse of the atom–cavity coupling rate g^{-1}, so that no appreciable loss of population from state $|e,0\rangle$ occurs during the preparation stage. We thus require $\Gamma, g \ll \tau_p^{-1} = 2\Omega_p/\pi$, which yields the following condition on the Rabi frequency of the pump pulse, $\Omega \gg \Gamma + g$. Once the atom is put to the excited state $|e\rangle$, it returns to the ground state $|g\rangle$ either via photon emission into the cavity mode, or via emission of a spontaneous photon into a random direction not constrained by the cavity geometry. In the latter case, no photon is added into the cavity mode, while in the former a photon is created in the cavity. Assuming that one of the cavity mirrors is partially transparent, this photon leaves the cavity with the rate $\kappa_{\rm tr}$, forming a single-photon pulse propagating in free space. The compound system is then restored to the initial state $|g,0\rangle$ and the whole process can be repeated again as many times as required.

Recall from Sect. 2.2.2, that the single-photon wavepacket (2.49) is characterized by the carrier frequency and envelope function whose Fourier transform determines the bandwidth of the wavepacket. Obviously, here the carrier frequency of the outgoing wavepacket is that of the cavity mode frequency ω, while its temporal shape is given by

$$R(t) \equiv |f(t)|^2 = \kappa_{\rm tr}|c_{g,1}(t)|^2 \,, \tag{5.87}$$

which replicates the shape of probability $|c_{g,1}(t)|^2$ for the cavity to contain a photon. During one cycle, the emission probability grows according to $P_{\rm emit}(t) = \int_{-\infty}^{t} R(t'){\rm d}t'$, and the total emission probability is just $P_{\rm emit}(\infty)$.

As an example, consider the atom–cavity system with the parameters of Fig. 5.2(b), namely $g = \Gamma$ and $\kappa_{\rm tr} \simeq 4\Gamma$ ($\kappa_{\rm abs} \ll \kappa_{\rm tr}$). Then the photon emission probability turns out to be $P_{\rm emit}(\infty) \simeq 0.4$, the main limiting factors for the efficient generation of single-photon pulses being the atomic spontaneous decay with the rate Γ and the photon absorption in the mirrors with the rate $\kappa_{\rm abs}$, which is negligible here. In the limit $\Gamma, \kappa_{\rm abs} \ll g \ll \kappa_{\rm tr}$, using (5.82b) we therefore have

$$R(t) = \frac{4g^2}{\kappa_{\rm tr}}\left[{\rm e}^{-\frac{1}{2}\kappa_{\rm tr}t} - {\rm e}^{-2g^2t/\kappa_{\rm tr}}\right]^2 \,, \tag{5.88}$$

which yields $P_{\rm emit}(\infty) \to 1$, i.e., ideal single-photon source. For optical transitions, however, Γ is large so that the above condition is difficult to satisfy in optical cavities, with the remarkable exception of solid-state photonic crystal nanocavities. Consequently, the efficiency, or reliability, of this directional single-photon source is typically smaller than 100%. In addition, one can not tailor the temporal shape $R(t)$ or the bandwidth of the pulse, which are determined solely by the parameters g and κ. Let us therefore describe a slightly different scheme which can provide, under realistic conditions, close to the ideal efficiency.

Single-Photon Pulses via Intracavity STIRAP

Consider a three-level atom with Λ configuration of levels as shown in Fig. 5.4. The atom interacts with the optical cavity on the transition $|g\rangle \leftrightarrow |e\rangle$ and with the classical field on the transition $|s\rangle \leftrightarrow |e\rangle$. We have already encountered in Sect. 3.6 a similar scheme with a three-level atom interacting with two classical fields in the Raman configuration. In the frame rotating with the frequencies of the pump field ω_p and cavity mode ω, the Hamiltonian of the system is given by

$$\mathcal{H} = -\hbar\big[\Delta_p\sigma_{ee} + (\Delta_p - \Delta)\sigma_{gg} + \Omega_p(\sigma_{se} + \sigma_{es}) - g(\sigma_{eg}a + a^\dagger\sigma_{ge})\big] \ , \quad (5.89)$$

where $\Delta_p = \omega_p - \omega_{es}$ is the pump field detuning from the atomic transition $|s\rangle \leftrightarrow |e\rangle$, and Ω_p is the corresponding Rabi frequency. We assume that the compound system is prepared initially in state $|s,0\rangle$, i.e., the atom is in state $|s\rangle$ and the cavity mode is empty, $|0\rangle$. Neglecting for the moment relaxation processes, the state vector of the system reads

$$|\Psi(t)\rangle = c_{s,0}(t)\,|s,0\rangle + c_{e,0}(t)\,|e,0\rangle + c_{g,1}(t)\,|g,1\rangle \ . \quad (5.90)$$

Then, under the Raman resonance condition $\Delta_p = \Delta$, the Hamiltonian (5.89) can be cast in the matrix form

$$\mathcal{H} = -\hbar \begin{bmatrix} 0 & \Omega_p & 0 \\ \Omega_p & \Delta & -g \\ 0 & -g & 0 \end{bmatrix} \ , \quad (5.91)$$

where the basis is $\{\,|s,0\rangle,\ |e,0\rangle,\ |g,1\rangle\}$. Recall from Sect. 3.6 that this Hamiltonian has a dark eigenstate

$$|D\rangle = \frac{1}{\sqrt{N_0}}[g\,|s,0\rangle + \Omega_p\,|g,1\rangle] \ , \quad (5.92)$$

with zero eigenvalue $\lambda_0 = 0$, and a pair of bright eigenstates

$$|B_\pm\rangle = \frac{1}{\sqrt{N_\pm}}[\Omega_p\,|s,0\rangle - \lambda_\pm\,|e,0\rangle - g\,|g,1\rangle] \ , \quad (5.93)$$

with corresponding eigenvalues $\lambda_\pm = -(\Delta/2) \pm \bar{\Omega}$ where $\bar{\Omega} = \sqrt{\Omega_p^2 + g^2 + (\Delta/2)^2}$. The normalization coefficients are $N_0 = g^2 + \Omega_p^2$ and $N_\pm = N_0 + \lambda_\pm^2$. For $\Omega_p = 0$, the dark state $|D\rangle$ coincides with the initial state $|s,0\rangle$, while in the limit $\Omega_p \gg g$ the dark state $|D\rangle$ approaches the desired state $|g,1\rangle$ containing a single photon in the cavity mode. Since $|D\rangle$ is not coupled to the state $|e,0\rangle$, it is immune to the atomic spontaneous decay from $|e\rangle$. Therefore, by adiabatically changing the pump field Rabi frequency from its initial value $\Omega_p(t_i) \ll g$ to some value $\Omega_p(t_f) > g$, we can expect that stimulated Raman adiabatic population transfer (STIRAP) between the initial $|e,0\rangle$ and the desired final $|g,1\rangle$ states will take place.

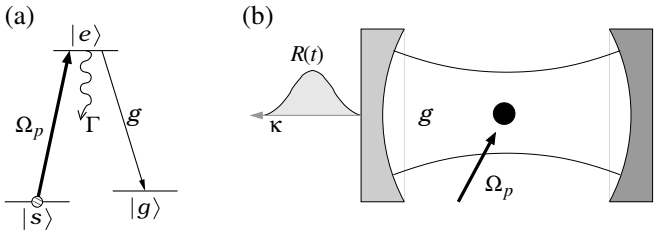

Fig. 5.4. Single-photon source via intracavity STIRAP. (a) A three-level atom is pumped by a classical field of Rabi frequency $\Omega_p(t)$ and is coupled to the cavity field with vacuum Rabi frequency g. (b) The compound system atom + cavity field initially in state $|s,0\rangle$ undergoes STIRAP transfer into the state $|g,1\rangle$ with a single photon in the cavity mode which escapes the cavity through a partially transmitting mirror with the rate κ, forming a single-photon wavepacket with temporal shape $R(t)$.

We need, however, to consider the effects of atomic and cavity field relaxation in more detail. Assuming that the lower atomic levels $|s\rangle$ and $|g\rangle$ are metastable (long-lived), the state $|e,0\rangle$ of the compound system decays via the atomic spontaneous emission with the rate Γ, while the state $|g,1\rangle$ decays due to the cavity-field relaxation with the rate κ. Thus, the eigenstates $|D\rangle$ and $|B_\pm\rangle$, whose energy separation $|\lambda_\pm - \lambda_0|$ is characterized by $\bar{\Omega}$, acquire certain widths determined by Γ and κ. As a result, the nonadiabatic coupling between the dark $|D\rangle$ and bright $|B_\pm\rangle$ eigenstates is small if they do not overlap, which requires that the condition $\bar{\Omega} > \Gamma + \kappa$ be satisfied at all times. Since the vacuum Rabi frequency g is constant, while $\Omega_p(t)$ is time-dependent, so that $\Omega_p(t_i) \ll g$ and $\Omega_p(t_f) > g$, at resonance $\Delta = 0$, the above requirement translates to the strong coupling condition $g > \Gamma, \kappa$. In addition, the adiabatic following condition (3.135) requires that $\Omega_p(t)$ changes sufficiently slowly for the condition $\max(\Omega_p)\,\tau_p \gg 1$, with τ_p being a characteristic raising time of $\Omega_p(t)$, to be satisfied.

To verify the possibility of intracavity STIRAP, we thus have to solve the Liouville equation for the density matrix ρ of the compound system,

$$\frac{\partial}{\partial t}\rho = -\frac{\mathrm{i}}{\hbar}[\mathcal{H},\rho] + \mathcal{L}_{\mathrm{at}}\rho + \mathcal{L}_{\mathrm{cav}}\rho\,, \tag{5.94}$$

where $\mathcal{H}$ is the Hamiltonian of (5.89), while $\mathcal{L}_{\mathrm{at}}\rho$ and $\mathcal{L}_{\mathrm{cav}}\rho$ describe, respectively, the atomic and cavity mode relaxations. The cavity Liouvillian $\mathcal{L}_{\mathrm{cav}}\rho$ is that of (5.15), and the atomic Liouvillian $\mathcal{L}_{\mathrm{at}}\rho$ is given by

$$\begin{aligned}\mathcal{L}_{\mathrm{at}}\rho &= \sum_l \tfrac{1}{2}\Gamma_{el}\big(2\,\sigma_{le}\rho\,\sigma_{el} - \sigma_{ee}\rho - \rho\,\sigma_{ee}\big)\\ &= \sum_l \Gamma_{el}\,\sigma_{le}\rho\,\sigma_{el} - \tfrac{1}{2}\Gamma\big(\sigma_{ee}\rho + \rho\,\sigma_{ee}\big)\,,\end{aligned} \tag{5.95}$$

where the index $l = s, g, \ldots$ runs over all the lower levels of the atom to which the upper level $|e\rangle$ can decay. Hence, Γ_{es} and Γ_{eg} represent the spontaneous decay rates from $|e\rangle$ to levels $|s\rangle$ and $|g\rangle$, respectively, while $\Gamma = \sum_l \Gamma_{el}$ is the total decay rate of $|e\rangle$. For the initial state $|s, 0\rangle$, the Hamiltonian $\mathcal{H}$ acts in the Hilbert space $\mathbb{H} = \{|s, 0\rangle, |e, 0\rangle, |g, 1\rangle\}$. Then the decay of the cavity field takes the system outside of space $\mathbb{H}$, to state $|g, 0\rangle \notin \mathbb{H}$. On the other hand, the decay of state $|e, 0\rangle$ due to the atomic relaxation can take the system to one of the states $|s, 0\rangle$, $|g, 0\rangle$ or $|l, 0\rangle$, where $|l\rangle$ denotes any lower atomic state other than $|g\rangle$ or $|s\rangle$. The states $|g, 0\rangle$ and $|l, 0\rangle$ are not in space $\mathbb{H}$, while $|s, 0\rangle \in \mathbb{H}$. This necessitates our use of the density matrix approach, since with the amplitude equations we could not properly take into account the decay channel $|e, 0\rangle \to |s, 0\rangle$.

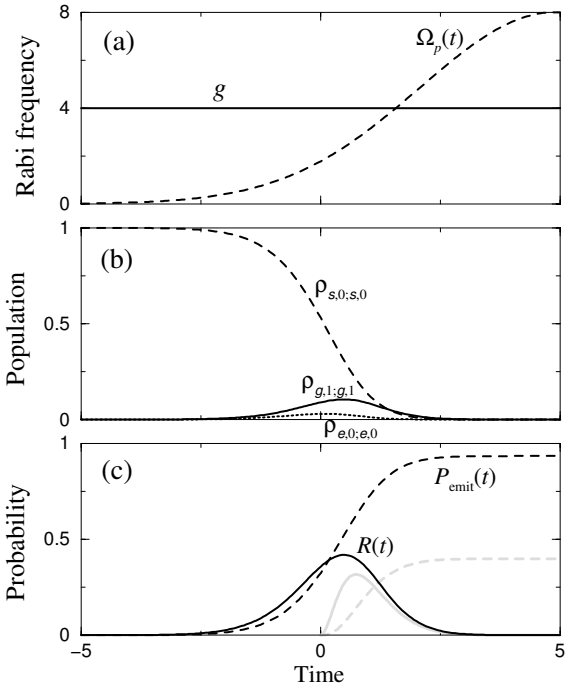

Fig. 5.5. Dynamics of the intracavity STIRAP with $g = \kappa = 4\Gamma$. (a) Rabi frequencies g and $\Omega_p(t)$; (b) populations $\rho_{s,0;s,0}(t)$, $\rho_{e,0;e,0}(t)$ and $\rho_{g,1;g,1}(t)$; and (c) emission rate $R(t)$ and probability $P_{\rm emit}(t)$. The light-gray curves in (c) correspond to $R(t)$ and $P_{\rm emit}(t)$ for an initially excited two-level atom with the parameters of Fig. 5.2, i.e., $g = \Gamma$ and $\kappa = 4\Gamma$. Time is measured in units of Γ^{-1}.

In Fig. 5.5, we plot the results of the numerical solution of the equations for all the relevant elements of the density matrix ρ (see Prob. 5.6). We find that, when the strong coupling condition is not quite satisfied, during the

evolution the intermediate excited state $|e,0\rangle$ acquires small but finite population $\rho_{e,0;e,0}$, which is due to nonadiabatic transitions. On the other hand, assuming the absorption in the cavity mirrors to be negligible, $\kappa_{\rm abs} \ll \kappa_{\rm tr} \simeq \kappa$, the probability $\rho_{g,1;g,1}$ of the single-photon state $|g,1\rangle$ decays due to the leakage of the cavity field through the partially transparent mirror, the outgoing photon pulse having the temporal shape $R(t) = \kappa_{\rm tr}\rho_{g,1;g,1}(t)$. Yet, for the parameters of Fig. 5.5, at the end of the process the photon emission probability $P_{\rm emit}(t_f)$ attains the value 0.93, which is close to the ideal. When we take $g = 8\Gamma$, with the other parameters unchanged, so as to better satisfy the strong coupling condition, we obtain completely adiabatic evolution of the system with negligible population of the excited state $|e,0\rangle$, achieving $P_{\rm emit}(t_f) \gtrsim 0.98$.

Under these conditions, using simple arguments, we can derive an analytic expression for the shape of the outgoing single-photon pulse $R(t)$. As the system adiabatically follows the dark state $|D(t)\rangle$ of (5.92), we expect that at any time $t \in [t_i, t_f]$ the ratio of populations of states $|s,0\rangle$ and $|g,1\rangle$ is given by

$$\frac{\rho_{s,0;s,0}(t)}{\rho_{g,1;g,1}(t)} = \cot^2\Theta(t)\ , \tag{5.96}$$

where the mixing angle $\Theta(t)$ is defined through $\cot\Theta(t) = g/\Omega_p(t)$. Next, since under adiabatic evolution, the excited state $|e,0\rangle$ is never significantly populated, the sum of populations of the initial $|s,0\rangle$ and final $|g,1\rangle$ states decays only via the cavity field relaxation,

$$\frac{\partial}{\partial t}\big[\rho_{s,0;s,0}(t) + \rho_{g,1;g,1}(t)\big] = -\kappa\rho_{g,1;g,1}(t)\ . \tag{5.97}$$

Using (5.96) with $\Omega_p(t) \neq 0$ for $t \in [t_i, t_f]$, one can now derive the rate equation for the population of state $|g,1\rangle$ (see Prob. 5.7), whose solution is

$$\rho_{g,1;g,1}(t) = \rho_{g,1;g,1}(t_i)\exp\left[-\int_{t_i}^{t} {\rm d}t' \frac{\kappa + \partial_{t'}\cot^2\Theta(t')}{1+\cot^2\Theta(t')}\right]\ . \tag{5.98}$$

At the initial time t_i, we assume that $g \gg \Omega_p(t_i) \neq 0$, and $\rho_{s,0;s,0}(t_i) = 1$. From (5.96) we then have $\rho_{g,1;g,1}(t_i) = \tan^2\Theta(t_i)$, which should be used in the above solution. It turns out that under the strong coupling condition $g > \kappa, \Gamma$, the analytic solution (5.98) is practically indistinguishable from the exact numerical solution of the full set of density matrix equations. This confirms the validity of the adiabatic approximation that led to our starting equations (5.96) and (5.97).

We can now write the expression for the pulse shape in the explicit form

$$R(t) = \kappa_{\rm tr}\frac{\Omega_p^2(t_i)}{g^2}\ \exp\left[\int_{t_i}^{t} {\rm d}t' \frac{2g^2\frac{\partial_{t'}\Omega_p(t')}{\Omega_p(t')} - \kappa\Omega_p^2(t')}{g^2+\Omega_p^2(t')}\right]\ , \tag{5.99}$$

which shows that, by carefully changing the pump field Rabi frequency $\Omega_p(t)$, and thereby the mixing angle $\Theta(t)$, we can manipulate at will the temporal characteristics of the outgoing pulse. In particular, we can fully control the timing and the temporal shape, or the bandwidth, of the single-photon pulse. Once the photon has left the cavity, we may recycle the system by switching off the pump field and preparing the atom in the initial state $|s\rangle$. We could then repeat the process to generate another photon with precise timing and pulse shape. This system can thus serve as a deterministic and efficient source of tailored single-photon pulses.

Problems

5.1. Verify the derivation of equations (5.11)–(5.14).

5.2. Using the master equation for the cavity field (5.14), derive the equations of motion for the expectation values of the field amplitude (5.16) and mean photon number (5.17).

5.3. A single-mode electromagnetic field (F) is coupled to a two-level system (atom A) through the master equation

$$\frac{\partial}{\partial t}\rho^{\mathrm{F}} = g\rho_{gg}^{\mathrm{A}}\left(2a\rho^{\mathrm{F}}a^{\dagger} - a^{\dagger}a\rho^{\mathrm{F}} - \rho^{\mathrm{F}}a^{\dagger}a\right) + g\rho_{ee}^{\mathrm{A}}\left(2a^{\dagger}\rho^{\mathrm{F}}a - aa^{\dagger}\rho^{\mathrm{F}} - \rho^{\mathrm{F}}aa^{\dagger}\right), \tag{5.100}$$

where g is the coupling constant, and ρ_{gg}^{A} and ρ_{ee}^{A} are the populations of the lower and upper levels of the two-level system, respectively. Assume that ρ_{gg}^{A} and ρ_{ee}^{A} are kept constant. Derive differential equations governing the evolution of the expectation values $\langle a\rangle$ and $\langle a^{\dagger}a\rangle$ and solve them.

5.4. An electromagnetic field consisting of two modes 1 and 2 is coupled to a two-level system through the master equation

$$\begin{aligned}\frac{\partial}{\partial t}\rho^{\mathrm{F}} = {} & g\rho_{gg}^{\mathrm{A}}\left(2a_1a_2\rho^{\mathrm{F}}a_1^{\dagger}a_2^{\dagger} - a_1^{\dagger}a_2^{\dagger}a_1a_2\rho^{\mathrm{F}} - \rho^{\mathrm{F}}a_1^{\dagger}a_2^{\dagger}a_1a_2\right) \\ & + g\rho_{ee}^{\mathrm{A}}\left(2a_1^{\dagger}a_2^{\dagger}\rho^{\mathrm{F}}a_1a_2 - a_1a_2a_1^{\dagger}a_2^{\dagger}\rho^{\mathrm{F}} - \rho^{\mathrm{F}}a_1a_2a_1^{\dagger}a_2^{\dagger}\right), \end{aligned} \tag{5.101}$$

where g is the effective coupling constant, a_j and $a_j^{\dagger}$ are creation and annihilation operators of the field mode $j = 1, 2$, and ρ_{gg}^{A} and ρ_{ee}^{A} are the populations of the lower and upper levels of the two-level system, respectively. Assume that ρ_{gg}^{A} and ρ_{ee}^{A} are kept constant.

(a) Derive differential equations that govern the evolution of the expectation values $\langle a_j\rangle$ and $\langle a_j^{\dagger}a_j\rangle$ and discuss their solvability.

(b) Perform the factorization of modes, i.e., take $\rho^{\mathrm{F}} \to \rho^{(1)} \otimes \rho^{(2)}$, and solve the resulting equations for the expectation values $\langle a_j\rangle$ and $\langle a_j^{\dagger}a_j\rangle$.

(c) Obtain differential equations for $\langle a_j^\dagger a_j \rangle$ without factorization, but for $\rho_{ee}^{\mathrm{A}} = 0$ and discuss their meaning.

5.5. Verify that $P(\alpha, t)$ given by (5.42) is the solution of the Fokker–Planck equation (5.40).

5.6. Using (5.94), derive the equations for all the elements of density matrix ρ in the basis $\{ |s,0\rangle, |g,0\rangle, |l,0\rangle, |e,0\rangle, |g,1\rangle \}$.

5.7. Using (5.96) and (5.97), derive the rate equation for population $\rho_{g,1;g,1}(t)$ and its solution (5.98).

6

Field Propagation in Atomic Media

In this chapter, we consider several illustrative examples of weak field propagation in atomic media. We derive the coupled evolution equations for the field and the atoms, which in general should be solved self consistently. Physically, depending on the amplitude and the pulse shape, the field interacts with the atoms in a certain linear or nonlinear way, which in turn influence the evolution of the field upon propagating in the medium. Thus the subject of this chapter contains elements of both quantum and nonlinear optics. Since in quantum information applications one typically considers weak quantum fields, such as single-photon or weak coherent pulses, our discussion will focus mainly on weak field propagation and interaction with optically dense atomic ensembles.

6.1 Propagation Equation for Slowly Varying Electric Field

In Chap. 3 we have seen that, when considering the interaction of an atom with a radiation field whose wavelength is large compared to the size of the atom, such as optical or microwave field, the dipole approximation gives the dominant contribution to the atom–field coupling. The resulting interaction Hamiltonian (3.30) is given by the scalar product of the atomic dipole moment and the electric field. We thus begin with the derivation of the propagation equation for the electric field, whose envelope varies slowly in space and time as compared to its wavelength and oscillation period, respectively.

The Maxwell equations in a macroscopic medium are given by (2.1). In a dielectric medium with no magnetization, the densities of currents $\boldsymbol{J}$ and free charges σ are zero, the magnetic field is $\boldsymbol{B} = \mu_0 \boldsymbol{H}$ while the displacement electric field is given by $\boldsymbol{D} = \varepsilon \boldsymbol{E} + \boldsymbol{P}$, where the permittivity ε may contain the contribution of a passive host material, if any, and $\boldsymbol{P}$ is the macroscopic polarization of the active medium. In what follows, we will be concerned with the situation in which the medium is represented by near-resonant atoms

whose response determines the polarization $\boldsymbol{P}$ and assume $\varepsilon = \varepsilon_0$. Taking the curl of (2.1a), exchanging the order of differentiation $\boldsymbol{\nabla} \times (\partial_t \boldsymbol{B}) = \partial_t (\boldsymbol{\nabla} \times \boldsymbol{B})$, and using (2.1b) together with the expressions for $\boldsymbol{B}$ and $\boldsymbol{D}$ above, we obtain

$$\boldsymbol{\nabla} \times (\boldsymbol{\nabla} \times \boldsymbol{E}) + \mu_0 \varepsilon_0 \frac{\partial^2 \boldsymbol{E}}{\partial t^2} = -\mu_0 \frac{\partial^2 \boldsymbol{P}}{\partial t^2} \ . \tag{6.1}$$

Using the vector identity $\boldsymbol{\nabla} \times \boldsymbol{\nabla} \times \boldsymbol{E} = \boldsymbol{\nabla}(\boldsymbol{\nabla} \cdot \boldsymbol{E}) - \nabla^2 \boldsymbol{E}$ and assuming that the electric field varies slowly in the plane transverse to the propagation direction, $\boldsymbol{\nabla} \cdot \boldsymbol{E} \simeq 0$, we arrive at the wave equation

$$\nabla^2 \boldsymbol{E} - \frac{1}{c^2} \frac{\partial^2 \boldsymbol{E}}{\partial t^2} = \mu_0 \frac{\partial^2 \boldsymbol{P}}{\partial t^2} \ . \tag{6.2}$$

As is typical in optics, we consider a unidirectional propagation of the field along the z axis, in which case the electric field and the induced polarization vectors can be expressed as

$$\boldsymbol{E}(\boldsymbol{r}, t) = \hat{\boldsymbol{e}} E(z, t) \ , \quad \boldsymbol{P}(\boldsymbol{r}, t) = \hat{\boldsymbol{e}} P(z, t) \ , \tag{6.3}$$

where $\hat{\boldsymbol{e}}$ is the unit polarization vector normal to the field propagation direction. The wave equation (6.2) then reduces to the 1D equation

$$\frac{\partial^2 E}{\partial z^2} - \frac{1}{c^2} \frac{\partial^2 E}{\partial t^2} = \mu_0 \frac{\partial^2 P}{\partial t^2} \ . \tag{6.4}$$

Let us now consider a classical quasi-monochromatic electric field with carrier frequency ω and wavevector $k = \omega/c$,

$$E(z, t) = \mathcal{E}(z, t) \mathrm{e}^{\mathrm{i}(kz - \omega t)} + \mathcal{E}^*(z, t) \mathrm{e}^{-\mathrm{i}(kz - \omega t)} \ , \tag{6.5}$$

where $\mathcal{E}(z, t)$ is a slowly varying in time and space envelope of the field, which in general is a complex function, $\mathcal{E} = \overline{\mathcal{E}} \mathrm{e}^{\mathrm{i}\varphi}$ with $\overline{\mathcal{E}}$ the real amplitude and φ the phase. This field induces the medium polarization

$$P(z, t) = \mathcal{P}(z, t) \mathrm{e}^{\mathrm{i}(kz - \omega t)} + \mathcal{P}^*(z, t) \mathrm{e}^{-\mathrm{i}(kz - \omega t)} \ , \tag{6.6}$$

where again $\mathcal{P}(z, t)$ is a slowly varying in time and space complex function, $\mathcal{P} = \overline{\mathcal{P}} \mathrm{e}^{\mathrm{i}\varphi}$. Substituting (6.5) and (6.6) into the 1D wave equation (6.4), and adopting the slowly varying envelope approximation,

$$\left| \frac{\partial \overline{\mathcal{E}}}{\partial t} \right| \ll \omega |\overline{\mathcal{E}}| \ , \quad \left| \frac{\partial \overline{\mathcal{E}}}{\partial z} \right| \ll k |\overline{\mathcal{E}}| \ , \quad \left| \frac{\partial \varphi}{\partial t} \right| \ll \omega \ , \quad \left| \frac{\partial \varphi}{\partial z} \right| \ll k \tag{6.7a}$$

$$\left| \frac{\partial \overline{\mathcal{P}}}{\partial t} \right| \ll \omega |\overline{\mathcal{P}}| \ , \quad \left| \frac{\partial \overline{\mathcal{P}}}{\partial z} \right| \ll k |\overline{\mathcal{P}}| \ , \tag{6.7b}$$

which amounts to assuming that the field variation is small on the scale of both the optical period ω^{-1} and the wavelength k^{-1}, we obtain the following propagation equation

$$\frac{\partial \mathcal{E}}{\partial z} + \frac{1}{c}\frac{\partial \mathcal{E}}{\partial t} = \mathrm{i}\frac{k}{2\varepsilon_0}\mathcal{P} \,. \tag{6.8}$$

In terms of real quantities, this equation reads

$$\left(\frac{\partial}{\partial z} + \frac{1}{c}\frac{\partial}{\partial t}\right)\overline{\mathcal{E}} = -\frac{k}{2\varepsilon_0}\mathrm{Im}\overline{\mathcal{P}} \,, \quad \overline{\mathcal{E}}\left(\frac{\partial}{\partial z} + \frac{1}{c}\frac{\partial}{\partial t}\right)\varphi = \frac{k}{2\varepsilon_0}\mathrm{Re}\overline{\mathcal{P}} \,. \tag{6.9}$$

In many problems of quantum and nonlinear optics involving the propagation of slowly varying optical fields in near-resonant media, equations (6.8) or (6.9) constitute the starting point of the discussion. In the following sections of this chapter, we discuss several aspects of weak pulse propagation in two and three-level atomic media.

In the remainder of this section, we outline a very useful in optics formalism of susceptibilities through which the polarization of the medium can be related to the applied field. In general, the induced polarization can be a very complicated nonlinear function of the field. Here, however, we will be interested in the case of weak field propagation in an isotropic medium, for which, to a good approximation, the polarization is a linear function of the field,

$$P(z,t) = \varepsilon_0 \int_{-\infty}^{\infty} \chi(t')E(z,t-t')\mathrm{d}t' \,, \tag{6.10}$$

where $\chi(t)$ is the linear susceptibility. For a monochromatic probe field of frequency ω, substituting $E(z,t) = \mathcal{E}(\omega)\mathrm{e}^{\mathrm{i}(kz-\omega t)} + \text{c.c.}$ into (6.10) and comparing the result with (6.6) we obtain the familiar relation

$$\mathcal{P} = \varepsilon_0 \chi(\omega)\mathcal{E}(\omega) \,, \tag{6.11}$$

where $\chi(\omega)$ is the Fourier transform of $\chi(t')$, $\chi(\omega) = \int \chi(t')\mathrm{e}^{\mathrm{i}\omega t'}\mathrm{d}t'$. Substituting this into (6.8) and taking into account that by definition $\mathcal{E}$ is time-independent, we have

$$\frac{\partial \mathcal{E}}{\partial z} = \mathrm{i}\frac{k}{2}\chi(\omega)\mathcal{E} \,, \tag{6.12}$$

with the solution

$$\mathcal{E}(z) = \mathcal{E}(0)\,\mathrm{e}^{\mathrm{i}\varphi(z)}\mathrm{e}^{-az} \,, \tag{6.13}$$

where $\varphi(z) = \frac{1}{2}k\,\mathrm{Re}\chi(\omega)z$ is the phase shift and $a \equiv \frac{1}{2}k\,\mathrm{Im}\chi(\omega)$ is the linear amplitude attenuation (for $a \geq 0$) coefficient. Thus, the real and imaginary parts of the linear susceptibility $\chi(\omega)$ describe, respectively, the dispersive and absorptive properties of the medium. Upon propagation in the medium, the intensity of the field $I = \frac{\varepsilon_0 c}{2}|E|^2$ is attenuated according to $I(z) = I(0)\,\mathrm{e}^{-2az}$ which is known as Beer's law of absorption.

We have just seen that when a is positive the amplitude and the intensity of the field are attenuated in the medium. It is possible though that a is negative, meaning that the absorption is replaced by amplification. Clearly, if such a situation is realized, the energy of the field will increase at the expense of energy stored in the medium. This in turn means that there should

be some mechanism in place that will pump the energy into the medium, which is in fact what happens in lasers. This pumping mechanism can provide the energy into the system with a certain rate, however high but bound. On the other hand, if the linear regime discussed above were valid for arbitrary propagation distances, the intensity of the field, or its energy for that matter, would grow exponentially and become arbitrarily large for sufficiently long distances. This of course can not happen in any realistic situation, as saturation effects will come into play once certain intensity of the propagating field is reached. Therefore, while the linear regime can adequately describe many practical situations involving field attenuation (or energy absorption) in the medium, rigorous treatment of amplification problems will necessarily require the consideration of the nonlinear response of the system which will certainly include the saturation.

Consider now a quasi-monochromatic electric field with the carrier frequency ω as in (6.5). We can express the envelope function $\mathcal{E}(t)$ quite generally through the Fourier integral

$$\mathcal{E}(t) = \int \mathcal{E}(\omega+\nu)\mathrm{e}^{-\mathrm{i}\nu t}\mathrm{d}\nu \,, \tag{6.14}$$

where $\mathcal{E}(\omega+\nu)$ is the amplitude of the frequency component $(\omega+\nu)$ of the probe field. The corresponding expression for the polarization is

$$\mathcal{P}(t) = \varepsilon_0 \int \chi(\omega+\nu)\mathcal{E}(\omega+\nu)\mathrm{e}^{-\mathrm{i}\nu t}\mathrm{d}\nu \,. \tag{6.15}$$

Assuming the susceptibility is a smooth function of frequency in the vicinity of ω, to first order in ν it is given by

$$\chi(\omega+\nu) \simeq \chi(\omega) + \frac{\partial\chi(\omega)}{\partial\omega}\nu + O(\nu^2) \,,$$

which after the substitution into (6.15) yields

$$\mathcal{P}(t) = \varepsilon_0\chi(\omega)\mathcal{E}(t) + \mathrm{i}\varepsilon_0\frac{\partial\chi(\omega)}{\partial\omega}\frac{\partial\mathcal{E}(t)}{\partial t} + \dots \,, \tag{6.16}$$

where we have used (6.14) and the resulting from it relation $\int \nu\mathcal{E}(\omega+\nu)\mathrm{e}^{-\mathrm{i}\nu t}\mathrm{d}\nu = \mathrm{i}\partial_t\mathcal{E}(t)$. With the polarization expressed as in (6.16), the propagation equation (6.8) becomes

$$\frac{\partial\mathcal{E}}{\partial z} + \frac{1}{v_g}\frac{\partial\mathcal{E}}{\partial t} = \mathrm{i}\frac{k}{2}\chi(\omega)\mathcal{E} \,, \tag{6.17}$$

where the group velocity v_g is given by

$$v_g = \left[\frac{1}{c} + \frac{k}{2}\frac{\partial\chi}{\partial\omega}\right]^{-1} = \frac{c}{1+\frac{\omega}{2}\frac{\partial\chi}{\partial\omega}} \,. \tag{6.18}$$

As will be seen shortly, v_g is equal to the velocity with which the peak of the probe pulse propagates in the medium. If in (6.16) we kept terms of higher order in ν, on the right-hand-side of (6.17) we would have had terms containing the second and higher derivatives of $\mathcal{E}$, such as $\frac{\partial^2\chi}{\partial\omega^2}\frac{\partial^2\mathcal{E}}{\partial t^2}$ known as the group velocity dispersion, which determine the pulse distortion. On the other hand, in the frequency region where $\chi(\omega)$ is approximately a linear function of ω, these terms vanish and the pulse whose Fourier bandwidth lies within this frequency region propagates in the medium without much distortion of its shape.

To solve the propagation equation (6.8), we introduce new variables $\zeta = z$ and $\tau = t - z/v_g$. Obviously, the old variables z and t are expressed through the new ones as $z = \zeta$ and $t = \tau + \zeta/v_g$ and we have

$$\frac{\partial}{\partial\zeta} = \frac{\partial z}{\partial\zeta}\frac{\partial}{\partial z} + \frac{\partial t}{\partial\zeta}\frac{\partial}{\partial t} = \frac{\partial}{\partial z} + \frac{1}{v_g}\frac{\partial}{\partial t} .$$

In terms of the new variables, (6.17) can be written as

$$\frac{\partial}{\partial\zeta}\mathcal{E}(\zeta) = \mathrm{i}\frac{k}{2}\chi\mathcal{E}(\zeta) , \tag{6.19}$$

where $\mathcal{E}(\zeta) \equiv \mathcal{E}(\zeta, \tau+\zeta/v_g)$. Its solution is $\mathcal{E}(\zeta) = \mathcal{E}(0)\exp[\frac{\mathrm{i}}{2}k\chi\zeta]$, from which we easily obtain

$$\mathcal{E}(z,t) = \mathcal{E}(0,\tau)\,\mathrm{e}^{\mathrm{i}\varphi(z)}\mathrm{e}^{-az} , \tag{6.20}$$

where the phase shift φ and absorption coefficient a are the same as in (6.13). This equation indicates that, given the boundary condition for the field at $z = 0$ and all times t', $\mathcal{E}(0,t')$, inside the medium, at coordinate $z \geq 0$ and time t, the envelope of the pulse is related to that at $z = 0$ but an earlier time $t' = \tau = t - z/v_g$ (for $v_g > 0$) which is called the retarded time. In addition, the field undergoes a phase shift and absorption with the propagation distance z as per (6.20).

What if instead of the boundary value problem, i.e., given the probe field envelope $\mathcal{E}$ at $z = 0$, we need to solve the initial value problem, meaning we know the field at time $t = 0$ for all z', $\mathcal{E}(z',0)$? Similarly to the above, we can introduce another set of variables $\zeta = z - v_g t$ and $\tau = t$, in terms of which (6.17) becomes

$$\frac{\partial}{\partial\tau}\mathcal{E}(\tau) = \mathrm{i}\frac{k}{2}\chi v_g\mathcal{E}(\tau) , \tag{6.21}$$

with the solution $\mathcal{E}(\tau) = \mathcal{E}(0)\exp[\frac{\mathrm{i}}{2}k\chi v_g\tau]$, where $\mathcal{E}(\tau) \equiv \mathcal{E}(\zeta + v_g\tau, \tau)$. Returning back to the old variables t and z, we have

$$\mathcal{E}(z,t) = \mathcal{E}(\zeta,0)\,\mathrm{e}^{\mathrm{i}\varphi(v_g t)}\mathrm{e}^{-av_g t} . \tag{6.22}$$

Thus inside the medium, at coordinate z and time $t > 0$, the envelope of the pulse is related to that at the initial time $t = 0$ but at a retarded point in

space $z' = \zeta = z - v_g t$. The phase-shift and absorption are now functions of time. Note that the physical equivalence of solutions (6.20) and (6.22) stems from the mathematical equivalence of the expansions of $\mathcal{E}(0, t - z/v_g)$ and $\mathcal{E}(z - v_g t, 0)$ is terms of temporal and spatial eigenmodes, respectively,

$$\begin{aligned}\mathcal{E}(0, t - z/v_g) &= \sum_\nu \mathcal{E}(\nu) \mathrm{e}^{-\mathrm{i}\nu(t - z/v_g)} = \sum_\nu \mathcal{E}(\nu) \mathrm{e}^{\mathrm{i}\nu/v_g (z - v_g t)} \\ &= \sum_q \mathcal{E}(q) \mathrm{e}^{\mathrm{i}q(z - v_g t)} = \mathcal{E}(z - v_g t, 0) \; . \end{aligned} \tag{6.23}$$

In the discussion above, we have tacitly assumed that $\frac{\partial \chi(\omega)}{\partial \omega} \geq 0$, which means that the group velocity of (6.18) can take values $0 \leq v_g \leq c$. It is possible, however, that the derivative of the medium susceptibility with respect to the frequency of the applied field is negative. Then the group velocity may exceed the speed of light or even become negative. Considering such a medium of finite length L, the group velocity exceeding c means that the peak of the pulse appears at the exit from the medium at a time $t = L/v_g$ which is shorter than the time L/c that the light pulse needs to propagate the distance L in free space. Even more dramatic is the case of the negative group velocity, for which the peak of the pulse appears at the exit from the medium even before the peak of the incident pulse enters the medium at $z = 0$. These observations are however not as mysterious as they may seem, if one realizes that such a "superluminal" pulse propagation is possible only in amplifying media, because in conventional atomic media the anomalous dispersion $\frac{\partial \chi(\omega)}{\partial \omega} < 0$ around the atomic resonance frequency is accompanied by a strong absorption of the pulse, as discussed in the following section. In an amplifying medium, however, it is possible that as the pulse enters the medium, its leading edge is amplified more strongly (or absorbed more weakly) than the rest of the pulse. Then the pulse is getting reshaped in the medium and its peak leaving the medium is nothing else than the amplified front of the incident pulse. It may therefore reach $z = L$ even before the peak of the incident pulse has entered the medium at $z = 0$. Of course, no information travels faster then light, since signal velocity can not exceed the lesser of the group velocity of an information carrying pulse and the phase velocity of all the frequency components of that pulse.

6.2 Field Propagation in a Two-Level Atomic Medium

In this section we employ the above formalism to describe the propagation of a weak probe field $E(z, t)$ through a near-resonant two-level atomic medium. The macroscopic polarization of the medium $P(z, t)$ of (6.6), induced by the applied electric field (6.5), is given by the expectation value of the dipole moment of all the atoms at position z and time t,

$$P(z, t) = \varrho_{\mathrm{a}}(z) \, \mathrm{Tr}\big[\wp \rho(z, t)\big] \; , \tag{6.24}$$

where $\wp = \boldsymbol{\wp} \cdot \hat{\boldsymbol{e}}$ is the projection of the dipole moment onto the field polarization direction $\hat{\boldsymbol{e}}$, and $\varrho_{\rm a}(z)$ is the number density of atoms which in the following will be assumed uniform over the entire interaction volume, $\varrho_{\rm a}(z) = \varrho_{\rm a}$. Expanding the trace and taking into account the fact that the diagonal matrix elements of $\wp$ are zero, we have

$$P(z,t) = \varrho_{\rm a}\big[\wp_{ge}\rho_{eg}(z,t) + \wp_{eg}\rho_{ge}(z,t)\big] \,. \tag{6.25}$$

Recall that in Sect. 4.1.3 we have studied the interaction of a two-level atom with a monochromatic field $\mathcal{E}$ employing the density matrix equations in the frame rotating with the frequency ω of the field. Since there we were dealing with a single atom at a fixed position, its spatial coordinate was taken as the origin, with the consequence that the spatial dependence of the field disappeared. Here we consider the field propagation and interaction with the atoms at various positions z. Therefore the off-diagonal density matrix elements in (6.25) are related to the corresponding slowly varying (sv) matrix elements of (4.42), by the transformation

$$\rho_{eg} = \rho_{eg}^{(\rm sv)} {\rm e}^{{\rm i}(kz-\omega t)} \,, \quad \rho_{ge} = \rho_{eg}^{*} = \rho_{ge}^{(\rm sv)} {\rm e}^{-{\rm i}(kz-\omega t)} \,.$$

Substituting this into (6.25) and comparing it with (6.6), for the slowly varying complex polarization $\mathcal{P}$ we obtain

$$\mathcal{P}(z,t) = \varrho_{\rm a}\wp_{ge}\rho_{eg}^{(\rm sv)}(z,t) \,, \tag{6.26}$$

and similarly for its complex conjugate $\mathcal{P}^*(z,t) = \varrho_{\rm a}\wp_{eg}\rho_{ge}^{(\rm sv)}(z,t)$. The field propagation equation (6.8) with the polarization given by (6.26), together with the density matrix equations (4.42) with $\Omega = \frac{\wp_{eg}}{\hbar}\mathcal{E}$ constitute the so-called Maxwell–Bloch equations, which in general require a self-consistent solution. Typically, for strong time-dependent fields $E(z,t)$, when the atomic saturation and dynamic effects are important, only numerical solutions of these equations are feasible. Simple analytic solutions of the Maxwell–Bloch equations can be obtained in the two opposite limiting cases: weak, long-pulsed or continuous-wave field propagation which is discussed below in some detail, and strong and short pulse propagation briefly outlined at the end of this section.

We thus consider the propagation and near-resonant interaction of the electromagnetic field with a medium of two-level atoms. The spatio-temporal evolution of the field is governed by the equation

$$\left(\frac{\partial}{\partial z} + \frac{1}{c}\frac{\partial}{\partial t}\right)\mathcal{E}(z,t) = {\rm i}\frac{\varrho_{\rm a}\omega\wp_{ge}}{2\varepsilon_0 c}\,\rho_{eg}^{(\rm sv)}(z,t) \,. \tag{6.27}$$

In turn, the atomic coherence $\rho_{eg}^{(\rm sv)}$ obeys the equation (dropping the superscript (sv))

$$\frac{\partial}{\partial t}\rho_{eg}(z,t) = ({\rm i}\Delta - \gamma_{eg})\rho_{eg}(z,t) - {\rm i}\frac{\wp_{eg}}{\hbar}\mathcal{E}(z,t)D(z,t) \,, \tag{6.28}$$

where $D = \rho_{ee} - \rho_{gg}$ is the population inversion and $\Delta = \omega - \omega_{eg}$ the detuning. As we are interested in weak field propagation, we may solve (6.28) to lowest (first) order in $\mathcal{E}$. To that end, we neglect saturation and take $D(z,t) = -1$ for all z and t, obtaining

$$\rho_{eg}^{(1)} = -\frac{\wp_{eg}}{\hbar} \frac{\mathcal{E}}{\Delta + \mathrm{i}\gamma_{eg}} \,. \tag{6.29}$$

This is obviously analogous to the solution obtained in Sect. 4.1.3 through the rate-equation approximation, which is valid for fields whose amplitudes vary little on a time-scale of γ_{eg}^{-1}. Consistently with this approximation, we neglect the time derivative in (6.27), which upon the substitution of $\rho_{eg}^{(1)}$ from (6.29) takes the form

$$\frac{\partial}{\partial z}\mathcal{E} = -\alpha\mathcal{E} \,. \tag{6.30}$$

Its solution is

$$\mathcal{E}(z) = \mathcal{E}(0)\,\mathrm{e}^{-\alpha z} \,, \tag{6.31}$$

where

$$\alpha = \frac{\varrho_\mathrm{a}\omega|\wp_{ge}|^2}{2\varepsilon_0 c\hbar} \frac{1}{\gamma_{eg} - \mathrm{i}\Delta} \tag{6.32}$$

is the complex linear absorption coefficient, whose real and imaginary parts determine the medium absorption $a = \mathrm{Re}(\alpha)$ and dispersion $\phi/z = \mathrm{Im}(\alpha)$, respectively. Near the resonance $\omega \sim \omega_{eg} \gg \Delta$, we can rewrite (6.32) as

$$\alpha = a_0 \frac{\gamma_{eg}}{\gamma_{eg} - \mathrm{i}\Delta} \,, \quad a_0 = \frac{\omega_{eg}|\wp_{ge}|^2}{2\varepsilon_0 c\hbar\gamma_{eg}} \varrho_\mathrm{a} \,, \tag{6.33}$$

where in the definition of the resonant absorption coefficient a_0 we have replaced ω by ω_{eg}. In the absence of atomic collisions and other additional sources of coherence relaxation, such that $\gamma_{eg} = \frac{1}{2}\Gamma$, we can express a_0 through the spontaneous decay rate of the excited atomic state

$$\Gamma = \frac{1}{4\pi\varepsilon_0} \frac{4\omega_{eg}^3|\wp_{ge}|^2}{3\hbar c^3} \,,$$

obtaining

$$a_0 = \frac{3\pi c^2}{\omega^2} \varrho_\mathrm{a} \equiv \sigma_0 \varrho_\mathrm{a} \,. \tag{6.34}$$

Thus the resonant absorption coefficient a_0 is given by the product of the absorption cross-section σ_0 and the atomic density ϱ_a.

Comparing (6.30) with (6.12), we see that the linear susceptibility for the two-level atomic medium is given by

$$\chi(\omega) = \frac{2a_0}{k} \frac{\mathrm{i}\gamma_{eg}}{\gamma_{eg} - \mathrm{i}\Delta} \,. \tag{6.35}$$

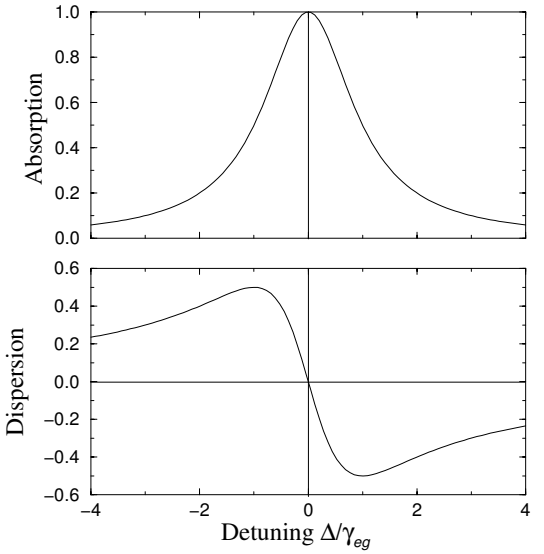

Fig. 6.1. Absorption and dispersion spectra of the two-level atomic medium for weak probe field $\mathcal{E}$ in units of resonant absorption coefficient a_0.

The corresponding absorption and dispersion spectra are shown in Fig. 6.1. At exact resonance $\Delta = 0$, the field is strongly attenuated, $\mathcal{E}(z) = \mathcal{E}(0)\,\mathrm{e}^{-a_0 z}$, and its intensity $I \propto |\mathcal{E}|^2$ is depleted with the propagation distance according to

$$I(z) = I(0)\,\mathrm{e}^{-2a_0 z}\ . \tag{6.36}$$

The quantity $2a_0 z = 2\sigma_0 \varrho_\mathrm{a} z$, is called optical depth of the medium, since it determines the fraction of the energy dissipated in a medium of number density ϱ_a and length z. Away from the resonance, the absorption spectrum is Lorentzian, given by

$$a = \tfrac{1}{2} k\,\mathrm{Im}\chi(\omega) = a_0\,\frac{\gamma_{eg}^2}{\Delta^2 + \gamma_{eg}^2} = \frac{a_0}{1 + \left(\frac{\Delta}{\gamma_{eg}}\right)^2}\ . \tag{6.37}$$

Let us note parenthetically that, if one were to consider a short pulse propagation in the two-level medium, the rate-equation approximation made in (6.29) would have been inconsistent with keeping the time derivative in the propagation equation (6.27). The perturbative solution for ρ_{eg} should then be modified as

$$\rho_{eg} = \rho_{eg}^{(1)} + \frac{1}{\mathrm{i}\Delta - \gamma_{ge}}\,\frac{\partial}{\partial t}\rho_{eg}^{(1)}\ ,$$

where $\rho_{eg}^{(1)}$ is given by (6.29). Upon substitution into (6.27), this would result in a modified group velocity, which in the frequency region around resonance is given by

$$v_g = \frac{c}{1 - c\frac{a_0}{\gamma_{eg}}} ,$$

corresponding to the anomalous dispersion $\frac{\partial \chi(\omega)}{\partial \omega} < 0$ around $\omega = \omega_{eg}$, as seen in Fig. 6.1. This dispersion, however, is accompanied by strong absorption and the resulting "superluminal" group velocity is of little physical interest, as we have noted at the end of the previous section.

In the above discussion, we assumed a homogeneously broadened atomic medium, meaning that all of the atoms have a common resonance frequency ω_{eg} and therefore their response to the applied probe field is homogeneous, given by (6.29). As noted before, the homogeneous width of the atomic resonance γ_{eg} consists of contributions from the atomic spontaneous decay (natural width) and other phase-relaxation processes, such as atomic collisions and laser phase fluctuations. Often, however, one encounters a situation in which various atoms respond to the applied field differently, primarily due to the variations of their resonant frequencies. For example, optically active dopants—atoms—in solid state host material typically experience different level-shifts due to the variations in the local environment, i.e., inhomogeneities in the crystal structure. Another example often encountered in quantum optics is the thermal atomic vapor. There the atoms moving with various velocities $\boldsymbol{v}$ see different Doppler-shifted frequencies ω' of the applied field, $\omega' = \omega - \boldsymbol{k} \cdot \boldsymbol{v}$ with $\boldsymbol{k}$ being the field wavevector. In turn, the effective resonant frequency of the moving atom, as it appears to the field, is given by $\omega'_{eg} = \omega_{eg}/(1 - v/c) \simeq \omega_{eg} + kv$, with $|v| \ll c$. In general, to calculate the medium polarization (6.26), one has to sum up the contributions of all the atoms weighed by the appropriate distribution function $W(\omega'_{eg})$ for the atomic resonant frequencies,

$$\mathcal{P}(z,t) = \varrho_{\mathrm{a}} \wp_{ge} \int \mathrm{d}\omega'_{eg} W(\omega'_{eg})\, \rho_{eg}(\omega'_{eg}) . \tag{6.38}$$

In particular, in the case of Doppler broadening of thermal atomic ensemble, the dependence of ρ_{eg} on the atomic velocity can be obtained from (6.29) by replacing Δ with the effective detuning $\Delta' = \omega - \omega'_{eg} = \Delta - kv$. The corresponding Maxwellian velocity distribution function is $W(v) = (u\sqrt{\pi})^{-1} \exp(-v^2/u^2)$ with $u = \sqrt{2k_{\mathrm{B}}T/M_{\mathrm{A}}}$ being the most probable velocity at temperature T. Consequently, the linear susceptibility for the Doppler-broadened two-level atomic medium becomes

$$\chi(\omega) = \frac{2a_0}{k} \int_{-\infty}^{\infty} \mathrm{d}v \, \frac{\mathrm{i}\gamma_{eg} W(v)}{\gamma_{eg} - \mathrm{i}(\Delta - kv)} , \tag{6.39}$$

and the resulting absorption spectrum is given by the convolution of the Gaussian and Lorentzian functions

$$a = \frac{a_0}{u\sqrt{\pi}} \int_{-\infty}^{\infty} \mathrm{d}v \, \frac{\exp\left(-\frac{v^2}{u^2}\right)}{1 + \left(\frac{\Delta - kv}{\gamma_{eg}}\right)^2} , \tag{6.40}$$

known as the Voigt profile, which in general does not yield simple analytical expressions. However, when the Doppler width is much larger than the homogeneous width, $ku \gg \gamma_{eg}$, we can evaluate the Gaussian at the line-center of the Lorentzian, $v = \Delta/k$ and pull it out of the integral. The remaining Lorentzian is then easily integrated, with the result

$$a = \frac{a_0 \gamma_{eg} \sqrt{\pi}}{ku} \exp\left[-\frac{\Delta^2}{(ku)^2}\right] . \tag{6.41}$$

In the opposite limit of a cold atomic gas, such that $\gamma_{eg} \gg ku$, the above expression (6.40) obviously reduces to (6.37).

Before closing this section, let us briefly address the case of strong and short input pulse, when the atomic relaxation can be neglected on the time-scale of pulse duration. McCall and Hahn have found that the pulse area, defined by

$$\theta(z) = \frac{2\wp_{eg}}{\hbar} \int_{-\infty}^{\infty} \mathcal{E}(z,t)\, \mathrm{d}t , \tag{6.42}$$

obeys the propagation equation

$$\frac{\partial}{\partial z}\theta(z) = -a \sin\left[\theta(z)\right] , \tag{6.43}$$

which is known as the pulse area theorem (see Prob. 6.1). Obviously, in the limit of small area pulses, so that $\theta(z) \ll 1$ and therefore $\sin\left[\theta(z)\right] \simeq \theta(z)$, this equation leads to the exponential absorption of the pulse according to Beer's law (6.13) or (6.31). In the case of strong pulse, (6.43) predicts that upon propagation the area of the pulse evolves towards the nearest even multiple of π, i.e., $\theta(z) \to 2n\pi$, where n is an integer. However, pulses with $n > 1$ are not stable and tend to break up into pulses with area $\theta = 2\pi$ which can propagate in the medium over long distances preserving their spatio-temporal shape given by

$$\mathcal{E}(z,t) = \frac{\hbar}{\tau_w \wp_{eg}} \operatorname{sech}\left(\frac{t - z/v_g}{\tau_w}\right) , \tag{6.44}$$

where τ_w is the temporal width of the pulse and $v_g = c/(1 + ca\tau_w) \simeq (a\tau_w)^{-1}$ is the corresponding group velocity. This effect is called self-induced transparency, which is a manifestation of optical soliton propagation in resonant atomic media.

6.3 Field Propagation in a Three-Level Atomic Medium

We discuss now weak field propagation in a three level atomic medium. We consider the scheme of Fig. 6.2 in which the probe field E interacts with the atoms on the $|g\rangle \leftrightarrow |e\rangle$ transition, while the second strong coherent field drives the atomic transition $|s\rangle \leftrightarrow |e\rangle$ with Rabi frequency Ω_d. We

will see that under the conditions of two-photon Raman resonance, the probe propagates in the medium without much attenuation and with the reduced group velocity, which is a consequence of the coherent population trapping (CPT) of atoms in the dark state $|D\rangle$ discussed in Sect. 3.6. Such absorption-free propagation of probe field in coherently–driven atomic media is called electromagnetically induced transparency (EIT). Although EIT can and has been observed in atomic media with Ξ, V and Λ level configurations, here we focus upon the Λ configuration, as in this case the absorption is particularly low, owing to the long relaxation times of the atomic ground state coherence.

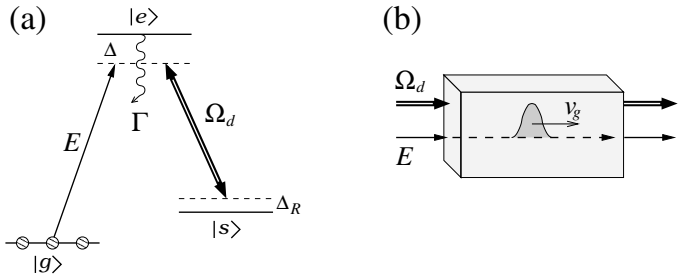

Fig. 6.2. Electromagnetically induced transparency in an atomic medium. (a) Level scheme of three-level Λ-atoms interacting with a strong cw driving field with Rabi frequency Ω_d on the transition $|s\rangle \leftrightarrow |e\rangle$ and a weak probe field E acting on the transition $|g\rangle \leftrightarrow |e\rangle$. The lower states $|g\rangle$ and $|s\rangle$ are long-lived (metastable), while the excited state $|e\rangle$ decays fast with the rate Γ. (b) Collinear geometry of the probe and driving field propagation in the atomic medium for Doppler-free EIT.

The Hamiltonian for the three-level atom interacting with two classical fields in the Λ configuration is given by (3.121), which in the notations of Fig. 6.2(a) becomes

$$\mathcal{H}_\Lambda(z) = -\hbar\big[\Delta\sigma_{ee} + \Delta_R\sigma_{ss}\big] - \big[\wp_{eg}\,\mathcal{E}\mathrm{e}^{\mathrm{i}kz}\sigma_{eg} + \hbar\Omega_d\,\mathrm{e}^{\mathrm{i}k_d z}\sigma_{es} + \mathrm{H.c.}\big]\,, \quad (6.45)$$

where $\Delta = \omega - \omega_{eg}$ is the detuning of the probe field from the $|g\rangle \leftrightarrow |e\rangle$ transition, and $\Delta_R = \Delta - \Delta_d = \omega - \omega_d - \omega_{sg}$ is the two-photon Raman detuning, with $\Delta_d = \omega_d - \omega_{es}$ being the driving field detuning from the $|s\rangle \leftrightarrow |e\rangle$ transition. In (6.45) we have explicitly shown the dependence of $\mathcal{H}_\Lambda$ on the atomic position z, with k_d being the projection of the driving field wavevector onto the probe field propagation direction z. Using the Liouville equation

$$\frac{\partial}{\partial t}\rho = -\frac{\mathrm{i}}{\hbar}[\mathcal{H}_\Lambda, \rho] + \mathcal{L}_\Lambda\rho\,, \quad (6.46)$$

which includes the relaxation matrix $\mathcal{L}_\Lambda\rho$ appropriate to the Λ configuration of atomic levels (see (5.95)), we obtain the following set of density matrix equations,

$$\frac{\partial}{\partial t}\rho_{gg} = \Gamma_{eg}\rho_{ee} + \frac{\mathrm{i}}{\hbar}(\wp_{ge}\,\mathcal{E}^{*}\mathrm{e}^{-\mathrm{i}kz}\rho_{eg} - \text{c.c.})\,, \tag{6.47a}$$

$$\frac{\partial}{\partial t}\rho_{ee} = -\Gamma\rho_{ee} + \frac{\mathrm{i}}{\hbar}(\wp_{eg}\,\mathcal{E}\mathrm{e}^{\mathrm{i}kz}\rho_{ge} - \text{c.c.}) + \mathrm{i}(\Omega_d\,\mathrm{e}^{\mathrm{i}k_d z}\rho_{se} - \text{c.c.})\,, \tag{6.47b}$$

$$\frac{\partial}{\partial t}\rho_{ss} = \Gamma_{es}\rho_{ee} + \mathrm{i}(\Omega_d^{*}\,\mathrm{e}^{-\mathrm{i}k_d z}\rho_{es} - \text{c.c.})\,, \tag{6.47c}$$

$$\frac{\partial}{\partial t}\rho_{eg} = (\mathrm{i}\Delta - \gamma_{eg})\rho_{eg} + \frac{\mathrm{i}}{\hbar}\wp_{eg}\,\mathcal{E}\mathrm{e}^{\mathrm{i}kz}(\rho_{gg} - \rho_{ee}) + \mathrm{i}\Omega_d\,\mathrm{e}^{\mathrm{i}k_d z}\rho_{sg}\,, \tag{6.47d}$$

$$\frac{\partial}{\partial t}\rho_{sg} = (\mathrm{i}\Delta_R - \gamma_{sg})\rho_{sg} - \frac{\mathrm{i}}{\hbar}\wp_{eg}\,\mathcal{E}\mathrm{e}^{\mathrm{i}kz}\rho_{se} + \mathrm{i}\Omega_d^{*}\mathrm{e}^{-\mathrm{i}k_d z}\rho_{eg}\,, \tag{6.47e}$$

$$\frac{\partial}{\partial t}\rho_{es} = (\mathrm{i}\Delta_d - \gamma_{es})\rho_{es} + \frac{\mathrm{i}}{\hbar}\wp_{eg}\,\mathcal{E}\mathrm{e}^{\mathrm{i}kz}\rho_{gs} + \mathrm{i}\Omega_d\,\mathrm{e}^{\mathrm{i}k_d z}(\rho_{ss} - \rho_{ee})\,, \tag{6.47f}$$

where Γ_{eg} and Γ_{es} are the spontaneous decay rates from level $|e\rangle$ to levels $|g\rangle$ and $|s\rangle$, respectively, while Γ is the total spontaneous decay rate of $|e\rangle$, which in addition to Γ_{eg} and Γ_{es} may also include the decay to other atomic levels. Finally, γ_{eg}, γ_{es} and γ_{sg} are the corresponding coherence relaxation rates, with γ_{sg} typically being much smaller than γ_{eg} and γ_{es} because the lower states $|g\rangle$ and $|s\rangle$ are long-lived (metastable). Since the Hamiltonian (6.45) corresponds to the frame rotating with the frequencies of the optical fields, the off-diagonal density matrix elements in (6.47) are slowly oscillating functions of time. Yet, their spatial oscillations are rapid, corresponding to the wavelengths of the optical fields. These fast spatial oscillations are removed via the transformations

$$\rho_{eg} = \rho_{eg}^{(\mathrm{sv})}\mathrm{e}^{\mathrm{i}kz}\,, \quad \rho_{es} = \rho_{es}^{(\mathrm{sv})}\mathrm{e}^{\mathrm{i}k_d z}\,, \quad \rho_{sg} = \rho_{sg}^{(\mathrm{sv})}\mathrm{e}^{\mathrm{i}(k-k_d)z}\,, \tag{6.48}$$

which results in a set of equations identical to (6.47) but without the exponential factors $\mathrm{e}^{\mathrm{i}kz}$ and $\mathrm{e}^{\mathrm{i}k_d z}$.

As discussed in the previous section, the propagation equation for the slowly varying in time and space amplitude $\mathcal{E}(z,t)$ of the probe field is given by (6.28). We are interested in the weak probe field interaction with the atoms initially prepared by the strong cw driving field in the ground state $|g\rangle$. More precisely, we assume that the driving field with Rabi frequency Ω_d is switched on long before the probe field arrives. Then, as the driving field saturates the transition $|s\rangle \leftrightarrow |e\rangle$, level $|s\rangle$ is being depleted due to the spontaneous decay from $|e\rangle$ to $|g\rangle$ with the rate Γ_{eg}, and eventually all atoms accumulate on level $|g\rangle$. This is the essence of optical pumping of atomic level $|g\rangle$. Once the process of optical pumping is over, the absorption of the driving field becomes negligible. With atoms so prepared, we can solve (6.47) to the lowest (first) order in the weak probe field $\mathcal{E}$, to obtain the expression for $\rho_{eg}^{(\mathrm{sv})}$ (we will drop from now on the superscript (sv)). In the stationary regime, from (6.47e) we have

$$\rho_{sg} \simeq -\frac{\Omega_d^{*}}{\Delta_R + \mathrm{i}\gamma_{sg}}\rho_{eg}\,,$$

where the term containing $\mathcal{E}\rho_{se}$ has been neglected due to the smallness of both $\mathcal{E}$ and ρ_{se}. Substituting this into (6.47d), dropping the time derivative, and taking $\rho_{gg} - \rho_{ee} \simeq 1$ as the probe is assumed too weak to cause depletion of ρ_{gg}, we obtain

$$\rho_{eg}^{(1)} = -\frac{\wp_{eg}}{\hbar} \frac{\mathcal{E}}{\Delta + \mathrm{i}\gamma_{eg} - |\Omega_d|^2(\Delta_R + \mathrm{i}\gamma_{sg})^{-1}} \,. \tag{6.49}$$

Similarly to the previous section, we substitute $\rho_{eg}^{(1)}$ into the propagation equation (6.27) without the time-derivative, and after comparing it with (6.12) we find the complex susceptibility for the probe field, which now takes the form

$$\chi(\omega) = \frac{2a_0}{k} \frac{i\gamma_{eg}}{\gamma_{eg} - i\Delta + |\Omega_d|^2(\gamma_{sg} - i\Delta_R)^{-1}} \,. \tag{6.50}$$

Obviously, in the limit of $\Omega_d \to 0$, this susceptibility reduces to that for the two-level atom (6.35). The absorption and dispersion spectra corresponding to the susceptibility of (6.50) are shown in Fig. 6.3 for the case of $\Omega_d = \gamma_{ge}$ and $\Delta_d = 0$, i.e., driving field is resonant with the transition $|s\rangle \leftrightarrow |e\rangle$ and therefore $\Delta_R = \Delta$. As seen, the interaction with the driving field results in a splitting of the absorption spectrum into two peaks separated by $2\Omega_d$, which is known as the Autler–Towns splitting. Meanwhile, at the line center the medium becomes transparent to the resonant field, provided the ground state coherence relaxation rate γ_{sg} is sufficiently small, $\gamma_{sg} \ll |\Omega_d|^2/\gamma_{eg}$, This is the essence of electromagnetically induced transparency (EIT).

At the exit from the optically dense medium of length L (optical depth $2a_0L > 1$), the intensity transmission coefficient, defined as $T_I \equiv I(L)/I(0) = \mathrm{e}^{-2aL}$, is given by

$$T_I(\omega) = \exp[-k\,\mathrm{Im}\chi(\omega)L] \,.$$

To determine the width of the transparency window $\delta\omega_{\mathrm{tw}}$, we expand $\mathrm{Im}\chi(\omega)$ in a power series in the vicinity of maximum transmission $\Delta_R = 0$. Under the EIT conditions $(\gamma_{eg}, \Delta_d, \Delta_d^2/\gamma_{eg})\gamma_{sg} \ll |\Omega_d|^2$, to lowest non-vanishing order in Δ_R, we then obtain

$$T_I(\omega) \simeq \exp\left(-\frac{\Delta_R^2}{\delta\omega_{\mathrm{tw}}^2}\right) \,, \quad \delta\omega_{\mathrm{tw}} = \frac{|\Omega_d|^2}{\gamma_{eg}\sqrt{2a_0L}} \,. \tag{6.51}$$

Considering next the dispersive properties of EIT, as shown in Fig. 6.3, the dispersion exhibits a steep and approximately linear slope in the vicinity of absorption minimum $\Delta_R = 0$. Therefore, a probe field slightly detuned from resonance by $\Delta_R < \delta\omega_{\mathrm{tw}}$, during the propagation would acquire a large phase-shift

$$\phi(L) \simeq \frac{a_0\gamma_{eg}}{|\Omega_d|^2}\Delta_R L \,, \tag{6.52}$$

while suffering only little absorption, as per equation (6.51).

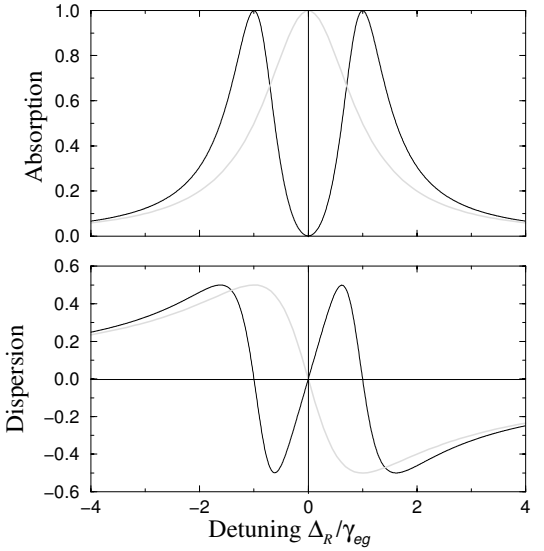

Fig. 6.3. Absorption and dispersion spectra ($\Delta_R = \Delta$) of a three-level atomic medium for weak probe field $\mathcal{E}$ in units of a_0, for $\Omega_d/\gamma_{eg} = 1$ and $\gamma_{sg}/\gamma_{eg} = 10^{-3}$. The light-gray curves correspond to the case of $\Omega_d = 0$ (two-level atom).

Let us now briefly address the consequences of inhomogeneous broadening in a thermal atomic ensemble. As we have established in the previous section, in the expression for the susceptibility (6.50), the detunings of the optical fields Δ and Δ_d should then be replaced by the effective Doppler-shifted detunings $\Delta' = \Delta - kv$ and $\Delta'_d = \Delta_d - k_d v$ (recall that k_d is the projection of the driving field wavevector onto the z direction). Consequently, the two-photon Raman detuning becomes $\Delta'_R = \Delta_R - (k - k_p)v$. It is thus obvious that when $k \simeq k_p$ the Raman detuning is practically unaffected by the atomic thermal motion. Such a situation can be realized when the probe and driving fields have similar frequencies and propagation directions, i.e., are collinear as shown in Fig. 6.2(b). Since both fields couple to the same upper level $|e\rangle$, they can have similar frequencies if the lower levels $|g\rangle$ and $|s\rangle$ are closely spaced in energy, i.e., nearly degenerate. This is in fact the case for most of the alkali atoms—the workhorse of experimental quantum optics—whose electronic ground state contains a manifold of hyperfine and Zeeman levels. A pair of such levels is then selected by properly adjusting the frequencies and polarizations of the probe and driving fields to serve as the lower metastable levels $|g\rangle$ and $|s\rangle$. Then, in the vicinity of Raman resonance $\Delta_R = 0$, the EIT is immune to the atomic thermal motion, provided $(k - k_p)\bar{v} < \delta\omega_{\rm tw}$ and $(k\bar{v}, \Delta_d k\bar{v}/\gamma_{eg})\gamma_{sg} \ll |\Omega_d|^2$, where $\bar{v} = \sqrt{3k_{\rm B}T/m_{\rm a}}$ is the mean thermal atomic velocity.

Next, we discuss a pulsed field propagation in the EIT medium. Equation (6.51) implies that for the absorption-free propagation, the bandwidth $\delta\omega$ of a near-resonant probe field should be within the transparency window, $\delta\omega < \delta\omega_{\rm tw}$. Alternatively, the temporal width τ_w of a Fourier-limited probe pulse should satisfy $\tau_w \gtrsim \delta\omega_{\rm tw}^{-1}$. As we know from Sect. 6.1, due to the steep slope of the dispersion in the vicinity of the absorption minimum $\Delta_R = 0$, a near-resonant probe pulse $\mathcal{E}(z,t)$ propagates in the EIT medium with greatly reduced group velocity

$$v_g = \frac{c}{1 + \frac{\omega}{2}\frac{\partial}{\partial\omega}[{\rm Re}\chi(\omega)]} = \frac{c}{1 + c\frac{a_0\gamma_{ge}}{|\Omega_d|^2}} \simeq \frac{|\Omega_d|^2}{a_0\gamma_{ge}} \ll c\,. \tag{6.53}$$

Therefore, upon entering the medium, the spatial envelope of the pulse is compressed by a factor of $v_g/c \ll 1$, while its peak amplitude remains unchanged. Since the dispersion slope is approximately linear around $\Delta_R = 0$, during propagation the shape of the pulse experiences little distortion.

The physical origin of this behavior is the coherent populations trapping of the atoms in the dark state $|D\rangle$ discussed in Sect. 3.6. Here, for the atoms located at various spatial coordinates z the dark state of the Hamiltonian (6.45) is given by

$$|D(z,t)\rangle = \cos\Theta\,|g\rangle - {\rm e}^{{\rm i}(k-k_p)z}\sin\Theta\,|s\rangle\,, \tag{6.54}$$

where

$$\cos\Theta = \frac{\Omega_d}{\sqrt{\Omega_d^2 + \Omega_p^2}}\,, \quad \sin\Theta = \frac{\Omega_p}{\sqrt{\Omega_d^2 + \Omega_p^2}}\,,$$

and $\Omega_p = \frac{\wp_{eg}}{\hbar}\mathcal{E}$ is the Rabi frequency of the probe, which is a function of space and time since $\mathcal{E} = \mathcal{E}(z,t)$. Before the probe pulse arrives, all atoms have been prepared in state $|g\rangle$ and the driving field is on, which means that $\Theta = 0$ and the atoms are in the dark state, $|D\rangle = |g\rangle$. As the probe pulse enters and propagates in the medium, every atom adiabatically follows the dark state (6.54), provided the field envelope changes in time sufficiently slowly, as required by the adiabatic criterion (3.135). Stated otherwise, the Fourier bandwidth of the pulse should be smaller than the Autler–Towns splitting of the atomic resonance, which determines the EIT transparency window $\delta\omega_{\rm tw}$. Upon propagation through the medium, as the probe pulse approaches some position z, the mixing angle for the atom at that position slightly rotates to adjust to the value $\Theta(z,t) = \arctan|\Omega_p(z,t)/\Omega_d|$. A small fraction of atomic population, proportional to $|\Omega_p/\Omega_d|^2$, is therefore transfered to state $|s\rangle$ by coherent Raman scattering, i.e., absorbing a photon from the leading edge of the pulse and re-emitting it into the driving field. At the end of the pulse, this population is transfered back to state $|g\rangle$ by the reverse process, absorbing a photon from the driving field and re-emitting it into the trailing edge of the probe pulse. Thus, upon propagation, photons are continuously "borrowed" by the atoms from the leading edge of the probe pulse, to be added later on to its tale. As a result, the pulse propagates without attenuation as a

whole, but with a reduced group velocity proportional to $|\Omega_d|^2$ and inversely proportional to the atomic density as per (6.53). Since the Raman scattering process is coherent, the probe pulse retains its coherent properties throughout propagation.

Thus far we have considered EIT under the condition of stationary Rabi frequency of the diving field. Let us now see what happens if the driving field is a function of time but uniform in space, $\Omega_d = \Omega_d(t)$. From (6.54) we see that in the dark state the ratio of the amplitudes c_s and c_g of states $|s\rangle$ and $|g\rangle$ is given by

$$\frac{c_s(z,t)}{c_g(z,t)} = -\frac{\Omega_p(z,t)}{\Omega_d(t)}\, \mathrm{e}^{\mathrm{i}(k-k_p)z} \,. \tag{6.55}$$

We consider a weak probe pulse, such that the number density of photons in the probe is much smaller than the number density of the atoms. Then c_g can not be affected significantly by the propagating probe and we can take it as $c_g(z,t) \simeq 1$ at all times t and space coordinates z. Once the probe pulse is fully accommodated in the medium, most of its energy has been coherently scattered into the driving field and it has been spatially compressed by a factor of $v_g/c \ll 1$. Suppose now that we switch the driving field off. Since in (6.55) c_s is bound, while $c_g \simeq 1$, the ratio Ω_p/Ω_d is also bound. In fact, the maximum value that the population $\rho_{ss} = |c_s|^2$ of the atomic state $|s\rangle$ can take is given by the ratio of the number density of photons in the probe to the number density of atoms, which is assumed very small. Thus, as $\Omega_d \to 0$, we must have $\Omega_p \to 0$ too. Intuitively, we can understand this result by noting that by switching off the driving field we rotate the mixing angle for every atom from its initial value $0 \le \Theta < \pi$ to $\Theta = \pi$. Therefore all the photons in the probe pulse are coherently scattered into the driving field and the corresponding number of atoms are transfered to the state $|s\rangle$. To put it otherwise, the photonic excitation initially propagating as a probe pulse is coherently converted into the Raman (or spin) excitation stored in the stationary atoms. Since this process is coherent, one can reverse it by switching on the driving field at a later time and releasing the probe pulse.

To describe this reversible "photon memory" more quantitatively, we will now derive a perturbative time-dependent solution of the density matrix equations (6.47), under the EIT conditions stated above. To first order in the probe field Rabi frequency Ω_p, from (6.47d) we have

$$\rho_{sg}(z,t) = -\frac{\frac{\wp_{eg}}{\hbar}\mathcal{E}(z,t)}{\Omega_d(t)} = -\frac{\Omega_p(z,t)}{\Omega_d(t)} \,, \tag{6.56}$$

while (6.47e) gives

$$\rho_{eg}(z,t) = -\frac{\mathrm{i}}{\Omega_d^*(t)}\left[\frac{\partial}{\partial t} - \mathrm{i}\Delta_R + \gamma_{sg}\right]\rho_{sg}(z,t) \,, \tag{6.57}$$

where again we have neglected the term containing $\Omega_p\rho_{se}$. Substituting this into the propagation equation (6.27) we obtain

$$\left(\frac{\partial}{\partial z}+\frac{1}{c}\frac{\partial}{\partial t}\right)\mathcal{E}(z,t)=-\frac{a_0\gamma_{eg}}{\Omega_d^*}\frac{\partial}{\partial t}\frac{\mathcal{E}(z,t)}{\Omega_d(t)}+\frac{a_0\gamma_{eg}}{|\Omega_d|^2}(\mathrm{i}\Delta_R-\gamma_{sg})\mathcal{E}(z,t)\ . \quad (6.58)$$

Note that if the driving field Rabi frequency Ω_d is constant in time, this equation becomes

$$\left(\frac{\partial}{\partial z}+\frac{1}{v_g}\frac{\partial}{\partial t}\right)\mathcal{E}=\frac{a_0\gamma_{eg}}{|\Omega_d|^2}(\mathrm{i}\Delta_R-\gamma_{sg})\mathcal{E}\ , \quad (6.59)$$

which describes the probe field propagation in the medium with the group velocity v_g as given by (6.53). Equation (6.59) is of the general form of the linear propagation equation (6.17). Hence, depending on the given boundary or initial conditions, its solution can be expressed as in (6.20) or (6.22). Evidently, the terms proportional to Δ_R and γ_{sg} on the right-hand-side of (6.59) are responsible, respectively, for the linear phase shift (6.52) and absorption of the probe.

Consider now the case of exact two-photon resonance $\Delta_R = 0$ and time-dependent but spatially-uniform Rabi frequency $\Omega_d(t)$ of the driving field, which for simplicity we take real. Substituting ρ_{eg} from (6.57) into (6.27) and multiplying the resulting equation by $c\frac{\wp_{eg}}{\hbar}$, we obtain the following propagation equation for the Rabi frequency of the probe field,

$$\left(\frac{\partial}{\partial t}+c\frac{\partial}{\partial z}\right)\Omega_p(z,t)=\frac{M}{\Omega_d(t)}\frac{\partial}{\partial t}\rho_{sg}(z,t)\ , \quad (6.60)$$

where $M = a_0\gamma_{eg}c$ is a constant proportional to the atomic density (recall that $a_0 \propto \varrho_{\mathrm{a}}$). In the above equation, we have neglected the probe absorption keeping in mind that the relevant time-scales should be short compared to the life-time of the ground state (Raman) coherence γ_{sg}^{-1}. Let us introduce a new field Ω_{D}, which we will call "dark field", via

$$\Omega_{\mathrm{D}}(z,t)=\cos\bar{\Theta}(t)\,\Omega_p(z,t)-\sin\bar{\Theta}(t)\,\sqrt{M}\rho_{sg}(z,t)\ , \quad (6.61)$$

where the collective mixing angle $\bar{\Theta}$ (not to be confused with the single-atom mixing angle Θ encountered above, even though the two are related) is defined through

$$\tan\bar{\Theta}(t)=\frac{\sqrt{M}}{\Omega_d(t)}\ ,$$

or, equivalently,

$$\cos\bar{\Theta}=\frac{\Omega_d}{\sqrt{\Omega_d^2+M}}\ ,\quad \sin\bar{\Theta}=\frac{\sqrt{M}}{\sqrt{\Omega_d^2+M}}\ .$$

Thus the dark field is a superposition of the probe field and atomic Raman coherence amplitudes; it is therefore sometimes called "dark-state polariton". Using the relation between the probe field Rabi frequency Ω_p and atomic

Raman coherence ρ_{sg} in (6.56), it is easy to verify that Ω_p and ρ_{sg} can be expressed through the dark-field amplitude $\Omega_{\rm D}$ as

$$\Omega_p = \cos\bar{\Theta}\Omega_{\rm D} \ , \quad \sqrt{M}\rho_{sg} = -\sin\bar{\Theta}\Omega_{\rm D} \ . \tag{6.62}$$

Substituting this relations into the propagation equation (6.60), after a few algebraic steps (Prob. 6.3) we arrive at the following equation for the dark field amplitude

$$\left(\frac{\partial}{\partial t} + c\cos^2\bar{\Theta}(t)\frac{\partial}{\partial z}\right)\Omega_{\rm D}(z,t) = 0 \ . \tag{6.63}$$

This equation has a simple solution

$$\Omega_{\rm D}(z,t) = \Omega_{\rm D}\left(z - \int_0^t v_g(t'){\rm d}t', t = 0\right) \ , \tag{6.64}$$

which describes a state- and shape-preserving pulse propagation with time-dependent group velocity $v_g(t) = c\cos^2\bar{\Theta}(t)$. Thus, once the probe pulse has been fully accommodated in the medium, one can stop it by rotating the mixing angle $\bar{\Theta}$ from its initial value $0 \le \bar{\Theta} < \pi/2$ to $\bar{\Theta} = \pi/2$, which amounts to switching off the driving field Ω_d. As a result, the probe field Rabi frequency Ω_p, or its amplitude $\mathcal{E}$ for that matter, is coherently mapped onto the atomic Raman coherence ρ_{sg} as per relations (6.62). At a later time, the probe pulse can be released from the medium on demand by switching the driving field on, which results in the reversal of the mapping. Before closing this section, let us emphasize again that in order to accommodate the probe pulse in the medium with negligible losses, its duration should exceed the inverse of the initial EIT bandwidth, while at the entrance its length should be compressed to the length of the medium, $\delta\omega_{\rm tw}^{-1}v_g \ll \tau_w v_g < L$, where v_g is the initial group velocity. These two conditions yield $(2a_0L)^{-1/2} \ll \tau_w v_g/L < 1$, which requires media with large optical depth $2a_0L \gg 1$.

Problems

6.1. Prove the pulse area theorem of (6.43). (*Hint*: See S. McCall and E. Hahn, Phys. Rev. Lett. **18**, 908 (1967); Phys. Rev. **183**, 457 (1969).)

6.2. Verify that for $\Delta_R = 0$ the dark state $|D(z,t)\rangle$ of (6.54) is indeed the eigenstate of Hamiltonian (6.45) with the eigenvalue 0.

6.3. From (6.60), using the relations (6.62) and keeping in mind that the collective mixing angle $\bar{\Theta}(t)$ is a function of time, derive the dark field propagation equation (6.63).

Part II

Quantum Information

Preamble

Information is represented, stored, processed, transmitted and readout by physical systems: "Information is physical," as Rolf Landauer has summarized. Until recently, information has largely been thought of in classical terms, quantum mechanics having played a supportive role in designing the equipment to store and process it. With the tremendous progress in semiconductor technology and ever shrinking size of microelectronics, presently a single transistor in a PC processor is as small as $\sim 60\,\mathrm{nm}$. According to Moore's low, every 18 months computer chips double in density and power. If this trend continues during the next 15–20 years, we'll have a single transistor represented by a single atom or molecule. Then quantum mechanical effects will begin playing an important role. This has in part motivated the birth of a new field—Quantum Information Theory—based on quantum principles, which extends and generalizes classical information theory. Quantum information theory is currently attracting enormous interest in view of its fundamental nature and its potentially revolutionary applications to computation and secure communication.

This Part of the book is devoted to quantum information and computation. In Chap. 7 we briefly outline the basic concepts of classical computation. This will prove useful in the description of the fundamental building blocks of quantum information in Chap. 8 and the principles of quantum computation in Chap. 9. We then conclude this Part and the whole book by Chap. 10, where we outline several representative quantum optical systems for quantum information processing.

7

Elements of Classical Computation

Computation is data processing. Computers process the input data, following a certain set of instructions called program, to proceed toward the result of computation contained in the output data. One distinguishes analog and digital computation. In analog computation, the computer basically imitates the physical process being simulated. In digital computation that most of us use on a daily basis, one "digitalizes" the parameters of the system to be modeled or analyzed and feeds this digital data into the computer input. The computation is then digital data processing.

In this chapter we review the basic concepts of classical computation. This is necessary in order to make the discussion on the theory of quantum information and computation more transparent. As will be seen in the chapters that follow, there are many parallels and analogies one can draw between classical and quantum computers, but there are also striking differences associated with the superposition principle that results in quantum parallelism.

7.1 Bits and Memory

In a classical digital computer, the elementary unit of information—bit a—is represented by a classical two-state system $a \in \{0, 1\}$, e.g., charge state of a capacitance, magnetization of a ferromagnetic material, or current direction of a transistor circuit. A bit thus stores 0 *or* 1. An n-bit memory (register) of the computer can exist in 2^n logical states

$$000\ldots0,\ 000\ldots1,\ldots,\ 111\ldots1\ .$$

Any integer number x, or a symbol associated with it, can be represented in binary units $x \equiv x_1x_2\ldots x_n$ $(x_i \in \{0, 1\})$ through

$$x = x_1 2^{n-1} + x_2 2^{n-2} + \ldots + x_n 2^0\ . \tag{7.1}$$

Thus, an 8-bit section of the memory, called byte, can store non-negative integer numbers in the range $[0, 255]$, or if the first bit is used to indicate sign, then the byte can store integer numbers in the range $[-127, 127]$.

Fractions $0.y$ are represented by binary fractions $0.y \equiv 0.y_1y_2 \ldots y_n$ ($y_i \in \{0, 1\}$) through

$$0.y = y_1 2^{-1} + y_2 2^{-2} + \ldots + y_n 2^{-n} \,. \tag{7.2}$$

A byte can then store fractional numbers in the range $[0.1)$ with the precision of $2^{-8} = 1/256$.

7.2 Circuits

Computation is a manipulation of the digital data according to a program which in turn reduces to a sequence of elementary arithmetic operations, examples of which are be given below.

7.2.1 Wires and Gates

Operation of a digital computer can schematically be represented by circuits. Circuits consist of wires that carry bits in space or in time (or both), and logic gates. Logic gate is a function $f : \{0, 1\}^k \to \{0, 1\}^l$ taking k input bits and returning l output bits. One usually distinguishes one-bit, two-bit or more-bit logic gates.

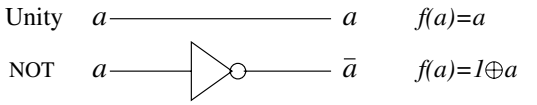

Fig. 7.1. Unity and NOT one-bit logic gates.

One-bit logic gates are shown in Fig. 7.1. These are the Unity operation that does not change the bit and therefore coincides with the wire, and the NOT gate that flips the bit $a \to \bar{a}$ changing 1 to 0, and 0 to 1.

Several two-bit logic gates are shown in Fig. 7.2. They take two input bits and return one output bit. The AND gate returns 1 if both input bits are in state 1, otherwise it returns 0. The OR gate returns 0 if both input bits are in state 0, otherwise it returns 1. The XOR gate output is conveniently represented by $a \oplus b$, where $\oplus$ is addition modulo 2 operation that returns 0 if $a = b$ and 1 if $a \neq b$. The action of the last two gates, NAND and NOR corresponds to applying the NOT gate to the output from the AND and OR gates, respectively. One can construct three- and more-bit gates as well. Examples of three-bit gates will be given in Sect. 7.4. As discussed at the end of this section, however, just a few fixed gates, supplemented by two additional operations, can

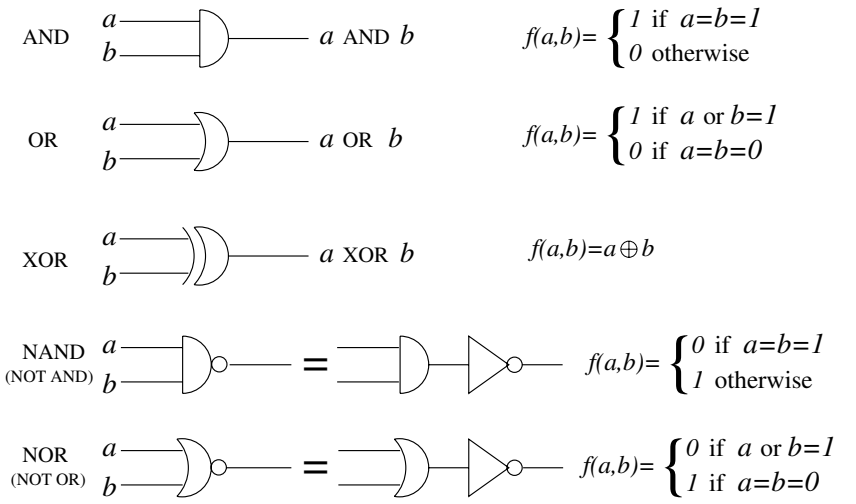

Fig. 7.2. AND, OR, XOR, NAND and NOR two-bit logic gates.

compute any function, and therefore are said to implement the Universal circuit construction. The two additional operations shown in Fig. 7.3 are the copying operation FANOUT and swapping operation CROSSOVER.

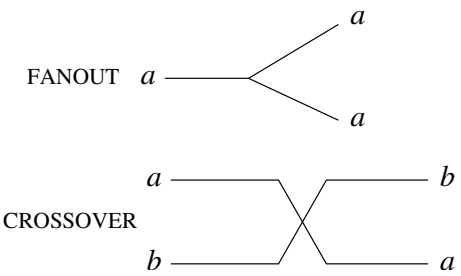

Fig. 7.3. FANOUT bit-copying and CROSSOVER bit-swapping operations.

7.2.2 Circuit Examples

Programming is translating an algorithm for performing certain task into a sequence of instructions for a computer. Hence algorithms define circuits to perform desired computations.

Let us consider now an example of circuit that can perform a useful operation, add two single-digit binary numbers x and y. The circuit for doing this is called half–adder circuit shown in Fig. 7.4. The output of this circuit is a two-digit number representing the sum of x and y. This sum can take values

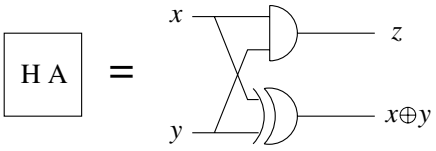

In x+y	Out $z, x\oplus y$
0+0	00
0+1	01
1+0	01
1+1	10

Fig. 7.4. Half–Adder circuit and the corresponding truth-table.

from 00 = 0 to 10 = 2, while the largest value that a two-digit binary number can hold is 11 = 3. It is therefore capable of holding the result of addition of three binary numbers x, y and z, which is realized by the full–adder circuit shown in Fig. 7.5. The circuit uses two half–adders and one OR gate, all together five two-bit gates.

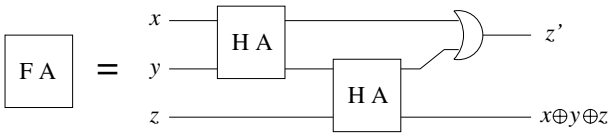

In x+y+z	Out z', $x\oplus y\oplus z$
0+0+0	00
0+0+1	01
0+1+0	01
0+1+1	10
1+0+0	01
1+0+1	10
1+1+0	10
1+1+1	11

Fig. 7.5. Full–Adder circuit and the corresponding truth-table.

It is not difficult now to construct a circuit adding two binary n-digit numbers $x = x_1x_2 \ldots x_n$ and $y = y_1y_2 \ldots y_n$, as shown in Fig. 7.6 for three-digit numbers. The generalization to arbitrary n is straightforward.

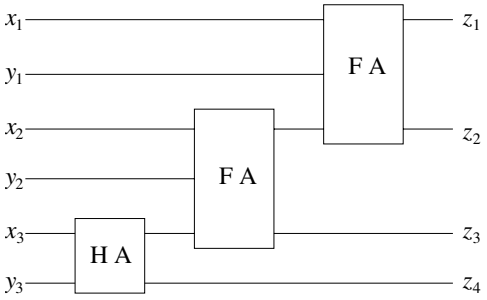

Fig. 7.6. Circuit adding two three-digit numbers $x = x_1x_2x_3$ and $y = y_1y_2y_3$.

7.2.3 Elements of Universal Circuit Construction

One of the main tenets of classical computation theory is that just a few fixed gates can be used to compute *any* function $f : \{0,1\}^n \to \{0,1\}^m$. It is easy to prove it for a Boolean function $f : \{0,1\} \to \{0,1\}$ taking one input bit and returning single output bit. There are four possible functions of this kind: the identity corresponding to a singe wire, the bit flip corresponding to a single NOT gate, the function returning 0 for any input, which can be implemented by applying the XOR on two copies of the input bit, and the function returning 1 for any input, which can be implemented by applying the XOR on two copies of the input bit followed by the NOT gate. The general proof for an arbitrary function $f : \{0,1\}^n \to \{0,1\}^m$ relies on induction and can be found in many textbooks on the theory of computation.

There are five basic elements in the Universal circuit construction:

1. Wires.
2. Ancilla (auxiliary) bits a_k prepared in a standard state, e.g., $a_k = 0$.
3. FANOUT copying operation.
4. CROSSOVER swapping operation.
5. Single bit NOT and two-bit AND and XOR gates.

In the last item, the required NOT, AND and XOR gates (as well as the OR gate) can be implemented using just NAND gate, as shown in Fig. 7.7. The NAND gate is therefore said to be universal.

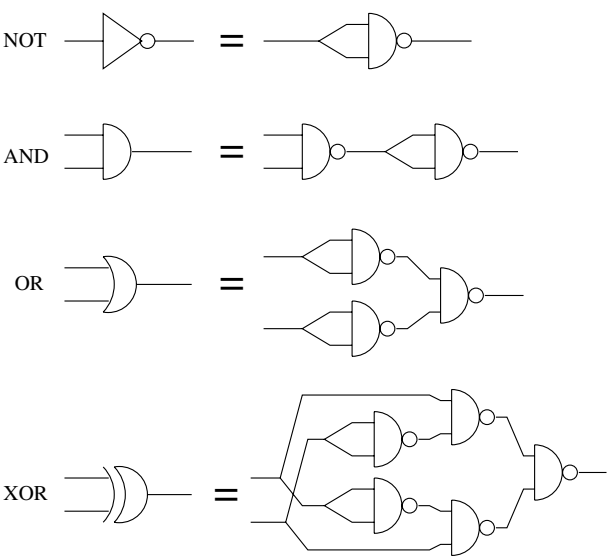

Fig. 7.7. Implementation of the NOT, AND, OR and XOR gates using the NAND gate.

7.3 Computational Resources

An important part of the analysis of computational problems is an estimation of the resources required to solve a given problem. The computational resources include the space, or memory (number of bits), required to hold and manipulate the data, and time, or complexity of the circuit (number of elementary steps) required to process the data. The vital question then is: What are the minimal resources needed to solve a given computational problem? The answer to this question ranks the problem among one or another complexity class.

Consider a problem of size N, where N is the number of bits containing the input and, possibly, the associated data required to process it. If the problem can be solved using resources which are bounded by a polynomial in N, then the problem can be solved efficiently. This means that if the problem is resized to $N' > N$, then the computational resources grow modestly (polynomially) with N, and the problem is said to be an easy or tractable problem. If, on the other hand, the problem requires resources which grow with N faster than any polynomial in N (e.g., exponentially), the problem cannot be solved efficiently on a computer, and it is said to be a hard or intractable problem.

Ranking the computational problems as easy or hard is rather coarse. While there are hard problems for which it is rigorously proven that the best algorithm needs resources growing exponentially in the problem size, for other cases there may exist efficient algorithms that are simply not known yet. Many algorithms are frequently used to solve moderate size problems that may be ranked as hard according the definition above. On the other hand, an easy problem of enormous size may be intractable and very costly for present-day computers. As expressed by Papadimitriou, however, "adopting polynomial worst-case performance as our criterion of efficiency results in an elegant and useful theory that says something meaningful about practical computation, and would be impossible without this simplification." The detailed study of complexity classes of computational problems is an important part of computer science and applied mathematics, which is beyond the scope of the present text.

7.4 Reversible Computation

The model of computation discussed until now is intrinsically irreversible. This is because the two-bit gates used to construct circuits are irreversible as they involve two input bits and only one output bit. Thus one cannot deduce the input of the gate from its output. Consider, as an example, the AND gate. The possible inputs are {00}, {01},{10} and {11}, and the outputs are 0 for the first three inputs and 1 for the last input. Thus with a 0 at the output, one cannot determine which of the three possible inputs were fed into the gate; this information is lost. Another example is the XOR gate, for which the

inputs {00} and {11} yield 0, and inputs {01} and {10} yield 1 at the output. Conversely, finding a 0 at the output can not disclose whether the input was {00} or {11} and similarly, finding a 1 at the output can not disclose whether the input was {01} or {10}.

In these examples, the number of input bits to the circuit is less then the number of output bits. The information carried by the excess bits is discarded which inevitably leads to energy dissipation according to the Landauer's principle: Erasing a single bit of information leads to dissipation of at least $k_B T \ln 2$ Joule of energy into the environment with temperature T. Alternatively one may say that the entropy of the environment increases by at least $k_B \ln 2$, as required by thermodynamics. This determines the fundamental lower limit of energy consumed and dissipated by the computer in the course of operation. Therefore if one realizes a reversible computation, which is not accompanied by bit erasure, one would reduce the energy dissipation. We should note, however, that present day computers consume more than $100 k_B T \ln 2$ Joule of energy per dissipated bit, which is quite far from the fundamental lower limit. Semiconductor nanotechnology is, however, evolving with enormous pace and perhaps in the not-very-distant future, the fundamental lower limit may be approached, in which case the construction of a reversible computer will become an important technological objective.

Toffoli (CCNOT) gate

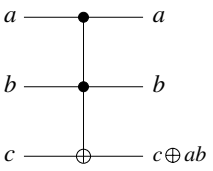

In *a,b,c*	Out *a',b',c'*
0 0 0	0 0 0
0 0 1	0 0 1
0 1 0	0 1 0
0 1 1	0 1 1
1 0 0	1 0 0
1 0 1	1 0 1
1 1 0	1 1 1
1 1 1	1 1 0

Fredkin (CSWAP) gate

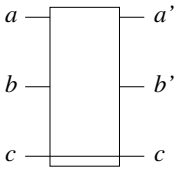

In *a,b,c*	Out *a',b',c'*
0 0 0	0 0 0
0 0 1	0 0 1
0 1 0	0 1 0
0 1 1	1 0 1
1 0 0	1 0 0
1 0 1	0 1 1
1 1 0	1 1 0
1 1 1	1 1 1

Fig. 7.8. Toffoli (Controlled-Controlled-NOT) gate and Fredkin (Controlled-SWAP) gate.

It turns out that employing the universal three-bit Toffoli or Fredkin gates, shown in Fig. 7.8, one can realize reversible circuit construction capable of universal computation. The action of the Toffoli gate is to flip the target bit c conditional upon the states of the two control bits a and b; the target bit is flipped $c \to \bar{c}$ if $a = b = 1$, otherwise it is unchanged. The Fredkin gate interchanges the target bits a and b conditional upon the state of the control bit c; the target bits are swapped $a \leftrightarrow b$ if $c = 1$, otherwise they are unchanged. It is easy to see that the output of either Toffoli or Fredkin gate uniquely determines the corresponding input and therefore no information is lost.

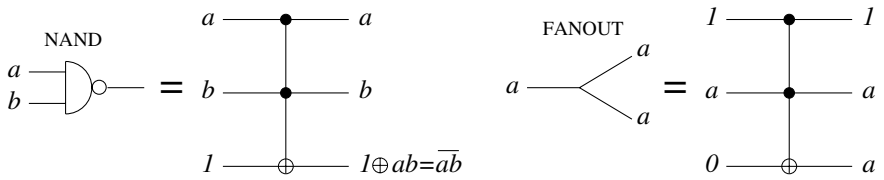

Fig. 7.9. Implementation of the NAND and FANOUT operations using the Toffoli gate.

Using a single ancilla bit, the Toffoli gate can implement the universal NAND and FANOUT operations, as shown in Fig. 7.9. Similarly, it is a simple exercise to show that the Fredkin gate can also be configured to simulate the NOT, AND, CROSSOVER and FANOUT operations (see Prob. 7.5). Therefore either of the three-bit reversible gates can be cascaded to simulate *any* classical circuit. In general, with a small resource overhead due to the use of ancilla bits, any irreversible circuit computing a function $f(x)$ can be efficiently simulated by a reversible circuit with the action $(x, y) \to (x, y \oplus f(x))$. Then reversal of the computation can be achieved by repeated application of the circuit $(x, y \oplus f(x)) \to (x, y \oplus f(x) \oplus f(x)) = (x, y)$.

Problems

7.1. What is the largest positive integer number that can be stored in a 8, 16 or 32 bit register?

7.2. What is the smallest positive real number that can be stored in a 8, 16 or 32 bit register?

7.3. Compose a circuit to add two 5 digit binary numbers.

7.4. Verify the implementations of the NOT, AND, OR and XOR gates using the NAND gates of Fig. 7.7. Compose a different implementation of the XOR gate using 6 NAND gates. (*Hint*: Combine the NAND gates with the OR and AND gates implemented by NAND gates.)

7.5. Implement the NOT, AND, FANOUT and CROSSOVER operations using the Fredkin gate.

8

Fundamentals of Quantum Information

We turn now to the description of the building blocks of quantum information theory. We introduce the quantum analog of the bit—qubit, single- and multiple-qubit logic gates and quantum circuits performing information processing. Any introduction to quantum information theory would be incomplete if it did not contain a discussion on the peculiar properties of the entanglement, which results, on the one hand, in the notorious non-locality of quantum mechanics, and on the other hand, in decoherence already studied in previous chapters in the general framework of a small quantum system coupled to a large reservoir. A significant part of this chapter is therefore devoted to the analysis of the role of entanglement in the fundamental tests of quantum mechanics, as well as its quantum information applications such as cryptography, teleportation and dense coding.

8.1 Quantum Bits and Memory

In quantum information theory, the elementary unit of information is a quantum bit—qubit. A qubit is represented by a quantum mechanical system with two orthogonal states conventionally denoted by $|0\rangle$ and $|1\rangle$. These states form the computational basis $\{|0\rangle, |1\rangle\}$, whereas their orthogonality implies $\langle 0|1\rangle = 0$. A qubit can be not only in one of the basis states, but also in any superposition state of the form

$$|\psi_1\rangle = \alpha\,|0\rangle + \beta\,|1\rangle\ , \tag{8.1}$$

where the coefficients α and β are arbitrary complex numbers normalized to unity according to $|\alpha|^2 + |\beta|^2 = 1$. Hence, unlike the classical bit which can only store a discrete variable taking two real values, the qubit can represent a continuum of states spanned by a unit vector in a two-dimensional complex vector space. Thus, when both coefficients of superposition (8.1) are nonzero, the qubit, in a sense, simultaneously contains both possible values of classical

bit 0 and 1, each having the corresponding probability amplitude α and β. As discussed in detail in Chap. 9, this fact is at the heart of all quantum algorithms that explore the superposition principle, combined with quantum interference to achieve the massive parallelism in solving certain computational problems that are otherwise intractable on classical computers.

A pair of qubits can exist is any state of the form

$$|\psi_2\rangle = c_{00}\,|00\rangle + c_{01}\,|01\rangle + c_{10}\,|10\rangle + c_{11}\,|11\rangle\ , \tag{8.2}$$

where the complex coefficients c_x ($x = 00, \ldots, 11$) are normalized as $\sum_x |c_x|^2 = 1$. In general, the compound state $|\psi_2\rangle$ is an entangled state of two qubits, meaning that it can not be factorized into a product state of the qubits $(\alpha\,|0\rangle + \beta\,|1\rangle) \otimes (\alpha'\,|0\rangle + \beta'\,|1\rangle)$. Only when the coefficients of (8.2) satisfy $c_{00} = \alpha\alpha'$, $c_{01} = \alpha\beta'$, $c_{10} = \beta\alpha'$ and $c_{11} = \beta\beta'$, is the decomposition into the product state possible, in which case the state is factorisable. Important examples of two-qubit (bipartite) entangled states are the Bell states, also known as Einstein–Podolsky–Rosen (EPR) states

$$|B_{00}\rangle = \tfrac{1}{\sqrt{2}}(\,|00\rangle + |11\rangle)\ , \quad |B_{01}\rangle = \tfrac{1}{\sqrt{2}}(\,|01\rangle + |10\rangle)\ , \tag{8.3a}$$

$$|B_{10}\rangle = \tfrac{1}{\sqrt{2}}(\,|00\rangle - |11\rangle)\ , \quad |B_{11}\rangle = \tfrac{1}{\sqrt{2}}(\,|01\rangle - |10\rangle)\ . \tag{8.3b}$$

These are maximally entangled states in the sense that if we discard the information pertaining to one of the qubits, the measurement performed on the other qubit of the pair would yield completely random result, as discussed in more detail in Sect. 8.5. The Bell states are widely employed in quantum communication protocols such as teleportation and dense coding, as well as in fundamental tests of the locality of quantum mechanics, described later in this chapter.

In general, an n-qubit register has 2^n mutually orthogonal states which, in the computational basis, are of the form $|x_1 x_2 \ldots x_n\rangle$, where $x_k \in \{0, 1\}$ for $1 \le k \le n$. Any state of the register can therefore be specified by 2^n complex amplitudes c_x, $x \equiv x_1 x_2 \ldots x_n$, via

$$|\psi_n\rangle = \sum_x c_x\,|x\rangle\ , \qquad \sum_x |c_x|^2 = 1\ . \tag{8.4}$$

Thus, even for a modest number of qubits $n < 100$, the number of amplitudes c_x specifying the state of quantum system is very large. Storing and manipulating such an amount of complex numbers with classical computers is an enormously costly task. Hence the inefficiency of classical computers in simulating quantum mechanics, as discussed in more detail in Sect. 9.3

Let us finally present the many qubit "analogs" of Bell states. One family of such fully-entangled multiqubit states is known as the Greenberger–Horne–Zeilinger states, or GHZ for short,

$$|\mathrm{GHZ}\rangle = \tfrac{1}{\sqrt{2}}(\,|000\ldots0\rangle \pm |111\ldots1\rangle)\ . \tag{8.5}$$

As discussed in Sect. 8.8.3, such states are even more compelling than the Bell states in revealing the non-local nature of quantum mechanics. Another family of multiqubit entangled states is called the W states, having the form

$$|\mathrm{W}_n\rangle = \frac{1}{\sqrt{N}}(\,|00\ldots01\rangle + |00\ldots10\rangle + \ldots + |01\ldots00\rangle + |10\ldots00\rangle)\,. \quad (8.6)$$

Thus a W state of n qubits consists of an equally weighted superposition of n states, each of which has exactly one qubit in state $|1\rangle$ and all the others in state $|0\rangle$.

8.2 Quantum Circuits

As in classical computers, the operation of quantum computers can be represented by circuits consisting of quantum wires that carry qubits and quantum logic gates. One distinguishes one-qubit and multiple-qubit logic gates, acting, respectively on one and many qubits. Since quantum computation is reversible, in any quantum logic gate the number of input and output qubits must be the same. In addition, only the quantum logic gates that preserve the norm $\sum_x |c_x|^2 = 1$ of the register's wavevector $|\psi_n\rangle$ for all times are allowed in quantum circuits. Therefore the logic gates can be represented by quantum mechanical unitary operators acting on the state of the register.

8.2.1 One Qubit Gates

Consider first single-qubit logic gates. A general one-qubit logic gate is described by a 2×2 unitary matrix $U = \begin{bmatrix} \alpha & \gamma \\ \beta & \delta \end{bmatrix}$ that transforms the qubit state $|0\rangle$ to $\alpha\,|0\rangle + \beta\,|1\rangle$ and state $|1\rangle$ to $\gamma\,|0\rangle + \delta\,|1\rangle$. Examples of one-qubit logic gates are shown in Fig. 8.1. These are the Unity I, Hadamard H, Pauli X, Y and Z, and Phase S gates. The matrix representation of operators corresponding to these gates is shown on the right of each gate. The action of the gate is therefore equivalent to the action of the corresponding operator on the input state of the qubit. For the Unity gate we have $I\,|\psi_1\rangle = |\psi_1\rangle$ which leaves the qubit state unchanged being thus equivalent to the wire. The Hadamard gate transforms the initial state of the qubit $|0\rangle$ or $|1\rangle$ to an evenly weighted superposition of its two basis states

$$H\,|0\rangle \to \frac{1}{\sqrt{2}}(\,|0\rangle + |1\rangle) \equiv |+\rangle\,,$$
$$H\,|1\rangle \to \frac{1}{\sqrt{2}}(\,|0\rangle - |1\rangle) \equiv |-\rangle\,.$$

We can cast this in a compact form, obtaining a very useful expression

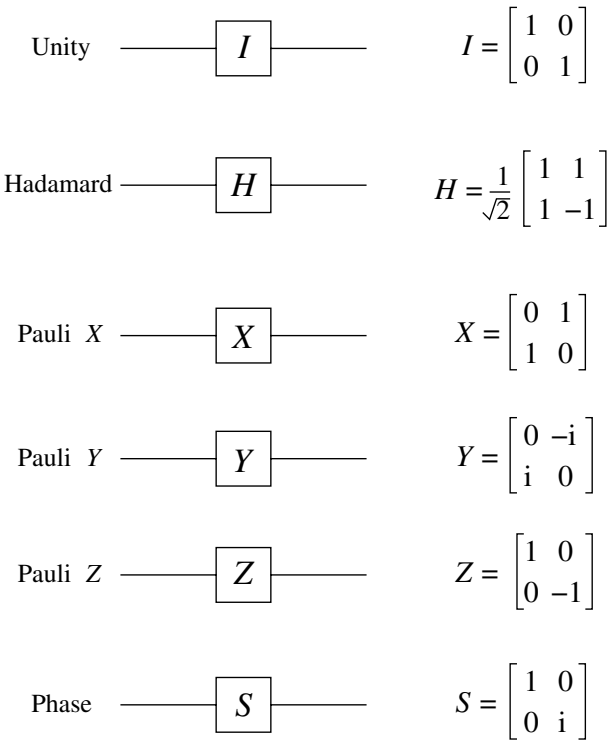

Fig. 8.1. Unity I, Hadamard H, Pauli X, Y and Z, and Phase S one-qubit logic gates.

$$H\,|x\rangle = \sum_z \frac{(-1)^{xz}\,|z\rangle}{\sqrt{2}}\ , \tag{8.7}$$

where $x, z \in \{0, 1\}$. Consequently, an arbitrary qubit state $|\psi_1\rangle$ given by (8.1) is transformed according to

$$H\,|\psi_1\rangle = \frac{1}{\sqrt{2}} \begin{bmatrix} 1 & 1 \\ 1 & -1 \end{bmatrix} \begin{bmatrix} \alpha \\ \beta \end{bmatrix} \to \frac{1}{\sqrt{2}} \begin{bmatrix} \alpha+\beta \\ \alpha-\beta \end{bmatrix} = \frac{1}{\sqrt{2}}[(\alpha+\beta)\,|0\rangle + (\alpha-\beta)\,|1\rangle]\ . \tag{8.8}$$

The X, Y and Z gates are equivalent to the Pauli spin-$\frac{1}{2}$ operators σ_x, σ_y, σ_z, respectively. The X gate flips the qubit state according to

$$\begin{aligned} X\,|0\rangle &\to |1\rangle\ , \\ X\,|1\rangle &\to |0\rangle\ , \\ X\,|\psi_1\rangle = \begin{bmatrix} 0 & 1 \\ 1 & 0 \end{bmatrix} \begin{bmatrix} \alpha \\ \beta \end{bmatrix} &\to \begin{bmatrix} \beta \\ \alpha \end{bmatrix} = (\beta\,|0\rangle + \alpha\,|1\rangle)\ , \end{aligned} \tag{8.9}$$

which is the quantum analog of the NOT gate. Similarly for the Y gate we have

$$
\begin{aligned}
Y\,|0\rangle &\to \mathrm{i}\,|1\rangle\ , \\
Y\,|1\rangle &\to -\mathrm{i}\,|0\rangle\ , \\
Y\,|\psi_1\rangle = \begin{bmatrix} 0 & -\mathrm{i} \\ \mathrm{i} & 0 \end{bmatrix} \begin{bmatrix} \alpha \\ \beta \end{bmatrix} &\to \begin{bmatrix} -\mathrm{i}\beta \\ \mathrm{i}\alpha \end{bmatrix} = -\mathrm{i}(\beta\,|0\rangle - \alpha\,|1\rangle)\ .
\end{aligned} \tag{8.10}
$$

The Z gate introduces the phase-shift π to the qubit state $|1\rangle$ while leaving state $|0\rangle$ unchanged

$$
\begin{aligned}
Z\,|0\rangle &\to |0\rangle\ , \\
Z\,|1\rangle &\to -\,|1\rangle\ , \\
Z\,|\psi_1\rangle = \begin{bmatrix} 1 & 0 \\ 0 & -1 \end{bmatrix} \begin{bmatrix} \alpha \\ \beta \end{bmatrix} &\to \begin{bmatrix} \alpha \\ -\beta \end{bmatrix} = (\alpha\,|0\rangle - \beta\,|1\rangle)\ .
\end{aligned} \tag{8.11}
$$

Note that if the qubit is prepared in either $|+\rangle$ or $|-\rangle$ states (using, e.g., the Hadamard gate), the action of the Z gate is to interchange these states, $Z\,|\pm\rangle \to |\mp\rangle$. Finally, the Phase gate S introduces the phase-shift $\pi/2$ to state $|1\rangle$ and leaves state $|0\rangle$ unchanged,

$$
\begin{aligned}
S\,|0\rangle &\to |0\rangle\ , \\
S\,|1\rangle &\to \mathrm{i}\,|1\rangle\ , \\
S\,|\psi_1\rangle = \begin{bmatrix} 1 & 0 \\ 0 & \mathrm{i} \end{bmatrix} \begin{bmatrix} \alpha \\ \beta \end{bmatrix} &\to \begin{bmatrix} \alpha \\ \mathrm{i}\beta \end{bmatrix} = (\alpha\,|0\rangle + \mathrm{i}\beta\,|1\rangle)\ .
\end{aligned} \tag{8.12}
$$

Its action can thus be thought of as "half-way" or square-root of the action of Z gate, as it is easy to check that $SS = Z$. Other useful relations between the single-qubit gates are $HH = XX = YY = ZZ = I$, $H = \frac{1}{\sqrt{2}}(X + Z)$, $XY = \mathrm{i}Z$, $XZ = -\mathrm{i}Y$, $YZ = \mathrm{i}X$, etc.

More generally, an arbitrary single qubit transformation U can be decomposed into the product of the rotation operators $R_y(\theta)$ and $R_z(\theta')$ and an overall phase factor given by $\mathrm{e}^{\mathrm{i}\alpha}$. The expressions for the rotation operators and their physical meaning are given in Sect. 8.4.

8.2.2 Two and More Qubit Gates

Consider now examples of two-qubit logic gates W shown in Fig. 8.2. These are the controlled-NOT (CNOT), SWAP, controlled-Z (CZ) and a general controlled-U gates, where U is any single-qubit unitary transformation. The CNOT is a quantum analog of the classical reversible XOR gate, $|a\rangle\,|b\rangle \to |a\rangle\,|a \oplus b\rangle$ $(a, b \in \{0, 1\})$, whereby the target (lower) qubit b is flipped if the control (upper) qubit a is in state $|1\rangle$, and is left unchanged if the control qubit state is $|0\rangle$. The SWAP is analogous to the classical CROSSOVER transformation, $|a\rangle\,|b\rangle \to |b\rangle\,|a\rangle$, it interchanges the states of the two qubits. The SWAP gate can be implemented by triple application of the CNOT as shown on the second line of Fig. 8.2. Another example of a two-qubit gate is the controlled-Z gate,

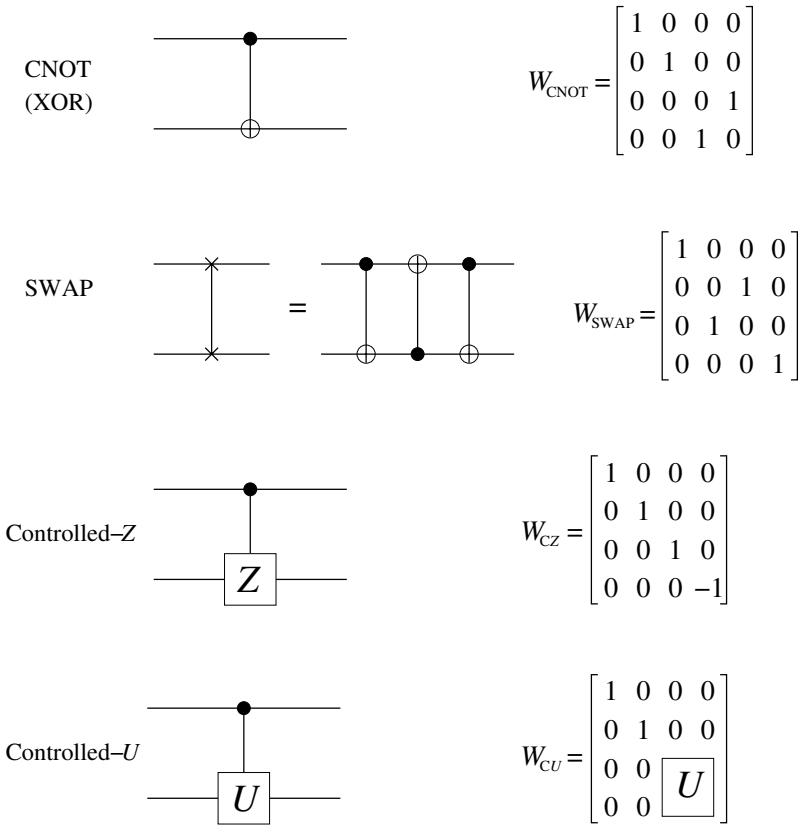

Fig. 8.2. CNOT (controlled-NOT), SWAP, controlled-Z and controlled-U two-qubit logic gates.

$|a\rangle\,|b\rangle \rightarrow (-1)^{ab}\,|a\rangle\,|b\rangle$, where the Z operator is applied to the target qubit conditional upon the state of the control qubit. More generally, any controlled-U transformation is realized by a circuit shown on the last line of Fig. 8.2, where the application of the U operator to the target qubit is triggered by the control qubit if its state is $|1\rangle$.

As in the case of one-qubit gates, the operators W corresponding to the two-qubit gates have convenient matrix representation shown on the right of each gate in Fig. 8.2. There we use the usual convention for numbering the rows and columns of the matrix, $|00\rangle$, $|01\rangle$, $|10\rangle$ and $|11\rangle$, where the first symbol in the kets indicates the state of the control qubit and the second symbol indicates the state of the target. The result of application of, e.g., the CNOT to the general two-qubit state (8.2) can be calculated via

$$W_{\text{CNOT}}\,|\psi_2\rangle = \begin{bmatrix} 1&0&0&0\\ 0&1&0&0\\ 0&0&0&1\\ 0&0&1&0 \end{bmatrix} \begin{bmatrix} c_{00}\\ c_{01}\\ c_{10}\\ c_{11} \end{bmatrix} = \begin{bmatrix} c_{00}\\ c_{01}\\ c_{11}\\ c_{10} \end{bmatrix}\,, \tag{8.13}$$

which shows that the coefficients of states $|10\rangle$ and $|11\rangle$ are interchanged. The same procedure is used to calculate the action of any two-qubit gate.

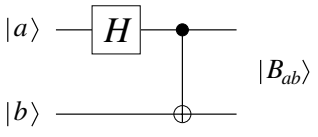

In	Out
$\|00\rangle$	$\frac{1}{\sqrt{2}}(\|00\rangle + \|11\rangle) = \|B_{00}\rangle$
$\|01\rangle$	$\frac{1}{\sqrt{2}}(\|01\rangle + \|10\rangle) = \|B_{01}\rangle$
$\|10\rangle$	$\frac{1}{\sqrt{2}}(\|00\rangle - \|11\rangle) = \|B_{10}\rangle$
$\|11\rangle$	$\frac{1}{\sqrt{2}}(\|01\rangle - \|10\rangle) = \|B_{11}\rangle$

Fig. 8.3. Circuit generating the four Bell states $|B_{ab}\rangle$ and the corresponding truth table.

As an example of a simple circuit, we show in Fig. 8.3 the generation of the four Bell states $|B_{ab}\rangle$ from the the initially unentangled pair of qubits $|a\rangle \otimes |b\rangle$ using the Hadamard and CNOT gates (see Prob. 8.1).

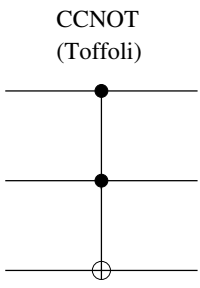

$$U_{\text{CCNOT}} = \begin{bmatrix} 1&0&0&0&0&0&0&0\\ 0&1&0&0&0&0&0&0\\ 0&0&1&0&0&0&0&0\\ 0&0&0&1&0&0&0&0\\ 0&0&0&0&1&0&0&0\\ 0&0&0&0&0&1&0&0\\ 0&0&0&0&0&0&0&1\\ 0&0&0&0&0&0&1&0 \end{bmatrix}$$

Fig. 8.4. CCNOT (controlled-controlled-NOT) or quantum Toffoli logic gate.

Next, in Fig. 8.4 we depict the three-qubit CCNOT (controlled-controlled-NOT) logic gate, which is the quantum analog of the classical universal Toffoli gate, $|a\rangle\,|b\rangle\,|c\rangle \rightarrow |a\rangle\,|b\rangle\,|ab \oplus c\rangle$, whereby the target (lower) qubit c is flipped if both control (upper) qubits a and b are in state $|1\rangle$, and is left unchanged otherwise. As discussed in Sect. 9.1.1, any multiqubit unitary transformation, including the quantum Toffoli gate, can be efficiently simulated by an appropriate circuit that involves only single- and two-qubit operations. In par-

ticular, the combination of the single-qubit and CNOT gates can implement any multiqubit gate with an arbitrary number of control and target qubits.

8.2.3 Qubit Measurement

Let us revisit some of the properties of quantum measurement, already discussed in Sect. 1.2.4, in their application to qubits. In discussing classical bits, we have tacitly assumed that one can easily measure the bit as many times as one wishes, without disturbing its state, and the result of the measurement is 0 if the bit state is 0, and 1 if the state is 1. This is indeed the case in classical information processing devises. In quantum mechanics the situation is drastically different: If one has a single copy of a quantum system—a qubit in an arbitrary state $|\psi_1\rangle = \alpha\,|0\rangle + \beta\,|1\rangle$, the measurement yields *either* $|0\rangle$ *or* $|1\rangle$. A single measurement does not allow one to infer the amplitudes α and β of the quantum state. Moreover, the no-cloning theorem, discussed in the following section, forbids one to clone an unknown quantum state so as to produce many copies of the system. In addition, the measuring process itself modifies the state of the system: If during the measurement one finds the system, e.g., in $|0\rangle$, the post-measurement state of the system will be $|\psi_1^{\rm pm}\rangle = \Pi_0\,|\psi_1\rangle/\sqrt{P_0} = |0\rangle$, where $\Pi_0 = |0\rangle\langle 0|$ is the projection operator and P_0 stands for the renormalization of the wavefunction. Similarly, finding the system in $|1\rangle$ yields the post-measurement state $|\psi_1^{\rm pm}\rangle = \Pi_1\,|\psi_1\rangle/\sqrt{P_1} = |1\rangle$, where $\Pi_1 = |1\rangle\langle 1|$. The probabilities of finding the system in state $|0\rangle$ or $|1\rangle$ are given, respectively, by $P_0 = \langle\psi_1|\,\Pi_0\,|\psi_1\rangle = |\alpha|^2$ and $P_1 = \langle\psi_1|\,\Pi_1\,|\psi_1\rangle = |\beta|^2$, but these probabilities can experimentally be determined only after many measurements on the ensemble of identical systems all being in state $|\psi\rangle$.

Consider now the measurement performed on a subset of a composite quantum system. The simplest example is a pair of qubits in state (8.2). If we measure the state of the first qubit with the result $|0\rangle$, the post-measurement state of the system collapses to

$$|\psi_2^{\rm pm}\rangle = \frac{\Pi_0^1\,|\psi_2\rangle}{\sqrt{P_0^1}} = \frac{c_{00}\,|00\rangle + c_{01}\,|01\rangle}{\sqrt{|c_0 0|^2 + |c_0 0|^2}} = |0\rangle\,\frac{c_{00}\,|0\rangle + c_{01}\,|1\rangle}{\sqrt{|c_0 0|^2 + |c_0 0|^2}}\,.$$

This shows, in particular, that even if the two qubits were initially entangled, after measuring the first qubit the state of the system becomes factorisable and, in general, the second qubit is left in a superposition state.

Fig. 8.5. Symbol designating qubit measurement in the computational basis.

The last, but not least, important ingredient of quantum circuits is the projective measurement, which is denoted by the symbol shown in Fig. 8.5.

It is applied at the end of the circuit to yield the result of computation, but often the measurement is also performed in the middle of computation to control the subsequent quantum gates, as is the case in, e.g., quantum error correction discussed in Sect. 9.4.

It is sufficient to perform the measurement on individual qubits only in the computational basis $\{|0\rangle, |1\rangle\}$. If we need to perform a measurement in some other orthogonal basis, we can apply a suitable unitary operator to transform the basis to the computational one and then measure. For example, if we want to perform a measurement that distinguishes the states $|\pm\rangle = \frac{1}{\sqrt{2}}(|0\rangle \pm |1\rangle)$, the required unitary transformation is the Hadamard gate H which transforms the basis $\{|+\rangle, |-\rangle\}$ to $\{|0\rangle, |1\rangle\}$.

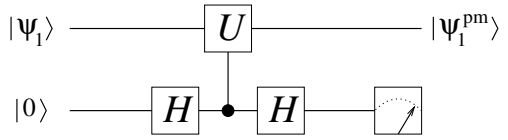

Fig. 8.6. Circuit for measuring the observable U.

Finally, suppose we want to measure an observable associated with an operator U acting on a qubit in state $|\psi_1\rangle$ and having the eigenvalues ± 1 and the corresponding eigenstates $|\psi_\pm\rangle$. The circuit for doing this is shown in Fig. 8.6. Recall that we can represent state $|\psi_1\rangle$ in terms of the eigenstates $|\psi_\pm\rangle$ as $|\psi_1\rangle = c_+ |\psi_+\rangle + c_- |\psi_-\rangle$. Following the steps of the circuit, we have

$$\begin{aligned} |\psi_1\rangle |0\rangle &\xrightarrow{H} \frac{1}{\sqrt{2}} |\psi_1\rangle (|0\rangle + |1\rangle) \xrightarrow{W_{CU}} \frac{1}{\sqrt{2}} (|\psi_1\rangle |0\rangle + U |\psi_1\rangle |1\rangle) \\ &= \frac{1}{\sqrt{2}} [(c_+ |\psi_+\rangle + c_- |\psi_-\rangle) |0\rangle + (c_+ |\psi_+\rangle - c_- |\psi_-\rangle) |1\rangle] \\ &\xrightarrow{H} c_+ |\psi_+\rangle |0\rangle + c_- |\psi_-\rangle |1\rangle \, . \end{aligned} \tag{8.14}$$

Consequently, detecting the lower (ancilla) qubit in state $|0\rangle$ or $|1\rangle$ indicates, respectively, the eigenvalue $+1$ or -1 of operator U, while the post-measurement state of the interrogated qubit collapses to the corresponding eigenstate of U,

$$|\psi_1^{\rm pm}\rangle = |\psi_\pm\rangle \, . \tag{8.15}$$

Note that in (8.14) we have only used the fact that U has just two eigenvalues ± 1; we did not explicitly rely on whether U corresponds to a single or many qubit observable. This measurement scheme can therefore be applied equally well to observables U acting on any number of qubits but having only two eigenvalues ± 1.

8.3 No-Cloning Theorem

In the previous section, we have identified the quantum analogs of the classical one- and multi-bit gates, including the CROSSOVER swapping operation that is realized by the quantum SWAP gate. What is still missing is the copying operation. At first sight it may seem that copying qubits is possible by employing the quantum CNOT gate,

$$W_{\text{CNOT}}\,|0\rangle\,|0\rangle \rightarrow |0\rangle\,|0\rangle\ ,$$
$$W_{\text{CNOT}}\,|1\rangle\,|0\rangle \rightarrow |1\rangle\,|1\rangle\ .$$

If the control qubit is in state $|0\rangle$ *or* $|1\rangle$, the target qubit initially prepared in state $|0\rangle$ after the action of CNOT gate acquires the state of the control. We thus obtain two copies of the control qubit. Consider now the control qubit in a general superposition state (8.1) with $\alpha, \beta \neq 0$,

$$W_{\text{CNOT}}(\alpha\,|0\rangle + \beta\,|1\rangle)\,|0\rangle \rightarrow \alpha\,|0\rangle\,|0\rangle + \beta\,|1\rangle\,|1\rangle \neq (\alpha\,|0\rangle + \beta\,|1\rangle)(\alpha\,|0\rangle + \beta\,|1\rangle)\ . \tag{8.16}$$

Unfortunately, the output state is an entangled state rather than the product state $|\psi_1\rangle\,|\psi_1\rangle$ of the two-qubits and the copying operation fails.

What we have encountered above is the manifestation of a fact crucial to quantum information theory called the no-cloning theorem, which states that an unknown quantum state cannot be cloned or copied. Before proving it, let us note that if the quantum state *is* known, then one can produce its copy, or clone, by first preparing the system in a known well-defined state, say one of its eigenstates, and then applying a sequence of unitary transformations that would result in the desired state. But if the state of a quantum system is not known, it can not be determined with a measurement performed on a single copy of the system.

To prove the no-cloning theorem, assume the opposite: There exists a unitary transformation $\mathcal{U}_{\text{clone}}$ such that, for *any* two states $|\psi\rangle \neq |\phi\rangle$ of the system (not necessarily a qubit) one has

$$\mathcal{U}_{\text{clone}}\,|\psi\rangle\,|0\rangle = |\psi\rangle\,|\psi\rangle\ , \tag{8.17a}$$
$$\mathcal{U}_{\text{clone}}\,|\phi\rangle\,|0\rangle = |\phi\rangle\,|\phi\rangle\ , \tag{8.17b}$$

where $|0\rangle$ denotes some well-defined initial state of the target system, whose dimension should be at least as large as that of the control system we wish to clone. Consider the state $|\sigma\rangle = \frac{1}{\sqrt{2}}(\,|\psi\rangle + |\phi\rangle)$. Since, as assumed, $\mathcal{U}_{\text{clone}}$ can produce a copy of any state, then one should have $\mathcal{U}_{\text{clone}}\,|\sigma\rangle\,|0\rangle = |\sigma\rangle\,|\sigma\rangle$. But from (8.17) one has

$$\begin{aligned}\mathcal{U}_{\text{clone}}\,|\sigma\rangle\,|0\rangle &= \mathcal{U}_{\text{clone}}\frac{1}{\sqrt{2}}(\,|\psi\rangle + |\phi\rangle)\,|0\rangle = \frac{1}{\sqrt{2}}(\,|\psi\rangle\,|\psi\rangle + |\phi\rangle\,|\phi\rangle)\\ &\neq |\sigma\rangle\,|\sigma\rangle = \frac{1}{2}(\,|\psi\rangle\,|\psi\rangle + |\psi\rangle\,|\phi\rangle + |\phi\rangle\,|\psi\rangle + |\phi\rangle\,|\phi\rangle)\ ,\end{aligned} \tag{8.18}$$

arriving at a contradiction which proves the theorem. □

We have thus seen that one can only clone a qubit being in one of its basis states and not in a superposition state. More generally, one can only clone quantum states that are orthogonal to each other, while an arbitrary superposition state cannot be cloned. This limitation on quantum information processing and communication devices has several important implications, such as the possibility of realizing secure quantum communication channels and the impossibility of communicating information faster than light (see Prob. 8.2).

8.4 Genuine Physical Qubits

So far we have considered the qubits as abstract mathematical objects—unit vectors in a two-dimensional complex vector space,—without specifying physical systems which can actually represent them. We outline now two simple quantum mechanical systems, spin-$\frac{1}{2}$ particle and single photon, both having just two orthogonal states (spin projection and photon polarization, respectively), which makes them natural qubit candidates. In general, any quantum mechanical system having a pair of well-characterized orthogonal states may serve as a qubit. The actual choice of the system is dictated by the practical considerations of the feasibility to robustly store and manipulate the quantum information imprinted on the system. Several such systems are considered in some detail in Chap. 10

8.4.1 Spin-$\frac{1}{2}$ Qubit

Let us recall the properties of a particle having intrinsic angular momentum—spin—equal to $\frac{1}{2}\hbar$, e.g., electron (see Sect. 3.1.2). The projection of the spin along any axis can take two values $\pm\frac{1}{2}$ (in units of $\hbar$). If one chooses a particular quantization direction z, the spin-up $|\uparrow_z\rangle$ and spin-down $|\downarrow_z\rangle$ eigenstates of the spin operator $\boldsymbol{s}$ along the z-axis will uniquely define the two basis states of the qubit according to $|0\rangle = |\uparrow_z\rangle$ and $|1\rangle = |\downarrow_z\rangle$. The spin operator is conveniently expressed through the dimensionless operator $\boldsymbol{\sigma}$ as $\boldsymbol{s} = \frac{1}{2}\boldsymbol{\sigma}$. The three spatial components of $\boldsymbol{\sigma}$ along the x, y and z axes are described, respectively, by the Pauli matrices

$$\sigma_x = \begin{bmatrix} 0 & 1 \\ 1 & 0 \end{bmatrix} , \quad \sigma_y = \begin{bmatrix} 0 & -\mathrm{i} \\ \mathrm{i} & 0 \end{bmatrix} , \quad \sigma_z = \begin{bmatrix} 1 & 0 \\ 0 & -1 \end{bmatrix} , \tag{8.19}$$

which obey the angular momentum commutation relations

$$[\sigma_x, \sigma_y] = 2\mathrm{i}\sigma_z , \quad [\sigma_y, \sigma_z] = 2\mathrm{i}\sigma_x , \quad [\sigma_z, \sigma_x] = 2\mathrm{i}\sigma_y . \tag{8.20}$$

Additionally, we have

$$\sigma_y\sigma_z + \sigma_z\sigma_y = 0\ ,\quad \sigma_z\sigma_x + \sigma_x\sigma_z = 0\ ,\quad \sigma_x\sigma_y + \sigma_y\sigma_x = 0\ , \tag{8.21}$$

or in a compact form $\sigma_i\sigma_j + \sigma_j\sigma_i = 2\delta_{ij}I$, i.e., the Pauli matrices anticommute. The frequently used pseudo-spin raising σ^+ and lowering σ^- operators are defined, as in Sect. 3.3.2, through

$$\sigma^+ = \tfrac{1}{2}[\sigma_x + \mathrm{i}\sigma_y] = \begin{bmatrix} 0 & 1 \\ 0 & 0 \end{bmatrix}\ ,\quad \sigma^- = \tfrac{1}{2}[\sigma_x - \mathrm{i}\sigma_y] = \begin{bmatrix} 0 & 0 \\ 1 & 0 \end{bmatrix}\ . \tag{8.22}$$

The density operator ρ for the spin-$\frac{1}{2}$ particle (or indeed any two-state quantum system, including the two-level atom) is obviously a 2×2 matrix. It can conveniently be expressed in terms of the Bloch vector $\boldsymbol{u} = (u_x, u_y, u_z)$ as

$$\rho = \tfrac{1}{2}(I + \boldsymbol{u}\cdot\boldsymbol{\sigma}) = \tfrac{1}{2}(I + u_x\sigma_x + u_y\sigma_y + u_z\sigma_z)\ . \tag{8.23}$$

The density matrix can then be visualized with the help of the Bloch sphere spanned by vector $\boldsymbol{u}$ whose direction corresponds to the direction of the expectation value of the spin. The length of the Bloch vector is limited by $0 \le |\boldsymbol{u}| \le 1$, the value 1 corresponding to the pure states of the spin lying on the surface of Bloch sphere with unit radius, while 0 indicates the completely mixed state $\rho = \frac{1}{2}I$.

Any unitary transformation U performed on a spin reduces to a product of an overall phase shift of the form $\mathrm{e}^{\mathrm{i}\alpha}$ and rotation of the spin by an angle θ about some axis $\hat{\boldsymbol{n}} = (n_x, n_y, n_z)$, $U = \mathrm{e}^{\mathrm{i}\alpha}R_{\hat{\boldsymbol{n}}}(\theta)$. The rotation operator $R_{\hat{\boldsymbol{n}}}(\theta)$ is given by

$$R_{\hat{\boldsymbol{n}}}(\theta) = \exp\left(-\mathrm{i}\theta\hat{\boldsymbol{n}}\boldsymbol{\sigma}/2\right) = I\cos\frac{\theta}{2} - \mathrm{i}(n_x\sigma_x + n_y\sigma_y + n_z\sigma_z)\sin\frac{\theta}{2}\ . \tag{8.24}$$

In particular, the rotations of the spin about the x, y and z axes are described, respectively, by the operators $R_x(\theta) = \mathrm{e}^{-\mathrm{i}\theta\sigma_x/2}$, $R_y(\theta) = \mathrm{e}^{-\mathrm{i}\theta\sigma_y/2}$ and $R_z(\theta) = \mathrm{e}^{-\mathrm{i}\theta\sigma_z/2}$, which in matrix form are given by

$$R_x(\theta) = \begin{bmatrix} \cos\frac{\theta}{2} & -\mathrm{i}\sin\frac{\theta}{2} \\ -\mathrm{i}\sin\frac{\theta}{2} & \cos\frac{\theta}{2} \end{bmatrix}\ , \tag{8.25a}$$

$$R_y(\theta) = \begin{bmatrix} \cos\frac{\theta}{2} & -\sin\frac{\theta}{2} \\ \sin\frac{\theta}{2} & \cos\frac{\theta}{2} \end{bmatrix}\ , \tag{8.25b}$$

$$R_z(\theta) = \begin{bmatrix} \exp(-\mathrm{i}\frac{\theta}{2}) & 0 \\ 0 & \exp(\mathrm{i}\frac{\theta}{2}) \end{bmatrix}\ . \tag{8.25c}$$

Then, any unitary transformation performed on the spin can be decomposed as

$$U = \mathrm{e}^{\mathrm{i}\alpha}R_z(\theta_1)R_y(\theta_2)R_z(\theta_3)\ , \tag{8.26}$$

where α and θ_i are real numbers, which is easy to prove by directly multiplying the rotation matrices and using the unitarity of U (see Sect. 9.1.1). Simple examples are $Y = \mathrm{e}^{\mathrm{i}\pi/2}R_y(\pi)$, $Z = \mathrm{e}^{\mathrm{i}\pi/2}R_z(\pi)$, $X = \mathrm{e}^{\mathrm{i}\pi/2}R_y(\pi)R_z(\pi)$ and $H = \mathrm{e}^{\mathrm{i}\pi/2}R_y(\pi/2)R_z(\pi)$. Also note that $R_{\hat{\boldsymbol{n}}}(2\pi) = -I$ for any $\hat{\boldsymbol{n}}$.

Qubit interference

Let us consider a noteworthy case illustrating quantum mechanical interference with a single qubit. Assume that a spin-$\frac{1}{2}$ particle is prepared in either $|\uparrow_x\rangle$ or $|\downarrow_x\rangle$ eigenstate of the σ_x operator, i.e., its spin is either parallel or antiparallel to the x axis. These states can be prepared by applying the Hadamard transformation to the particle being initially in state $|\uparrow_z\rangle$ or $|\downarrow_z\rangle$,

$$H|\uparrow_z\rangle = \frac{1}{\sqrt{2}}(|\uparrow_z\rangle + |\downarrow_z\rangle) = |\uparrow_x\rangle \,,$$
$$H|\downarrow_z\rangle = \frac{1}{\sqrt{2}}(|\uparrow_z\rangle - |\downarrow_z\rangle) = |\downarrow_x\rangle \,.$$

If we now measure the z-component of the spin, we will naturally obtain a random result of spin pointing up or down with equal probabilities $\frac{1}{2}$ for either state $|\uparrow_x\rangle$ or $|\downarrow_x\rangle$,

$$\langle\uparrow_x|\,\Pi_{\uparrow_z}|\uparrow_x\rangle = \langle\uparrow_x|\,\Pi_{\downarrow_z}|\uparrow_x\rangle = \frac{1}{2} \,, \quad \langle\downarrow_x|\,\Pi_{\uparrow_z}|\downarrow_x\rangle = \langle\downarrow_x|\,\Pi_{\downarrow_z}|\downarrow_x\rangle = \frac{1}{2} \,,$$

where $\Pi_i = |i\rangle\langle i|$ is the corresponding projection operator. But what if the particle was prepared in the state $|\psi_{\rm cs}\rangle = \frac{1}{\sqrt{2}}(|\uparrow_x\rangle + |\downarrow_x\rangle)$ which is a coherent superposition of $|\uparrow_x\rangle$ and $|\downarrow_x\rangle$? Then measuring along the z axis, we *always* find the particle spin pointing up and *never* pointing down,

$$\langle\psi_{\rm cs}|\,\Pi_{\uparrow_z}|\psi_{\rm cs}\rangle = 1 \,, \quad \langle\psi_{\rm cs}|\,\Pi_{\downarrow_z}|\psi_{\rm cs}\rangle = 0 \,.$$

This apparent paradox is resolved when one realizes that adding coherently $|\uparrow_x\rangle$ and $|\downarrow_x\rangle$ results in state $|\psi_{\rm cs}\rangle$ which is equivalent to $|\uparrow_z\rangle$.

8.4.2 Photon Polarization Qubit

Another genuine two-level quantum system is a linearly-polarized single photon in a well-defined spatial mode $\boldsymbol{k}$. Assuming that the photon propagates along the horizontally oriented z-axis ($\boldsymbol{k} = \hat{z}k$), its vertical $|\updownarrow\rangle$ and horizontal $|\leftrightarrow\rangle$ polarizations along the x and y axes, respectively, uniquely define the two basis states of the qubit according to $|0\rangle = |\updownarrow\rangle$ and $|1\rangle = |\leftrightarrow\rangle$. As we already know from Part I, the two orthogonal polarization modes of the photon are described by the creation and annihilation operators $a^\dagger_\updownarrow$, $a_\updownarrow$ and $a^\dagger_\leftrightarrow$, $a_\leftrightarrow$ which obey the standard bosonic commutation relations

$$[a_i, a_j] = [a_i^\dagger, a_j^\dagger] = 0 \,, \quad [a_i, a_j^\dagger] = \delta_{ij} \quad (i,j = \updownarrow, \leftrightarrow) \,. \tag{8.27}$$

In the case of a single photon, it is useful to note the formal analogy between the creation $a_i^\dagger$ and annihilation a_i operators and the raising σ^+ and lowering σ^- operators,

$$\sigma^+ \longleftrightarrow a^\dagger_{\leftrightarrow} a_{\updownarrow} \,, \tag{8.28a}$$

$$\sigma^- \longleftrightarrow a^\dagger_{\updownarrow} a_{\leftrightarrow} \,, \tag{8.28b}$$

$$\sigma_z \longleftrightarrow a^\dagger_{\leftrightarrow} a_{\leftrightarrow} - a^\dagger_{\updownarrow} a_{\updownarrow} \,. \tag{8.28c}$$

This correspondence, however formal, allows one to apply many results pertaining to the two-level atomic or spin systems directly to single-photon systems, and vice versa.

Rotations of photon polarization about the propagation axis z can be described by the rotation operator

$$R(\theta) = \begin{bmatrix} \cos\theta & -\sin\theta \\ \sin\theta & \cos\theta \end{bmatrix} \,. \tag{8.29}$$

Unlike the case of spin-$\frac{1}{2}$ particle, one cannot rotate the photon-polarization qubit about the x or y axes, since the transverse gauge condition $\boldsymbol{\nabla} \cdot \boldsymbol{A} = 0$ requires that the polarization direction be orthogonal to the propagation direction z. However, one can easily construct an operator $T(\varphi)$, defined as

$$T(\varphi) = \begin{bmatrix} 1 & 0 \\ 0 & \mathrm{e}^{\mathrm{i}\varphi} \end{bmatrix} \,, \tag{8.30}$$

which introduces the phase-shift φ to the qubit state $|1\rangle$ and leaves state $|0\rangle$ unchanged. Then, any unitary transformation U performed on a photon-polarization qubit can be decomposed into the product of rotation and phase-shift operations as

$$U = \mathrm{e}^{\mathrm{i}\alpha} T(\varphi_1) R(\theta) T(\varphi_2) \,, \tag{8.31}$$

where α, θ and φ_i are some real numbers. For example, $X = R(\pi/2)T(\pi)$, $Y = \mathrm{e}^{\mathrm{i}\pi/2} R(\pi/2)$, $Z = T(\pi)$, and $H = R(\pi/4)T(\pi)$, while $R(\pi) = -I$.

Qubit interference

The example of Sect. 8.4.1, illustrating quantum interference with spin-$\frac{1}{2}$ qubit, has also its photonic qubit counterpart. Consider the setup depicted in Fig. 8.7(a). The vertically $|\updownarrow\rangle$ polarized photon is blocked by the horizontally x-oriented polarizer, which projects the photon state onto the state $|\leftrightarrow\rangle$, $|\langle\leftrightarrow | \updownarrow\rangle|^2 = 0$. The horizontally $|\leftrightarrow\rangle$ polarized photon goes through the x-oriented polarizer with unit probability $|\langle\leftrightarrow | \leftrightarrow\rangle|^2 = 1$, but is blocked by the following vertically y-oriented polarizer, $|\langle\updownarrow | \leftrightarrow\rangle|^2 = 0$. Thus, neither a vertically nor a horizontally polarized photon can pass the system of two crossed polarizers. Perhaps surprisingly, inserting between the crossed polarizers another polarizer oriented at 45° with respect to either x or y axes, results in a finite probability of detecting the photon at the exit from the system, Fig. 8.7(b). To calculate the corresponding probabilities, note first that going through the 45°-oriented polarizer results in projecting the

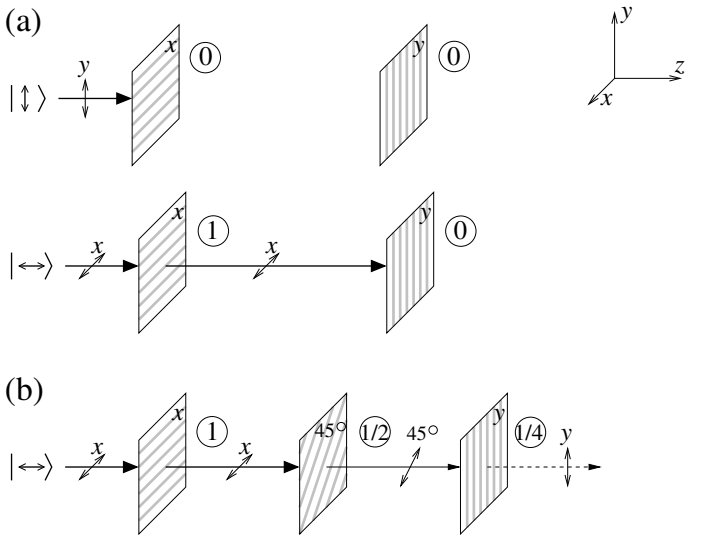

Fig. 8.7. Quantum interference with single photon: (a) Neither a vertically $|\updownarrow\rangle$ nor a horizontally $|\leftrightarrow\rangle$ polarized photon can go through two crossed polarizers. (b) Inserting between the crossed polarizers another polarizer at 45° allows the horizontally polarized photon to pass with probability $\frac{1}{4}$.

state of the photon onto the state $|+\rangle = \frac{1}{\sqrt{2}}(|\updownarrow\rangle + |\leftrightarrow\rangle)$. The probability for the photon to go through the first polarizer is $\langle\leftrightarrow|\,\Pi_{\leftrightarrow}|\leftrightarrow\rangle = 1$, and its state remains unchanged $\Pi_{\leftrightarrow}|\leftrightarrow\rangle/\sqrt{\langle\leftrightarrow|\,\Pi_{\leftrightarrow}|\leftrightarrow\rangle} = |\leftrightarrow\rangle$, where $\Pi_i = |i\rangle\langle i|$ is the projection operator describing the action of the corresponding polarizer. Next, the probability of going through the second polarizer is $\langle\leftrightarrow|\,\Pi_+|\leftrightarrow\rangle = \frac{1}{2}$. If the photon does pass the 45°-oriented polarizer, its state is given by $\Pi_+|\leftrightarrow\rangle/\sqrt{\langle\leftrightarrow|\,\Pi_+|\leftrightarrow\rangle} = |+\rangle$. Finally, the probability of going through the last polarizer is $\langle+|\,\Pi_\updownarrow|+\rangle = \frac{1}{2}$. Again, if the photon does pass the y-oriented polarizer, its state collapses to $\Pi_\updownarrow|+\rangle/\sqrt{\langle+|\,\Pi_\updownarrow|+\rangle} = |+\rangle$. The total probability for the photon to pass the system and be detected by a perfect (unit efficiency) photodetector is therefore given by the product of probabilities of all three events, $1 \times \frac{1}{2} \times \frac{1}{2} = \frac{1}{4}$. We can thus follow the evolution of the photon wavefunction, conditional upon detecting a photon after the last polarizer,

$$|\leftrightarrow\rangle \xrightarrow{x} |\leftrightarrow\rangle \xrightarrow{45^\circ} |+\rangle \xrightarrow{y} |\updownarrow\rangle\,,$$

where the symbol above the evolution arrow indicates the corresponding polarizer.

8.5 Entanglement, Decoherence and Quantum Erasure

Consider now some of the peculiar properties of entanglement, which plays a fundamental role in quantum information theory. Our aim here is to illustrate the connection between entanglement and decoherence using the simplest possible setup—a pair of qubits A and B in the entangled state

$$|\psi_2\rangle = \alpha\,|0^{\rm A}\rangle\,|0^{\rm B}\rangle + \beta\,|1^{\rm A}\rangle\,|1^{\rm B}\rangle\ . \tag{8.32}$$

Obviously, the probability of detecting this two-qubit system in state $|0^{\rm A}\rangle\,|0^{\rm B}\rangle$ is $|\alpha|^2$ and in state $|1^{\rm A}\rangle\,|1^{\rm B}\rangle$ is $|\beta|^2$. An inherent property of the bipartite entangled state (8.32) is that measuring the state of only qubit B and finding it in either state $|0^{\rm B}\rangle$ or $|1^{\rm B}\rangle$ instantly prepares qubit A in the same state $|0^{\rm A}\rangle$ or $|1^{\rm A}\rangle$. So the expectation value $\langle\mathcal{A}\rangle$ of some operator $\mathcal{A}$ acting only on qubit A is given by $\langle\mathcal{A}\rangle = \langle 0^{\rm A}|\,\mathcal{A}\,|0^{\rm A}\rangle$ if qubit B is found in $|0^{\rm B}\rangle$, and $\langle\mathcal{A}\rangle = \langle 1^{\rm A}|\,\mathcal{A}\,|1^{\rm A}\rangle$ if qubit B is found in $|1^{\rm B}\rangle$. But what if, for some reason, we do not (or can not) measure the state of qubit B. We are then led to the following question: What is the expectation value of $\mathcal{A}$ acting on qubit A, irrespective of any measurement on qubit B? It is given by

$$\langle\mathcal{A}\rangle = \langle\psi_2|\,\mathcal{A}\,|\psi_2\rangle = |\alpha|^2\,\langle 0^{\rm A}|\,\mathcal{A}\,|0^{\rm A}\rangle + |\beta|^2\,\langle 1^{\rm A}|\,\mathcal{A}\,|1^{\rm A}\rangle = {\rm Tr}(\rho^{\rm A}\mathcal{A})\ , \tag{8.33}$$

where

$$\rho^{\rm A} = |\alpha|^2\,|0^{\rm A}\rangle\langle 0^{\rm A}| + |\beta|^2\,|1^{\rm A}\rangle\langle 1^{\rm A}| = {\rm Tr}_{\rm B}(\rho) \tag{8.34}$$

is the reduced density operator of qubit A, obtained by taking the partial trace of the total density operator of the system $\rho = |\psi_2\rangle\langle\psi_2|$ with respect to qubit B. The mixed state described by (8.34) is very different form the single qubit pure superposition state

$$|\psi_1\rangle = \alpha\,|0^{\rm A}\rangle + \beta\,|1^{\rm A}\rangle\ . \tag{8.35}$$

To see that, compare the density operator for state (8.35),

$$\rho^{\rm A}_{\rm pure} = |\psi_1\rangle\langle\psi_1| = |\alpha|^2\,|0^{\rm A}\rangle\langle 0^{\rm A}| + |\beta|^2\,|1^{\rm A}\rangle\langle 1^{\rm A}| + \alpha\beta^*\,|0^{\rm A}\rangle\langle 1^{\rm A}| + \alpha^*\beta\,|1^{\rm A}\rangle\langle 0^{\rm A}|\ ,$$

with $\rho^{\rm A}$ of (8.34). In the mixed state, the non-diagonal elements of the density operator, $\langle 0^{\rm A}|\,\rho^{\rm A}_{\rm pure}\,|1^{\rm A}\rangle = \alpha\beta^*$ and $\langle 1^{\rm A}|\,\rho^{\rm A}_{\rm pure}\,|0^{\rm A}\rangle = \alpha^*\beta$,—coherences—are missing. Thus entangling systems A and B and then discarding the information pertaining to B, which mathematically amounts to taking the partial trace of the total density operator with respect to B, results in decoherence—loss of coherence by system A.

Consider a simple example illustrating the difference between spin-$\frac{1}{2}$ particles being, respectively, in the pure superposition state

$$|\psi_1\rangle = \frac{1}{\sqrt{2}}(\,|\uparrow_z\rangle + |\downarrow_z\rangle)$$

and the mixed state

$$\rho_{\text{mixed}} = \frac{1}{2} |\uparrow_z\rangle\langle\uparrow_z| + \frac{1}{2} |\downarrow_z\rangle\langle\downarrow_z| \ .$$

If we measure the x component of the spin, for the pure state we obtain $|\uparrow_x\rangle$ with probability 1, $\langle\psi_1|\Pi_{\uparrow_x}|\psi_1\rangle = 1$, while for the mixed state, obtaining $|\uparrow_x\rangle$ and $|\downarrow_x\rangle$ is equally probable, since $\text{Tr}(\Pi_{\uparrow_x}\rho_{\text{mixed}}) = \text{Tr}(\Pi_{\downarrow_x}\rho_{\text{mixed}}) = \frac{1}{2}$, where $\Pi_i = |i\rangle\langle i|$ is the corresponding projection operator. Actually, in the mixed state ρ_{mixed}, the probability of obtaining any direction of spin is $\frac{1}{2}$, i.e., the spin orientation is completely random, while in the pure state $|\psi_1\rangle$ the spin is pointing in the x direction.

Consider now the maximally entangled state of two spin-$\frac{1}{2}$ particles

$$|\psi_2\rangle = \frac{1}{\sqrt{2}}(|\uparrow_z^{\text{A}}\rangle|\uparrow_z^{\text{B}}\rangle + |\downarrow_z^{\text{A}}\rangle|\downarrow_z^{\text{B}}\rangle) = \frac{1}{\sqrt{2}}(|\uparrow_x^{\text{A}}\rangle|\uparrow_x^{\text{B}}\rangle + |\downarrow_x^{\text{A}}\rangle|\downarrow_x^{\text{B}}\rangle) \ ,$$

where the second equality is easy to check by direct substitution of $|\uparrow_x\rangle, |\downarrow_x\rangle = \frac{1}{\sqrt{2}}(|\uparrow_z\rangle \pm |\downarrow_z\rangle)$. According to (8.34), the state of particle A is given by an incoherent mixture of spin states $|\uparrow_z^{\text{A}}\rangle$ and $|\downarrow_z^{\text{A}}\rangle$,

$$\rho^{\text{A}} = \text{Tr}_{\text{B}}(|\psi_2\rangle\langle\psi_2|) = \frac{1}{2} |\uparrow_z^{\text{A}}\rangle\langle\uparrow_z^{\text{A}}| + \frac{1}{2} |\downarrow_z^{\text{A}}\rangle\langle\downarrow_z^{\text{A}}| \ ,$$

and the outcome of spin measurement along the x axis is completely random, $\text{Tr}(\Pi^{\text{A}}_{\uparrow_x}\rho^{\text{A}}) = \text{Tr}(\Pi^{\text{A}}_{\downarrow_x}\rho^{\text{A}}) = \frac{1}{2}$. The states $|\uparrow_z^{\text{A}}\rangle$ and $|\downarrow_z^{\text{A}}\rangle$ can not interfere because due to the perfect correlations between particles A and B, there exists a possibility to infer the state of particle A by measuring the spin of particle B along the z axis. The actual fact, whether we do or do not measure the spin of B thereby revealing the state of A, does not matter. The mere fact of the existence of the possibility, even in principle, to gain this information, is enough to destroy the coherence.

But what if we do measure the spin of particle B, but along the x rather than z axis? Rewriting $|\psi_2\rangle$ as

$$|\psi_2\rangle = \frac{1}{2}[(|\uparrow_z^{\text{A}}\rangle + |\downarrow_z^{\text{A}}\rangle)|\uparrow_x^{\text{B}}\rangle + (|\uparrow_z^{\text{A}}\rangle - |\downarrow_z^{\text{A}}\rangle)|\downarrow_x^{\text{B}}\rangle] \ ,$$

it is easily seen that depending on the outcome of the measurement on B, the state of particle A is projected onto either $\frac{1}{\sqrt{2}}(|\uparrow_z^{\text{A}}\rangle + |\downarrow_z^{\text{A}}\rangle)$ if $|\uparrow_x^{\text{B}}\rangle$, or $\frac{1}{\sqrt{2}}(|\uparrow_z^{\text{A}}\rangle - |\downarrow_z^{\text{A}}\rangle)$ if $|\downarrow_x^{\text{B}}\rangle$, i.e., pure superposition state. We thus find that measuring the spin of particle B along the x axis erases the information on particle A and restores coherence in the appropriate basis $\{|\uparrow_z\rangle, |\downarrow_z\rangle\}$. Such a measurement is referred to as quantum eraser.

8.6 Quantum Teleportation and Dense Coding

We can now describe two interesting quantum protocols called quantum teleportation and dense coding, enabling efficient communication of quantum and

classical information, respectively. Both protocols use EPR entanglement between two distant spatial locations as the information resource.

Quantum teleportation

Assume that two distant parties, customarily called Alice and Bob, wish to exchange some quantum information using a classical communication channel, such as telephone or Internet. Specifically, Alice needs to communicate to Bob one qubit of information

$$|\psi\rangle = \alpha\,|0\rangle + \beta\,|1\rangle\ . \tag{8.36}$$

If Alice knows precisely the state of the qubit, she can simply contact Bob via a classical channel and tell him the values of coefficients α and β of (8.36). Bob then, possessing one qubit prepared in a well-defined initial state, such as, e.g., $|0\rangle$, can apply the necessary unitary transformation realized by a sequence of one qubit gates (rotations and phase shifts), to attain the state $|\psi\rangle$. But what if Alice does not know the state of the qubit she needs to send to Bob. A single measurement on that qubit will not disclose the complete information about the coefficients α and β and, moreover, will destroy the qubit state. Also, the no-cloning theorem does not allow Alice to clone a qubit in an arbitrary quantum state, so as to perform many measurements and infer its state with high precision. It turns out that quantum teleportation can overcome these obstacles, as discussed below.

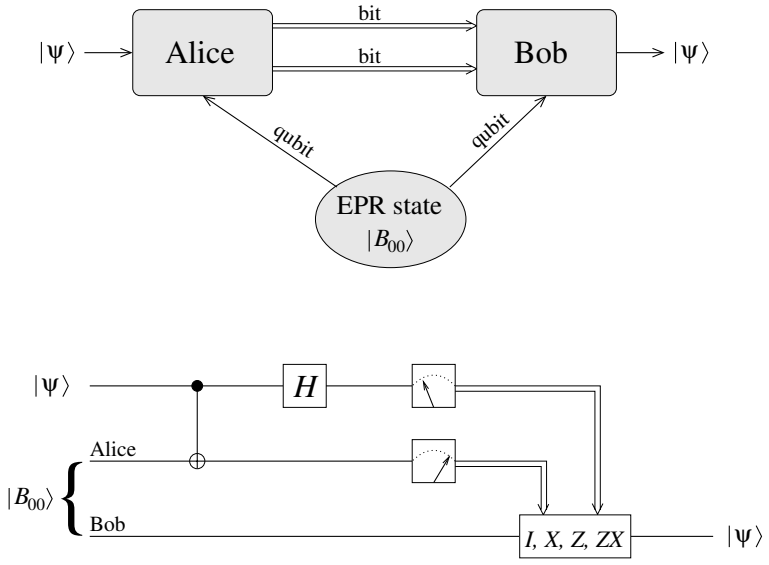

Fig. 8.8. Quantum teleportation scheme and the corresponding circuit.

Suppose Alice and Bob share a pair of qubits in the entangled state $|B_{00}\rangle = \frac{1}{\sqrt{2}}(\,|0^{\rm A}\rangle\,|0^{\rm B}\rangle + |1^{\rm A}\rangle\,|1^{\rm B}\rangle)$. This state may have been prepared at an earlier time using the circuit of Fig. 8.3, either by Alice and Bob coming to close contact with each other, or by a third party at a different location, who then has sent one qubit of the entangled pair to Alice and the other qubit to Bob, as shown in Fig. 8.8. The initial state $|\psi_3^{(0)}\rangle$ of the system of three qubits is then given by

$$|\psi_3^{(0)}\rangle = |\psi\rangle\,|B_{00}\rangle = \frac{1}{\sqrt{2}}[\alpha\,|0\rangle(\,|0^{\rm A}\rangle\,|0^{\rm B}\rangle + |1^{\rm A}\rangle\,|1^{\rm B}\rangle) + \beta\,|1\rangle(\,|0^{\rm A}\rangle\,|0^{\rm B}\rangle + |1^{\rm A}\rangle\,|1^{\rm B}\rangle)]\,, \tag{8.37}$$

the first two qubits being at Alice's location and the last qubit at Bob's location. Alice applies the CNOT transformation to her two qubits, with the control qubit being the qubit to be teleported to Bob. The resulting state is

$$|\psi_3^{(1)}\rangle = \frac{1}{\sqrt{2}}\left[\alpha\,|0\rangle(\,|0^{\rm A}\rangle\,|0^{\rm B}\rangle + |1^{\rm A}\rangle\,|1^{\rm B}\rangle) + \beta\,|1\rangle(\,|1^{\rm A}\rangle\,|0^{\rm B}\rangle + |0^{\rm A}\rangle\,|1^{\rm B}\rangle)\right]\,. \tag{8.38}$$

She then applies the Hadamard transformation to the first qubit, with the result

$$|\psi_3^{(2)}\rangle = \frac{1}{2}[\alpha(\,|0\rangle + |1\rangle)(\,|0^{\rm A}\rangle\,|0^{\rm B}\rangle + |1^{\rm A}\rangle\,|1^{\rm B}\rangle) + \beta(\,|0\rangle - |1\rangle)(\,|1^{\rm A}\rangle\,|0^{\rm B}\rangle + |0^{\rm A}\rangle\,|1^{\rm B}\rangle)]\,,$$

which can be cast in a more useful form

$$|\psi_3^{(2)}\rangle = \frac{1}{2}[\,|00^{\rm A}\rangle(\alpha\,|0^{\rm B}\rangle + \beta\,|1^{\rm B}\rangle) + |01^{\rm A}\rangle(\alpha\,|1^{\rm B}\rangle + \beta\,|0^{\rm B}\rangle) + |10^{\rm A}\rangle(\alpha\,|0^{\rm B}\rangle - \beta\,|1^{\rm B}\rangle) + |11^{\rm A}\rangle(\alpha\,|1^{\rm B}\rangle - \beta\,|0^{\rm B}\rangle)]\,. \tag{8.39}$$

Finally, Alice measures the two qubits in her possession and communicates the result to Bob with two classical bits of information, which encode the four possible states $|00\rangle$, $|01\rangle$, $|10\rangle$, and $|11\rangle$. As seen from (8.39), the measurement outcome $|00\rangle$ reveals that the state of Bob's qubit is equivalent to the original state $|\psi\rangle$ that was to be teleported. So, if Bob receives from Alice a two-bit message 00, he knows that the state of his qubit, as is, coincides with $|\psi\rangle$ and he does not change it, which is indicated by the Unity I operation in the lower part of Fig. 8.8. If, on the other hand, Bob receives message 01, he applies the X (NOT) transformation to his qubit, whose state then becomes $|\psi\rangle$. Similarly, messages 10 or 11 instruct Bob to apply, respectively, the Z or ZX transformations, to attain state $|\psi\rangle$.

Thus, in quantum teleportation, a single qubit in an arbitrary state can be transferred, or teleported, using just two bits of information sent from one spatial location to another via classical communication channel. Note that the qubit is not physically transferred from one place to the other, rather, it is its

state that is transferred from Alice to Bob. The entangled qubit pair shared by Alice and Bob prior to the teleportation is a crucial ingredient of the protocol. This entanglement between the distant parties can not be established using only classical communication channel; to establish the entanglement, either Alice and Bob should come to a contact with each other some time before the actual execution of the teleportation protocol, or a third party should prepare the entangled state and send its two constituent qubits to Alice and Bob. The third party may even be represented by, say, Alice, who will then also need to physically transfer one qubit to Bob via quantum communication channel, e.g., photon waveguide. The reader may then ask: "if there is a quantum communication channel capable of transmitting qubits, why would one need to teleport them any way?" There are number of reasons for that. For example, if Alice and Bob met and established an entanglement which they can preserve for a long time, then quantum teleportation is an efficient and secure way of exchanging quantum information. Another example of the usefulness of teleportation is when Alice and Bob have access to a reliable classical channel but unreliable quantum channel, which can, with some probability, corrupt the entangled state during its communication. There exist entanglement purification and error correction protocols which, in combination with quantum teleportation, can implement reliable quantum information transfer between different spatial locations.

Dense coding

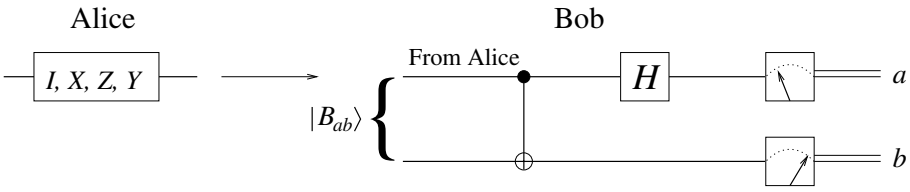

Fig. 8.9. Circuit realizing dense coding.

Consider next a related and, in some sense, inverse problem. As before, Alice and Bob possess two qubits in the entangled $|B_{00}\rangle$ state, but can communicate with each other using a reliable quantum communication channel, rather than classical channel. First of all, note that a reliable quantum channel allows one to transmit reliably classical information as well, since the two possible states 0 and 1 of a classical bit can be represented by a qubit being in state $|0\rangle$ and $|1\rangle$, respectively. Our objective here is to show that Alice, applying local transformations to her qubit and then sending it to Bob, can communicate two bits of classical information, as shown in Fig. 8.9. Depending on which of the four possible two-bit sequences 00, 01, 10, or 11 Alice

wants to encode, she acts on her qubit with I, X, Z, or Y gates, respectively. The resulting two qubit states are

$$I_A\,|B_{00}\rangle = \frac{1}{\sqrt{2}}(\,|0^{\mathrm{A}}\rangle\,|0^{\mathrm{B}}\rangle + |1^{\mathrm{A}}\rangle\,|1^{\mathrm{B}}\rangle) = |B_{00}\rangle\,, \tag{8.40a}$$

$$X_A\,|B_{00}\rangle = \frac{1}{\sqrt{2}}(\,|1^{\mathrm{A}}\rangle\,|0^{\mathrm{B}}\rangle + |0^{\mathrm{A}}\rangle\,|1^{\mathrm{B}}\rangle) = |B_{01}\rangle\,, \tag{8.40b}$$

$$Z_A\,|B_{00}\rangle = \frac{1}{\sqrt{2}}(\,|0^{\mathrm{A}}\rangle\,|0^{\mathrm{B}}\rangle - |1^{\mathrm{A}}\rangle\,|1^{\mathrm{B}}\rangle) = |B_{10}\rangle\,, \tag{8.40c}$$

$$Y_A\,|B_{00}\rangle = \frac{\mathrm{i}}{\sqrt{2}}(\,|1^{\mathrm{A}}\rangle\,|0^{\mathrm{B}}\rangle - |0^{\mathrm{A}}\rangle\,|1^{\mathrm{B}}\rangle) = \mathrm{i}\,|B_{11}\rangle\,, \tag{8.40d}$$

Bob, upon receiving Alice's qubit, applies the CNOT transformation followed by the Hadamard gate, as shown in Fig. 8.9. The states (8.40) are then transformed as

$$|B_{00}\rangle \xrightarrow{\text{CNOT}} \frac{1}{\sqrt{2}}(\,|00^{\mathrm{B}}\rangle + |10^{\mathrm{B}}\rangle) \xrightarrow{H} |00^{\mathrm{B}}\rangle\,, \tag{8.41a}$$

$$|B_{01}\rangle \xrightarrow{\text{CNOT}} \frac{1}{\sqrt{2}}(\,|11^{\mathrm{B}}\rangle + |01^{\mathrm{B}}\rangle) \xrightarrow{H} |01^{\mathrm{B}}\rangle \tag{8.41b}$$

$$|B_{10}\rangle \xrightarrow{\text{CNOT}} \frac{1}{\sqrt{2}}(\,|00^{\mathrm{B}}\rangle - |10^{\mathrm{B}}\rangle) \xrightarrow{H} |10^{\mathrm{B}}\rangle\,, \tag{8.41c}$$

$$\mathrm{i}\,|B_{11}\rangle \xrightarrow{\text{CNOT}} \frac{\mathrm{i}}{\sqrt{2}}(\,|11^{\mathrm{B}}\rangle - |01^{\mathrm{B}}\rangle) \xrightarrow{H} -\mathrm{i}\,|11^{\mathrm{B}}\rangle\,. \tag{8.41d}$$

He can then measure the two qubits in the computational basis and distinguish the four possibilities 00, 01, 10, and 11, corresponding to two bits of classical information. Thus, employing the entanglement between two spatial locations and transmitting only one qubit, one can communicate two bits of classical information. The protocol for doing this is therefore called dense coding.

8.7 Quantum Cryptography

Cryptography is a means of secure communication between two or more parties over an insecure communication channel. Suppose Alice and Bob wish to secretly exchange information over a long distance, uncompromised by the possible presence of a third party—eavesdropper Eve—located somewhere along the communication channel. One strategy for doing this is to employ the public key cryptosystem, the most widely used example of which is the RSA (Rivest–Shamir–Adleman) protocol. The underlying idea behind the public key cryptosystem is to use for message encryption a one-way function which is easy to compute by everyone but enormously hard to invert without possessing the clue, or private key. In the RSA protocol, such an inverse function involves the factorization of a large (a few hundred digit long) integer, which

is intractable for classical computers using existing algorithms. Employing the quantum Fourier transform algorithm, Shor has shown that integer factorization becomes tractable on quantum computers, which will thus threaten the security of currently used public key cryptosystems. This is one of the most tempting motivations to realize a practically useful quantum computer.

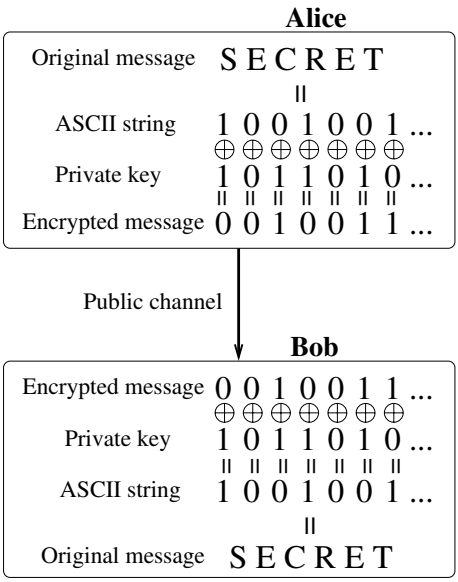

Fig. 8.10. Private key cryptosystem.

There is however, an alternative, absolutely secure protocol based on the private key cryptosystem, known as the one–time pad, or Vernam's cipher. In this protocol, Alice and Bob share a private key—random string of N bits—which only they two know. When Alice needs to communicate to Bob a secret message via public communication channel, she first converts it into ASCII binary string containing $M \leq N$ bits and then uses the private key to encrypt the message and send it to Bob. The encryption procedure is realized by adding the random bits of the private key, one by one, to the message string using addition modulo 2 operation, as shown in Fig. 8.10. The fact that the private key string is not shorter than the message string ensures that each random bit is used only once. This guaranties absolute secrecy since the encrypted message sent through the channel does not contain any repetitive structure and is completely random. Bob, upon receiving the encrypted message, can decrypt it by binary adding the same string of random bits of the private key. This results in undoing the encrypting transformation, and after converting the binary string into usual alphabet, Bob can read the original message.

So far the cryptography protocol above is not difficult to perform, provided Alice and Bob share a common private key. The most difficult and costly part of the protocol is reliable private key distribution. Alice and Bob may have met before and generated the key in private. But the key should be used only once and destroyed afterwords, in order not to compromise the secrecy of communication. Once they run out of random bits, they should meet again to generate and agree on the new random string. Otherwise Alice and Bob should rely on a third party for the key distribution, but can they trust him? Fortunately, quantum information theory offers an alternative secure way of private key distribution. In fact the most advanced application of quantum information today is quantum key distribution, generally refereed to as quantum cryptography. We thus outline below three essentially equivalent protocols, demonstrating slightly different, yet complimentary aspects of quantum mechanics.

8.7.1 BB84 Protocol

In 1984 Bennett and Brassard suggested the first quantum protocol for private key distribution, which since then has been experimentally implemented. Its essence is as follows. Alice and Bob establish two communication channels, one quantum and another one classical and, possibly, public. Alice sends to Bob through the quantum channel $2N$ qubits (e.g., single-photons), each prepared in one of the four states $|0\rangle$, $|1\rangle$, $|+\rangle = \frac{1}{\sqrt{2}}(|0\rangle + |1\rangle)$, or $|-\rangle = \frac{1}{\sqrt{2}}(|0\rangle - |1\rangle)$, randomly chosen. States $|0\rangle$ and $|+\rangle$ correspond to the value 0 of Alice's random bit, and states $|1\rangle$ and $|-\rangle$ correspond to 1. Bob, upon receiving the qubits, measures them one by one in randomly chosen basis $\{|0\rangle, |1\rangle\}$ or $\{|+\rangle, |-\rangle\}$. He then assigns 0 to his random bit, if the measurement yields $|0\rangle$ or $|+\rangle$, and 1, if it is $|1\rangle$ or $|-\rangle$. Next, Bob and Alice communicate with each other via the classical channel (e.g., telephone), to find out whether any of the qubits were lost and for which qubits Bob used the correct measurement basis. In the absence of losses, out of $2N$ qubits received and measured by Bob, on the average in half of the cases he used the correct basis. If some of the qubits did not reach Bob for whatever reason, Alice can generate and send a new string of qubits to compensate for the lost ones. After comparing the bases, Alice and Bob discard those bits for which they did not agree on the bases and are thus left with N random bits of private key.

So far we have not considered the consequences of the possible presence of an eavesdropper Eve, somewhere along the quantum channel. To infer the private key, Eve, similarly to Bob, has to measure the qubits in the randomly chosen basis and record the result of the measurement (recall that according to the no-cloning theorem, Eve can not clone the qubits). Then she has to generate each detected qubit in the measured state and send it to Bob, since otherwise Alice will discard all the lost qubits and substitute them with new ones. When Eve's basis is correct, Bob receives a qubit in the correct state. But when Eve's basis is incorrect, on the average in $N/2$ cases, after projecting

onto the correct basis, Bob's measurement yields in half of those cases ($N/4$ bits) the wrong outcome. To detect the presence of an eavesdropper, Bob and Alice can randomly choose some $m < N$ bits out of their common string and publicly compare them. If the values of about $m/4$ bits do not coincide, they realize that Eve was trying to eavesdrop, so they have to erase all the bits and start all over again. If, on the other hand, all m bits are the same, then the probability that Eve remained undetected is $(3/4)^m$, which for, say, $m = 400$ is an incredibly small number $(3/4)^m \sim 10^{-50}$.

8.7.2 B92 Protocol

In 1992 Bennett suggested a somewhat simplified protocol, called B92, in which Alice, instead of the four pairwise orthogonal states, employs only two nonorthogonal states $|0\rangle$ and $|+\rangle$, corresponding to values 0 and 1 of her random bit. Bob, upon receiving the qubits, measures them in randomly chosen basis $\{|0\rangle, |1\rangle\}$ or $\{|+\rangle, |-\rangle\}$. If Bob uses the $\{|0\rangle, |1\rangle\}$ basis, he assigns value 1 to his random bit, while the $\{|+\rangle, |-\rangle\}$ basis corresponds to value 0. In addition to the random string of bits, Bob uses a control string where he records the measurement result, 0 for states $|0\rangle$ or $|+\rangle$, and 1 otherwise. That is, Bob's random bits correspond to the measurement bases, rather than to the measurement results. He then communicates with Alice to tell her the values of the control bits, without disclosing the measurement bases recorded in his random string. To establish a common private key, Alice and Bob preserve only those random bits that correspond to control bits having value 1, and discard all of the other bits.

It is easy to verify that, in the absence of the eavesdropper Eve, the control bit containing 1 guarantees that the associated random bits of Alice and Bob are the same. Suppose that Alice sends to Bob a qubit in state $|0\rangle$ corresponding to value 0 of her random bit. If Bob decides to measure this qubit in the $\{|+\rangle, |-\rangle\}$ basis, he assigns 0 to his random bit and finds with probability $\frac{1}{2}$ state $|+\rangle$ recording 0 in the control sting, and with probability $\frac{1}{2}$ state $|-\rangle$ recording 1. Alice and Bob, after communicating with each other, preserve the random bit 0 corresponding to the value 1 of the control bit. So far the presence or absence of Eve has not been detected. Let us see what happens if Bob decides to use the $\{|0\rangle, |1\rangle\}$ basis. His random bit is then 1 and in the absence of Eve he is certain to find the $|0\rangle$ state and assign 0 to the control bit, an event leading to discarding such a bit. But if Eve was tapping the quantum channel, with probability $\frac{1}{2}$ she would use the wrong $\{|+\rangle, |-\rangle\}$ basis and corrupt the state of the qubit. So with probability $\frac{1}{4}$ Bob's measurement would yield state $|1\rangle$ and the corresponding value 1 of the control bit. After communicating with each other, Alice and Bob would keep this bit having opposite values at their sites. (Equivalent reasoning applies to the case when Alice sends to Bob a qubit in state $|1\rangle$ corresponding to value 1 of her random bit.) Hence, similarly to the BB84 protocol, sacrificing a relatively small number of random bits, Alice and Bob can discover whether

Eve has attempted to intercept the qubits. The relative disadvantage of the B92 scheme is that on the average only a quarter of the qubits are eventually used to establish the private key.

8.7.3 EPR Protocol

Private key distribution between two distant parties can be accomplished more economically with the help of EPR entanglement, as proposed by Ekert in 1991 (see also Bennett, Brassard and Mermin (1992)). Suppose Alice and Bob share $N + m$, $(m < N)$ pairs of entangled qubits, all in state $|B_{00}\rangle = \frac{1}{\sqrt{2}}(\,|0^{\mathrm{A}}\rangle\,|0^{\mathrm{B}}\rangle + |1^{\mathrm{A}}\rangle\,|1^{\mathrm{B}}\rangle)$. As noted in Sect. 8.6, such entangled pairs may have been prepared at some earlier time, either by Alice and Bob having had prior contact with each other, or by a third party, Eve, at a different location, who has then sent one qubit of each pair to Alice and the other qubit to Bob. To test the fidelity of the entanglement or, alternatively, the honesty of Eve, who provided them with the entangled pairs, Alice and Bob select at random a subset of m pairs and perform measurements in jointly determined random bases $\{\,|0\rangle,\,|1\rangle\}$ or $\{\,|+\rangle,\,|-\rangle\}$. As we know from Sect. 8.5, the EPR state $|B_{00}\rangle$ can equivalently be represented as $|B_{00}\rangle = \frac{1}{\sqrt{2}}(\,|+^{\mathrm{A}}\rangle\,|+^{\mathrm{B}}\rangle + |-^{\mathrm{A}}\rangle\,|-^{\mathrm{B}}\rangle)$. Therefore, if the measurement results for all m pairs are perfectly correlated, Alice and Bob can be confident that Eve did not attempt to cheat and honestly provided them with pure entangled states $|B_{00}\rangle$ (see Prob. 8.3). After that, whenever the private key is required, Alice and Bob can generate it by measuring the remaining N entangled qubit pairs in a jointly determined basis. Note that once Alice has measured her qubit in any basis, Bob's qubit is instantly projected onto the same basis. If Bob does not communicate with Alice beforehand and chooses his measurement basis randomly and independently of Alice, this protocol becomes essentially equivalent to the BB84 protocol.

In reality, due to the unavoidable imperfections in the measuring devices and communication channels, all three cryptography protocols described above will suffer from errors and losses, even in the absence of any eavesdropper. Nevertheless, provided the error probability is below certain minimal threshold, one can purify the private key using privacy amplification and error correction techniques, some of which are outlined in Sect. 9.4.

8.8 Einstein–Podolsky–Rosen Paradox

In the preceding sections we have encountered several useful applications of bipartite entanglement for quantum communication tasks, such as teleportation, dense coding and EPR private key generation. These examples employ, and at the same time illustrate, a highly nonclassical property of quantum entanglement, namely the correlation and instantaneous action at a distance, with seemingly no causal dependence between two or more constituents of

the entangled multiparticle system. This counterintuitive nonlocality of correlations on the one hand, and the inherently probabilistic description of the measurement outcome on the other hand, have been the subject of debate since the early days of quantum mechanics. With the conviction that any complete physical theory must obey the usual causality and locality rules, in 1935 Einstein, Podolsky and Rosen—EPR—conjectured that quantum theory is incomplete. Their reasoning employed a coordinate–momentum entangled pair of particles to show that by simply choosing which observable to measure on one of the particles, one can predict with arbitrary precision the outcome of the corresponding measurement on the other particle, without in any way disturbing it. This, as they argued, contradicts one of the cornerstones of quantum mechanics, the Heisenberg uncertainty principle $\Delta\mathcal{Q}\,\Delta\mathcal{P} \geq \hbar/2$, stating that two non-commuting operators, e.g., position $\mathcal{Q}$ and momentum $\mathcal{P}$ operators with $[\mathcal{Q},\mathcal{P}] = \mathrm{i}\hbar$, can not be determined simultaneously with arbitrary precision.

Following Bohm, let us reformulate the EPR arguments as pertaining to a Gedankenexperiment involving spin-$\frac{1}{2}$ particles, which are generic two-state systems—qubits. Consider the entangled state of two such particles, A and B,

$$|\psi_2\rangle = \frac{1}{\sqrt{2}}(\,|\uparrow_z^{\mathrm{A}}\rangle\,|\uparrow_z^{\mathrm{B}}\rangle + |\downarrow_z^{\mathrm{A}}\rangle\,|\downarrow_z^{\mathrm{B}}\rangle) = \frac{1}{\sqrt{2}}(\,|\uparrow_x^{\mathrm{A}}\rangle\,|\uparrow_x^{\mathrm{B}}\rangle + |\downarrow_x^{\mathrm{A}}\rangle\,|\downarrow_x^{\mathrm{B}}\rangle)\,, \quad (8.42)$$

which, in the qubit notation, is Bell's $|B_{00}\rangle$ state. A possible physical realization of the entangled state (8.42) of two spin-$\frac{1}{2}$ particles, flying apart from each other along the y axis, is outlined later in this section. Two parties, Alice and Bob, separated by a considerable distance (such that no interaction between the particles can take place), trap the particles A and B at their sites. Bob can measure the spin state of his particle either along the z or x axis. The observables are thus the operators σ_z and σ_x which do not commute, $[\sigma_z,\sigma_x] = 2\mathrm{i}\sigma_y$. These operators have the eigenvalues ±1 and the corresponding eigenvectors are $|\uparrow_z\rangle$, $|\downarrow_z\rangle$ for σ_z, and $|\uparrow_x\rangle$, $|\downarrow_x\rangle$ for σ_x.

(i) Suppose Bob decides to measure the state of B along the z axis. If the measurement yields the eigenvalue $+1$ of the σ_z operator, the two-particle wavefunction (8.42) collapses to

$$|\psi_2^{\mathrm{pm}}\rangle = \frac{\Pi_{\uparrow_z}^{\mathrm{B}}\,|\psi_2\rangle}{\sqrt{\langle\psi_2|\,\Pi_{\uparrow_z}^{\mathrm{B}}\,|\psi_2\rangle}} = |\uparrow_z^{\mathrm{A}}\rangle\,|\uparrow_z^{\mathrm{B}}\rangle\,.$$

Similarly, if Bob's measurement yields the -1 eigenvalue of σ_z, the wavefunction (8.42) collapses to

$$|\psi_2^{\mathrm{pm}}\rangle = \frac{\Pi_{\downarrow_z}^{\mathrm{B}}\,|\psi_2\rangle}{\sqrt{\langle\psi_2|\,\Pi_{\downarrow_z}^{\mathrm{B}}\,|\psi_2\rangle}} = |\downarrow_z^{\mathrm{A}}\rangle\,|\downarrow_z^{\mathrm{B}}\rangle\,.$$

Accordingly, immediately after the measurement, Bob can predict with certainty the outcome of the σ_z measurement on particle A.

(ii) Suppose next that Bob decides to measure the spin state of his particle along the x axis. In analogy with (i), finding the $+1$ eigenvalue of the σ_x operator leads to the state

$$|\psi_2^{\rm pm}\rangle = \frac{\mathit{\Pi}^{\rm B}_{\uparrow_x}\,|\psi_2\rangle}{\sqrt{\langle\psi_2|\,\mathit{\Pi}^{\rm B}_{\uparrow_x}\,|\psi_2\rangle}} = |\uparrow^{\rm A}_x\rangle\,|\uparrow^{\rm B}_x\rangle\,,$$

while the -1 eigenvalue of σ_x results in

$$|\psi_2^{\rm pm}\rangle = \frac{\mathit{\Pi}^{\rm B}_{\downarrow_x}\,|\psi_2\rangle}{\sqrt{\langle\psi_2|\,\mathit{\Pi}^{\rm B}_{\downarrow_x}\,|\psi_2\rangle}} = |\downarrow^{\rm A}_x\rangle\,|\downarrow^{\rm B}_x\rangle\,,$$

so that, after the measurement, Bob can predict with certainty the outcome of the σ_x measurement on particle A.

Here comes the "paradox". If the events at Alice's and Bob's sites are spacelike separated, a local measurement on particle B can not modify the state of particle A. But, depending on whether Bob decides to measure the spin of particle B either along the z or x axis, particle A instantly finds itself in the eigenstate of one of the two noncommuting operators σ_z or σ_x.

EPR thus state: "If, without in any way disturbing a system, one can predict with certainty (i.e., with probability equal to unity) the value of a physical quantity, then there exists an element of physical reality corresponding to this quantity." In quantum mechanics, the precise knowledge of one physical quantity (observable), described by, e.g., operator σ_z, precludes the knowledge of another physical quantity, described by the noncommuting operator σ_x. EPR therefore conclude that "the description of reality as given by a wave function is not complete." Anticipating a possible criticism, based on the assertion that "two or more physical quantities can be regarded as simultaneous elements of reality only when they can be simultaneously measured or predicted", EPR respond: "No reasonable definition of reality could be expected to permit this," because then the reality of, e.g., the z or x components of the spin of particle A would depend upon the process of measurement carried out by Bob on particle B, which does not disturb particle A in any way.

8.8.1 Local Hidden Variable and Bell's Inequality

One could then conjecture that the EPR's "physical reality" can perhaps be described by some hidden variable, or a set of such variables, which are not known and can not be measured or determined by quantum mechanics. Quantum mechanics in its present form would therefore be an incomplete theory, and if these variables exist and could be included in a more complete theory, that theory would be capable of predicting the outcome of any measurement deterministically.

Assume for a moment that hidden variables exist. Then the measurement is fundamentally deterministic, but appears probabilistic because some degrees of freedom of the system (described by the hidden variables) are not known. To illustrate the idea, let us consider again the spin-$\frac{1}{2}$ particle. Suppose that the particle is prepared initially in state $|\uparrow_z\rangle$ and that a hidden variable λ determines the outcome of spin measurement on that particle along any axis $\hat{n}_\theta$ characterized by the rotation angle θ about the y axis. Since during the preparation stage we have no control over the hidden variable, it is reasonable to assume that λ is a random number uniformly distributed over the unit interval $0 \le \lambda \le 1$ with the probability distribution $\rho(\lambda) = \text{const}$ which is normalized as $\int_0^1 \rho(\lambda)\mathrm{d}\lambda = 1$. Then the spin measurement along the axis $\hat{n}_\theta$ rotated by the angle θ yields the spin-up state $|\uparrow_\theta\rangle$ if $0 \le \lambda < \cos^2\frac{\theta}{2}$, and the spin-down state $|\downarrow_\theta\rangle$ if $\cos^2\frac{\theta}{2} \le \lambda \le 1$. For example, in the case of $\theta = \pi/2$, we have $\hat{n}_{\pi/2} = \hat{x}$. Then the $|\uparrow_x\rangle$ state is obtained if $0 \le \lambda < \frac{1}{2}$, while the $|\downarrow_x\rangle$ state is obtained if $\frac{1}{2} \le \lambda \le 1$.

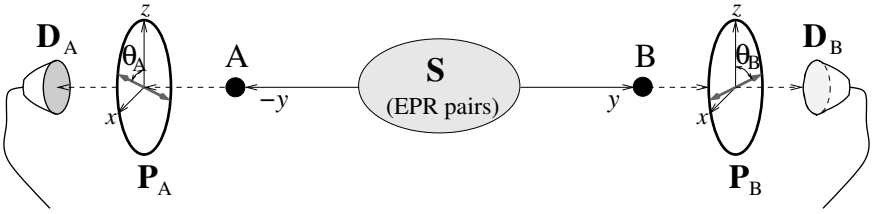

Fig. 8.11. Schematic representation of Bell's setup: **S** is the source of correlated (entangled) particles A and B, measured by corresponding apparatuses each consisting of analyzer $\mathbf{P}_i$ and detector $\mathbf{D}_i$.

Considering the case of two spatially separated but correlated particles, Bell, however, has shown that certain statistical predictions of quantum mechanics are incompatible with hidden variable theories based on local realism. Let us outline his arguments following the treatment of Clauser and Horne. Suppose that EPR correlated (entangled) particles A and B are produced by a source of such particles, one pair at a time. The particles A and B fly in the opposite directions towards their respective analyzer–detector apparatuses. Each apparatus has an adjustable parameter characterized by variable θ, which may denote, e.g., the angle of the analyzer defining the measurement axis for spin-$\frac{1}{2}$ particles or for photon polarization, as shown schematically in Fig. 8.11. For fixed values of the parameters θ_A and θ_B, the probability $p_\mathrm{AB}(\lambda, \theta_\mathrm{A}, \theta_\mathrm{B})$ of simultaneous detection of both particles is a function of a hidden variable, or a set of such, collectively denoted by λ. Since the two apparatuses are assumed to be separated by sufficiently large distance, according to Einstein's locality constraint, the space-like separated detection events can not influence one another. Then the joint probability p_AB should factorize into

the product of individual detection probabilities p_{A} and p_{B}, according to

$$p_{\mathrm{AB}}(\lambda, \theta_{\mathrm{A}}, \theta_{\mathrm{B}}) = p_{\mathrm{A}}(\lambda, \theta_{\mathrm{A}})\, p_{\mathrm{B}}(\lambda, \theta_{\mathrm{B}})\ . \tag{8.43}$$

At the system preparation and detection stages, we can neither control nor determine the hidden variables λ. Let us therefore characterize λ by some probability distribution $\rho(\lambda)$ normalized in the usual way $\int_{\Gamma} \rho(\lambda)\mathrm{d}\lambda = 1$, where Γ encompasses the complete range of possible values of λ ($\lambda \in \Gamma$). Performing many identical measurements with fixed parameters of the system, the observed ensemble averaged probabilities are given by

$$P_{\mathrm{A}}(\theta_{\mathrm{A}}) = \int_{\Gamma} p_{\mathrm{A}}(\lambda, \theta_{\mathrm{A}})\rho(\lambda)\mathrm{d}\lambda\ , \tag{8.44a}$$

$$P_{\mathrm{B}}(\theta_{\mathrm{B}}) = \int_{\Gamma} p_{\mathrm{B}}(\lambda, \theta_{\mathrm{B}})\rho(\lambda)\mathrm{d}\lambda\ , \tag{8.44b}$$

$$P_{\mathrm{AB}}(\theta_{\mathrm{A}}, \theta_{\mathrm{B}}) = \int_{\Gamma} p_{\mathrm{AB}}(\lambda, \theta_{\mathrm{A}}, \theta_{\mathrm{B}})\rho(\lambda)\mathrm{d}\lambda\ . \tag{8.44c}$$

Below we use a theorem from number theory, stating that for any four numbers x_1, x_2, y_1, y_2, such that $0 \le x_{1,2}, y_{1,2} \le 1$, the inequality

$$-1 \le x_1 y_1 - x_1 y_2 + x_2 y_1 + x_2 y_2 - x_2 - y_1 \le 0 \tag{8.45}$$

is always satisfied (Prob. 8.4). Let us denote by θ_{A}, θ'_{A} and θ_{B}, θ'_{B} four possible values of the parameters of apparatuses measuring particles A and B, respectively. Since for any θ_{A}, θ_{B} and λ, physically meaningful probabilities must satisfy $0 \le p_{\mathrm{A}}(\lambda, \theta_{\mathrm{A}}), p_{\mathrm{B}}(\lambda, \theta_{\mathrm{B}}) \le 1$, we can use (8.45) to write

$$\begin{aligned} -1 \le\ & p_{\mathrm{A}}(\lambda, \theta_{\mathrm{A}})p_{\mathrm{B}}(\lambda, \theta_{\mathrm{B}}) - p_{\mathrm{A}}(\lambda, \theta_{\mathrm{A}})p_{\mathrm{B}}(\lambda, \theta'_{\mathrm{B}}) \\ & + p_{\mathrm{A}}(\lambda, \theta'_{\mathrm{A}})p_{\mathrm{B}}(\lambda, \theta_{\mathrm{B}}) + p_{\mathrm{A}}(\lambda, \theta'_{\mathrm{A}})p_{\mathrm{B}}(\lambda, \theta'_{\mathrm{B}}) \le p_{\mathrm{A}}(\lambda, \theta'_{\mathrm{A}}) + p_{\mathrm{B}}(\lambda, \theta_{\mathrm{B}})\ . \end{aligned} \tag{8.46}$$

Multiplying all terms of this inequality by $\rho(\lambda)$ and integrating over λ taking into account (8.43), we obtain

$$\begin{aligned} -1 \le\ & P_{\mathrm{AB}}(\theta_{\mathrm{A}}, \theta_{\mathrm{B}}) - P_{\mathrm{AB}}(\theta_{\mathrm{A}}, \theta'_{\mathrm{B}}) \\ & + P_{\mathrm{AB}}(\theta'_{\mathrm{A}}, \theta_{\mathrm{B}}) + P_{\mathrm{AB}}(\theta'_{\mathrm{A}}, \theta'_{\mathrm{B}}) \le P_{\mathrm{A}}(\theta'_{\mathrm{A}}) + P_{\mathrm{B}}(\theta_{\mathrm{B}})\ . \end{aligned} \tag{8.47}$$

If, due to, e.g., rotational invariance, the probabilities $P_{\mathrm{A}}(\theta_{\mathrm{A}})$ and $P_{\mathrm{B}}(\theta_{\mathrm{B}})$ are constant and the joint probability $P_{\mathrm{AB}}(\theta_{\mathrm{A}}, \theta_{\mathrm{B}}) = P_{\mathrm{AB}}(\Delta\theta)$ is a function of only the angle difference $\Delta\theta = |\theta_{\mathrm{A}} - \theta_{\mathrm{B}}|$, by choosing the four angles so that

$$|\theta_{\mathrm{A}} - \theta_{\mathrm{B}}| = |\theta'_{\mathrm{A}} - \theta_{\mathrm{B}}| = |\theta'_{\mathrm{A}} - \theta'_{\mathrm{B}}| = \frac{1}{3}|\theta_{\mathrm{A}} - \theta'_{\mathrm{B}}| = \phi\ ,$$

from (8.47) we obtain the so-called Bell's inequality

$$S(\phi) = \frac{3P_{\rm AB}(\phi) - P_{\rm AB}(3\phi)}{P_{\rm A} + P_{\rm B}} \leq 1 \,. \tag{8.48}$$

Below we show that in the cases of EPR correlated spin-$\frac{1}{2}$ particles and polarization-entangled single photons, such rotational invariance is indeed satisfied and that for a certain range of angles ϕ, the values of function $S(\phi)$ exceed 1, violating Bell's inequality (8.48). This proves that any hidden variable theory based on Einstein's conviction of local realism is incompatible with certain predictions of quantum mechanics, which can be tested experimentally.

8.8.2 Violations of Bell's Inequality

We outline now two physical schemes for testing Bell's inequality (8.48) against experimentally confirmed predictions of quantum mechanics.

Entangled spin-$\frac{1}{2}$ particles

Consider first two spin-$\frac{1}{2}$ particles A and B in the entangled state

$$|\psi_2\rangle = \frac{1}{\sqrt{2}}(|\uparrow_z^{\rm A}\rangle|\uparrow_z^{\rm B}\rangle + |\downarrow_z^{\rm A}\rangle|\downarrow_z^{\rm B}\rangle) \,. \tag{8.49}$$

In a real experiment, these particles could be, e.g., Hg atoms. Then the entangled state (8.49) could be realized in two steps: First, a Hg_2 molecule is photodissociated into the singlet state $\frac{1}{\sqrt{2}}(|\uparrow_z^{\rm A}\rangle|\downarrow_z^{\rm B}\rangle - |\downarrow_z^{\rm A}\rangle|\uparrow_z^{\rm B}\rangle)$, whose two constituent particles (atoms) A and B fly in opposite directions, parallel and anti-parallel to the y axis, respectively. Next, a longitudinal magnetic field is applied to one of the particles to rotate its spin around the y axis by angle π, realizing thereby the σ_y transformation that results in state (8.49), to within the trivial overall phase factor $e^{i\pi/2}$ which can be omitted.

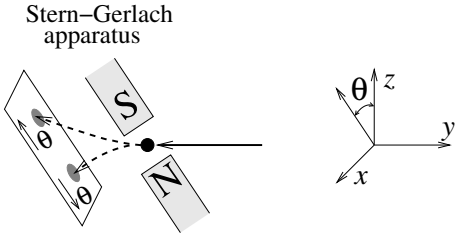

Fig. 8.12. Spin-$\frac{1}{2}$ particle passing through a Stern–Gerlach apparatus rotated by angle θ with respect to the z axis.

Let us first determine the probability of detecting a spin-$\frac{1}{2}$ particle in the spin-up state $|\uparrow_\theta\rangle$ along the axis rotated by angle θ with respect to the z

axis. Such a measurement can be realized by letting the particle pass a Stern–Gerlach apparatus and detecting its upward deflected component, as sketched in Fig. 8.12. This amounts to projecting the state of the particle onto the state $|\uparrow_\theta\rangle$, which can be obtained by applying the rotation operator $R_y(\theta)$ to state $|\uparrow_z\rangle$ (see Sect. 8.4),

$$|\uparrow_\theta\rangle = R_y(\theta)\,|\uparrow_z\rangle = \mathrm{e}^{-\mathrm{i}\theta\sigma_y/2}\,|\uparrow_z\rangle = \cos\frac{\theta}{2}\,|\uparrow_z\rangle + \sin\frac{\theta}{2}\,|\downarrow_z\rangle\ .$$

The probability $P(\theta)$ of detecting the particle in state $|\uparrow_\theta\rangle$ is then given by the expectation value of the projection operator $\Pi_\theta = |\uparrow_\theta\rangle\langle\uparrow_\theta|$, $P(\theta) = \langle\Pi_\theta\rangle$. If we now have a system of two spin-$\frac{1}{2}$ particles A and B, each analyzed by its own Stern–Gerlach apparatus rotated by the corresponding angle $\theta_{\mathrm{A,B}}$, the joint detection probability $P_{\mathrm{AB}}(\theta_{\mathrm{A}},\theta_{\mathrm{B}})$ is given by the expectation value of the product of two projection operators $\Pi^{\mathrm{A}}_{\theta_{\mathrm{A}}} = |\uparrow^{\mathrm{A}}_{\theta_{\mathrm{A}}}\rangle\langle\uparrow^{\mathrm{A}}_{\theta_{\mathrm{A}}}|$ and $\Pi^{\mathrm{B}}_{\theta_{\mathrm{B}}} = |\uparrow^{\mathrm{B}}_{\theta_{\mathrm{B}}}\rangle\langle\uparrow^{\mathrm{B}}_{\theta_{\mathrm{B}}}|$, $P_{\mathrm{AB}}(\theta_{\mathrm{A}},\theta_{\mathrm{B}}) = \langle\Pi^{\mathrm{A}}_{\theta_{\mathrm{A}}}\Pi^{\mathrm{B}}_{\theta_{\mathrm{B}}}\rangle$.

We can now easily calculate all detection probabilities for a pair of particles in the entangled state (8.49). For P_{A} and P_{B} we have

$$P_{\mathrm{A}}(\theta_{\mathrm{A}}) = P_{\mathrm{B}}(\theta_{\mathrm{B}}) = \frac{1}{2} \tag{8.50}$$

for any θ_{A} and θ_{B}, while for the joint detection probability P_{AB} we obtain

$$P_{\mathrm{AB}}(\theta_{\mathrm{A}},\theta_{\mathrm{B}}) = \frac{1}{2}\cos^2\left(\frac{\theta_{\mathrm{A}}-\theta_{\mathrm{B}}}{2}\right)\ . \tag{8.51}$$

Equations (8.50) and (8.51) show that the rotational invariance assumed in the derivation of function $S(\phi)$ is indeed satisfied in this case. Choosing the four detection angles as $\theta_{\mathrm{A}} = 0$, $\theta_{\mathrm{B}} = \pi/4$, $\theta'_{\mathrm{A}} = \pi/2$ and $\theta'_{\mathrm{B}} = 3\pi/4$ yields $\phi = \pi/4$. From (8.48) we then obtain

$$S(\phi) = \frac{3}{2}\cos^2\left(\frac{\phi}{2}\right) - \frac{1}{2}\cos^2\left(\frac{3\phi}{2}\right) \simeq 1.2 \not\leq 1\ , \tag{8.52}$$

which clearly violates Bell's inequality. Hence, the predictions of quantum mechanics, which have been verified in many experiments, contradict and thereby invalidate the hidden variable theories based on Einstein's local realism. This leads to the inescapable conclusion that quantum mechanics is a nonlocal theory.

Entangled photons

We now describe an optical scheme for testing Bell's inequality (8.48) using pairs of photons in the entangled state

$$|\psi_2\rangle = \frac{1}{\sqrt{2}}(\,|\updownarrow^{\mathrm{A}}\rangle\,|\updownarrow^{\mathrm{B}}\rangle + |\leftrightarrow^{\mathrm{A}}\rangle\,|\leftrightarrow^{\mathrm{B}}\rangle)\ . \tag{8.53}$$

In fact, most of the experimental tests of Bell's inequalities have been performed using polarization-entangled photon pairs. These include a series of pioneering experiments by Aspect and coworkers, using atomic radiative cascade, as well as a number of experiments by several teams using nonlinear crystals to realize spontaneous parametric down-conversion. In the former experiments, a high-efficiency source of pairs of photons, at frequencies $\omega_{\rm A} = 2\pi \times 7.102 \times 10^{14}$ rad/s and $\omega_{\rm B} = 2\pi \times 5.44 \times 10^{14}$ rad/s, was obtained by two-photon excitation of state $4p^2\,{}^1S_0$, via the intermediate state $3d4p\,{}^1P_1$, of the $4p^2\,{}^1S_0 \xrightarrow{\omega_{\rm A}} 4s4p\,{}^1P_1 \xrightarrow{\omega_{\rm B}} 4s^2\,{}^1S_0$ radiative cascade in calcium. The polarization entanglement of the photons comes about because of angular momentum conservation. Since relative to photons, the atoms are massive objects, their recoil during photon emission is negligible. Therefore, in addition to the polarization entanglement, the propagation directions of the two photons are also strongly correlated, due to energy and momentum conservation. In the experiments with nonlinear crystals possessing the $\chi^{(2)}$ nonlinearity, a pump photon at frequency ω_p is converted into a pair of photons (called signal and idler) with the frequencies $\omega_s \equiv \omega_{\rm A}$ and $\omega_i \equiv \omega_{\rm B}$ such that $\omega_s + \omega_i = \omega_p$. Here again, angular momentum conservation imposes polarization entanglement between the photons, while the phase-matching conditions result in a finite angle between the propagation directions of the photons, which makes it possible to redirect each photon to its own measuring apparatus. The measurements in different bases are realized by detecting photons that go through the usual optical polarizers rotated by the corresponding angle θ. This amounts to projecting the state of each photon onto the corresponding state $|\theta\rangle$, obtained by rotating the vertical polarization state $|\updownarrow\rangle$ with the rotation operator $R(\theta)$ of (8.29),

$$|\theta\rangle = R(\theta)\,|\updownarrow\rangle = \cos\theta\,|\updownarrow\rangle + \sin\theta\,|\leftrightarrow\rangle\ .$$

Then the individual and joint detection probabilities $P_{\rm A}(\theta_{\rm A}) = \langle \Pi^{\rm A}_{\theta_{\rm A}} \rangle$, $P_{\rm B}(\theta_{\rm B}) = \langle \Pi^{\rm B}_{\theta_{\rm B}} \rangle$ and $P_{\rm AB}(\theta_{\rm A}, \theta_{\rm B}) = \langle \Pi^{\rm A}_{\theta_{\rm A}} \Pi^{\rm B}_{\theta_{\rm B}} \rangle$ are given by the expectation values of the corresponding projection operators $\Pi^{\rm A}_{\theta_{\rm A}} = |\theta^{\rm A}_{\rm A}\rangle\langle\theta^{\rm A}_{\rm A}|$ and $\Pi^{\rm B}_{\theta_{\rm B}} = |\theta^{\rm B}_{\rm B}\rangle\langle\theta^{\rm B}_{\rm B}|$.

When the two photons are in the entangled state (8.53), similarly to the case of spin-$\frac{1}{2}$ particles, the quantum mechanical calculation of the detection probabilities yields

$$P_{\rm A}(\theta_{\rm A}) = P_{\rm B}(\theta_{\rm B}) = \frac{1}{2}\ , \tag{8.54}$$

$$P_{\rm AB}(\theta_{\rm A}, \theta_{\rm B}) = \frac{1}{2}\cos^2\left(\theta_{\rm A} - \theta_{\rm B}\right)\ . \tag{8.55}$$

Choosing the four detection angles as $\theta_{\rm A} = 0$, $\theta_{\rm B} = \pi/8$, $\theta'_{\rm A} = \pi/4$ and $\theta'_{\rm B} = 3\pi/8$, we obtain $\phi = \pi/8$ and, correspondingly,

$$S(\phi) = \frac{3}{2}\cos^2(\phi) - \frac{1}{2}\cos^2(\phi) \simeq 1.2 \not\leq 1\ , \tag{8.56}$$

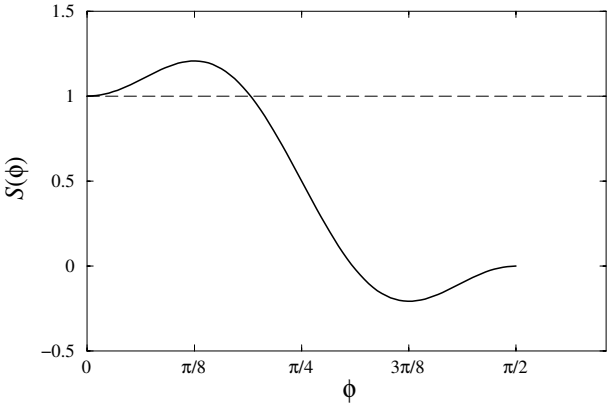

Fig. 8.13. Variation of the function $S(\phi)$ with angle ϕ, as given by (8.56). The dashed line represents the upper bound of Bell's inequality (8.48).

which again violates Bell's inequality, refuting any hidden variable theory based on local realism. As shown in Fig. 8.13, where we plot the function $S(\phi)$, inequality (8.48) is violated for the values of angle ϕ in the range $0 < \phi < 3\pi/16$. The strongest violation, however, is attained in the vicinity of $\phi \simeq \pi/8$.

8.8.3 Greenberger–Horne–Zeilinger Equality

We have seen above that certain statistical predictions of quantum mechanics, which require averaging over a large number of measurements by repeating the experiment many times, violate Bell's inequality (8.48). In 1989 Greenberger, Horne and Zeilinger—GHZ—discovered a more powerful test of the existence of elements of reality which may be hidden from us due to our inability to control and detect them for whatever reason. In the experiment proposed by GHZ, such elements of reality, if existing, would reveal themselves in just a single measurement, and in complete violation of the predictions by quantum mechanics.

Following GHZ, instead of the EPR entangled state of two spin-$\frac{1}{2}$ particles, we consider the three particle entangled state

$$|\psi_3\rangle = \frac{1}{\sqrt{2}}(\,|\uparrow_z^{\rm A}\rangle\,|\uparrow_z^{\rm B}\rangle\,|\uparrow_z^{\rm C}\rangle - |\downarrow_z^{\rm A}\rangle\,|\downarrow_z^{\rm B}\rangle\,|\downarrow_z^{\rm C}\rangle)\,. \tag{8.57}$$

As before, let us assume that all three constituent particles A, B and C of this state are separated from each other by sufficiently large distances, so that the measurement performed at each particle site can not influence the other two. Consider three composite operators, $S_1 = \sigma_x^{\rm A}\sigma_y^{\rm B}\sigma_y^{\rm C}$, $S_2 = \sigma_y^{\rm A}\sigma_x^{\rm B}\sigma_y^{\rm C}$, and $S_3 = \sigma_y^{\rm A}\sigma_y^{\rm B}\sigma_x^{\rm C}$, where the superscript of each Pauli operator indicates the

particle upon which that operator acts. Using (8.19), it is easy to see that all three operators S_i $(i = 1, 2, 3)$ mutually commute,

$$[S_1, S_2] = [S_2, S_3] = [S_3, S_1] = 0 \; .$$

In addition, the GHZ state (8.57) is a simultaneous eigenstate of these operators, with the eigenvalue $+1$,

$$S_1 \, |\psi_3\rangle = S_2 \, |\psi_3\rangle = S_3 \, |\psi_3\rangle = +1 \, |\psi_3\rangle \; . \tag{8.58}$$

This means that the product of the result of three spin measurements as given by the operators S_i (i.e., any two spins along the y axis and the third spin along the x axis), has to be $+1$. Consider, for example, operator S_1: If the measurements on particles B and C result in the $+1$ eigenvalue of $\sigma_y^{\rm B}$ and -1 eigenvalue of $\sigma_y^{\rm C}$, then measuring $\sigma_x^{\rm A}$ on particle A has to yield the eigenvalue -1, i.e., the state is $|\downarrow_x^{\rm A}\rangle\,|\uparrow_y^{\rm B}\rangle\,|\downarrow_y^{\rm C}\rangle$. Other possible outcomes of the S_1 measurement are $|\uparrow_z^{\rm A}\rangle\,|\uparrow_y^{\rm B}\rangle\,|\uparrow_y^{\rm C}\rangle$, $|\uparrow_z^{\rm A}\rangle\,|\downarrow_y^{\rm B}\rangle\,|\downarrow_y^{\rm C}\rangle$, and $|\downarrow_x^{\rm A}\rangle\,|\downarrow_y^{\rm B}\rangle\,|\uparrow_y^{\rm C}\rangle$. Equivalent reasoning applies to the operators S_2 and S_3.

Consider next the operator $S_4 = \sigma_x^{\rm A}\sigma_x^{\rm B}\sigma_x^{\rm C}$. Using the equalities $\sigma_y^2 = I$ and $\sigma_y\sigma_x = -\sigma_x\sigma_y$, it is easy to show that $S_4 = -S_1S_2S_3$. Since all three operators S_1, S_2 and S_3 have the eigenvalue $+1$, the eigenvalue of S_4 is -1,

$$S_4 \, |\psi_3\rangle = -1 \, |\psi_3\rangle \; . \tag{8.59}$$

Thus, all of the possible outcomes of the S_4 measurement on state (8.57) are $|\downarrow_x^{\rm A}\rangle\,|\downarrow_x^{\rm B}\rangle\,|\downarrow_x^{\rm C}\rangle$, $|\downarrow_x^{\rm A}\rangle\,|\uparrow_x^{\rm B}\rangle\,|\uparrow_x^{\rm C}\rangle$, $|\uparrow_z^{\rm A}\rangle\,|\downarrow_x^{\rm B}\rangle\,|\uparrow_x^{\rm C}\rangle$ and $|\uparrow_z^{\rm A}\rangle\,|\uparrow_x^{\rm B}\rangle\,|\downarrow_x^{\rm C}\rangle$.

Let us now assign to the operators σ_x^j and σ_y^j $(j = {\rm A,B,C})$ the corresponding "elements of reality" m_x^j and m_y^j, each having the value $+1$ or -1 which is revealed by the relevant measurement. From (8.58) we have

$$m_x^{\rm A} m_y^{\rm B} m_y^{\rm C} = 1 \; , \;\; m_y^{\rm A} m_x^{\rm B} m_y^{\rm C} = 1 \; , \;\; m_y^{\rm A} m_y^{\rm B} m_x^{\rm C} = 1 \; . \tag{8.60}$$

Multiplying the three equalities and taking into account that $(m_y^j)^2 = 1$, we obtain

$$\begin{aligned} &(m_x^{\rm A} m_y^{\rm B} m_y^{\rm C})(m_y^{\rm A} m_x^{\rm B} m_y^{\rm C})(m_y^{\rm A} m_y^{\rm B} m_x^{\rm C}) \\ &\quad = m_x^{\rm A} m_x^{\rm B} m_x^{\rm C} (m_y^{\rm A})^2 (m_y^{\rm B})^2 (m_y^{\rm C})^2 \\ &\qquad = m_x^{\rm A} m_x^{\rm B} m_x^{\rm C} = 1 \; . \end{aligned} \tag{8.61}$$

On the other hand, the quantum mechanical prediction from (8.59) is

$$m_x^{\rm A} m_x^{\rm B} m_x^{\rm C} = -1 \; , \tag{8.62}$$

which contradicts (8.61). Several recent experiments by Zeilinger and coworkers, using three- and four-photon GHZ states have clearly confirmed the quantum mechanical result, refuting the hypothesis of the existence of elements of reality.

8.9 Entropy and Information Theory

A pivotal theme of information theory—both classical and quantum—is the quantification of the information, produced by a source, through the smallest amount of memory needed to faithfully represent it, or the minimum amount of communication needed to reliably convey it. In classical information theory, this reduces to the compressibility of information characterized by a given probability distribution of its source, the measure of which is Shannon's entropy. In quantum information theory, it is the von Neumann entropy that plays the same role. A novel feature of quantum information theory, not having a classical counterpart, is quantum entanglement, which, as we have already seen, is a vital information resource; hence the necessity of verifying and quantifying the entanglement, which is a very active topic of current research. Our aim in this section is to outline certain aspects of information theory, whose detailed discussion is beyond the scope of this book.

The Shannon Entropy

Consider a message composed of a long string of letters $x^{(1)}, x^{(2)}, \ldots, x^{(n)}$ chosen from a binary alphabet, e.g., $x \in \{0, 1\}$. Assume that the letters in the message are statistically independent, with 0 appearing with probability $p_0 \equiv p$ and 1 with probability $p_1 = 1 - p$. When n is very large, a typical message would contain about np zeros and $n(1-p)$ ones. The number of such messages is given by the binomial coefficient $\binom{n}{np}$ which can be approximated as

$$\binom{n}{np} \simeq 2^{nH_{\text{bin}}(p)} ,$$

where the function

$$H_{\text{bin}}(p) = -p \log_2 p - (1-p) \log_2 (1-p) \tag{8.63}$$

is referred to as the Shannon entropy of a binary source. Clearly $0 \leq H_{\text{bin}}(p) \leq 1$, with $H_{\text{bin}}(p) = 0$ when $p = 0$ or 1, and $H_{\text{bin}}(p) = 1$ when $p = \frac{1}{2}$. Let us assign to each typical message a positive integer number, which can be represented by a binary string of length $nH_{\text{bin}}(p)$. Then, to convey a typical message between two parties, instead of sending the message itself, it is enough to sent the binary string identifying that message. That string is shorter than the original message, since $H_{\text{bin}}(p) < 1$ for any $p \neq \frac{1}{2}$. This procedure thus yields data compression. The fact that for $p = \frac{1}{2}$, corresponding to maximum Shannon entropy, the data can not be compressed points to a physical interpretation of these concepts: $p = \frac{1}{2}$ means completely random distribution of zeros and ones in a typical message string in which the sequence of letters contains no pattern. As such, the message has to be transferred as a whole and no compression can achieve the same result. It then makes perfect sense that maximum entropy is associated with maximum information. And it is

no accidental coincidence that maximum entropy in statistical physics is also associated with complete randomness.

The above result can be generalized to the case of an alphabet containing $k \geq 2$ letters, i.e., $x \in \{x_1, x_2, \ldots, x_k\}$. Assuming that each letter x_j appears with the corresponding probability p_j ($\sum_j p_j = 1$), a typical message of length $n \gg 1$ would have np_1 instances of x_1, np_2 instances of x_2, etc. The total number of permutations in such message strings is given by

$$\frac{n!}{\prod_j (np_j)!} \simeq 2^{nH(X)} \,,$$

where

$$H(X) \equiv H(p_1, p_2, \ldots, p_k) = \sum_j -p_j \log_2 p_j \tag{8.64}$$

is the Shannon entropy of the ensemble $X = \{x_j, p_j\}$. Again, we can assign to each typical message a positive integer number, and send that number to the receiver using only $nH(p)$ bits. Importantly, as the length n of the message grows, the probability of having to deal with an atypical message, in which the statistical weights of various letters x_j deviate from the typical ones np_j, quickly approaches zero. Therefore, the above procedure achieves (asymptotically as $n \to \infty$) optimal data compression with the rate $H(X)$, which is Shannon's noiseless coding theorem.

The Von Neumann Entropy

Generalizing now the notion of entropy to quantum ensembles, for a quantum system characterized by the density operator ρ, the so-called von Neumann entropy $S(\rho)$ of ρ is defined as

$$S(\rho) = -\mathrm{Tr}(\rho \log_2 \rho) \,. \tag{8.65}$$

The von Neumann entropy is invariant under unitary basis transformations, $S(\mathcal{U}\,\rho\,\mathcal{U}^\dagger) = S(\rho)$, which follows from (1.48). Choosing an orthogonal basis $\{\,|\psi_i\rangle\}$ in which ρ is diagonal,

$$\rho = \sum_i \lambda_i \,|\psi_i\rangle\langle\psi_i| \;\,,$$

where λ_i are the eigenvalues of ρ, we can write

$$S(\rho) = -\sum_i \lambda_i \log_2 \lambda_i = H(Y) \,, \tag{8.66}$$

which shows that the von Neumann entropy $S(\rho)$ reduces to the Shannon entropy $H(Y)$ for the ensemble $Y = \{\,|\psi_i\rangle, \lambda_i\}$. Clearly, if the system is in a pure state $\rho = \,|\Psi\rangle\langle\Psi|\,$, its entropy vanishes, $S(\rho) = 0$. Conversely, the entropy

attains the maximum $S(\rho) = \log_2 N$ in the case of a completely mixed state $\rho = \frac{1}{N}\sum_i |\psi_i\rangle\langle\psi_i| = \frac{1}{N} I$, where N is the dimension of the corresponding Hilbert space.

We can now outline the quantum analog of the classical data compression, which is known as Schumacher's quantum noiseless coding theorem. Consider a quantum source which produces messages composed of sequences of $n \gg 1$ qubits represented by, e.g., polarization states of photons. Assume that the possible states of the qubits are drawn for a set of distinct pure states $\{|\psi_j\rangle\}$, not necessarily orthogonal to each other, with each state occurring with the respective probability p_j ($\sum_j p_j = 1$). Thus, each qubit in a message is characterized by the density operator $\rho = \sum_j p_j |\psi_j\rangle\langle\psi_j|$ and the whole message is described by the tensor product density operator $\rho^{\otimes n} = \rho \otimes \rho \otimes \cdots \otimes \rho$ which spans an $N = 2^n$ dimensional Hilbert space $\mathbb{H}^{(N)}$. We can diagonalize $\rho^{\otimes n}$ through an appropriate unitary transformation. The corresponding orthogonal basis states will be represented by the products of eigenstates $|x_0\rangle$ and $|x_1\rangle$ of individual qubits, while the eigenvalues of $\rho^{\otimes n}$ will be products of eigenvalues $p_0 = p$ and $p_1 = 1 - p$ of ρ. In this basis, the information content of $\rho^{\otimes n}$ is essentially that of a classical source producing message strings corresponding to $|x^{(1)}, x^{(2)}, \ldots, x^{(n)}\rangle$ with probabilities $p^{(1)}p^{(2)}\ldots p^{(n)}$. The von Neumann entropy $S(\rho)$ of ρ is obviously equal to the Shannon entropy $H_{\rm bin}(p)$ of (8.63). This means that we have about $M = 2^{nH_{\rm bin}(p)}$ orthogonal message strings, which can be encoded in a quantum system whose Hilbert space $\mathbb{H}^{(M)}$ is M dimensional. This requires only $nS(\rho) = nH_{\rm bin}(p)$ qubits, whose product space can therefore accommodate all the typical quantum messages with high fidelity. Since $H_{\rm bin}(p) < 1$ for any $p \neq \frac{1}{2}$, quantum data compression is thereby achieved. Only for completely random qubits $\rho = \frac{1}{2} I$ ($p = \frac{1}{2}$), in which case $S(\rho) = 1$ ($H_{\rm bin}(p) = 1$), no compression is possible ($M = N$), in complete analogy with the classical case.

Entropy as a Measure of Entanglement

Consider a two-component (bipartite) quantum system A+B in a pure state $|\Phi\rangle$. To test whether the subsystems are entangled or not, following the prescription of Sect. 1.3.3, we can perform the Schmidt decomposition of $|\Phi\rangle$. If this decomposition has more than one term, i.e., the Schmidt number is greater than one, $|\Phi\rangle$ is an entangled state, and the reduced density operator of one of the subsystems, say A, represents a mixed state, $\rho^{\rm A}_{\rm mixed} = {\rm Tr}_{\rm B}(\,|\Phi\rangle\langle\Phi|\,) = \sum_i p_i\, |\psi^{\rm A}_i\rangle\langle\psi^{\rm A}_i|$. On the other hand, for a factorisable state of the form $|\Phi\rangle = |\Psi^{\rm A}\rangle \otimes |\Psi^{\rm B}\rangle$, the Schmidt number is one, while the reduced density operator of A represents a pure state $\rho^{\rm A}_{\rm pure} = |\Psi^{\rm A}\rangle\langle\Psi^{\rm A}|$. Recall that the von Neumann entropy of a pure state $\rho^{\rm A}_{\rm pure}$ is zero, $S(\rho^{\rm A}_{\rm pure}) = 0$, while it is maximized to $S(\rho^{\rm A}_{\rm mixed}) = \log_2 N$ for a mixed state $\rho^{\rm A}_{\rm mixed}$ with all $p_i = 1/N$, which results from a maximally entangled state. Thus the von Neumann entropy is a monotonic function of entanglement between a pair of subsystems and is invariant under local unitary transformations, which do not

affect the entanglement. Therefore the von Neumann entropy of the density matrix for either subsystem of a bipartite system can serve as a convenient measure of entanglement, and is often referred to simply as the entropy of entanglement.

Considering now a two-component quantum system in a mixed state represented by the density operator ρ, one measure of entanglement is the so-called entanglement of formation $E(\rho)$, which is the minimum average entropy of entanglement of an ensemble of pure states $\{|\Phi\rangle\}$ that represents $\rho = \sum_{\Phi} P_{\Phi} |\Phi\rangle\langle\Phi|$. In general, for multistate subsystems the entanglement of formation is difficult to calculate, but in the simplest case of subsystems represented by two-state quantum systems (qubits), $E(\rho)$ can be expressed through the concurrence $C(\rho)$ defined as $C(\rho) = \max\{0, \lambda_1 - \lambda_2 - \lambda_3 - \lambda_4\}$, where $\lambda_1, \ldots, \lambda_4$ are the square roots of the eigenvalues of matrix $\rho\tilde{\rho}$, taken in decreasing order. Here $\tilde{\rho} \equiv \sigma_y^{\mathrm{A}} \sigma_y^{\mathrm{B}} \rho^* \sigma_y^{\mathrm{A}} \sigma_y^{\mathrm{B}}$, with ρ^* being the complex conjugate of ρ, and $\sigma_y^{\mathrm{A,B}}$ the Pauli matrices acting on the corresponding qubits. Several other measures of entanglement of bipartite quantum systems have been suggested, including the distillable entanglement and logarithmic negativity. All of these measures reduce to the (von Neumann) entropy of entanglement in the case of pure states, and they share the important property of being the entanglement monotones, i.e., they do not increase under local operations and classical communication between the parties.

Quantifying entanglement of bipartite quantum systems is an important and difficult problem attracting at present much attention. In the general case of mixed states, the various measures of entanglement are nonequivalent, leading to much debate in the scientific community. The entanglement of three- and more-component systems represents an even more difficult problem. Usually one performs the pairwise decompositions of the compound system in all possible ways and then computes the measures of bipartite entanglements. This procedure, however, is capable of characterizing only certain aspects of multiparticle entanglement and for some states even fails to detect genuine entanglement. The characterization of multiparticle entanglement thus requires much further research.

Before closing this section, let us note that most of the experiments aimed at detecting entanglement between quantum systems employ the so-called entanglement witnesses. In general, entanglement witnesses are linear inequalities for expectation (mean) values of appropriate physical observables, which upon violating the inequalities verify the presence of entanglement in a bipartite system. The Bell inequalities described in the previous section are perhaps the most representative examples of entanglement witnesses.

Problems

8.1. Verify the truth table of Fig. 8.3.

8.2. Show that, if perfect cloning of quantum states were possible, then two distant parties, Alice and Bob, sharing a pair of entangled qubits in state $|B_{11}\rangle = \frac{1}{\sqrt{2}}(\,|0^{\rm A}\rangle\,|1^{\rm B}\rangle - |1^{\rm A}\rangle\,|0^{\rm B}\rangle)$, could communicate information with superluminal velocity. (*Hint*: Let Alice measure her qubit in either $\{\,|0\rangle,\,|1\rangle\}$ or $\{\,|+\rangle,\,|-\rangle\}$ basis. Now show that if Bob could perfectly clone his qubit, he would be able, with some probability, to find out Alice's basis.)

8.3. In the EPR protocol for quantum cryptography, in order to eavesdrop on the private key, Eve may employ the strategy of generating the three qubit entangled states $|{\rm GHZ}\rangle = \frac{1}{\sqrt{2}}(\,|000\rangle + |111\rangle)$ and then sending the first qubit to Alice, the second one to Bob and keeping the third qubit to her own. Show that when Alice and Bob test the fidelity of their pairs by performing measurements in jointly determined random bases, on the average in one out of four measurements the correlation between the qubit states is violated. (*Hint*: Express the $|{\rm GHZ}\rangle$ state in the $\{\,|+\rangle,\,|-\rangle\}$ basis.)

8.4. Prove that for any given four positive numbers x_1, x_2, y_1, y_2, such that $0 \le x_{1,2}, y_{1,2} \le 1$, the inequality

$$-1 \le x_1y_1 - x_1y_2 + x_2y_1 + x_2y_2 - x_2 - y_1 \le 0$$

is always satisfied. (*Hint*: See J. F. Clause and M. A. Horne, Phys. Rev. D **10**, 526 (1974).)

8.5. Verify expressions (8.50) and (8.51) for the individual and joint detection probabilities $P_{\rm A}(\theta_{\rm A})$, $P_{\rm B}(\theta_{\rm B})$ and $P_{\rm AB}(\theta_{\rm A}, \theta_{\rm B})$ for a pair of particles in the entangled state (8.49). Also, calculate $P_{\rm A}(\theta_{\rm A})$, $P_{\rm B}(\theta_{\rm B})$ and $P_{\rm AB}(\theta_{\rm A}, \theta_{\rm B})$ for the two-particle singlet state $\frac{1}{\sqrt{2}}(\,|\uparrow_z^{\rm A}\rangle\,|\downarrow_z^{\rm B}\rangle - |\downarrow_z^{\rm A}\rangle\,|\uparrow_z^{\rm B}\rangle)$.

8.6. Given a pair of qubits in the pure entangled state $|\psi_2\rangle = \alpha\,|0^{\rm A}\rangle\,|1^{\rm B}\rangle + \beta\,|1^{\rm A}\rangle\,|0^{\rm B}\rangle$, calculate the concurrence $C(\rho)$ defined on the previous page. Show that for any two-qubit pure state $|\psi_2\rangle$, the concurrence is equal to

$$C(\psi_2) = |\langle\psi_2|\tilde{\psi}_2\rangle|\ , \quad \text{with} \quad |\tilde{\psi}_2\rangle \equiv \sigma_y^{\rm A}\sigma_y^{\rm B}\,|\psi_2^*\rangle\ . \tag{8.67}$$

(*Hint*: See W. K. Wootters, Phys. Rev. Lett. **80**, 2245 (1998).)

9

Principles of Quantum Computation

In this chapter, after an outline of the general principles of operation of a quantum computer, we present several representative quantum algorithms for data processing and error correction. As we will see, these quantum algorithms can outperform their classical counterparts. The material here also serves to motivate the discussion in the next chapter pertaining to the physical implementations of quantum computation.

9.1 Operation of Quantum Computer

In the previous chapter we have studied the building blocks of a quantum information processing devise. These are the qubits which constitute the register where quantum information is stored, and the quantum logic gates which manipulate that quantum information. We discuss now the Universal set of quantum gates and the principal steps involved in quantum computation.

9.1.1 Universal Gates for Quantum Computation

The Universal set of quantum gates, capable or realizing any unitary transformation on a multiqubit register, consists of the single-qubit rotational operations, such as $R_y(\theta)$ and $R_z(\theta')$ for spin-$\frac{1}{2}$ qubits or $R(\theta)$ and $T(\varphi)$ for photon-polarization qubits, and the CNOT two-qubit logic gate. This is to be contrasted with the reversible classical computation, where the universal logic gate—the Toffoli (or Fredkin) gate—involves three bits. As we show below, however, any three-qubit controlled-controlled-U operation (including the quantum Toffoli gate) can be decomposed into a sequence of two-qubit operations, which in turn can be implemented using the single-qubit rotations and CNOT gate.

Consider a general unitary operation U on a single qubit,

$$U = \begin{bmatrix} \mathrm{e}^{-\mathrm{i}\beta}\cos\gamma & -\mathrm{e}^{-\mathrm{i}\delta}\sin\gamma \\ \mathrm{e}^{\mathrm{i}\delta}\sin\gamma & \mathrm{e}^{\mathrm{i}\beta}\cos\gamma \end{bmatrix}, \tag{9.1}$$

where, for simplicity, we disregard an overall phase factor $\mathrm{e}^{\mathrm{i}\alpha}$. From the definition of the rotation operators R_y and R_z in (8.25) and matrix multiplication, it follows that there exist real numbers θ_1, θ_2, and θ_3, such that $U = R_z(\theta_1)R_y(\theta_2)R_z(\theta_3)$. Indeed, by choosing the three angles θ_i according to $\theta_1 + \theta_3 = 2\beta$, $\theta_1 - \theta_3 = 2\delta$, and $\theta_2 = 2\gamma$, we find that the product of the three rotations yields the right-hand-side of (9.1).

Next, we show that for any unitary matrix U, there exist matrices A, B and C such that $ABC = I$ and $AXBXC = U$. Indeed, by choosing $A = R_z(\theta_1)R_y(\theta_2/2)$, $B = R_y(-\theta_2/2)R_z(-(\theta_1+\theta_3)/2)$, and $C = R_z((\theta_3-\theta_1)/2)$, we have

$$\begin{aligned} ABC &= R_z(\theta_1)R_y\left(\frac{\theta_2}{2}\right)R_y\left(-\frac{\theta_2}{2}\right)R_z\left(-\frac{\theta_1+\theta_3}{2}\right)R_z\left(\frac{\theta_3-\theta_1}{2}\right) \\ &= R_z(\theta_1)R_z(-\theta_1) = I\,. \end{aligned} \tag{9.2}$$

Using the equalities $XX = I$, $XR_y(\theta)X = R_y(-\theta)$, and $XR_z(\theta)X = R_z(-\theta)$, we see that

$$\begin{aligned} AXBXC &= R_z(\theta_1)R_y\left(\frac{\theta_2}{2}\right)XR_y\left(-\frac{\theta_2}{2}\right)R_z\left(-\frac{\theta_1+\theta_3}{2}\right)XR_z\left(\frac{\theta_3-\theta_1}{2}\right) \\ &= R_z(\theta_1)R_y\left(\frac{\theta_2}{2}\right)XR_y\left(-\frac{\theta_2}{2}\right)XXR_z\left(-\frac{\theta_1+\theta_3}{2}\right)XR_z\left(\frac{\theta_3-\theta_1}{2}\right) \\ &= R_z(\theta_1)R_y(\theta_2)R_z(\theta_3) = U\,, \end{aligned} \tag{9.3}$$

which proves the statement.

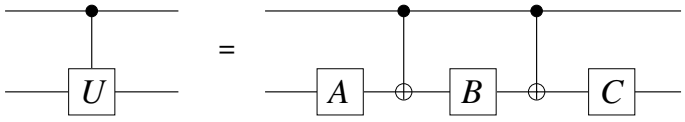

Fig. 9.1. Circuit generating the controlled-U gate.

Now it is easy to see that any two-qubit controlled-U operation can be simulated by the circuit of Fig. 9.1, which involves only the single-qubit operations A, B, and C, and the two-qubit CNOT gates. Indeed, if the control (upper) qubit is in state $|0\rangle$, then the $ABC = I$ transformation is applied to the target (lower) qubit, while if the control qubit state is $|1\rangle$, the target qubit undergoes the transformation $AXBXC = U$.

It turns out that not only the CNOT gate but almost any two-qubit logic gate is universal. In particular, the CZ (controlled-Z) and $\sqrt{\text{SWAP}}$ (square-root of SWAP) gates are almost as good as the CNOT gate, since we can easily construct circuits implementing the CNOT transformation $W^{\text{AB}}_{\text{CNOT}}$ between qubits A and B through the $W^{\text{AB}}_{\text{CZ}}$ and $W^{\text{AB}}_{\sqrt{\text{SWAP}}}$ transformations,

$$W^{\mathrm{AB}}_{\mathrm{CNOT}} = R^{\mathrm{B}}_y(\pi/2)\, W^{\mathrm{AB}}_{\mathrm{CZ}}\, R^{\mathrm{B}}_y(-\pi/2)\,, \tag{9.4a}$$

$$W^{\mathrm{AB}}_{\mathrm{CNOT}} = R^{\mathrm{A}}_z(-\pi)\, R^{\mathrm{B}}_z(\pi)\, W^{\mathrm{AB}}_{\sqrt{\mathrm{SWAP}}}\, R^{\mathrm{A}}_z(2\pi)\, W^{\mathrm{AB}}_{\sqrt{\mathrm{SWAP}}}\,, \tag{9.4b}$$

where the $\sqrt{\mathrm{SWAP}}$ gate, defined via $\left(W^{\mathrm{AB}}_{\sqrt{\mathrm{SWAP}}}\right)^2 = W^{\mathrm{AB}}_{\mathrm{SWAP}}$, has the following matrix representation,

$$W^{\mathrm{AB}}_{\sqrt{\mathrm{SWAP}}} = \begin{bmatrix} 1 & 0 & 0 & 0 \\ 0 & \frac{1+\mathrm{i}}{2} & \frac{1-\mathrm{i}}{2} & 0 \\ 0 & \frac{1-\mathrm{i}}{2} & \frac{1+\mathrm{i}}{2} & 0 \\ 0 & 0 & 0 & 1 \end{bmatrix} = \frac{1}{\sqrt{2}} \begin{bmatrix} \sqrt{2} & 0 & 0 & 0 \\ 0 & \mathrm{e}^{\mathrm{i}\pi/4} & \mathrm{e}^{-\mathrm{i}\pi/4} & 0 \\ 0 & \mathrm{e}^{-\mathrm{i}\pi/4} & \mathrm{e}^{\mathrm{i}\pi/4} & 0 \\ 0 & 0 & 0 & \sqrt{2} \end{bmatrix}. \tag{9.5}$$

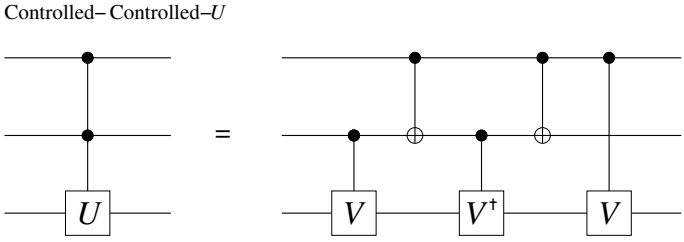

Fig. 9.2. Circuit generating the three-qubit controlled-controlled-U gate.

Consider, finally, multi-qubit operations. An example of the three-qubit controlled-controlled-U gate and its decomposition into a sequence of two-qubit operations is shown in Fig. 9.2, where the operator V is defined via $VV = U$ (see Prob. 9.1). When U corresponds to the X or NOT gate, and therefore $V = \frac{1}{2}(1-\mathrm{i})(I+\mathrm{i}X)$, this circuit realizes the universal quantum Toffoli or CCNOT gate. This CCNOT gate can further be used to implement multiqubit gates having any number of control and target qubits.[1] In analogy with the reversible classical computer discussed in Sect. 7.4, using an equivalent sequence of quantum logic gates, any function $f(x) : \{0,1\}^k \to \{0,1\}^l$ is computed via the transformation $|x, y\rangle \xrightarrow{U_f} |x, y \oplus f(x)\rangle$, as shown in Fig. 9.3. The unitary transformation U_f leaves the "data" register of k qubits containing the argument $x \in \{0,1\}^k$ of the function unchanged, while the value of the function is written into the "target" register of l qubits $y \in \{0,1\}^l$ via the addition modulo 2 operation, $|y \oplus f(x)\rangle$.

[1] Of course, if a particular physical system is capable of explicitly realizing unitary transformations involving more than two qubits, implementing thereby multiqubit logic gates, it is an advantageous but not a fundamental factor, since single- and two-qubit gates suffice to construct any multiqubit transformation.

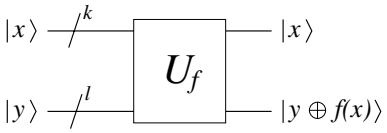

Fig. 9.3. Unitary transformation U_f for the evaluation of function $f(x)$. Symbol "$/^n$" is a short-hand notation for a set of n qubits.

9.1.2 Building Blocks of a Quantum Computer

In preparation for the discussion of the physical implementations of quantum information processing in the next chapter, let us list here the necessary ingredients of an envisioned quantum computer. The quantum computer is composed of (i) register containing K qubits; (ii) one- and two-qubit (and possibly $k(>2)$-qubit) logic gates applied to the register according to the particular algorithm; and (iii) measuring apparatus applied to the desired qubits at the end of (and, possibly, during) the program execution, which projects the qubit state onto the computational basis $\{|0\rangle, |1\rangle\}$.

The operation of the quantum computer consists of the following principal steps:

1. *Initialization*—Prepare all K qubits of the register in a well-defined initial state, such as, e.g., $|0\ldots000\rangle$.
2. *Input*—Load the input data using the logic gates.
3. *Computation*—Perform the desired unitary transformation by applying the sequence of logic gates according to the program.
4. *Output*—Measure the final state of the register in the computational basis.

In the following sections we consider several representative quantum algorithms for data processing and error correction.

9.2 Quantum Algorithms

Before we embark upon a detailed discussion, let us outline two general principles pertaining to most of the existing quantum algorithms. The first principle instructs us as to how to prepare the input state of the register, in order to make the best use of quantum parallelism. It may be formulated as follows:

(i) Prepare the input state of the register in a superposition state of all possible "classical" inputs x

$$|\psi^{\text{in}}\rangle = \sum_x c_x |x\rangle \ , \qquad \sum_x |c_x|^2 = 1 \ . \tag{9.6}$$

Note that many problems are intractable on classical computers simply because there are too many possible inputs that should be processed and analyzed by a computer before the actual problem is solved. This usually requires either an enormous amount of CPU time, if a sequential processing of the input data is performed on a single processor, or enormous number of simultaneously working processors, to vastly parallelize the algorithm execution. On the other hand, owing to the quantum superposition principle, a single quantum register is capable of simultaneously storing and processing all of the classical inputs at once.

The second principle has to do with the measurement which should yield an intelligible result of computation, expressed in terms of classical quantities. It states:

(ii) Design an algorithm in which all of the computational paths interfere with each other to yield with high probability the output state y

$$|\psi^{\text{out}}\rangle \simeq c_y\,|y\rangle\ , \qquad |c_y|^2 \simeq 1\ , \quad \sum_{y'\neq y} |c_{y'}|^2 \ll 1\ . \tag{9.7}$$

We thus recognize that the required output state y, containing the sought after solution of the problem, is an eigenstate of the quantum register. It is thus a classical state, since no superposition is involved, and a single measurement reveals y with almost unit probability $|c_y|^2 \simeq 1$. If the algorithm execution is not too costly in terms of the hardware involved, we may allow for several repetitions of the algorithm, followed by the measurements, and the condition on c_y can be somewhat relaxed to $|c_y|^2 > 1/2$. Then if we perform say N_r repetitions of the cycle (i)-(ii), all resulting in the same state y, the probability of obtaining an erroneous output $P_{\text{error}}(N_r) = (1 - |c_y|^2)^{N_r}$ rapidly goes to zero with increasing N_r.

Designing good quantum algorithms is a very difficult task requiring profound insight and ingenuity, particularly because we think largely in classical terms, with the quantum world often being rather counterintuitive.

9.2.1 Deutsch Algorithm

We begin with this simple algorithm, involving only two qubits, representing therefore a "toy problem", aimed at demonstrating the power of quantum parallelism employed in other quantum algorithms capable of performing useful tasks.

Suppose we are given some Boolean function $f(x) : \{0,1\} \to \{0,1\}$ of a single-bit argument x and the corresponding quantum "black-box" or "oracle" U_f evaluating that function via $|x, y\rangle \xrightarrow{U_f} |x, y \oplus f(x)\rangle$ (see. Prob. 9.2). Our aim is to determine a property of function f, i.e., whether it is constant $f(0) = f(1)$ of balanced $f(0) \neq f(1)$. On a classical computer, we would need to evaluate $f(x)$ twice, once for $x = 0$ and once for $x = 1$, and then

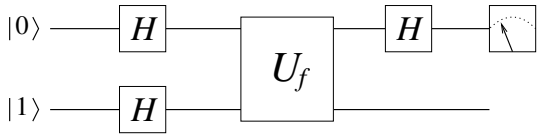

Fig. 9.4. Circuit implementing the Deutsch algorithm.

compare the results. A quantum computer, however, allows us to characterize the function by calling U_f only once. This is achieved by preparing the data qubit in an equally weighted superposition state of both classical inputs $x = 0$ and $x = 1$ and evaluating $f(x)$ for both x at the same time, followed by interfering the output of U_f and a single measurement that unambiguously reveals the function. The quantum circuit for doing this is shown in Fig. 9.4. Let us follow the states of the register through this circuit. The initial state of the two qubits is

$$|\psi_2^{(0)}\rangle = |0\rangle\,|1\rangle\,. \tag{9.8}$$

After applying the Hadamard gates to the data and target qubits, we have

$$|\psi_2^{(1)}\rangle = \frac{1}{2}(\,|0\rangle + |1\rangle)(\,|0\rangle - |1\rangle)\,. \tag{9.9}$$

Next, the U_f transformation leads to

$$|\psi_2^{(2)}\rangle = \begin{cases} \pm\frac{1}{2}(\,|0\rangle + |1\rangle)(\,|0\rangle - |1\rangle) & \text{if } f(0) = f(1) \\ \pm\frac{1}{2}(\,|0\rangle - |1\rangle)(\,|0\rangle - |1\rangle) & \text{if } f(0) \neq f(1). \end{cases}$$

Realizing that $|x\rangle(\,|0\rangle - |1\rangle)/\sqrt{2} \xrightarrow{U_f} (-1)^{f(x)}\,|x\rangle(\,|0\rangle - |1\rangle)/\sqrt{2}$, we can cast $|\psi_2^{(2)}\rangle$ in a more compact form

$$|\psi_2^{(2)}\rangle = \sum_{x=0,1} \frac{(-1)^{f(x)}\,|x\rangle}{\sqrt{2}}\;\frac{|0\rangle - |1\rangle}{\sqrt{2}}. \tag{9.10}$$

Finally, after applying the Hadamard gate to the data qubit, we have

$$|\psi_2^{(3)}\rangle = \begin{cases} \pm\,|0\rangle\frac{1}{\sqrt{2}}(\,|0\rangle - |1\rangle) & \text{if } f(0) = f(1) \\ \pm\,|1\rangle\frac{1}{\sqrt{2}}(\,|0\rangle - |1\rangle) & \text{if } f(0) \neq f(1), \end{cases}$$

or, alternatively,

$$|\psi_2^{(3)}\rangle = \pm\,|f(0) \oplus f(1)\rangle\frac{1}{\sqrt{2}}(\,|0\rangle - |1\rangle). \tag{9.11}$$

Thus, measurement on the data qubit yields state $|f(0)\oplus f(1)\rangle$, which is $|0\rangle$ if $f(0) = f(1)$ $[f(0)\oplus f(1) = 0]$, and is $|1\rangle$ if $f(0) \neq f(1)$ $[f(0)\oplus f(1) = 1]$. This illustrates the power of superposition employed in quantum computation.

9.2.2 Deutsch–Jozsa Algorithm

The Deutsch-Jozsa algorithm is a generalization of the above algorithm to the multiqubit case. Namely, suppose that a Boolean function $f(x) : \{0,1\}^k \to \{0,1\}$ of a k-bit argument $x \equiv x_1 x_2 \ldots x_k$ is computed by the quantum black-box U_f via $|x, y\rangle \xrightarrow{U_f} |x, y \oplus f(x)\rangle$. As before, our aim is to determine whether the function is constant $f(x) = \text{const}$, i.e., its value is the same for all $0 \leq x < 2^k$, or balanced, meaning that $f(x) = 0$ for exactly half of all possible x, and $f(x) = 1$ for the other half of the values of x. We are guaranteed that f is either constant or balanced. On a classical computer, we would need to evaluate $f(x)$ at least twice for two different arguments x and x', provided that the values of f for x and x' are different, in which case we know that the function is balanced. If however, the values of f are the same, we need to call U_f with yet another argument $x'' \neq x, x'$, and compare the output with the previous values of f. Again, if these values are different, we learn that f is balanced, otherwise we have to test more x. Only after $2^k/2+1$ queries of the function with different arguments yielding the same result we can be certain that the function is constant. The quantum circuit of Fig. 9.5, however, can give a definite answer to that problem after only a single evaluation of f for a superposition of all x.

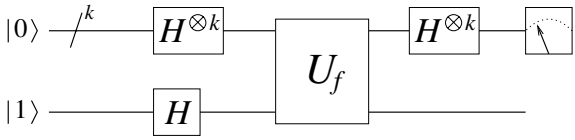

Fig. 9.5. Circuit implementing the Deutsch–Jozsa algorithm.

Let us follow the states of the register through this circuit. The data register is composed of k qubits, initially all in state $|0\rangle$, and the target is a single qubit, initially in state $|1\rangle$. Thus, the initial state of the system is

$$|\psi_{k+1}^{(0)}\rangle = |0\rangle^{\otimes k} |1\rangle \, . \tag{9.12}$$

Applying the Hadamard gates to the data and target qubits, we prepare the data register in the equally weighted superposition state of all possible x,

$$|\psi_{k+1}^{(1)}\rangle = \sum_x \frac{|x\rangle}{\sqrt{2^k}} \, \frac{|0\rangle - |1\rangle}{\sqrt{2}} \, . \tag{9.13}$$

Since the target qubit is prepared in state $(|0\rangle - |1\rangle)/\sqrt{2}$, the U_f transformation leads to

$$|\psi_{k+1}^{(2)}\rangle = \sum_x \frac{(-1)^{f(x)} |x\rangle}{\sqrt{2^k}} \, \frac{|0\rangle - |1\rangle}{\sqrt{2}} \, . \tag{9.14}$$

Finally, the Hadamard transformation is applied to all k qubits of the data register, which yields the state

$$|\psi_{k+1}^{(3)}\rangle = \sum_z \sum_x \frac{(-1)^{x\cdot z+f(x)}\,|z\rangle}{2^k}\,\frac{|0\rangle - |1\rangle}{\sqrt{2}}\,. \tag{9.15}$$

Here we have used the multiqubit generalization of (8.7),

$$H^{\otimes k}\,|x_1\ldots x_k\rangle = \sum_{z_1,\ldots,z_k} \frac{(-1)^{x_1z_1+\ldots+x_kz_k}\,|z_1\ldots z_k\rangle}{\sqrt{2^k}}\,,$$

which, in a compact form, is

$$H^{\otimes k}\,|x\rangle = \sum_z \frac{(-1)^{x\cdot z}\,|z\rangle}{\sqrt{2^k}}\,,$$

where $x\cdot z = x_1z_1+\ldots+x_kz_k$ is the bitwise dot product of x and z.

The remarkable property of the final state (9.15) is that the amplitude c_0 of the state $|z=0\rangle = |0\rangle^{\otimes k}$ of the data register is given by

$$c_0 = \langle\psi_{k+1}^{(3)}|0\rangle^{\otimes k}\,\frac{|0\rangle - |1\rangle}{\sqrt{2}} = \sum_x \frac{(-1)^{f(x)}}{2^k}\,.$$

Therefore, if the function f is constant, all 2^k terms enter this sum with the same sign ("+" for $f(x)=0$ and "−" for $f(x)=1$) and we have $c_0=\pm1$. On the other hand, if the function f is balanced, exactly half of the terms enter this sum with the "+" sigh, and the other half enter with the "−" sign, which results in $c_0=0$. Thus, if the function f is constant, the measurement of the data register yields, with the probability $|c_0|^2=1$, the output state $|0\rangle^{\otimes k}$, i.e., all qubits are in state $|0\rangle$. If, on the other hand, the measurement yields $|c_0|^2=0$, i.e, at least one of qubits of the data register is found in state $|1\rangle$, the function f is balanced.

We have thus seen that, despite of its limited use for practical applications, the Deutsch–Jozsa algorithm unambiguously demonstrates the potential power of a quantum computer. In what follows, we describe two very useful quantum algorithms that can significantly speed up and efficiently solve two classes of important problems involving search/minimization and Fourier transform.

9.2.3 Grover Algorithm

The quantum search algorithm was invented by Grover, and it offers a quadratic speed-up over classical algorithms for searching an unsorted database. Suppose we have a list of $N=2^k$ elements d_x stored in a computer memory. The index x, taking N different integer values $x=0,1,\ldots,N-1$, identifies

the position of each element in the list. We are searching for the position x_w of an element d_w satisfying certain condition $C(d_x)$, e.g., $d_{x_w} = d_w$. To that end, we are given a black-box—oracle U_f—evaluating a function $f(x)$ that returns 1, if x points to the desired element d_w, and zero otherwise, i.e.,

$$f(x) = \begin{cases} 1 & \text{if } C(d_x) = \text{TRUE} \\ 0 & \text{if } C(d_x) = \text{FALSE} . \end{cases}$$

Our aim is thus to find the index x_w for which $f(x_w) = 1$.

Table 9.1. Schematic representation of a telephone directory.

x	Name	Phone/address
0	A	d_0
1	B	d_1
	...	
$N-1$	Z	d_{N-1}

To better visualize the problem at hand, consider a list of entries in Table 9.1 which is a schematic representation of a telephone directory sorted according to the names in alphabetic order. Suppose we know the telephone number or address of a person whose name we want to find. For that purpose, the telephone directory is a usual unsorted database. To find out the person's name, we would need to identify the line x_w that contains also his telephone number and address.

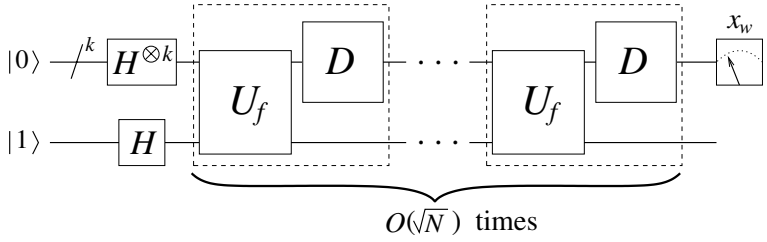

Fig. 9.6. Circuit implementing Grover's search algorithm.

For simplicity, let us assume that only one element in the database satisfies condition C. A typical classical algorithm would have to evaluate the function f for each entry in the database, starting from say $x = 0$, until it finds the position x_w of the desired element. On the average, $N/2$ queries of the oracle U_f are needed, before x_w is identified. We describe now a quantum search algorithm that is capable of finding x_w, with a probability approaching unity

after only about $\sqrt{N}$ calls of U_f. The corresponding quantum circuit is shown in Fig. 9.6. Initially, the data register composed of k qubits is prepared in state $|0\rangle \equiv |0\rangle^{\otimes k}$ and the single-qubit target register is in state $|1\rangle$. As in the Deutsch–Josza algorithm, application of the Hadamard gates to the data and target qubits prepares the data register in an equally weighted superposition state of all x,

$$H^{\otimes k}\,|0\rangle = \frac{1}{\sqrt{N}} \sum_x |x\rangle \equiv |s\rangle \;, \tag{9.16}$$

and the target register state is $(|0\rangle - |1\rangle)/\sqrt{2}$. After the preparation, we call the oracle, followed by the D transformation detailed below, $O(\sqrt{N})$ times and finally measure the state of the data register. With a probability close to unity, the resulting output, given by a sequence of 0s and 1s, is a binary representation of index x_w of the desired element.

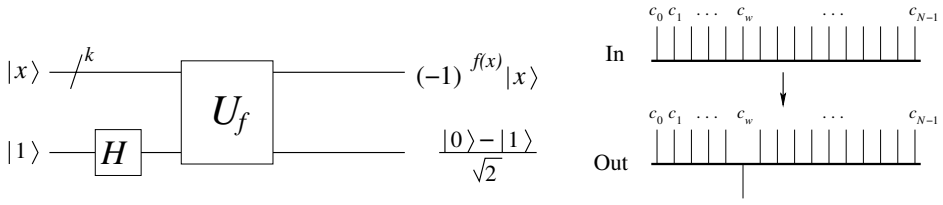

Fig. 9.7. Oracle U_f acting upon state $|x\rangle$ induces a phase-shift $(-1)^{f(x)}$. When the input is a superposition state, only amplitude c_w of the required state flips its sign.

Let us consider in detail the two core transformations used by the algorithm, the oracle U_f and Grover's operator D. As shown in Fig. 9.7, the oracle takes as an input a k-bit data register in state $|x\rangle$ and a single-bit target register prepared in state $(|0\rangle - |1\rangle)/\sqrt{2}$. The combined state is thus $|\psi^{\rm in}_{k+1}\rangle = |x\rangle\,(|0\rangle - |1\rangle)/\sqrt{2}$. At the output, the state of the data register acquires a phase-shift $(-1)^{f(x)}$,

$$|\psi^{\rm out}_{k+1}\rangle = U_f\,|\psi^{\rm in}_{k+1}\rangle = (-1)^{f(x)}\,|x\rangle\,\frac{|0\rangle - |1\rangle}{\sqrt{2}} \;.$$

That is, only the sought after state $|x_w\rangle$, for which $f(x_w) = 1$, flips its sign while all other states $|x\rangle$ remain unchanged. Therefore, if at the input the data register is prepared in a superposition state of all $0 \le x < 2^k$, $|\psi^{\rm in}_{k+1}\rangle = \sum_x c_x\,|x\rangle\,(|0\rangle - |1\rangle)/\sqrt{2}$, at the output the amplitude c_w of state $|x_w\rangle$ will change its sign,

$$|\psi^{\rm out}_{k+1}\rangle = U_f\,|\psi^{\rm in}_{k+1}\rangle = \left(-c_w\,|x_w\rangle + \sum_{x\neq x_w} c_x\,|x\rangle\right)\,\frac{|0\rangle - |1\rangle}{\sqrt{2}} \;. \tag{9.17}$$

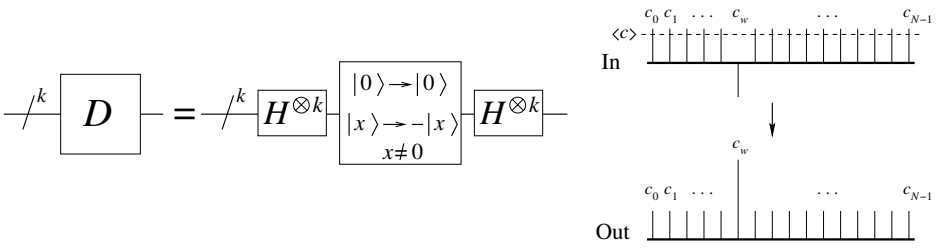

Fig. 9.8. Inversion about the average transformation D is realized by the sequence of $H^{\otimes k}$, conditional phase-shift $|0\rangle \rightarrow |0\rangle$, $|x\rangle \rightarrow -|x\rangle$ $(1 \leq x < 2^k)$, and $H^{\otimes k}$ transformations. This operation enhances the amplitude c_w of the flipped state.

The second transformation, known as "inversion about the average", is described by the operator

$$D = H^{\otimes k}(2\,|0\rangle\langle 0| - I)H^{\otimes k} = 2\,|s\rangle\langle s| - I\,, \tag{9.18}$$

with $|s\rangle$ given by (9.16), which acts upon the data register. From definition (9.18), it follows that this operation can be realized by the circuit of Fig. 9.8, where the conditional phase-shift operation, $|0\rangle \rightarrow |0\rangle$ and $|x\rangle \rightarrow -|x\rangle$ $(1 \leq x < 2^k)$, is sandwiched between two k-qubit Hadamard transforms $H^{\otimes k}$. Operator D, applied to the data register in an arbitrary superposition state $|\psi_k^{\text{in}}\rangle = \sum_x c_x\,|x\rangle$, yields

$$|\psi_k^{\text{out}}\rangle = D\,|\psi_k^{\text{in}}\rangle = \sum_x (2\langle c\rangle - c_x)\,|x\rangle\,, \tag{9.19}$$

where $\langle c\rangle \equiv \sum_x c_x/N$ is the averaged value of all c_x. That is, every amplitude c_x is transformed according to $c_x \rightarrow 2\langle c\rangle - c_x$. As a result, the amplitude c_w of state $|x_w\rangle$, that was flipped by the U_f, becomes $c_w = 3/\sqrt{N} - O(N^{-3/2})$, while all of the other $N-1$ amplitudes c_x $(x \neq x_w)$ are given by $c_x = 1/\sqrt{N} - O(N^{-3/2})$.

Returning to the complete search algorithm of Fig. 9.6, we see that after every iteration of the $[U_f D]$ sequence, the amplitude c_w increases by $O(1/\sqrt{N})$. Therefore after $O(\sqrt{N})$ iterations, the probability to find the data register in state $|x_w\rangle$ approaches $O(1)$, i.e., $|c_w|^2 \sim 1$, and the measurement yields x_w, which is the position of the desired element.

The quantum search algorithm described above is rather general, since many other problems, such as minimization, solution finding, and even factorization[2] can be reduced to a search problem. A straightforward generalization of the Grover algorithm is possible for the case when the database contains more than one element satisfying a given condition C. As noted at the end of Sect. 9.1.1, the implementation of quantum oracle U_f involves resources (auxiliary qubits and quantum logic gates) that are proportional to those needed

[2]The factorization problem can actually be solved even more efficiently, using the quantum Fourier transform algorithm described in the following section.

to compute the function f classically using bits and reversible logic gates. In that respect, it has been proven that Grover's algorithm is optimal—there is no other algorithm that can do better in searching an unsorted database.

9.2.4 Quantum Fourier Transform

The Fourier transform is an important operation used in a large class of mathematical problems. Many real-world physical and computational problems, that usually deal with a discretized set of data, are efficiently analyzed and solved employing the discrete Fourier transform, which amounts to transforming one set of complex numbers $x_0, x_1, \ldots, x_{N-1}$ to another set $y_0, y_1, \ldots, y_{N-1}$, according to

$$y_n = \frac{1}{\sqrt{N}} \sum_{j=0}^{N-1} \exp\left(\frac{2\pi \mathrm{i} jn}{N}\right) x_j \ . \tag{9.20}$$

The set $\{x_j\}$ can conveniently be thought of as representing a vector in an N dimensional complex vector space, and the set $\{y_j\}$ is then a rotated vector, since transformation (9.20) is norm-preserving, $\sum |y_j|^2 = \sum |x_j|^2$. For computational convenience, the dimension of the vector is usually taken such that $N = 2^k$. To accomplish the discrete Fourier transform, a straightforward application of (9.20) requires about $N \times N = 2^{2k}$ steps of computation. There exists, however, a more economical classical algorithm, called fast Fourier transform—FFT—that performs the transformation in $N \log(N) = k2^k$ computational steps. We describe now a quantum Fourier transform (QFT) algorithm, invented by Shor, that offers an impressive exponential speed-up over the best known classical FFT algorithm.

Let us use integers j and n, such that $0 \leq j, n \leq 2^k - 1$, to represent the basis states $|j\rangle$ and $|n\rangle$ of a k-qubit quantum register. Recall from Sect. 7.1 that j and n have the binary representation $j \equiv j_1 j_2 \ldots j_k$ and $n \equiv n_1 n_2 \ldots n_k$. The quantum Fourier transform operation U_{QFT} is defined via

$$|j\rangle \xrightarrow{\mathrm{QFT}} \frac{1}{\sqrt{N}} \sum_{n=0}^{N-1} \exp\left(\frac{2\pi \mathrm{i} jn}{N}\right) |n\rangle \ . \tag{9.21}$$

Then, if the input state of the register is prepared as $|\psi_k^{\mathrm{in}}\rangle = \sum_{j=0}^{N-1} x_j |j\rangle$, and the U_{QFT} transforms every $|j\rangle$ according to (9.21), for the output state we have

$$\begin{aligned} |\psi_k^{\mathrm{out}}\rangle = U_{\mathrm{QFT}} |\psi_k^{\mathrm{in}}\rangle &= \sum_{j=0}^{N-1} x_j \left[\frac{1}{\sqrt{N}} \sum_{n=0}^{N-1} \exp\left(\frac{2\pi \mathrm{i} jn}{N}\right) |n\rangle\right] \\ &= \sum_{n=0}^{N-1} \left[\frac{1}{\sqrt{N}} \sum_{j=0}^{N-1} \exp\left(\frac{2\pi \mathrm{i} jn}{N}\right) x_j\right] |n\rangle = \sum_{n=0}^{N-1} y_n |n\rangle \ , \end{aligned} \tag{9.22}$$

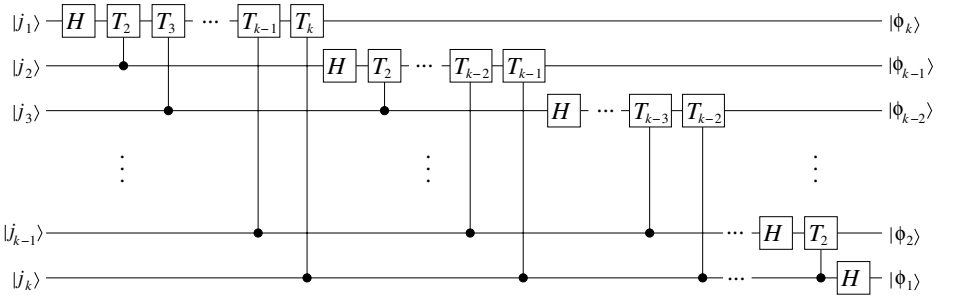

Fig. 9.9. Circuit implementing the quantum Fourier transform.

where the amplitudes y_n are given by (9.20).

The circuit realizing the quantum Fourier transform is shown in Fig. 9.9, where the T_l operation is defined as

$$T_l = \begin{bmatrix} 1 & 0 \\ 0 & \mathrm{e}^{\frac{2\pi \mathrm{i}}{2^l}} \end{bmatrix} ,$$

while H denotes the usual Hadamard gate. This circuit is based on the following product representation for the Fourier transformed register,

$$\begin{aligned}
|j\rangle &\equiv |j_1 \dots j_k\rangle \\
&\xrightarrow{\text{QFT}} \frac{1}{2^{k/2}} \sum_{n=0}^{2^k-1} \exp\left(\frac{2\pi \mathrm{i} j n}{2^k}\right) |n\rangle \\
&= \frac{1}{2^{k/2}} \sum_{n_1=0}^{1} \dots \sum_{n_k=0}^{1} \exp\left(2\pi \mathrm{i} j \sum_{l=1}^{k} \frac{n_l}{2^l}\right) |n_1 \dots n_k\rangle \\
&= \frac{1}{2^{k/2}} \sum_{n_1=0}^{1} \dots \sum_{n_k=0}^{1} \prod_{l=1}^{k} \exp\left(\frac{2\pi \mathrm{i} j n_l}{2^l}\right) |n_l\rangle \\
&= \frac{1}{2^{k/2}} \prod_{l=1}^{k} \left[\sum_{n_l=0}^{1} \exp\left(\frac{2\pi \mathrm{i} j n_l}{2^l}\right) |n_l\rangle\right] \\
&= \prod_{l=1}^{k} \frac{|0\rangle + \mathrm{e}^{\frac{2\pi \mathrm{i} j}{2^l}} |1\rangle}{\sqrt{2}} = \prod_{l=1}^{k} |\phi_l\rangle \\
&\equiv \frac{|0\rangle + \mathrm{e}^{2\pi \mathrm{i}\, 0.j_k} |1\rangle}{\sqrt{2}} \; \frac{|0\rangle + \mathrm{e}^{2\pi \mathrm{i}\, 0.j_{k-1} j_k} |1\rangle}{\sqrt{2}} \; \dots \; \frac{|0\rangle + \mathrm{e}^{2\pi \mathrm{i}\, 0.j_1 j_2 \dots j_k} |1\rangle}{\sqrt{2}} ,
\end{aligned} \tag{9.23}$$

where in the last step we have used the decomposition $j = j_1 2^{k-1} + \dots + j_k 2^0$, binary fraction representation (7.2), and the fact that $\mathrm{e}^{2\pi \mathrm{i} r} = 1$, r being any integer (see Prob. 9.3).

To see that the circuit of Fig. 9.9 indeed realizes transformation (9.23), observe that the action of the Hadamard gate on a qubit in state $|j_m\rangle$ ($j_m \in \{0,1\}$) can be cast as

$$|j_m\rangle \xrightarrow{H} \frac{|0\rangle + \mathrm{e}^{2\pi \mathrm{i}\, 0.j_m}\,|1\rangle}{\sqrt{2}}\ ,$$

while an application of the controlled-T_l operation between the control qubit in state $|j_c\rangle$ and target qubit in state $(\,|0\rangle + |1\rangle)/\sqrt{2}$, gives

$$|j_c\rangle\,\frac{|0\rangle + |1\rangle}{\sqrt{2}} \xrightarrow{T_l^{j_c}} |j_c\rangle\,\frac{|0\rangle + \mathrm{e}^{j_c \frac{2\pi \mathrm{i}}{2^l}}\,|1\rangle}{\sqrt{2}} = |j_c\rangle\,\frac{|0\rangle + \mathrm{e}^{2\pi \mathrm{i}\, 0.\overbrace{0\ldots0}^{l-1} j_c}\,|1\rangle}{\sqrt{2}}\ .$$

Let us follow through the circuit the evolution of the state of the first qubit,

$$\begin{aligned} |j_1\rangle \xrightarrow{H} \frac{|0\rangle + \mathrm{e}^{2\pi \mathrm{i}\, 0.j_1}\,|1\rangle}{\sqrt{2}} \xrightarrow{T_2^{j_2}} \frac{|0\rangle + \mathrm{e}^{2\pi \mathrm{i}\, 0.j_1 j_2}\,|1\rangle}{\sqrt{2}} \xrightarrow{T_3^{j_3}} \cdots \\ \cdots \xrightarrow{T_k^{j_k}} \frac{|0\rangle + \mathrm{e}^{2\pi \mathrm{i}\, 0.j_1 j_2 \ldots j_k}\,|1\rangle}{\sqrt{2}} = |\phi_k\rangle\ . \end{aligned} \tag{9.24}$$

Similarly, for the second qubit we have

$$\begin{aligned} |j_2\rangle \xrightarrow{H} \frac{|0\rangle + \mathrm{e}^{2\pi \mathrm{i}\, 0.j_2}\,|1\rangle}{\sqrt{2}} \xrightarrow{T_2^{j_3}} \frac{|0\rangle + \mathrm{e}^{2\pi \mathrm{i}\, 0.j_2 j_3}\,|1\rangle}{\sqrt{2}} \xrightarrow{T_3^{j_4}} \cdots \\ \cdots \xrightarrow{T_{k-1}^{j_k}} \frac{|0\rangle + \mathrm{e}^{2\pi \mathrm{i}\, 0.j_2 j_3 \ldots j_k}\,|1\rangle}{\sqrt{2}} = |\phi_{k-1}\rangle\ , \end{aligned} \tag{9.25}$$

and so on for all the qubits through the last one

$$|j_k\rangle \xrightarrow{H} \frac{|0\rangle + \mathrm{e}^{2\pi \mathrm{i}\, 0.j_k}\,|1\rangle}{\sqrt{2}} = |\phi_1\rangle\ . \tag{9.26}$$

We then use the SWAP operations (not shown in Fig. 9.9) between the first and the last qubits, the second and one before the last qubits, etc., to reverse the order of qubits, obtaining finally (9.23). In doing this, we apply k logic gates to the first qubit, $k-1$ gates to the second one, etc., all together $k(k+1)/2$ gates. At the end, we use $k/2$ SWAP gates, if k is even, or $(k-1)/2$ SWAP gates, if k is odd. So all in all, we need $k(k+2)/2$ gates, or $O(k^2)$ steps of computation, which is exponentially better than the classical FFT algorithm.

Given such an impressive speed-up, one is then tempted to assume that the quantum Fourier transform can be used to efficiently solve a great variety of classical problems. This is, however, not entirely true, and to-date only a limited number of problems have been shown to be amenable to the QFT algorithm. All of them are examples of a general problem known as the (Abelian) hidden subgroup problem. It includes the order-finding and prime factorization which employ the phase estimation procedure of Prob. 9.5, as well as

period-finding and discrete logarithm determination. Other possible applications of the QFT algorithm include efficient simulations of certain quantum systems, such as particles confined in potentials of specific shapes, whose classical counterparts exhibit chaos. One of the main complications associated with the use of the quantum Fourier transform for a broader range of applications is that it is usually very difficult to prepare the input state of a quantum register as $|\psi_k^{\rm in}\rangle = \sum_{j=0}^{2^k-1} x_j\,|j\rangle$, which is typically an entangled state of k qubits. Also, even if state $|\psi_k^{\rm in}\rangle$ is successfully prepared and the transformation (9.22) is accomplished, measuring reliably the amplitudes y_n of the output state in a single (or few) runs is usually not possible, unless the input represents a periodic function, in which case at the output only one or just a few states $|n\rangle$ have appreciable probabilities $|y_n|^2$.

9.3 Quantum Computer Simulating Quantum Mechanics

Finally, let us briefly discuss simulations of quantum systems by quantum computers. One of the most important applications of modern (classical) computers involves analysis, design and simulation of complex physical systems, such as constructions and buildings, cars and aircraft, and even weapons, to name just a few. However, classical computers are inefficient in simulating quantum systems. As reviewed in Chap. 1, a typical quantum mechanical problem can be formulated as follows. Given a compound system S composed of subsystems A,B,C,..., each having a finite number of states $N_{\rm A}, N_{\rm B}, N_{\rm C}, \ldots$, respectively, then the number of states $N_{\rm S}$ spanning the complete system S (the dimension of its Hilbert space) is given by the product $N_{\rm S} = N_{\rm A} \times N_{\rm B} \times N_{\rm C} \ldots$ At an initial time t_0, the state of the system $|\Psi^{\rm S}(t_0)\rangle$ is known and, provided the subsystems are unentangled, it is given by the tensor product $|\Psi^{\rm S}(t_0)\rangle = |\Psi_0^{\rm A}\rangle \otimes |\Psi_0^{\rm B}\rangle \otimes |\Psi_0^{\rm C}\rangle \ldots$ of the initial states $|\Psi_0^j\rangle$ of subsystems $j = {\rm A,B,C,}\ldots$ The time-evolution of the system is governed by the Schrödinger equation

$$\mathrm{i}\hbar \frac{\partial}{\partial t}\,|\Psi^{\rm S}\rangle = \mathcal{H}^{\rm S}\,|\Psi^{\rm S}\rangle\ , \tag{9.27}$$

where the Hamiltonian of the systems $\mathcal{H}^{\rm S} = \sum \mathcal{H}^j + \mathcal{V}$ is composed of the sum of free Hamiltonians of each subsystem $\mathcal{H}^j$ plus the term $\mathcal{V}$ describing the interactions between them. At time $t > t_0$, the state vector evolves into

$$|\Psi^{\rm S}(t)\rangle = \mathcal{U}_{\rm S}(t)\,|\Psi^{\rm S}(t_0)\rangle\ . \tag{9.28}$$

where $\mathcal{U}_{\rm S}(t) \equiv \exp[-\frac{\mathrm{i}}{\hbar}\mathcal{H}^{\rm S}(t-t_0)]$ is the evolution operator. Except for a few special cases, analytic expressions for the evolution operator $\mathcal{U}_{\rm S}(t)$ are usually not attainable, because exponentiating operators is very difficult. Thus to solve the problem of determining the state of the system $|\Psi^{\rm S}(t)\rangle$, in most cases one would have to use computers.

On a classical computer, solving the Schrödinger equation amounts to integrating N_{S} differential equations

$$\frac{\partial}{\partial t}c_n = -\frac{\mathrm{i}}{\hbar}\sum_m \mathcal{H}_{nm}c_m \ , \quad \mathcal{H}_{nm} \equiv \langle n|\,\mathcal{H}^{\mathrm{S}}\,|m\rangle \ , \tag{9.29}$$

for N_{S} complex amplitudes c_n representing the state vector $|\Psi^{\mathrm{S}}\rangle = \sum_{n=1}^{N_{\mathrm{S}}} c_n\,|n\rangle$. Each amplitude requires at least 64, or better 128 bits of memory to store its value. Adding one more subsystem of dimension M increases the dimension N_{S} of system's Hilbert space M times! Assuming that the subsystems have a comparable number of states $N_j \sim N$, we see that the dimension of the Hilbert space of the total system grows exponentially with the number of subsystems n_s, $N_{\mathrm{S}} \sim N^{n_s}$. As remarked by Caves, "Hilbert space is a big place." Even for a modest system composed of only a few ($n_s \lesssim 10$) interacting subsystems, each having say $N \sim 10-100$ relevant eigenstates, we have to store and process a huge number ($N_{\mathrm{S}} \sim 10^{10}$) of complex probability amplitudes. If the size of the system is somewhat larger, even the best classical computers today and in the foreseeable future will not be able to cope with such amounts of data, not to mention the amount of energy required to process it.

If we realize a scalable quantum computer, however, these problems would become tractable. To be able to store and process all the data associated with a quantum system of size N_{S} we need to have a register containing k qubits so that $2^k \gtrsim N_S$. That is, the size of the Hilbert space of the computer's register should be comparable or only slightly larger than that of the system. The computation would then proceeds in four steps outlined in Sect. 9.1: First, we initialize the register to a known initial state $|00\ldots0\rangle$. We then load the input by preparing the register in a state $|\psi_k\rangle$ corresponding to the initial state $|\Psi^{\mathrm{S}}(t_0)\rangle$ of the system to be simulated. Since the initial state is usually a simple product state of subsystems, no entanglement is present and this step can be accomplished easily using only a small number of logic gates. Next comes the difficult part—simulation of the dynamics due to the Hamiltonian $\mathcal{H}^{\mathrm{S}}$. For that we need to design a sequence of logic gates $U_1, U_2, \ldots U_l$, whose application to the register results in the evolution operator $\mathcal{U}_{\mathrm{S}}(t)$ according to $U_l U_{l-1} \ldots U_1 = \mathcal{U}_{\mathrm{S}}(t)$. This transformation can be simulated efficiently, if the interaction Hamiltonian can be represented as a sum $\mathcal{V} = \sum_l V^l$ involving a finite number of terms, polynomial in the size of the total system, each element V^l acting only on a small number of subsystems at a time. This is the case for many physical systems of interest, where the interaction between the subsystems usually involves only two- or few-body interactions. Finally, we measure the quantum register whose state corresponds to that of the simulated system. If the measured state is not an eigenstate of the register, we may have to perform many repetitions of this cycle, to attain a reliable probability distribution for the final state of the system. Provided the number of required repetitions does not grow exponentially with the system's size, but only polynomially, we can claim that quantum computers can efficiently

simulate quantum mechanics. Thus we see that this is essentially an analog computation, since, upon the program execution, the quantum computer imitates another physical system being simulated, as envisioned by Richard Feynman as early as 1982.

9.4 Error Correction and Fault–Tolerant Computation

Errors are inevitable, happen all the time everywhere, and computers are no exception. Though the hardware of modern digital computers is extremely reliable, telecommunication networks are more prone to errors caused by noise and imperfections. One can think of two complementary ways of coping with errors—passive and active stabilization of information. The former consists of suppressing the noise and the sensitivity to it by improving the hardware and making it more reliable, while the latter employs redundancy in combination with appropriate software to encode and decode the information that can be recovered after being partially corrupted.

Semiconductor technology, which is at the heart of modern high-performance computers, is already very well developed and there is constant improvement in its reliability. The technology associated with quantum information processing is just beginning to be developed and there is a long way to go before one can assert that it is as reliable as modern digital information technology. A quantum system in a superposition state can undergo uncontrolled evolution resulting in the destruction of coherence. Broadly speaking, this loss of coherence can be attributed to two sources, classical noise and decoherence. The noise is associated with the interaction of the systems with stray, yet classical, electric or magnetic fields which change the system's state vector in an uncontrollable way. That is, the evolution of the systems is governed by the Schrödinger equation (1.117) with some Hamiltonian $\mathcal{H}$ which we, however, do not know and can not control. Decoherence, on the other hand, is caused by the coupling of the system to its environment or a reservoir, even when the latter is in a vacuum state. Then the evolution of the state vector of the system alone does not obey the Schrödinger equation, rather, the total state vector of the system plus the environment does. But then the system–environment interaction results in their entanglement so that the state vector of the system alone is no longer well-defined. The state of the system does not exhibit coherence and is described by the density operator obtained after tracing over the environment degrees of freedom.

Since in quantum computation and communication protocols the qubits store superposition states, the information encoded in qubits is very fragile. Fortunately, there exist methods to protect that information and even correct the errors with the help of quantum error correcting codes. In this section, we will briefly dwell upon the subject of error correction and fault–tolerant quantum computation. This is already a mature field, interdisciplinary in its essence as it involves an interplay of mathematics, quantum mechanics and

related disciplines. Here we aim merely at a simple introduction to this subject. For further details the reader is referred to the more specialized literature on the subject.

9.4.1 Classical Error Correction

Before describing schemes for quantum error correction, it may be illuminating to first consider their classical counterparts. As discussed in Chap. 7, in a classical computer the elementary unit of information—bit—is represented by a physical device being in one of its two possible, easily distinguishable states 0 and 1. The information is written in a string of such bits. When this information is stored or sent through a communication channel, a single-bit error amounts to the bit flip $0 \leftrightarrow 1$, i.e., 0 is replaced by 1 or vice versa.

Let us assume that the probability p for the error to occur on any given bit is independent on the values of the other bits in the string. Then the simplest method to protect the information against the single-bit errors is to encode every bit into three bits via

$$0 \to 000 \ , \quad 1 \to 111 \ . \tag{9.30}$$

Such redundant bit-strings encoding single (physical) bits are called logical bits and often designated as $0_L \equiv 000$ and $1_L \equiv 111$. At the readout, the value of the actual bit is inferred from majority voting. Its essence is to assign to the original bit the value of the majority of the bits contained in the logical bit, i.e., if the logical bit contains 000, 001, 010, or 100, the actual bit is assigned 0; while in the case of 111, 110, 101, or 011, it is assigned 1. Obviously, the majority voting fails when in the logical bit-string more than one error occur. The probability $P_{\rm err}$ of the majority voting protocol to fail is then given by the sum of the probabilities that any two bits or all three bits flip. These probabilities are given, respectively, by

$$p_2 = 3p^2(1-p) \ , \quad p_3 = p^3 \ ,$$

the factor 3 in the equation for p_2 coming from the fact that there are three possible ways of the double-error to occur. The total probability then reads

$$P_{\rm err} = p_2 + p_3 = 3p^2 - 2p^3 \ , \tag{9.31}$$

which is smaller than single-bit error probability p when $p < \frac{1}{2}$. Thus the repetition code of (9.30) yields an improved reliability of storing the information in an error-prone physical system or sending it through a noisy communication channel. This reliability can further be improved by using longer encoding strings and other more elaborate and often system-dependent strategies for designing error correcting codes. All of them, however, make use of the redundancy in information encoding that allows for the restorability of the original information.

9.4.2 Quantum Error Correction

Consider now a qubit in state

$$|\psi_1\rangle = \alpha\,|0\rangle + \beta\,|1\rangle\ . \tag{9.32}$$

Since the coefficients α and β take arbitrary complex values, constrained only by the normalization $|\alpha|^2 + |\beta|^2 = 1$, a continuum of errors can corrupt the qubit state. Any single qubit error, however, can be expanded in terms of the original uncorrupted state (9.32) and three kinds of errors:

1. Bit-flip error that interchanges the basis states, $|0\rangle \leftrightarrow |1\rangle$. It can thus be associated with the X operator applied to the qubit, resulting in state $X\,|\psi_1\rangle = \beta\,|0\rangle + \alpha\,|1\rangle$.
2. Phase-flip error that flips the sign of the superposition (9.32). The corresponding operator is Z, with the action $Z\,|\psi_1\rangle = \alpha\,|0\rangle - \beta\,|1\rangle$.
3. Bit and phase flip error, which is the combination of both errors above. The corresponding operator is $XZ = -\mathrm{i}Y$, resulting in $XZ\,|\psi_1\rangle = \beta\,|0\rangle - \alpha\,|1\rangle$.

Obviously, no error corresponds to the Unity operator I applied to the qubit (9.32). If we characterize a general single qubit error by operator $\mathcal{E}_{\mathrm{err}}$, we see that it can be expanded in terms of the operators I, X, Z and XZ as

$$\mathcal{E}_{\mathrm{err}} = \sqrt{1 - p_x - p_z - p_{xz}}\,I + \sqrt{p_x}\,X + \sqrt{p_z}\,Z + \sqrt{p_{xz}}\,XZ\ , \tag{9.33}$$

where p_i are the probabilities of the corresponding errors.

To be able to reliably store and communicate quantum information, we need to design error correcting codes capable of reliably detecting and correcting the three types of errors mentioned above. A straightforward application of the repetition code used for classical bits, followed by the majority voting scheme, is impossible due to the following fundamental limitations:

- The no-cloning theorem (Sect. 8.3) forbids one to produce exact copies of a qubit in an arbitrary state.
- The projective measurement of the qubit (Sect. 8.2.3) does not yield complete information about the qubit state and destroys the quantum information content stored in it.

Thus a more clever procedure is needed. The general strategy used in quantum error correcting codes can be summarized as follows.

1. Encode the state of a qubit in a collective (typically entangled) state of several qubits. This state belongs to a cleverly chosen code subspace $\mathbb{S}_{\mathrm{C}}$ of the Hilbert space of the multiqubit block having the following core property: an arbitrary single-qubit error on any qubit in the block takes its state to an orthogonal subspace uniquely associated with that particular qubit and the error type. That is, every possible error in the error correcting code leads to a state that is orthogonal to the original uncorrupted state and all other states obtained by single-qubit errors.

2. Perform multiqubit measurements on the encoding block, which can clearly distinguish between the uncorrupted state and all other states resulting from any single-qubit error. Such measurements do not disclose the encoded data, but reveal the *error syndrome* that identifies the type and location of the error.
3. Knowing the error syndrome, perform the error correction by applying the appropriate transformation to the corrupted qubit.

We thus see that in the above scheme, the encoding of the qubit state is nonlocal while the errors are local, provided they act on every qubit in the register independently, which is usually a reasonable assumption for many practical cases. Therefore such local (single-qubit) errors are not fatal and collective measurements allow us to identify and correct the errors without disclosing and destroying the quantum information. In what follows, we illustrate these principles using simple examples.

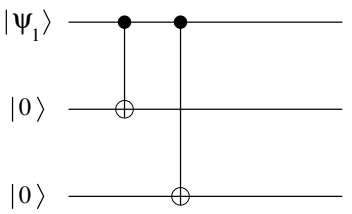

Fig. 9.10. Circuit for implementing a bit-flip error correcting code.

Let us assume for the moment that only the bit-flip errors X can corrupt our qubits. Using the circuit of Fig. 9.10, we can encode a single qubit with three qubits via

$$|0\rangle \rightarrow |000\rangle \equiv |0_L\rangle\,, \quad |1\rangle \rightarrow |111\rangle \equiv |1_L\rangle\,. \tag{9.34}$$

Then an arbitrary superposition of single-qubit basis states $|0\rangle$ and $|1\rangle$ is transformed into the corresponding superposition of logical states (also called code words) $|0_L\rangle$ and $|1_L\rangle$,

$$|\psi_1\rangle = \alpha\,|0\rangle + \beta\,|1\rangle \rightarrow \alpha\,|0_L\rangle + \beta\,|1_L\rangle = \alpha\,|000\rangle + \beta\,|111\rangle = |\psi_3\rangle\,. \tag{9.35}$$

A bit-flip error can now affect any qubit of (9.35) with probability p_x which we assume to be the same for all the qubits. If the first qubit flips, the state (9.35) turns into $\alpha\,|100\rangle + \beta\,|011\rangle$; similarly, flips of the second or the third qubit result in states $\alpha\,|010\rangle + \beta\,|101\rangle$ or $\alpha\,|001\rangle + \beta\,|110\rangle$, respectively. As noted above, measuring any one qubit in the block will not reveal the possible error and, what is even worse, will destroy the superposition (9.35). But we can perform collective measurements on the encoding block, which will identify the error, if any, without affecting the amplitudes α and β. The complete

set of measurements for determining the error syndrome is given by the four projection operators

$$\Pi_{00} = |000\rangle\langle 000| + |111\rangle\langle 111| \ , \tag{9.36a}$$
$$\Pi_{01} = |100\rangle\langle 100| + |011\rangle\langle 011| \ , \tag{9.36b}$$
$$\Pi_{10} = |010\rangle\langle 010| + |101\rangle\langle 101| \ , \tag{9.36c}$$
$$\Pi_{11} = |001\rangle\langle 001| + |110\rangle\langle 110| \ . \tag{9.36d}$$

The meaning of the indices will become clear shortly. If no error occurs, we have $\langle \Pi_{00} \rangle = 1$, since Π_{00} is the identity operator for any state of the form (9.35). Suppose now that the bit-flip error affects the first qubit, $\alpha\,|000\rangle + \beta\,|111\rangle \rightarrow \alpha\,|100\rangle + \beta\,|011\rangle$. The syndrome measurement then yields

$$\langle \Pi_{01} \rangle = 1 \ , \quad \langle \Pi_{00} \rangle = \langle \Pi_{10} \rangle = \langle \Pi_{11} \rangle = 0 \ ,$$

while the measurement does not affect the superposition, since

$$\Pi_{01}(\alpha\,|100\rangle + \beta\,|011\rangle) = \alpha\,|100\rangle + \beta\,|011\rangle \ .$$

We have thus learned that the first qubit has flipped. To recover the original state, we need to apply the X_1 transformation to the first qubit. Similarly, the measurement result $\langle \Pi_{10} \rangle = 1$ or $\langle \Pi_{11} \rangle = 1$ tells us that the bit flip has affected qubit 2 or 3, respectively, and instructs us to apply the X_2 or X_3 gate to the corresponding qubit.

How can we implement in practice all four projection operators (9.36)? For that, we can use two ancilla qubits, both prepared initially in state $|0\rangle$. Employing the measurement scheme of Fig. 8.6 (see Sect. 8.2.3), we use the first ancilla to measure the two-qubit observable corresponding to operator $U_1 = Z_2 Z_3$, and the second ancilla to measure $U_2 = Z_1 Z_3$. Note that both operators $U_{1,2}$ have eigenvalues ± 1; the $+1$ eigenvalue of each U_i indicates that the two qubits are in the same state, otherwise the eigenvalue is -1. In effect, the operator U_1 compares the states of qubits 2 and 3, while the operator U_2 compares the states of qubits 1 and 3. The projective measurement of each ancilla yields one bit of information, whereby "0" indicates the eigenvalue $+1$ and "1" the eigenvalue -1 of the corresponding operator U_i. Thus, after measuring both ancillas, the result xy ($x, y \in \{0, 1\}$) signifies that for the corresponding projection operator Π_{xy} we have $\langle \Pi_{xy} \rangle = 1$.

Let us determine what happens if any two or all three qubits flip. Apparently, in that case our error correcting scheme fails as it results in the wrong state $\beta\,|000\rangle + \alpha\,|111\rangle$, where the amplitudes α and β are interchanged. The failure probability is thus given by the sum of probabilities that any two or all three qubits flip,

$$P_{\text{err}} = 3p_x^2 - 2p_x^3 \ , \tag{9.37}$$

which is smaller than p_x when $p_x < \frac{1}{2}$, exactly as for the classical three-bit error correcting code.

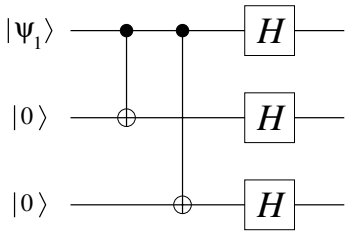

Fig. 9.11. Circuit for implementing the phase flip error correcting code.

Suppose now that only the phase-flip errors Z can corrupt our qubits with probability p_z. Note that in the rotated by the Hadamard transformation basis $\{|+\rangle, |-\rangle\}$ the phase flip error $|0\rangle \to |0\rangle$, $|1\rangle \to -|1\rangle$ interchanges the basis states, $|+\rangle \leftrightarrow |-\rangle$ (see Sect. 8.2.1). In analogy with the three qubit bit-flip code, we can therefore employ the circuit of Fig. 9.11 to encode a single qubit with three qubits via

$$|0\rangle \to |++\!+\rangle \equiv |0_L\rangle\,, \quad |1\rangle \to |--\!-\rangle \equiv |1_L\rangle\,. \tag{9.38}$$

Consequently, an arbitrary single-qubit superposition state is encoded as

$$|\psi_1\rangle = \alpha\,|0\rangle + \beta\,|1\rangle \to \alpha\,|0_L\rangle + \beta\,|1_L\rangle = \alpha\,|++\!+\rangle + \beta\,|--\!-\rangle = |\psi_3\rangle\,. \tag{9.39}$$

If a phase flip affects, say, the first qubit of the code, this state is transformed to $\alpha\,|-\!+\!+\rangle + \beta\,|+\!-\!-\rangle$, and similarly for qubits 2 and 3. The four projection operators for the syndrome diagnosis are given by (9.36) with the replacements $0 \to +$ and $1 \to -$. To detect the phase flip, we need to compare the states of qubits 2 and 3, and qubits 1 and 3. Recall that states $|+\rangle$ and $|-\rangle$ are the eigenstates of operator X, and the corresponding eigenvalues are $+1$ and -1. Then the operators comparing the states of the corresponding qubits are $U_1 = X_2X_3$ and $U_2 = X_1X_3$. Thus, measuring the two ancilla qubits and detecting the error, if any, we apply the Z operator to the corresponding qubit and undo the flipped phase.

It is not difficult now to combine the bit-flip and phase-flip error correcting codes discussed above to obtain a code capable of correcting both types of errors as well as their combination XZ. Such a code is shown in Fig. 9.12 and is called the Shor code after Peter Shor who invented it. This code is an example of *concatenated code*, whereby the encoding is implemented using a hierarchy of levels of concatenation of more elementary codes. Thus, in the first part of the circuit of Fig. 9.12, we use the phase flip code (9.38) to encode the qubit that we want to protect. We then use the bit flip code (9.34) to encode each of the three qubits as $|\pm\rangle \to (|000\rangle \pm |111\rangle)/\sqrt{2}$. We thus obtain three clusters each containing three qubits. The resulting nine-qubit logical states encoding the single-qubit basis states $|0\rangle$ and $|1\rangle$ are given by

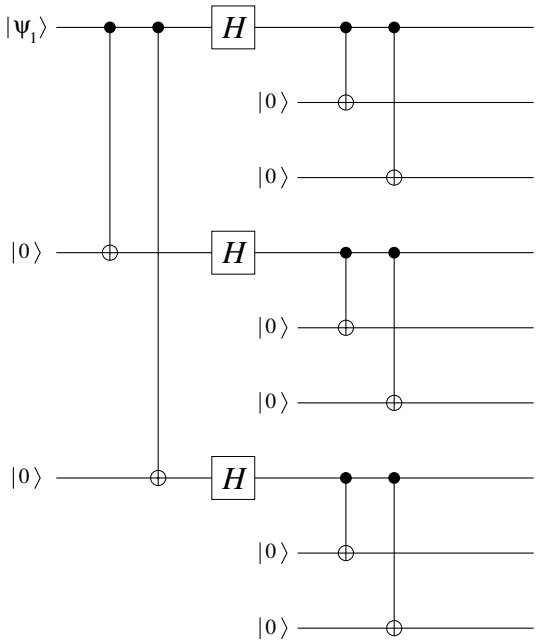

Fig. 9.12. Circuit for implementing the Shor nine-qubit error correcting code.

$$|0\rangle \rightarrow |+++\rangle$$
$$\rightarrow \frac{(|000\rangle + |111\rangle)(|000\rangle + |111\rangle)(|000\rangle + |111\rangle)}{2\sqrt{2}} \equiv |0_L\rangle\,, \quad (9.40a)$$
$$|1\rangle \rightarrow |---\rangle$$
$$\rightarrow \frac{(|000\rangle - |111\rangle)(|000\rangle - |111\rangle)(|000\rangle - |111\rangle)}{2\sqrt{2}} \equiv |1_L\rangle\,. \quad (9.40b)$$

Any single qubit state of the form (9.32) is thus encoded as

$$|\psi_1\rangle = \alpha|0\rangle + \beta|1\rangle$$
$$\rightarrow \alpha|0_L\rangle + \beta|1_L\rangle$$
$$= \alpha\frac{(|000\rangle + |111\rangle)^{\otimes 3}}{2\sqrt{2}} + \beta\frac{(|000\rangle - |111\rangle)^{\otimes 3}}{2\sqrt{2}} = |\psi_9\rangle\,. \quad (9.41)$$

We now want to detect a singe qubit error that may have occurred in any of the three clusters. As in the case of the three-qubit bit-flip code, within each cluster we compare the states of qubits 2 and 3 by measuring Z_2Z_3 and the states of qubits 1 and 3 by measuring Z_1Z_3. If a bit-flip occurred, the measurement will detect it and instruct us to apply the X transformation to the flipped qubit to correct the error. Consider next the phase-flip errors. Within each cluster, a single (or triple, etc) phase-flip changes the sign of the

superposition as $|000\rangle + |111\rangle \leftrightarrow |000\rangle - |111\rangle$. Two (or four, etc) phase-flips within the same cluster do not change its state and therefore do not result in an error. If a single phase-flip occurs in only one cluster, we can detect it by comparing the sign of clusters 2 and 3 and the sign of clusters 1 and 3. The corresponding six-qubit observables are $X_4X_5X_6X_7X_8X_9$ and $X_1X_2X_3X_7X_8X_9$. To correct the phase-error, if any, we apply the Z transformation to any qubit of the cluster where the sign-flip occurred. We thus see that the Shor code is capable of correcting any single qubit flip (per cluster) and any single phase flip, as well as any combination of the two, be it in the same qubit or in different qubits of the code. The number of necessary ancilla qubits used to perform the measurements can be calculated as follows: two ancillas per cluster for bit-flip measurement plus two more ancillas for phase-flip measurement, altogether $2 \times 3 + 2 = 8$ qubits.

Historically, the Shor code invented in 1995, is the first quantum error correcting code. Shortly thereafter, more sophisticated and economical quantum error correcting codes were invented, such as the seven-qubit Steane code and even a five-qubit code, the latter containing the minimum number of qubits required to correct an arbitrary single-qubit error in the encoding block. There exist also larger codes capable of encoding more physical qubits and correcting multiple-qubit errors in the block. Many important quantum error correcting codes are conveniently characterized by the parameters $[n, k, d]$, where n is the number of physical qubits in the encoding block, k is the number of encoded logical qubits and d is the minimum (Hamming) distance that determines the number of correctable errors $t = (d-1)/2$. A general theory of quantum error-correction has been developed, which builds upon the stabilizer formalism—a very powerful mathematical method for designing and classifying a wide class of operations in quantum mechanics. A good introduction to this subject can be found in the book by Nielsen and Chuang (2000).

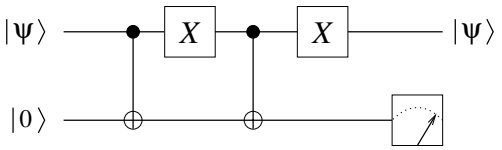

Fig. 9.13. Circuit for detecting leakage error.

So far we have neglected one more type of errors, the leakage errors, resulting in qubit loss. In general, such an error occurs when the qubit leaks out of its two-dimensional Hilbert space to a larger (possibly infinite-dimensional) space. To detect the leakage error, one can use the circuit of Fig. 9.13. There we assume that if the state of the interrogated qubit $|\psi\rangle$ is neither $|0\rangle$ nor $|1\rangle$ (nor any coherent or incoherent combination of the two), the controlled by that qubit operation, CNOT, is not executed. As such, measuring the ancilla qubit in state $|0\rangle$ tells us that the leakage has indeed occurred, otherwise the

ancilla's state is $|1\rangle$. Then to recover the lost qubit, one replaces it with a fresh qubit prepared in a standard state, e.g., $|0\rangle$, followed by the syndrome measurement and, if necessary, the recovery operation.

We note finally that in the analysis above we have assumed that the errors affecting different qubits are not correlated. This indirectly implies that each qubit couples to its own different noisy environment causing the decoherence. Depending on the particular system, this may or may not be a good approximation, especially for adjacent qubits. More precisely, if the scale of correlations within the common noise and/or the environment is large as compared to the interqubit separation, then the assumption of uncorrelated errors could be unjustified. Fortunately, for such cases there exists a complementary class of error-correcting or, rather, error-avoiding codes called noiseless quantum codes. Such codes implement the passive stabilization of quantum information by employing precisely the long-range correlations present in the environment. The basic idea behind the noiseless quantum codes is to encode the information in a decoherence free subspace $\mathbb{S}_{\rm DF}$ of the total Hilbert space of a multiqubit block, each qubit of which interacts in a symmetric fashion with the same set of modes of the environment. As the simplest example, consider a pair of qubits each represented by a two-level system, such as spin-$\frac{1}{2}$ particle in a magnetic field or two-level atom. Then the decoherence free subspace of this system contains just one state, the singlet state $\frac{1}{\sqrt{2}}(\,|01\rangle - |10\rangle)$. Provided the distance between the qubits is much smaller than the wavelength of radiation associated with the energy separation between the qubit basis states, the singlet state is, to a large extent, decoupled from the environment. A more practical code is realized by using a four-qubit block, which allows for the encoding of one qubit in the decoherence free subspace containing the logical states

$$|0_L\rangle = \tfrac{1}{2}(\,|0101\rangle - |0110\rangle + |1001\rangle - |1010\rangle)\,,$$
$$|1_L\rangle = \tfrac{1}{2}(\,|0101\rangle + |0110\rangle - |1001\rangle - |1010\rangle)\,.$$

In the case of larger even number of qubits k localized within a wavelength of the radiation field, the number $n_{\rm sng}$ of such stable singlet states is given by

$$n_{\rm sng} = \frac{k!}{(k/2)!(k/2+1)!}\,,$$

which can be used to encode more qubits in the noiseless code. In quantum optics, these states are known as sub-radiant states which were studied by Dicke some 50 years ago in connection with the, in some sense, inverse problem of super-radiance in an ensemble of two-level atoms.

9.4.3 Fault–Tolerant Quantum Computation

The error correcting codes stabilize the quantum information that is stored in the computer memory or sent through the quantum communication channel. Information processing by quantum computers, however, also involves

the application of logic gates which should be executed reliably. In fact, even the error correcting protocols themselves use the logic gates at all stages—information encoding, decoding, error detection and correction. The flawless execution of quantum logic gates therefore seems to be critical for reliable quantum computation. In practice, however, we can not expect that the gates operate with perfect reliability, so we need to design strategies for implementing reliable quantum computation with unreliable quantum logic gates—fault–tolerant quantum computation. Fortunately, the fault–tolerant quantum computation appears to be possible and our aim here is to outline its basic principles.

The main idea behind the fault–tolerant computation is to encode the data using the error correcting codes and then perform the information processing directly with the encoded data, without ever decoding it, except, perhaps, at the end of computation. That is, every time we need to apply a quantum logic gate, we do not decode the relevant qubits making them vulnerable to permanent damage. Rather, we replace the logic gate of the original circuit with an encoded gate whose action on the corresponding encoding blocks of qubits is equivalent to the action of the required gate applied to the original circuit. Then, under the appropriate conditions outlined below, if we perform the error detection and correction frequently enough, we avoid the accumulation of not only the memory errors but also the errors introduced by the failed logic gates.

The procedure for realizing the encoded gates should be designed so that individual errors do not propagate and spread over a larger number of qubits, but remain localized to a single or few qubits within the encoding block, so that the error correcting protocols remain effective in identifying and removing the errors. The gates used by the error-correcting circuits should adhere to the same principle as well. Depending on the particular error-correcting code employed, the realization of the universal set of encoded logic gates is different. In the case of the convenient $[7, 1, 3]$ (Steane) code, the encoded Hadamard H, Phase S and Pauli X, Y and Z gates are realized by the application of the corresponding transformation to each qubit in the encoding block, while the encoded CNOT gate is implemented by a bitwise application of the CNOT operation between pairs of qubits in the encoding blocks. These gates alone can not accomplish the universal quantum computation, which in addition requires either arbitrary single qubit rotation or, ultimately, the universal Toffoli CCNOT gate. To complete the universal set of gates, there exist explicit, although involved constructions to implement the CCNOT gate between any three blocks each encoding a single-qubit.

As noted above, in addition to memory errors, imperfections in gate operations introduce errors as well. One can quantify the reliability of a quantum gate with the parameter F called the fidelity. Suppose that in the ideal case a gate described by an operator U is expected to transform the state of the register $|\psi\rangle$ to $|\psi_f\rangle = U|\psi\rangle$, while the actual imperfect gate U' leads to the state $|\psi'_f\rangle = U'|\psi\rangle$. The fidelity of this gate is then given by the overlap of

states $|\psi_f\rangle$ and $|\psi'_f\rangle$ (sometimes also called Loschmidt echo),

$$F = |\langle\psi_f|\psi'_f\rangle|^2 = |\langle\psi|\, U^\dagger U' \,|\psi\rangle|^2 \,, \tag{9.42}$$

while the probability of the gate failure is $p = 1 - F$.

As discussed above, the simplest error-correcting codes can correct single-qubit errors but fail when two or more errors occur in the encoding block. Using the stabilizer formalism, one can in principle construct codes capable of correcting any desired number of errors t per block. As we increase t, both the block size itself and the complexity q (number of logic gates) of the error-detecting and correcting circuit increases sharply, typically, as a power law $q \propto t^b$ with $b \simeq 3-4$. For a given code correcting t errors, however, once $t+1$ or more errors occur in the encoding block, the computation crashes. For the probability $P_{\rm fail}$ that the error-correcting code fails we thus have

$$P_{\rm fail} \gtrsim (t^b p)^{t+1} \,. \tag{9.43}$$

With increasing t, eventually we reach the point when the number of computational steps in the corresponding circuit becomes so large that $P_{\rm fail}$ overtakes p, while for yet larger $t \gtrsim p^{-1/b}$ the failure probability of the code simply blows up. Therefore, to minimize $P_{\rm fail}$, we have to keep $t < p^{-1/b}$. Then, to be able to reliably perform Q steps of computation, with each step followed by the error correction, from the condition $QP_{\rm fail} < 1$ we obtain

$$p < (\log Q)^{-b} \,. \tag{9.44}$$

That is, given the error probability per qubit $p > 0$, which is due to either memory failure or gate failure or both, only a limited by (9.44) number of computational steps can be accomplished reliably while an arbitrarily long quantum computation is impossible.

Fortunately, by concatenating error correcting codes as shown in Fig. 9.14, we can overcome this limitation. Suppose that each qubit in the original quantum circuit is encoded with a simple code of size n capable of correcting only single-qubit errors, e.g., the Shor or Steane code. This is the first level of encoding in Fig. 9.14. Then each qubit in the code is in turn encoded with the same or similar code. Continuing this procedure, we can obtain L levels of concatenation, whereby each qubit of the original circuit is encoded in a block of size n^L qubits. At each level of concatenation, the error correcting procedure would fail if at least two errors occur in the same sub-block. After the first-level encoding, the failure probability is given by cp^2, where c contains the number of ways two simultaneous errors can occur, and for simplicity we assume $p \ll 1$ which allows us to neglect the higher order contributions of p. But if we further encode each qubit of the first level code and perform the error detection and correction in each sub-block in parallel, then the failure would occur only when two sub-blocks simultaneously fail, which has the probability $c\,(cp^2)^2$. Continuing this argument, after L levels of concatenation, the failure probability becomes $(cp)^{2^L}/c$. In the mean time, if the complexity of the

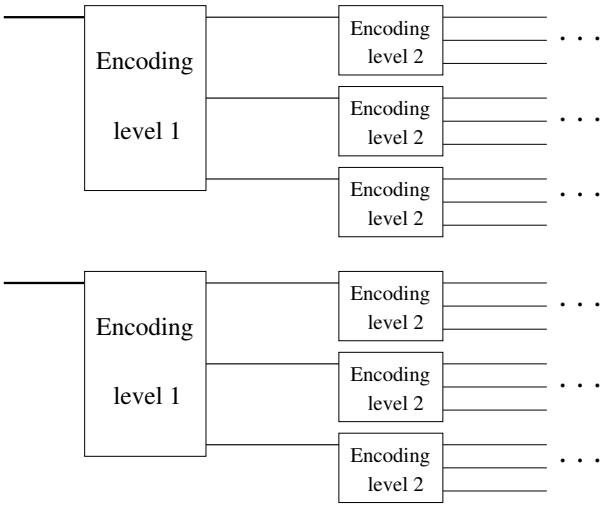

Fig. 9.14. Encoding qubits using concatenated codes.

highest level error-correcting circuit is q, the concatenated code involves $\sim q^L$ logical operations. We thus get significantly better scaling for reducing failure probability by increasing the circuit complexity, as compared to the case of multiple-qubit error-correcting codes expressed by (9.43). In fact, provided the error probability p is below certain threshold value $p_{\rm th}$, using the concatenated codes we can realize arbitrarily long quantum computation with any desired precision ϵ. To see this, suppose the problem we want to solve involves Q elementary steps of computation—logic gates of the original circuit. For a tractable problem, the number of logic gates is some polynomial function of the size n of the problem, $Q = \text{poly}(n)$. To achieve the computation precision ϵ, each gate has to be simulated with accuracy of ϵ/Q, so we must perform L levels of concatenation such that

$$\frac{(cp)^{2^L}}{c} \leq \frac{\epsilon}{Q} \,. \tag{9.45}$$

For any given ϵ, we can find an appropriate L to satisfy condition (9.45), provided $p < 1/c \equiv p_{\rm th}$. This is the *threshold theorem* for quantum computation, which asserts that one can tolerate a certain level of noise and perform reliable quantum computation by only polynomially increasing the complexity of the quantum circuit to incorporate the error-correction. Depending on the parameters of the system, such as the character of noise, measurement efficiency and speed, and the particular combination of the error-correcting codes used in the concatenation procedure, the estimates of the threshold value $p_{\rm th}$ vary between 10^{-5} and 10^{-3}, which have important implications in the design of suitable physical systems, some of which are described in the following chapter.

Problems

9.1. Verify that the circuit in Fig. 9.2 implements the controlled-controlled-U logic gate. Construct a circuit implementing the Toffoli gate using the single-qubit Hadamard H and two-qubit CNOT and controlled-S gates, where S is the Phase gate of Fig. 8.1.

9.2. Construct circuits implementing the oracles U_f for evaluating constant or balanced Boolean functions $f(x)$.

9.3. Fill in the missing steps in (9.23).

9.4. Construct a circuit implementing the inverse quantum Fourier transform $\mathrm{QFT}^\dagger$ defined as

$$|j\rangle \stackrel{\mathrm{QFT}^\dagger}{\longrightarrow} \frac{1}{\sqrt{N}} \sum_{n=0}^{N-1} \exp\left(-\frac{2\pi \mathrm{i} jn}{N}\right) |n\rangle \ . \tag{9.46}$$

9.5. The problem of phase estimation can be formulated as follows: Given a unitary operator U and its eigenvector $|u\rangle$, find the phase φ of the corresponding eigenvalue $\mathrm{e}^{2\pi \mathrm{i}\varphi}$.

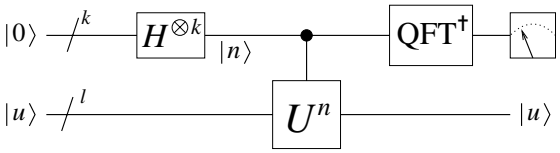

Fig. 9.15. Phase estimation circuit.

The binary representation for the phase $0 \le \varphi < 1$ is $\varphi = 0.\varphi_1\varphi_2 \ldots \varphi_N$ ($N = 2^k$). Suppose we are given a black-box performing a controlled-U^n operation, where $0 \le n \le 2^k - 1$. The circuit for phase estimation is shown in Fig. 9.15. It yields

$$|0\rangle\,|u\rangle \stackrel{H^{\otimes k}}{\longrightarrow} \frac{1}{2^{k/2}} \sum_{n=0}^{2^k-1} |n\rangle\,|u\rangle \stackrel{U^n}{\longrightarrow} \frac{1}{2^{k/2}} \sum_{n=0}^{2^k-1} \mathrm{e}^{2\pi \mathrm{i}\varphi n} |n\rangle\,|u\rangle \stackrel{\mathrm{QFT}^\dagger}{\longrightarrow} |\varphi_1 \ldots \varphi_N\rangle\,|u\rangle \ , \tag{9.47}$$

where $\mathrm{QFT}^\dagger$ denotes the inverse quantum Fourier transform (9.46). Verify the steps involved in (9.47).

10

Physical Implementations of Quantum Computation

In this closing chapter of the book, we dwell upon various schemes for the physical implementation of quantum computation. We begin with an outline of the necessary requirements on physical systems for implementing quantum information processing. We then describe a simple model system in which basic quantum gates between Rydberg atoms and microwave cavity field are realized. The sections that follow deal with several representative schemes for scalable quantum computation with trapped ions, atoms, photons and electrons. Some of the systems are only in the proposal stage, while for others significant experimental progress, although on a small scale, has recently been achieved.

10.1 Requirements for Physical Implementations of Quantum Information Processing

Identifying and studying suitable candidate systems for physical implementations of quantum information processing and communication has by now become a major subfield of quantum optics, as well as related disciplines of quantum physics. Let us therefore outline the main ingredients that a physical system should possess in order to be, at least in principle, a viable candidate for the implementation of quantum computation. As classified by DiVincenzo, they are:

- *Quantum Register*: A scalable physical system with well characterized states representing qubits, which in turn compose the quantum register.
- *Initialization*: The ability to prepare the state of the register in a known initial state, such as $|000\ldots0\rangle$.
- *Universal set of gates*: The ability to implement the universal set of quantum logic gates, typically arbitrary single-qubit unitary transformations U and two-qubit conditional gates W.

- *Low error and decoherence rate*: High fidelity of gate operation, with error probability per gate $< 10^{-3}$, and qubit decoherence times much longer than the gate operation time.
- *Read-out*: The ability to reliably measure the states of individual qubits in the computational basis with error probability $< \frac{1}{2}$.

In addition to quantum computation, quantum information science concerns itself with quantum communication applications, which include distributed quantum computation, quantum teleportation, dense coding and quantum key distribution. Thus, one more requirement is needed to assist with that task:

- *Communication*: The ability to faithfully transmit or teleport qubits between distant locations.

Having identified the basic requirements, we turn now to some actual schemes for the physical implementation of quantum computation.

10.2 Rydberg Atoms in Microwave Cavity

An almost ideal physical setup for realizing the Jaynes–Cummings model studied in Sect. 3.3.2 involves Rydberg atoms interacting with a single mode of a microwave cavity. This scheme is not practical for quantum computation applications, as far as scalability is concerned, but it is very useful, both theoretically and experimentally, in illustrating the basic principles underlying the manipulation of physical qubits. In addition, the scheme allows for the experimental preparation and studies of the so-called Schrödinger cat states, which are quantum superposition states of large (mesoscopic or even macroscopic) systems.

Conventionally, the term Rydberg atoms is used to designate atoms excited to states with large principal quantum numbers $n \gtrsim 20$, referred to as Rydberg states. High lying Rydberg states, in particular the circular ones, having the maximum allowed values of the orbital angular momentum l and its projection m on the z-axis, are very long lived. Yet, the dipole matrix elements for the transitions between the Rydberg states, proportional to the radius of the circular orbit, are very large.

Through elaborate and sophisticated experimental techniques, developed and perfected over the last twenty years or so by Haroche and coworkers, as well as by others, the atoms can be put in a controlled fashion to circular Rydberg states. Typically, two or three circular Rydberg states of rubidium atoms with principal quantum numbers $n = 51$, $n = 50$, and $n = 49$ designated, respectively, as $|e\rangle$, $|g\rangle$ and $|s\rangle$ are involved in the experiments, in which the atoms cross one by one a superconducting microwave cavity, as shown in Fig. 10.1. The radiative lifetimes of $|e\rangle$, $|g\rangle$ and $|s\rangle$ are of the order of 30 ms, while the frequencies of the transitions $|e\rangle \leftrightarrow |g\rangle$ and $|g\rangle \leftrightarrow |s\rangle$

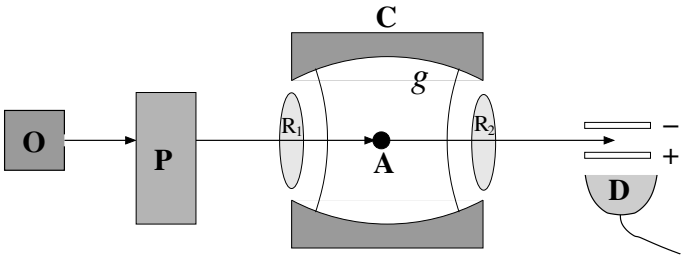

Fig. 10.1. Schematic representation of the set-up: Rubidium atoms effusing from oven O are velocity–selected and prepared in a required circular Rydberg state in zone P. The atoms then pass one by one through the microwave cavity C and finally detected by field ionization detector D. In the Ramsey field zones $R_{1,2}$ microwave pulses can coherently drive the atomic transitions $|g\rangle \leftrightarrow |e\rangle$ or $|s\rangle \leftrightarrow |g\rangle$.

are 51.1 GHz and 54.3 GHz, respectively. At the entrance to and exit from the cavity, the atoms can be prepared in an arbitrary superposition state by classical microwave pulses, know as Ramsey pulses $R_{1,2}$. The cavity sustains a Gaussian mode at frequency ω, which is near-resonant with the transition $|e\rangle \leftrightarrow |g\rangle$, i.e., $\omega \simeq \omega_{eg}$. The quality factor $Q = \omega/\kappa$ of the cavity mode is $Q \simeq 3 \times 10^8$, which implies a lifetime of a cavity photon κ^{-1} around 1 ms. The distance between the cavity mirrors is $L \simeq 27$mm, the mode waist is $w \simeq 6$mm, which together with the large atomic dipole moment $\wp_{eg} \gtrsim 10^3\, ea_0$ (with e the electron charge and a_0 the Bohr radius) translates into an atom–field coupling strength g in the range of several tens of kHz. The atom–field interaction time $t_{\rm int}$ is determined by the transit time of the atoms through the cavity, $t_{\rm int} = \sqrt{\pi} w/v_a$. The atomic velocity v_a, and thereby the interaction time, can be controlled with very high precision, with $t_{\rm int}$ being around a few μs, so that the interaction is over before either the atom or the cavity photon(s) have any appreciable chance to decay. The atoms can then be detected state–selectively by a sensitive field-ionization detector.

We thus consider the interaction of a single mode cavity field with a Rydberg atom having the lower $|g\rangle$ and upper $|e\rangle$ levels. The setup described above represents a remarkably clean realization of the Jaynes–Cummings model in which, during the atom–field interaction, relaxation can, to a very good approximation, be neglected. The Hamiltonian of the system is then given by (3.57) which, in the frame rotating with the cavity mode frequency ω, can be written as

$$\mathcal{H} = -\hbar\Delta\sigma_+\sigma_- + \hbar g(\mathrm{e}^{\mathrm{i}\varphi}\sigma_+ a + \mathrm{e}^{-\mathrm{i}\varphi} a^\dagger \sigma_-) \,, \tag{10.1}$$

where $\Delta = \omega - \omega_{eg}$ is the atom–cavity mode detuning, while φ is a phase factor containing the phases of the atomic dipole moment $\wp_{eg}$ and the cavity field. This phase is essentially arbitrary and has been included here purely for the sake of convenience.

Let us assume resonant interaction $\Delta = 0$ and set the phase $\varphi = -\pi/2$. Then, from the solution of the Jaynes–Cummings model in Sect. 3.3.2 we know that, if an atom A in state $|e\rangle$ enters an empty cavity C at time $t = 0$, the state of the system evolves in time according to

$$|\Psi_{e,0}(t)\rangle = \cos(gt)\,|e,0\rangle + \sin(gt)\,|g,1\rangle\ . \tag{10.2}$$

If, instead, the atom is initially in state $|g\rangle$ while the cavity contains one photon, the state of the system at time $t \geq 0$ is

$$|\Psi_{g,1}(t)\rangle = \cos(gt)\,|g,1\rangle - \sin(gt)\,|e,0\rangle\ . \tag{10.3}$$

The state $|g,0\rangle$ does not evolve in time, since $\mathcal{H}\,|g,0\rangle = 0$.

We shall be interested in times at which the atom has exited the cavity, $t = t_{\rm int}$. Although there is nothing literally pulsed as the atom travels through the cavity, since the atom is exposed to the cavity field for an interval determined by the transit time, we shall refer to the quantity $\vartheta = 2gt_{\rm int}$ as the (vacuum Rabi) pulse area, which has a meaning similar to the pulse area $\theta = 2\Omega\tau$ of a classical field introduced in Sect. 3.3.1, although the two should not be confused. Note that, as a result of the interaction, after the atom leaves the cavity, the state of the system A+C is an entangled state, with the entanglement persisting when A and C are separated; which is why this entanglement can be referred to as non-local. Ignoring detection imperfections, for the initial state $|e,0\rangle$, the probability that the atom will be found by the detector in level $|e\rangle$ is

$$P_{e,0}(e) = \tfrac{1}{2}\big[1 + \cos(\vartheta)\big]\ .$$

Similarly, for the initial state $|g,1\rangle$, the probability for detecting the atom in level $|e\rangle$ is

$$P_{g,1}(e) = \tfrac{1}{2}\big[1 - \cos(\vartheta)\big]\ .$$

10.2.1 Logic Gates and Multiparticle Entanglement

We can envisage the atom and the cavity mode each representing a qubit. By properly choosing the interaction time $t_{\rm int}$, and thereby the pulse area ϑ, we can then realize various quantum gates and generate atom–cavity entangled states, as described below.

Quantum Gates with Rabi Pulses

When $\vartheta = \pi/2$, we have the following transformations

$$|e,0\rangle \to \tfrac{1}{\sqrt{2}}(\,|e,0\rangle + |g,1\rangle)\ , \quad |g,1\rangle \to \tfrac{1}{\sqrt{2}}(\,|g,1\rangle - |e,0\rangle)\ . \tag{10.4}$$

Thus, in an appropriate basis, the output states are equivalent to the EPR, or Bell states of (8.3). Note that the atom–cavity field entanglement is also

produced when the cavity contains n photons. For example, with the atom initially in level $|e\rangle$, we have

$$|\Psi_{e,n}(t_{\rm int})\rangle = \cos\left(g\sqrt{n+1}\,t_{\rm int}\right)|e,n\rangle + \sin\left(g\sqrt{n+1}\,t_{\rm int}\right)|g,n+1\rangle\ ,$$

and the maximally entangled state is attained at time $t_{\rm int} = \pi/4g\sqrt{n+1}$, which is by a factor of $\sqrt{n+1}$ faster than for the initially empty cavity. This assumes of course that the cavity field can be prepared in a Fock state of arbitrary number of photons, an issue that represents a non-trivial problem of ongoing research.

When $\vartheta = \pi$, the atom and the cavity field exchange a single excitation according to

$$|e,0\rangle \rightarrow |g,1\rangle\ , \quad |g,1\rangle \rightarrow -|e,0\rangle\ . \tag{10.5}$$

This transformation, to within a sign change of the final state $-|e,0\rangle$ (which is equivalent to a change of its phase by π), is analogous to the SWAP gate of Fig. 8.2. By the same token, the transformation (10.4) realized by the $\pi/2$-pulse is analogous to the $\sqrt{\rm SWAP}$ gate of (9.5). Considering now initial states of the compound system A+C involving linear superpositions of one of its subsystems and using the above properties of the π pulse, we obtain

$$(c_g|g\rangle + c_e|e\rangle)|0\rangle \rightarrow |g\rangle(c_g|0\rangle + c_e|1\rangle)\ , \tag{10.6a}$$

$$(c_0|0\rangle + c_1|1\rangle)|g\rangle \rightarrow |0\rangle(c_0|g\rangle - c_1|e\rangle)\ . \tag{10.6b}$$

The π-pulse therefore maps the state of one subsystem into the other.

The last case in this catalog is the transformation due to the $\vartheta = 2\pi$ pulse,

$$|e,0\rangle \rightarrow -|e,0\rangle \qquad |g,1\rangle \rightarrow -|g,1\rangle\ , \tag{10.7}$$

which means that a full Rabi cycle introduces a global phase-shift π for both initial states $|e,0\rangle$ and $|g,1\rangle$. Since the state $|g,0\rangle$ can not be affected by the atom–field coupling, the phase shift of the atom entering the cavity in level $|g\rangle$ is conditioned upon the presence of a photon in the cavity. Thus, if the cavity mode is in a superposition state of zero and one photon, we obtain

$$(c_0|0\rangle + c_1|1\rangle)|g\rangle \rightarrow (c_0|0\rangle - c_1|1\rangle)|g\rangle\ . \tag{10.8}$$

If we now assume that the atom is either in the resonant state $|g\rangle$ or in a spectator state $|s\rangle$, which is far off-resonant and therefore not interacting with the cavity field, upon crossing the cavity the following transformation takes place,

$$\begin{array}{rcl} |0\rangle|s\rangle \rightarrow & & |0\rangle|s\rangle \\ |1\rangle|s\rangle \rightarrow & & |1\rangle|s\rangle \\ |0\rangle|g\rangle \rightarrow & & |0\rangle|g\rangle \\ |1\rangle|g\rangle \rightarrow & - & |1\rangle|g\rangle \end{array}\ , \tag{10.9}$$

which is equivalent to the controlled-Z (CZ) logic gate of Fig. 8.2 between a pair of qubits represented here by the cavity mode C and the atom A, with

the qubit basis states $|s\rangle \equiv |0\rangle$ and $|g\rangle \equiv |1\rangle$. In combination with two single-qubit rotations $R_y^{\rm A}(-\pi/2)$ and $R_y^{\rm A}(\pi/2)$, the CZ gate $W_{\rm CZ}^{\rm CA}$ can be converted into the CNOT gate $W_{\rm CNOT}^{\rm CA}$, as per (9.4a). To that end, at the entrance to the cavity in the first Ramsey zone $\rm R_1$, we submit the atom to a classical microwave pulse of area $\theta_1 = \pi/2$ and phase $\varphi_1 = -\pi/2$ resonantly driving the atomic transition $|s\rangle \leftrightarrow |g\rangle$. According to (3.47), this pulse realizes the required rotation operation $R_y^{\rm A}(-\pi/2)$,

$$\mathcal{U}_{sg}^{(1)} = \begin{bmatrix} \cos\frac{\pi}{4} & {\rm i}{\rm e}^{-{\rm i}\pi/2}\sin\frac{\pi}{4} \\ {\rm i}{\rm e}^{{\rm i}\pi/2}\sin\frac{\pi}{4} & \cos\frac{\pi}{4} \end{bmatrix} = \frac{1}{\sqrt{2}}\begin{bmatrix} 1 & 1 \\ -1 & 1 \end{bmatrix} = R_y^{\rm A}(-\pi/2)\,. \qquad (10.10)$$

Next, as the atom crosses the cavity, the compound system undergoes the $W_{\rm CZ}^{\rm CA}$ transformation of (10.9). Finally, at the exit from the cavity in the second Ramsey zone $\rm R_2$, we submit the atom to a classical microwave pulse of area $\theta_2 = \pi/2$ and phase $\varphi_2 = \pi/2$, resulting in the $R_y^{\rm A}(\pi/2)$ rotation,

$$\mathcal{U}_{sg}^{(2)} = \begin{bmatrix} \cos\frac{\pi}{4} & {\rm i}{\rm e}^{{\rm i}\pi/2}\sin\frac{\pi}{4} \\ {\rm i}{\rm e}^{-{\rm i}\pi/2}\sin\frac{\pi}{4} & \cos\frac{\pi}{4} \end{bmatrix} = \frac{1}{\sqrt{2}}\begin{bmatrix} 1 & -1 \\ 1 & 1 \end{bmatrix} = R_y^{\rm A}(\pi/2)\,. \qquad (10.11)$$

Summarizing the above steps, we obtain the following evolution table,

$$\begin{array}{ccccccccc} & R_y^{\rm A}(-\pi/2) & & & W_{\rm CZ}^{\rm CA} & & & R_y^{\rm A}(\pi/2) & \\ |0\rangle\,|s\rangle & \longrightarrow & |0\rangle\,\frac{1}{\sqrt{2}}(\,|s\rangle - |g\rangle) & \longrightarrow & |0\rangle\,\frac{1}{\sqrt{2}}(\,|s\rangle - |g\rangle) & \longrightarrow & |0\rangle\,|s\rangle \\ |0\rangle\,|g\rangle & \longrightarrow & |0\rangle\,\frac{1}{\sqrt{2}}(\,|s\rangle + |g\rangle) & \longrightarrow & |0\rangle\,\frac{1}{\sqrt{2}}(\,|s\rangle + |g\rangle) & \longrightarrow & |0\rangle\,|g\rangle \\ |1\rangle\,|s\rangle & \longrightarrow & |1\rangle\,\frac{1}{\sqrt{2}}(\,|s\rangle - |g\rangle) & \longrightarrow & |1\rangle\,\frac{1}{\sqrt{2}}(\,|s\rangle + |g\rangle) & \longrightarrow & |1\rangle\,|g\rangle \\ |1\rangle\,|g\rangle & \longrightarrow & |1\rangle\,\frac{1}{\sqrt{2}}(\,|s\rangle + |g\rangle) & \longrightarrow & |0\rangle\,\frac{1}{\sqrt{2}}(\,|s\rangle - |g\rangle) & \longrightarrow & |1\rangle\,|s\rangle \end{array}\,,$$

which realizes the CNOT logic gate, with the control qubit C represented by the cavity mode with states $\{\,|0\rangle,\,|1\rangle\}$, and the target qubit A being the atom with states $\{\,|s\rangle,\,|g\rangle\}$.

Two- and Three-Particle Entanglement

We have seen above that, when an excited atom $\rm A_1$ crosses an initially empty cavity with the pulse area set to $\vartheta = \pi/2$, a maximally entangled state of the system $\rm A_1 + C$ is created,

$$|e^{\rm A_1}, 0^{\rm C}\rangle \to \tfrac{1}{\sqrt{2}}(\,|e^{\rm A_1}, 0^{\rm C}\rangle + |g^{\rm A_1}, 1^{\rm C}\rangle)\,. \qquad (10.12)$$

A subsequent detection of the atom either in state $|e\rangle$ or state $|g\rangle$ would instantly project the cavity field on the corresponding zero-photon state $|0\rangle$ or one-photon state $|1\rangle$, even though the two subsystems can be separated by a large distance. We can read-out the field state by sending a second atom $\rm A_2$ initially in state $|g\rangle$, with the pulse area set to $\vartheta = \pi$. According to (10.6b), the state of the cavity field is then mapped into the state of atom $\rm A_2$, with

the final state of the field being $|0\rangle$. Thus, if we do not perform a detection, we create an entangled state of two atoms

$$\tfrac{1}{\sqrt{2}}\big(\,|e^{\mathrm{A}_1}, g^{\mathrm{A}_2}\rangle - |g^{\mathrm{A}_1}, e^{\mathrm{A}_2}\rangle\big)\,, \tag{10.13}$$

which, with the convention $|e\rangle \equiv |0\rangle$ and $|g\rangle \equiv |1\rangle$, is the Bell state $|B_{11}\rangle$ of (8.3).

Employing the CZ logic gate described above, we can also generate a maximally entangled state of three and more subsystems. To that end, assume that a first atom A_1 prepared in state $|e\rangle$ crosses an initially empty cavity with the pulse area set to $\vartheta = \pi/2$. The resulting entangled state of the system $\mathrm{A}_1 + \mathrm{C}$ is given by (10.12). A second atom, initially in state $|s\rangle$, before entering the cavity undergoes a $R_y^{\mathrm{A}_2}(-\pi/2)$ rotation in the Ramsey zone R_1, with the result $|s^{\mathrm{A}_2}\rangle \to \frac{1}{\sqrt{2}}\big(\,|s^{\mathrm{A}_2}\rangle - |g^{\mathrm{A}_2}\rangle\big)$. It then crosses the cavity with the pulse area set to $\vartheta = 2\pi$. The combined state of the three subsystems, A_1, C and A_2, undergoes the following transformation

$$\begin{aligned}&\tfrac{1}{2}\big[\,|e^{\mathrm{A}_1}\rangle\,|0^{\mathrm{C}}\rangle\big(\,|s^{\mathrm{A}_2}\rangle - |g^{\mathrm{A}_2}\rangle\big) + |g^{\mathrm{A}_1}\rangle\,|1^{\mathrm{C}}\rangle\big)\big(\,|s^{\mathrm{A}_2}\rangle - |g^{\mathrm{A}_2}\rangle\big)\big]\\ &\overset{W_{\mathrm{CZ}}^{\mathrm{CA}_2}}{\longrightarrow} \tfrac{1}{2}\big[\,|e^{\mathrm{A}_1}\rangle\,|0^{\mathrm{C}}\rangle\big(\,|s^{\mathrm{A}_2}\rangle - |g^{\mathrm{A}_2}\rangle\big) + |g^{\mathrm{A}_1}\rangle\,|1^{\mathrm{C}}\rangle\big)\big(\,|s^{\mathrm{A}_2}\rangle + |g^{\mathrm{A}_2}\rangle\big)\big]\,.\end{aligned} \tag{10.14}$$

At the exit from the cavity, the second atom undergoes a $R_y^{\mathrm{A}_2}(\pi/2)$ rotation in the Ramsey zone R_2. Then the final state of the compound system $\mathrm{A}_1{+}\mathrm{A}_2{+}\mathrm{C}$, becomes

$$\tfrac{1}{\sqrt{2}}\big(\,|e^{\mathrm{A}_1}\rangle\,|s^{\mathrm{A}_2}\rangle\,|0^{\mathrm{C}}\rangle + |g^{\mathrm{A}_1}\rangle\,|g^{\mathrm{A}_2}\rangle\,|1^{\mathrm{C}}\rangle\big)\,, \tag{10.15}$$

which, with the convention $|e^{\mathrm{A}_1}\rangle \equiv |0\rangle$, $|g^{\mathrm{A}_1}\rangle \equiv |1\rangle$ and $|s^{\mathrm{A}_2}\rangle \equiv |0\rangle$, $|g^{\mathrm{A}_2}\rangle \equiv |1\rangle$, is the maximally–entangled three-particle Greenberger–Horne–Zeilinger (GHZ) state

$$|\mathrm{GHZ}\rangle = \tfrac{1}{\sqrt{2}}\big(\,|000\rangle + |111\rangle\big)\,. \tag{10.16}$$

In a similar manner, one can generate four and more-particle GHZ states (see Prob. 10.1).

10.2.2 Schrödinger Cat States of the Cavity Field

The superposition principle, according to which a perfectly legitimate state of a quantum system can be a linear superposition of two or more of its distinguishable eigenstates, is perhaps the most conspicuous feature of quantum mechanics that sets it apart from classical mechanics. There is no conceptual or even experimental difficulty in dealing with such superpositions in small systems involving one or few atoms, photons, etc., examples of which are encountered throughout this book. On the other hand, it is obvious that contemplating analogous superpositions of macroscopic (classical) systems borders the absurd. This absurdity was brought to a climax by Schrödinger in a Gedankenexperiment in which he imagined a cat in a box together with a

radioactive nucleus emitting a gamma ray which when emitted would kill the cat. The argument was that, since it is perfectly legitimate to consider that at a later time the nucleus can be in a superposition of its excited and ground state, it would appear equally legitimate to consider the cat in a superposition of the states "dead" and "alive". Then the quantitative question is: Can we reach this macroscopic limit by increasing the size of the quantum system? Although it had become clear for some time that the answer had to do with the fact that a macroscopic system can not be separated from the environment due to which quantum superpositions are subject to decoherence, it is only recently that it has been possible to devise experiments involving superpositions in mesoscopic systems. Microwave cavity fields interacting with Rydberg atoms have proven to be convenient experimental systems leading to the realization of bona fide models for the Schrödinger cat (or rather kitten) arrangement. A particular advantage of this system is that it is simple enough from the theoretical point of view to provide a quantitative understanding of the essential physics, as discussed below. Whether it will ever be possible to test this issue in truly macroscopic systems will for the moment remain an intriguing question.

Preparation of Schrödinger Cat States

Consider a microwave cavity field interacting with a Rydberg atom on the transition $|g\rangle \leftrightarrow |e\rangle$. Let us assume that the cavity mode contains n photons, while the detuning $\Delta = \omega - \omega_{eg}$ and the atom–field coupling constant g are chosen so that the resonant energy exchange between the atom and the field is suppressed, which requires $g\sqrt{n} < |\Delta|$. Then, if the atom is in level $|g\rangle$, the coupling induces an ac Stark shift of the energy of the combined state $|g, n\rangle$ given by $g^2 n/\Delta$. Similarly, for the atom in level $|e\rangle$, the energy of state $|e, n\rangle$ is shifted by the amount $-g^2(n+1)/\Delta$. Thus, upon the interaction during the transit time $t_{\rm int}$, the states $|g, n\rangle$ and $|e, n\rangle$ acquire the corresponding phases φn and $-\varphi(n+1)$, where $\varphi \equiv g^2 t_{\rm int}/\Delta$.

Let us now assume that the cavity field is initially prepared in a coherent state $|\alpha\rangle$ with a small amplitude $|\alpha| < |\Delta|/g$. This can be accomplished by injecting into the cavity a classical field from a microwave source using a small hole in one of the cavity mirrors. If the atom enters the cavity in level $|g\rangle$, upon interaction the combined state of the system $|g, \alpha\rangle$ undergoes the following transformation

$$\begin{aligned} |g, \alpha\rangle \;&=\; \mathrm{e}^{-\frac{1}{2}|\alpha|^2} \sum_{n=0}^{\infty} \frac{\alpha^n}{\sqrt{n!}} \, |g, n\rangle \\ &\longrightarrow \mathrm{e}^{-\frac{1}{2}|\alpha|^2} \sum_{n=0}^{\infty} \frac{\alpha^n}{\sqrt{n!}} \, \mathrm{e}^{\mathrm{i}\varphi n} \, |g, n\rangle = \, |g, \alpha \mathrm{e}^{\mathrm{i}\varphi}\rangle \; . \end{aligned} \tag{10.17}$$

Similarly, for the atom entering the cavity in level $|e\rangle$ we have

$$|e,\alpha\rangle \;=\; \mathrm{e}^{-\frac{1}{2}|\alpha|^2}\sum_{n=0}^{\infty}\frac{\alpha^n}{\sqrt{n!}}\,|e,n\rangle$$

$$\longrightarrow \mathrm{e}^{-\frac{1}{2}|\alpha|^2}\sum_{n=0}^{\infty}\frac{\alpha^n}{\sqrt{n!}}\,\mathrm{e}^{-\mathrm{i}\varphi(n+1)}\,|e,n\rangle = \mathrm{e}^{-\mathrm{i}\varphi}\,|e,\alpha\mathrm{e}^{-\mathrm{i}\varphi}\rangle\;. \quad (10.18)$$

Before entering the cavity, we can prepare the atom in the superposition state $\frac{1}{\sqrt{2}}\big(\,|g\rangle + \mathrm{i}\,|e\rangle\big)$. To that end, in the first Ramsey zone R_1, we apply to the atom initially in state $|g\rangle$ a classical microwave pulse of area $\theta_1 = \pi/2$ and phase $\varphi_1 = 0$ resonantly driving the atomic transition $|g\rangle \leftrightarrow |e\rangle$. Then at the exit from the cavity, the state of the system is

$$\frac{1}{\sqrt{2}}\big(\,|g,\alpha\mathrm{e}^{\mathrm{i}\varphi}\rangle + \mathrm{i}\mathrm{e}^{-\mathrm{i}\varphi}\,|e,\alpha\mathrm{e}^{-\mathrm{i}\varphi}\rangle\big)\;,$$

which, upon setting $\varphi = \pi/2$ and denoting $\mathrm{i}\alpha \equiv \beta$, becomes

$$\frac{1}{\sqrt{2}}\big(\,|g,\beta\rangle + \,|e,-\beta\rangle\big)\;. \quad (10.19)$$

If after the atom exits the cavity, we measure its state and find it in either $|g\rangle$ or $|e\rangle$, we immediately project the cavity field on the state $|\beta\rangle$ or $|-\beta\rangle$, respectively. But what if before measuring the state of the atom, we submit it in the second Ramsey zone R_2 to another microwave pulse of area $\theta_2 = \pi/2$ and phase $\varphi_2 = \pi/2$. Then, the state (10.19) is transformed to

$$\frac{1}{2}\big(\,|g,\beta\rangle - \,|g,-\beta\rangle + \,|e,\beta\rangle + \,|e,-\beta\rangle\big)\;. \quad (10.20)$$

Now, if upon measurement the state of the atom is found to be either $|g\rangle$ or $|e\rangle$, the field is projected on the corresponding state

$$|\Psi_{\mathrm{cat}}\rangle = \frac{1}{\sqrt{N}}\big(\,|\beta\rangle + \mathrm{e}^{\mathrm{i}\phi}\,|-\beta\rangle\big)\;, \quad (10.21)$$

where the phase $\phi = \pi$ if the atom is in $|g\rangle$ and $\phi = 0$ if it is in $|e\rangle$. The normalization factor N is given by

$$N = \big(\langle\beta| + \mathrm{e}^{-\mathrm{i}\phi}\langle-\beta|\,\big)\big(\,|\beta\rangle + \mathrm{e}^{\mathrm{i}\phi}\,|-\beta\rangle\big) = 2\big[1+\cos(\phi)\,\mathrm{e}^{-2|\beta|^2}\big]\;,$$

which for $|\beta|^2 \gg 1$ approaches 2, again due to the fact that the overlap between two coherent states decreases as their distance on the complex plain increases. Thus, in the limit of $|\beta|^2 \gg 1$, we have an experimental realization of a Schrödinger cat state

$$|\Psi_{\mathrm{cat}}\rangle = \frac{1}{\sqrt{2}}\big(\,|\beta\rangle + \mathrm{e}^{\mathrm{i}\phi}\,|-\beta\rangle\big)\;. \quad (10.22)$$

Why can that claim be made? Two necessary and sufficient reasons: (i) If $|\beta|$ is large, the states $|\beta\rangle$ and $|-\beta\rangle$ are fully quantum mechanical objects

and practically orthogonal, since the distance between them is $2|\beta|^2 \gg 1$. (ii) Again for $|\beta|$ large, the states $|\beta\rangle$ and $|-\beta\rangle$ at the same time correspond to practically macroscopic (classical) objects. We have therefore the quantum description of two objects whose size we can make as large as we wish. We can then explore the question of how fast this quantum mechanical superposition disappears, as the size of the object increases; which is the idea behind the Schrödinger cat argument. In some sense and metaphorically, $|\beta\rangle$ can be the cat alive and $|-\beta\rangle$ the cat dead, or the other way around. Exploration of these issues requires that we introduce dissipation through coupling to an environment, which is properly done through the master equation. In preparation for that, let us first note that the density operator corresponding to the pure state of the field (10.21) is

$$\rho = |\Psi_{\rm cat}\rangle\langle\Psi_{\rm cat}| = \frac{1}{N}\big(\,|\beta\rangle\langle\beta| + |-\beta\rangle\langle-\beta| + \mathrm{e}^{\mathrm{i}\phi}\,|-\beta\rangle\langle\beta| + \mathrm{e}^{-\mathrm{i}\phi}\,|\beta\rangle\langle-\beta|\,\big)\,. \tag{10.23}$$

If the phase ϕ is completely randomized, through, e.g., discarding the information pertaining to the state of the atom, we obtain the corresponding mixed state density operator

$$\rho_{\rm mixed} = \frac{1}{N}\big(\,|\beta\rangle\langle\beta| + |-\beta\rangle\langle-\beta|\,\big)\,. \tag{10.24}$$

Formally then, the question to be explored is how fast the pure density operator tends to the mixed, as a function of the "size" of the system, in the presence of dissipation.

Dissipation and Decoherence of the Field

Here we wish to explore the rate with which the density operator of the field, prepared in a pure Schrödinger cat state, approaches a mixed state; in other words, the rate with which a quantum superposition approaches a classical mixture, as a function of the size of the system. Assume that we have created the pure state with density operator ρ given by (10.23). This is a situation in which the use of characteristic functions introduced in Sect. 2.4.2 is quite convenient. Following Davidovich *et al.* (1996), consider the normally ordered characteristic function

$$C_{\rm N}(\gamma,t) = \mathrm{Tr}\big(\rho(t)\,\mathrm{e}^{\gamma a^\dagger}\,\mathrm{e}^{-\gamma^* a}\big)\,, \tag{10.25}$$

with γ being c-numbers. At time $t = 0$ the density operator $\rho(0)$ is that of (10.23), and we have

$$C_{\rm N}(\gamma,0) = \frac{1}{N}\big[\mathrm{e}^{\gamma\beta^*-\gamma^*\beta} + \mathrm{e}^{-\gamma\beta^*+\gamma^*\beta} + \mathrm{e}^{-2|\beta|^2}\big(\mathrm{e}^{\mathrm{i}\phi}\mathrm{e}^{\gamma\beta^*+\gamma^*\beta} + \mathrm{e}^{-\mathrm{i}\phi}\mathrm{e}^{-\gamma\beta^*-\gamma^*\beta}\big)\big]\,, \tag{10.26}$$

which is easily obtained by calculating the trace in the coherent state representation (see Prob. 10.2). Recall from Sect. 5.1.3 that when coupled to a

Markovian reservoir at zero temperature, the time evolution of a coherent state $|\beta\rangle$ is given by $|\beta \mathrm{e}^{-\kappa t/2}\rangle$, where κ is the cavity field decay rate. As a result, the above characteristic function acquires the time development

$$C_{\mathrm{N}}(\gamma, t) = C_{\mathrm{N}}(\gamma \mathrm{e}^{-\kappa t/2}, 0) \,. \tag{10.27}$$

This means that in (10.26), γ and γ^* should be replaced by $\gamma \mathrm{e}^{-\kappa t/2}$ and $\gamma^* \mathrm{e}^{-\kappa t/2}$, respectively, with the result

$$\begin{aligned} C_{\mathrm{N}}(\gamma, t) = \frac{1}{N} \big[& \mathrm{e}^{(\gamma\beta^* - \gamma^*\beta)\mathrm{e}^{-\kappa t/2}} + \mathrm{e}^{(-\gamma\beta^* + \gamma^*\beta)\mathrm{e}^{-\kappa t/2}} \\ & + \mathrm{e}^{-2|\beta|^2} \big(\mathrm{e}^{\mathrm{i}\phi} \mathrm{e}^{(\gamma\beta^* + \gamma^*\beta)\mathrm{e}^{-\kappa t/2}} + \mathrm{e}^{-\mathrm{i}\phi} \mathrm{e}^{(-\gamma\beta^* - \gamma^*\beta)\mathrm{e}^{-\kappa t/2}} \big) \big] \,. \end{aligned} \tag{10.28}$$

Comparing this expression to (10.25), we deduce an expression for $\rho(t)$ in the presence of dissipation, namely

$$\begin{aligned} \rho(t) = \frac{1}{N} \big[& |\beta \mathrm{e}^{-\kappa t/2}\rangle\langle \beta \mathrm{e}^{-\kappa t/2}| + |-\beta \mathrm{e}^{-\kappa t/2}\rangle\langle -\beta \mathrm{e}^{-\kappa t/2}| \\ & + \mathrm{e}^{-2|\beta|^2(1-\mathrm{e}^{-\kappa t})} \big(\mathrm{e}^{\mathrm{i}\phi} |-\beta \mathrm{e}^{-\kappa t/2}\rangle\langle \beta \mathrm{e}^{-\kappa t/2}| \\ & + \mathrm{e}^{-\mathrm{i}\phi} |\beta \mathrm{e}^{-\kappa t/2}\rangle\langle -\beta \mathrm{e}^{-\kappa t/2}| \big) \big] \,. \end{aligned} \tag{10.29}$$

This expression displays explicitly the effect of dissipation on quantum coherence as a function of time and the size of the system. The first feature to note is the exponential decay of the amplitudes of the coherent states with rate $\kappa/2$, as expected in the coupling of a quantum system to a Markovian reservoir. Beyond this decay of the amplitude, however, we note that the last two terms incorporating the coherence are multiplied by the factor $\exp\big[-2|\beta|^2(1-\mathrm{e}^{-\kappa t})\big]$ which decreases at a different rate, depending on the size $|\beta|^2$ of the system. To reveal its significance, consider the behavior of the density operator for times such that $\kappa t \ll 1$. For such short times, exponential decay of the amplitudes has had practically no effect. Yet the last two terms of (10.29) have decayed at a rate $\Gamma_{\mathrm{D}} \simeq 2|\beta|^2\kappa$, which is obtained by using the relation $(1-\mathrm{e}^{-\kappa t}) \simeq \kappa t$. Clearly, the rate Γ_{D} is much larger than κ if $|\beta|^2 \gg 1$. And thus we have the answer to the question of how fast quantum superposition (coherence) decays as a function of the size of the system, in the presence of dissipation, i.e., coupling to an environment. Appropriately then, Γ_{D} is referred to as rate of decoherence.

It is now evident that a large (macroscopic) system, prepared initially in a pure superposition state of the form $|\Psi_{\mathrm{cat}}\rangle \propto \big(|\beta\rangle + |-\beta\rangle \big)$ and coupled to an environment, which is inevitable for macroscopic systems, quickly losses coherence. For times t such that $\Gamma_{\mathrm{D}}^{-1} \ll t \ll \kappa^{-1}$, its density operator reduces from the pure density operator of (10.23) to the density operator of a statistical mixture as in (10.24). As Haroche and collaborators have demonstrated in a series of elegant experiments, this rate of decoherence can be measured by sequentially sending two atoms through the cavity and measuring their state.

10.3 Ion-Trap Quantum Computer

Historically, the ion-trap quantum computer is the first complete and realistic proposal, put forward by Cirac and Zoller (1995), for the physical implementation of quantum computation. In the ion-trap quantum computer, the qubits are represented by internal electronic states of single alkali–like ions, such as singly-charged ions from group II of the periodic table, e.g., $^{9}\mathrm{Be}^{+}$ or $^{40}\mathrm{Ca}^{+}$. These ions are placed in a linear Paul trap which consists of four parallel conducting rods—electrodes,—each having radius of the order of 1 mm. The distance from the surface of each electrode to a common axis, to be taken as the x-axis, is comparable to the radius of the electrodes. A sinusoidally oscillating rf (radio-frequency) potential $V_0 \cos(\omega_{\mathrm{rf}} t)$ is applied to two opposite electrodes, while the other pair of electrodes is maintained at rf ground (nominal zero). For sufficiently high frequency ω_{rf} of the rf oscillations, a charged ion of mass M_{I} feels a time-averaged effective (pseudo)potential $M_{\mathrm{I}}\nu_{\perp}^2/2$, where $\nu_{\perp} \propto V_0/\omega_{\mathrm{rf}}$ is the frequency associated with the transverse motion in the plain perpendicular to the x-axis, typically in the MHz range. A chain of ions at low enough temperatures ($T \lesssim 10\,\mu\mathrm{K}$) can then be strongly trapped by the effective potential in the transverse direction. To confine the positively charged ions in the axial direction, static potentials are applied from the opposite sides, as shown in Fig. 10.2(a). The axial confinement is relatively weak, with the frequency ν_x of the harmonic potential along the x axis being typically a few times smaller than $\nu_{\perp}$. As the ions strongly repel each other via the Coulomb force, they tend to form a linear ionic crystal, in which single ions are approximately equidistantly spaced by a few tens of μm. This allows one to spatially resolve individual ions by focused laser beams.

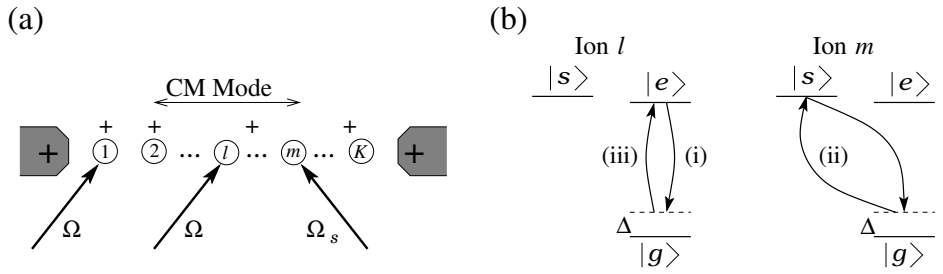

Fig. 10.2. Scheme of the ion-trap quantum computer. (a) Lineal ion-trap with K equidistantly spaced ions. (b) Sequence of laser pulses realizing the CZ logic gate between ions l and m.

The dynamics of the trapped ions can conveniently be described in terms of the normal modes of the ionic crystal. Since we are dealing with a chain of ions strongly confined in the transverse direction, and more weakly in the axial direction, for low enough temperatures and properly tuned laser frequencies

(to be detailed below), we can concentrate only on the axial degrees of freedom of the ions. The normal mode with the lowest frequency is the center-of-mass (CM) mode, corresponding to all of the ions oscillating together, as a rigid body, with the frequency ν_x. The next so-called breathing mode has frequency $\sqrt{3}\nu_x$, and all other modes have even higher frequencies. A remarkable feature of this system is that the frequency difference between successive modes is independent on the number K of ions in the trap.

Let us denote by $|g\rangle$ and $|e\rangle$ two internal metastable (long-lived) states of individual ions representing the qubit basis states $|0\rangle$ and $|1\rangle$. The transition $|g\rangle \leftrightarrow |e\rangle$ can be a weak quadrupole transition, or it can be a two-photon (Raman) transition. For simplicity, we assume that $|g\rangle \leftrightarrow |e\rangle$ is a single-photon transition and denote by $\Omega = \wp_{ge}|\mathcal{E}|/\hbar$ the Rabi frequency of the applied field having amplitude $\mathcal{E}$, frequency ω, phase φ and projection of the wavevector $\boldsymbol{k}$ onto the x direction k_x. We have already studied in Sect. 3.4 the dynamics of a laser–driven two-level atom/ion confined in a 1D harmonic trap and subject to a coherent laser field. Recall that the Lamb–Dicke parameter $\eta \equiv k_x\,\Delta x_0 = k_x[\hbar/(2M_{\rm I}\nu_x)]^{1/2}$ quantifies the amplitude of oscillations in the trap relative to the wavelength of the applied field. In the Lamb–Dicke regime $\eta \ll 1$, depending on the detuning $\Delta = \omega - \omega_{eg}$ of the applied field, we can selectively drive the carrier ($\Delta = 0$), the red sideband ($\Delta = -\nu_x$) or the blue sideband ($\Delta = \nu_x$) resonances. The situation for K ions is completely analogous, the only difference being that the single-ion Lamb–Dicke parameter should be divided by the factor $\sqrt{K}$, which is due to the fact that the effective mass of the CM motion of the ionic crystal is K times larger then the single-ion mass. The interaction Hamiltonians for the cases of the carrier, red sideband and blue sideband resonances are then given by

$$\mathcal{V}_{ge}^{\rm car} = -\hbar\Omega\big[\mathrm{e}^{\mathrm{i}\varphi}\,|e\rangle\langle g| + \mathrm{e}^{-\mathrm{i}\varphi}\,|g\rangle\langle e|\,\big]\,, \tag{10.30a}$$

$$\mathcal{V}_{ge}^{\rm rsb} = -\hbar\frac{\Omega\eta}{\sqrt{K}}\big[\mathrm{i}\,\mathrm{e}^{\mathrm{i}\varphi}\,|e\rangle\langle g|\,b - \mathrm{i}\,\mathrm{e}^{-\mathrm{i}\varphi}\,|g\rangle\langle e|\,b^\dagger\big]\,, \tag{10.30b}$$

$$\mathcal{V}_{ge}^{\rm bsb} = -\hbar\frac{\Omega\eta}{\sqrt{K}}\big[\mathrm{i}\,\mathrm{e}^{\mathrm{i}\varphi}\,|e\rangle\langle g|\,b^\dagger - \mathrm{i}\,\mathrm{e}^{-\mathrm{i}\varphi}\,|g\rangle\langle e|\,b\big]\,, \tag{10.30c}$$

where $b^\dagger$ and b are the creation and annihilation operators for the CM phonon mode. Thus, applying a laser field with the proper phase φ and pulse area $\theta = 2\Omega\tau$ to the carrier resonance ($\omega = \omega_{eg}$) of a particular ion, we can realize an arbitrary single-qubit unitary transformation $\mathcal{U}_{ge}^{\rm car}(\theta)$ as per (3.47). On the other hand, laser pulses acting on the red-sideband ($\omega = \omega_{eg} - \nu_x$) and the blue-sideband ($\omega = \omega_{eg} + \nu_x$) resonances can couple the internal and motional degrees of freedom of the ions. For example, if an ion l is in level $|e^{{\rm I}_l}\rangle$ and the CM mode contains n phonons, a laser field tuned to the red-sideband resonance would induce oscillations on the transition $|e^{{\rm I}_l}\rangle\,|n\rangle \leftrightarrow |g^{{\rm I}_l}\rangle\,|n+1\rangle$ with the effective Rabi frequency $\frac{\Omega\eta}{\sqrt{K}}\sqrt{n+1}$.

For the implementation of two-qubit gates described shortly, another excited ionic level, denoted as $|s\rangle$, must be employed as an auxiliary level. The

transition $|g\rangle \leftrightarrow |s\rangle$ can selectively be driven by a different laser field with amplitude $\mathcal{E}_s$ and frequency $\omega_s \simeq \omega_{sg}$. This field does not couple to the qubit transition $|g\rangle \leftrightarrow |e\rangle$, due to the proper polarization and/or frequency selection. All of the above properties of qubit transition equally apply to the transition $|g\rangle \leftrightarrow |s\rangle$. In particular, by choosing $\omega_s = \omega_{sg}$, we can drive the carrier resonance of the required ion with the Rabi frequency $\Omega_s = \wp_{gs}|\mathcal{E}_s|/\hbar$, while tuning the laser to the red-sideband resonance ($\omega_s = \omega_{sg} - \nu_x$), we can induce the transitions $|g^{\mathrm{I}_m}\rangle\,|n\rangle \leftrightarrow |s^{\mathrm{I}_m}\rangle\,|n-1\rangle$ with the effective Rabi frequency $\frac{\Omega_s \eta_s}{\sqrt{K}}\sqrt{n}$, where $\eta_s \equiv k_x^{(s)} \Delta x_0$ is the corresponding Lamb–Dicke parameter.

We assume that the chain of ions can initially be prepared in the ground motional state, in which the CM mode contains zero phonons. This can be accomplished by laser cooling of the ions using a strong, dipole-allowed cycling transition from the ionic ground state $|g\rangle$ to some excited state $|c\rangle$ which decays rapidly, with the rate Γ_{cg}, back to $|g\rangle$. When we apply a laser field tuned to the red sideband resonance of the transition $|g\rangle \leftrightarrow |c\rangle$, the excitation of the ion is accompanied by the absorption of a phonon, $|g\rangle\,|n\rangle \rightarrow |c\rangle\,|n-1\rangle$. In the Lamb–Dicke regime $\eta_c \equiv (\omega_{cg}/c)\Delta x_0 \ll 1$, the state $|c\rangle\,|n-1\rangle$ preferentially decays to the state $|g\rangle\,|n-1\rangle$, accomplishing thereby one cooling cycle. After n such cycles, we end up in the ground state of the system $|g\rangle\,|0\rangle$. Further interaction of the system in state $|g\rangle\,|0\rangle$ with the laser field is suppressed due to the detuning $\Delta = -\nu_x$. This completes the initialization of the quantum register.

The same rapidly decaying excited state $|c\rangle$ can be used to read-out the internal states of individual ions. To that end, we apply a strong laser field to the interrogated ion so as to saturate the carrier resonance of the transition $|g\rangle \leftrightarrow |c\rangle$ (see Sect. 4.1.3 and Prob. 4.3). If before applying the field the ion is in state $|g\rangle$, then it will fluoresce thereby scattering the laser photons, with the rate $\Gamma_{cg}/2$, which can be detected by a photodetector. If, on the other hand, the ion is in state $|e\rangle$, the application of the laser field to the empty transition $|g\rangle \leftrightarrow |c\rangle$ will not cause any fluorescence and the detector will register no signal. This is the essence of the electron shelving or quantum jump technique which can achieve 100% detection efficiency of single trapped atoms/ions.

We can now describe the realization of the CZ gate between any pair of ions l and m in the chain. This involves a three step process schematically shown in Fig. 10.2(b). Initially the CM mode is assumed in the ground motional state $|0\rangle$. In step (i) we apply to ion l a laser pulse tuned to the red sideband resonance of the transition $|g\rangle \leftrightarrow |e\rangle$. The duration of the pulse is $\tau = \pi\sqrt{K}/(2\Omega\eta)$, so that the effective pulse area is $\theta_{\mathrm{eff}} \equiv 2\frac{\Omega\eta}{\sqrt{K}}\tau = \pi$. Then, if the combined state of the system "ion l+CM mode" is $|g^{\mathrm{I}_l}\rangle\,|0\rangle$, no transformation takes place, since the field is detuned by the amount $|\Delta| = \nu_x$ assumed much larger than the effective Rabi frequency $\Omega\eta/\sqrt{K}$. If, however, the system is initially in state $|e^{\mathrm{I}_l}\rangle\,|0\rangle$, after the pulse, it is transformed to $-\mathrm{e}^{\mathrm{i}\varphi}\,|g^{\mathrm{I}_l}\rangle\,|1\rangle$. We

denote this unitary transformation by $\mathcal{U}^{\rm rsb}_{ge;{\rm I}_l}(\pi)$. Next, in step (ii) we apply to ion m a laser pulse of effective area $\theta_{\rm eff} = 2\pi$ (pulse duration $\tau = \pi\sqrt{K}/(\Omega\eta)$) resonant with the red sideband of the transition $|g\rangle \leftrightarrow |s\rangle$. Clearly, this pulse does not affect ion m if its state is $|e^{{\rm I}_m}\rangle$. Also, if the combined state of the system "ion m+CM mode" is $|g^{{\rm I}_m}\rangle\,|0\rangle$, no transformation takes place due to the large detuning $|\Delta_s| = \nu_x$. Only the state $|g^{{\rm I}_m}\rangle\,|1\rangle$ undergoes a full 2π Rabi cycle acquiring a π phase shift, i.e., changing the sign. The corresponding unitary operator will be denoted by $\mathcal{U}^{\rm rsb}_{gs;{\rm I}_m}(2\pi)$. Finally, in step (iii) we repeat (i). Namely, we apply to ion l a laser pulse of effective area $\theta_{\rm eff} = \pi$ resonant with the red sideband of the transition $|g\rangle \leftrightarrow |e\rangle$. This accomplishes the reverse transformation $\mathcal{U}^{\rm rsb}_{ge;{\rm I}_l}(\pi)\,|g^{{\rm I}_l}\rangle\,|1\rangle \to {\rm e}^{-{\rm i}\varphi}\,|e^{{\rm I}_l}\rangle\,|0\rangle$. Note that at the end of (iii) the laser phase φ will cancel, provided it has the same value as in step (i). Thus the absolute phase of the laser field should be constant through the three-step process, but otherwise arbitrary. We can therefore take $\varphi = 0$. The following evolution table may be useful in guiding the reader through the above steps,

$$
\begin{array}{ccccccccc}
 & & \mathcal{U}^{\rm rsb}_{ge;{\rm I}_l}(\pi) & & & \mathcal{U}^{\rm rsb}_{gs;{\rm I}_m}(2\pi) & & \mathcal{U}^{\rm rsb}_{ge;{\rm I}_l}(\pi) & \\
|g^{{\rm I}_l}\rangle\,|g^{{\rm I}_m}\rangle\,|0\rangle & \longrightarrow & |g^{{\rm I}_l}\rangle\,|g^{{\rm I}_m}\rangle\,|0\rangle & \longrightarrow & |g^{{\rm I}_l}\rangle\,|g^{{\rm I}_m}\rangle\,|0\rangle & \longrightarrow & |g^{{\rm I}_l}\rangle\,|g^{{\rm I}_m}\rangle\,|0\rangle \\
|g^{{\rm I}_l}\rangle\,|e^{{\rm I}_m}\rangle\,|0\rangle & \longrightarrow & |g^{{\rm I}_l}\rangle\,|e^{{\rm I}_m}\rangle\,|0\rangle & \longrightarrow & |g^{{\rm I}_l}\rangle\,|e^{{\rm I}_m}\rangle\,|0\rangle & \longrightarrow & |g^{{\rm I}_l}\rangle\,|e^{{\rm I}_m}\rangle\,|0\rangle \\
|e^{{\rm I}_l}\rangle\,|g^{{\rm I}_m}\rangle\,|0\rangle & \longrightarrow & -\,|g^{{\rm I}_l}\rangle\,|g^{{\rm I}_m}\rangle\,|1\rangle & \longrightarrow & |g^{{\rm I}_l}\rangle\,|g^{{\rm I}_m}\rangle\,|1\rangle & \longrightarrow & |e^{{\rm I}_l}\rangle\,|g^{{\rm I}_m}\rangle\,|0\rangle \\
|e^{{\rm I}_l}\rangle\,|e^{{\rm I}_m}\rangle\,|0\rangle & \longrightarrow & -\,|g^{{\rm I}_l}\rangle\,|e^{{\rm I}_m}\rangle\,|1\rangle & \longrightarrow & -\,|g^{{\rm I}_l}\rangle\,|e^{{\rm I}_m}\rangle\,|1\rangle & \longrightarrow & -\,|e^{{\rm I}_l}\rangle\,|e^{{\rm I}_m}\rangle\,|0\rangle
\end{array}
\quad .
$$

This corresponds to the CZ logic gate $W^{{\rm I}_l{\rm I}_m}_{\rm CZ}$ between two qubits represented by ions l and m. Note that at the end of the process, the CM mode is restored to its ground state $|0\rangle$. It serves therefore as the quantum data bus that conveys information between the qubits but does not store it for a very long time, suppressing thus a severe source of decoherence in this system.

As we already know, arbitrary single-qubit unitary transformations $\mathcal{U}^{\rm car}_{ge}(\theta)$ can be realized using laser fields driving the carrier resonance of individual ions, which together with the two-qubit CZ gate implement the Universal set of quantum gates in this system. In particular, if we apply the rotation operations $R^{{\rm I}_m}_y(-\pi/2)$ and $R^{{\rm I}_m}_y(\pi/2)$ to ion m before and after the execution of $W^{{\rm I}_l{\rm I}_m}_{\rm CZ}$, we will implement the CNOT logic gate, with the control qubit represented by ion l and the target qubit by ion m. Three- and more-qubit gates can also be constructed in a similar way (see Prob. 10.3), which makes this system a particularly attractive candidate for the physical implementation of quantum computation.

Recently, remarkable experimental progress in coherent manipulations of up to eight laser–cooled and trapped ions has been achieved. In principle, this number can be increased to up to a few dozens of ions, still maintaining their resolvability and accessibility by focused laser beams. Trapping hundreds, or even thousands of ions in a single trap, however, does not appear to be technologically feasible. Various architectures for realizing a large-scale integrated ion-trap quantum computer have been studied. In one of such schemes,

suggested by Kielpinski *et al.* (2002), in order to circumvent the difficulties associated with single large ion trap quantum register, it has been proposed to use many small sub-registers, each containing a small number of ions, and connect these sub-registers to each other via controlled qubit (ion) transfer to the interaction region (entangler) represented by yet another ion trap.

10.4 Cavity QED-Based Quantum Computer

Cavity QED provides a fertile ground for the exploration and study of many aspect of quantum information. A large number of cavity QED based schemes for the physical implementation of quantum information processing and communication have been suggested, and few of them tested experimentally, such as the one described in Sect. 10.2. Here we outline one proposal, by Pellizzari *et al.* (1995), which possesses the important property of scalability to a relatively large number of qubits represented by single atoms placed in an optical cavity. In a certain sense, this scheme constitutes an optical analog of the ion-trap quantum computer, as here the photon mode of the cavity plays the role of the quantum data bus which conveys information between the qubits.

Consider K multilevel atoms placed in a standing-wave optical cavity, as shown in Fig. 10.3(a). The qubit basis states are represented by the lower long-lived (metastable) states corresponding to the hyperfine and Zeeman sublevels of the electronic ground states of the atoms. Individual atoms can be addressed by focused laser beams. As we know from Sect. 3.6, the transition between the lower atomic levels $|s\rangle$ and $|g\rangle$ can be driven by a pair of optical fields in the Raman configuration. When we apply to a particular atom two classical fields, each having a (single-photon) Rabi frequency Ω and detuned from the intermediate excited level $|e'\rangle$ by the same amount $\Delta \gg \Omega, \gamma_{e'}$, they induce two-photon transitions between $|s\rangle$ and $|g\rangle$ with the effective Rabi frequency $\Omega_{\text{eff}} = \Omega^2/\Delta$ (Fig. 10.3(b)). Then, just as in the case of a two-level atom subject to a single resonant pulse, by properly choosing the duration τ and the phases of the two pulsed fields, we can realize any unitary transformation $\mathcal{U}_{gs}(\theta_{\text{eff}})$ on the atomic transition $|g\rangle \leftrightarrow |s\rangle$, where $\theta_{\text{eff}} = 2\Omega_{\text{eff}}\tau$ is the effective two-photon pulse area. We can thus implement arbitrary single-qubit gates.

Next we show that, employing the cavity mode C as the quantum data bus, we can transfer an arbitrary superposition state $|\psi_1\rangle = c_s|s\rangle + c_g|g\rangle$ between any pair of atoms A_l and A_m. For simplicity, we assume that all of the atoms interact with the cavity field on the transition $|e\rangle \leftrightarrow |g\rangle$ with equal coupling strengths $g_j = \wp_{eg}\epsilon_\omega/\hbar$, i.e., the atoms being fixed at the antinodes of the cavity mode so that $\sin(kz_j) = -1$, where z_j is the position of atom $j = 1, 2, \ldots, K$. Consider for now only three atomic levels, $|s\rangle$, $|e\rangle$ and $|g\rangle$, with the transition $|s\rangle \leftrightarrow |e\rangle$ driven by a resonant optical field focused upon the corresponding atom. In the frame rotating with the frequencies of the cavity and driving fields, the Hamiltonian of the compound system A_l+A_m+C reads

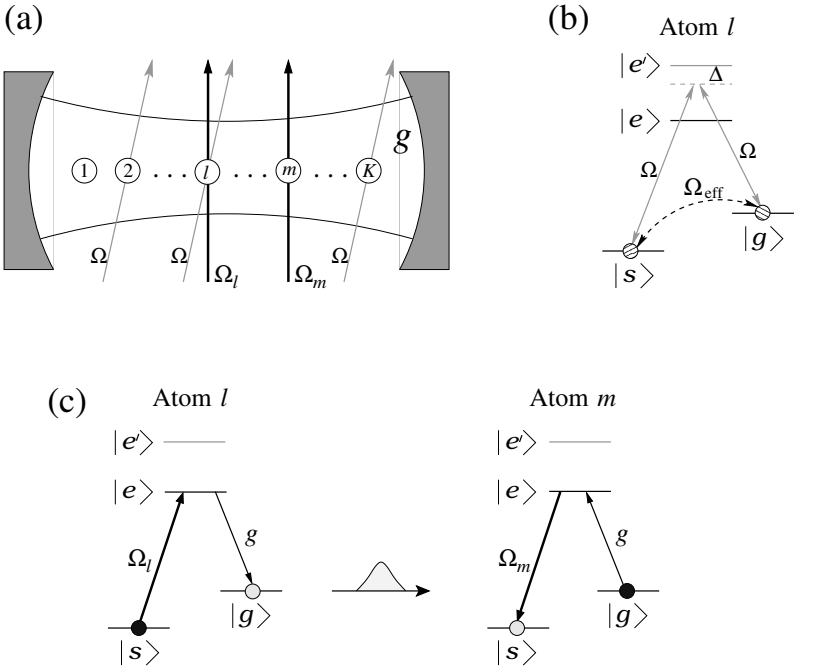

Fig. 10.3. Scheme of a cavity QED quantum computer. (a) Standing-wave optical cavity containing K multilevel atoms, each interacting with a common cavity mode with vacuum Rabi frequency g and selectively addressed by focused laser beams. (b) A pair of optical fields with Rabi frequencies Ω applied to a particular atom can drive the two-photon (Raman) transition between the lower metastable levels $|s\rangle$ and $|g\rangle$ via the intermediate excited level $|e'\rangle$. (c) The cavity mode resonant with the transition $|g\rangle \leftrightarrow |e\rangle$ can transfer the atomic coherence between atoms l and m addressed by laser pulses with Rabi frequencies Ω_l and Ω_m.

$$\mathcal{H} = -\hbar\big[\Omega_l\,\sigma_{se}^{\mathrm{A}_l} - g_l\,\sigma_{eg}^{\mathrm{A}_l} a + \Omega_m\,\sigma_{se}^{\mathrm{A}_m} - g_m\,\sigma_{eg}^{\mathrm{A}_m} a + \mathrm{H.\,c.}\big]\,, \tag{10.31}$$

where $\sigma_{\mu\nu}^{\mathrm{A}_j}$ is the transition operator of atom $j(= l, m)$, Ω_j is the Rabi frequency of the corresponding driving field, a is the annihilation operator of the cavity mode, and H. c. denotes the Hermitian conjugate. We assume that atom m is initially prepared in level $|g^{\mathrm{A}_m}\rangle$ and the cavity is empty, $|0^{\mathrm{C}}\rangle$. Then, if atom l is in level $|g^{\mathrm{A}_l}\rangle$, the compound system is decoupled from the Hamiltonian (10.31), i.e., $\mathcal{H}\,|g^{\mathrm{A}_l}\rangle\,|g^{\mathrm{A}_m}\rangle\,|0^{\mathrm{C}}\rangle = 0$. We need therefore only consider the evolution of the system initially in state $|s^{\mathrm{A}_l}\rangle\,|g^{\mathrm{A}_m}\rangle\,|0^{\mathrm{C}}\rangle$. The above Hamiltonian can then be cast in the matrix form as

$$\mathcal{H} = -\hbar \begin{bmatrix} 0 & \Omega_l & 0 & 0 & 0 \\ \Omega_l & 0 & -g_l & 0 & 0 \\ 0 & -g_l & 0 & -g_m & 0 \\ 0 & 0 & -g_m & 0 & \Omega_m \\ 0 & 0 & 0 & \Omega_m & 0 \end{bmatrix} , \tag{10.32}$$

where the basis is $\{|s,g,0\rangle, |e,g,0\rangle, |g,g,1\rangle, |g,e,0\rangle, |g,s,0\rangle\}$ with the first symbol in each ket referring to the state of atom l, the second to that of atom m and the last symbol to the state of the cavity mode. It is easy to verify that this Hamiltonian has a dark eigenstate (see Prob. 10.4)

$$|D\rangle = \frac{1}{\sqrt{N_0}}[g\,\Omega_m\,|s,g,0\rangle + \Omega_l\Omega_m\,|g,g,1\rangle + g\,\Omega_l\,|g,s,0\rangle] , \tag{10.33}$$

with zero eigenvalue $\lambda_0 = 0$. The normalization coefficient is obviously $N_0 = \Omega_l^2\Omega_m^2 + g^2(\Omega_l^2 + \Omega_m^2)$, and consistently with the assumption above, we have taken $g_l = g_m = g$. For $\Omega_m \gg \Omega_l \simeq 0$, the dark state coincides with the initial state, $|D\rangle = |s,g,0\rangle$, while in the opposite limit $\Omega_l \gg \Omega_m \simeq 0$ we have $|D\rangle = |g,s,1\rangle$. Therefore if the two classical fields are pulsed in a way such that the pulse on atom m precedes the pulse on atom l, i.e., $\Omega_m \gg \Omega_l$ at an early time, and $\Omega_m \ll \Omega_l$ at a later time, while $g = \text{const}$ throughout, then complete transfer of the system from the initial state $|s,g,0\rangle$ to the final state $|g,s,1\rangle$ can be achieved. This requires that the state vector of the system adiabatically follows the dark state $|D\rangle$, which implies the condition $g\tau, \max(\Omega_i)\,\tau \gg 1$, where τ is the pulse duration. The situation is analogous to the stimulated Raman adiabatic population transfer (STIRAP) in a three-state system studied in Sect. 3.6, representing thus an extension of STIRAP to a five-state cavity QED system. Also recall from Sect. 5.3, that, in addition to the adiabatic following condition stated above, an efficient intracavity STIRAP requires the strong coupling condition $g, \max(\Omega_i) > \Gamma, \kappa$, where Γ and κ are the atomic and cavity field relaxation rates. Under these conditions,we can then realize the transformation

$$\left(c_s\,|s^{\mathrm{A}_l}\rangle + c_g\,|g^{\mathrm{A}_l}\rangle\right)|g^{\mathrm{A}_m}\rangle\,|0^{\mathrm{C}}\rangle \rightarrow |g^{\mathrm{A}_l}\rangle\left(c_s\,|s^{\mathrm{A}_m}\rangle + c_g\,|g^{\mathrm{A}_m}\rangle\right)|0^{\mathrm{C}}\rangle , \tag{10.34}$$

whereby an arbitrary superposition state of atom l is transfered to atom m. Note that the cavity mode is populated only for a short time during the transfer process and, upon its completion, is restored to the vacuum state $|0\rangle$. It plays therefore the role of the quantum data bus, as the center-of-mass phonon mode does in the ion-trap quantum computer.

We can now describe the realization of the CNOT gate between a pair of atoms l and m in the cavity. To this end, we need to employ additional atomic levels represented by degenerate Zeeman sublevels of states $|s\rangle$, $|e\rangle$ and $|g\rangle$, which are assumed to have nonzero values of angular momentum, such as the hyperfine states with $F > 0$. The relevant level structure is shown in Fig. 10.4, where each atom involves two parallel Λ configurations. The qubit states of

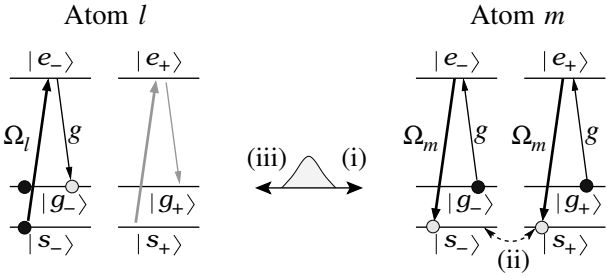

Fig. 10.4. Level scheme of atoms l and m and the sequence of transformations realizing the CNOT gate.

atom l are represented by $|g_-^{\mathrm{A}_l}\rangle \equiv |0\rangle$ and $|s_-^{\mathrm{A}_l}\rangle \equiv |1\rangle$, while those of atom m are $|g_-^{\mathrm{A}_m}\rangle \equiv |0\rangle$ and $|g_+^{\mathrm{A}_m}\rangle \equiv |1\rangle$. This asymmetry between the qubit encoding in different atoms is insignificant, since using appropriate Raman pulses one can always interchange states $|s_-\rangle$ and $|g_+\rangle$ in any atom. The qubit initially stored in atom l will serve as a "mobile" control qubit, while that in atom m will be the target qubit. In step (i) we map the state of atom l (control qubit) onto atom m using the STIRAP procedure described above. If atom l was in $|g_-^{\mathrm{A}_l}\rangle$, the combined state of the system $\mathrm{A}_l + \mathrm{A}_m$ remains unchanged. If, however, atom l was in $|s_-^{\mathrm{A}_l}\rangle$, after the STIRAP pulses, it ends up in $|g_-^{\mathrm{A}_l}\rangle$, while the target qubit stored in atom m as a superposition of $|g_-^{\mathrm{A}_m}\rangle$ and $|g_+^{\mathrm{A}_m}\rangle$ is transfered to the corresponding superposition of $|s_-^{\mathrm{A}_m}\rangle$ and $|s_+^{\mathrm{A}_m}\rangle$. Next, in step (ii) we interchange states $|s_-^{\mathrm{A}_m}\rangle$ and $|s_+^{\mathrm{A}_m}\rangle$ of atom m using an effective two-photon (Raman) π-pulse. Finally, in step (iii) we reverse (i), i.e., we apply the inverse sequence of STIRAP pulses to atoms l and m. By doing this, we map the state of the control qubit back onto atom l, while the target qubit is transfered to the superposition of $|g_-^{\mathrm{A}_m}\rangle$ and $|g_+^{\mathrm{A}_m}\rangle$ of atom m. These steps are conveniently illustrated by the following evolution table,

$$
\begin{array}{ccccccccc}
 & & (i) & & & (ii) & & (iii) & \\
|g_-^{\mathrm{A}_l}\rangle\,|g_-^{\mathrm{A}_m}\rangle & \longrightarrow & |g_-^{\mathrm{A}_l}\rangle\,|g_-^{\mathrm{A}_m}\rangle & \longrightarrow & |g_-^{\mathrm{A}_l}\rangle\,|g_-^{\mathrm{A}_m}\rangle & \longrightarrow & |g_-^{\mathrm{A}_l}\rangle\,|g_-^{\mathrm{A}_m}\rangle \\
|g_-^{\mathrm{A}_l}\rangle\,|g_+^{\mathrm{A}_m}\rangle & \longrightarrow & |g_-^{\mathrm{A}_l}\rangle\,|g_+^{\mathrm{A}_m}\rangle & \longrightarrow & |g_-^{\mathrm{A}_l}\rangle\,|g_+^{\mathrm{A}_m}\rangle & \longrightarrow & |g_-^{\mathrm{A}_l}\rangle\,|g_+^{\mathrm{A}_m}\rangle \\
|s_-^{\mathrm{A}_l}\rangle\,|g_-^{\mathrm{A}_m}\rangle & \longrightarrow & |g_-^{\mathrm{A}_l}\rangle\,|s_-^{\mathrm{A}_m}\rangle & \longrightarrow & |g_-^{\mathrm{A}_l}\rangle\,|s_+^{\mathrm{A}_m}\rangle & \longrightarrow & |s_-^{\mathrm{A}_l}\rangle\,|g_+^{\mathrm{A}_m}\rangle \\
|s_-^{\mathrm{A}_l}\rangle\,|g_+^{\mathrm{A}_m}\rangle & \longrightarrow & |g_-^{\mathrm{A}_l}\rangle\,|s_+^{\mathrm{A}_m}\rangle & \longrightarrow & |g_-^{\mathrm{A}_l}\rangle\,|s_-^{\mathrm{A}_m}\rangle & \longrightarrow & |s_-^{\mathrm{A}_l}\rangle\,|g_-^{\mathrm{A}_m}\rangle
\end{array}
\,.
$$

Clearly, the above input–output relations correspond to the truth table of the CNOT logic gate between a pair of qubits represented by atoms l and m, which together with arbitrary single-qubit (-atom) unitary transformations $\mathcal{U}_{gs}$ implement the Universal set of quantum gates in this system.

10.5 Optical Quantum Computer

Recall from Sect. 8.4 that photons with their two orthogonal polarization states are natural candidates for representing qubits. Photons have the advantage of being very robust and versatile carriers of quantum information, as they can propagate quickly over long distances in optical fibers, without undergoing much absorption and decoherence. Here we thus present an envisaged quantum computer with photonic qubits.

A schematic representation of an optical quantum computer is shown in Fig. 10.5. In the initialization section of the computer, deterministic sources of single photons generate single-photon pulses with precise timing and well-defined polarization and pulse–shapes. A collection of such photons constitutes the quantum register. The qubit basis states are represented by the vertical $|\updownarrow\rangle \equiv |0\rangle$ and horizontal $|\leftrightarrow\rangle \equiv |1\rangle$ polarization states of the photons. The preparation of an initial state of the register and the execution of the program according to the desired quantum algorithm is implemented by the quantum processor. This amounts to the application of a certain sequence of single-qubit U and two-qubit W unitary transformations, whose physical realization is described below. Finally, the result of computation is read-out by a collection of efficient polarization–sensitive photon detectors.

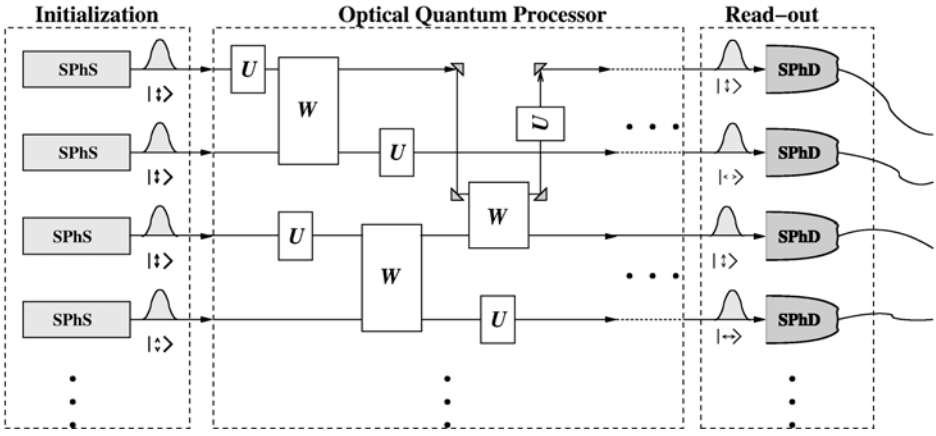

Fig. 10.5. Schematic representation of a quantum computer with photonic qubits. Qubit initialization is realized by deterministic single-photon sources (SPhS). Information processing is implemented by the quantum processor with single-qubit U and two-qubit W logic gates. Read-out of the result of computation is accomplished by efficient single-photon detectors (SPhD).

According to Sect. 8.4.2, for the photon-polarization qubit $|\psi_1\rangle = \alpha\,|\updownarrow\rangle + \beta\,|\leftrightarrow\rangle$, the combination of the polarization rotation $R(\theta)$ and phase-shift operations $T(\varphi)$ can realize any single-qubit unitary transformation U given

by (8.31). Together with a two-photon conditional operation realizing either the CNOT or the equivalent CZ gate, we can then implement the Universal set of quantum gates.

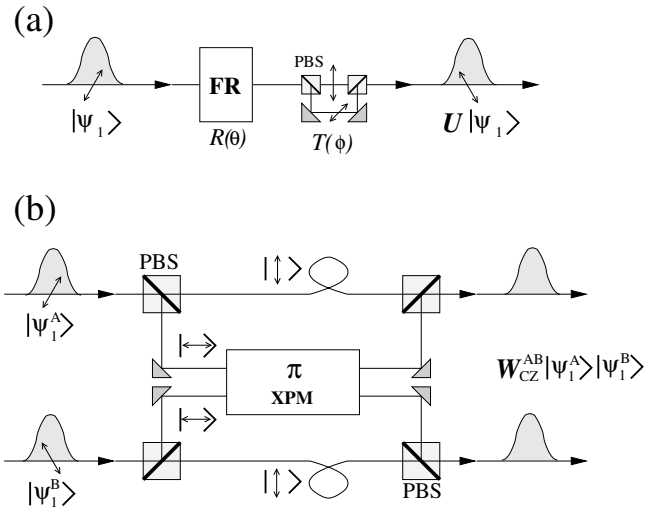

Fig. 10.6. Physical implementations of quantum logic gates. (a) Single-qubit logic gates U are implemented with a sequence of two linear–optics operations: $R(\theta)$—Faraday rotation (FR) of photon polarization by angle θ about the propagation direction; $T(\varphi)$—relative phase-shift φ of the photon's $|\leftrightarrow\rangle$ and $|\updownarrow\rangle$ polarized components due to their optical paths difference. (b) Two-qubit controlled-Z (CZ) gate W_{CZ} is realized using polarizing beam-splitters (PBS) and π cross-phase modulation (XPM).

In Fig. 10.6(a) we show the possible implementations of the polarization rotation of a photon by angle θ about the propagation direction, $R(\theta)$, and the relative phase-shift φ of the $|\updownarrow\rangle$ and $|\leftrightarrow\rangle$ polarized components of the photon, $T(\varphi)$. Both operations are easy to realize with standard linear optical elements. Recall from classical optics that linear polarization can be decomposed into left- and right-circular polarization components. In a circular–birefringent medium, these two orthogonal polarizations propagate with different phase velocities due to the different refraction indexes $n_{\text{L}} \neq n_{\text{R}}$. Then, upon passing through the medium of length L, the left- and right-circular polarization components acquire a phase difference $\delta\varphi = 2\pi L\delta n/\lambda$, which translates into the rotation of the linear polarization by the angle $\theta = \frac{1}{2}\,\delta\varphi$. Thus, the rotation angle θ can be controlled by the difference of the refraction indices $\delta n \equiv n_{\text{R}} - n_{\text{L}}$, which in a medium susceptible to the Zeeman effect can be manipulated by a longitudinal magnetic field $\boldsymbol{B} = \hat{z}B$ leading to $\delta n \propto B$. This is the essence of the magneto-optical Faraday effect. In turn, the $T(\varphi)$ operation is nothing more than the phase shift $\varphi = \delta s/\lambda$ due to the optical

path difference $\delta s = s_{\leftrightarrow} - s_{\updownarrow}$ between the photon's $|\leftrightarrow\rangle$ and $|\updownarrow\rangle$ polarized components

A possible realization of the CZ logic gate $W_{\mathrm{CZ}}^{\mathrm{AB}}$ between two photonic qubits A and B is shown in Fig. 10.6(b). There, after passing through a polarizing beam-splitter, the vertically polarized component $|\updownarrow\rangle$ of each photon is transmitted, while the horizontally polarized component $|\leftrightarrow\rangle$ is directed into the active medium, wherein the two-photon state $|\Phi_{\mathrm{in}}\rangle = |\leftrightarrow^{\mathrm{A}}\rangle\,|\leftrightarrow^{\mathrm{B}}\rangle$ acquires a conditional phase-shift $\varphi_c = \pi$. This is possible when the Hamiltonian governing the evolution of the two optical field modes in the active medium has the form

$$\mathcal{H} = -\hbar\xi\, a_{\mathrm{A}}^{\dagger} a_{\mathrm{A}}\, a_{\mathrm{B}}^{\dagger} a_{\mathrm{B}}\ , \tag{10.35}$$

where ξ is the so-called cross-phase modulation (XPM) coefficient, while $a_j^{\dagger}$ and a_j are the creation and annihilation operators of the corresponding mode $j = \mathrm{A,B}$. Then, during the interaction, the input state evolves according to

$$|\Phi(t)\rangle = \mathrm{e}^{-\frac{\mathrm{i}}{\hbar}\mathcal{H}t}\,|\Phi_{\mathrm{in}}\rangle = \mathrm{e}^{\mathrm{i}\xi t}\,|\leftrightarrow^{\mathrm{A}}\rangle\,|\leftrightarrow^{\mathrm{B}}\rangle\ , \tag{10.36}$$

where we have used the fact that there is only one photon in each mode j, therefore $a_j^{\dagger} a_j\,|1^j\rangle = |1^j\rangle$. At the exit from the medium of length L, the accumulated conditional phase shift is then $\varphi_c = \xi t_{\mathrm{out}}$, where $t_{\mathrm{out}} = L/v_g$ is the interaction time, with v_g being the light velocity inside the medium. For $\varphi_c = \pi$ we then obtain $|\Phi_{\mathrm{out}}\rangle = -\,|\Phi_{\mathrm{in}}\rangle$. Attaining large conditional phase-shift within a reasonable interaction length L (of a few centimeters) requires, however, a very large value of the coefficient ξ and long interaction time (small group velocity v_g), which conventional media can not provide. Developing schemes for achieving giant cross-phase modulation is therefore crucial for the implementation of deterministic optical quantum logic gates, which is an active topic of current research. Recently, several promising proposals towards this goal, based on electromagnetically induced transparency (EIT) in atomic media, have been reported. After leaving the medium, the $|\leftrightarrow\rangle$ component of each photon is recombined with its $|\updownarrow\rangle$ component on another polarizing beam-splitter. Complete temporal overlap of the two polarization components of each photon can be achieved by delaying the $|\updownarrow\rangle$ component in a fiber loop or sending it though an EIT medium, in which the light propagates with a small group velocity $v_g \ll c$ (see Sect. 6.3). At the output, we then have the transformation

$$\begin{array}{l}
|\updownarrow^{\mathrm{A}}\rangle\,|\updownarrow^{\mathrm{B}}\rangle \to \ \ |\updownarrow^{\mathrm{A}}\rangle\,|\updownarrow^{\mathrm{B}}\rangle \\
|\updownarrow^{\mathrm{A}}\rangle\,|\leftrightarrow^{\mathrm{B}}\rangle \to \ \ |\updownarrow^{\mathrm{A}}\rangle\,|\leftrightarrow^{\mathrm{B}}\rangle \\
|\leftrightarrow^{\mathrm{A}}\rangle\,|\updownarrow^{\mathrm{B}}\rangle \to \ \ |\leftrightarrow^{\mathrm{A}}\rangle\,|\updownarrow^{\mathrm{B}}\rangle \\
|\leftrightarrow^{\mathrm{A}}\rangle\,|\leftrightarrow^{\mathrm{B}}\rangle \to -|\leftrightarrow^{\mathrm{A}}\rangle\,|\leftrightarrow^{\mathrm{B}}\rangle
\end{array}\ ,$$

which corresponds to the truth-table of the CZ logic gate between a pair of qubits represented by photons A and B.

Another important prerequisite for the optical quantum computer is the availability of single-photon sources. Currently, the most accessible scheme

for generating single photons relies on the process of spontaneous parametric down-conversion, in which a single pump photon of frequency ω_p and wave vector $\boldsymbol{k}_p$ is converted to two polarization- and momentum-correlated photons (signal and idler) of frequencies ω_s and ω_i and wave vectors $\boldsymbol{k}_s$ and $\boldsymbol{k}_i$, such that $\omega_p = \omega_s + \omega_i$ and $\boldsymbol{k}_p = \boldsymbol{k}_s + \boldsymbol{k}_i$. The crystal thus produces pairs of entangled photons in state

$$|\psi_2\rangle = \tfrac{1}{\sqrt{2}}(\,|\updownarrow^s\rangle\,|\leftrightarrow^i\rangle + |\leftrightarrow^s\rangle\,|\updownarrow^i\rangle)\,. \tag{10.37}$$

Then, if we detect one photon of the pair, say the idler, along a particular direction $\boldsymbol{k}_i$ and polarization $|\leftrightarrow^i\rangle$, we know that there is one signal photon in the mode with $\boldsymbol{k}_s = \boldsymbol{k}_f - \boldsymbol{k}_i$ and in state $|\updownarrow^s\rangle$. This, however, is not a deterministic source of single-photons, as it relies on the spontaneous generation of entangled photon pairs and conditional detection of one photon, which projects the other photon onto the desired polarization and momentum state. Hence, we can not control the timing and the temporal characteristics of the single-photon pulses. If we need to initialize the quantum register with a certain number of qubits represented by the signal photons, we will need a coincidence detection of the corresponding number of idler photons, which for a large register is a very unlikely event. Thus, for an efficient initialization of the register, deterministic sources of single photons are required. In Sect. 5.3 we have presented one such deterministic and efficient source of tailored single-photon pulses based on intracavity STIRAP with a single atom.

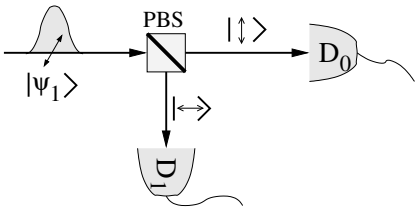

Fig. 10.7. Photonic qubit measurement in the computational basis $\{\,|0\rangle, |1\rangle\}$ is implemented with a polarizing beam-splitter (PBS) and two photodetectors D_0 and D_1.

To complete the description of the optical quantum computer, we need to consider a measurement scheme capable of reliably detecting the polarization states of single photons. When the photonic qubit $|\psi_1\rangle = \alpha\,|\updownarrow\rangle + \beta\,|\leftrightarrow\rangle$ goes though a polarizing beam-splitter, its vertically and horizontally polarized components are sent to two different spatial modes—photonic channels. Placing efficient photon detectors at each channel would therefore accomplish the projective measurement of the qubits in the computational basis $\{\,|0\rangle, |1\rangle\}$, as shown in Fig. 10.7. Avalanche photodetectors, mentioned in the beginning of Sect. 2.3, have very high quantum efficiencies of $\eta \gtrsim 70\%$ and can therefore realize reliable qubit measurements. Finally, all of the constituent parts of the

optical quantum computer described above can be interconnected by optical fibers, according to the algorithm or program under execution.

10.6 Quantum Dot Array Quantum Computer

The other genuine two-state system discussed in Sect. 8.4 is a spin-$\frac{1}{2}$ particle, such as an isolated electron. Here we outline a promising proposal by Loss and DiVincenzo (1998) for implementing scalable quantum computation with single electrons trapped in semiconductor quantum dots. A schematic representation of a typical structure is shown in Fig. 10.8. An approximately 5 nm thick layer of AlGaAs is sandwiched between two thicker layers of GaAs. The lower substrate of GaAs is n-doped so as to provide free electrons which tend to accumulate at the upper interface between the AlGaAs and GaAs, forming a so-called 2D electron gas. This is due to an effect analogous to the total internal reflection of optical waves from the interface of two transparent media possessing different refraction indices. Here the two semiconductor species posses different "refraction indices" for electron waves. An array of metallic contacts, also called gates, is lithographically imprinted on the top of the upper GaAs layer about $50-100$ nm above the 2D electron gas. Externally controlled voltages applied to these gates can then restrict the movement of the electrons in the two remaining directions. In particular, 3D potential wells for the electrons can be induced in the regions marked by dashed circles in Fig. 10.8, where the shorter gates define the depths of the potential in the surface plain, while the longer gates define the potential barriers between the neighboring potential minima. The electrons can then be confined in these regions, conventionally called quantum dots.

We thus consider a lateral array of K nearly identical quantum dots doped with electrons. This system is described by the second–quantized Hamiltonian

$$\begin{aligned}\mathcal{H} = &\sum_{j,s} E_{js} a_{js}^{\dagger} a_{js} + \frac{\hbar}{2} \sum_{j} U \mathcal{N}_j (\mathcal{N}_j - 1) \\ &+ \hbar \sum_{i<j,s} J_{ij,s} (a_{is}^{\dagger} a_{js} + a_{js}^{\dagger} a_{is}) + \hbar \sum_{i<j} V_{ij} \mathcal{N}_i \mathcal{N}_j \ , \end{aligned} \tag{10.38}$$

the first two terms being responsible for the intradot effects and the last two describing the interdot interactions, with $i, j = 1, 2, \ldots, K$ denoting the dot index. Here $a_{js}^{\dagger}$ and a_{js} are the (fermionic) creation and annihilation operators for an electron in state s with single-particle energy E_{js} and orbital wavefunction $\Psi_{js}(\boldsymbol{r})$.

$$U = \frac{e^2}{8\pi\varepsilon_r\varepsilon_0} \int \mathrm{d}^3 r \int \mathrm{d}^3 r' \, \frac{|\Psi_{js}(\boldsymbol{r})|^2 |\Psi_{js'}(\boldsymbol{r}')|^2}{|\boldsymbol{r} - \boldsymbol{r}'|} \simeq \frac{e^2}{C_g} \ ,$$

is the on-site Coulomb repulsion, with $C_g \simeq 8\varepsilon_r\varepsilon_0 R$ being the self-capacitance for 2D disk-shaped quantum dot ($\varepsilon_r \simeq 13$ for GaAs). $\mathcal{N}_j = \sum_s a_{js}^{\dagger} a_{js}$ is the

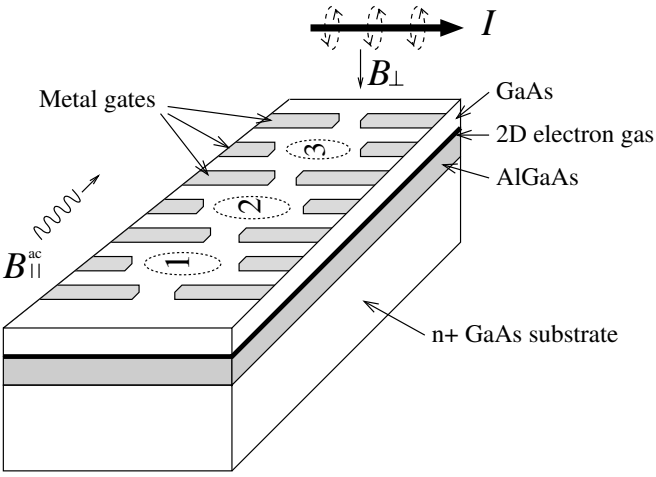

Fig. 10.8. Scheme of a semiconductor heterostructure for implementing quantum computation with single electrons confined in individual quantum dots, three of which are indicated.

total electron number operator of the jth dot.

$$J_{ij,s} = \frac{\hbar^2}{2m_{\mathrm{e}}^*} \int \mathrm{d}^3 r \, \Psi_{is}^*(\boldsymbol{r}) \nabla^2 \Psi_{js}(\boldsymbol{r}) \; ,$$

with m_{e}^* being the electron effective mass ($m_{\mathrm{e}}^* \simeq 0.067 m_e$ in GaAs), are the coherent tunnel matrix elements which are given by the overlap of the electronic wavefunctions $\Psi_{is}(\boldsymbol{r})$ and $\Psi_{js}(\boldsymbol{r})$ of adjacent dots ($j = i + 1$) and can therefore be controlled by the external voltage applied to the gates defining the corresponding interdot tunneling barriers. Finally, $V_{ij} \simeq U(C/C_g)^{|i-j|}$, with $C \ll C_g$ being the interdot capacitance, describe the interdot electrostatic interaction. In general, the index s refers to both orbital and spin states of an electron. In the Coulomb blockade and tight-binding regime, the on-site Coulomb repulsion and single-particle level–spacing $\Delta E \simeq \hbar^2 \pi / (m_{\mathrm{e}}^* R^2)$ are much larger than the tunneling rates, $U > \Delta E/\hbar \gg J_{ij,s}$. Under these conditions, the Hamiltonian (10.38), also known as the extended Mott–Hubbard Hamiltonian, provides a very accurate description of the system. Usually, the matrix elements $V_{ij} = V$ are non-vanishing for the nearest neighbors only ($j = i + 1$), and are further suppressed in the presence of free carriers in the substrate, where image charges can almost completely screen the interdot Coulomb repulsion, in which case $V \approx 0$. Typically, in ~ 50 nm size GaAs/AlGaAs quantum dots, separated from each other by ~ 100 nm, one has $0 \leq J_{ij} \lesssim 0.05$ meV, $\Delta E \sim 0.4$ meV, $U \sim 10$ meV, while the thermal energy can be made very small at the dilution–refrigerator temperatures $T \sim 2 - 10$ mK, in which case $k_{\mathrm{B}} T \sim 0.2 - 1$ μeV.

By carefully manipulating the voltages applied to the metal gates, one can deplete the 2D electron gas under the gates and then dope each quantum dot with a single electron occupying the lowest energy level. In this case, the spin state of an individual electron can represent a qubit with basis states $|\uparrow\rangle \equiv |0\rangle$ and $|\downarrow\rangle \equiv |1\rangle$, where the quantization z-axis is taken normal to the surface of the structure. If we apply a static magnetic field $B_\perp(x)$ perpendicular to the surface, but having a large gradient along the lateral x direction, it will induce a Zeeman shift of the spin-up and spin-down components of the electrons according to $E_{j\uparrow,\downarrow} = \pm\mu_{\rm B} g_{\rm e} B_\perp(x_j)$, where $\mu_{\rm B}$ is the Bohr magneton, $g_{\rm e}$ is the gyromagnetic factor of the electron in the semiconductor, and x_j is the position of jth dot. Then, as in the case of a two-level atom driven by a resonant ac electric field, by using an ac magnetic field $B_\parallel^{\rm ac}$, whose frequency ω is resonant with the frequency $\omega_{j\uparrow\downarrow} = (E_{j\uparrow} - E_{j\downarrow})/\hbar$ of the transition $|\uparrow^j\rangle \leftrightarrow |\downarrow^j\rangle$, we can selectively address the electron localized at position x_j. Thus we have a typical case of magnetic resonance, in which the electron oscillates between its spin-up and spin-down state with the Rabi frequency $\Omega = \mu_{\rm e} B_\parallel^{\rm ac}/\hbar$, where $\mu_{\rm e}$ is the electron magnetic moment. Clearly, the Rabi frequency should be smaller than the difference of the Zeeman splitting for the electrons localized at various quantum dots, so that the field drives resonantly only the required spin. Then, by properly choosing the phase and duration τ of the ac magnetic field, one can realize any unitary transformation $\mathcal{U}_{\uparrow\downarrow}(\theta)$ on the qubit transition $|\uparrow\rangle \leftrightarrow |\downarrow\rangle$, with $\theta = 2\Omega\tau$ being the corresponding pulse area.

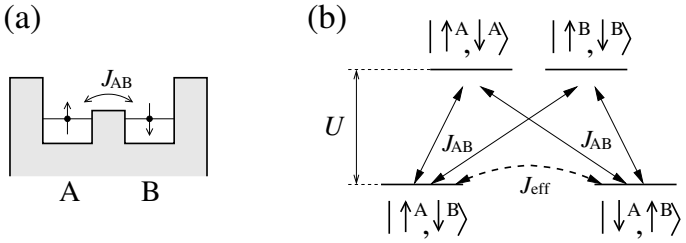

Fig. 10.9. (a) A pair of quantum dots A and B, each doped with a single electron, interact via electron tunneling with the rate $J_{\rm AB}$. (b) Adiabatic elimination of the nonresonant (virtual) states $|\uparrow^{\rm A},\downarrow^{\rm A}\rangle$ and $|\uparrow^{\rm B},\downarrow^{\rm B}\rangle$, with two electrons located at the same dot, yields an effective spin-exchange interaction with the rate $J_{\rm eff} = 2J_{\rm AB}^2/U$.

Let us now outline a possible implementation of a two-qubit gate. Consider a pair of neighboring quantum dots A and B, each containing a single electron in the ground energy level, as shown in Fig. 10.9(a). When $B_\perp = 0$, the $|\uparrow\rangle$ and $|\downarrow\rangle$ states of the electrons are degenerate, i.e., have the same energy, which we set as the zero-point energy. The Hamiltonian (10.38) then reduces to

$$\mathcal{H} = \sum_{s=\uparrow,\downarrow} J_{\mathrm{AB},s}(a^{\dagger}_{\mathrm{A}s}a_{\mathrm{B}s} + a^{\dagger}_{\mathrm{B}s}a_{\mathrm{A}s}) + \frac{\hbar}{2}\sum_{j=\mathrm{A,B}} U\mathcal{N}_j(\mathcal{N}_j - 1)\ . \qquad (10.39)$$

Assume that the tunnel matrix elements couple only equivalent energy and spin states of the neighboring dots with the same rate $J_{\mathrm{AB}} = J_{\mathrm{AB},s}$. The total number of electrons in the system under consideration is 2, therefore the expectation value of the electron number operator $\mathcal{N}_j = a^{\dagger}_{j\uparrow}a_{j\uparrow} + a^{\dagger}_{j\downarrow}a_{j\downarrow}$ of each dot can only take the values $\langle\mathcal{N}_j\rangle = 0, 1,$ or 2. The value $\langle\mathcal{N}_{\mathrm{A}}\rangle = \langle\mathcal{N}_{\mathrm{B}}\rangle = 1$ is realized for the states $|s^{\mathrm{A}}, s^{\mathrm{B}}\rangle$ with two electrons located at different dots, while $\langle\mathcal{N}_{\mathrm{A}}\rangle = 2$ and $\langle\mathcal{N}_{\mathrm{B}}\rangle = 0$, or $\langle\mathcal{N}_{\mathrm{A}}\rangle = 0$ and $\langle\mathcal{N}_{\mathrm{B}}\rangle = 2$ are possible when both electrons are at the same dot. Since electrons are fermions, the Pauli exclusion principle precludes the occupation of the ground energy level of the same dot by two electrons having the same spin s. Let us therefore consider the dynamics of the system initially prepared in one of the states $|\uparrow^{\mathrm{A}}, \downarrow^{\mathrm{B}}\rangle$ or $|\downarrow^{\mathrm{A}}, \uparrow^{\mathrm{B}}\rangle$, i.e., each dot contains one electron, and the spins of the electrons are opposite. When $J_{\mathrm{AB}} \neq 0$, each electron can tunnel to the other dot, resulting in states $|\uparrow^{\mathrm{A}}, \downarrow^{\mathrm{A}}\rangle$ and $|\uparrow^{\mathrm{B}}, \downarrow^{\mathrm{B}}\rangle$ with two electrons located at the same dot (see Fig. 10.9(b)). But since $U \gg J_{\mathrm{AB}}$, these states are largely nonresonant and never significantly populated. We can therefore eliminate them adiabatically, obtaining an effective coupling rate $J_{\mathrm{eff}} = 2J^2_{\mathrm{AB}}/U$ between the states $|\uparrow^{\mathrm{A}}, \downarrow^{\mathrm{B}}\rangle$ and $|\downarrow^{\mathrm{A}}, \uparrow^{\mathrm{B}}\rangle$. The procedure is completely analogous to the adiabatic elimination of an intermediate excited state in a three-level Λ system described in Sect. 3.6. Here the factor 2 in the expression for J_{eff} comes about because we have two intermediate states and therefore two parallel paths for the transition $|\uparrow^{\mathrm{A}}, \downarrow^{\mathrm{B}}\rangle \leftrightarrow |\downarrow^{\mathrm{A}}, \uparrow^{\mathrm{B}}\rangle$. Thus, by lowering the potential barrier and thereby allowing for electron tunneling between the neighboring quantum dots, we can realize a spin-exchange interaction with the rate J_{eff}. If we turn the interdot tunneling on for time $t_{\mathrm{int}} = \pi/(2J_{\mathrm{eff}})$, so that the exchange "pulse area" is $\vartheta \equiv 2J_{\mathrm{eff}}t_{\mathrm{int}} = \pi$, the following transformation will take place:

$$\begin{array}{l} |\uparrow^{\mathrm{A}}\rangle|\uparrow^{\mathrm{B}}\rangle \rightarrow |\uparrow^{\mathrm{A}}\rangle|\uparrow^{\mathrm{B}}\rangle \\ |\uparrow^{\mathrm{A}}\rangle|\downarrow^{\mathrm{B}}\rangle \rightarrow |\downarrow^{\mathrm{A}}\rangle|\uparrow^{\mathrm{B}}\rangle \\ |\downarrow^{\mathrm{A}}\rangle|\uparrow^{\mathrm{B}}\rangle \rightarrow |\uparrow^{\mathrm{A}}\rangle|\downarrow^{\mathrm{B}}\rangle \\ |\downarrow^{\mathrm{A}}\rangle|\downarrow^{\mathrm{B}}\rangle \rightarrow |\downarrow^{\mathrm{A}}\rangle|\downarrow^{\mathrm{B}}\rangle \end{array}\ ,$$

which corresponds to the SWAP gate between a pair of qubits represented by the spins of electrons localized at neighboring quantum dots A and B. In the above table, we have omitted the phase factors, keeping in mind that they can be amended by appropriate single-qubit transformations before or after the exchange interaction. Similarly, if we pulse the interdot tunneling for time $t_{\mathrm{int}} = \pi/(4J_{\mathrm{eff}})$ ("pulse area" is $\vartheta = \pi/2$), the $\sqrt{\mathrm{SWAP}}$ transformation will take place. Recall that $\sqrt{\mathrm{SWAP}}$ is a universal two-qubit gate, since in combination with appropriate single-qubit rotations, it can implement the CNOT gate as per (9.4b).

Recently, significant experimental progress in fabricating semiconductor heterostructures containing several quantum dots has been achieved. Coher-

ent manipulations of single electrons, as well as coherent interactions between pairs of electrons has been demonstrated. Scaling such structure up to tens of even hundreds of qubits, however, requires overcoming several physical and technological obstacles. Thus, when the electrons are subject to a common static inhomogeneous magnetic field, as the total number of electrons increases, it becomes increasingly difficult to resonantly resolve individual electron-spins without affecting the neighboring electrons. Another problem is associated with the fact that the exchange interaction can be implemented between the nearest neighbors only, and there is no efficient mechanism of transferring the information between distant qubits. As a way around such difficulties, we can envision an integrated quantum computer composed of many sub-registers, each containing only a few electrons localized at individual quantum dots. Within each sub-register, single qubit transformations can be implemented by the combination of static and oscillating magnetic fields, while two-qubit gates are mediated by the spin-exchange interactions between electrons trapped in adjacent quantum dots. The sub-registers would be embedded in a two-dimensional array, or grid, of empty quantum dots. It has been shown by Nikolopoulos *et al.* (2004), that by carefully manipulating the tunnel-couplings between the dots, this two-dimensional grid could, in principle, realize a flexible quantum channel, capable of connecting any pair of qubits within the integrated quantum computer.

10.7 Overview and Closing Remarks

In this book, we have focused on the standard (circuit) model of quantum information processing and communication, which involves qubits (two-state quantum systems) and deterministic, unitary and therefore reversible quantum gates. Alternative models do exist and are currently attracting considerable attention. For example, quantum continuous variables, such as the quadrature variables of electromagnetic fields or collective spin states of atomic ensembles, are being explored for quantum simulations as well as quantum information storage and communication purposes. Another model of quantum computation involves probabilistic quantum logic with qubits, conditioned on the successful outcome of measurements on auxiliary qubits resulting in an effective qubit–qubit interaction (entanglement). This paradigm is currently being applied in the context of linear optics quantum information processing. A related idea towards realizing a one-way quantum computation with initially prepared highly entangled multiqubit cluster states of the quantum register is also being explored. The information processing would then employ qubit measurements and conditional feed-forward manipulations resulting in the effective quantum logic.

In this last chapter, we have described several representative schemes pertaining to the physical implementation of the circuit model of quantum computation. In particular, we have discussed quantum optical schemes based on

the manipulation of atoms in cavities and ion-traps, as well as the manipulation of single-photons with linear and nonlinear optical elements. We have also outlined a solid-state proposal based on an array of quantum dots doped with single electrons. We did not touch upon the implementations of various quantum information processing tasks with nuclear magnetic resonance (NMR) schemes. Briefly, the principles of operation of the liquid-state NMR are similar to those of the quantum-dot array quantum computer, the main differences being that the qubits are represented by the nuclear spins of individual atoms bound to a large molecule. As in the case of the electron spins, single qubit rotations are realized with ac magnetic fields, while the inter-qubit coupling is always present due to the spin-exchange interaction between the nuclear spins. A huge number of such molecules in a liquid solvent serve as many quantum registers operating in parallel. The measurement amounts to the detection of the average magnetization of the whole sample. The liquid-state NMR schemes, although rather successful in terms of the number of qubits realized so far, are not scalable, the main limitations being the impossibility of robust initialization in the thermal ensemble of such processors, as well as difficulties in resolving the NMR frequencies of individual qubits and the measurement signal, as the number of qubits becomes larger than a dozen or so. Scalable NMR based schemes have been proposed for solid state systems with appropriate dopants implanted at a regular separation from each other in a solid (semiconductor) matrix. Alternative solid-state candidate systems involve superconducting circuits with charge, flux or phase qubits.

These, as well as many other schemes, are attracting increasing attention in the quest for scalable quantum information processing and communication. It is not clear at this time, which scheme will eventually prove to be the most practical one. However, even if no practical quantum computer is ever built, the advances in technology, as well as the understanding of the fundamental physics gained in the process, will most likely prove useful even in possibly unexpected contexts.

Problems

10.1. Devise the sequence of operations for the Rydberg atoms crossing a microwave cavity to generate the maximally-entangled four (and more) particle GHZ states.

10.2. Verify expressions (10.26), (10.28) and (10.29).

10.3. Devise the sequence of operations for the ion-trap quantum computer to implement the three-qubit CCZ (controlled-controlled-Z) and CCNOT (quantum Toffoli) gates. Generalize this procedure to the case of multiqubit gates C^k-Z and C^k-NOT involving $k > 2$ control qubits and one target qubit.

10.4. Find the eigenstates and eigenvalues of (10.32). Then derive the conditions for adiabatic following of the dark state $|D\rangle$ of (10.33).

10.5. Verify that the cross-phase modulation (XPM) Hamiltonian (10.35) results in the evolution equation (10.36) for two single-photon fields. Now assume that at the input to the XPM medium, each mode $j = \mathrm{A,B}$ is prepared in the corresponding coherent state $|\alpha^j\rangle$, i.e., $|\Phi_{\mathrm{in}}\rangle = |\alpha^{\mathrm{A}}\rangle\,|\alpha^{\mathrm{B}}\rangle$. How does this input state evolve upon the interaction? Prove that for $\varphi = \xi t_{\mathrm{out}} = \pi$, the output state is given by

$$|\Phi_{\mathrm{out}}\rangle = \tfrac{1}{2}\big(\,|\alpha^{\mathrm{A}}\rangle + |-\alpha^{\mathrm{A}}\rangle\big)\,|\alpha^{\mathrm{B}}\rangle + \tfrac{1}{2}\big(\,|\alpha^{\mathrm{A}}\rangle - |-\alpha^{\mathrm{A}}\rangle\big)\,|-\alpha^{\mathrm{B}}\rangle\,. \tag{10.40}$$

Further Reading

Books

Quantum Theory

- C. Cohen-Tannoudji, B. Diu and F. Laloë, *Quantum Mechanics, Vols. I and II* (Wiley, 1977).
- A. Messiah, *Quantum Mechanics* (Dover, 2000).
- L. D. Landau and E. M. Lifshits, *Quantum Mechanics—Nonrelativistic theory* (Pergamon, 1981).
- T. F. Jordan, *Linear Operators for Quantum Mechanics* (Wiley, 1969).
- K. Gottfried and T.-M. Yan, *Quantum Mechanics: Fundamentals* (Springer, 2003).
- E. Merzbacher, *Quantum Mechanics* (Wiley, 1998).
- J. J. Sakurai, *Advanced Quantum Mechanics* (Addison-Wesley, 1967).
- C. Cohen-Tannoudji, J. Dupont-Roc and G. Grynberg, *Photons and Atoms: Introduction to Quantum Electrodynamics* (Wiley, 1989).
- J. A. Wheeler and W. H. Zurek, *Quantum Theory and Measurement* (Princeton University Press, 1984).
- J. S. Bell, *Speakable and Unspeakable in Quantum Mechanics* (Cambridge University Press, 1988).
- A. Peres, *Quantum Theory: Concepts and Methods* (Kluwer Academic/Springer, 1995).
- D. Giulini, E. Joos, C. Kiefer, J. Kupsch, I.-O. Stamatescu and H. D. Zeh, *Decoherence and the Appearance of a Classical World in Quantum Theory* (Springer, 2003).
- P. D. Drummond and Z. Ficek (editors), *Quantum Squeezing* (Springer, 2003).
- L. Jacak, P. Hawrylak and A. Wojs, *Quantum Dots* (Springer, 1998).

Quantum and Nonlinear Optics

- J. R. Klauder and E. C. G. Sudarshan, *Fundamentals of Quantum Optics* (Dover, 2006).
- R. Loudon, *The Quantum Theory of Light* (Oxford University Press, 2000).

- M. Sargent III, M. O. Scully and W. E. Lamb, Jr., *Laser Physics* (Addison-Wesley, 1974).
- H. Carmichael, *An Open Systems Approach to Quantum Optics* (Springer, 1993).
- D. Walls and G. J. Milburn, *Quantum Optics* (Springer, 1995).
- P. Meystre and M. Sargent III, *Elements of Quantum Optics* (Springer, 1999).
- M. O. Scully and M. S. Zubairy, *Quantum Optics* (Cambridge University Press, 1997).
- L. Allen and J. H. Eberly, *Optical Resonance and Two-Level Atoms* (Wiley, 1975).
- C. Cohen-Tannoudji, J. Dupont-Roc and G. Grynberg, *Atom-Photon Interactions: Basic Processes and Applications* (Wiley, 1992).
- G. S. Agarwal, *Quantum Statistical Theories of Spontaneous Emission and Their Relation to Other Approaches*, Springer Tracts Mod. Phys. **70** (Springer, 1974).
- C. W. Gardiner and P. Zoller, *Quantum Noise: A Handbook of Markovian and Non-Markovian Quantum Stochastic Methods with Applications to Quantum Optics* (Springer, 2004).
- W. P. Schleich, *Quantum Optics in Phase Space* (Wiley, 2001).
- U. Leonhardt, *Measuring the Quantum State of Light* (Cambridge University Press, 1997).
- H.-P. Breuer and F. Petruccione, *The Theory of Open Quantum Systems* (Oxford University Press, 2002).
- W. H. Louisell, *Quantum Statistical Properties of Radiation* (Wiley, 1973).
- L. Mandel and E. Wolf, *Optical Coherence and Quantum Optics* (Cambridge University Press, 1995).
- Y. Yamamoto and A. Imamoğlu, *Mesoscopic Quantum Optics* (Wiley, 1999).
- R. R. Puri, *Mathematical Methods of Quantum Optics* (Springer, 2001).
- Z. Ficek and S. Swain, *Quantum Interference and Coherence: Theory and Experiments* (Springer, 2005).
- C. Gerry and P. Knight, *Introductory Quantum Optics* (Cambridge University Press, 2004).
- V. Vedral, *Modern Foundations of Quantum Optics* (Imperial College Press, 2005).
- W. Vogel, D.-G. Welsch and S. Wallentowitz, *Quantum Optics* (Wiley, 2006).
- M. Bloembergen, *Nonlinear Optics* (World Scientific, 1996).
- Y. R. Shen, *The Principles of Nonlinear Optics* (Wiley, 1984).
- R. W. Boyd, *Nonlinear Optics* (Academic Press, 2002).
- F. G. Major, V. N. Gheorghe and G. Werth, *Charged Particle Traps: Physics and Techniques of Charged Particle Field Confinement* (Springer, 2004).

Quantum Information and Computation

- C. E. Shannon and W. Weaver, *The Mathematical Theory of Communication* (University of Illinois Press, 1949).
- D. Slepian (editor), *Key papers in the development in information theory* (IEEE, 1974).
- R. W. Hamming, *Coding and information theory* (Prentice Hall, 1986).
- H. R. Lewis and C. H. Papadimitriou, *Elements of the Theory of Computation* (Prentice Hall, 1997).

- A. Yu. Kitaev, A. H. Shen and M. N. Vyalyi, *Classical and Quantum Computation* (American Mathematical Society, 2002).
- J. Preskill, *Lecture Notes for Physics 229: Quantum Information and Computation* (1998), `http://www.theory.caltech.edu/people/preskill/ph229/`.
- M. A. Nielsen and I. L. Chuang, *Quantum Information and Quantum Computation* (Cambridge University Press, 2000).
- D. Bouwmeester, A. Ekert and A. Zeilinger (editors), *The Physics of Quantum Information: Quantum Cryptography, Quantum Teleportation, Quantum Computation* (Springer, 2000).
- G. Alber, T. Beth, M. Horodecki, P. Horodecki, R. Horodecki, M. Rötteler, H. Weinfurter, R. Werner and A. Zeilinger, *Quantum Information* (Springer, 2001).
- H.-K. Lo, S. Popescu and T. Spiller (editors), *Introduction to Quantum Computation and Information* (World Scientific, 2001).
- J. Stolze and D. Suter, *Quantum Computing: A Short Course from Theory to Experiment* (Wiley, 2004).
- W.-H. Steeb and Y. Hardy, *Problems & Solutions in Quantum Computing & Quantum Information* (World Scientific, 2004).
- D. C. Marinescu and G. M. Marinescu, *Approaching Quantum Computing* (Prentice Hall, 2004).
- M. Hirvensalo, *Quantum Computing* (Springer, 2004).
- P. Kaye, R. Laflamme and M. Mosca, *An Introduction to Quantum Computing* (Oxford University Press, 2006).
- M. Hayashi, *Quantum Information: An Introduction* (Springer, 2006).
- G. Benenti, G. Casati and G. Strini, *Principles of Quantum Information and Computation: Basic Concepts* (World Scientific, 2004).
- G. Benenti, *Principles of Quantum Computation and Information: Basic Tools and Special Topics* (World Scientific, 2006).

Selected References

Chapter 1

- D. Stoler, *Equivalence classes of minimum uncertainty packets*, Phys. Rev. D **1**, 3217 (1970).
- W.H. Zurek, *Decoherence, einselection, and the quantum origins of the classical*, Rev. Mod. Phys. **75**, 715 (2003).
- M. Schlosshauer, *Decoherence, the measurement problem, and interpretations of quantum mechanics*, Rev. Mod. Phys. **76**, 1267 (2004).

Chapter 2

- R. Hanbury-Brown and R. Q. Twiss, *Correlation between photons in two coherent beams of light*, Nature **177**, 27 (1956).
- R. J. Glauber, *The quantum theory of optical coherence*, Phys Rev. **130**, 2529 (1963);
  R. J. Glauber, *Coherent and incoherent states of the radiation field*, Phys Rev. **131**, 2766 (1963).

- E. C. G. Sudarshan, *Equivalence of semiclassical and quantum mechanical descriptions of statistical light beams*, Phys. Rev. Lett. **10**, 277 (1963).
- L. Mandel and E. Wolf, *Coherence properties of optical fields*, Rev. Mod. Phys. **37**, 231 (1965).
- K. E. Cahill and R. J. Glauber, *Density operators and quasiprobability distributions*, Phys Rev. **177**, 1822 (1969).
- D. F. Walls, *Squeezed states of light*, Nature **306**, 141 (1983).

Chapter 3

- V. Weisskopf and E. Wigner, *Berechnung der naturlichen Linienbreite auf Grund der Diracschen Lichttheorie*, Z. Phys. **63**, 54 (1930).
- E. T. Jaynes and F. W. Cummings, *Comparison of quantum and semiclassical radiation theory with application to the beam maser*, Proc. IEEE **51**, 89 (1963).
- E. Arimondo, *Coherent population trapping in laser spectroscopy*, Prog. Opt. **35**, 257 (1996).
- K. Bergmann, H. Theuer and B.W. Shore, *Coherent population transfer among quantum states of atoms and molecules*, Rev. Mod. Phys. **70**, 1003 (1998).
- D. Leibfried, R. Blatt, C. Monroe and D. Wineland, *Quantum dynamics of single trapped ions*, Rev. Mod. Phys. **75**, 281 (2003).

Chapter 4

- H. J. Kimble, M. Dagenais and L. Mandel, *Photon antibunching in resonance fluorescence*, Phys. Rev. Lett. **39**, 691 (1977).
- R. Dum, P. Zoller and H. Ritsch, *Monte Carlo simulation of the atomic master equation for spontaneous emission*, Phys. Rev. A **45**, 4879 (1992);
  C. W. Gardiner, A. S. Parkins and P. Zoller, *Wave-functions stochastic differential equations and quantum-jump simulation methods*, Phys. Rev. A **46**, 4463 (1992).
- J. Dalibard, Y. Castin and K. Mølmer, *Wave-function approach to dissipative processes in quantum optics*, Phys. Rev. Lett. **68**, 580 (1992).
- M. B. Plenio and P. L. Knigh, *The quantum-jump approach to dissipative dynamics in quantum optics*, Rev. Mod. Phys. **70**, 101 (1998).

Chapter 5

- E. M. Purcell, *Spontaneous emission probabilities at radio frequencies*, Phys. Rev. **69**, 681 (1946).
- D. Kleppner, *Inhibited spontaneous emission*, Phys. Rev. Lett. **47**, 233 (1981).
- P. Goy, J.-M. Raimond, M. Gross and S. Haroche, *Observation of cavity-enhanced single-atom spontaneous emission*, Phys. Rev. Lett. **50**, 1903 (1983).
- S. Haroche and J.-M. Raimond, *Radiative properties of Rydberg atoms in cavities*, Advances in Atomic and Molecular Physics **20**, 347 (1985).
- A. Kuhn, M. Hennrich and G. Rempe, *Deterministic single-photon source for distributed quantum networking*, Phys. Rev. Lett. **89**, 067901 (2002);
  J. McKeever, A. Boca, A. D. Boozer, R. Miller, J. R. Buck, A. Kuzmich and H. J. Kimble, *Deterministic generation of single photons from one atom trapped*

in a cavity, Science **303**, 1992 (2004);
M. Keller, B. Lange, K. Hayasaka, W. Lange and H. Walther, *Continuous generation of single photons with controlled waveform in an ion-trap cavity system*, Nature **431**, 1075 (2004).
- G. Khitrova, H. M. Gibbs, M. Kira, S. W. Koch and A. Scherer, *Vacuum Rabi splitting in semiconductors*, Nature Physics **2**, 81 (2006).

Chapter 6

- S. McCall and E. Hahn, *Self-induced transparency by pulsed coherent light*, Phys. Rev. Lett. **18**, 908 (1967); Phys. Rev. **183**, 457 (1969).
- G. L. Lamb, Jr., *Analytical descriptions of ultrashort optical pulse propagation in a resonant medium*, Rev. Mod. Phys. **43**, 99 (1971).
- S. E. Harris, *Electromagnetically induced transparency*, Phys. Today **50**(7), 36 (1997).
- L. V. Hau, S. E. Harris, Z. Dutton Z and C. H. Behroozi, *Light speed reduction to 17 metres per second in an ultracold atomic gas*, Nature **397**, 594 (1999).
- M. Fleischhauer and M. D. Lukin, *Dark-state polaritons in electromagnetically induced transparency*, Phys. Rev. Lett. **84**, 5094 (2000); Phys. Rev. A **65**, 022314 (2002).
- C. Liu, Z. Dutton, C. H. Behroozi and L. V. Hau, *Observation of coherent optical information storage in an atomic medium using halted light pulses*, Nature **409**, 490 (2001);
D. F. Phillips, A. Fleischhauer, A. Mair, R. L. Walsworth and M. D. Lukin, *Storage of light in atomic vapor*, Phys. Rev. Lett. **86**, 781 (2001).
- M. Fleischhauer, A. Imamoğlu and J. P. Marangos, *Electromagnetically induced transparency: Optics in coherent media*, Rev. Mod. Phys. **77**, 633 (2005).

Chapter 7

- R. Landauer, *Irreversibility and heat generation in the computing process*, IBM J. Res. Dev. **3**, 183 (1961).
- E. Fredkin and T. Toffoli, *Conservative logic*, Int. J. Theor. Phys. **21**, 219 (1982).
- C. H. Bennett and R. Landauer, *The fundamental physical limits of computation*, Scientific American **253**(1), 38 (1985);
R. Landauer, *Information is physical*, Phys. Today **44**(5) 23 (1991).
- A. Galindo and M. A. Martin-Delagado, *Information and computation: Classical and quantum aspects*, Rev. Mod. Phys. **74**, 347 (2002).

Chapter 8

- V. Scarani, S. Iblisdir, N. Gisin and A. Acin, *Quantum cloning*, Rev. Mod. Phys. **77**, 1225 (2005).
- M. O. Scully, B. G. Englert and H. Walther, *Quantum optical tests of complementarity*, Nature **351** 111 (1991).
- A. Einstein, B. Podolsky and N. Rosen, *Can quantum-mechanical description of physical reality be considered complete?*, Phys. Rev. **47**, 777 (1935);
N. Bohr, *Can quantum-mechanical description of physical reality be considered complete?*, Phys. Rev. **48**, 696 (1935).

- J. S. Bell, *On the Einstein Podolsky Rosen paradox*, Physics **1**, 195 (1964);
  J. S. Bell, *On the problem of hidden variables in quantum mechanics*, Rev. Mod. Phys. **38**, 447 (1966).
- J. F. Clauser, M. A. Horne, A. Shimony and R.A. Holt, *Proposed experiment to test local hidden-variable theories*, Phys. Rev. Lett. **23**, 880 (1969);
  J. F. Clauser and M. A. Horne, *Experimental consequences of objective local theories*, Phys. Rev. D **10**, 526 (1974).
- A. Aspect, P. Grangier and G. Roger, *Experimental realization of Einstein–Podolsky–Rosen–Bohm Gedankenexperiment: A new violation of Bell's inequalities*, Phys. Rev. Lett. **49**, 91 (1982).
- A. Zeilinger, *Experiment and the foundations of quantum physics*, Rev. Mod. Phys. **71**, S288 (1999);
  R. Werner and M. Wolf, *Bell inequalities and entanglement*, Quant. Inf. Comput. **1**(3) 1, (2001).
- D. M. Greenberger, M. Horne and A. Zeilinger, in *Bell's Theorem, Quantum Theory, and Conceptions of the Universe*, edited by M. Katafos (Kluwer Academic, 1988), p 73;
  D. M. Greenberger, M. A. Horne, A. Shimony and A. Zeilinger, *Bell's theorem without inequalities*, Am. J. Phys. **58**, 1131 (1990).
- C. H. Bennett, G. Brassard, C. Crepeau, R. Jozsa, A. Peres and W. K. Wootters, *Teleporting an unknown quantum state via dual classical and Einstein–Podolsky–Rosen channels*, Phys. Rev. Lett. **70**, 1895 (1993).
- C. H. Bennett and S. J. Wiesner, *Communication via one- and two-particle operators on Einstein–Podolsky–Rosen states*, Phys. Rev. Lett. **69**, 2881 (1992).
- C. H. Bennett, G. Brassard, S. Popescu, B. Schumacher, J. A. Smolin and W. K. Wootters, *Purification of noisy entanglement and faithful teleportation via noisy channels*, Phys. Rev. Lett. **76**, 722 (1996).
- C. H. Bennett and G. Brassard, in *Proceedings of IEEE International Conference on Computers, Systems, and Signal Processing*, Bangalore, India, (IEEE, 1984) p. 175;
  C. H. Bennett, *Quantum cryptography using any two nonorthogonal states*, Phys. Rev. Lett. **68**, 3121 (1992);
  A. K. Ekert, *Quantum cryptography based on Bell's theorem*, Phys. Rev. Lett. **67**, 661 (1991);
  C. H. Bennett, G. Brassard and N. D. Mermin, *Quantum cryptography without Bell's theorem*, Phys. Rev. Lett. **68**, 557 (1992).
- N. Gisin, G. Ribordy, W. Tittel and H. Zbinden, *Quantum cryptography*, Rev. Mod. Phys. **74**, 145 (2002).
- D. C. H. Bennett and D. P. DiVincenzo, *Quantum information and computation*, Nature **404**, 247 (2000).
- A. Galindo and M. A. Martin-Delagado, *Information and computation: Classical and quantum aspects*, Rev. Mod. Phys. **74**, 347 (2002).
- C. E. Shannon, *A mathematical theory of communication*, Bell Syst. Thech. J. **27**, 379 (1948); **27**, 623 (1948); **28**, 656 (1949).
- B. Schumacher, *Quantum coding*, Phys. Rev. A **51**, 2738 (1995).
- C. H. Bennett, D. P. DiVincenzo, J. A. Smolin and W. K. Wootters, *Mixed-state entanglement and quantum error correction*, Phys. Rev. A **54**, 3824 (1996).
- W. K. Wootters, *Entanglement of formation of an arbitrary state of two qubits*, Phys. Rev. Lett. **80**, 2245 (1998);

P. Rungta, V. Bužek, C. M. Caves, M. Hillery and G. J. Milburn, *Universal state inversion and concurrence in arbitrary dimensions*, Phys. Rev. A **64**, 042315 (2001).

Chapter 9

- A. Barenco, C. H. Bennett, R. Cleve, D. P. DiVincenzo, N. Margolus, P. Shor, T. Sleator, J. A. Smolin and H. Weinfurter, *Elementary gates for quantum computation*, Phys. Rev. A **52**, 3457 (1995).
- D. Deutsch, *Quantum theory, the Church-Turing principle, and the universal quantum computer*, Proc. Roy. Soc. London **400**, 97 (1985).
- A. Steane, *Quantum computing*, Rep. Prog. Phys. **61**, 117 (1998).
- L. K. Grover, *Quantum mechanics helps in searching for a needle in a haystack*, Phys. Rev. Lett. **79**, 325(1997).
- P. W. Shor, *Algorithms for quantum computation, discrete log and factorizing*, in *Proceedings of the 35th Annual Symposium on Foundations of Computer Science*, edited by S. Goldwasser (IEEE Computer Society, 1994) p. 124;
  A. Ekert and R. Jozsa, *Quantum computation and Shor's factoring algorithm*, Rev. Mod. Phys. **68**, 733 (1996).
- D. S. Abrams and S. Lloyd, *Quantum algorithm providing exponential speed increase for finding eigenvalues and eigenvectors*, Phys. Rev. Lett. **83**, 5162 (1999).
- S. Lloyd, *Universal quantum simulators*, Science **273**, 1073 (1996).
- P. W. Shor, *Scheme for reducing decoherence in quantum computer memory*, Phys. Rev. A **52**, R2493 (1995).
- A. M. Steane, *Error correcting codes in quantum theory*, Phys. Rev. Lett. **77**, 793 (1996);
  D. P. DiVincenzo and P. W. Shor, *Fault-tolerant error correction with efficient quantum codes*, Phys. Rev. Lett. **77**, 3260 (1996).
- E. Knill, R. Laflamme and W. H. Zurek, *Resilient quantum computation*, Science **279**, 342 (1998).
- J. Preskill, *Fault-tolerant quantum computation*, in *Introduction to Quantum Computation and Information*, edited by H.-K. Lo, S. Popescu and T. Spiller (World Scientific, 2001), p. 213.
- P. Zanardi and M. Rasetti, *Noiseless quantum codes*, Phys. Rev. Lett. **79**, 3306 (1997);
  D. A. Lidar, I. L. Chuang and K. B. Whaley, *Decoherence-free subspaces for quantum computation*, Phys. Rev. Lett. **81**, 2594 (1998).

Chapter 10

- D. P. DiVincenzo, *The physical implementation of quantum computation*, Fortschr. Phys. **48**, 771 (2000).
- J.-M. Raimond, M. Brune and S. Haroche, *Manipulating quantum entanglement with atoms and photons in a cavity*, Rev. Mod. Phys. **73**, 565 (2001);
  L. Davidovich, M. Brune, J.-M. Raimond and S. Haroche, *Mesoscopic quantum coherence in cavity QED: Preparation and decoherence monitoring schemes*, Phys. Rev. A **53**, 1295 (1996).

- J, I. Cirac and P. Zoller, *Quantum computations with cold trapped ions*, Phys. Rev. Lett. **74**, 4091 (1995);
  A. Steane, *The ion trap quantum information processor*, Appl. Phys. B. **64**, 623 (1997).
- M. G. Raizen, J. M. Gilligan, J. C. Bergquist, W. M. Itano and D. J. Wineland, *Ionic crystals in a linear Paul trap*, Phys. Rev. A **45**, 6493 (1992).
- D. Kielpinski, C. Monroe and D. J. Wineland, *Architecture for a large-scale ion-trap quantum computer*, Nature **417**, 709 (2002).
- T. Pellizzari, S. A. Gardiner, J, I. Cirac and P. Zoller, *Decoherence, continuous observation, and quantum computing: A cavity QED model*, Phys. Rev. Lett. **75**, 3788 (1995).
- D. Petrosyan, *Towards deterministic optical quantum computation with coherently driven atomic ensembles*, J. Opt. B **7**, S141 (2005).
- C. K. Hong and L. Mandel, *Experimental realization of a localized one-photon state*, Phys. Rev. Lett. **56**, 58 (1986).
- P. Grangier, G. Roger and A. Aspect, *Experimental evidence for a photon anticorrelation effect on a beam splitter: A new light on single-photon interferences*, Europhys. Lett. **1**, 173 (1986).
- D. Loss and D.P. DiVincenzo, *Quantum computation with quantum dots*, Phys. Rev. A **57** 120 (1998).
- L. Vandersypen, R. Hanson, L. Willems van Beveren, J. Elzerman, J. Greidanus, S. De Franceschi and L. Kouwenhoven, *Quantum computing with electron spins in quantum dots*, in *Quantum Computing and Quantum Bits in Mesoscopic Systems* (Kluwer Academic, 2002).
- G. M. Nikolopoulos, D. Petrosyan and P. Lambropoulos, *Coherent electron wavepacket propagation and entanglement in array of coupled quantum dots*, Europhys. Lett. **65** 297 (2004); J. Phys.: Condens. Matter **16**, 4991 (2004);
  D. Petrosyan and P. Lambropoulos, *Coherent population transfer in a chain of tunnel coupled quantum dots*, Optics Commun. (2006), in press.
- D. Deutsch, *Quantum computational networks*, Proc. R. Soc. London A **425**, 73 (1989).
- S. L. Braunstein and P. van Loock, *Quantum information with continuous variables*, Rev. Mod. Phys. **77**, 513 (2005).
- E. Knill, R. Laflamme and G. J. Milburn, *A scheme for efficient quantum computation with linear optics*, Nature **409**, 46 (2001).
- R. Raussendorf and H. J. Briegel, *A one-way quantum computer*, Phys. Rev. Lett. **86** 5188 (2001).
- L. M. K. Vandersypen and I. L. Chuang, *NMR techniques for quantum control and computation*, Rev. Mod. Phys. **76**, 1037 (2004).
- B. Kane, *A silicon-based nuclear spin quantum computer*, Nature **393**, 133 (1998);
  D. P. DiVincenzo, *Real and realistic quantum computers*, Nature **393**, 113 (1998).
- D. Esteve, *Superconducting qubits*, in *Proceedings of the Les Houches 2003 Summer School on Quantum Entanglement and Information Processing*, edited by D. Esteve and J.-M. Raimond (Elsevier, 2004).
- C. Monroe, *Quantum information processing with atoms and photons*, Nature **416**, 238 (2002).
- P. Zoller *et al.*, *Quantum information processing and communication*, Eur. Phys. J. D **36**, 203 (2005).

Index